Identification de nouveaux gènes de prédisposition aux paranganglioms

Alexandre Buffet

UNIVERSITÉ PARIS DESCARTES

THÈSE de DOCTORAT

Pour l'obtention du grade de DOCTEUR DE L'UNIVERSITÉ PARIS DESCARTES
Ecole Doctorale : Hématologie, Oncogenèse, Biothérapie
Spécialité : Oncogenèse

présentée et soutenue publiquement
par **Alexandre BUFFET**
Le mardi 25 septembre 2018

IDENTIFICATION DE NOUVEAUX GÈNES DE PRÉDISPOSITION AUX PARAGANGLIOMES

Jury :

Pr Pierre LAURENT-PUIG	Président
Pr Anne-Paule GIMENEZ-ROQUEPLO	Directeur de thèse
Pr Anne BARLIER	Rapporteur
Dr Rodrigue ROSSIGNOL	Rapporteur
Pr Bernard GOICHOT	Membre invité
Dr Judith FAVIER	Membre invité

Ce travail de thèse a été réalisé au sein de l'unité INSERM U970 au centre de recherche cardiovasculaire de l'HEGP (PARCC@HEGP) dirigé par le Dr Alain Tedgui, au sein de l'équipe 13 « Phéochromocytomes et paragangliomes, de la génétique à la thérapie ciblée » du Pr Anne-Paule Gimenez-Roqueplo.

Je tiens tout d'abord à remercier très sincèrement les membres du jury :

Le Pr Pierre Laurent-Puig pour m'avoir fait l'honneur d'accepter de présider ce jury de thèse.
Le Pr Anne Barlier et le Dr Rodrigue Rossignol pour avoir accepté d'être rapporteur de cette thèse.
Le Pr Bernard Goichot pour avoir accepté de participer à ce jury.

Je tiens à remercier sincèrement le Pr Anne-Paule Gimenez-Roqueplo pour son encadrement lors de ce travail de quatre ans, sa rigueur et sa patience.

Je remercie vivement Judith Favier pour son aide au cours de cette thèse, son optimisme, ses encouragements (même si je continue à penser que le verre est toujours à moitié vide).

Je tiens à remercier l'ensemble des membres de l'équipe 13 (Nelly, coach Aurélie, Luis, Estelle, Mini Judith, Yasmin) pour leurs bonnes humeurs, leurs aides au quotidien, et leurs conseils.

Je remercie également l'ensemble des techniciens et ingénieurs du laboratoire de génétique moléculaire de l'HEGP pour avoir eu la gentillesse de m'accepter sur la plateforme et leurs coups de mains. Un grand merci également à Laurène pour ton aide et ta bonne humeur lors de notre tour de France.

Un grand merci aux membres du BDE (Hélène, Mini Judith, Rami, Kelly) pour cette bonne humeur perpétuelle dans laquelle nous avons pu travailler.

Je tiens aussi à remercie du fond du cœur l'équipe de Génétique du CHU de Toulouse, pour m'avoir transmis votre passion pour la génétique clinique et moléculaire.

Un grand merci à Lucile, Aline, Caroline, Emilie, Elise, Pascale pour les goutés/restos/ cafés/apéros réguliers et indispensables à ces quatre ans !
Enfin un grand merci à mes parents pour leur soutien sans faille tout au long de ces années.

RÉSUMÉ

Les paragangliomes (PGL) sont des tumeurs neuroendocrines rares, génétiquement déterminées dans 40 % des cas. Malgré les évolutions récentes des connaissances sur la génétique des PGL, il reste toujours environ 15 % des patients pour lesquels aucune cause génétique ne peut être identifiée alors que leur présentation clinique évoque une forme génétiquement déterminée. De plus, il n'a jamais été démontré que l'identification d'une mutation constitutionnelle dans l'un de ces gènes de prédisposition avait un impact positif sur la prise en charge et l'évolution des patients. Mon travail de thèse a été organisé autour de deux grands objectifs : 1) évaluer le bénéfice pour les patients de l'identification d'une mutation constitutionnelle sur un gène de prédisposition au moment du diagnostic du PGL ; 2) mettre en évidence de nouveaux gènes de prédisposition aux PGL et/ou de nouveaux mécanismes d'inactivation des gènes de prédisposition connus pouvant expliciter les formes suspectes d'être génétiques sans mutation identifiée.

Grâce à une étude rétrospective multicentrique rassemblant 221 patients ayant un PGL secondaire à une mutation sur les gènes *SDHB, SDHD, SDHC* ou *VHL*, j'ai pu observer que les patients ayant bénéficié de l'analyse génétique au moment du diagnostic de leur PGL avaient été mieux suivis que ceux ayant bénéficié du diagnostic génétique à distance de leur prise en charge initiale. La connaissance d'un statut génétique positif dans la période du diagnostic du PGL a permis de dépister des PGL plus petits en cas de récidive et une maladie métastatique moins étendue en cas de malignité et d'améliorer la survie. Ces résultats valident les recommandations internationales qui proposent un test génétique à tous patients avec PGL au moment du diagnostic initial.

Sur le plan fondamental, j'ai identifié par une stratégie de séquençage d'exome des mutations dans un nouveau gène de prédisposition au PGL, *SLC25A11*, qui code pour le transporteur mitochondrial du 2-oxoglutarate/malate et montré que les mutations constitutionnelles de *SLC25A11* prédisposent à des formes malignes de PGL. J'ai de plus démontré que les tumeurs humaines ainsi que le modèle expérimental cellulaire inactivé pour ce gène développent une pseudo-hypoxie et une hyperméthylation globale de l'ADN expliquant la tumorigenèse secondaire à l'inactivation de ce gène. L'identification de ce nouveau gène de prédisposition étend le champ des dysfonctions mitochondriales dans la tumorigenèse et dans la cancérogénèse des PGL et révèle un nouveau lien entre mitochondrie et cancer.

ABSTRACT

Paragangliomas (PGL) are rare neuroendocrine tumors, genetically determined in around 40% of cases. Despite recent developments in PGL genetics, there is still about 15% of patients for whom no genetic cause can be identified, while their clinical presentation is suspicious of a genetic form. Moreover, it has never been demonstrated that the identification of a germline mutation in any of the PPGL predisposition genes has a positive impact on the patients' management and clinical outcome.

My PhD research project has been organized around two main objectives: 1) to evaluate the benefits for the patients of the identification of a germline mutation on one susceptibility gene at the time of PGL diagnosis; 2) to search for new PGL genes and / or new mechanisms of inactivation of the previously known genes, which could explain PGL suspected to be a genetic form but without detected mutation.

Thanks to a retrospective multicenter study involving 221 patients with a PGL due to a mutation on the *SDHB, SDHD, SDHC* or *VHL* genes, I observed that the patients who benefited from the genetic analysis at the time of the diagnosis of PGL had a better follow-up than those who had the data of their genetic test later on after the initial PGL diagnosis. Knowledge of a positive genetic status in the PGL diagnosis period favored the detection of smaller recurrent PGLs and less extensive metastatic disease and improved the median of survival. These results validate the international recommendations of offering a PPGL genetic testing to all affected patients at the time of initial diagnosis.

I identified germline mutations in a novel PGL gene, *SLC25A11* with a whole-exome sequencing strategy, which encodes for the mitochondrial 2-oxoglutarate/malate carrier and showed that *SLC25A11* germline mutations predispose to malignant PGL. I demonstrated that human tumors as well as the knockout of *slc25a11* gene in a murine experimental model induces a pseudo-hypoxia and a global hypermethylation of the DNA, which explains the tumourigenesis secondary to the inactivation of this gene. The identification of this new PGL susceptibility gene expands the role of mitochondrial dysfunction in paraganglioma tumorigenesis and reveals a new pathway linking metabolic defects and cancer.

SOMMAIRE

LISTE DES FIGURES

LISTE DES TABLES

LISTE DES ABBRÉVIATIONS

CMT : carcinome médullaire de la thyroïde

COMT : catéchol-O-méthyl transférase

CVD : cyclophosphamide, vincristine, dacarbazine

^{18}F-DOPA : ^{18}F-dihydroxyphénylalanine

^{18}F-FDG : ^{18}F-Fluorodeoxyglucose

GIST : tumeur gastrointestinale stromale

HPTH : hyperparathyroïdie

HRLCC : Hereditary Leiomyomatosis and Renal Cell Cancer

HTA : hypertension artérielle

IHC : immunohistochimies

^{123}I-MIBG : ^{123}I-métaiodobenzylguanidine

L-DOPA : dihydrophénylélthylamine

MAO : monoamine oxydase

3-MT : 3-méthoxytyramine

NEM2 : néoplasies endocriniennes multiples de type 2

NF1 : neurofibromatose de type 1

NGS : séquençage de nouvelle génération à haut débit

PA : pression artérielle

PGL : paragangliome

PH : phéochromocytome

PNMT : Phényléthanolamine N-méthyltransférase

SDH : succinate déshydrogénase

TCGA : The Cancer Genome Atlas

TEP : tomographie par émission de positons

VHL : maladie de von Hippel-Lindau

WT : sauvage

INTRODUCTION

Les Paragangliomes et Phéochromocytomes
-
Présentation Générale

Génétique des paragangliomes et phéochromocytomes

PARTIE 1 : LES PARAGANGLIOMES ET PHÉOCHROMOCYTOMES : PRÉSENTATION GÉNÉRALE

I- DÉFINITION ET LOCALISATION

Les paragangliomes (PGL) sont des tumeurs neuroendocrines rares (OMIM 171300 et OMIM 606864) qui se développent aux dépens des paraganglions qui forment les systèmes parasympathiques ou sympathiques extra-surrénaliens et la médullo-surrénale. Les phéochromocytomes (PH) sont définis comme des PGL développés spécifiquement aux dépens de la médullo-surrénale.

Ces tumeurs hypervascularisées ont une distribution large dans l'organisme. Un PGL peut donc être diagnostiqué dans différentes localisations (**Figure 1**) :

- dans la région cervicale, ils peuvent se développer à partir des ganglions du système nerveux parasympathique (glomus tympanique et jugulaire dans la tête, et glomus carotidien et vagal dans le cou),
- dans les régions thoraciques, abdominales et pelviennes, ils peuvent se développer à partir de la chaine ganglionnaire du système nerveux sympathique, c'est à dire le long des chaines ganglionnaires para-aortiques, le long des chaines ganglionnaires pré-vertébrales et para-vertébrales thoraciques et abdominales, au niveau de l'organe de Zuckerkandl, en avant de la bifurcation aortique et dans la vessie. Des localisations plus rares ont été décrites au niveau du pelvis (ovaires, testicules, prostate, urètre) ou du système digestif (foie, ampoule de Vater, estomac, pancréas).
- dans la médulla de la glande surrénale.

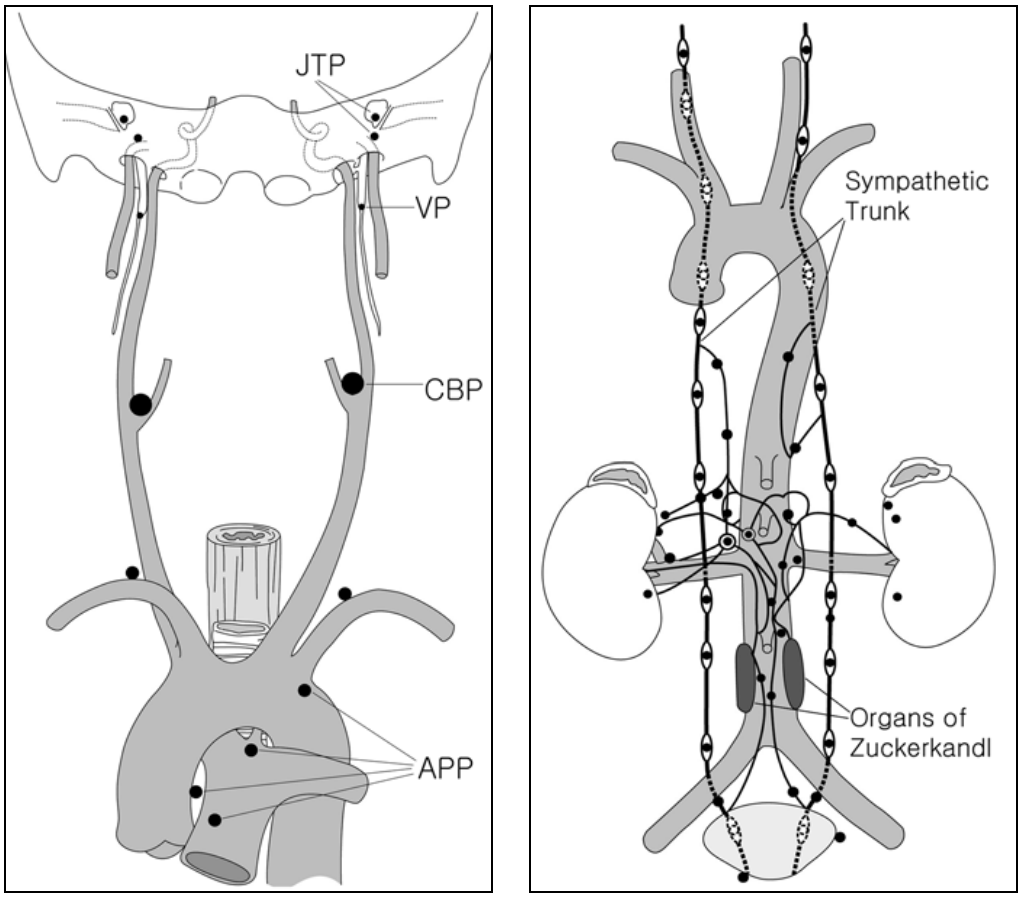

Figure 1 : Localisation anatomique des principaux paraganglions dans la région cervicale (à gauche) et thoraco-abdomino-pelvienne (à droite) (d'après (1)). JTP : paraganglion jugulotympanique, VP : paraganglion vagal, CBP : paraganglion carotidien, APP : paraganglions aortiques.

Comme de nombreuses tumeurs neuroendocrines, les PGL peuvent être sécrétants. Certains PGL ont ainsi la particularité de pouvoir produire des catécholamines. Dans ce cas, la tumeur sera dite fonctionnelle.

II- ORIGINE EMBRYOLOGIQUE

Les cellules neuroendocrines qui formeront les cellules chromaffines des PGL et PH sont des cellules d'origines neuroectodermiques dérivées de la crête neurale.
Ces crêtes neurales se forment au cours de la vie embryonnaire, lors de la jonction du tube neural et de l'ectoderme dorsal à la fin de la gastrulation. Elles donnent

naissance à des cellules pluripotentes qui vont migrer dans l'embryon, coloniser différents types de tissus et se différencier en différents types cellulaires. Elles sont à l'origine de la quasi-totalité du système nerveux périphérique, des mélanocytes, des os, cartilages et tissus conjonctifs de la face, des cellules C de la thyroïde et des cellules chromaffines des paraganglions (**Figure 2**) (2, 3).

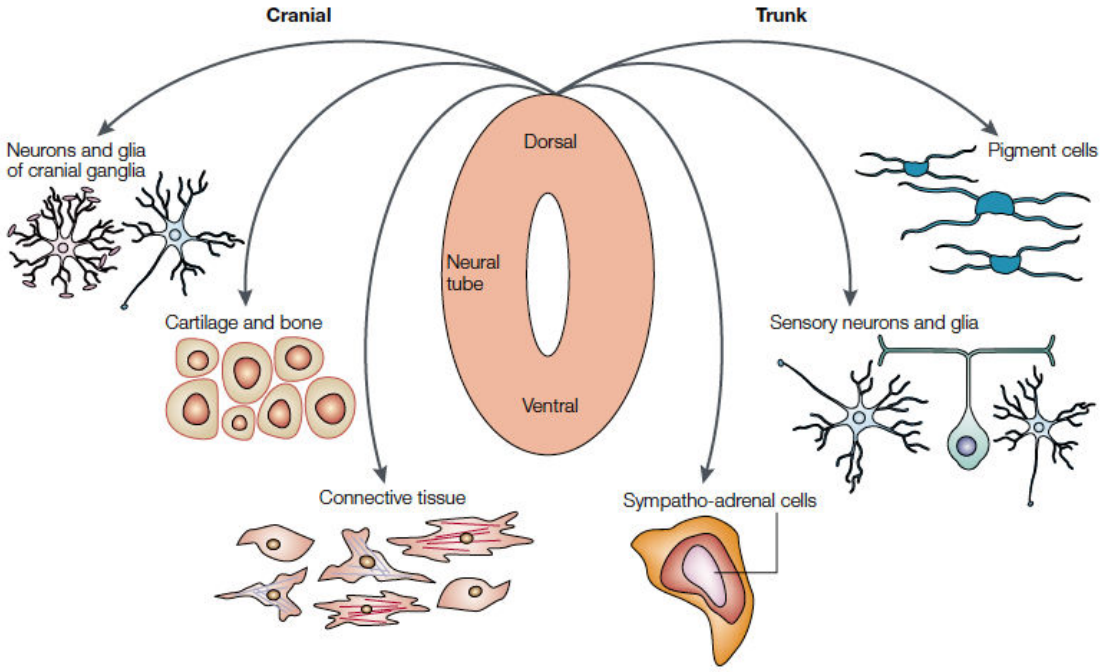

Figure 2 : Différents types cellulaires dérivant de la migration des cellules de la crête neurale (d'après (3))

Des données très récentes suggèrent que le développement des cellules chromaffines des systèmes nerveux sympathiques, parasympathiques et de la médullo-surrénale passeraient par des étapes différentes selon leurs localisations anatomiques. En effet, le système nerveux sympathique se développerait en une seule étape à partir de précurseurs issus directement de la crête neurale (4). Par contre, le système nerveux parasympathique se développerait en deux étapes. Des cellules de Schwann précurseurs multipotentes migreraient de la crête neurale pour former des niches cellulaires le long des axones puis migreraient le long de ces axones pour former ensuite le système nerveux parasympathique (5). La médullo-

surrénale quant à elle se développerait en associant les deux mécanismes précédemment décrits (4).

III- SÉCRÉTION

Les PGL et PH sont des tumeurs pouvant être responsables d'une morbidité et mortalité cardiovasculaire causées par la production intermittente ou continue de catécholamines (dopamine, adrénaline, noradrénaline). Les catécholamines sont synthétisées à partir de la tyrosine, issue de l'alimentation ou du métabolisme de la phénylalanine. La première étape de la synthèse des catécholamines à partir de la tyrosine débute par l'étape limitante de la réaction. La tyrosine va être métabolisée par la tyrosine hydroxylase en L-DOPA (dihydrophényléthylamine) dans le cytoplasme des cellules du système sympathique et de la médullo-surrénale. Cette étape est sous le rétrocontrôle des catécholamines qui vont inhiber leur propre synthèse (6).

La dopa décarboxylase transforme la L-DOPA en dopamine, puis après transfert intra-vésiculaire, la dopamine est transformée en noradrénaline par la dopamine β hydroxylase. Finalement, la noradrénaline sera transformée en adrénaline dans le cytoplasme par la PNMT (Phényléthanolamine N-méthyltransférase) dans la médullosurrénale et dans les neurones adrénergiques du système nerveux central (**Figure 3**).

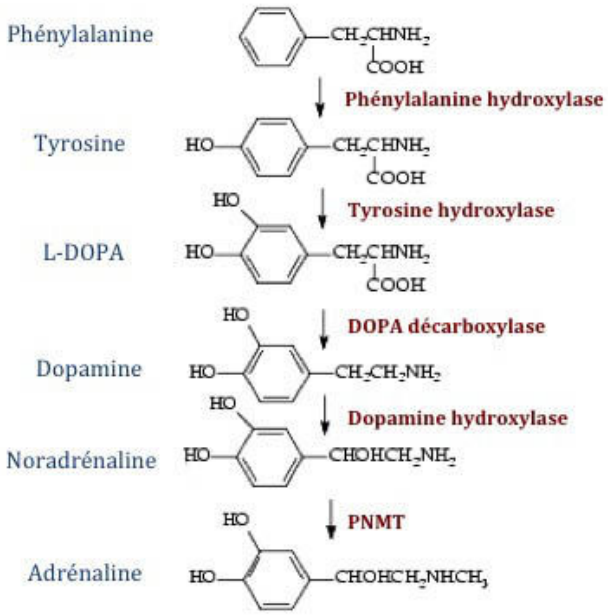

Figure 3 : Voie de synthèse des catécholamines.

Les catécholamines sont ensuite stockées dans les cellules chromaffines sous forme libre dans le cytoplasme (20 % des catécholamines, ou pool libre) ou dans des granules (80 % des catécholamines, ou pool de réserve), des transporteurs vésiculaires assurant leur transport d'un pool à l'autre. Les catécholamines sont ensuite sécrétées par exocytose et relarguées dans la circulation, et une partie est toutefois recaptée pour être de nouveau stockée afin de reconstituer le pool de réserve (7). La sécrétion est déclenchée par la stimulation des récepteurs nicotiniques à l'acétylcholine au niveau de la médullo-surrénale ou par l'activation des canaux sodiques voltages dépendants dans les neurones sympathiques (8).

Après sécrétion, les catécholamines seront inactivées au niveau de la médullo-surrénale ou des organes périphériques (notamment le foie et le rein) par la monoamine oxydase (MAO) et la catéchol-O-méthyl transférase (COMT) (7) puis sulfo-conjuguées et éliminées par voie urinaire

IV- ÉPIDÉMIOLOGIE

Les PGL et PH sont des pathologies rares, dont l'incidence est estimée entre 2 et 8 par million (9). Ces pathologies touchent autant les hommes que les femmes. Dans un centre tertiaire, la prévalence des PH a été estimée à 1 à 2 /100 000 adultes par an (10).

Toutefois la prévalence de ces pathologies augmente chez les sujets hypertendus, où elle est évaluée entre 0,2 et 0,6% des patients et elle atteint 4% chez les patients présentant une masse surrénalienne découverte de façon fortuite (11-13).

Malheureusement l'épidémiologie de ces tumeurs est difficile à déterminer du fait des formes pauci-symptomatiques ou asymptomatiques, et de la clinique aspécifique. Plusieurs études ont ainsi démontré qu'elles étaient sous diagnostiqués. Sur des séries autopsiques, un PH était découvert dans 0,05 % des cas, suggérant une incidence bien supérieure à celle qui est actuellement considérée (14).

V- DIAGNOSTIC

1- **Signes cliniques**

Les PGL/PH peuvent se révéler soit par un syndrome de compression (le plus souvent pour les PGL de la tête et du cou), soit par des manifestations catécholaminergiques si le PGL est fonctionnel, soit de façon incidente à l'occasion d'un examen d'imagerie. Néanmoins, du fait de symptômes souvent aspécifiques quand ils sont présents et de la rareté de la pathologie, il a été estimé que le délai moyen entre l'apparition des premiers symptômes et le diagnostic de PGL serait d'environ 3 ans (15). La sécrétion de catécholamines entraîne une hypertension artérielle (HTA) dans plus de 80 % des cas, soit permanente soit paroxystique, expliquée par l'augmentation des résistances périphériques, de la fréquence cardiaque et par l'hyperaldostéronisme secondaire. Une hypotension est également possible en cas de sécrétion préférentielle de dopamine (16). A côté de cette HTA les patients peuvent également présenter des malaises prototypiques,

correspondants à des décharges de catécholamines, connus sous la dénomination de « triade de Ménard » : céphalées, sueurs et palpitations. Les signes de cette triade peuvent survenir associés entre eux ou de façon isolée. Les céphalées sont présentes dans 60 à 90 % des cas, les sueurs dans 55 à 75 % des cas et les palpitations dans 50 à 70 % des cas. Ils sont classiquement associés à une pâleur après le malaise ce qui distingue la crise catécholaminergique du malaise vagal. L'association de ces trois signes au cours d'un malaise a une spécificité de 90 % pour le diagnostic de PGL fonctionnel (17, 18). D'autres symptômes liés à la production catécholaminergique peuvent survenir comme par exemple l'anxiété, l'amaigrissement, une intolérance au glucose ou un diabète, et chez l'enfant un syndrome polyuro-polydypsique et/ou des douleurs abdominales et/ou des troubles du comportement. De plus, 10 à 15 % des PGL fonctionnels sont diagnostiqués suite à une complication aigue comme une cardiopathie adrénergique, un accident vasculaire cérébral, ou une hypertension artérielle maligne (19).

En cas de PGL non fonctionnel, le PGL peut être découvert sur des signes de compression (nerveuse, vasculaire, urétérale…). C'est souvent le cas des PGL qui se développent dans la région cervicale. Ces PGL peuvent être découverts soit devant une tuméfaction cervicale ou des signes de compression des nerf crâniens environnants : par exemple, hypoacousie et/ou acouphènes en cas de compression du nerf auditif, paralysie faciale en cas de compression du nerf facial, ou troubles de la déglutition en cas de compression du nerf vague ou glossopharygien (20).
Enfin, on estime qu'environ 25% des PGL/PH sont découverts de façon fortuite à l'occasion d'une imagerie (incidentalomes) (15).

2- **Indications de la mise en place d'une démarche diagnostique**

La recherche de PGL/PH se justifie :
- chez les patients ayant une HTA résistante définie comme une pression artérielle systolique supérieure ou égale à 140 et/ou une PA diastolique supérieure ou égale à 90 mm Hg malgré une trithérapie à dose efficace contenant au moins un diurétique,

- chez les patients ayant des symptômes pouvant être d'origine catécholaminergique,
- chez les patients ayant une labilité tensionnelle importante objectivée,
- chez les patients de moins de 50 ans, diabétiques, hypertendus, ayant un indice de masse corporelle inférieur à 25,
- chez les patients présentant un incidentalome surrénalien,
- chez les patients présentant des symptômes évocateurs d'un syndrome de masse cervical, thoracique, abdominal ou pelvien,
- chez les patients atteints d'une maladie génétique prédisposant aux PGL/PH ou chez des sujets chez qui le dépistage génétique a montré qu'ils étaient à risque de développer un PGL/PH (21).

3- **Diagnostic biologique**

Le diagnostic biologique de PGL/PH permet principalement de mettre en évidence un PGL fonctionnel, élément d'une importance capitale pour la prise en charge du patient.

Il repose sur la mise en évidence d'une hypersécrétion de catécholamines. Du fait de leur excellente sensibilité et spécificité, le dosage des métabolites issus de la dégradation de l'adrénaline et de la noradrénaline (l'adrénaline est dégradée par la COMT en métanéphrines et la noradrénaline en normétanéphrines) au niveau urinaire ou plasmatique est indiqué en première intention (21). Chez les patients présentant un PH ou PGL fonctionnel, plus de 94 % des métanéphrines (MN) et normétanéphrines (NMN) plasmatiques proviennent du métabolisme intra-tumoral des catécholamines, un processus qui se produit en permanence et qui est indépendant du relargage des catécholamines (22, 23). Ces MN et NMN sont ensuite éliminées par voie urinaire sous forme sulfo-conjuguée. Ainsi les dosages des NMN et MN urinaires reflètent les NMN et MN conjuguées alors que les NMN et MN plasmatique reflètent les NMN et MN libres (24).

Le dosage des NMN et MN urinaires ou plasmatiques a été démontré comme supérieur aux dosages des catécholamines urinaires et plasmatiques antérieurement utilisés (25).

Ces dosages sont actuellement effectués par des techniques de chromatographie liquide à haute performance (HPLC) ou de spectrométrie de masse ce qui permet une bonne reproductibilité et permet de séparer les NMN des MN (on parle alors de métanéphrines fractionnées) (26). La sensibilité de ces dosages pour le diagnostic de PGL fonctionnel est supérieure à 95 % dans la plupart des études tant pour les dosages des MN/NMN libres plasmatiques que pour les dosages des MN/NMN urinaires fractionnées des 24 heures, et la spécificité est supérieure à 85 %. Les dosages plasmatiques sont équivalents aux urinaires et plus simples pour le patient, les dosages urinaires se faisant sur un recueil complet des urines de 24 heures (25, 27-30). Le diagnostic est hautement probable devant une élévation au-dessus de trois fois la normale et suspecté en dessous lorsque l'élévation se situe entre 2 et 3 fois la normale.

A côté du dosage des MN et NMN, qui est reconnu comme étant le gold standard pour le diagnostic d'une hyperproduction catécholaminergique, le groupe de Graeme Eisenhofer a suggéré de compléter les explorations biologiques par le dosage de la 3-méthoxytyramine (3-MT) plasmatique et/ou urinaire. En effet, certains PGL notamment cervicaux ne produisent que de la dopamine. Ce marqueur serait donc élevé chez 10 à 28 % des patients avec un PGL cervical (alors que moins de 5 % de ces patients auraient une élévation des MN ou NMN) (31-33). Il avait été suggéré que la 3-MT pourrait être aussi un facteur diagnostique et pronostique dans les formes malignes de PGL (34), ce qui n'a pas été confirmé dans les études suivantes (31, 35).

Le profil sécrétoire mis en évidence lors de ces dosages (prédominance soit des MN ou des NMN) va dépendre de l'expression de la PNMT dans le PGL et, comme nous le verrons plus loin, du statut génétique du PGL (36).

Les résultats de ces dosages peuvent être biaisés par certains médicaments qui peuvent induire des faux positifs en raison d'interférences avec le métabolisme des catécholamines ou avec la méthode de dosage (21) ou en raison des conditions de prélèvement. Ainsi, le dosage des MN/NMN plasmatiques doit être réalisé sur un

prélèvement sanguin effectué chez un patient allongé pendant au moins 30 minutes, et le dosage des 3-MT doit être fait après une nuit de jeun (21).
La chromogranine A étant moins sensible et moins spécifique que les dosages de NMN et MN, elle n'est généralement pas utilisée pour le diagnostic de PGL (37, 38). Elle peut être utile pour la surveillance des patients, opérés ou ayant une forme métastatique, qui présenteraient une élévation de la chromogranine A au moment du diagnostic.

Les tests dynamiques anciennement utilisés (test à la clonidine, test au glucagon), parfois dangereux, ont été abandonnés au profit du dosage de métanéphrines et normétanéphrines.

4- **Diagnostic topographique**

Une fois le diagnostic évoqué, du fait de la mise en évidence d'un excès de catécholamines ou de symptômes liés à un syndrome compression, un diagnostic topographique précis est nécessaire pour localiser le(s) PGL responsable(s).

a- Imageries conventionnelles

Pour la région thoracique, abdominale et pelvienne les recommandations internationales sur la prise en charge des PGL/PH publiées en 2014 ont suggéré de réaliser une tomodensitométrie (TDM). Une imagerie par résonance magnétique (IRM) pourrait être envisagée en cas de contre-indications au TDM (21).
Pour la région cervicale, l'angio-IRM est l'examen de référence pour le dépistage des PGL de la sphère ORL.
Ces examens ont une excellente sensibilité (98 et 100 % respectivement) mais une spécificité moindre (70 et 67 % respectivement) (18).

b- Imageries fonctionnelles

Depuis de nombreuses années, différents traceurs de médecine nucléaire ont été développés pour aider au diagnostic des PGL. Dans une méta-analyse réalisée par

la Mayo Clinic dans le contexte des recommandations internationales de prise en charge, l'apport des examens de médecine nucléaire à l'imagerie conventionnelle est considéré comme faible puisqu'ils ont permis de détecter 24 PGL supplémentaires chez 1445 cas index (39). Toutefois, ces différentes études ont été menées dans des « centres experts » de la pathologie, et ces examens de médecine nucléaire ont toute leur place dans des « centres non experts » comme l'a démontré l'étude PGL.EVA menée chez les patients avec PGL *SDHx*-dépendants (40). De plus, leur spécificité par rapport à l'imagerie conventionnelle est souvent une aide au diagnostic.

- *Scintigraphie à la ^{123}I-métaiodobenzylguanidine (^{123}I-MIBG)*

La MIBG est un dérivé proche de la noradrénaline, captée via le transporteur noradrénergique NET (NorEpinephrine Transporter) et qui permet son accumulation sélective dans les tumeurs produisant des catécholamines. Elle s'accumule dans les tissus chromaffines après stockage dans les vésicules de sécrétion par le transport VMAT. Cette scintigraphie du corps entier, réalisée grâce à un marquage à l'iode 123, peut révéler des atteintes multifocales et des localisations secondaires, à condition qu'elles secrètent des catécholamines.

La sensibilité est bonne pour les localisations surrénaliennes (supérieure à 90 %), par contre elle chute à 50-60 % pour les localisations extra-surrénaliennes ainsi que pour la détection de métastases (41-43). Dans le cas d'une forme métastatique, cette scintigraphie ouvre l'opportunité d'un traitement par ^{131}I-MIBG, ainsi le PGL/PH métastatique est la seule indication retenue pour cette scintigraphie par les recommandations internationales (21).

- *Scintigraphie des récepteurs de la somatostatine par ^{111}In-pentetréotide (Octréoscan®)*

Le pentetréotide est un analogue de la somatostatine qui présente une affinité excellente pour les récepteurs de la somatostatine de sous-types 2 et 5 et plus modérée pour les sous-types 3 et 4. Les PGL expriment préférentiellement les récepteurs de la somatostatine de sous-types 3 et 4 (44).

La sensibilité est bonne dans les localisations thoraciques et cervicales et les PGL *SDHx*-dépendants (supérieure à 95 %), mais nettement moins bonne pour les localisations surrénaliennes (40, 41, 45, 46). Ces scintigraphies ont été progressivement remplacées par la tomographie par émission de positons (TEP) (cf ci-après) à partir du moment où ce nouvel examen a été largement disponible en routine clinique.

- *TEP au ^{18}F-Fluorodeoxyglucose (^{18}F-FDG)*

Le ^{18}F-FDG est le traceur le plus utilisé en oncologie. L'examen repose sur l'utilisation d'un analogue du glucose marqué au fluor 18 permettant de mettre en évidence l'augmentation de la consommation tissulaire de glucose induite par la transformation néoplasique. Cette fixation sera d'autant plus marquée que la prolifération tumorale est intense dans les tumeurs malignes.

Les PGL fixent fréquemment le ^{18}FDG, notamment les tumeurs avec mutation *SDHx* et *VHL*, qui présentent une surexpression des transporteurs du glucose GLUT1 et GLUT3 du fait de la pseudo-hypoxie (47, 48). La sensibilité de cet examen se situe entre 80 à 100 %, notamment chez les patients avec un PGL métastatique *SDHB*-dépendant, mais la spécificité est faible (43, 47, 49).

- *TEP à la dihydroxyphénylalanine marquées au fluor 18 (^{18}F-DOPA)*

Les PGL ont la capacité de capter avec une haute affinité la F-DOPA mais également de la décarboxyler en F-FDA. Elle sera ainsi stockée dans les vésicules de sécrétion permettant l'imagerie (50).

La sensibilité globale de cet examen a été estimée dans une méta-analyse à 79 % et la spécificité à 95 % chez 275 patients (51). Ce traceur a une forte affinité pour les PGL cervicaux *SDHD*-dépendants (51, 52), mais une sensibilité inférieure à celle du ^{18}FDG dans les PGL *SDHB*-dépendants (50). En effet, la sensibilité chez les patients porteurs d'une mutation *SDHB* a été évaluée à 20 % (53, 54).

- *TEP aux analogues de la somatostatine marqués au Gallium 68*

Trois peptides sont actuellement disponibles sur le marché : DOTATOC, DOTATATE

et DOTANOC. Il ne semble pas y avoir de supériorité diagnostique entre ces trois traceurs bien que DOTANOC ait une plus haute affinité pour les récepteurs de la somatostatine de sous type 2, 3 et 5 (55-57).
Sur les petites séries rétrospectives publiées jusqu'alors, il semblerait que cet examen soit prometteur pour le diagnostic des formes métastatiques *SDHB*-dépendants et pour les localisations cervicales. Une méta-analyse publiée en 2018 confirmerait la bonne sensibilité de cet examen pour les PGL cervicaux (58). Cependant la TEP aux analogues de la somatostatine marqués au Gallium 68 n'a pas été, pour l'instant, comparée à l'imagerie de référence (AngioIRM) dans les PGL cervicaux (59, 60).

5- **Diagnostic histologique**

Historiquement, le diagnostic histologique des PH reposait sur la coloration au bichromate de potassium, qui conduisait à une coloration brune caractéristique (due à la présence de sels de chrome) des cellules contenant des catécholamines, d'où leur nom de cellules « chromaffines ». Ces techniques de coloration sont désormais abandonnées au profit de techniques plus récentes d'immunohistochimie (IHC).
La majorité des PGL/PH ont une structure caractéristique en coloration HES. En effet, les cellules tumorales sont organisées en niches séparées par des capillaires et entourées par des cellules sus-tentaculaire. Cette structure est aussi nommée « Zellballen », et a été décrite pour la première fois au 19^{éme} siècle par Alfred Kohn dans des paraganglions (61) (**Figure 4**). Toutefois, cette structure n'est pas toujours présente et le diagnostic histologique des PGL/PH repose essentiellement sur la mise en évidence d'une positivité pour les marqueurs généraux des tumeurs neuroendocrines que sont la chromogranine A et la synaptophysine, en association avec un réseau caractéristique de cellules sus-tentaculaires visibles grâce au marquage de la protéine S100. Un immunomarquage plus spécifique sur les enzymes impliquées dans la synthèse des catécholamines comme la tyrosine hydroxylase peut également être utilisée (62).

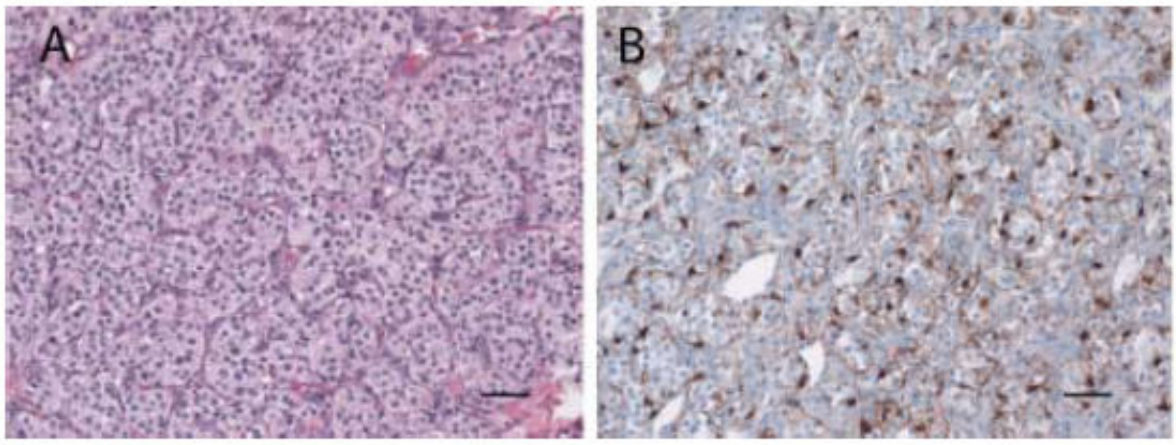

Figure 4 : **Histologie d'un PGL**. HES d'un PGL montrant des ilots de Zellballen (A) et immunohistochimie anti protéine S100 mettant en évidence des cellules sus-tentaculaires autour des Zellballen (B) (D'après (61))

VI- PRISE EN CHARGE THÉRAPEUTIQUE

La prise en charge thérapeutique des patients avec un PGL/PH va dépendre du caractère fonctionnel ou non de la tumeur et de sa localisation. Le seul traitement curatif des PGL est la chirurgie, mais l'acte chirurgical peut être difficile du fait du risque de décharges catécholaminergiques, du caractère hypervasculaire de ces tumeurs et de leurs rapports intimes avec le réseau vasculo-nerveux locorégional.
En cas de chirurgie, si le patient a un PGL fonctionnel, une préparation du patient est recommandée sept à quatorze jours avant la chirurgie reposant sur une réhydratation et un traitement par alpha-bloquants complété en cas de tachycardie secondaire à ce traitement par l'introduction d'un béta-bloquant, ceci afin de limiter le risque et l'impact de décharges catécholaminergiques au cours du geste chirurgical et notamment lors de la mobilisation de la tumeur (63, 64).

Pour les PGL cervicaux, la chirurgie peut être discutée. En effet, le risque d'atteinte, lors de la procédure chirurgicale, d'un nerf crânien responsable d'une paralysie définitive est non négligeable et dépend de la localisation et de la taille de la tumeur et de son envahissement vasculaire (65). Une méta-analyse récente a évalué le

risque de paralysie d'un nerf crânien à 3 % chez les patients ayant un PGL carotidien sans envahissement vasculaire, alors que ce risque s'élève à 32 % en cas d'englobement complet de la carotide par le PGL (66). Certaines équipes accompagnent ce geste chirurgical d'une embolisation préopératoire du PGL (67, 68). Toutefois cette procédure s'accompagne d'un risque non-négligeable d'accident vasculaire cérébral (de 0 à 18 % selon les études) (67-69). De plus, une méta-analyse sur 470 patients publiée en 2016 a démontré que l'embolisation pré-chirurgicale ne réduisait pas le taux de saignement peropératoire, ni le temps chirurgical, ni le risque de paralysie des nerfs crâniens par rapport à la chirurgie seule (70). L'indication chirurgicale est possible pour le traitement d'un PGL du glomus carotidien de petite taille. Pour les tumeurs volumineuses envahissant la carotide, ou proches de la base du crâne, des traitements par radiothérapie ou radiochirurgie sont de plus en plus souvent proposés pour éviter la morbidité secondaire au geste chirurgical. Ils permettent une stabilisation tumorale dans 92 à 100 % des cas (suivi moyen, selon les séries de la littérature, de 3 à 13 ans). Il n'a pas été rapporté d'effets indésirables graves suite à la radiothérapie ou la radiochirurgie (71, 72). Une publication récente a mis en lumière les résultats prometteurs de la proton-thérapie (73).

VII- LE PROBLÈME DE LA MALIGNITE DES PGL/PH

Dix à 15 % des PGL sont d'évolution maligne (15), le diagnostic de malignité étant porté sur la présence d'une dissémination métastatique à distance d'un site paraganglionnaire (classification WHO 2016). Il est désormais recommandé d'abandonner l'appellation PGL/PH « malin » pour la remplacer par PGL/PH « métastatique ». Cette dissémination métastatique se fait le plus souvent aux dépens des ganglions lymphatiques, des os, du foie, et du poumon (15, 74). Cette évolution métastatique est synchrone dans 30 % des cas et métachrone dans 70 % des cas (75), les métastases métachrones pouvant survenir dans un délai très variable allant de 3 mois à 30 ans (15, 76). Le pronostic à 5 ans de ces formes

métastatiques est inférieur à 50 % (77, 78), mais presque la moitié des patients avec une forme métastatique d'emblée sont stables sans traitement à un an de suivi (74). Ces formes métastatiques posent donc un problème de diagnostic et de suivi car un patient avec une forme apparemment bénigne après la chirurgie peut développer des métastases des années plus tard.

1- **Diagnostic des formes métastatiques**

a- Critères clinico-biologiques

D'un point de vue clinico-biologique, différentes études de cohortes ont mis en évidence qu'en analyses multivariées, la taille du PGL au diagnostic et une localisation extra-surrénalienne étaient les facteurs de risque les plus robustes de malignité (79-81), l'âge au diagnostic de PGL ne sortant pas dans toutes les études. Dans les différentes études, la présence d'une mutation constitutionnelle du gène *SDHB* apparait comme un facteur de malignité et de mauvais pronostic. Ce point sera développé en détail dans le chapitre *Génétique* de ce travail (15, 76, 81-84).

b- Critères histologiques

Il n'y a actuellement pas de critères histologiques fiables permettant le diagnostic de malignité (85, 86). Différents scores histologiques ont été proposés pour essayer de diagnostiquer les formes malignes. Le plus largement utilisé est le score de PASS (Pheochromocytoma of the Adrenal Scaled Score), mis au point en 2002 sur 100 phéochromocytomes. Il s'agit d'un score composé de douze items comportant des critères de morphologie cellulaire et tissulaire et d'invasivité. Chaque item est associé à un score différent (**Table 1**). Un score cumulé supérieur ou égal à 4/20 est en faveur de la malignité.

Items	Points
Anomalies cellulaires :	
- Nids larges et irréguliers	2
- Cellules spumeuses	2
Cellularité élevée	2
Nécrose	2
Invasion :	
- Capsulaire	1
- Vasculaire	1
Mitoses :	
- > 3/10 grands champs	2
- atypiques	2
Monotonie cellulaire	2
Extension au tissu adipeux	2
Pléomorphisme nucléaire	1
Hyperchromasie du noyaux	1
Score maximum	20

Table 1 : **Score de PASS.** Un score supérieur ou égal à 4 serait en faveur de la malignité.

Ce score souffrait dès sa conception d'un défaut important. En effet, le suivi des patients n'était pas connu dans la série princeps (87). Les publications suivantes évaluant ce score par des experts internationaux de la pathologie ont montré une variabilité inter-observateurs mais aussi intra-observateur importante (86, 88).

Récemment un nouveau score a été proposé, le score de GAPP (Grading of Adrenal Pheochromocytoma and Paraganglioma). Ce score reprend les items du PASS en supprimant les items dont l'interprétation est peu reproductible et en y ajoutant l'évaluation de la prolifération par le Ki67 et le phénotype sécrétoire. Ce score permet de séparer les PGL en trois groupes de différenciation différente : PGL bien différencié (Grade 1), modérément différencié (Grade 2) et peu différencié (Grade 3) (**Table 2**). Ce score serait corrélé à la vitesse de progression de la maladie métastatique et à la survie des patients (85). Malheureusement, cette classification ne permet pas non plus de différencier les PGL malins des autres car 10 % des PGL

malins sont classés en Grade 1 selon le score de GAPP (89). Ce score de GAPP a ensuite été modifié en score M-GAPP, qui reprend les différents items du GAPP mais en y ajoutant l'immunohistochimie anti-SDHB, ce qui améliorerait sa sensibilité (89).

Items	Points
Anomalies cellulaires :	
- Zellballen	0
- Nids larges et irréguliers	1
- Pseudo-rosettes	1
Cellularité :	
- Faible (<150 cellules/champ)	0
- Modérée (150-250 cellules/champ)	1
- Elevée (> 250 cellules/champ)	2
Nécrose	2
Invasion	
Capsulaire ou vasculaire	1
Index Ki67 (%)*	
- < 1 %	0
- 1-3 %	1
- > 3 %	2
Sécrétion :	
- Adrénaline	0
- Noradrénaline	1
- Non fonctionnel	0
Score maximum	10

Table 2 : Score de GAPP. Le score maximum permet de définir le grade de la tumeur : Grade 1 entre 0-2 points ; Grade 2 entre 3-6 ; Grade 3 entre 7-10. Les items en rouge sont les items déjà présents dans le score de PASS.
*Un champ est défini sous grossissement x400.

Mon équipe d'accueil a proposé l'utilisation de l'architecture vasculaire comme critère de malignité. En effet, les PGL malins présentent une architecture vasculaire désorganisée et anarchique (90). Toutefois ce critère évalué en aveugle par les anatomopathologistes du consortium ENSAT-Cancer sur une série de 184 tumeurs a montré qu'il posait également des problèmes de reproductibilité d'interprétation par les experts (91).

2- **Prise en charge des formes métastatiques**

Le traitement des formes métastatiques est tout d'abord symptomatique. Il vise à contrôler le retentissement de l'excès de catécholamines dans la circulation, responsable des symptômes catécholaminergiques souvent sévères (HTA malaises, constipation..), voire du décès du patient.

Différentes possibilités de traitement existent. Le thésaurus français établi par le centre national de référence COMETE-CANCER indique que :

- La radiothérapie métabolique à l'^{131}I-MIBG permet une amélioration des symptômes chez près de 80% des patients, une rémission partielle dans 30 à 50% des cas et une rémission complète dans seulement 5 à 13% des cas (16, 92).
- Pour les tumeurs fixant l'octréotide, la radiothérapie métabolique utilisant les dérivés de la somatostatine est une option. Toutefois, peu de patients ayant bénéficié de ce traitement ont été rapportés, la plus large série comportant 28 patients (93). Les nouveaux traceurs couplés à l'^{90}Yttrium ou le ^{177}Lutétium semblent avoir des résultats prometteurs dans les PGL malins sur les premières petites séries publiées, avec 10 à 20 % de réponse objective et 46 à 60 % de stabilisation (93-95).
- La chimiothérapie de type CVD (Cyclophosphamide, Vincristine, Dacarbazine) est efficace chez 55% des patients (11% de rémission complète et 44% de rémission partielle) mais cette réponse n'est que transitoire (durée médiane de réponse de 20 mois) (96, 97).
- Le témozolomide a été proposé récemment comme alternative à la chimiothérapie intra-veineuse. Ce traitement, si la tumeur présente une sous-expression de l'enzyme MGMT, présente une bonne efficacité (réponse partielle dans 33 % des cas et stabilité dans 47 % des cas, avec une survie sans progression de 13,3 mois) et ceux d'autant plus que le patient est porteur d'une mutation *SDHB* (98).
- L'interféron semble être une alternative dans certains cas. En effet, la seule étude dans la littérature sur le sujet chez 14 patients ayant un PGL métastatique avec des lésions osseuses prédominantes a mis en évidence une stabilisation chez 9 patients et une réponse partielle chez 3 patients avec une survie sans progression de 17 mois

(99).

- Enfin le sunitinib est en cours d'évaluation dans une étude prospective randomisée en double aveugle évaluant le sunitinib contre placebo (FIRSTMAPPP) dans le PGL/PH malin progressif. Une étude antérieure rétrospective chez 14 patients avait mis en évidence une réponse partielle chez trois patients et une stabilisation chez cinq. De façon intéressante, chez ces huit patients, six étaient porteurs d'une mutation *SDHB* ou *VHL* (100).

PARTIE 2 : LA GÉNÉTIQUE CONSTITUTIONNELLE ET TUMORALE DES PARAGANGLIOMES ET PHÉOCHROMOCYTOMES

Une des grandes caractéristiques PGL/PH est leur fort déterminisme génétique, pour lequel des progrès marquants ont été effectués ces quinze dernières années. En effet, il était considéré avant les années 2000 que les PH obéissaient à la règle des 10 % : 10 % de formes extra-surrénaliennes, 10 % de formes malignes, 10 % de formes multiples, et 10 % de formes génétiquement déterminés qui s'intégraient dans des formes syndromiques (101). Les années 2000, avec la découverte de mutations constitutionnelles dans les gènes *SDHD*, *SDHC* puis *SDHB* (102-104) ont changé cette vision et ont permis de comprendre que les PGL et PH étaient le même type de tumeur. Actuellement, grâce au progrès des méthodes d'exploration génétique, il est considéré qu'environ 40 % des PGL sont génétiquement déterminés, secondaires à des mutations constitutionnelles de transmission autosomique dominante dans une quinzaine de gènes de prédisposition. La probabilité d'identifier une mutation constitutionnelle dans un gène de prédisposition est d'autant plus forte que le patient présente un PGL précoce (avant 35 ans), des PGL multiples, des lésions syndromiques, ou des antécédents familiaux de PGL (84). Toutefois, ces caractéristiques ne sont pas indispensables, et il est identifié une mutation constitutionnelle dans un gène de prédisposition au PGL/PH chez environ 12 % des patients avec un PH et 16% des patients avec un PGL de présentation apparemment sporadique (84, 105, 106).

Mis à part le proto-oncogène *RET* et le gène *HIF2A* qui sont des oncogènes, tous les autres gènes de prédisposition au PGL/PH sont des gènes suppresseurs de tumeurs, c'est-à-dire que le mécanisme de tumorigenèse nécessite l'association d'une mutation constitutionnelle et d'un deuxième événement génétique somatique comme une perte d'hétérozygotie, une mutation ou une hyperméthylation sur l'autre allèle, comme dans le modèle des « two hits » de Knudson (107).

A- GÉNÉTIQUE CONSTITUTIONNELLE DES PGL

I- LES FORMES SYNDROMIQUES

1-La neurofibromatose de type 1 (gène *NF1*)

Le gène *NF1*, localisé sur le chromosome 17q11.2 est un des gènes les plus longs chez l'humain, avec 60 exons qui codent pour une protéine de 2839 acides aminés. Ce gène code pour la neurofibromine qui, en inhibant la protéine RAS, est impliquée dans la suppression de la voie de signalisation RAS-RAF-MAPK.

Les mutations de ce gène sont responsables de la neurofibromatose de type 1 (NF1) ou maladie de von Recklinghausen, pathologie à forte pénétrance de transmission autosomique dominante et dont la prévalence est estimée à 1/3000 (108). Le diagnostic est relativement simple cliniquement chez l'adulte. Il repose sur les 7 critères du consensus du NIH (**Table 3**) (109). Le diagnostic est posé dans 95 % des cas dès l'âge de 11 ans sur ces seuls critères cliniques (110).

Deux critères ou plus sont suffisants parmi la liste ci dessous pour faire le diagnostic de NF1
≥ 6 taches café au lait - > 0,5 cm avant la puberté, - > 1,5 cm après la puberté
Ephélides axillaires ou inguinales
≥ 2 neurofibromes quelques soit le type ou 1 neurofibrome plexiforme
≥ 2 nodules de Lisch
Une lésion osseuse évocatrice
Un gliome des voies optiques
Un apparenté au premier degré avec un NF1

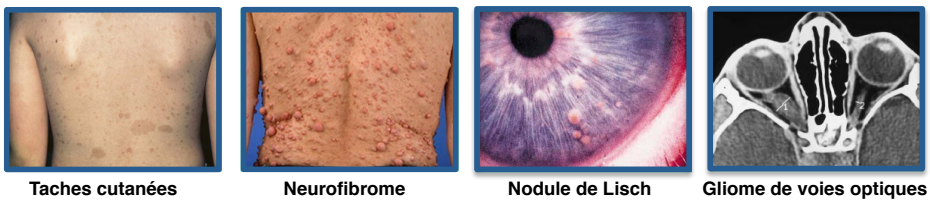

Taches cutanées | Neurofibrome | Nodule de Lisch | Gliome de voies optiques

Table 3 : **Critères diagnostiques de la Neurofibromatose de type 1 selon le consensus du NIH.**

Les patients avec une neurofibromatose de type 1 développent des PGL dans 0,1 à 5,7 % des cas, plutôt vers l'âge de 40 ans (84, 111-113). Il s'agit, dans la grande majorité des cas, de PH sécrétant de l'adrénaline, métastatiques dans 10 % des cas et bilatéraux dans 20 à 40 % des cas (84, 113, 114). De façon intéressante, ces PH sont découverts de façon incidente dans 30 % des cas (113, 115), et moins de 20 % des patients présentent des symptômes catécholaminergiques (112). Le diagnostic de NF1 chez un patient avec un PH nécessite donc un examen clinique et un interrogatoire sur l'histoire familiale attentif. Toutefois, il a été mis en évidence une mutation constitutionnelle du gène *NF1* chez quatre patients avec un PH initialement considéré comme sporadique. Ces patients avaient en réalité des critères modérés de la maladie lors de la réévaluation clinique spécialisée ou une histoire familiale de NF1 passée inaperçue (114, 116). Ces données ont été récemment confirmées par la réalisation du séquençage systématiquement du gène *NF1* par Next Generation Sequencing dans l'ADN constitutionnel de 1029 patients avec un PGL d'apparence sporadique. Dans cette étude, trois patients porteurs d'une mutation *NF1* ont été identifiés. Ils présentaient eux-aussi des signes cliniques modérés de la maladie (117).

2- La maladie de von Hippel-Lindau (gène *VHL*)

Le gène *VHL* est un gène suppresseur de tumeur, composé de 3 exons, localisé en position chromosomique 3p25. Il code pour une protéine faisant partie d'un complexe protéique responsable de l'ubiquitination et de la dégradation dans le protéasome des sous unité alpha des facteurs de transcription de réponse à l'hypoxie (HIF 1 et 2) (118).

Les mutations constitutionnelles de ce gène *VHL* induisent le développement de la maladie de von Hippel-Lindau (VHL), maladie de transmission autosomique dominante dont l'incidence est de 1/36 000. Cette pathologie dont la pénétrance est

quasi complète à 65 ans (119), est caractérisée par le développement avec une expressivité variable de différentes tumeurs :

- cancers du rein à cellules claires (70 % à l'âge de 60 ans (119)),
- PGL (24 % des patients),
- hémangioblastomes rétiniens et/ou du système nerveux central (80 % et 75 % des patients respectivement),
- tumeurs neuroendocrines (5-17 % des patients) et/ou kystes pancréatiques (80 % des patients) (120),
- tumeurs du sac endolymphatique (10-15 % des patients) (121, 122),
- cystadénomes épididymaires ou du ligament large.

Deux grands cadres phénotypiques ont été décrits chez les patients atteints, basés sur le risque de développer un PGL/PH : le VHL de type 1, où le risque de développer un PH est bas, et où les mutations mises en évidence sont plus fréquemment des mutations tronquantes, et le VHL de type 2, où le risque de développer un PH est important. Ce VHL de type 2 est subdivisé en 3 sous-groupes : le type 2A où le risque de cancer du rein est important, le type 2B ou le risque de cancer du rein est faible, et enfin le type 2C où les patients ne développent théoriquement que des PH ou des PGL (**Figure 5**) (123, 124). Les mutations responsables du VHL de type 2 sont plutôt des mutations faux sens qui, si elles mènent à une altération importante de la fonction de la protéine VHL, seront plutôt responsable d'un VHL de type 2A ou 2B, alors que si l'altération de la fonction est faible, seront responsables d'un VHL de type 2C (125, 126).

Pour compléter le tableau de ces corrélations génotype/phénotype, il a été décrit par plusieurs équipes que les patients porteurs d'une délétion de *VHL* emportant la partie 5' du gène *VHL* et le gène *C3orf10* avait un risque de cancer du rein moindre que les autres patients ayant un VHL de type 1 causée par une délétion plus courte n'emportant pas le gène *C3orf10* (127, 128).

Toutefois les corrélations génotypes-phénotypes de ses différentes formes ne sont pas parfaites (127).

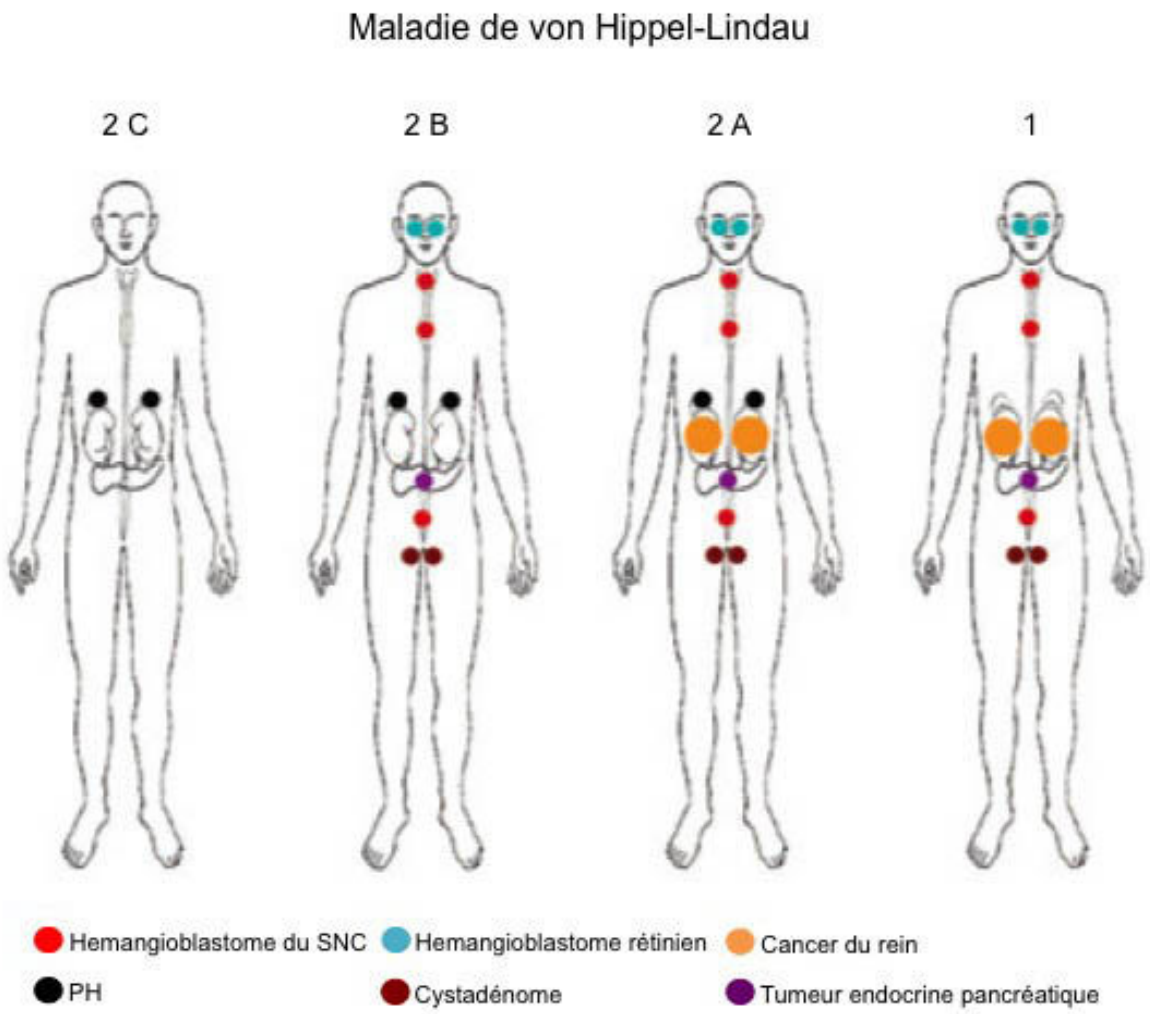

Figure 5 : Différences phénotypiques dans la maladie de von Hippel-Lindau (d'après (129)).

Les patients porteurs d'une mutation dans le gène *VHL* développent souvent un PGL avant l'âge de 20 ans, de location surrénalienne ou abdominale, et volontiers bilatéral durant le suivi (40 à 60 % des cas). Ces PGL sécrètent de la noradrénaline car il y a une sous expression de la PNMT secondaire à l'hyperméthylation du promoteur du gène codant pour cette enzyme (130) (**Voir l'article 3 donné en Annexes**). Il est retrouvé des antécédents familiaux de VHL ou des lésions syndromiques associés au PGL/PH dans deux tiers des cas (84, 131). De façon exceptionnelle une mutation dans le gène *VHL* peut être mise en évidence chez des patients avec des PGL cervicaux (132).

3- **Les néoplasies endocriniennes multiples de type 2 (gène *RET*)**

Le proto-oncogène *RET* est un gène de 21 exons localisé sur le chromosome 10q11.2. Ce gène code pour un récepteur à tyrosine kinase qui comporte plusieurs domaines : quatre domaines cadhérine-like qui permettent la dimérisation, un domaine riche en cystéine, et un domaine tyrosine kinase qui permet l'activation du récepteur et la transactivation du signal (133). Physiologiquement, le récepteur RET est activé par la phosphorylation de son domaine tyrosine kinase, secondaire à sa dimérisation et à son interaction avec son co-récepteur GFRA. Cette dimérisation du récepteur RET fait suite à l'interaction du récepteur GFRA avec son ligand le GDNF (**Figure 6**). Ceci va conduire à l'autophosphorylation de RET et son activation, qui va mener à l'activation des voies des PI3K-AKT et des voies des MAPK-ERK kinases.

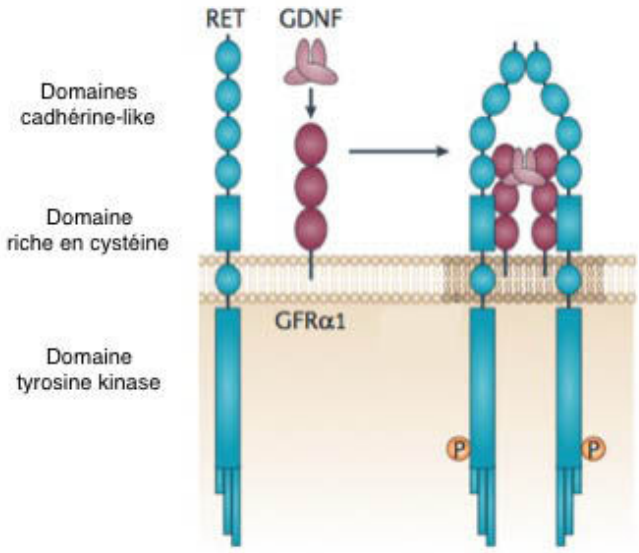

Figure 6 : Représentation schématique du récepteur RET et de son interaction avec son corécepteur GFRA (d'après (133)).

Les mutations gain de fonction du gène *RET* sont responsables des néoplasies endocriniennes multiples de type 2 (NEM2), touchant 1/30 000 individus. Ces mutations de transmission autosomique dominante sont des mutations récurrentes survenant dans les exons 8, 10, 11, 13, 14, 15, 16, qui entrainent une auto-activation du récepteur RET. Trois tableaux cliniques différents sont issus de ces mutations activatrices avec de bonnes corrélations génotype-phénotype :

- les NEM2A ou syndrome de Sipple (70% à 80 % des cas), caractérisées par l'occurrence d'un carcinome médullaire de la thyroïde (CMT), d'un PH et d'une hyperparathyroïdie (HPTH). Certains patients peuvent aussi développer un lichen amyloïde.
- les NEM2B ou syndrome de Gorlin (5 % des cas), caractérisées par l'occurrence d'un CMT, d'un PH, de neuromes muqueux, d'une gangliomatose de l'estomac et de l'intestin, et d'un habitus marfanoïde.
- les carcinomes médullaires de la thyroïde familiaux ou syndrome de Farndon (10 à 12 % des cas) caractérisés par le développement isolé d'un CMT (134).

La gravité de la NEM2A et son pronostic reposent sur le CMT. Des corrélations entre le génotype et l'agressivité du CMT sont bien établies. Les mutations responsables de la NEM2B (p.Met918Thr) donnent les CMT de développement le plus précoce et les plus agressifs. Les mutations *RET* ont ainsi été classées en fonction de l'agressivité du CMT en 3 niveaux (Moderate, High, Highest) par l'American Thyroid Association (**Table 4**) (135).

Mutation *RET*	Exon	Risque de CMT	Incidence des PH	Incidence de l'HPTH
G533C	8	MODERATE	+	-
C609F/G/R/S/Y	10	MODERATE	+/++	+
C611F/G/S/Y/W	10	MODERATE	+/++	+
C618F/R/S	10	MODERATE	+/++	+
C620F/R/S	10	MODERATE	+/++	+
C630R/Y	11	MODERATE	+/++	+
D631Y	11	MODERATE	+++	-
C634F/G/R/S/W/Y	11	HIGH	+++	++
K666E	11	MODERATE	+	-
E768D	13	MODERATE	-	-
L790F	13	MODERATE	+	-
V804L	14	MODERATE	+	+
V804M	14	MODERATE	+	+
A833F	15	HIGH	+++	-
S891A	15	MODERATE	+	+
R912P	16	MODERATE	-	-
M918T	16	HIGHEST	+++	-

Table 4 : Corrélations génotypes/phénotypes dans les NEM2 (d'après (136)).
+ : environ 10 %, ++ : 20-30 %, +++ : environ 50 %.

Les PH sont présents chez environ 50 % des patients avec une NEM2A ou NEM2B. (134) et peuvent révéler une NEM2 dans 6-13 % des cas (137, 138). Ces PH se développent généralement vers l'âge de 30 ans. Ils sécrètent de l'adrénaline. Deux tiers des patients développent des PH bilatéraux (84, 137, 139). Un seul cas de PGL a été décrit dans le cadre de la NEM2 chez un patient porteur d'une mutation du codon 620, ayant un PGL cervical diagnostiqué en même temps qu'un CMT (140).

4- Les syndromes PGL-polyglobulie (gènes *EPAS1* et *EGLN1*)

Les gènes *EPAS1* (aussi dénommé *HIF2A*, 16 exons, chromosome 2p21) et *EGLN1* (aussi dénommé *PHD2*, 5 exons chromosome 1q42.2) codent pour deux protéines qui interviennent comme VHL dans la voie de l'hypoxie. *EPAS1* code pour la sous-unité alpha du facteur de réponse à l'hypoxie HIF2 et *EGLN1* pour une des prolines hydroxylases permettant l'hydroxylation de HIF2α et ainsi la fixation de VHL (**Figure 7**).

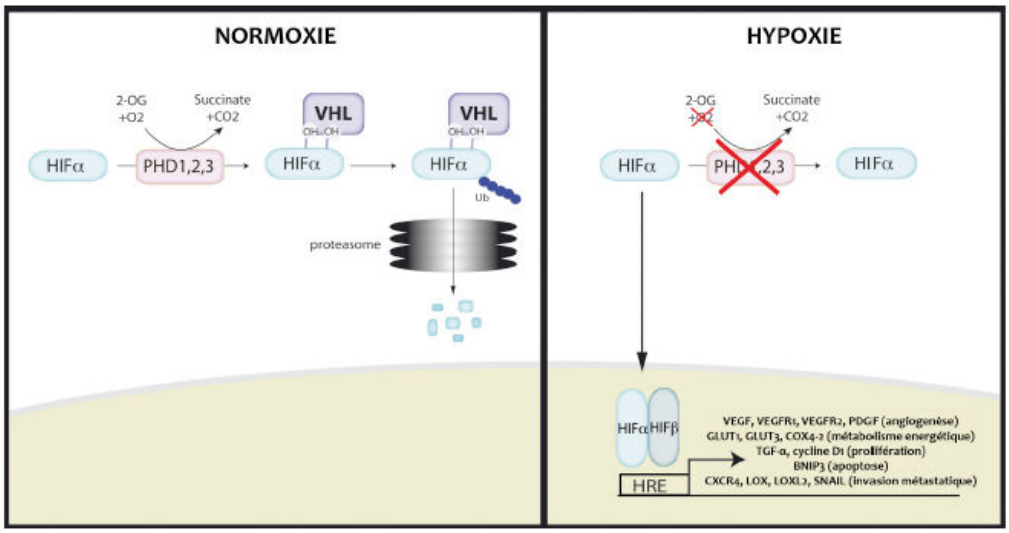

Figure 7 : Représentation schématique de la voie de régulation de l'hypoxie (d'après (141)).

Les mutations constitutionnelles gain de fonction de *EPAS1* et perte de fonction de *EGLN1* sont connues depuis de nombreuses années pour être impliquées dans les polyglobulies congénitales de transmission autosomique dominante (142-144).

La première mutation constitutionnelle de *EGLN1* a été décrite en 2008 chez un patient ayant une polyglobulie et un PGL abdominal (145). La mutation était une mutation perte de fonction associée à une perte d'hétérozygotie dans le PGL. Ces données ont été confirmées récemment avec la description d'un nouveau patient ayant des PGL multiples et porteur d'une mutation *EGLN1* (146).

L'équipe de Karel Pacak a décrit en 2012 les premières mutations somatiques de *EPAS1*. Ces mutations sont des mutations gain de fonction et ont été retrouvées chez des patients avec polyglobulie congénitale, somatostatinome et PGL (147). Depuis d'autres équipes, dont la notre, ont confirmé ces données : les patients avec mutations *EPAS1* ont des PGL ou des PH, sécrétant préférentiellement de la noradrénaline et/ou de l'EPO, multiples dans la moitié des cas et volontiers précoces (147-151). Une polyglobulie est retrouvée dans moins de la moitié des cas et des somatostatinomes uniques ou multiples sont présents dans un quart des cas.
Toutes ces mutations de *EPAS1* sont localisées dans les exons 9 et 12, qui codent pour les deux prolines hydroxylées par les PHD et qui permettent donc la dégradation de HIF2α. Ainsi ces mutations mènent à une stabilisation anormale de HIF2α et à une activation inappropriée de la voie de réponse à l'hypoxie. De surcroit, ces différentes mutations peuvent être présentes au niveau tumoral, mais aussi à l'état de mosaïque somatique ou de mosaïque constitutionnelle. Dans ce dernier cas, elles peuvent être transmissibles à la descendance (151) .

Les mutations somatiques de *EPAS1* ont très récemment été impliquées dans les PGL et PH qui se développent chez les patients avec cardiopathie cyanogène. En effet, les patients ayant une cardiopathie cyanogène ont une probabilité de développer des PH plus importante que celle de la population générale (152). Cela serait dû à la présence de mutations somatiques *EPAS1* dans ces PH comme le suggère un article de l'équipe de Patricia Dahia (153). L'hypoxie chronique pourrait favoriser l'émergence de ces mutations somatiques de *EPAS1*.

II- LES PARAGANGLIOMES ET PHEOCHROMOCYTOMES HEREDITAIRES

1- Les gènes *SDHx* (*SDHA, SDHB, SDHC, SDHD, SDHAF2*)

Les gènes *SDHx* (*SDHA, SDHB, SDHC, SDHD* et *SDHAF2*) représentent presque la moitié des gènes mutés au niveau constitutionnel dans les PGL (84, 131, 154, 155). Ils représentent les gènes majeurs de prédisposition à cette pathologie. Les gènes *SDHx* sont des gènes nucléaires. Les gènes *SDHA, SDHB, SDHC et SDHD* codent pour les 4 sous-unités de la succinate déshydrogénase (SDH) ou complexe II mitochondrial, un enzyme localisée dans la membrane interne de la mitochondrie. Cette enzyme est au carrefour de deux voies métaboliques : elle permet d'oxyder le succinate en fumarate dans le cycle de Krebs, et intervient dans le transfert d'électrons de la chaine respiratoire mitochondriale. La SDH contient deux sous-unités d'ancrage SDHC, SDHD, et deux sous-unités catalytiques SDHA et SDHB (**Figure 8**). Le gène *SDHAF2* code quant à lui pour une protéine indépendante de la SDH, mais essentielle à l'assemblage du complexe, responsable de la flavination de SDHA.

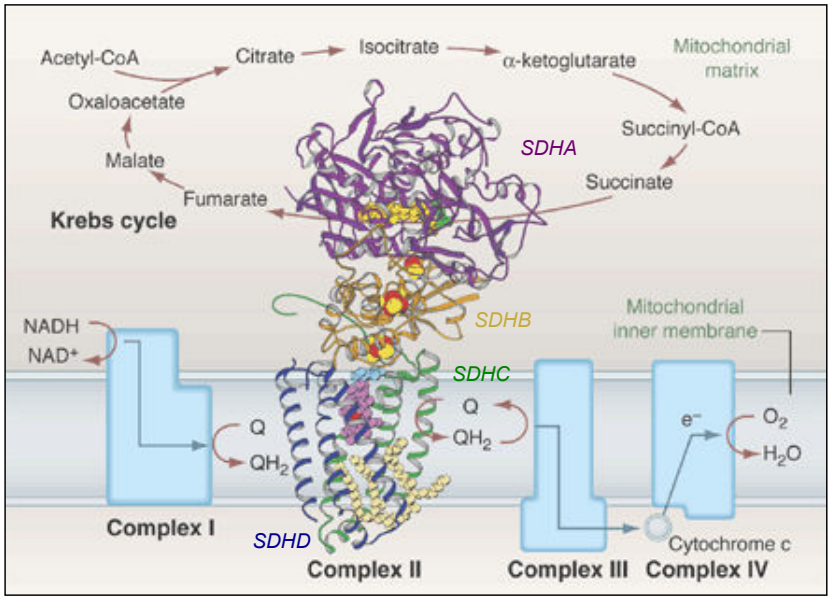

Figure 8 : Représentation schématique de la succinate déshydrogénase (d'après (156)).

La découverte dans les années 2000, que les gènes *SDHx* étaient des gènes suppresseurs de tumeurs responsables de la tumorigenèse des PGL a révolutionné les connaissances sur la génétique des PGL (102-104). Une mutation constitutionnelle dans un de ces gènes associée à une perte d'hétérozygotie au niveau somatique mène à une perte de l'activité de la SDH, responsable d'une accumulation de succinate dans le cytoplasme qui va se comporter comme un oncométabolite (83, 157). Ces mutations se transmettent simplement de façon autosomique dominante pour les gènes *SDHA, SDHB, et SDHC* mais de façon autosomique dominante associé à un mécanisme évoquant une empreinte génomique maternelle pour *SDHD* et *SDHAF2*.

La majorité des PGL *SDHx*-déterminés sont secondaires à des mutations dans les gènes *SDHD* et *SDHB*, alors que les mutations dans *SDHC* et *SDHA* sont rares (155, 158, 159). Les patients porteurs de ces mutations développent des PGL vers l'âge de 36 ans, alors que les PGL sporadiques apparaissent habituellement vers 50 ans (105). Ces PGL, s'ils sont fonctionnels, sécrètent de la noradrénaline ou de la dopamine du fait de l'inactivation par un mécanisme épigénétique de la PNMT dans la tumeur (157, 160). Des phénotypes différents sont observés selon le gène *SDHx* muté ce qui permet d'orienter les analyses moléculaires (**Table 5**).

	SDHB	***SDHC***	***SDHD***	***SDHA***	***SDHAF2***
PHEO unique	++	-	+	+	-
PGL TAP	**+++**	+	++	+	-
PGL cervical	++	++	**+++**	++	**+++**
PH bilatéral	+	-	+	-	-
PGL multiples	++	+	**+++**	-	+
PGL métastatiques	**+++**	+/-	+/-	+/-	-

Table 5 : Phénotype des patients porteurs d'une mutation constitutionnelle dans les gènes *SDHx* (d'après (84, 105, 131, 155, 161)). TAP : thoraco-abdomino-pelvien.

a- Le gène *SDHD*

Le gène *SDHD* code pour l'une des deux sous-unités d'ancrage de la succinate déshydrogénase. Il comporte 4 exons et est localisé en 11q23. Ce gène fut le premier gène *SDHx* impliqué dans la tumorigenèse des PGL, grâce à des études de liaison menées dans des grandes familles hollandaises et américaines (102).

Les PGL héréditaires secondaires aux mutations *SDHD* se transmettent selon le mode autosomique dominant soumis à empreinte maternelle, ce qui fait que le phénotype des patients va varier selon le parent transmetteur.
Les mutations dans le gène *SDHD,* quand elles sont héritées de la branche paternelle sont plutôt responsables de PGL cervicaux (plus de 97 % des patients), multiples dans deux tiers des cas. La pénétrance des mutations *SDHD* a été évaluée à 86 % à l'âge de 50 ans. Il est retrouvé une histoire familiale de PGL dans la branche paternelle dans 60 à 80 % des cas (105, 158).

Du fait de l'empreinte maternelle, il était considéré jusqu'à récemment que les mutations *SDHD* transmises par la branche maternelle n'étaient pas responsables du développement de PGL. Toutefois, quelques cas de violation de la règle de l'empreinte génomique maternelle ont été décrits (162-164). Mon équipe d'accueil, dans une étude prospective, a récemment estimé que les patients ayant hérité de la mutation *SDHD* de la branche maternelle ont un risque d'environ 5 % de développer un PGL dans leur vie. De surcroit, il semblerait que ces patients développent principalement des PH uniques (165).

Les premières explications à cette violation de l'empreinte dans les PGL *SDHD*-dépendants ont été apportées par Hensen *et al.* puis par Burnichon *et al.* Le développement des PGL *SDHD*-dépendants serait secondaire à la perte d'hétérozygotie qui, au niveau somatique, emporte l'intégralité du chromosome 11 et induirait la perte d'un allèle d'un second gène suppresseur de tumeur localisé dans la région chromosomique 11p15, bien connue comme étant soumise à empreinte, ce

deuxième gène étant hyperméthylé sur l'allèle paternel. Ainsi, en cas de mutation *SDHD* d'origine paternelle, la perte d'hétérozygotie somatique permettrait l'inactivation bi-allélique de *SDHD* et du deuxième gène suppresseur de tumeur (dont la seule copie restante serait hyperméthylée et donc inactive).

Dans le cas de mutation *SDHD* sur l'allèle maternel, la perte d'hétérozygotie ne serait pas suffisante pour induire la tumorigenèse car le second gène suppresseur de tumeur ne serait pas inactivé (il resterait le second allèle non hyperméthylé). Le développement de PGL n'aurait lieu que si un autre évènement somatique se produit. Il s'agit d'une recombinaison entre l'allèle paternel et maternel qui ne laisse en place que l'allèle paternel hyperméthylé du second gène suppresseur de tumeur dans le tissu (**Figure 9**) (166). La complexité de ce mécanisme, qui nécessite 3 différents évènements génétiques (mutation constitutionnelle, recombinaison et perte d'hétérozygotie au niveau somatique) dans la même cellule d'un paraganglion, explique le fait que les PGL se développent très rarement chez les patients porteurs d'une mutation *SDHD* d'origine maternelle.

Toutefois cette explication repose sur l'hypothèse théorique qu'il n'y a pas de centre de l'empreinte à proximité directe de *SDHD.* Or, il a été proposé un putatif centre de l'empreinte à 125 kb en aval de *SDHD* à proximité d'un gène codant pour un long ARN non codant, ce qui n'a jamais été confirmé expérimentalement jusqu'alors (167).

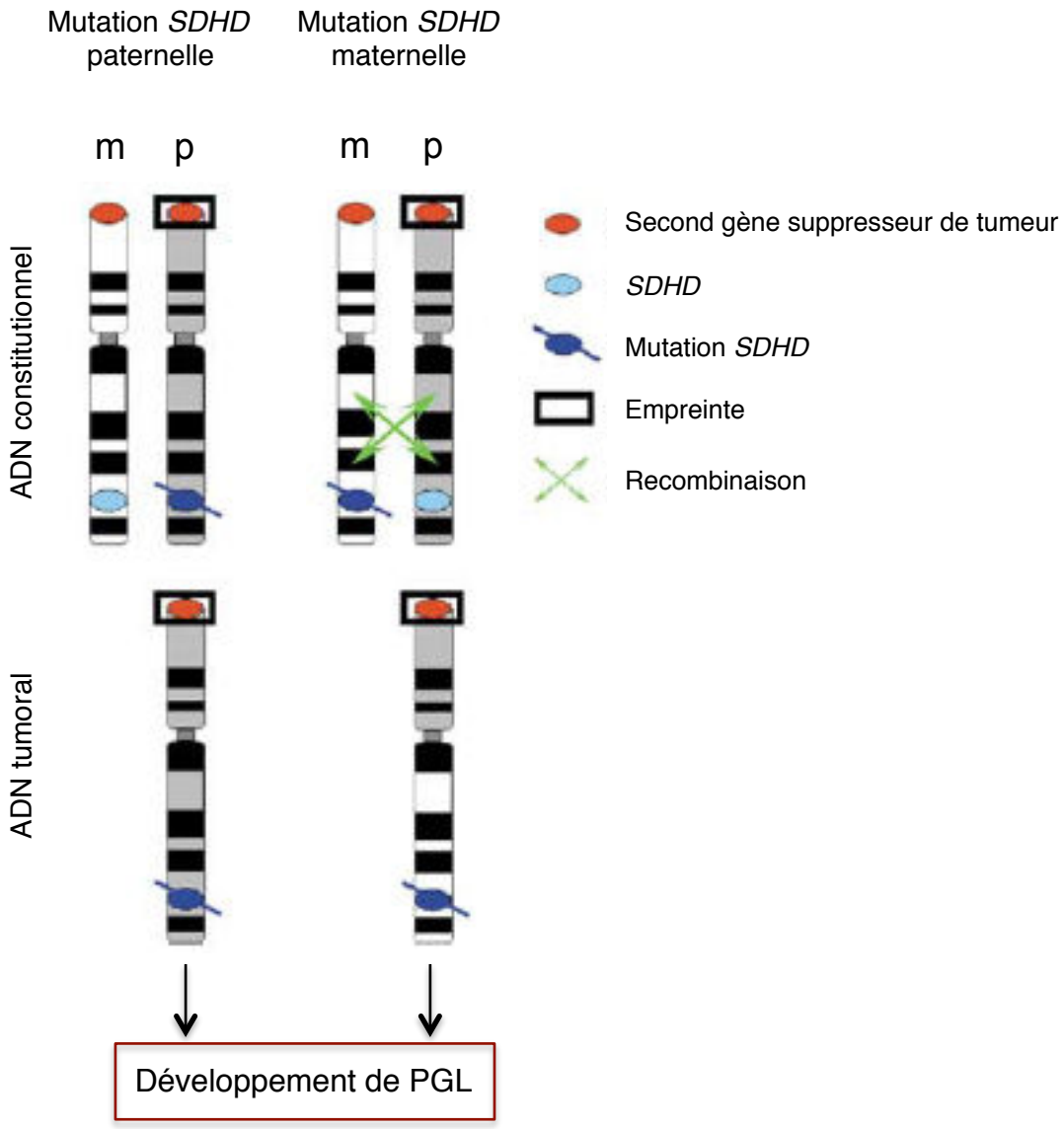

Figure 9 : Mécanisme proposé pour expliquer la possible violation de l'empreinte maternelle dans les PGL *SDHD*-dépendants (d'après (166)). m : allèle maternel, p : allèle paternel

b- Le gène *SDHB*

Le gène *SDHB* code pour l'une des deux sous-unités catalytiques de la succinate déshydrogénase. Il comporte 8 exons et est localisé en position chromosomique 1p36.

Les mutations constitutionnelles dans le gène *SDHB* prédisposent au développement des PGL abdominaux dans 60 % des cas, et cervicaux dans 40 % des cas. Seules

20 % des patients ont une forme multiple. L'âge moyen au diagnostic de PGL est comme pour *SDHD,* de 30 ans environ (84, 131, 161). La pénétrance des mutations *SDHB* est estimée à 50 % à l'âge de 50 ans (168, 169). Ces données de pénétrance ont été contestées récemment par une étude sur 673 patients porteurs d'une mutation *SDHB* où la pénétrance était estimée à 22 % à 60 ans. Mais contrairement aux études précédentes, cette étude couplait des cas index et des apparentés (plus de 2 apparentés pour un cas index) dans son calcul de pénétrance ce qui explique probablement ce résultat (170).

Par ailleurs, les mutations du gène *SDHB* prédisposent à la malignité et sont le principal facteur prédictif de malignité chez les patients avec un PGL (15, 76, 81-84). En effet, environ la moitié des patients porteurs d'un PGL *SDHB*-dépendant ont une forme métastatique, et une mutation constitutionnelle du gène *SDHB* est retrouvée chez 36 % des patients avec un PGL malin, alors qu'une forme maligne n'est retrouvé que chez 5 % des patients porteurs d'une mutation dans les gènes *SDHD* et *SDHC* (**Figure 10**) (105, 158).

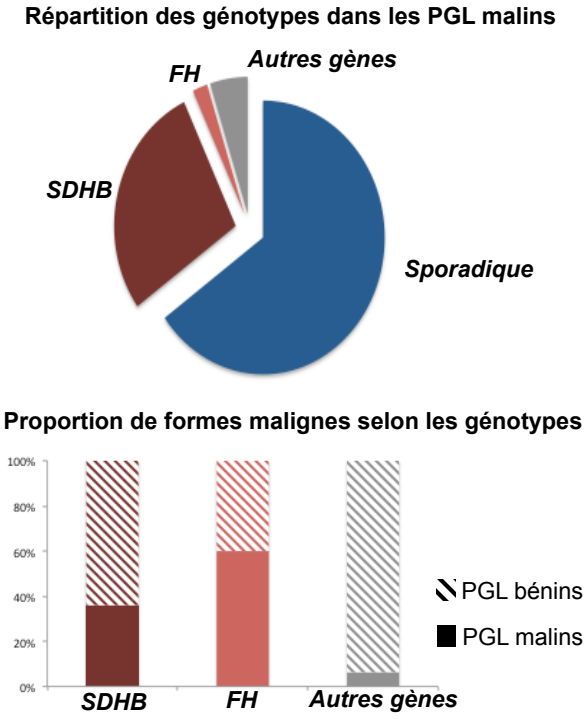

Figure 10 : Répartition des génotypes dans les PGL malins et proportion de PGL malins selon les génotypes (d'après (83, 84, 171)).

De plus, dans une étude princeps ayant inclus rétrospectivement 54 patients ayant un PGL malin, les patients avec un PGL *SDHB*-dépendant avaient un plus mauvais pronostic que les patients ayant un PGL malin non *SDHB*-dépendant. La survie globale des patients ayant un PGL malin *SDHB*-dépendant était de 42 mois après le diagnostic de première métastase versus 244 mois chez les patients ayant un PGL malin non *SDHB*-dépendant (**Figure 11**) (76). Cette association entre mutations *SDHB* et mauvais pronostic a été confirmée dans une série pédiatrique (172, 173). Les raisons de ce phénotype malin et de cette agressivité spécifique des mutations *SDHB* n'étaient pas connues au début de mon travail.

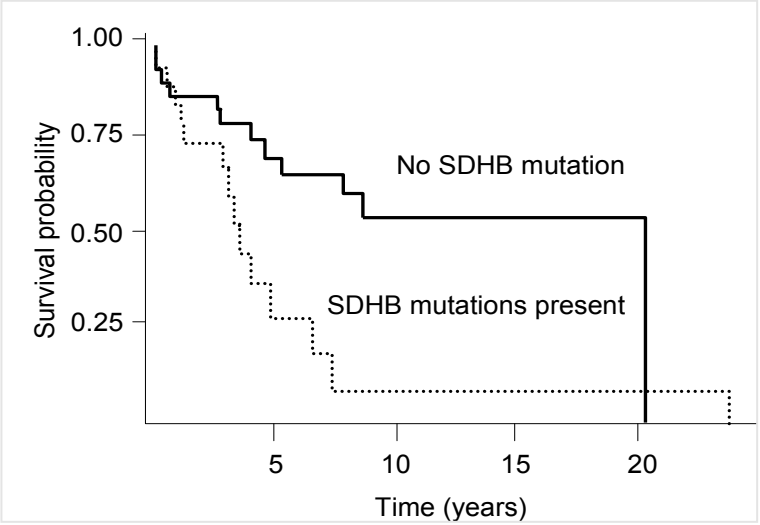

Figure 11 : Survie globale des patients avec PGL après le diagnostic de la première métastase (d'après (76)).

c- Les gènes *SDHC, SDHA, SDHAF2*

Ces trois gènes sont plus rarement mutés chez des patients avec PGL/PH.

Le gène *SDHC* code pour l'une des deux sous-unités d'ancrage de la succinate déshydrogénase. Il comporte 6 exons et est localisé en 1q23.

Les mutations dans le gène *SDHC* prédisposent au développement de PGL cervicaux dans la majorité des cas, avec une histoire familiale dans un quart des cas, mais aussi aux autres localisations de la maladie (105).

Le gène *SDHA* code pour l'une des deux sous-unités catalytiques de la succinate déshydrogénase. Il comporte 15 exons et est localisé en 5p15.
Les mutations dans le gène *SDHA* représentent moins de 10 % des mutations identifiées chez les patients avec PGL/PH. La première mutation a été mise en évidence par mon équipe d'accueil initialement chez une patiente avec un PGL abdominal fonctionnel révélé par une HTA gravidique (174). Le phénotype est un peu mieux connu grâce à une étude récente sur 30 patients ayant un PGL porteurs d'une mutation constitutionnelle dans le gène *SDHA* : 70 % des patients ont un PGL cervical, et 16 % un PGL thoracique ou abdominal (175).

Le gène *SDHAF2* code pour une protéine permettant la flavination de la sous-unité SDHA essentielle à la stabilisation du complexe et donc à la fonction de la succinate déshydrogénase (176). Il comporte 4 exons et est localisé en 11q13. Deux familles ont été décrites en 2009 et 2010 aux Pays Bas et en Espagne portant la même mutation. Les membres de cette famille avaient uniquement des PGL cervicaux uniques ou multiples bénins (176-178). Depuis lors, seuls 3 patients supplémentaires ont été décrits avec le même phénotype (179, 180).

d- Les mutations *SDHx* prédisposent à d'autres tumeurs que les PGL/PH

Les mutations *SDHx* ont aussi été impliquées dans la genèse d'autres tumeurs :
- Elles ont été décrites chez quelques patients avec cancer du rein (181). Elles seraient impliquées dans 0,05 à 0,2 % des cancers du rein, principalement des carcinomes à cellules claires (182). Deux à 3% des patients porteurs d'une mutation *SDHx* développeraient un cancer du rein (168, 170). Même si tous les génotypes ont été impliqués, il s'agit plutôt de patients jeunes, porteurs d'une mutation *SDHB.* Ces cancers du rein *SDHx*-dépendants sont reconnus maintenant comme une forme à part entière de cancer du rein par l'OMS (OMS 2016). Cependant il est important de souligner que la preuve formelle de l'implication de la mutation *SDHx* par un immunomarquage SDHB négatif est apportée dans un faible nombre de cas publiés.

- Elles ont été également impliquées dans les tumeurs gastrointestinales stromales (GIST) sans mutation dans les gènes *PDGFRA* et *KIT*. Elles prédisposent principalement à la survenue de GIST survenant chez l'enfant ou l'adulte jeune, gastriques, multiples et malignes (183). En effet, 85 % des GIST de l'adulte et 15 % des GIST pédiatriques sont secondaires à des mutations somatiques des gènes *KIT* ou *PDGFRA*, les GIST sans mutation dans ces deux gènes étant appelés GIST Wild-Type (WT). Parmi ces GIST WT, plus de 80 % sont secondaires à des mutations somatiques ou constitutionnelles des gènes *SDHx* (183). Alors que *SDHB* est le gène le plus souvent muté dans les cancers du rein *SDHx*-dépendants, *SDHA* serait le gène majeur des GIST *SDHx*-dépendants (183).
En outre, parmi ces GIST *SDHx*-dépendants, il a été décrit au début de ma thèse un nouveau mécanisme mutationnel des gènes *SDHx* : il s'agit des « épimutations » du promoteur de *SDHC* (184) qui sont des hyperméthylations du promoteur qui empêchent sa transcription.

- Enfin elles ont été impliquées dans les adénomes hypophysaires mais leurs implications dans la tumorigenèse reste débattue notamment car, comme pour les cancers du rein évoqués plus haut, les données d'immunohistochimie sont le plus souvent absentes ou contradictoires dans les cas publiés (185).

2- **Le gène *FH***

Le gène *FH* code pour la fumarate hydratase, une enzyme du cycle de Krebs qui catalyse l'étape qui suit celle de la succinate déshydrogénase, permettant l'hydratation du fumarate en malate (**Figure 8**).
Les mutations constitutionnelles de ce gène de 8 exons localisé en 1q42, étaient connues pour être responsables du syndrome HRLCC (Hereditary Leiomyomatosis and Renal Cell Cancer) ou syndrome de Reed (186). Les patients atteints développent des léiomyomes cutanés dans 70 % des cas et de façon rare, des leiomyosarcomes cutanés. Les femmes présentent des léiomyomes utérins dans plus de 80 % des cas, dès l'âge de 30 ans (187). Enfin dans 15% à 19% des cas il

est retrouvé un carcinome rénal papillaire de type 2, qui est de mauvais pronostic (188, 189). En effet, environ 47 % des ces cancers du rein sont métastatiques d'emblée et 35 % le deviendront dans les 3 ans qui suivent le diagnostic. En outre, la survie médiane des patients avec cancer du rein est de 18 mois, ce qui fait du cancer du rein le principal facteur pronostic de ce syndrome (187).

Nous avons démontré récemment que ce gène *FH* était également impliqué dans les PGL. Nous avons mis en évidence les premières mutations constitutionnelles de ce gène chez 1 % des patients avec PGL, dont 40 % avaient des PGL malins (**Figure 10**) ou multiples sécrétant de la noradrénaline ou non sécrétant (157, 171, 190). De façon intéressante, une seule patiente avait des manifestations de HLRCC (léiomyomes utérins), les autres étaient indemnes de ces manifestations.

3- **Le gène *TMEM127***

L'implication de *TMEM127* dans la prédisposition au PGL a été mise en évidence en 2010 dans une grande famille présentant de nombreux sujets atteints d'un PH, grâce à une analyse de liaison génétique puis de séquençage à haut débit de la région chromosomique identifiée comme contenant le gène (191). Ce gène de 4 exons, localisé en 2q11, est un régulateur négatif de la voie mTOR. TMEM127 interagirait avec un complexe multi-protéique à la surface du lysosome pour réprimer la stimulation de mTOR par les acides aminés (192).

TMEM127, qui représente 1 à 2 % des gènes mutés dans les PGL, prédispose aux PH sécrétant de l'adrénaline, dont 15 à 66 % sont bilatéraux et qui se développent après 35 ans (193-195). Une histoire familiale est retrouvée dans 15 à 30 % des cas. La pénétrance est de 32 % avant 65 ans (194).
Ce gène a également été impliqué dans la prédisposition aux carcinomes rénaux à cellules claires (196).

4- **Le gène *MAX***

Le gène *MAX* est le premier gène de prédisposition au PGL identifié par une stratégie utilisant le whole-exome sequencing (197). Il est composé de 5 exons et localisé en 14q23. Il s'agit d'un facteur de transcription de type leucine zipper qui est un membre du réseau protéique MYC/MAX/MXD, intervenant dans la prolifération cellulaire, la différenciation et l'apoptose. La protéine MAX peut former des hétérodimères avec les oncogènes MYC ou les protéines MXD. Son association avec MYC lui permet de se fixer sur ses gènes cibles via un motif du promoteur (Boite E) pour induire la transformation et la prolifération, alors que son interaction avec les protéines MXD induit une réponse opposée (198). De plus la protéine MAX est capable de former un homodimère qui réprime les cibles de l'hétérodimère MYC/MAX (199).

Les mutations de *MAX* sont retrouvées dans environ 1 % des PGL. Il prédispose aux PGL sécrétant de la noradrénaline qui se développent en moyenne autour de l'âge de 34 ans. La majorité des patients porteurs d'une mutation *MAX* présentent un PH ou un PGL abdominal, la moitié d'entre eux développent une forme bilatérale synchrone ou métachrone. Une histoire familiale est retrouvée dans 40 % des cas (200).
De façon récente, il a été mis en évidence des mutations *MAX* chez des patients avec adénomes hypophysaires mais pour le moment, l'association reste toujours à démontrer (201).

III- LES GÈNES DE PRÉDISPOSITION PLUS RARES

Certains gènes ont été impliqués que dans un nombre très limité de patients, comme par exemple *MDH2, MET, H3F3A, MERTK*, *KMT2D* et *KIF1B*, et la réalité de leur implication reste à encore démontrer dans des études plus larges

1- **Le gène *MDH2***

La malate déshydrogénase existe sous deux isoformes, l'une dans le cytosol (codée par le gène *MDH1*) et l'autre dans la matrice mitochondriale (codée par le gène *MDH2*). C'est une enzyme du cycle du Krebs qui catalyse l'étape suivant celle de la fumarate hydratase où elle oxyde le L-malate en oxaloacétate **(Figure 12).** La forme mitochondriale intervient également dans la navette malate-aspartate, essentielle à la respiration cellulaire.

Le premier patient porteur d'une mutation constitutionnelle du gène *MDH2* a été décrit très récemment. Il s'agissait d'un patient qui avait des PGL multiples métastatiques sécrétant de la noradrénaline. (202). Les mutations de ce gène semblent être rarement impliquées dans la prédisposition aux PGL. Dans une cohorte internationale à laquelle notre laboratoire a participé, seul 4 patients porteurs d'une mutation constitutionnelle de ce gène ont été mis en évidence sur les 830 patients analysés (203) (**Voir l'article 8 donné en Annexes**).

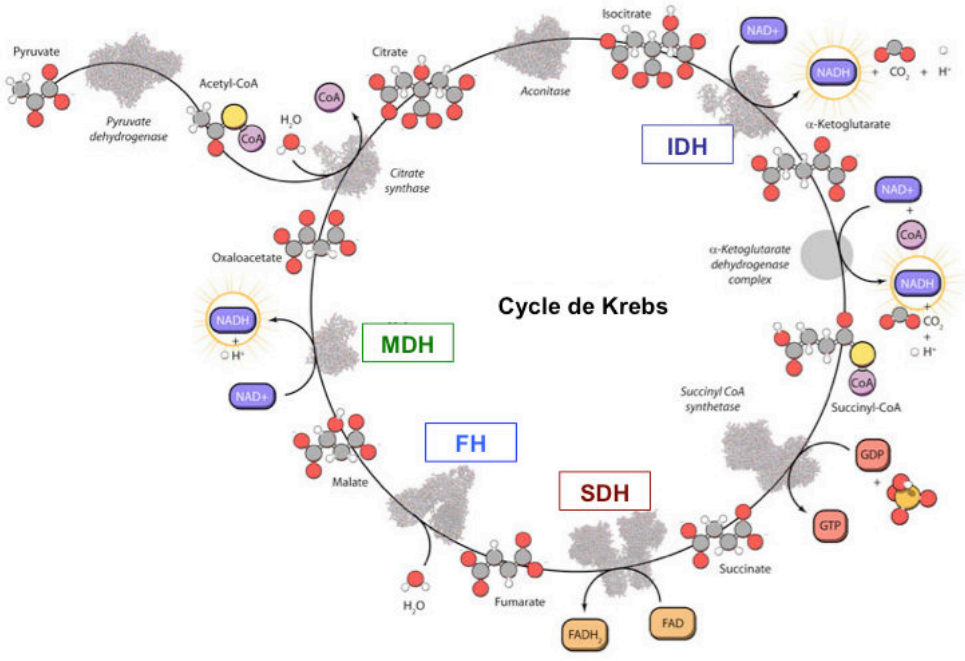

Figure 12 : Cycle de Krebs. Les enzymes SDH, FH et MDH sont impliquées dans la prédisposition aux PGL.

2- **Le gène *MET***

L'oncogène *MET* est impliqué dans les carcinomes rénaux papillaires de type 1. Il code pour un récepteur à tyrosine kinase comme RET.
Des mutations somatiques de ce gène ont été décrites en premier par mon équipe d'accueil dans les PGL (130), et récemment au niveau constitutionnel dans une famille de PH (204).

3- **Le gène *KIF1B***

Seule deux mutations constitutionnelles ont été décrites depuis 2008 (205, 206) dans ce putatif gène suppresseur de tumeurs. Toutefois, l'implication de ce gène dans la prédisposition aux PGL n'a jamais été prouvée formellement et il n'y a pas à l'heure actuelle de test fonctionnel disponible permettant de prouver la pathogénicité de ces variants génétiques identifiés sur ce gène comportant 1816 acides aminés.

4- **Le gène *H3F3A***

Une seule équipe a décrit une mutation récurrente à l'état de mosaïque somatique sur un hot spot de mutation déjà impliquée dans les tumeurs osseuses à cellules géantes. Il s'agissait de deux patients qui avaient des PGL multiples associés à des tumeurs osseuses à cellules géantes (204).

5- **Le gène *MERTK***

Deux patients ayant un PGL et un CMT ont été décrits récemment comme porteurs d'une mutation constitutionnelle de ce gène, qui code pour un récepteur à tyrosine kinase. Toutefois l'implication de ce gène reste à prouver (204).

6- **Le gène *GOT2***

En 2017, en utilisant une approche de séquençage à haut débit ciblé sur les différents gènes impliqués dans le métabolisme mitochondrial, l'équipe de M. Robledo a mis en évidence une mutation gain de fonction de *GOT2* (207) chez un patient avec des PGL multiples et métastasiques. Ce gène code pour la transaminase glutamique-oxaloacétique mitochondriale faisant partie de la navette malate-aspartate.

7- **Le gène *DNMT3A***

Grâce à une approche de whole-exome sequencing, il a été mis en évidence début 2018 deux mutations constitutionnelles activatrices dans le gène *DNMT3A* chez deux patients avec des PGL familiaux (208).

B- LA GÉNÉTIQUE TUMORALE DES PGL/PH

Si jusqu'à 40% des patients atteints de PGL peuvent être porteurs de mutations constitutionnelles dans l'un des nombreux gènes de prédisposition, des mutations dans l'ADN tumoral des PGL ont également été décrites dans différents gènes. Mon équipe d'accueil a identifié l'importance de ces mutations somatiques dans les PGL, qui sont retrouvées dans presque 30 % des PGL, ce qui porte à 70 % le nombre de PGL génétiquement déterminés (116, 130, 209).

Les gènes mutés au niveau somatique peuvent être divisés en deux groupes :
- soit les mutations sont identifiées dans des gènes de prédisposition connus aux PGL, comme *NF1, VHL, RET, EPAS1, MET,…* ce qui en fait dans ce cas le « driver » de la tumorigenèse du PGL (116, 130, 204, 209, 210). Dans ce groupe les mutations *NF1* sont de loin les plus fréquentes (116, 211).
- soit les mutations sont identifiées dans des gènes connus pour être impliqués dans l'oncogenèse (*HRAS, TP53, CDKN2A, FGFR1, ATRX…*) (130, 210, 212-215).

En dehors de ces deux groupes de gènes il a été mis en évidence sur la cohorte de PGL/PH sur laquelle a été menée l'étude de génomique intégrative du The Cancer Genome Atlas (TCGA) des mutations somatiques du gène *CSDE1*. Ces mutations activeraient la voie Wnt-βcaténine. Ces travaux n'ayant pas été répliqués, il n'est pas certain pour le moment que ce gène soit responsable de la tumorigenèse des PGL (210).

Bien qu'il n'y ait pas de risque de transmission de ces mutations somatiques à la descendance, la mise en évidence de ces mutations est importante pour connaître la biologie de la tumeur du patient et explique entre autres le phénotype sécrétoire de ces PGL. En effet, un PGL avec une mutation somatique dans le gène *VHL* secrétera préférentiellement de la noradrénaline, alors qu'un PGL avec une mutation somatique *NF1* ou *RET* sécrétera préférentiellement de l'adrénaline (116, 206, 209). De surcroit, certaines données récentes suggèrent que l'identification d'une mutation somatique dans les gènes *ATRX*, ou *KMT2D* pourrait être un prédicteur de l'agressivité de la tumeur ou de sa taille respectivement (213, 216).

C- LA VALIDATION DES VARIANTS GÉNÉTIQUES IDENTIFIÉS

Du fait de la complexité génétique des PGL et du nombre important de variants de signification inconnue, accélérée récemment par les techniques de séquençage haut débit mises en place en routine diagnostique, il est devenu nécessaire de développer des tests fonctionnels pour valider les variants mis en évidence dans les différents gènes de prédisposition aux PGL.
Actuellement les immunohistochimies (IHC) anti-SDHA (217), SDHB (218), SDHD (219), MAX (200) et 2-succinyl cystéine (171) sont utilisées pour valider les variants génétiques identifiés.
Ainsi, une immunohistochimie anti-SDHA négative sera en faveur d'une mutation *SDHA* alors qu'une IHC anti-SDHB négative sera en faveur d'une mutation dans un

gène *SDHx* de façon non spécifique. En cas d'IHC anti-SDHB non contributive, l'IHC anti-SDHD positive permet d'orienter vers une mutation dans une des gènes *SDHx*.
En dehors des gènes *SDHx,* l'IHC anti-MAX permettra de valider la présence d'une mutation tronquante de la protéine MAX si elle est négative, et une IHC anti 2-succinyl cystéine positive orientera vers une mutation *FH*.
A côté de ces IHC, il a été développé des approches basées sur la quantification de certains métabolites, et en particulier du succinate dans les tumeurs *SDHx*. Ainsi, la spectrométrie de masse ou la résonnance magnétique nucléaire peuvent être utilisées sur les tumeurs congelées pour valider l'accumulation du succinate, signe d'une mutation sur un gène *SDHx* (220, 221).
Récemment, mon équipe a développé une séquence de spectrométrie par résonnance magnétique qui permet de détecter l'accumulation de succinate in vivo dans les tumeurs, lors d'une séance d'imagerie par IRM, et ainsi d'orienter le diagnostic vers une mutation d'un gène S*DHx* avant que le patient ne soit opéré de son PGL (221-223) (**Voir l'article 5 donné en Annexes**).

D- L'IMPLICATION DE CES GÈNES DANS LA TUMORIGENÈSE

Les données récentes issues des études de génomique, ont permis de mieux comprendre les mécanismes de la tumorigenèse des PGL/PH (**Figure 13**). En effet, les études de transcriptomique menées sur des cohortes de PGL, ont montré que que les PGL se répartissaient en trois grands clusters, reflétant trois mécanismes de tumorigenèse différents (209, 210).
Le premier cluster (cluster C1) se subdivise en deux, un sous groupe regroupant les tumeurs secondaires aux mutations *SDHx*, et *FH* (cluster C1A), et un deuxième sous-groupe regroupant les PGL secondaires aux mutations *VHL* (cluster C1B). Ces deux sous-groupes sont caractérisés par une signature moléculaire suggérant une activation de la voie de la réponse hypoxique. Il a été démontré que cette activation passe par la stabilisation anormale des facteurs de transcription HIF-1 et HIF-2 mènant à ce qu'on appelle la « pseudo-hypoxie ». Les protéines HIFs sont des facteurs de transcription hétérodimériques associant une sous-unité exprimée de

façon constitutionnelle (HIF1β) à une des sous-unités induite par l'hypoxie (HIF1α ou HIF2α). En situation physiologique et normoxique, les HIFα sont dégradés rapidement grâce à l'hydroxylation de deux prolines par les prolyl-hydroxylases (PHD), permettant la fixation de VHL et ainsi leur polyubiquitination et leur dégradation dans le protéasome. En absence d'O_2, les PHD ne peuvent plus assurer l'hydroxylation des HIFα, qui sont donc stabilisés et transloqués dans le noyau.

Les mutations des gènes *SDHx* et *FH* mènent respectivement à l'accumulation de succinate et de fumarate dans les PGL, où ils jouent un rôle d'inhibiteur compétitif des dioxygénases dépendantes du 2-oxoglutarate (2-OG) (dont les PHD), et conduisent donc à une stabilisation anormale des HIFs (224, 225). L'activation de la pseudo-hypoxie induit l'expression de gènes cibles impliqués entre autres dans la prolifération cellulaire (Cyclin D1), l'angiogenèse (VEGF, Angiopoeitine, VEGFR1 et 2, PDGF), la survie et la transition epithélio-mésenchymateuse (LOXL2, Twist) (226). Toutefois la pseudo-hypoxie n'est pas le seul mécanisme de la tumorigenèse associé à l'accumulation de succinate. Mon équipe d'accueil a démontré que des modifications épigénétiques intervenaient également dans les PGL *SDHx* et *FH*-dépendants (157, 224). En effet, l'accumulation de succinate et de fumarate dans ces PGL est responsable de l'inhibition de l'activité d'autres dioxygénases dépendantes du 2-oxoglutarate, les enzymes TET, impliquées dans la déméthylation de l'ADN, et les enzymes JmJ, impliquées dans la déméthylation des histones, conduisant ainsi à une hyperméthylation globale de l'ADN et à des modifications structurelles de la chromatine. Ces modifications mènent à la sous-expression de différents gènes, notamment de GST, et de gènes répresseurs des processus métastatiques, ainsi qu'à la sous-expression des gènes impliqués dans la différenciation chromaffine (157). Enfin il a été démontré en 2018 que l'accumulation de succinate et de fumarate menait également à l'inhibition des enzymes KDM4A et KDM4B qui seraient responsable d'une suppression de la recombinaison homologue dans les tumeurs *SDHx* et *FH*-dépendantes (227).

Le deuxième grand mécanisme de tumorigenèse des PGL implique la voie des MAP kinase et la voie mTOR et est retrouvé dans les PGL secondaires aux mutations des gènes *RET*, *NF1*, *TMEM127*, et *MAX* (cluster C2). Le gène *RET* code pour un récepteur à activité tyrosine kinase activant la voie des MAP kinase. La GTPase NF1 est impliquée dans la régulation de la voie de l'oncogène Ras, première étape de la voie des MAP kinases et qui régule la voie AKT/mTOR et, comme évoqué plus haut, la protéine TMEM127 réprime l'activation secondaire aux acides aminés de mTOR. Enfin, les mécanismes exacts de l'activation de ces voies dans les PGL secondaires aux mutations *MAX* ne sont pas encore bien connus mais font également intervenir la signalisation mTOR (192, 200, 209).

Finalement il a été récemment mis en évidence un troisième cluster sur le transcriptome grâce aux études menées dans le cadre du TCGA. Celui-ci est marqué par une activation de la voie de Wnt-βcatenine, une voie impliquée dans la tumorigenèse de nombreuses tumeurs. Des mutations somatiques dans le gène *CSDE1* intervenant dans cette voie ont été mises en évidence ainsi que l'amplification d'un gène de fusion (*UBTF-MAML3*) (210).

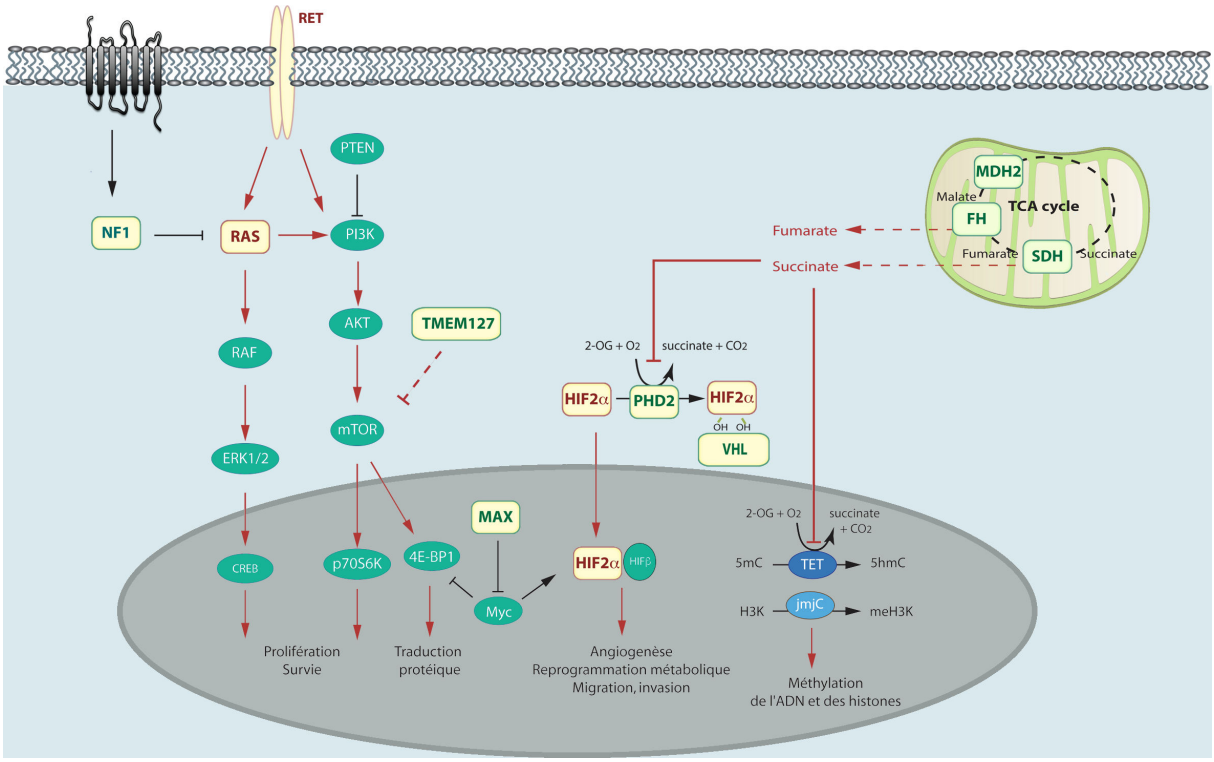

Figure 13 : Voie de tumorigenèse des PGL selon le génotype. Les protéines entourées en vert sont codées par des gènes suppresseurs de tumeur et celle entourées en rouge par des oncogènes.

E- LES IMPLICATIONS DE LA GÉNÉTIQUE POUR LES PATIENTS AYANT UN PGL

I- LE TEST GÉNÉTIQUE

Devant cette forte composante génétique dans la genèse des PGL, il est désormais recommandé de proposer systématiquement, à chaque patient atteint d'un PGL, de bénéficier de l'analyse de ces différents gènes au niveau constitutionnel. Ce test génétique permet de proposer un suivi adapté au cas index selon son génotype et un test pré-symptomatique chez les apparentés si une mutation constitutionnelle est mise en évidence. Néanmoins, le bénéfice d'un test génétique chez le cas index n'a jamais été formellement prouvé.

Les procédures de réalisation de ces tests génétiques, symptomatiques ou pré-symptomatiques ont été parfaitement définies sur le plan légal par l'article R.1131-1 du Code de la Santé Publique.

Les tests étaient antérieurement orientés selon le phénotype du patient comme rapporté en synthèse sur la **Table 6**, la fréquence des mutations (**Figure 14**), et dans certains cas sur les résultats d'immunohistochimies anti-SDHB, SDHA, MAX sur le tissu tumoral inclus en paraffine (200, 217, 218).

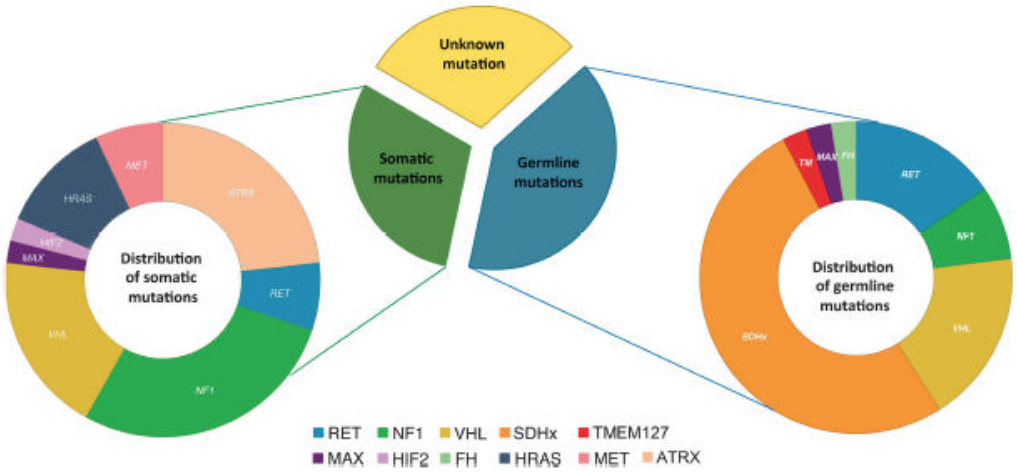

Figure 14 : Répartition des mutations constitutionnelles et somatiques (d'après (228)).

Cette approche est de moins en moins utilisée avec la généralisation récente du séquençage haut débit utilisé pour séquencer l'ensemble des gènes de prédisposition à l'aide d'un panel dédié. Cette technologie permet désormais de séquencer sans *a priori* et en une seule fois l'intégralité des gènes du PGL (229). Toutefois, la description détaillée du phénotype du patient et les analyses immunohistochimiques peuvent permettre de valider les variations génétiques de signification inconnue qui sont beaucoup plus fréquentes avec les nouvelles techniques de séquençage haut débit (NGS). Des recommandations internationales sur la pratique du test génétique du PGL par NGS ont été récemment publiées (229).

Gène	Fréquence des mutations	Age au diagnostic	Localisation préférentielle	PGL multiples	PGL malins	Type de catécholamine
NF1	3 %	40-50 ans	PH	20-40 %	Rare	Adré
VHL	7 %	20-30 ans	PH/PGLA	40-60 %	Rare	Norad
RET	6 %	30-40 ans	PH	66 %	Rare	Adré
EPAS1	1 %	20-30 ans	PH/PGLTAP	50 %	Rare	Norad, EPO
EGLN1	2 patients	NC	PGLA	NC	Rare	Norad
SDHA	< 5 %	35-40 ans	PGLC>PGLA	< 5 %	Rare	Norad, Dopa, NS
SDHB	10 %	30-40 ans	PGLA>PGLC	20 %	40 %	Norad, Dopa, NS
SDHC	1 %	35-40 ans	PGLC	30 %	Rare	Norad, Dopa, NS
SDHD	9 %	30-40 ans	PGLC	66 %	Rare	Norad, Dopa, NS
SDHAF2	< 1 %	30-40 ans	PGLC	75 %	Rare	NS
FH	1 %	30-40 ans	PGLA	40 %	60 %	Norad, Dopa, NS
TMEM127	1-2 %	35-40 ans	PH	15-66 %	Rare	Adré
MAX	1 %	35-40 ans	PH	50 %	Rare	Norad

Table 6 : Synthèse des différents phénotypes secondaires aux mutations des principaux gènes de prédisposition au PGL. PGLA : PGL abdominal, PGL C : PGL cervical, PGL TAP : PGL thoraco-abdomino-pelvien, Adré : sécrétion préférentielle d'adrénaline, Norad : sécrétion de noradrénaline, Dopa : sécrétion de dopamine, NS : non sécrétant, NC : non connu.

Malgré les tests génétiques systématiques et les évolutions technologiques au cours des années, il reste environ 10 à 15 % des patients avec PGL suspects d'une forme

héréditaire (précoce, multiples, familiaux) pour lesquels aucune cause génétique n'a été mise en évidence (159).

Enfin, l'intérêt de la génétique tumorale dans les PGL/PH est en cours d'évaluation par mon équipe d'accueil dans le cadre du PRTK COMETE TACTIC.

II- INTERET DU STATUT GENETIQUE POUR LE SUIVI DU CAS INDEX ET DES APPARENTES

Les recommandations américaines et européennes sur la prise en charge du PGL ont mis l'accent sur le fait que les patients avec une forme génétique de PGL devaient être suivis de façon adaptée à leur génotype par un centre expert (21, 230). La mise en évidence d'une mutation constitutionnelle permettra de surveiller l'occurrence des différentes lésions syndromiques. En effet, dans le cadre des formes syndromique de PGL des recommandations existent sur le rythme de dépistage des différentes lésions syndromique notamment pour la maladie de von Hippel-Lindau et pour les néoplasies endocriniennes multiples de type 2 (**Table 7** et **Table 8**).

Lésions	Modalités	Âge	Fréquence
PGL/PH	Mesure de la PA Dosage des métanéphrines	5 ans	1 an
Hémangioblastome rétinien	Fond de l'oeil	5 ans	1 an
Hémangioblastome du SNC	IRM	15 ans	2 ans
Tumeur du sac endolymphatique	IRM	18 ans	1 à 2 ans
Cancer du rein	Échographie abdominale	5 ans	1 an
	IRM/échographie abdominale	18 ans	1 an
Tumeur pancréatique	IRM/échographie abdominale	18 ans	1 an

Table 7 : Recommandations de suivi des patients avec une maladie de von Hippel-Lindau établies par le centre national de référence PREDIR. PA : Pression artérielle

Mutation	Tumeurs	Âge	Prise en charge
Moderate	CMT	5 ans	Calcitonine et échographie cervicale annuelles*
	PH	16 ans	Dosage des métanéphrines annuel
	HPTH	16 ans	Calcémie annuelle
High	CMT	Avant 5 ans	Thyroïdectomie prophylactique
	PH	11 ans	Dosage des métanéphrines annuel
	HPTH	11 ans	Calcémie annuelle
Highest	CMT	Avant 1 an	Thyroïdectomie prophylactique
	PH	11 ans	Dosage des métanéphrines annuel
	HPTH	11 ans	Calcémie annuelle

Table 8 : Recommandations américaines de suivi des patients avec une NEM2 selon le groupe à risque défini par le génotype (d'après (136)) * si la surveillance annuelle est acceptée par la famille, la thyroïdectomie prophylactique pourra être réalisée si la calcitonine est supérieure à 30 pg/ml (231)

En dehors de ces situations syndromiques, ils n'y pas de recommandations bien établies pour la surveillance des patients avec PGL génétiquement déterminés, et les propositions de suivi reposent sur des avis d'experts. De surcroit, il n'y a pas de preuve que le suivi de ces formes génétiques change la prise en charge des patients, l'histoire naturelle de la maladie, et soit véritablement bénéfique pour lui. La **Table 9** reprend les recommandations de suivi proposées par mon équipe d'accueil dans *Nature Reviews Endocrinology* en 2015 (154).

Gène	Âge au dépistage	Surveillance des adultes asymptomatiques
SDHB	6 ans	- Pression artérielle annuelle - Dosage des dérivés méthoxylés plasmatiques ou urinaires annuel - IRM corps entier tous les 2 à 3 ans - TEP ^{18}FDG-TEP si anomalie à l'IRM
SDHD	6 ans	- Pression artérielle annuelle - Dosage des dérivés méthoxylés plasmatiques ou urinaires annuel - IRM corps entier tous les 2 à 3 ans - TEP FDOPA si anomalie à l'IRM
SDHC **ou** ***SDHA***	6 ans	- Pression artérielle annuelle - Dosage des dérivés méthoxylés plasmatiques ou urinaires annuel - IRM corps entier tous les 2 à 3 ans
VHL	5 ans	Cf Table 7
FH	10 ans	- Pression artérielle annuelle - Dosage des dérivés méthoxylés plasmatiques ou urinaires annuel - Examen gynécologique annuel - IRM abdominal annuel
RET	Selon le génotype	Cf Table 8
NF1	non nécessaire, clinique	- Pression artérielle et examen physique annuel - Si HTA : dosage des dérivés méthoxylés plasmatiques ou urinaires et imagerie abdominale - Examen ophtalmologique annuel jusqu'à 8 ans puis tous les 2 ans
TMEM127 **ou** ***MAX***	10 ans	- Pression artérielle annuelle - Dosage des dérivés méthoxylés plasmatiques ou urinaires annuel - IRM abdominale tous les 2 à 3 ans

Table 9 : Propositions de suivi des patients porteurs d'une mutation constitutionnelle dans un des principaux gènes de prédisposition au PGL (d'après (154, 232)).

Enfin, des études rétrospectives menées sur un petit nombre de patients traités par témozolomide ou sunitinib ont montré que les patients répondeurs seraient fréquemment porteurs de mutations sur le gène *SDHB* (98, 100). Ainsi, la mise en évidence d'une mutation chez un patient avec un PGL malin peut potentiellement changer son traitement pour orienter vers ces thérapies en cas de mutation *SDHB.*

Par ailleurs, la mise en évidence d'une mutation dans un de ces gènes de prédisposition permet de proposer, comme il s'agit d'une maladie de transmission

autosomique dominante, un dépistage pré-symptomatique aux apparentés dans le cadre prévue par la loi (article R.1131-5 du Code la Santé Publique), et si ils sont porteurs de la mutation de les faire entrer dans un protocole de suivi adapté dans un centre expert (**Table 9**).

OBJECTIFS ET PRÉSENTATION DU TRAVAIL DE THÈSE

Comme nous l'avons vu, l'identification d'une quinzaine de gènes de prédisposition au PGL a permis, au cours de ces quinze dernières années, de comprendre la tumorigenèse des PGL et d'identifier de nouvelles pistes thérapeutiques pour traiter les formes malignes. Néanmoins plusieurs questions restaient en suspens au moment où j'ai entamé ce travail de thèse (2014).

La première partie de ma thèse est un travail de recherche clinique, où j'ai tenté de répondre à la question : *Quel est l'impact de la mise en évidence d'une mutation constitutionnelle dans l'un des gènes de prédisposition au PGL sur la prise en charge et l'évolution des cas index, en dehors de la possibilité d'offrir un dépistage génétique familial aux apparentés à risque ?*
Du fait de la rareté de la pathologie il était difficile de réaliser une étude prospective sur le sujet. Toutefois, grâce aux différents projets de recherche clinique mis en œuvre par mon laboratoire d'accueil ces dernières années et notamment la constitution des cohortes COMETE et PGL.NET puis du registre national du paragangliome héréditaire PGL.R (105, 233), un nombre conséquent de patients ayant un PGL porteurs d'une mutation constitutionnelle dans un gène de prédisposition au PGL sont suivis dans les différents centre français qui prennent en charge cette pathologie, depuis presque 10 ans pour la plupart, ce qui permet de collecter des données cliniques avec un long délai de suivi. Le premier objectif de mon travail de thèse fut donc d'évaluer l'intérêt de l'identification d'une mutation constitutionnelle dans un gène de prédisposition au PGL pour la prise en charge des cas index. Ce travail a bénéficié d'un financement du Groupe d'Etude des Tumeurs Endocrines (GTE).

L'objectif de la deuxième partie de ma thèse était de mettre en évidence de nouveaux gènes de prédisposition au PGL et/ou de nouveaux mécanismes mutationnels dans les gènes de prédisposition connus.
En effet, comme évoqué plus haut, environ 10 à 15 % des patients ont un phénotype

évoquant une forme héréditaire alors qu'aucune mutation dans l'un des gènes de prédisposition connus n'a été mise en évidence.

La première partie de ce travail a donc porté sur l'identification de nouveaux gènes de prédisposition. Pour ce faire, j'ai utilisé les échantillons biologiques et les annotations biocliniques de la cohorte de PPGL du réseau COMETE ainsi que les données multi-omiques précédemment obtenues par mon équipe d'accueil.

La seconde partie s'est intéressée à l'identification de nouveaux mécanismes mutationnels dans les gènes de prédispositions connus.

CHAPITRE 1

Impact d'un test génétique positif chez les patients ayant un PGL

I- CONTEXTE

La génétique constitutionnelle des PGL a rapidement évolué ces dernières années, en passant de l'identification de mutation dans 3 gènes de prédisposition avant les années 2000 à actuellement la possibilité de mettre en évidence une mutation dans une quinzaine de gènes de prédisposition. Les différentes séries rétrospectives de la littérature ont permis de mieux comprendre quels étaient les phénotypes attendus suite à l'identification d'une mutation constitutionnelle dans l'un de ces gènes de prédisposition, et quels étaient les risques de développer une forme multiple, maligne ou syndromique de PGL (84, 105, 131, 155, 161).

De surcroit, cette évolution majeure a conduit les experts chargés d'établir les recommandations internationales de l'Endocrine Society sur la prise en charge des PGL/PH à proposer la réalisation de l'analyse moléculaire des différents gènes de prédisposition chez tous les patients avec un diagnostic de PGL/PH (21).

Toutefois, en dehors de l'intérêt pour l'enquête familiale, il n'a jamais été formellement prouvé que l'identification d'une mutation dans un gène de prédisposition au PGL changeait le suivi et l'évolution clinique des cas index, et était bénéfique pour le patient. Cette question a d'ailleurs aussi été soulevée lors des recommandations sur la prise en charge des patients ayant un PGL de l'Endocrine Society (21).

L'objectif de ce premier chapitre de ma thèse était donc d'évaluer l'impact d'un test génétique positif sur la prise en charge des cas index.

II- TRAVAUX PERSONNELS

J'ai mené une étude rétrospective multicentrique dans 24 centres tertiaires prenant en charge des patients avec PGL génétiquement déterminés. Ces différents patients ont été recrutés grâce aux différents projets de recherche clinique mis en œuvre par mon laboratoire d'accueil ces dix dernières années et notamment la constitution des cohortes COMETE et PGL.NET puis du registre national du paragangliome héréditaire PGL.R (105, 233), et ce travail a été réalisé sous l'égide du Groupe des

Tumeurs Endocrines.

Ce travail représente le premier article de ma thèse, dont le manuscrit est en préparation. Je me suis rendu dans ces 24 centres dans 20 villes et j'ai analysé les dossiers de 221 patients avec PGL/PH. Ces patients étaient porteurs d'une mutation constitutionnelle dans un des gènes *SDHB, SDHD, SDHC,* ou *VHL*, qui sont les gènes majeurs dans les PGL/PH. Pour démontrer l'impact du test génétique sur la prise en charge du patient et son évolution, j'ai donc séparé en deux groupes ces 221 patients que j'ai ensuite comparés : un groupe ayant eu le diagnostic de PGL et le diagnostic génétique dans le même temps et un groupe ayant eu le diagnostic génétique plusieurs années après le diagnostic de PGL.

ARTICLE 1

Positive impact of the knowledge of genetic status on the management and clinical outcome of patients with paraganglioma and/or pheochromocytoma

Buffet A, Ben Aim L, Leboulleux S, Drui D, Vezzosi D, Libé R, Ajzenberg C, Bernardeschi D, Cariou B, Chabolle F, Chabre O, Darrouzet V, Delemer B, Desailloud R, Goichot B, Esvant A, Herman P, Laboureau S, Lefebvre H, Pierre P, Raingeard I, Reznik Y, Sadoul JL, Schlumberger M, Tabarin A, Tauveron I, Zenaty D, Bertherat J, Baudin E, Favier J, Amar L, Gimenez-Roqueplo AP ; French Group of Endocrine Tumors (GTE)

Manuscrit en préparation

Positive impact of genetic test on the management and outcome of patients with paraganglioma and/or pheochromocytoma

Alexandre Buffet[1,5], Laurène Ben Aim[2], Sophie Leboulleux[3], Delphine Drui[4], Delphine Vezzosi[5], Rossella Libé[6], Christiane Ajzenberg[7], Daniele Bernardeschi[8], Bertrand Cariou[4], Frédéric Chabolle[9], Olivier Chabre[10], Vincent Darrouzet[11], Brigitte Delemer[12], Rachel Desailloud[13], Bernard Goichot[14], Annabelle Esvant[15], Philippe Herman[16], Sandrine Laboureau[17], Hervé Lefebvre[18], Peggy Pierre[19], Isabelle Raingeard[20], Yves Reznik[21], Jean-Louis Sadoul[22], Martin Schlumberger[3], Antoine Tabarin[23], Igor Tauveron[24], Delphine Zenaty[25], Jérôme Bertherat[6,26], Eric Baudin[3], Judith Favier[1], Laurence Amar[26,27], Anne-Paule Gimenez-Roqueplo[1,2,26] ; French Group of Endocrine Tumors (GTE)

[1] INSERM, UMR970, Paris-Centre de Recherche Cardiovasculaire, Paris ; équipe labellisée par la Ligue contre le Cancer

[2] Assistance Publique-Hôpitaux de Paris, Hôpital Européen Georges Pompidou, Service de Génétique, Paris

[3] Département de Médecine Nucléaire et d'Oncologie Endocrinienne, Gustave Roussy, Villejuif

[4] Service d'Endocrinologie, Centre Hospitalier Universitaire de Nantes, Hôpital Nord Laënnec, Nantes

[5] Service d'Endocrinologie, Hôpital Larrey, CHU de Toulouse, Toulouse

[6] Assistance Publique, Hôpitaux de Paris, Hôpital Cochin, Service d'Endocrinologie "Centre de référence maladies rares de la surrénale", Paris

[7] Assistance Publique, Hôpitaux de Paris, Service de Médecine Interne et Endocrinologie, Hôpital Henri Mondor, Créteil

[8] Assistance Publique-Hôpitaux de Paris, Hôpital Universitaire Pitié-Salpêtrière, Service d'ORL, unité d'otologie, implantologie auditive et chirurgie de la base du crâne, Paris

[9] Service d'ORL et de Chirurgie Cervico-faciale, Hôpital Foch, Suresnes, France

[10] Service d'Endocrinologie, CHU de Grenoble-Alpes, La Tronche, Grenoble

[11] Service d'ORL et de Chirurgie Cervico-faciale, Hôpital Pellegrin, CHU de Bordeaux, Bordeaux

[12] Service d'Endocrinologie, Hôpital Robert Debré, CHU de Reims, Reims

[13] Service d'Endocrinologie, Hôpital Nord, CHU d'Amiens-Picardie, Amiens

[14] Service de Médecine Interne, Endocrinologie et Nutrition, Hôpitaux Universitaires de Strasbourg, Faculté de Médecine, Université de Strasbourg, Strasbourg

[15] Service d'Endocrinologie, CHU de Rennes, Rennes

[16] Assistance Publique, Hôpitaux de Paris, Service ORL-CCF, hôpital Lariboisière, université Paris VII, AP-HP, Paris

[17] Service d'Endocrinologie, Centre Hospitalier Universitaire d'Angers, Angers

[18] Service d'Endocrinologie, Diabète et Maladies Métaboliques, INSERM U1239, Centre Hospitalier Universitaire de Rouen, Rouen, France

[19] Service d'Endocrinologie, Hôpital Bretonneau, CHU de Tours, Tours

[20] Service d'Endocrinologie, CHU Montpellier, Hôpital Lapeyronie, Montpellier

[21] Service d'Endocrinologie, CHU de Caen, Caen, France

[22] Service d'Endocrinologie, Hôpital de L'Archet, CHU de Nice, Nice

[23] Service d'Endocrinologie, Hôpital Haut-Lévêque, CHU de Bordeaux, Pessac

[24] Service d'Endocrinologie, Hôpital Gabriel Montpied, CHU de Clermont-Ferrand, Clermont-Ferrand

[25] Assistance Publique-Hôpitaux de Paris, Hôpital Universitaire Robert Debré, Service d'Endocrinologie Diabétologie Pédiatrique, Centre de Référence des Maladies Endocriniennes Rares de la Croissance et du développement, Paris

[26] Université Paris Descartes, PRES Sorbonne Paris Cité, Faculté de Médecine, F-75006 Paris, France

[27] Assistance Publique-Hôpitaux de Paris, Hôpital Européen Georges Pompidou, Service d'hypertension artérielle et médecine vasculaire, Paris

Short Title: Clinical impact of genetic testing in paraganglioma

Keywords: Paraganglioma, pheochromocytoma, *SDHB*, *SDHD*, *VHL*, follow-up

Précis

Our study shows how knowledge of the genetic status at the time of PPGL diagnosis has a positive impact on the management and clinical outcome of patients with a germline *SDHx* or *VHL* mutation.

Corresponding author:
Anne-Paule Gimenez-Roqueplo
Service de Génétique,
Hôpital Européen Georges Pompidou,
20 rue Leblanc, 75908 Paris cedex 15, France.
Tel: 33 1 56 09 38 81
Fax: 33 1 56 09 38 84
Email: anne-paule.gimenez-roqueplo@egp.aphp.fr

Financial support: This study was supported by the Groupe d'Etude des Tumeurs Endocrines by a PFIZER and KEOCYT grant and by INSERM, which granted the PGL.R registry.
A. Buffet received a financial support from ITMO Cancer AVIESAN (Alliance Nationale pour les Sciences de la Vie et de la Santé, National Alliance for Life Sciences & Health) within the framework of the Cancer Plan and from la Fondation pour la Recherche Médicale (FDT20170436955).

Disclosure: The author reports no conflicts of interest in this work.

ABSTRACT

Context

Paragangliomas and pheochromocytomas (PPGL) are characterized by a strong genetic component with up to 40 % of patients carrying a germline mutation in a PPGL susceptibility gene, and international guidelines recommend that genetic screening should be proposed to all patients with PPGL.

Objective

Our objective was to evaluate how a positive genetic test impacts the management and outcome of patients with *SDHx* or *VHL*-related PPGL.

Design

We performed a multicentric retrospective study on 221 propositus carrying a *SDHB, SDHD, SDHC* or *VHL* germline mutation. Patients were divided into two groups: *Genetic* patients, who were informed of their genetic status within the year following the first PPGL diagnosis, and *Historic* patients who only benefited from the genetic test at least seven years after initial PPGL diagnosis.

Results

Compared to *Historic* patients, *Genetic* patients had a better follow-up, with a higher number of examinations and a reduced number of patients lost to follow-up (9.6% *versus* 72 %). During follow-up, smaller (18.7 mm *versus* 27.6, p=0.0128) new PPGL and metastases as well as lower metastatic spread were observed in *Genetic* patients. Importantly, these differences were reversed in the *Historic* cohort after genetic testing. *Genetic* patients who developed metachronous metastases had a better 5-year survival than *Historic* ones (p=0.0127).

Conclusion

Altogether our data suggest that the early knowledge of the genetic status has a positive impact on the management and on the clinical outcome of the patients with a germline *SDHx* or *VHL* mutation.

INTRODUCTION

Pheochromocytomas and paragangliomas (PPGL) are rare neuroendocrine tumors with an estimated prevalence of one in 10,000 (1-3). These tumors can be found in the head and neck region, as well as in thoracic, abdominal and pelvic area. PGL located in the adrenal medulla are called pheochromocytoma. These tumors can produce catecholamines and cause severe hypertension (HTA) and cardiovascular morbidity. Since 2000 and the identification of *SDHD*, *SDHC* and *SDHB* germline mutations in PPGL, the understanding of PPGL genetic determinism has significantly improved. Nowadays, it is known that up to 40% of patients with PPGL carry a germline mutation in one of the 17 susceptibility genes reported so far (three proto-oncogenes: *RET*, *EPAS1* and *GOT2* and 14 tumor suppressor genes: *SDHB, SDHD, SDHC, SDHA, SDHAF2, FH, MDH2, VHL, NF1, TMEM127, MAX, GOT2, SLC25A11, DNMT3A*) (4-7). The great majority (70 to 80%) of germline mutations detected in PPGL susceptibility genes are found in *SDHB, SDHD* and *VHL* genes (4,8-10). Various studies have shown that a mutation in one of these susceptibility genes can predispose the patient to the development of multiple and/or metastatic PPGL, or to other syndromic lesions (8,9,11-13). In accordance with the international recommendations, genotyping of PPGL susceptibility genes is therefore proposed to all patients with PPGL (14,15). However, it has actually never been shown whether the identification of a germline mutation in one PPGL susceptibility gene changes the outcome of mutation-carriers. The lack of such studies assessing the clinical benefits of the PPGL genetic test has been stressed by the experts of the Task Force in charge of the Endocrine Society Clinical Practice Guideline for the management of PPGL (14). In this context, our main objective was to evaluate the impact of a positive genetic test on the management and the clinical outcome of propositus patients with PPGL, in a retrospective multicentric study of a large cohort of 221 patients carrying a germline mutation in one of the four major PPGL susceptibility genes (*SDHB, SDHD, SDHC* and *VHL)*.

PATIENTS AND METHODS

Patients

Baseline and follow-up clinical and biological data of 271 propositus patients with PPGL carrying a germline mutation in one of the four major susceptibility genes (*SDHB, SDHD, SDHC* and *VHL)* were retrospectively collected in each clinical site by two investigators (AB & LB) in 24 tertiary centers in France. Each patient had signed a written informed consent for genetic analyses. Mutation screening of the major PPGL susceptibility genes were carried out in the Genetics Department of Hôpital Européen Georges Pompidou in Paris as previously reported (8,11,16). Patients' mutations are reported in **Supplemental Table 1**. This study has been approved by the CPP Ile de France II (IRB 00001072) and endorsed by the French Group of Endocrine Tumours (GTE).

The 271 cases were divided into two groups (named "*Genetic*" and "*Historic*") according to the delay between diagnosis of the first PPGL and announcement of a positive genetic result to the affected patient by the geneticist or the physician. In order to have comparable groups we divided the cohort as follows:

- Patients of the *Genetic* group were defined as patients who were delivered the result from their PPGL genetic test during a maximum delay of 12 months (1 year) after the diagnosis of their first PPGL. This delay includes the first genetic consultation, blood sampling for the test, processing of the sample in the genetics department, transmission of the results to the geneticist or the physician and finally consultation during which the geneticist/physician informed the patient. This group contains 125 patients that were first investigated between the years 1996 to 2013, and the mean of their follow-up was 7 years (range 1-17 years).
- Patients of the *Historic* group were defined as patients who benefited from the PPGL genetic test retrospectively. In order to have patients with a period of follow-up without knowledge of their genetic status comparable to that of the mean follow-up of the *Genetic*

group of patients (7 years), we selected patients who had at least seven years of follow-up after the first PPGL diagnosis, and who had benefited from a PPGL genetic test after these seven years of follow-up. This group contains 96 patients (named *Historic* patients). *Historic* patients were first investigated between 1963 and 2006, and the mean of their follow-up was 21 years (range 4-53 years). For the follow-up analyses, we did analyze this group during two periods: in the first seven years of follow-up (before the genetic test) and after the genetic test.

The fifty remaining patients were excluded from the study because they didn't fit with the definition of the two groups.

We defined 1) a 'follow-up examination' as a medical consultation associated with the assessment of metanephrines measurements and/or at least a PPGL imaging by conventional imaging (contrast-enhanced computed tomography (CT-scan) or gadolinium-enhanced magnetic resonance imaging (MRI)) or scintigraphic imaging (^{123}I-metaiodobenzylguanidine scintigraphy or somatostatin receptor scintigraphy) or positron emission tomography imaging (PET) (^{18}FDG PET or ^{18}FDOPA PET), 2) a 'complete follow-up' by at least a head and neck, thoracic, abdominal and pelvic conventional imaging (MRI and/or CT-scan) and plasma or urine metanephrines measurements after first PPGL diagnosis (4), 3) a 'lost of follow-up period' as a period of time for at least 3 years when the patient did not benefit from any medical consultation. This cut off 3 years was chosen because 1 to 3 years is the time interval for the imaging follow-up of genetically determined PPGL suggested by several experts in the field (4,17-21).

Statistical analysis

Statistical analyses were performed with Graph-Pad Prism software version 5.0 (La Jolla California, USA). As data exhibit a non-Gaussian distribution, results are expressed on mean, median and range and were compared by two-sided Mann and Whitney U test or Kruskal-Wallis test for quantitative variables and two-sided Fisher exact test for qualitative variables

were applied. Censored data were analyzed and plotted by Kaplan–Meier method and compared by two-sided log-rank test. $P<0.05$ was considered to be significant.

RESULTS

Baseline characteristics of *Historic* and *Genetic* patients (Table 1)

The mean delay between the first PPGL diagnosis and the results of PPGL genetic testing was of 199 months for the *Historic* patients and of 9.7 months' *Genetic* patients ($p<0.0001$). *Historic* patients were significantly younger at the time of the first PPGL diagnosis than *Genetic* (29.3 *versus* 39 years, $p< 0.0001$). Patients of both groups presented an equivalent number of single, multiple and metastatic PPGL and a similar tumor size measured by conventional imaging at diagnosis. Catecholamine production was evaluated in 55 % of the *Historic* patients *versus* 86.4 % of the *Genetic* ($p<0.0001$). We did observe a significant increase in the number of patients with family history of PPGL as well as an excess of *SDHD*-mutated patients in the *Historic* group. All significant data, except family history of PPGL, remained the same when we repeated the statistical analyses without the *SDHD*-mutated patients (**Supplemental Table 2**). The number of *SDHB*, *SDHC* or *VHL* mutated patients was not significantly different between both groups.

Genetic patients had benefited from a better follow-up than *Historic* patients (**Table 2**).

The quality of the follow-up during the first seven years after the diagnosis appeared significantly better for *Genetic* patients compared to *Historic* ones. *Genetic* patients benefited from a higher number of follow-up examinations and complete follow-up by years compared to *Historic* patients ($p<0.0001$). We identified a period of loss of follow-up in 72 % of *Historic* patients compared to 9.6 % (69 patients out of 96 *versus* 12 out of 125, $p<0.0001$) for the *Genetic* patients. Furthermore, 54 % of Historic patients had no follow-up examinations during their 7 first years of follow-up. The subsequent knowledge of their genetic status significantly improves the follow-up of these patients ($p<0.05$). All these data were not affected by the *SDHD* positive status (**Supplemental Table 3**).

***Genetic* patients experienced a less severe course of their disease compared to *Historic* patients before the genetic test.**

We, and others, have previously shown that *SDHD* mutation carriers have a significant increase in multiple PPGL compared with other *SDH*x mutation carriers (11,12). However, despite a higher number of *SDHD*-mutated patients, *Historic* patients had an equivalent number of new PPGL during their first seven years of follow-up than the *Genetic* ones (**Table 2**), suggesting that new tumors may have be under-detected in the *Historic* group. Moreover, new PPGL diagnosed during the follow-up had a smaller size at diagnosis in the *Genetic* group compared to the *Historic* group (18.7 mm *versus* 27.6 mm respectively, p=0.0128) (**Figure 1**). Interestingly, when detected in the period following the genetic test, new PPGL *Historic* patients were of comparable size to that of the *Genetic* group (16.3 mm, p=0.4132) (**Supplemental Table 3**). All these data were not affected by the *SDHD* positive status (**Supplemental Table 4** and **Supplemental Figure 1**).

52 *Historic* patients (54 %) were lost to follow-up during the whole seven years following the initial diagnosis. We thus evaluated the PPGL number and size in these *Historic* patients at the first follow-up examination after the period of loss of follow-up (occurring between 9 to 38 years after the initial diagnosis) but before the genetic test. Twenty two out of 54 patients (40.7 %) carried a new PPGL after 16.7 years of loss of follow-up (range 5-38). These patients had larger PPGL than the *Genetic* group (31.9 mm *versus* 18.7, p<0.0001) (**Supplemental figure 2**).

During the 7 first years of follow-up, occurrence of metachronous metastases in patients with an apparently benign PPGL at first diagnosis was observed in 13.5 % of *Historic* patients (11 *SDHB*-mutated patients, one *SDHC*-mutated patient, one *SDHD*-mutated patient), compared to 8.8 % of the *Genetic ones* (10 *SDHB*-mutated patients, 1 *SDHC*-mutated patient)(p=0.5163) (**Table 2**).

However, at the time of this diagnosis of malignancy, the size of the greatest metastasis (65.7 vs 23.3 mm, p=0.0184) and the total number of invaded organs by metastases (1,9 vs 1,3 p=0.0213) were significantly lower in the *Genetic* patients (**Figure 1**). Finally, the percentage of

patients with more than 5 different metastases detected by imaging was significantly smaller in the *Genetic* group compared to the *Historic* one (18.2 % versus 69 %, p=0.0188). After the genetic test, only two patients of the *Historic* group had a new metastatic PPGL, with metastasis size and metastatic spread comparable with the *Genetic* patients (**Supplemental Table 3 and Supplemental Table 4**).

Patients in the *Genetic* group have a better survival

Because most of the new metastatic patients of *Genetic* group were followed an average of 5 years following the diagnosis of the first metastasis, we assessed the 5-year survival of new metastatic patients in the *Genetic* patients and in *Historic* patients before the genetic test.

Patients with a metastatic PPGL diagnosed during their follow-up had a better survival at 5 years in the *Genetic* group compared to patients of the *Historic* group (p=0.0127) (**Figure 2**).

DISCUSSION

For the first time to our knowledge, this study demonstrates that performing the PPGL genetic test early after the first PPGL diagnosis has a positive impact on the management and on the clinical outcome of the patients carrying *SDHx* or *VHL* mutations. Knowing the genetic status of patients allows a better quality of follow-up and leads, at the time of new clinical events, to the diagnosis of smaller PPGL at recurrence and less extensive metachronous metastatic disease and, at the end, to a better survival of patients with metastatic PPGL.

We observed a higher number of *SDHD*-mutated patients in the *Historic* group compared to the *Genetic* one, which probably explains the increased number of PPGL familial histories and the younger age at PPGL diagnosis of these patients. We hypothesize that the patients of the *Historic* group did present more clinical symptoms in favor of a genetic form at the time of their genetic testing than the *Genetic* patients. Nevertheless, we have checked that this difference in the number of *SDHD*-mutated patients within the two groups did not introduce any biases in the results of our study.

The patients of the *Historic* and *Genetic* groups have been diagnosed for their first PPGL at a different time period. The *Historic* patients were diagnosed during the 1990's and the *Genetic* patients during the 2000's. This point raises the hypothesis of another potential bias due to the technical advances in imaging during the same period of time. However, there was no significant difference in the number of single, multiple and metastatic PPGL as well as in the size of tumors at the initial diagnosis between the two groups. Furthermore, all but 3 patients had a recurrence in the 2000's after a loss of follow-up period in the *Historic* group, and PPGL size in these patients was significantly higher than in the *Genetic* group, suggesting that the performances of imaging methods did not affect our data.

Many previous studies have highlighted the higher risk of metastatic disease in *SDHB*-mutated patients (8,9,11-13,22). In former retrospective series, patients with an *SDHB*-related metastatic PPGL had a worse overall survival than the non *SDHB*-related PPGL (23-27). Herein, patients of the *Historic* group with a metastatic PPGL, have a 5-year median survival of 50 % before the

genetic test, which is comparable to other studies (23,27,28). The survival dramatically increases with the knowledge of the genetic status (100% of survival at 5, years, more than 50 % of patients are still alive at 10 years), which is probably due to the higher quality of the follow-up and a change in the patients' management in accordance with the genetic risk. After the previous demonstrations of a positive impact of the identification of germline mutations in frequent cancers susceptibility genes such as *BRCA1* and *BRCA2* mutations in invasive epithelial ovarian and breast cancers, *APC* mutations in the familial adenomatous polyposis colon cancer, and *MMR* genes in the Lynch syndrome (29-31), our study clearly shows the positive impact of the identification of a *SDHx* or a *VHL* mutation in the management, clinical outcome and survival of patients with PPGL. It reveals, for the first time, the clinical benefits of the practice of oncogenetics for patients with a rare cancer and strongly strengthens the recommendations of the Endocrine Society to consider PPGL genetic testing in all patients affected by PPGL (14).

ACKNOWLEDGMENTS

We thank Catherine Tritscher for administrative assistance, Luz Marc, Sarah Cazenave, and Jerome Cartry for technical assistance.

REFERENCES

1. Stenstrom G, Svardsudd K. Pheochromocytoma in Sweden 1958-1981. An analysis of the National Cancer Registry Data. Acta medica Scandinavica 1986; 220:225-232
2. Beard CM, Sheps SG, Kurland LT, Carney JA, Lie JT. Occurrence of pheochromocytoma in Rochester, Minnesota, 1950 through 1979. Mayo Clinic proceedings 1983; 58:802-804
3. Baysal BE. Hereditary paraganglioma targets diverse paraganglia. Journal of medical genetics 2002; 39:617-622
4. Favier J, Amar L, Gimenez-Roqueplo AP. Paraganglioma and phaeochromocytoma: from genetics to personalized medicine. Nature reviews Endocrinology 2015; 11:101-111
5. Remacha L, Curras-Freixes M, Torres-Ruiz R, Schiavi F, Torres-Perez R, Calsina B, Leton R, Comino-Mendez I, Roldan-Romero JM, Montero-Conde C, Santos M, Perez LI, Pita G, Alonso MR, Honrado E, Pedrinaci S, Crespo-Facorro B, Percesepe A, Falcioni M, Rodriguez-Perales S, Korpershoek E, Ramon-Maiques S, Opocher G, Rodriguez-Antona C, Robledo M, Cascon A. Gain-of-function mutations in DNMT3A in patients with paraganglioma. Genetics in medicine : official journal of the American College of Medical Genetics 2018;
6. Remacha L, Comino-Mendez I, Richter S, Contreras L, Curras-Freixes M, Pita G, Leton R, Galarreta A, Torres-Perez R, Honrado E, Jimenez S, Maestre L, Moran S, Esteller M, Satrustegui J, Eisenhofer G, Robledo M, Cascon A. Targeted Exome Sequencing of Krebs Cycle Genes Reveals Candidate Cancer-Predisposing Mutations in Pheochromocytomas and Paragangliomas. Clinical cancer research : an official journal of the American Association for Cancer Research 2017; 23:6315-6324
7. Buffet A, Morin A, Castro-Vega LJ, Habarou F, Lussey-Lepoutre C, Letouze E, Lefebvre H, Guilhem I, Haissaguerre M, Raingeard I, Padilla-Girola M, Tran T, Tchara L, Bertherat J, Amar L, Ottolenghi C, Burnichon N, Gimenez-Roqueplo AP, Favier J. Germline Mutations in the Mitochondrial 2-Oxoglutarate/Malate Carrier SLC25A11 Gene Confer a Predisposition to Metastatic Paragangliomas. Cancer research 2018; 78:1914-1922
8. Amar L, Bertherat J, Baudin E, Ajzenberg C, Bressac-de Paillerets B, Chabre O, Chamontin B, Delemer B, Giraud S, Murat A, Niccoli-Sire P, Richard S, Rohmer V, Sadoul JL, Strompf L, Schlumberger M, Bertagna X, Plouin PF, Jeunemaitre X, Gimenez-Roqueplo AP. Genetic testing in pheochromocytoma or functional paraganglioma. Journal of clinical oncology : official journal of the American Society of Clinical Oncology 2005; 23:8812-8818
9. Neumann HP, Bausch B, McWhinney SR, Bender BU, Gimm O, Franke G, Schipper J, Klisch J, Altehoefer C, Zerres K, Januszewicz A, Eng C, Smith WM, Munk R, Manz T, Glaesker S, Apel TW, Treier M, Reineke M, Walz MK, Hoang-Vu C, Brauckhoff M, Klein-Franke A, Klose P, Schmidt H, Maier-Woelfle M, Peczkowska M, Szmigielski C, Eng C, Freiburg-Warsaw-Columbus Pheochromocytoma Study G. Germ-line mutations in nonsyndromic pheochromocytoma. The New England journal of medicine 2002; 346:1459-1466
10. Buffet A, Venisse A, Nau V, Roncellin I, Boccio V, Le Pottier N, Boussion M, Travers C, Simian C, Burnichon N, Abermil N, Favier J, Jeunemaitre X, Gimenez-Roqueplo AP. A decade (2001-2010) of genetic testing for pheochromocytoma and

paraganglioma. Hormone and metabolic research = Hormon- und Stoffwechselforschung = Hormones et metabolisme 2012; 44:359-366

11. Burnichon N, Rohmer V, Amar L, Herman P, Leboulleux S, Darrouzet V, Niccoli P, Gaillard D, Chabrier G, Chabolle F, Coupier I, Thieblot P, Lecomte P, Bertherat J, Wion-Barbot N, Murat A, Venisse A, Plouin PF, Jeunemaitre X, Gimenez-Roqueplo AP, network PN. The succinate dehydrogenase genetic testing in a large prospective series of patients with paragangliomas. The Journal of clinical endocrinology and metabolism 2009; 94:2817-2827

12. Mannelli M, Castellano M, Schiavi F, Filetti S, Giacche M, Mori L, Pignataro V, Bernini G, Giache V, Bacca A, Biondi B, Corona G, Di Trapani G, Grossrubatscher E, Reimondo G, Arnaldi G, Giacchetti G, Veglio F, Loli P, Colao A, Ambrosio MR, Terzolo M, Letizia C, Ercolino T, Opocher G, Italian Pheochromocytoma/Paraganglioma N. Clinically guided genetic screening in a large cohort of italian patients with pheochromocytomas and/or functional or nonfunctional paragangliomas. The Journal of clinical endocrinology and metabolism 2009; 94:1541-1547

13. Eisenhofer G, Timmers HJ, Lenders JW, Bornstein SR, Tiebel O, Mannelli M, King KS, Vocke CD, Linehan WM, Bratslavsky G, Pacak K. Age at diagnosis of pheochromocytoma differs according to catecholamine phenotype and tumor location. The Journal of clinical endocrinology and metabolism 2011; 96:375-384

14. Lenders JW, Duh QY, Eisenhofer G, Gimenez-Roqueplo AP, Grebe SK, Murad MH, Naruse M, Pacak K, Young WF, Jr., Endocrine S. Pheochromocytoma and paraganglioma: an endocrine society clinical practice guideline. The Journal of clinical endocrinology and metabolism 2014; 99:1915-1942

15. Plouin PF, Amar L, Dekkers OM, Fassnacht M, Gimenez-Roqueplo AP, Lenders JW, Lussey-Lepoutre C, Steichen O, Guideline Working G. European Society of Endocrinology Clinical Practice Guideline for long-term follow-up of patients operated on for a phaeochromocytoma or a paraganglioma. European journal of endocrinology 2016; 174:G1-G10

16. Group NGSiPS, Toledo RA, Burnichon N, Cascon A, Benn DE, Bayley JP, Welander J, Tops CM, Firth H, Dwight T, Ercolino T, Mannelli M, Opocher G, Clifton-Bligh R, Gimm O, Maher ER, Robledo M, Gimenez-Roqueplo AP, Dahia PL. Consensus Statement on next-generation-sequencing-based diagnostic testing of hereditary phaeochromocytomas and paragangliomas. Nature reviews Endocrinology 2017; 13:233-247

17. Taieb D, Kaliski A, Boedeker CC, Martucci V, Fojo T, Adler JR, Jr., Pacak K. Current approaches and recent developments in the management of head and neck paragangliomas. Endocrine reviews 2014; 35:795-819

18. Eijkelenkamp K, Osinga TE, de Jong MM, Sluiter WJ, Dullaart RP, Links TP, Kerstens MN, van der Horst-Schrivers AN. Calculating the optimal surveillance for head and neck paraganglioma in SDHB-mutation carriers. Familial cancer 2017; 16:123-130

19. Benn DE, Gimenez-Roqueplo AP, Reilly JR, Bertherat J, Burgess J, Byth K, Croxson M, Dahia PL, Elston M, Gimm O, Henley D, Herman P, Murday V, Niccoli-Sire P, Pasieka JL, Rohmer V, Tucker K, Jeunemaitre X, Marsh DJ, Plouin PF, Robinson BG. Clinical presentation and penetrance of pheochromocytoma/paraganglioma syndromes. The Journal of clinical endocrinology and metabolism 2006; 91:827-836

20. Daniel E, Jones R, Bull M, Newell-Price J. Rapid-sequence MRI for long-term surveillance for paraganglioma and phaeochromocytoma in patients with succinate dehydrogenase mutations. European journal of endocrinology 2016; 175:561-570

21. Tufton N, Shapiro L, Srirangalingam U, Richards P, Sahdev A, Kumar AV, McAndrew L, Martin L, Berney D, Monson J, Chew SL, Waterhouse M, Druce M, Korbonits M, Metcalfe K, Drake WM, Storr HL, Akker SA. Outcomes of annual surveillance imaging in an adult and paediatric cohort of succinate dehydrogenase B mutation carriers. Clinical endocrinology 2017; 86:286-296

22. Andrews KA, Ascher DB, Pires DEV, Barnes DR, Vialard L, Casey RT, Bradshaw N, Adlard J, Aylwin S, Brennan P, Brewer C, Cole T, Cook JA, Davidson R, Donaldson A, Fryer A, Greenhalgh L, Hodgson SV, Irving R, Lalloo F, McConachie M, McConnell VPM, Morrison PJ, Murday V, Park SM, Simpson HL, Snape K, Stewart S, Tomkins SE, Wallis Y, Izatt L, Goudie D, Lindsay RS, Perry CG, Woodward ER, Antoniou AC, Maher ER. Tumour risks and genotype-phenotype correlations associated with germline variants in succinate dehydrogenase subunit genes SDHB, SDHC and SDHD. Journal of medical genetics 2018;

23. Amar L, Baudin E, Burnichon N, Peyrard S, Silvera S, Bertherat J, Bertagna X, Schlumberger M, Jeunemaitre X, Gimenez-Roqueplo AP, Plouin PF. Succinate dehydrogenase B gene mutations predict survival in patients with malignant pheochromocytomas or paragangliomas. The Journal of clinical endocrinology and metabolism 2007; 92:3822-3828

24. Assadipour Y, Sadowski SM, Alimchandani M, Quezado M, Steinberg SM, Nilubol N, Patel D, Prodanov T, Pacak K, Kebebew E. SDHB mutation status and tumor size but not tumor grade are important predictors of clinical outcome in pheochromocytoma and abdominal paraganglioma. Surgery 2017; 161:230-239

25. King KS, Prodanov T, Kantorovich V, Fojo T, Hewitt JK, Zacharin M, Wesley R, Lodish M, Raygada M, Gimenez-Roqueplo AP, McCormack S, Eisenhofer G, Milosevic D, Kebebew E, Stratakis CA, Pacak K. Metastatic pheochromocytoma/paraganglioma related to primary tumor development in childhood or adolescence: significant link to SDHB mutations. Journal of clinical oncology : official journal of the American Society of Clinical Oncology 2011; 29:4137-4142

26. Bausch B, Wellner U, Bausch D, Schiavi F, Barontini M, Sanso G, Walz MK, Peczkowska M, Weryha G, Dall'igna P, Cecchetto G, Bisogno G, Moeller LC, Bockenhauer D, Patocs A, Racz K, Zabolotnyi D, Yaremchuk S, Dzivite-Krisane I, Castinetti F, Taieb D, Malinoc A, von Dobschuetz E, Roessler J, Schmid KW, Opocher G, Eng C, Neumann HP. Long-term prognosis of patients with pediatric pheochromocytoma. Endocrine-related cancer 2014; 21:17-25

27. Gimenez-Roqueplo AP, Favier J, Rustin P, Rieubland C, Crespin M, Nau V, Khau Van Kien P, Corvol P, Plouin PF, Jeunemaitre X, Network C. Mutations in the SDHB gene are associated with extra-adrenal and/or malignant phaeochromocytomas. Cancer research 2003; 63:5615-5621

28. Jimenez C, Rohren E, Habra MA, Rich T, Jimenez P, Ayala-Ramirez M, Baudin E. Current and future treatments for malignant pheochromocytoma and sympathetic paraganglioma. Current oncology reports 2013; 15:356-371

29. Bolton KL, Chenevix-Trench G, Goh C, Sadetzki S, Ramus SJ, Karlan BY, Lambrechts D, Despierre E, Barrowdale D, McGuffog L, Healey S, Easton DF, Sinilnikova O, Benitez J, Garcia MJ, Neuhausen S, Gail MH, Hartge P, Peock S, Frost

D, Evans DG, Eeles R, Godwin AK, Daly MB, Kwong A, Ma ES, Lazaro C, Blanco I, Montagna M, D'Andrea E, Nicoletto MO, Johnatty SE, Kjaer SK, Jensen A, Hogdall E, Goode EL, Fridley BL, Loud JT, Greene MH, Mai PL, Chetrit A, Lubin F, Hirsh-Yechezkel G, Glendon G, Andrulis IL, Toland AE, Senter L, Gore ME, Gourley C, Michie CO, Song H, Tyrer J, Whittemore AS, McGuire V, Sieh W, Kristoffersson U, Olsson H, Borg A, Levine DA, Steele L, Beattie MS, Chan S, Nussbaum RL, Moysich KB, Gross J, Cass I, Walsh C, Li AJ, Leuchter R, Gordon O, Garcia-Closas M, Gayther SA, Chanock SJ, Antoniou AC, Pharoah PD, Embrace, kConFab I, Cancer Genome Atlas Research N. Association between BRCA1 and BRCA2 mutations and survival in women with invasive epithelial ovarian cancer. Jama 2012; 307:382-390

30. Barrow P, Khan M, Lalloo F, Evans DG, Hill J. Systematic review of the impact of registration and screening on colorectal cancer incidence and mortality in familial adenomatous polyposis and Lynch syndrome. The British journal of surgery 2013; 100:1719-1731

31. Baretta Z, Mocellin S, Goldin E, Olopade OI, Huo D. Effect of BRCA germline mutations on breast cancer prognosis: A systematic review and meta-analysis. Medicine 2016; 95:e4975

TABLES AND FIGURES LEGENDS

Table 1: **Baseline characteristics of patients and PPGL in the *Historic* and *Genetic* groups.** Results are shown as means (medians; range) or number of patients (percent).

Table 2: **Main characteristics of the follow-up within the three groups.** Results are shown means (medians; range) or number of patients (percent).

* p< 0.05 versus Historic before the genetic test

$ p< 0.05 versus Historic after the genetic test

Figure 1: Size of new PPGL (A) and metastases (B), number of invaded organs by metastases at the diagnosis of malignancy (C), and percent of patient with up to five metastases at diagnosis of malignancy (D) in the different groups.

Historic before: *Historic* patients before the genetic test

* p<0.05 versus *Historic* group before the genetic test

Figure 3: Survival of patients affected by a metastatic PPGL, with the first metastasis diagnosed during their follow up with the knowledge of their positive genetic status for the Genetic patients and before the genetic diagnostic for the Historic patients.

Table 1: Baseline characteristics of patients and PPGL in *Historic* and *Genetic* groups. Results are shown as means (medians; range) or number of patients (percent).

	Historic	***Genetic***	***Historic* vs *Genetic***
Total number of patients (n)	96	125	p
Sex ratio, F/M (n)	54/42	61/64	0.2809
Age at first PPGL diagnosis (years)	29.3 (29; 7-66)	39 (39; 10-75)	**<0.0001**
Year of first PPGL diagnosis	1990 (1991; 1963-2009)	2007 (2007; 1996-2013)	**<0.0001**
PPGL size (mm)	44 (40; 5-150)	44.3 (40; 9-180)	0.7568
Single PPGL [n,(%)]	77 (80)	93 (74.4)	0.3374
Multiple PPGL [n,(%)]	19 (20)	32 (25.6)	0.3374
Number of PPGL by patients (n)	1.2 (1; 1-4)	1.4 (1; 1-5)	0.2244
Synchronous metastatic PPGL [n,(%)]	4 (4)	15 (12)	0.0518
Catecholamine producing PPGL [n,(%)]	35 (36)	59 (47.2)	0.1313
Absence of catecholamine assessment at first diagnosis [n,(%)]	43 (45)	17 (13.6)	**<0.0001**
Family history of PPGL [n,(%)]	26 (27)	20 (16)	**0.0471**
Delay between first PPGL diagnosis and genetic testing (months)	199 (180; 84-504)	9.7 (11; 4-12)	**<0.0001**
Age at genetic diagnosis (years)	45.9 (46; 18-78)	39.5 (40; 11-75)	**0.0015**
SDHB-mutated patients [n,(%)]	34 (35)	61 (48.8)	0.0552
SDHD-mutated patients [n,(%)]	38 (40)	24 (19.2)	**0.0014**
SDHC-mutated patients [n,(%)]	7 (7)	14 (11.2)	0.3637
VHL-mutated patients [n,(%)]	17 (18)	26 (20.8)	0.6101

Table 2: Main characteristics of the follow-up within the three groups. Results are done in means (medians; range) or number of patients (percent).
* p< 0.05 versus Historic before the genetic test
$ p< 0.05 versus Historic after the genetic test

	Historic		***Genetic***
	Before genetic test	**After genetic test**	
Total number of patients (n)	96	78	125
Follow-up duration (years)	6.9 (7; 4-7)	6.2 (6; 1-14)	7 (7; 1-17)
Number of follow-up examinations by years	0.42 (0.14; 0.14-4.3)	1* (0.7; 0-9)	0.96* (0.7; 0.27-4.7)
Number of complete follow-up by years	0.13 (0; 0-4.3)	0.9* (0.6; 0-9)	0.89* (0.66; 0-4.7)
Patients with a loss of follow-up period [n,(%)]	69 (72)	0 (0)*	12 (9.6)*
New PPGL [n,(%)]	18 (18.8)	20 (25.6)	24 (19.2)
Diagnosis delay of new PPGL (years)	4.3 (4; 1-7)	19.6 (20; 8-51)	3.4 (2; 1-9)
New metastatic patients [n,(%)]	13 (13.5)	2 (2.6)*	11 (8.8)$
Diagnosis delay of new metastases (years)	4.5 (4.5; 1-7)	16.5 (16.5; 16-17)	3.7 (4; 1-10)

Figure 1: Size of New PPGL (A) and metastases (B), number of invaded organs by metastasis at the diagnosis of malignancy (C), and percent of patient with up to five metastases at the diagnosis of malignancy (D) in the different groups.
Historic before: *Historic* patients before the genetic test
* p<0.05 versus *Historic* group before the genetic test

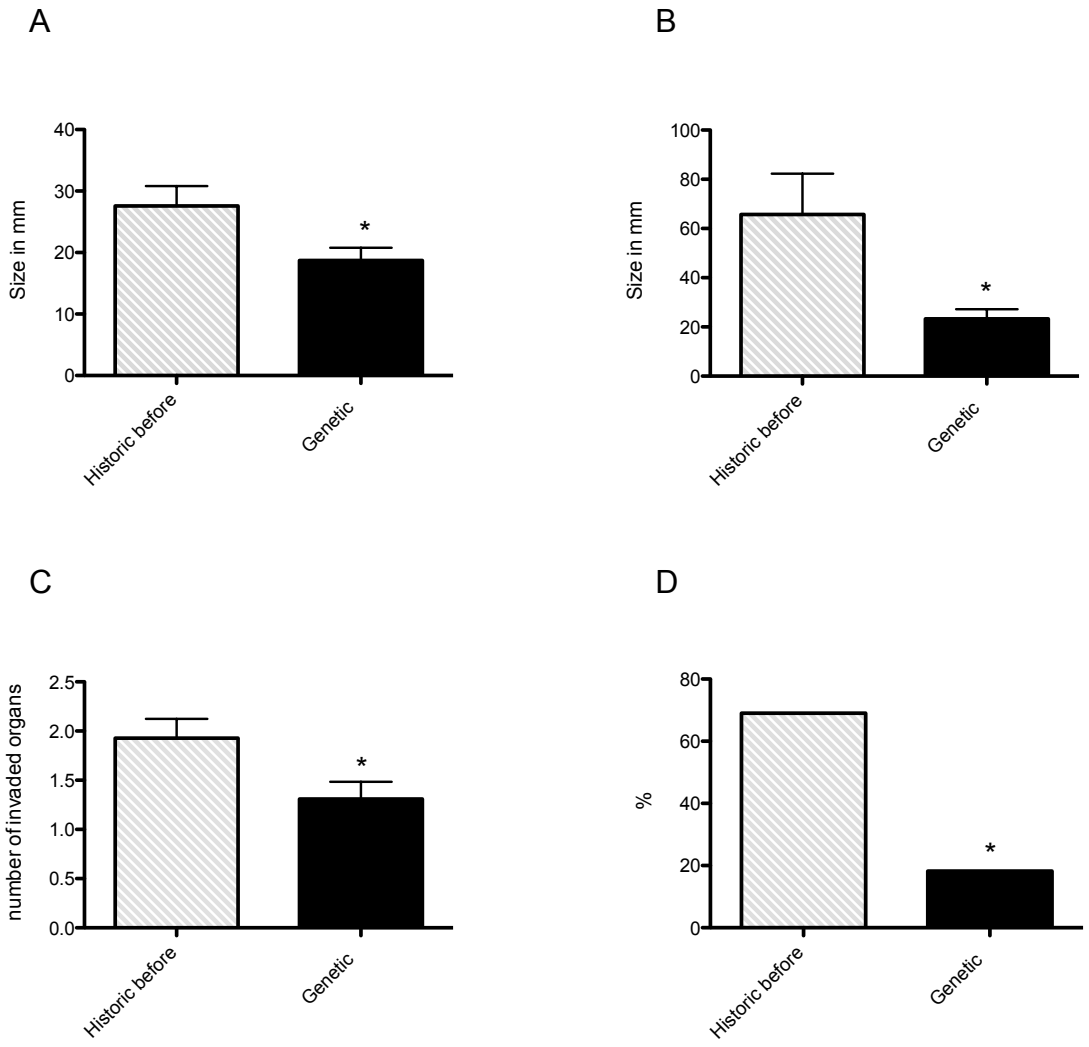

Figure 3: Survival of patients affected by a metastatic PPGL, with the first metastasis diagnosed during their follow up with the knowledge of their positive genetic status for the *Genetic* patients and before the genetic diagnostic for the *Historic* patients.

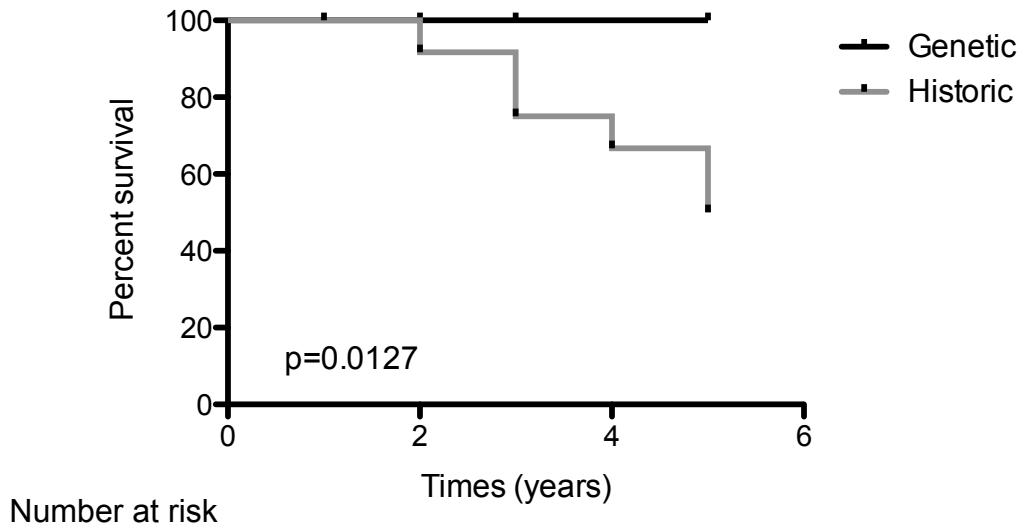

Number at risk

Historic	13	13	12	11	9	8
Genetic	11	11	11	10	10	9

Supplemental Data

Positive impact of genetic test on the management and outcome of patients with paraganglioma and/or pheochromocytoma

Alexandre Buffet, Laurène Ben Aim, Sophie Leboulleux, Delphine Drui, Delphine Vezzosi, Rossella Libé, Christiane Ajzenberg, Daniele Bernardeschi, Bertrand Cariou, Frédéric Chabolle, Olivier Chabre, Vincent Darrouzet, Brigitte Delemer, Rachel Desailloud, Bernard Goichot, Annabelle Esvant, Philippe Herman, Sandrine Laboureau, Hervé Lefebvre, Peggy Pierre, Isabelle Raingeard, Yves Reznik, Jean-Louis Sadoul, Martin Schlumberger, Antoine Tabarin, Igor Tauveron, Delphine Zenaty, Jérôme Bertherat, Eric Baudin, Laurence Amar, Anne-Paule Gimenez-Roqueplo ; French Group of Endocrine Tumors (GTE)

Supplemental Table 1: *SDHx* and *VHL* mutations in the 221 patients of the study.

Gene	cDNA mutation	Protein alteration	Number of patients
SDHB	c.1-?_72+?del	p.?	4
	c.1-?_765+?del	p.?	1
	c.1-16416_72+3877del	p.?	1
	c.72+1G>A	p.?	1
	c.73-?_843+?del	p.?	1
	c.79C>T	p.(Arg27Ter)	2
	c.127G>C	p.(Ala43Pro)	3
	c.136C>G	p.(Arg46Gly)	1
	c.137G>A	p.(Arg46Gln)	4
	c.166_170del	p.(Pro56TyrfsTer5)	2
	c.167C>T	p.(Pro56Leu)	1
	c.175C>T	p.(Gln59Ter)	1
	c.182A>C	p.(Tyr61Ser)	1
	c.200+1G>A	p.?	3
	c.201-?_286+?del	p.?	1
	c.201-1G>A	p.?	1
	c.203G>A	p.(Cys68Tyr)	1
	c.206G>T	p.(Gly69Val)	4
	c.260T>C	p.(Lys87Ser)	1
	c.268C>T	p.(Arg90Ter)	2
	c.274T>C	p.(Ser92Pro)	1
	c.286+1G>A	p.?	1
	c.287-2A>G	p.?	1
	c.287-6_287-3del	p.?	1
	c.293G>A	p.(Cys98Tyr)	1
	c.314_316del	p.(Ile105del)	2
	c.332T>G	p.(Leu111Arg)	1
	c.384C>A	p.(Tyr128Ter)	1
	c.392delC	p.(Pro131HisfsTer5)	2
	c.423+1G>A	p.?	4
	c.424-3C>G	p.?	1
	c.493del	p.(Glu165LysfsTer10)	1
	c.505C>T	p.(Gln169Ter)	1
	c.565T>C	p.(Cys189Arg)	1
	c.583_585del	p.(Ser195del)	1
	c.587G>A	p.(Cys196Tyr)	2
	c.587G>T	p.(Cys196Phe)	1
	c.589C>T	p.(Pro197Ser)	1
	c.591delC	p.(Ser198AlafsTer22)	1
	c.598T>A + c.603G>A	p.(Trp200Arg + p.Trp201Ter)	2
	c.617A>G	p.(Tyr206Cys)	1
	c.620_621del	p.(Leu207ArgfsTer14)	4
	c.626C>T	p.(Pro209Leu)	2

	c.654G>A	p.(Trp218Ter)	1
	c.688C>T	p.(Arg230Cys)	2
	c.689G>A	p.(Arg230His)	3
	c.701T>C	p.(Leu234Pro)	1
	c.713delT	p.(Phe238SerfsTer10)	6
	c.718_721delCTAT	p.(Leu240ThrfsTer7)	2
	c.724C>T	p.(Arg242Cys)	2
	c.725G>A	p.(Arg242His)	3
	c.745T>G	p.(Cys249Gly)	1
	c.746G>A	p.(Cys249Tyr)	1
	c.758G>A	p.(Cys253Tyr)	2
	c.761C>T	p.(Pro254Leu)	1
SDHC	c.1-?_c.20+?del	p.?	1
	c.1A>G	p.(Met1?)	2
	c.43C>T	p.(Arg15Ter)	2
	c.49del	p.(His17ThrfsTer30)	1
	c.77+2dup	p.?	2
	c.148C>T	p.(Arg50Cys)	1
	c.182G>A	p.(Trp61Ter)	2
	c.214C>T	p.(Arg72Cys)	1
	c.215G>A	p.(Arg72His)	1
	c.239-242dupGTGC	p.?	1
	c.377A>G	p.(Tyr126Cys)	1
	c.379C>T	p.(His127Tyr)	1
	c.385T>C	p.(Trp129Arg)	2
	c.397C>T	p.(Arg133Ter)	1
	c.409T>C	p.(Trp137Arg)	1
	c.489dup	p.(Met164TyrfsTer43)	1
SDHD	c.1-?_314+1_315-1del	p.?	1
	c.1-?_480+?del	p.?	6
	c.2T>C	p.(Met1?)	4
	c.64C>T	p.(Arg22Ter)	2
	c.94_95del	p.(Ala33IlefsTer35)	1
	c.112C>T	p.(Arg38Ter)	3
	c.129G>A	p.(Trp43Ter)	4
	c.148_149insA	p.(His50fsTer68)	1
	c.149dup	p.(His50GlnfsTer19)	1
	c.169+1G>T	p.?	1
	c.170-1G>T	p.?	6
	c.191_192del	p.(Leu64ProfsTer4)	2
	c.202dup	p.(Ser68LysfsTer46)	1
	c.239T>G	p.(Leu80Arg)	1
	c.242C>T	p.(Pro81Leu)	3
	c.242delC	p.(Pro81ArgfsTer5)	1
	c.260delC	p.(Pro87LeufsTer48)	1
	c.274G>T	p.(Asp92Tyr)	1

	c.275_286del	p.(Asp92_Leu95del)	1
	c.290G>T	p.(Arg70Met)	1
	c.302T>C	p.(Leu101Pro)	1
	c.305A>C	p.(His102Pro)	2
	c.312C>G	p.(His104Gln)	1
	c.315-?_480+?del	p.?	2
	c.315-2A>C	p.?	2
	c.316G>C	p.(Gly106Arg)	1
	c.337_340delGACT	p.(Asp113MetfsTer21)	1
	c.341A>G	p.(Tyr114Cys)	3
	c.405del	p.(Phe136LeufsTer32)	2
	c.446T>A + 448_450del	p.(Ile149Asn + Cys150del)	4
	trans (6;11) (p22;q23)	p.?	1
VHL	c.1-?_642+?del	p.?	2
	c.161insT	p.(Met54AsnfsTer78)	1
	c.203C>G	p.(Ser68Trp)	1
	c.239G>C	p.(Ser80Asn)	1
	c.244C>G	p.(Arg82Gly)	1
	c.292T>C	p.(Tyr98His)	2
	c.320G>A	p.(Arg107His)	1
	c.334T>C	p.(Tyr112His)	2
	c.340+1G>A	p.?	1
	c.365C>T	p.(Ala122Val)	1
	c.374A>C	p.(His125Pro)	1
	c.376G>A	p.(Asp126Asn)	1
	c.406C>T	p.(Pro154Ser)	2
	c.466T>C	p.(Tyr156His)	1
	c.467A>G	p.(Tyr156Cys)	7
	c.482G>A	p.(Arg161Gln)	4
	c.497T>C	p.(Val166Ala)	1
	c.499C>T	p.(Arg167Trp)	3
	c.500G>A	p.(Arg167Gln)	8
	c.764T>A	p.(Leu184His)	1

Supplemental table 2: Baseline characteristics of patients and PPGL in *Historic* and *Genetic* groups without *SDHD*-mutated patients. Results are shown as means, (medians; range) or number of patients (percent).

	Historic **without *SDHD***	***Genetic*** **without *SDHD***	***Historic*** **vs *Genetic***
Total number of patients (n)	58	101	p
Sex ratio, F/M (n)	34/24	47/54	0.1873
Age at PPGL diagnosis (years)	28.8 (27.5; 7-66)	38.5 (39; 10-71)	**0.0002**
Year of PPGL diagnosis	1991 (1993; 1963-2006)	2007 (2008; 1996-2013)	**<0.0001**
PPGL size (mm)	51.5 (50; 10-150)	49.4 (41; 10-180)	0.4584
Single PPGL [n,(%)]	53 (91.4)	85 (84.2)	0.2312
Multiple PPGL [n,(%)]	5 (8.6)	16 (15.8)	0.2312
Number of PPGL by patients (n)	1.1 (1; 1-2)	1.2 (1; 1-5)	0.1782
Metastatic PPGL [n,(%)]	4 (7)	15 (14.9)	0.2036
Catecholamine producing PPGL [n,(%)]	31 (53.4)	58 (57.4)	0.7402
Absence of catecholamine assessment at first diagnosis [n,(%)]	18 (31)	13 (12.9)	**0.007**
Family history of PPGL [n,(%)]	8 (13.8)	14 (13.9)	1
Delay between first PPGL diagnosis and genetic testing (months)	192 (168; 84-504)	9.7 (11; 4-12)	**<0.0001**
Age at genetic diagnosis (years)	44.8 (45.5; 18-78)	39 (40; 11-71)	**0.0288**
SDHB-mutated patients [n,(%)]	34 (58.6)	61 (60.4)	0.8675
SDHD-mutated patients [n,(%)]	0	0	NA
SDHC-mutated patients [n,(%)]	7 (12)	14 (13.9)	0.8124
VHL-mutated patients [n,(%)]	17 (29.3)	26 (25.7)	0.7113

Supplemental table 3: Sizes of new PPGL and metastases, and metastatic spread in *Historic* patients before and after the genetic test and in *Genetic* patients.
* p< 0.05 versus Historic before

	Historic		***Genetic***
	Before genetic test	**After genetic test**	
Total number of patients (n)	96	78	125
New PPGL size (mm)	27.6 (25; 10-80)	16.3* (12; 7-70)	18.7* (16; 7-60)
New metastasis size (mm)	65.7 (60; 22-150)	8 (8; 6-10)	23.3* (25; 8-45)
Number of invaded organs [n,(%)]	1.9 (2; 1-3)	1.5 (1.5; 1-2)	1.3* (1; 1-3)
Number of patients with >5 metastases at malignancy diagnosis [n,(%)]	9 (69)	0 (0)	2* (18.2)

Supplemental table 4: Main characteristics of the follow-up within the three groups without *SDHD*-mutated patients. Results are done in means (medians; range) or number of patients (percent).
* p< 0.05 versus Historic before

	Historic **without *SDHD***		***Genetic*** **without *SDHD***
	Before genetic test	**After genetic test**	
Total number of patients (n)	58	44	101
Follow-up duration (years)	6.9 (7; 4-7)	6.2 (6; 1-14)	6.7 (6; 1-17)
Number of follow-up examinations by years	0.42 (0.14; 0.14-4.3)	1.2* (0.7; 0-9)	1* (0.8; 0.3-4.7)
Number of complete follow-up by years	0.21 (0; 0-4.3)	1.1* (0.6; 0-9)	1* (0.7; 0-4.7)
Patients with a lost of follow-up period [n,(%)]	41 (70.6)	0* (0)	9* (8.9)
New PPGL [n,(%)]	5 (8.6)	8 (18.2)	14 (13.8)
Diagnosis delay of new PPGL (years)	3.8 (4; 2-5)	3.4 (2; 1-9)	4.5 (5; 1-9)
New metastatic patients [n,(%)]	11 (19)	2* (4.5)	11 (10.9)
Diagnosis delay of new metastasis (years)	4.5 (4.5; 1-7)	4 (4; 1-7)	3.7 (4; 1-10)

Supplemental Figure 1: Size of New PPGL (A) and metastases (B), number of invaded organs by metastasis at the malignancy diagnosis (C), and percent of patient with up to five metastases at malignancy diagnosis (D) in the different groups without *SDHD*-mutated patients.
Historic before: *Historic* patients before the genetic test
* p<0.05 versus *Historic* group before the genetic test

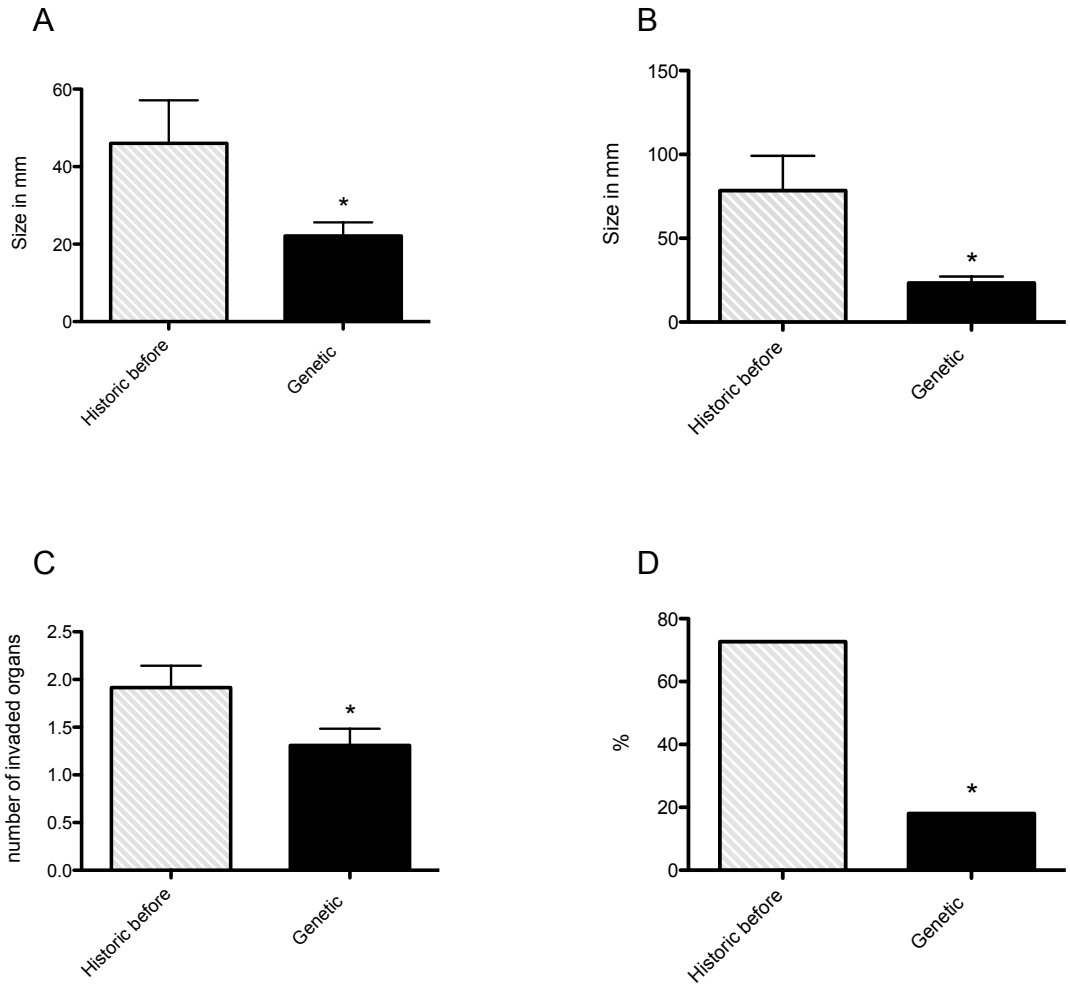

Supplemental Figure 2: New PPGL size in *Genetic* patients and in *Historic* patients before the genetic test and after lost of follow-up (LOF).
* p<0.0001

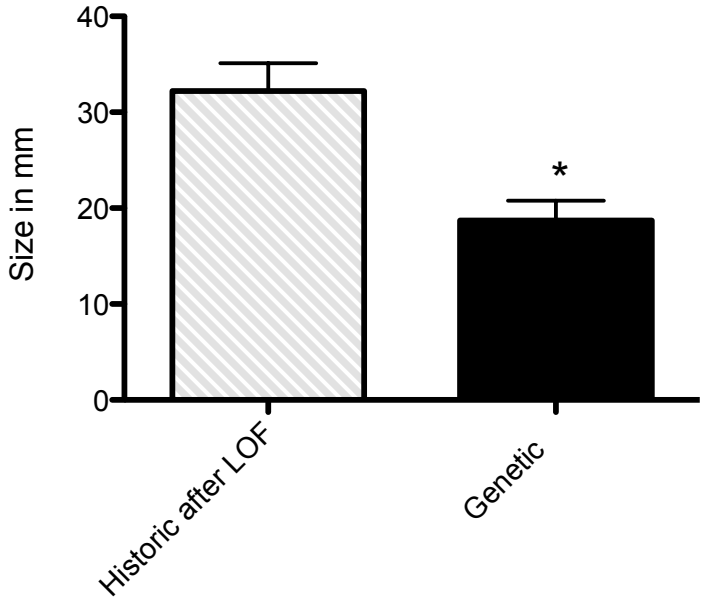

CHAPITRE 2

Identification d'un nouveau gène de prédisposition au paragangliome

I- CONTEXTE

Le deuxième objectif de ma thèse était d'identifier de nouveaux gènes de prédisposition au PGL/PH. Pour ce faire, nous avons utilisé les tumeurs incluses dans le réseau COMETE. Depuis de nombreuses années mon équipe d'accueil collecte, via le réseau COMETE, les ADN constitutionnels, les tumeurs et les données cliniques de patients opérés de phéochromocytomes et de paragangliomes fonctionnels pris en charge dans l'Unité d'Hypertension artérielle de l'Hôpital Européen Georges Pompidou (HEGP) dirigée par le Pr PF. PLOUIN puis par le Pr M.AZIZI et dans le service d'Endocrinologie de l'Hôpital Cochin dirigé par le Pr X. BERTAGNA puis par le Pr J. BERTHERAT (233). Une partie de cette cohorte (202 PGL/PH) a pu bénéficier du Programme Carte d'Identité des Tumeurs de la Ligue Contre le Cancer et obtenir la réalisation et l'analyse successive de différentes « omiques » (transcriptome, méthylome, miRnome, SNP-array) de ces tumeurs.

Ainsi, 13 tumeurs de 13 patients qui avaient précédemment eu une caractérisation génomique complète par analyse intégrative multi-omique dans le cadre du programme carte d'identité des tumeurs (130), ont bénéficié également du séquençage d'exome à partir d'ADN constitutionnel et tumoral. Ce séquençage avait été réalisé au laboratoire avant mon arrivée.

Les caractéristiques cliniques des patients atteints sont rapportées dans la **Table 10**.

Echantillons	Age	Localisation	Sécrétion	Transcriptome	Méthylome	Mutation
HS_021	68	PH B	Mixte	C2B	M3	
HS_042	46	PGL A B	NS	C1A	M1	
HS_091	64	PH B	NMN	C2B	M3	
HS_113	28	PH B	NMN	C2B	M3	
HS_125	21	PH B	NMN	C2B	M3	
HS_129	36	PH B	NMN	C2B	M3	
HS_130	58	PH B	Mixte	C2B	M3	*METs*
HS 151	27	PGL A M	Mixte	C2A	M3	
HS_164	60	PH B	NMN	C2B	M3	
HS_165	47	PH B	NMN	C2B	M3	
HS_168	47	PGL A B	NMN	C2B	M3	
HS_178	37	PH B	NMN	C2B	M3	*METs*
HS 179	70	PH B	NMN	C2B	M3	

Table 10 : Caractéristiques cliniques des 13 patients et génomiques des 13 tumeurs dont l'ADN a été analysé par whole-exome sequencing.

PGL A : PGL abdominal, B : PGL bénin, M : PGL malin, Mixte : sécrétion de normétanéphrines et métanephrines concomitantes, NS : non sécrétant, *METs* : mutation somatique du gène *MET*.

Onze de ces 13 tumeurs se classaient de façon préférentielle dans le cluster M3 du méthylome, où se classent les tumeurs dont l'ADN est hypométhylé et dans le cluster C2B du transcriptome, siège d'une activation de la voie des MAP Kinase et de mTOR, mais pour lequel le mécanisme génétique en cause restait méconnu dans la grande majorité des cas (seules deux mutations somatiques de l'oncogène *MET* avaient été précédemment retrouvées (130)).

Une tumeur se classait dans le cluster C2A du transcriptome, siège d'une activation de la voie des MAP Kinase et de mTOR, dans lequel il est habituellement retrouvé les tumeurs secondaires aux mutations *RET, NF1, TMEM127* et *MAX*. Aucune mutation somatique dans l'un de ces gènes n'avait été mise en évidence dans cette tumeur. Enfin une tumeur se classait dans le cluster C1A, dont la caractérisation est l'objet du chapitre suivant.

II- TRAVAUX PERSONNELS

1- **Interprétation du whole-exome sequencing du PGL pseudo-*SDHx***

Je me suis donc intéressé en premier lieu au patient HS_042 car il s'agissait de la dernière tumeur 'pseudo-*SDHx*' qui se classait systématiquement avec les tumeurs *SDHx*-dépendantes dans les différentes analyses de génomique, notamment dans le cluster C1A pseudo-hypoxique du transcriptome et M1 hyperméthylé du méthylome. Chez ce patient, aucune mutation sur un gène de prédisposition codant notamment pour une protéine du cycle de Krebs n'avait été identifiée, ni au niveau constitutionnel ni somatique.

En croisant les données du whole-exome sequencing et les données des multi-omiques, j'ai pu identifier une mutation constitutionnelle dans le gène *SLC25A11* qui code pour le transporteur mitochondrial du 2-oxoglutarate/malate (OGC). La mise en évidence des mutations et la démonstration fonctionnelle du rôle de ce nouveau gène dans la genèse des PGL ont fait l'objet du deuxième article de ma thèse publié au mois d'avril 2018 dans la revue *Cancer Research*.

ARTICLE 2

Germline Mutations in the Mitochondrial 2-Oxoglutarate/Malate Carrier *SLC25A11* Gene Confer a Predisposition to Metastatic Paragangliomas.

Buffet A, Morin A, Castro-Vega LJ, Habarou F, Lussey-Lepoutre C, Letouzé E, Lefebvre H, Guilhem I, Haissaguerre M, Raingeard I, Padilla-Girola M, Tran T, Tchara L, Bertherat J, Amar L, Ottolenghi C, Burnichon N, Gimenez-Roqueplo AP, Favier J.

Cancer Res. 2018 Apr 15;78(8):1914-1922

Published OnlineFirst February 5, 2018; DOI: 10.1158/0008-5472.CAN-17-2463

Genome and Epigenome

Cancer Research

Germline Mutations in the Mitochondrial 2-Oxoglutarate/Malate Carrier *SLC25A11* Gene Confer a Predisposition to Metastatic Paragangliomas

Alexandre Buffet[1,2], Aurélie Morin[1,2], Luis-Jaime Castro-Vega[1,2], Florence Habarou[2,3], Charlotte Lussey-Lepoutre[1,2], Eric Letouzé[2,4,5,6,7], Hervé Lefebvre[8], Isabelle Guilhem[9], Magalie Haissaguerre[10], Isabelle Raingeard[11], Mathilde Padilla-Girola[1], Thi Tran[1,2], Lucien Tchara[3], Jérôme Bertherat[2,12,13], Laurence Amar[1,2,13,14], Chris Ottolenghi[2,3], Nelly Burnichon[1,2,15], Anne-Paule Gimenez-Roqueplo[1,2,13,15], and Judith Favier[1,2]

Abstract

Comprehensive genetic analyses have identified germline *SDHB* and *FH* gene mutations as predominant causes of metastatic paraganglioma and pheochromocytoma. However, some suspicious cases remain unexplained. In this study, we performed whole-exome sequencing of a paraganglioma exhibiting an *SDHx*-like molecular profile in the absence of *SDHx* or *FH* mutations and identified a germline mutation in the *SLC25A11* gene, which encodes the mitochondrial 2-oxoglutarate/malate carrier. Germline *SLC25A11* mutations were identified in six other patients, five of whom had metastatic disease. These mutations were associated with loss of heterozygosity, suggesting that *SLC25A11* acts as a tumor-suppressor gene. Pseudohypoxic and hypermethylator phenotypes comparable with those described in *SDHx*- and *FH*-related tumors were observed both in tumors with mutated *SLC25A11* and in *Slc25a11*$^{\Delta/\Delta}$ immortalized mouse chromaffin knockout cells generated by CRISPR-Cas9 technology. These data show that *SLC25A11* is a novel paraganglioma susceptibility gene for which loss of function correlates with metastatic presentation.

Significance: A gene encoding a mitochondrial carrier is implicated in a hereditary cancer predisposition syndrome, expanding the role of mitochondrial dysfunction in paraganglioma. *Cancer Res; 78(8); 1914–22. ©2018 AACR.*

Introduction

Pheochromocytomas and paragangliomas (PPGL) are neuroendocrine tumors with a very strong genetic component. Up to 40% of patients with PPGL carry a germline mutation in one of the 13 susceptibility genes reported so far (two proto-oncogenes and 11 tumor-suppressor genes; for review, see ref. 1). Mutations in *SDHx* genes (*SDHA, SDHB, SDHC, SDHD*), encoding the tricarboxylic acid (TCA) cycle enzyme succinate dehydrogenase (or mitochondrial complex II) account for approximately 50% of the germline mutations identified in affected patients and cause multiple or metastatic PPGL (2). These mutations abolish succinate dehydrogenase (SDH) activity, resulting in the accumulation of its substrate, succinate, which acts as an oncometabolite by inhibiting 2-oxoglutarate (2-OG)–dependent dioxygenases. These include hypoxia-inducible factors (HIF) prolyl-hydroxylases (PHD), ten-eleven translocation enzymes (TET) DNA demethylases (which catalyze the conversion of 5-methylcytosine (5-mC) into 5-hydroxymethylcytosine (5-hmC; ref. 3) and JmjC-domain containing histone demethylases (which promote

[1]INSERM, UMR970, Paris-Centre de Recherche Cardiovasculaire, Paris, France; Equipe labellisée Ligue contre le Cancer. [2]Université Paris Descartes, PRES Sorbonne Paris Cité, Faculté de Médecine, Paris, France. [3]Assistance Publique-Hôpitaux de Paris, Hôpital Necker-Enfants Malades, Service de Biochimie Métabolique, Paris, France. [4]Programme Cartes d'Identité des Tumeurs, Ligue Nationale Contre Le Cancer, Paris, France. [5]INSERM, UMR-1162, Génomique Fonctionnelle des Tumeurs Solides, Equipe Labellisée Ligue Contre le Cancer, Institut Universitaire d'Hématologie, Paris, France. [6]Université Paris 13, Sorbonne Paris Cité, Unité de Formation et de Recherche Santé, Médecine, Biologie Humaine, Bobigny, France. [7]Université Paris Diderot, Paris, France. [8]Service d'Endocrinologie, Diabète et Maladies Métaboliques, INSERM U982, Centre Hospitalier Universitaire de Rouen, Rouen Cedex, France. [9]Service d'Endocrinologie-Diabétologie-Nutrition, CHU de Rennes, Hôpital Sud, Rennes, France. [10]Service d'Endocrinologie, Hôpital Haut-Lévêque, CHU de Bordeaux, Pessac, France. [11]Service d'Endocrinologie, CHU Montpellier, Hôpital Lapeyronie, Montpellier Cedex 5, France. [12]Service d'Endocrinologie "Centre de référence maladies rares de la surrénale", Hôpital Cochin, Assistance Publique, Hôpitaux de Paris, Paris, France. [13]Centre Expert National COMETE-Cancer de la surrénale, Paris, France. [14]Assistance Publique-Hôpitaux de Paris, Hôpital Européen Georges Pompidou, Service d'hypertension artérielle et médecine vasculaire, Paris, France. [15]Assistance Publique-Hôpitaux de Paris, Hôpital Européen Georges Pompidou, Service de Génétique, Paris, France.

Note: Supplementary data for this article are available at Cancer Research Online (http://cancerres.aacrjournals.org/).

A.-P. Gimenez-Roqueplo and J. Favier jointly supervised the work.

Corresponding Authors: Judith Favier, INSERM, 56 rue Leblanc, 75015 Paris, France. Phone: 33-1-5398-8041; Fax: 33-1-5398-7952; E-mail: judith.favier@inserm.fr; and Anne-Paule Gimenez-Roqueplo, anne-paule.gimenez-roqueplo@inserm.fr

doi: 10.1158/0008-5472.CAN-17-2463

Published OnlineFirst February 5, 2018; DOI: 10.1158/0008-5472.CAN-17-2463

lysine demethylation of histones; ref. 4). Inhibition of PHD, TET and JmjC-domain-containing proteins respectively result in a pseudohypoxic signature and a hypermethylator phenotype (5, 6). We previously reported the first integrated multi-omics study performed on a large collection of 202 PPGL that remarkably classified tumors according to their genotype (7). Unsupervised classifications revealed that *SDHx*-mutated PPGL systematically clustered together across the genomic platforms. These tumors formed the so-called cluster 1A (pseudohypoxic) in the transcriptome study, the cluster M1 (hypermethylated) following methylome analysis and the cluster Mi1 in the miRnome-based classification (7). Intriguingly, two tumors were classified within the *SDHx*-related clusters in these data sets (Fig. 1A and B; Supplementary Fig. S1), even though both did not carry any germline or somatic *SDHx* mutations. In the first tumor, whole-exome sequencing identified the first PPGL-causative germline mutation in the *FH* gene, encoding fumarate hydratase, another TCA cycle enzyme (6) previously known to predispose to hereditary leiomyomatosis and renal cell carcinoma (HLRCC). Subsequent study identified *FH* mutations in four additional patients with PPGL, who had a high incidence of the metastatic forms of the disease (8). The aim of the present study was to identify the mutation causing the second tumor with an *SDHx*-like genomic profile.

Patients and Methods

Patients

The tumor and blood samples were prospectively collected by the French COMETE Network. This study was conducted in accordance with the Declaration of Helsinki and was approved by the local ethics committee (Comité de Protection des Personnes (CPP) Ile de France II, June 2012). Each patient signed a written informed consent for genetic analyses. The procedures used for PPGL diagnosis were in accordance with both internal and international clinical practice guidelines (2, 9). Germline DNA was extracted from leukocytes according to standard protocols. Tumor DNA extraction was performed using the AllPrep Kit (Qiagen) and the DNA Mini Kit (Qiagen) for frozen tumor and paraffin-embedded tissue, respectively. DNA was quantified and its purity assessed with a NanoDrop ND-1000 spectrophotometer (Labtech). Mutation analyses of the major PPGL susceptibility genes were performed as previously described in the Genetic department of Hôpital Européen Georges Pompidou in Paris (2). Two groups of patients for whom no known mutation in a PPGL predisposition gene had been identified were enrolled: a first group of 267 patients with a clinical history suggestive of a hereditary PPGL (multiple tumors, early onset or family history of PPGL) and a second group of 372 patients with apparently sporadic PPGL (Table 1).

Whole-exome sequencing

Exome sequencing was performed by IntegraGen Genomics (Evry, France) as previously described (6). The germline mutation identified in the *SLC25A11* gene was validated by Sanger sequencing.

Next-generation sequencing on known PPGL susceptibility genes

PPGL susceptibility genes coding regions and exon-intron boundaries (*SDHx*, *VHL*, *EPAS1*, *EGLN1*, *EGLN2*, *NF1*, *RET*, *TMEM127*, *MAX*, *FH* and *MDH2* genes) were amplified using the SDH MASTR Kit V2.0 (Multiplicom, Belgium). Libraries were sequenced on MiSeq platform (Illumina) using v3 chemistry according to the standard protocol. Alignment and variant calling were performed using SeqNEXT (JSI medical systems) and PolyDiag (Paris Descartes university) software.

Genome editing in *SLC25A11* gene by the CRISPR–Cas9 method

Targeted gRNA was designed *in silico* by using http://crispr.genome-engineering.org/ as previously described (10). gRNA was transcribed *in vitro* using the kit PrecisionX Cas9 SmartNuclease RNA system (System Biosciences CAS510A-KIT). Briefly, targeted oligonucleotides were annealed to form double strands, and then cloned into SmartNuclease Linearized T7 gRNA Vector. The resulting recombinant vector was linearized by EcoRI digestion. The generated template was used to produce gRNA by *in vitro* transcription. gRNA was then purified (miRNeasy minikit, Qiagen) and its purity was assessed using the Experion RNA StdSens Analysis Kit (Bio-Rad).

Wild-type immortalized mouse chromaffin cells (WT imCC), previously generated by our laboratory (6), were transfected with 0.6 μg of gRNA (RNA i-MAX; Life Technologies) and 2 μg of Cas9 (System Biosciences CAS940A-1) and YFP plasmids (Lipofectamine 2000; Life Technologies). Fluorescent cells were cloned by FACS sorting. Clones were screened by direct sequencing of the targeted sequence of murine *Slc25a11* gene. Two consecutive transfections were performed: the first generated three heterozygous clones out of 70, and the second performed on heterozygous clones generated 51 homozygous clones out of 129. Predicted exonic off-target sequences were screened by direct sequencing (*KRT9* exon 2, *TMEM260* exon 16, *ALDH2* exon 10, *KANK1* exon 19, *FCRLB* exon 2). *Mycoplasma* contamination was ruled out using the PCR *Mycoplasma* Test kit I/C (PromKine, PK-CA91-1048). All experiments were performed between passages 15 and 20.

Slc25a11$^{\Delta/\Delta}$ clones transfection by *Slc25a11* plasmid

Slc25a11$^{\Delta/\Delta}$ clone 6 was transfected with 2 μg of *Slc25a11*-expressing vector (ORIGENE, MR204477) using Lipofectamine 2000 (Life Technologies). Twenty-four hours later, selection was performed by Geneticin (Sigma, G8168, 800 μg/mL) and selected cells were cloned by limited dilution under Geneticin selection.

5-methylcytosine and 5-hydroxymethylcytosine ELISA

200 ng of denatured DNA was added to the Reacti-Bind Coating Solution (Thermo, 17250) and incubated in a 96-well plate at 37°C for one hour. After blocking for 30 minutes with a blocking buffer [PBS1X, 5 g/l BSA, and 0,5% of Kathon CG/ICP (Supelco 5-0127)], anti-5-methylcytosine (1/5,000, Calbiochem, NA81) or anti 5-hydroxy-methylcytosine (1/200, Actif Motif, 39759) and secondary antibody (1/1,000) were added to the wells and incubated at 37°C overnight. The plate was then incubated with Streptavidin-HRP (BD Biosciences, 554066) for 30 minutes. Finally, revelation was performed by adding a solution of 5 mg/mL of TMB (Sigma), citrate 0,1 mol/L pH 5 and 3% hydrogen peroxide. Reaction was stopped with sulfuric acid and the absorbance was read at 450 nm. The experiments were performed three times.

Published OnlineFirst February 5, 2018; DOI: 10.1158/0008-5472.CAN-17-2463

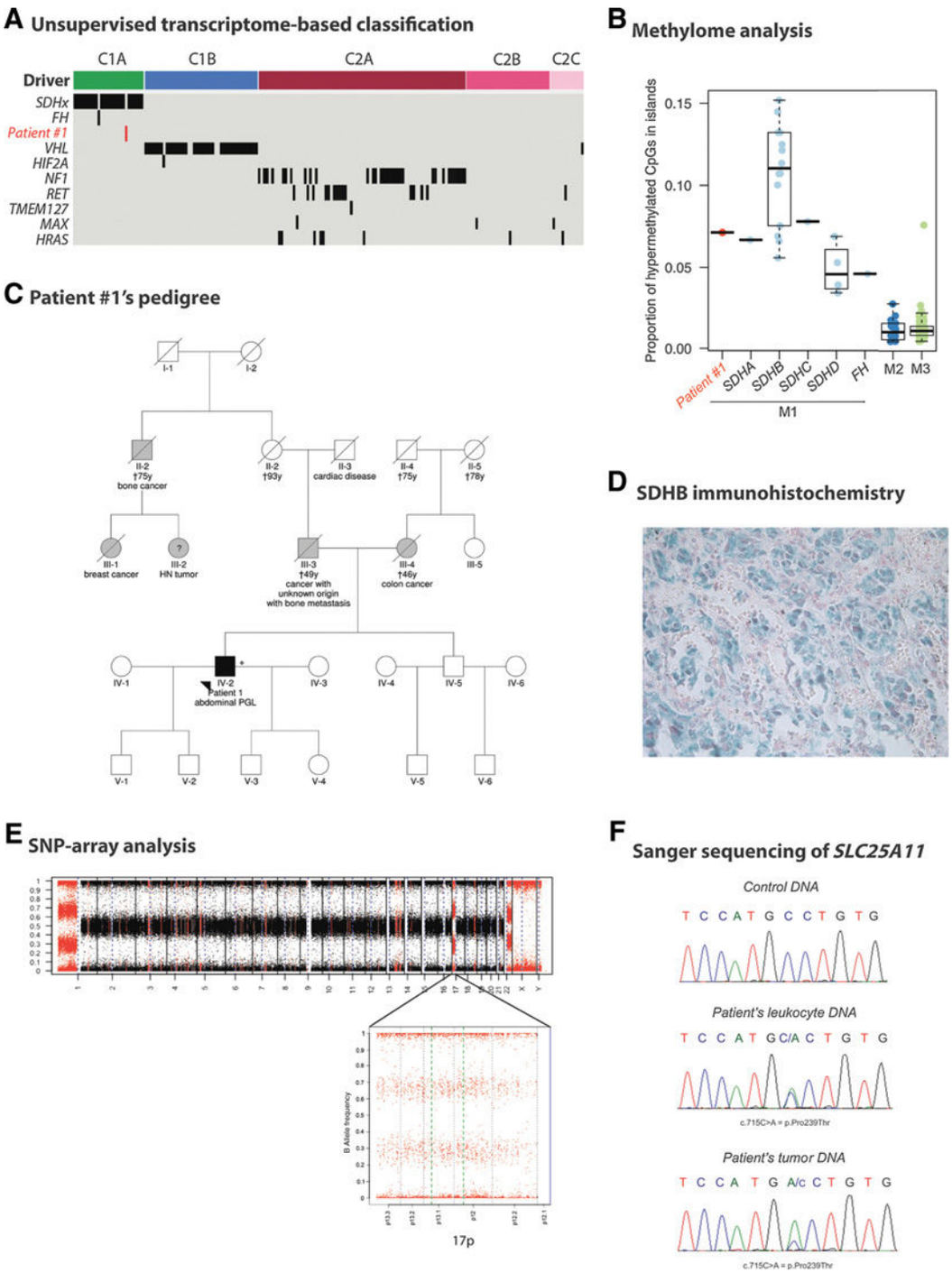

Figure 1.

Identification of an *SLC25A11* mutation in a patient with a paraganglioma. **A,** Transcriptome-based classification of 188 PPGL collected by the COMETE cohort reveals five clusters strongly associated with driver mutations. The paraganglioma of patient #1 classifies within cluster C1A together with *SDHx*- and *FH*-mutated tumors. **B,** The proportion of probes located within CpG islands that are hypermethylated with respect to normal samples (beta value difference > 0.2) is represented as a function of tumor subtype. Hypermethylated (M1) tumors are divided according to the mutated driver gene. The paraganglioma of patient #1 classifies within cluster M1 together with *SDHx*- and *FH*-mutated tumors. **C,** Pedigree of patient #1 (black box) shows several cases of cancers (gray boxes) in his family. **D,** Positive SDHB IHC of the patient #1's paraganglioma. **E,** B alleles frequency plots generated by SNP array analysis of the patient #1's paraganglioma show a 17p copy neutral LOH. **F,** Electropherograms of Sanger sequencing of the exon 6 of *SLC25A11* gene showing the c.715C>A mutation at heterozygous state from germline and at homozygous state from tumor DNA of patient #1 compared with a control DNA.

Published OnlineFirst February 5, 2018; DOI: 10.1158/0008-5472.CAN-17-2463

Table 1. Main clinical and tumor features of patients from the validation cohort

Clinical feature	Number of patients	Percentage
Benign PPGL	**518**	**81%**
Single HN PGL	74	
Single TAP PGL	180	
Single PCC	189	
Unknown localization	1	
Multiple HN PGL	25	
Multiple TAP PGL	12	
Bilateral PCC	17	
HN + TAP PGL	5	
PCC + TAP PGL	14	
Unknown localization	1	
Metastatic PPGL	**121**	**19%**
Single HN PGL	13	
Single TAP PGL	32	
Single PCC	66	
Unknown localization	3	
Multiple HN PGL	1	
Multiple TAP PGL	2	
Bilateral PCC	3	
PCC + TAP PGL	1	
	639	

Abbreviations: HN, head and neck PGL; PCC, pheochromocytoma; TAP, thoracic and abdominopelvic PGL.

Statistical analysis

Data were analyzed by one-way ANOVA. The results were considered to be significant if $P < 0.05$. Statistics tests were carried out using the Graph-Pad software.

Results

Characterization of the unexplained *SDHx*-like tumor

The unexplained tumor with a pseudo-*SDHx* profile (Fig. 1A and B; Supplementary Fig. S1) was a nonsecreting abdominal paraganglioma diagnosed in a 46 years-old patient (Patient #1). Genetic counseling revealed a family history of cancer, with his father deceased at 49 from a cancer of unknown origin discovered by bone metastases, a paternal uncle with bone cancer, and a paternal cousin with a head and neck tumor (Fig. 1C). Unfortunately, it was not possible to retrieve neither more specific clinical information regarding the relatives of the paternal branch suspected to be affected, nor tumors or DNA samples. Patient #1's tumor was positive for SDHB by immunochemistry (Fig. 1D) confirming the absence of *SDHx* mutations (11). Whole-exome sequencing performed on leukocyte DNA identified 2,343 germline genetic variations (2,213 SNVs and 130 InDels). After filtration of the common polymorphisms described in the dbSNP, ExAC or 1000 Genome databases, 218 variations remained. We hypothesized that similar to *SDHx* and *FH* genes, the causative gene could be a tumor suppressor, and searched for variations associated with a loss of heterozygosity (LOH) using SNP array in tumor DNA (Fig. 1E). We found 54 variations, of which 11 were classified as pathogenic according to *in silico* analyses (Supplementary Table S1). Among them, we identified a candidate genetic variation [c.715C>A, p.(Pro239Thr)] in the *SLC25A11* gene (NM_003562), encoding the mitochondrial 2-oxoglutarate/malate carrier (OGC) protein. The presence of the *SLC25A11* variation, heterozygous in germline and homozygous in tumor DNA, was confirmed by Sanger sequencing (Fig. 1F). OGC is part of the malate/aspartate shuttle (MAS) and mediates the transport of 2-OG from the mitochondrial matrix to the cytoplasm in an electroneutral exchange for malate (Fig. 2A). The proline at position 239 is part of a PX[D/E]XX[K/R]X[K/R] signature sequence motif (PROSITE PS50920, PFAM PF00153), which is highly conserved across species, particularly in the SLC25 family of mitochondrial transporters (12). Mutagenesis of this amino acid in bovine OGC results in a severe defect of 2-OG transport activity (12). We performed OGC immunohistochemistry (IHC)

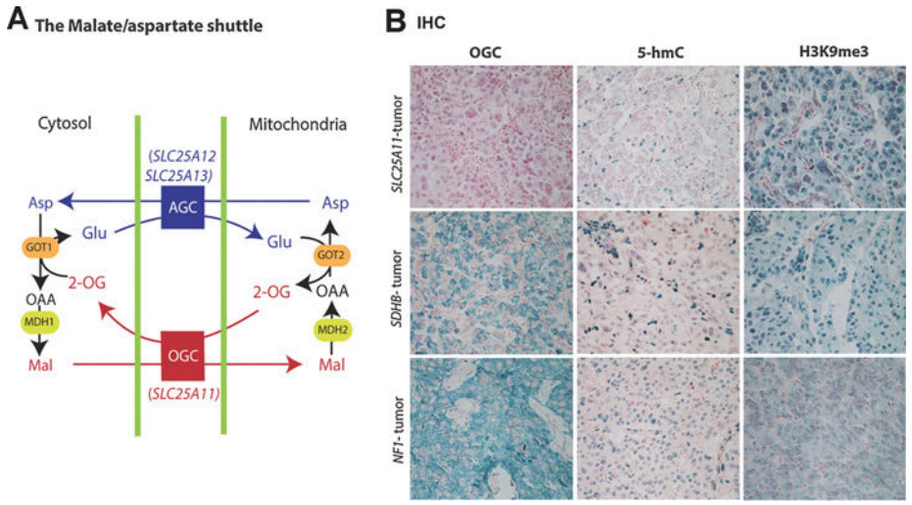

Figure 2.

SLC25A11 mutation is associated with loss of OGC, hypermethylator phenotype, and metabolic reprogramming. **A,** Schematic presentation of the malate–aspartate shuttle, composed of the OGC (encoded by *SLC25A11*) and the aspartate–glutamate carriers (AGC, encoded by *SLC25A12* and *13* genes). Asp, aspartate; Glu, glutamate; Mal, malate; OAA, oxaloacetate. **B,** OGC IHC in the *SLC25A11*-mutated paraganglioma from patient #1 shows no immunostaining, whereas a strong granular staining expected from a mitochondrial protein is observed in *SDHB* and *NF1*-mutated tumors. 5-hmC and H3K9 IHC in *SLC25A11*-mutated paraganglioma from patient #1 show an immunostaining, suggesting DNA and histone methylation.

Published OnlineFirst February 5, 2018; DOI: 10.1158/0008-5472.CAN-17-2463

Table 2. Clinical, genetic, and immunohistological characteristics of *SLC25A11* mutation carriers

	Sex	Age	Tumor location	Meta	Delay for meta diagnosis	Secretion	cDNA mutation	Protein alteration	LOH	OGC IHC	5-hmC IHC	H3me3 IHC
Patient #1	M	46	A PGL	No	NA	No	c.715C>A	p.(Pro239Thr)	Yes	Neg	Neg	Pos
Patient #2	F	51	A PGL	Yes	sync	NM	c.439A>G	p.(Met147Val)	Yes	Neg	Pos	Pos
Patient #3	M	67	A PGL	Yes	3 years	NM	c.248+3A>G	p.?	ND	ND	ND	ND
Patient #4	F	32	HN PGL	No	NA	No	c.708C>T	p.(Ala236Ala)	Yes	Neg	Neg	Pos
Patient #5	F	87	A PGL	Yes	sync	NM	c.25delG	p.(Ala9ProfsTer4)	ND	ND	ND	ND
Patient #6	F	59	A PGL	Yes	3 years	NM	c.421G>A	p.(Glu141Lys)	Yes	Neg	Neg	Pos
Patient #7	F	74	A PGL	Yes	sync	NM	c.107_108del	p.(Thr36SerfsTer71)	Yes	Neg	Neg	Pos

Abbreviations: Meta, metastases; A PGL, abdominal paraganglioma; HN PGL, head and neck paraganglioma; sync, synchronous; NM, normetanephrines; LOH, Loss of heterozygosity; H3me3, H3K9me3 and H3K27me3; Neg, negative; Pos, positive; ND, not determined; NA, not applicable.

on the paraffin-embedded tumor. We observed no OGC protein in the PGL carrying the *SLC25A11* mutation in contrast with the 20 PPGL tumors without *SLC25A11* mutations used as controls (6 *SDHx*, 1 *FH*, 3 *RET*, 4 *NF1*, 1 *TMEM127*, 3 *MAX*, 2 sporadic cases; Fig. 2B; Supplementary Table S2). 5-hmC and H3K9me3 IHC further validated a hypermethylated phenotype affecting both DNA and histones, as previously described in *SDHx*-mutated tumors (6, 13). Altogether these data suggested that germline [c.715C>A, p.(Pro239Thr)] *SLC25A11* mutation associated with somatic loss of the wild-type allele causes the patient's PGL.

SLC25A11 gene sequencing on a large cohort of PPGL

To establish the frequency of *SLC25A11* mutations in patients with PPGL, the 8 exons and exon/intron junctions of the gene were sequenced by Sanger method in a large cohort of 639 patients for whom no germline mutation had been identified in the major PPGL susceptibility genes (*SDHx*, *RET*, *VHL*, *TMEM127*, *MAX*, *FH*), nor in the recently described *MDH2* gene (14). These patients had a mean age at diagnosis of 34.8 years ± 15.6 (Table 1) and among them, 121 (19%) had a metastatic disease. Eighty-one (13%) had multiple PPGL and 13 (2%) reported a family history of the disease. We identified six patients with germline *SLC25A11* mutations (Table 2; Supplementary Table S3). Five patients had a single metastatic abdominal PGL and one a head and neck PGL; none had a known family history of PPGL (Supplementary Fig. S2 and Supplementary Clinical Data). All six mutations (2 missense, 2 frameshifts, one intronic and one silent mutation) were predicted to be deleterious *in silico* (Table 2). None of these variants was present in the dbSNP nor ExAC databases. The missense mutations affected highly conserved amino acids (Supplementary Fig. S3A) located in the signature protein sequence or in the alpha matrix helix, both well known to be critical for OGC function (Supplementary Fig. S3B; refs. 12, 15, 16). Interestingly, the silent p.Ala236Ala mutation was associated with a marked decrease in *SLC25A11* mRNA levels in leukocytes (Supplementary Fig. S3C). LOH was identified in tumor DNA of the three patients for whom tumor tissue was available (Supplementary Fig. S3D) and all evaluable tumors were negative for OGC by IHC (Table 2; Supplementary Fig. S4). Next-generation sequencing (NGS) performed on tumor DNA of patient #1, #4 and #6 showed no somatic mutation in *SDHx*, *VHL*, *EPAS1*, *EGLN1*, *EGLN2*, *NF1*, *RET*, *TMEM127*, *MAX*, *FH* and *MDH2* genes. We had not enough material to performed NGS on PGL of patient #2. We carried out 5-hmC (Supplementary Fig. S5), H3K9me3 (Supplementary Fig. S6) and H3K27me3 IHC (Supplementary Fig. S7) to establish whether these tumors displayed a hypermethylator phenotype, as the one we observed in the initial *SLC25A11*-mutated case. In all but one of the *SLC25A11*-mutated tumors (patient #2), 5-hmC immunolabelling was less intense in tumor cells than in endothelial or sustentacular cells (Table 2; Supplementary Fig. S5), whereas H3K9me3 and H3K27me3 were positive in all cases (Table 2; Supplementary Fig. S6 and S7). Hence, *SLC25A11* mutations apparently mediate the inhibition of TET and JmjC-domain containing demethylases, as we previously reported in *SDHx*- and *FH*-mutated PPGL (6).

Slc25a11 knockout in immortalized mouse chromaffin cells

To fully demonstrate that *SLC25A11* is a new tumor-suppressor gene, we generated a knockout (KO) of the *Slc25a11* gene using the CRISPR/Cas9 approach in wild-type immortalized mouse chromaffin cells (WT imCC; ref. 6; Supplementary Fig. S8A). Two $Slc25a11^{\Delta/\Delta}$ clones (c4 and c6) were selected for analyses. These clones carried a homozygous c.720delG and a heterozygous c.720_733del14 variant in the *Slc25a11* gene (Supplementary Fig. S8B and S8C), both leading to premature stop codons in exon 7. The corresponding mutation results in the loss of the third signature sequence motif and the H56 alpha matrix helix (Supplementary Fig. S8D). A rescue was then performed by stably transfecting an *Scl25a11*-expressing vector in the $Slc25a11^{\Delta/\Delta}$clone 6 (clone c6-R). Western blot analysis of OGC protein levels revealed a loss of the transporter in both $Slc25a11^{\Delta/\Delta}$ clones, and its re-expression in the c6-R cells (Supplementary Fig. S8E). Both $Slc25a11^{\Delta/\Delta}$ clones exhibited nuclear translocation of HIF2α similar to $Sdhb^{-/-}$ cells, which was not seen in WT imCC, nor in the c6-R cells (Fig. 3A). We used an ELISA method to quantify the levels of 5-mC and 5-hmC in the different cell types. As expected, 5-mC levels were 2-fold higher in $Sdhb^{-/-}$ imCCs than in WT cells. Similarly, both $Slc25a11^{\Delta/\Delta}$ clones displayed an approximately 2-fold increase in 5-mC content, reflecting a hypermethylated phenotype, which was reversed in the *Slc25a11*-rescued cells (Fig. 3B). Accordingly, 5-hmC levels in WT imCC and c6-R were higher than in $Sdhb^{-/-}$ and $Slc25a11^{\Delta/\Delta}$ cells (Fig. 3C). Hence, *Slc25a11* inactivation promotes both a pseudohypoxic and a hypermethylated phenotype. We next evaluated the proliferation, migration and adhesion capacities of $Slc25a11^{\Delta/\Delta}$ imCCs in comparison to those of wild-type, $Sdhb^{-/-}$ and *Slc25a11*-rescued cells. *Slc25a11*-deficient cells displayed a decrease in proliferation, compared to WT cells, which was much less marked than that observed in *Sdhb*-deficient cells (Supplementary Fig. S8F). They showed increased adhesion as compared to WT cells, which was however inferior to that observed in $Sdhb^{-/-}$ imCC (Fig. 3D). *Slc25a11* KO cells demonstrated a 2-fold increase in collective migration as compared with the WT and c6-R cells and comparable with the $Sdhb^{-/-}$ imCC (Fig. 3E). Altogether, these *in vitro* data obtained with two different *Slc25a11* KO clones and the reversion of the phenotypes shown by the rescue experiments clearly demonstrate that loss of *Slc25a11* gene mediates

Published OnlineFirst February 5, 2018; DOI: 10.1158/0008-5472.CAN-17-2463

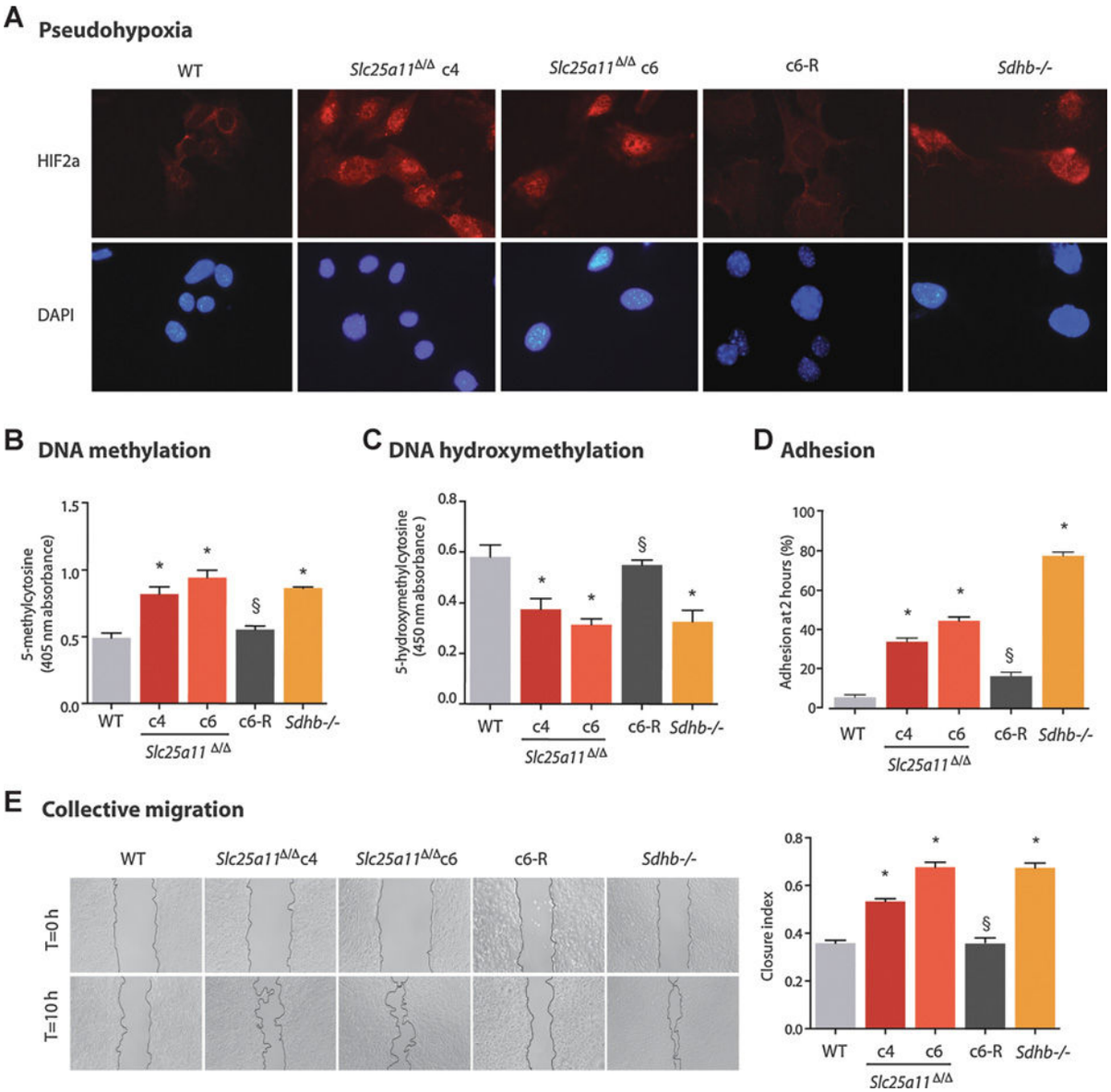

Figure 3.

Characterization of *Slc25a11*$^{\Delta/\Delta}$ immortalized mouse chromaffin cells. **A,** Immunofluorescence showing HIF2 nuclear localization in *Slc25a11*$^{\Delta/\Delta}$ (clones c4 and c6) and *Sdhb*$^{-/-}$ imCCs, whereas the signal is restricted to the cytoplasm in WT cells and *SLC25A11* rescued cells (c6-R). **B,** 5-methylcytosine quantification by ELISA in all cell types reveals the hypermethylator phenotype of *Slc25a11*$^{\Delta/\Delta}$ *cells* at comparable level with that observed in *Sdhb*-deficient imCCs. **C,** 5-hydroxymethylcytosine quantification by ELISA in all cell types shows a decrease level of 5-hmC quantification in *Slc25a11*-deficient cells at comparable level with *Sdhb*-deficient imCCs. **D,** Increased adhesion in *Slc25a11*$^{\Delta/\Delta}$ and *Sdhb*$^{-/-}$ as compared with WT and c6-R imCCs. **E,** Scratch test experiments reveal that collective migration is increased in *Slc25a11*$^{\Delta/\Delta}$ and *Sdhb*$^{-/-}$ imCCs compared with WT and c6-R cells. Data are mean ± SEM; *, $P < 0.01$ versus WT; §, $P < 0.01$ c4 and c6 versus c6R.

pseudo-hypoxic signature, hypermethylator phenotype and the acquisition of metastatic properties.

To decipher the mechanism linking SLC25A11 loss of function and this phenotype, we performed metabolomic analysis in the different cell types, which showed normal levels of succinate (Supplementary Fig. S8G) but higher levels of aspartate and glutamate, and lower levels of 2-OG in *Slc25a11*$^{\Delta/\Delta}$ cells (Fig. 4A). Interestingly, treating *Slc25a11*$^{\Delta/\Delta}$ cells with 2-OG reversed the migratory phenotype, demonstrating the role of this metabolite in the SLC25A11 tumorigenic cascade (Fig. 4B). Metabolomic analysis performed on the frozen tumor of patients #1, #6 and #7 showed normal succinate levels (Supplementary Fig. S9) whereas, consistent with MAS dysfunction and *in vitro* data, aspartate and glutamate concentrations were elevated in all three *SLC25A11*-mutated tumors compared with control PPGL samples from the cluster 1A (2 *SDHB* and 1 *SDHD*-mutated cases)

Published OnlineFirst February 5, 2018; DOI: 10.1158/0008-5472.CAN-17-2463

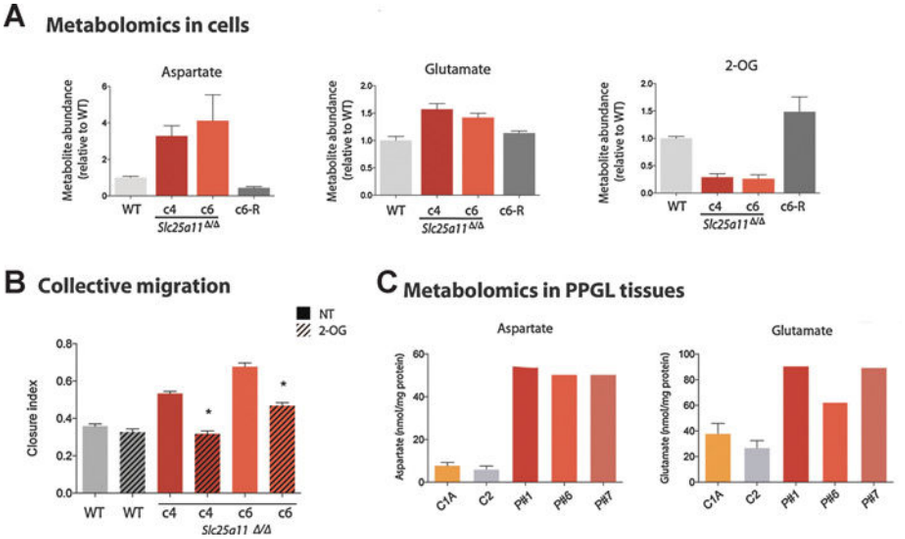

Figure 4.

A, Metabolomic profiling in the different cell types shows increased levels of intracellular aspartate and glutamate in *Slc25a11*-deficient cells (clones c4 and c6) versus WT, whereas 2-OG is decreased in *Slc25a11*$^{\Delta/\Delta}$ cells. Aspartate and glutamate both decrease, whereas 2-OG increases in *SLC25A11* rescued cells (c6-R). **B,** 2-OG treatment (hashed bars) reverses the collective migration capacities of *Slc25a11*-deficient cells (clones c4 and c6). **C**, Metabolomic analysis of the *SLC25A11*-mutated paraganglioma of patients #1, #6, and #7 reveals that aspartate and glutamate steady-state levels are increased as compared with control tumors from the cluster 1A (2 *SDHB*, 1 *SDHD* PPGL) or the cluster 2 (3 *RET*, 1 *TMEM127*, 1 sporadic PPGL). *, $P < 0.01$ versus WT.

or the cluster 2 (3 *RET*, 1 *TMEM127* and 1 sporadic case; Fig. 4C). 2-OG levels were highly variable between tumors homogenates and did not show such decrease (Supplementary Fig. S9).

Discussion

We identified *SLC25A11* as a new tumor-suppressor gene implicated in the predisposition to metastatic paraganglioma. This gene encodes a carrier that participates to malate–asparate shuttle (MAS) by mediating the transport of 2-OG from the mitochondrial matrix to the cytoplasm in an electroneutral exchange with malate. MAS is composed of OGC (*SLC25A11*) and of two aspartate–glutamate carriers: CITRIN *(SLC25A13)* and ARALAR (*SLC25A12*; Fig. 2). This shuttle regenerates NADH pool in mitochondrial matrix to allow complex I function (17). After the identification of 7 PPGL predisposing genes encoding TCA cycle enzymes *(SDHA, B, C, D, SDHAF2, FH* and *MDH2)*, it is the first time that a gene encoding a mitochondrial carrier is implicated in PPGL tumorigenesis. Interestingly, patients with CITRIN deficiency caused by homozygous germline mutation in *SLC25A13* have an increased risk of hepatocellular carcinoma following hepatic inflammation and fibrosis (18). Also, heterozygous germline mutations in the *SLC25A13* gene have been implicated in hepatocellular carcinoma in Asiatic population, suggesting a potential role for MAS in tumorigenesis (19). Nevertheless, mutations in *SLC25A13* reported in the latter study are frequent in Asiatic population raising the question of their actual pathogenicity (20).

More strikingly, a gain-of-function mutation in the *GOT2* gene, encoding the mitochondrial aspartate aminotransferase was very recently reported in a PGL patient, further reinforcing the link between MAS dysfunction and PPGL (21). The aspartate aminotransferase catalyzes the interconversion of aspartate and 2-OG to oxaloacetate and glutamate. Our metabolomics data show a marked increase in aspartate and glutamate in both *SLC25A11*-mutated human samples and KO mouse cells associated with a decrease in 2-OG in the KO cells. Various derivatives of glutamate and aspartate were previously shown to be potent inhibitors of HIF prolyl hydroxylases (22). Furthermore, these changes associated with the decrease in 2-OG levels may suggest an increased GOT2 activity in *SLC25A11*-deficent cells. This could lead to an alteration of the 2-OG/succinate ratio and to the subsequent inhibition of 2-OG dependent enzymes. This is consistent with the recent data on *GOT2* activating mutation, where the aspartate/glutamate ratio is also increased (21). Hence, although further studies will be needed, these observations may explain the link between MAS dysfunction and tumorigenesis.

We show that *SLC25A11* gene mutations account for 1% of all PPGL, a frequency equivalent to the recently identified PPGL susceptibility genes (*SDHA*, *TMEM127*, *MAX*, *FH*; refs. 1, 8, 14). Although these data will need to be confirmed in an independent cohort, our analysis of more than 600 patients does suggest that *SLC25A11* gene should now be screened in patients with PPGL, especially for those with a malignant phenotype. It is still unclear what will be the penetrance of the disease in affected families. The information we could obtain on few relatives of the *SLC25A11*-mutation carriers were suggestive of family history of cancers (cases reported with bone metastases of unknown primitive cancer, leukemia, as well as colon, breast, prostate and throat cancers) but not precise enough to allow drawing definite conclusions. So, it should further be assessed whether *SLC25A11*-mutations may confer an increased risk to other type of cancers. Moreover, *SLC25A11* somatic mutations or copy-number alterations have been reported in various types of cancers in The Cancer Genome Atlas (TCGA) project or the Catalog Of Somatic Mutations In Cancer (COSMIC) database (Supplementary Table S4), and 33 of these 145 samples were shown to present an underexpression of *SLC25A11* mRNA, thus strengthening the hypothesis of a role of *SLC25A11* in the tumorigenesis of other types of cancers. Interestingly, a low expression of *SLC25A11* is associated with a reduced survival in renal and pancreatic cancers, according to the TCGA studies (23).

It is worth noting that *SLC25A11* gene mutations are strongly associated with the development of metastatic PPGL as 5% of all metastatic patients in our cohort were *SLC25A11* mutations carriers and a malignant phenotype was observed in 5 out of the

7 (71%) *SLC25A11* mutation carriers (Table 2). In particular, we found germline *SLC25A11* mutations in 5 out of 30 (17%) patients with a single, apparently sporadic metastatic abdominal PGL (Table 1). In PPGL, malignancy diagnosis is made at the time of the diagnosis of the first metastasis (24) and the identification of an *SDHB* or an *FH* mutation are a risk factor for malignant disease. This study suggests that similar to *SDHB* and *FH* mutations, *SLC25A11* could be considered as a new genetic risk factor of metastatic PPGL. This observation is important for the follow-up of mutation carriers and may also have some important consequences on their therapeutic management. *SDHx*, *FH*- and now *SLC25A11*-mutated tumors should be managed as the so-called 'Cluster 1A' associated tumors. They display pseudo-hypoxic and hypermethylator phenotypes that probably participate to the acquisition of some metastatic properties (6, 25). Hence, antiangiogenic therapies or demethylating agents such as low-dosed 5-aza-deoxycytidine may be of therapeutic benefit for these specific patients. Similarly, it has recently been shown that *MGMT* promoter methylation in *SDHB*-metastatic PPGL confers an increased response to temozolomide (6, 26). Hence, *SCL25A11*-mutated carriers may also benefit from such therapy.

In conclusion, we show, using a large cohort of affected patients and an *in vitro* experimental model generated by CRISPR/Cas9 technology, that *SLC25A11* is a new tumor-suppressor gene conferring a predisposition to metastatic PPGL. The data reported here show how a mitochondrial dysfunction driven by a transporter inactivation can lead to tumorigenesis, and further broadens the field of mitochondrial genetic defects and cancer.

Disclosure of Potential Conflicts of Interest

No potential conflicts of interest were disclosed.

Authors' Contributions

Conception and design: A. Buffet, N. Burnichon, A.-P. Gimenez-Roqueplo, J. Favier

Development of methodology: A. Morin, J. Favier

Acquisition of data (provided animals, acquired and managed patients, provided facilities, etc.): L.-J. Castro-Vega, F. Habarou, C. Lussey-Lepoutre, E. Letouzé, H. Lefebvre, I. Guilhem, M. Haissaguerre, M. Padilla-Girola, T. Tran, L. Tchara, J. Bertherat, L. Amar, C. Ottolenghi, A.-P. Gimenez-Roqueplo

Analysis and interpretation of data (e.g., statistical analysis, biostatistics, computational analysis): A. Buffet, L.-J. Castro-Vega, F. Habarou, E. Letouzé, N. Burnichon, A.-P. Gimenez-Roqueplo, J. Favier

Writing, review, and/or revision of the manuscript: A. Buffet, L.-J. Castro-Vega, F. Habarou, I. Raingeard, J. Bertherat, N. Burnichon, A.-P. Gimenez-Roqueplo, J. Favier

Administrative, technical, or material support (i.e., reporting or organizing data, constructing databases): A.-P. Gimenez-Roqueplo

Study supervision: A.-P. Gimenez-Roqueplo, J. Favier

Acknowledgments

We thank Profs. Pierre-François Plouin and Xavier Bertagna for making this work possible through the COMETE Network. We also thank Jean-Michael Mazzella, Mélanie Menara, Aurélien de Reyniès, Nabila Elarouci, Dr. Rossella Libé, Prof. Antoine Tabarin, Prof. Cécile Badoual, Dr Tchao Méatchi, Dr. Mathilde Sibony, Dr Frédérique Tissier, Prof. Nathalie Rioux-Leclercq, Dr. François Le Gall, Dr. Françoise Gobet, Prof. Béatrice Vergier, Dr. Isabelle Pellegrin, Dr. Joel Edery, and Dr. Nathalie Carrere for their help, Estelle Robidel, Maëva Ruel, Irmine Ferrara, Stefani Mazurkiewics, Christophe Simian and Marie Fontenille for technical assistance, Catherine Tritscher for administrative assistance and Pr. Bertrand Tavitian for helpful discussion. We also thank all members of the Genetics Department and Biological Resources Center and Tumor Bank Platform, Hôpital européen Georges Pompidou (BB-0033-00063), all the members of the Tumor BioBank-biological resource center of Rouen University Hospital, all the members of the Centre de Ressources Biologiques Plurithématique Bordeaux Biothèques Santé (BB-0033-00036) and the Mass spectrometry platform of the Biology Department of the Necker Hospital (Christophe Merlette). This work has received funding from the Agence Nationale de la Recherche (ANR-2011-JCJC-00701 MODEOMAPP), the European Union Seventh Framework Program (FP7/2007-2013) under grant agreement n° 259735, the Plan Cancer: Appel à projets Epigénétique et Cancer 2013 (EPIG201303 METABEPIC), the European Union's Horizon 2020 research and innovation program under grant agreement No 633983 and by the Institut National du Cancer and the Direction Générale de l'Offre de Soins (PRT-K 2014, COMETE-TACTIC, INCa-DGOS_8663). A. Buffet received a financial support from ITMO Cancer AVIESAN (Alliance Nationale pour les Sciences de la Vie et de la Santé, National Alliance for Life Sciences & Health) within the framework of the Cancer Plan and from la Fondation pour la Recherche Médicale (FDT20170436955). C. Lussey-Lepoutre and N. Burnichon are funded by the Cancer Research for Personalized Medicine - CARPEM project (Site de Recherche Intégré sur le Cancer - SIRIC). The group is supported by the Ligue Nationale contre le Cancer (Equipe Labellisée). This work is part of the "Cartes d'Identité des Tumeurs (CIT) program" funded and developed by the `Ligue Nationale contre le Cancer' (http://cit.ligue-cancer.net).

The costs of publication of this article were defrayed in part by the payment of page charges. This article must therefore be hereby marked *advertisement* in accordance with 18 U.S.C. Section 1734 solely to indicate this fact.

Received August 15, 2017; revised December 14, 2017; accepted January 31, 2018; published first February 5, 2018.

References

1. Favier J, Amar L, Gimenez-Roqueplo AP. Paraganglioma and phaeochromocytoma: from genetics to personalized medicine. Nat Rev Endocrinol 2015;11:101–11.
2. Burnichon N, Rohmer V, Amar L, Herman P, Leboulleux S, Darrouzet V, et al. The succinate dehydrogenase genetic testing in a large prospective series of patients with paragangliomas. J Clin Endocrinol Metab 2009; 94:2817–27.
3. Pastor WA, Aravind L, Rao A. TETonic shift: biological roles of TET proteins in DNA demethylation and transcription. Nat Rev Mol Cell Biol 2013; 14:341–56.
4. Klose RJ, Kallin EM, Zhang Y. JmjC-domain-containing proteins and histone demethylation. Nat Rev Genet 2006;7:715–27.
5. Selak MA, Armour SM, MacKenzie ED, Boulahbel H, Watson DG, Mansfield KD, et al. Succinate links TCA cycle dysfunction to oncogenesis by inhibiting HIF-alpha prolyl hydroxylase. Cancer Cell 2005;7:77–85.
6. Letouze E, Martinelli C, Loriot C, Burnichon N, Abermil N, Ottolenghi C, et al. SDH mutations establish a hypermethylator phenotype in paraganglioma. Cancer Cell 2013;23:739–52.
7. Castro-Vega LJ, Letouze E, Burnichon N, Buffet A, Disderot PH, Khalifa E, et al. Multi-omics analysis defines core genomic alterations in pheochromocytomas and paragangliomas. Nat Commun 2015;6:6044.
8. Castro-Vega LJ, Buffet A, De Cubas AA, Cascon A, Menara M, Khalifa E, et al. Germline mutations in FH confer predisposition to malignant pheochromocytomas and paragangliomas. Hum Mol Genet 2014;23:2440–6.
9. Lenders JW, Duh QY, Eisenhofer G, Gimenez-Roqueplo AP, Grebe SK, Murad MH, et al. Pheochromocytoma and paraganglioma: an endocrine society clinical practice guideline. J Clin Endocrinol Metab 2014;99: 1915–42.
10. Hsu PD, Scott DA, Weinstein JA, Ran FA, Konermann S, Agarwala V, et al. DNA targeting specificity of RNA-guided Cas9 nucleases. Nat Biotechnol 2013;31:827–32.

Published OnlineFirst February 5, 2018; DOI: 10.1158/0008-5472.CAN-17-2463

11. Menara M, Oudijk L, Badoual C, Bertherat J, Lepoutre-Lussey C, Amar L, et al. SDHD immunohistochemistry: a new tool to validate SDHx mutations in pheochromocytoma/paraganglioma. J Clin Endocrinol Metab 2015;100:E287–91.
12. Cappello AR, Curcio R, Valeria Miniero D, Stipani I, Robinson AJ, Kunji ER, et al. Functional and structural role of amino acid residues in the even-numbered transmembrane alpha-helices of the bovine mitochondrial oxoglutarate carrier. J Mol Biol 2006;363:51–62.
13. Killian JK, Kim SY, Miettinen M, Smith C, Merino M, Tsokos M, et al. Succinate dehydrogenase mutation underlies global epigenomic divergence in gastrointestinal stromal tumor. Cancer Discov 2013;3:648–57.
14. Cascon A, Comino-Mendez I, Curras-Freixes M, de Cubas AA, Contreras L, Richter S, et al. Whole-exome sequencing identifies MDH2 as a new familial paraganglioma gene. J Natl Cancer Inst 2015;107.
15. Miniero DV, Cappello AR, Curcio R, Ludovico A, Daddabbo L, Stipani I, et al. Functional and structural role of amino acid residues in the matrix alpha-helices, termini and cytosolic loops of the bovine mitochondrial oxoglutarate carrier. Biochim Biophys Acta 2011;1807:302–10.
16. Stipani V, Cappello AR, Daddabbo L, Natuzzi D, Miniero DV, Stipani I, et al. The mitochondrial oxoglutarate carrier: cysteine-scanning mutagenesis of transmembrane domain IV and sensitivity of Cys mutants to sulfhydryl reagents. Biochemistry 2001;40:15805–10.
17. Monne M, Palmieri F. Antiporters of the mitochondrial carrier family. Curr Top Membr 2014;73:289–320.
18. Ohura T, Kobayashi K, Tazawa Y, Nishi I, Abukawa D, Sakamoto O, et al. Neonatal presentation of adult-onset type II citrullinemia. Hum Genet 2001;108:87–90.
19. Chang KW, Chen HL, Chien YH, Chen TC, Yeh CT. SLC25A13 gene mutations in Taiwanese patients with non-viral hepatocellular carcinoma. Mol Genet Metab 2011;103:293–6.
20. Dong H, Zhang H, Liang J, Yan H, Chen Y, Shen Y, et al. Digital karyotyping reveals probable target genes at 7q21.3 locus in hepatocellular carcinoma. BMC Med Genet 2011;4:60.
21. Remacha L, Comino-Mendez I, Richter S, Contreras L, Curras-Freixes M, Pita G, et al. Targeted exome sequencing of Krebs cycle genes reveals candidate cancer predisposing mutations in pheochromocytomas and paragangliomas. Clin Cancer Res 2017;23:6315–24.
22. Mole DR, Schlemminger I, McNeill LA, Hewitson KS, Pugh CW, Ratcliffe PJ, et al. 2-oxoglutarate analogue inhibitors of HIF prolyl hydroxylase. Bioorg Med Chem Lett 2003;13:2677–80.
23. Chandrashekar DS, Bashel B, Balasubramanya SAH, Creighton CJ, Ponce-Rodriguez I, Chakravarthi B, et al. UALCAN: a portal for facilitating tumor subgroup gene expression and survival analyses. Neoplasia 2017;19:649–58.
24. Gimenez-Roqueplo AP, Favier J, Rustin P, Rieubland C, Crespin M, Nau V, et al. Mutations in the SDHB gene are associated with extra-adrenal and/or malignant phaeochromocytomas. Cancer Res 2003;63:5615–21.
25. Loriot C, Domingues M, Berger A, Menara M, Ruel M, Morin A, et al. Deciphering the molecular basis of invasiveness in Sdhb-deficient cells. Oncotarget 2015;6:32955–65.
26. Hadoux J, Favier J, Scoazec JY, Leboulleux S, Al Ghuzlan A, Caramella C, et al. SDHB mutations are associated with response to temozolomide in patients with metastatic pheochromocytoma or paraganglioma. Int J Cancer 2014;135:2711–20.

Published OnlineFirst February 5, 2018; DOI: 10.1158/0008-5472.CAN-17-2463

Cancer Research
The Journal of Cancer Research (1916–1930) | The American Journal of Cancer (1931–1940)

AACR American Association for Cancer Research

Germline Mutations in the Mitochondrial 2-Oxoglutarate/Malate Carrier *SLC25A11* Gene Confer a Predisposition to Metastatic Paragangliomas

Alexandre Buffet, Aurélie Morin, Luis-Jaime Castro-Vega, et al.

Cancer Res 2018;78:1914-1922. Published OnlineFirst February 5, 2018.

Supplementary data for

Germline mutations in the mitochondrial 2-oxoglutarate/malate carrier *SLC25A11* gene confer a predisposition to metastatic paragangliomas.

A. Buffet, A. Morin, L-J. Castro-Vega, F. Habarou, C. Lussey-Lepoutre, E. Letouzé, H. Lefebvre, I. Guilhem, M. Haissaguerre, I. Raingeard, M. Padilla-Girola, T.Tran, L Tchara, J. Bertherat, L. Amar, C. Ottolenghi, N. Burnichon, A-P. Gimenez-Roqueplo[†], J. Favier[†]

correspondence to: J.F. (judith.favier@inserm.fr) or
A-P.G-R. (anne-paule.gimenez-roqueplo@inserm.fr)

TABLE OF CONTENTS

SUPPLEMENTARY METHODS

Direct sequencing of *SLC25A11* gene

Direct sequencing of the eight exons and exon-intron boundaries of the *SLC25A11* gene was performed by Sanger method. Specific primers to amplify small amplicons were designed for *SLC25A11* gene sequencing of DNA extracted from paraffin embedded tissues. Primers sequences are available upon request. The sequencing reactions were performed using the BigDye Terminator v3.1 kit (Life Technologies), in an ABI Prism3730XL DNA Analyzer (Perkin Elmer Applied Biosystems, Foster City, CA). We assessed the potential pathogenicity of variants with Alamut®-Mutation Interpretation Software version 2.3.2 (http://www.interactivebiosoftware.com/software.html).

RT-qPCR on leukocyte RNA

Total leukocyte RNA was extracted on Paxgene tube (PreAnalytiX) by the Maxwell 16 IVD Instrument (Maxwell 16 LEV simply RNA Blood Kit, Promega). RNA was quantified and its purity assessed with a NanoDrop ND-1000 spectrophotometer (Labtech). After a reverse transcription, quantitative PCR was performed on *SLC25A11* transcript from patient #4 and three controls on the C1000 Touch (Biorad).

Immunohistochemical analyses

Immunohistochemistry (IHC) was performed on 6 micrometers sections from paraffin-embedded tumors. Anti-5-hmC (1/1200, Active Motifs, 39759), H3K9me3 (1/1000, Active Motifs, 39161), H3K27me3 (1/1000, Active Motif, 39156), SDHB (1/500, Sigma-Aldrich, HPA002868) IHC and interpretation were performed as previously described (1). Anti-OGC IHC was carried out with the anti-SLC25A11 antibody produced in rabbit (HPA021167, Sigma-Aldrich) at a 1:10 dilution and following antigen retrieval by boiling slides in Tris-EDTA buffer (pH9) for 45 min. Revelation was achieved with Histogreen in all cases. Images were acquired with a Leica DM400B microscope with Leica Application Suite software version 2.8.1, and a Leica DFC420C camera.

Western blot

Protein extracts were prepared with RIPA lysis buffer. Equal quantities of proteins were separated on acrylamide 12 % gels and transferred to PVDF membranes. The membranes were incubated overnight at 4°C with primary antibody (anti-SLC25A11 (1/1000, Abcam ab80464) or anti-SDHA (1/5000, Abcam ab14715)). The membranes were washed in PBS, 0.05% tween-20, and incubated with horseradish-peroxidase-conjugated anti-rabbit or anti-mouse antibodies (Bio-FX). The bound antibodies were revealed by chemiluminescence using ECL (Pierce) and the results read with a LAS-4000 Mini (Fuji). The experiment was performed independently three times and representative results are shown.

Immunofluorescence

Cells were cultured on glass slides until 80% confluence. They were then washed in PBS and fixed for 10 min in ice-cold 4% paraformaldehyde. The slides were incubated with primary antibody for 2 hours at room temperature (anti HIF2-alpha, R&D systems, AF2997) and then washed with PBS. The slides were incubated with the secondary antibody, conjugated with Alexa Fluor 594 (1/2000, Invitrogen), was incubated for 1 h, at room temperature in the dark and then washed with PBS. The slides were finally mounted in Vectashield, containing DAPI, to stain the nuclei. Image acquisition was performed using an Axioimager Z1 Zeiss, with apotome system. The experiment was performed three times.

Cell migration assay

Cells were treated 48 hours by 5 mM of dimethyl 2-oxoglutarate (Sigma Aldrich). Non-treated and treated cells were seeded in 6-well dishes. Twelve hours later, when the cells were confluent, a wound was made in the cell layer and cells were maintained in standard medium for 10 hours. The relative cell migration was established by calculating the closure index by the analysis of 10 images for each time point using imageJ software. The experiment was performed three times, in duplicates.

Cell proliferation

50.000 cells were plated on 6-well plates. Growth curves were established by counting cells after two, four and six days. The experiment was performed three times, in duplicates.

Cell adhesion

After complete detachment from their plates by trypsin EDTA 0,05 % (Gibco), cells were plated in 12-wells plates. Cell adhesion was evaluated by taking picture two hours after plating. Adherent and non-adherent cells were identified on the basis of their morphology. The experiment was performed three times.

Metabolite quantification

Snap-frozen tumor samples (from patient #1, #6 and from 5 tumors classified in cluster 2 by the transcriptome used as controls (one sporadic, one *TMEM127*- and 3 *RET*-mutated PPGL), aliquots of 100 µl of cell pellets resuspensions, and the supernatant from imCC cultures (WT, *Sdhb-/-* clone (c8) and two *Slc25a11*$^{\Delta/\Delta}$ clones (clones 4 and 6) and *Slc25a11*-rescued cells (c6-R)) were processed by methanol precipitation or organic extraction with ethylacetate, derivatized with N,O-bis(trimethylsilyl) trifluoroacetamide with 1% trimethylchlorosilane, and analyzed by gas chromatography-tandem mass spectrometry on a GC-MS triple quadrupole (Scion TQ, Brüker Daltonics). Organic acids were identified according to retention time and mass spectra in selected reaction monitoring mode based on standard spectral reference libraries. Amino acids were quantified both by this method and by liquid chromatography tandem mass spectrometry (Acquity TQD, Waters). Stable isotope labeled internal standards included U-^{13}C4 fumarate, U-^{13}C4 succinate, U-^{13}C4 malate, 1,2,3,4-$^{13}C_4$ 2-oxoglutarate, 2,3,3,4,4-D_5 glutamate and 2,3,3-D_3-aspartate from Cambridge Isotope Laboratories.

SUPPLEMENTARY CLINICAL DATA

Patient #1

An abdominal mass was incidentally discovered in this 46-years old male during a doppler evaluation performed for surveillance of smoking complications. An abdominal CT scan revealed a 34 mm image evocating of Zuckerkandl PGL and a 6 mm right basal pulmonary nodule. The patient had no clear familial history of PPGL, but a paternal cousin had had surgery for a cervical tumor and his father died of a metastatic cancer of unknown origin at 49 years old. His blood pressure was normal as well as urinary concentrations of total metanephrine and normetanephrine. ^{111}In-pentetreotide scintigraphy (Octreoscan) was normal whereas ^{123}I-MIBG scintigraphy revealed a unique fixation on the abdominal PGL. He underwent surgery and the pathological analysis of the tumor diagnosed a 37 mm PGL without any lymph node metastasis and rare intravascular bolus. Thirteen years later, no recurrence has been detected and the size of pulmonary nodule was stable under 1 cm.

Patient #2

The patient was a 51 years old female, with no familial history of the disease, who suffered from arterial hypertension since she was 41 years old. She presented with upper gastrointestinal bleedings and gastroscopy revealed a duodenal tumor. Abdominal CT scan showed that the 40 mm tumor was located between duodenum and pancreas. The patient underwent a cephalic duodenopancreatectomy. Pathological analysis diagnosed a gangliocytic PGL of the ampulla of Vater with metastases in two lymph nodes. Ten years later she is disease free.

Patient #3

The patient had an arterial hypertension since he was 52 years old, which became resistant, ten years later. At 67 years old, he complained of nycturia associated with other symptoms (palpitations, headaches, diaphoresis) evocating of catecholamine-secreting tumor. Urinary total metanephrine measurements showed an increase in

normetanephrines. Abdominal CT scan revealed a 50 mm tumor in the bladder corresponding to a unique fixation on ^{123}I-MIBG scintigraphy. The patient underwent a partial cystectomy and pathological exam diagnosed paraganglioma. Three years later, the recurrence of hypertension led to new investigations that diagnosed multiple secreting metastatic locations in the lymph nodes that were not treated. The patient died 10 years after first surgery, of other causes.

Patient #4

The patient was a 32 years old female with a carotid body PGL discovered during a thyroid echography. This cervical mass had actually been observed by the patient by self-examination five years before, but not investigated. Urinary normetanephrine and metanephrine concentrations were normal. Head and neck MRI showed a 40 mm unique PGL developed from the carotid body. No other PGL was detected by thoraco-abdominal and pelvic CT scan neither by ^{111}In-pentetreotide scintigraphy. The tumor was operated on and pathological exam confirmed the diagnosis of PGL. 5 years later the patient is still disease free

Patient #5

The patient was a 87 years old female who presented with intestinal occlusion. The abdominal scan showed a retroperitoneal 46 mm tumor, corresponding to a unique fixation on ^{123}I-MIBG scintigraphy. The patient suffered from paroxystic and permanent arterial hypertension and urinary normetanephrines were elevated. She underwent surgery and the pathological analysis diagnosed a 55 mm PGL with local invasion, especially in the vena cava. The patient died 5 years later after metastatic diffusion of the disease.

Patient #6

At 59 years old, this patient complained of lumbar pains. She benefited from a CT scan that showed a 70 mm retroperitoneal tumor. Urinary normetanephrines concentration was highly increased. She underwent surgery and pathological analysis diagnosed a PGL

associated with intravascular and capsular invasions. One month later, an abdominal CT scan showed a residual tumor, which was treated by radiotherapy. Three years later, thoracic lymphatic metastases were diagnosed by F-DOPA and ^{18}F-FDG TEP scan and were treated by surgical resection. Six month later, pulmonary and liver metastases appeared and a treatment by a long-acting somatostatin analog (lanreotid) was begun. After 6 month of treatment the disease is stable.

Patient #7

The patient was operated at 74 years old of a 33 mm skull tumor the invading subarachnoid space. Pathological analysis diagnosed PGL metastasis. Thorax and abdominal CT showed a 40 mm right retroperitoneal PGL, and a unique retroperitoneal fixation on ^{123}I-MIBG scintigraphy, and ^{18}F-FDG TEP scan. The ^{111}In-pentetreotide scintigraphy was negative. She had a HTA for ten years and urinary normetanephrines concentrations were highly increased. She underwent surgery and pathological analysis diagnosed a metastatic PGL associated with capsular invasions and three lymph nodes metastasis. Four month later, urinary normetanephrines concentrations decreased but was still above the upper limit of the norm. ^{18}F-FDG TEP scan showed an iliac metastasis and a jugular lymph node. Two years later the iliac metastasis increased and pulmonary, mediastinal and peritoneal metastasis appeared. The patient was treated by iliac external radiotherapy and ^{131}I-MIBG therapy, but the disease was still progressive. She was treated for three months by interferon and then enrolled in the first FIRSTMAPPP randomized trial (ClinicalTrials.gov Identifier: NCT01371201). She died rapidly after the inclusion.

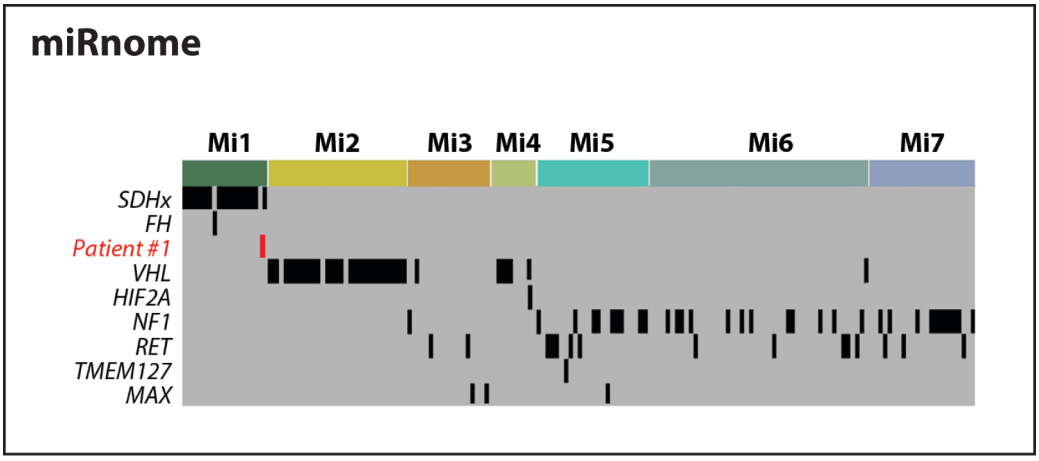

Fig. S1. Mirnome-based classification of tumors of the COMETE cohort. Patient #1's PGL (in red) classifies in the Mi1 cluster together with *SDHx*- and *FH*-mutated PPGL.

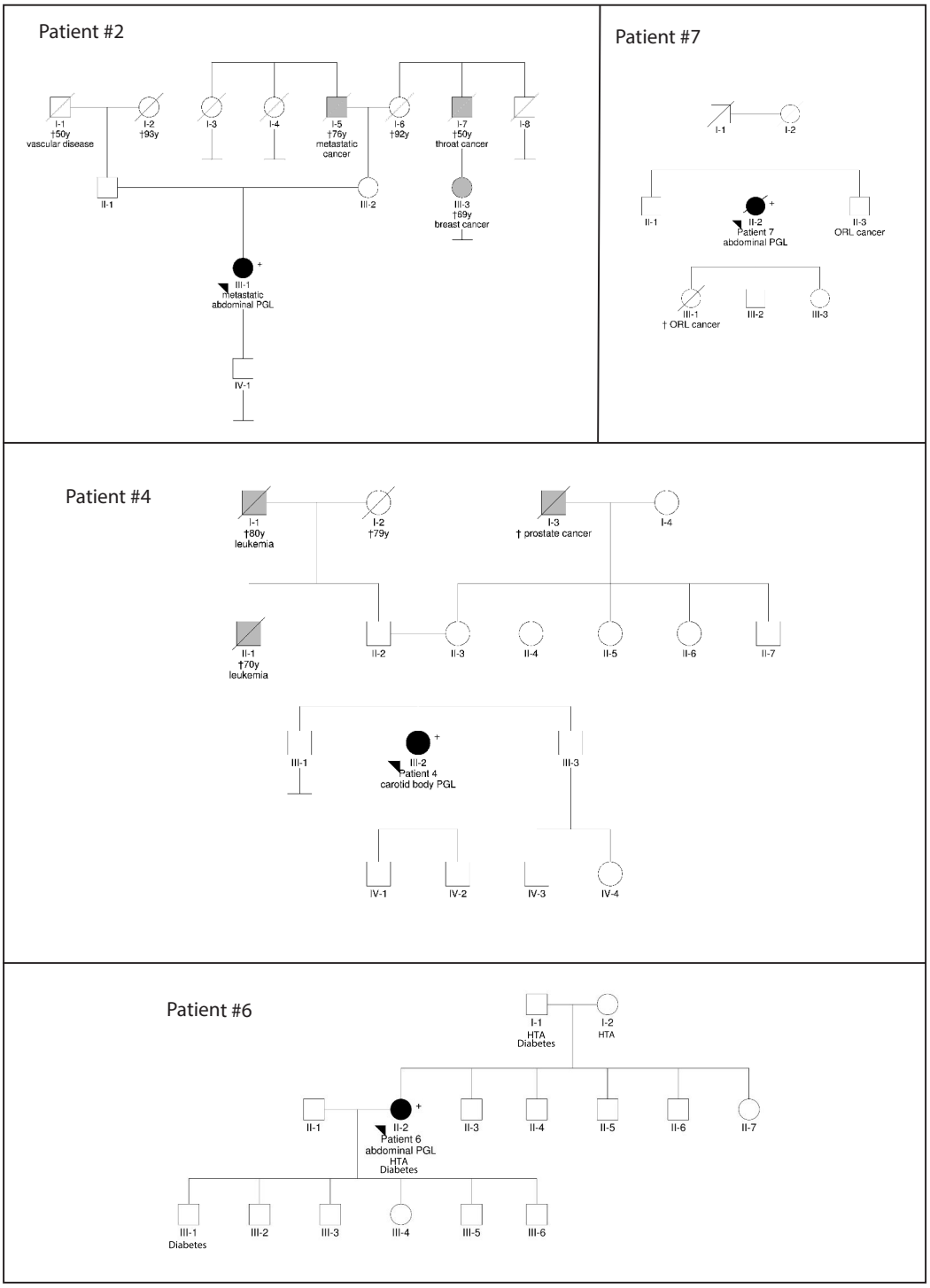

Fig. S2. **Family pedigrees of *SLC25A11*-mutated patients.** Index cases are shown in black, relatives with cancers are shown in grey. HTA: hypertension.

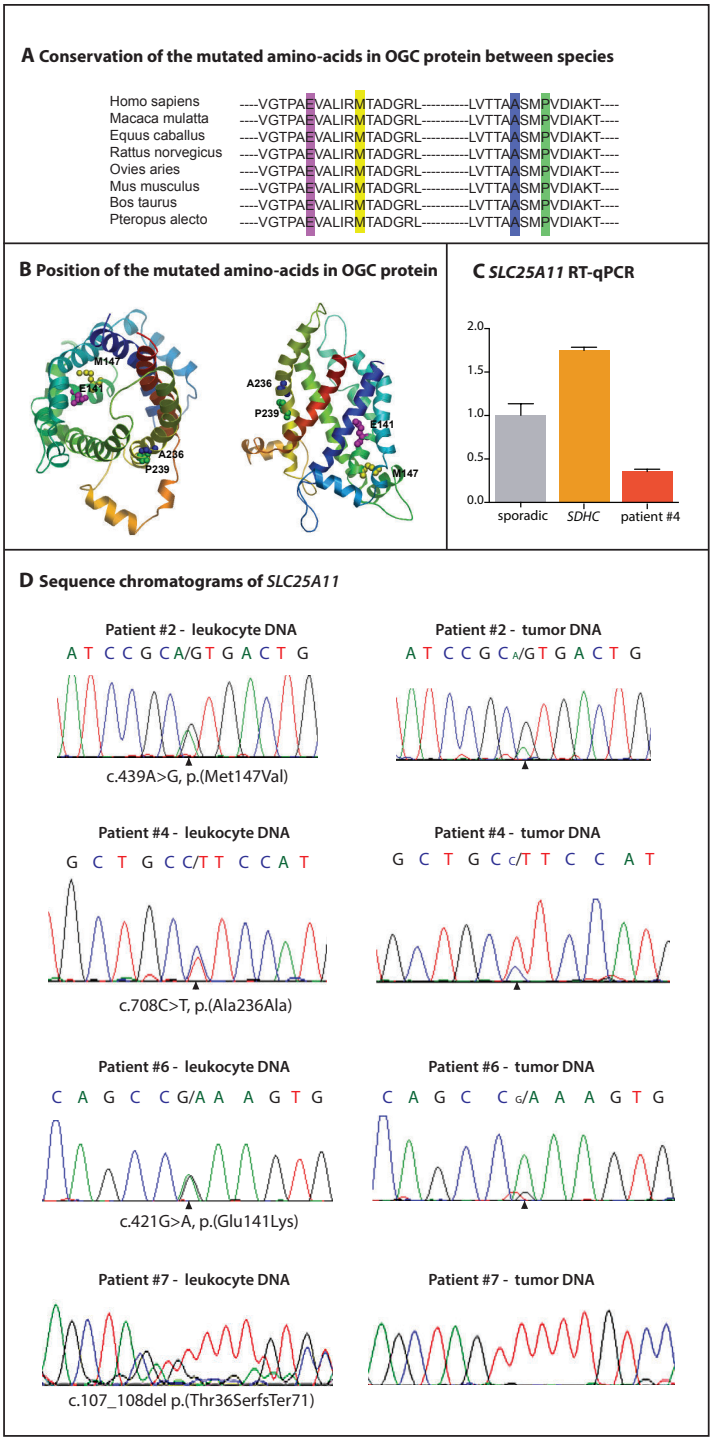

Fig. S3. Germline and tumor *SLC25A11* mutations. Conservation of mutated amino acid residues identified in *SLC25A11* gene across species (A). Localization of mutated amino acids on a 3D modelization of the OGC protein (by Swiss Model); up view (left) or side view (right) (B). RT-qPCR on leukocyte RNA suggests the degradation of the mutated mRNA in patient's #4 tumor, as compared to leukocyte RNA from a patient with a sporadic and an SDHC-mutated PGL (C). Sequence traces are shown for the 4 patients for whom tumor tissues were available (patients #2, #4, #6 and #7). All sequence traces exhibit a germline heterozygous mutation and a corresponding tumoral LOH (arrows) (D).

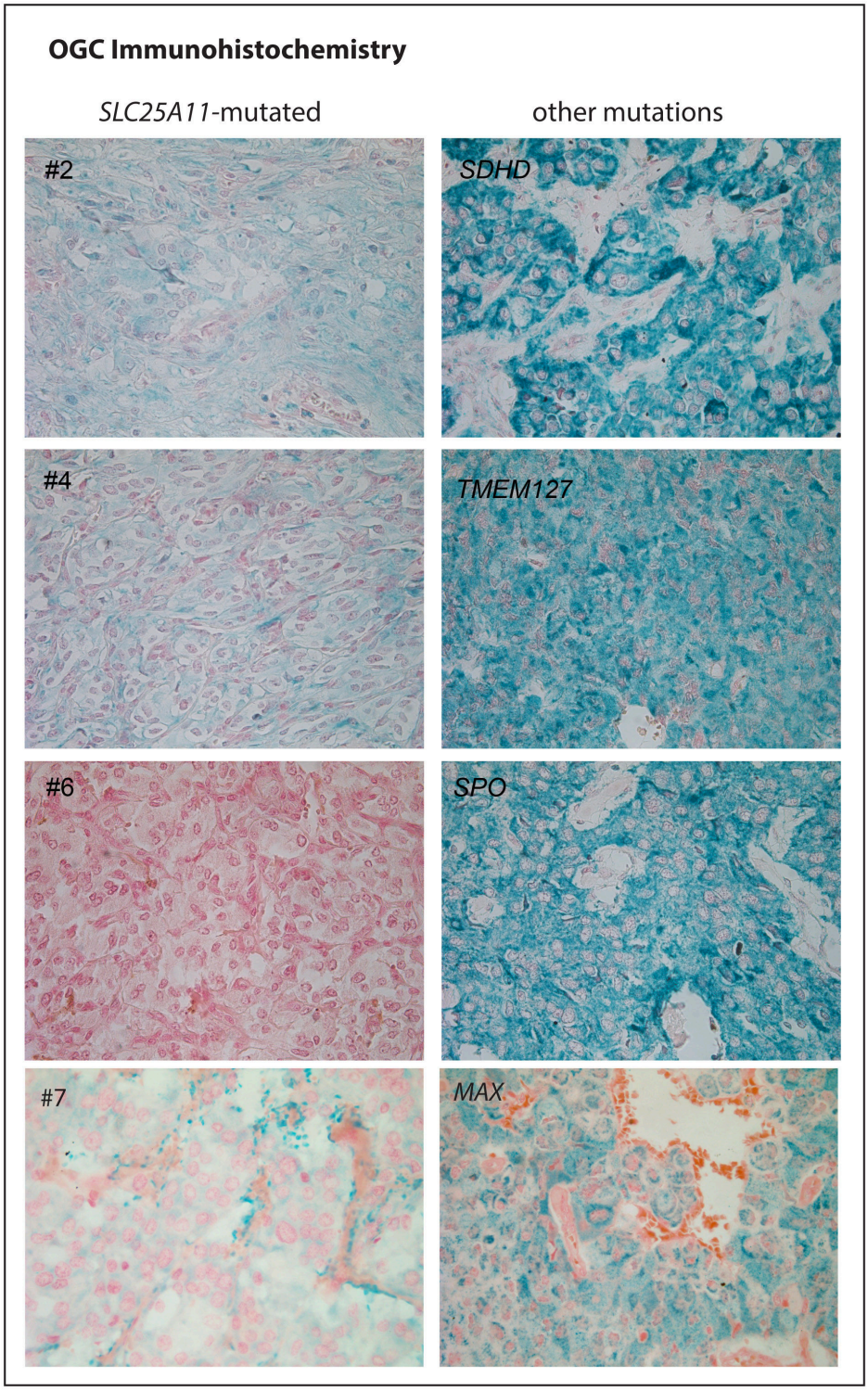

Fig. S4. OGC immunohistochemistry in *SLC25A11*-mutated tumors. Tumors from patients #2, #4 and #7 show a very low, weak diffuse OGC immunostaining, which is completely negative in

tumor tissue from patient #6. In contrast, control tumors without *SLC25A11* mutations (*SDHD*, *TMEM127*, sporadic (SPO) and *MAX* PPGL) display a strong granular staining, as expected from a mitochondrial protein.

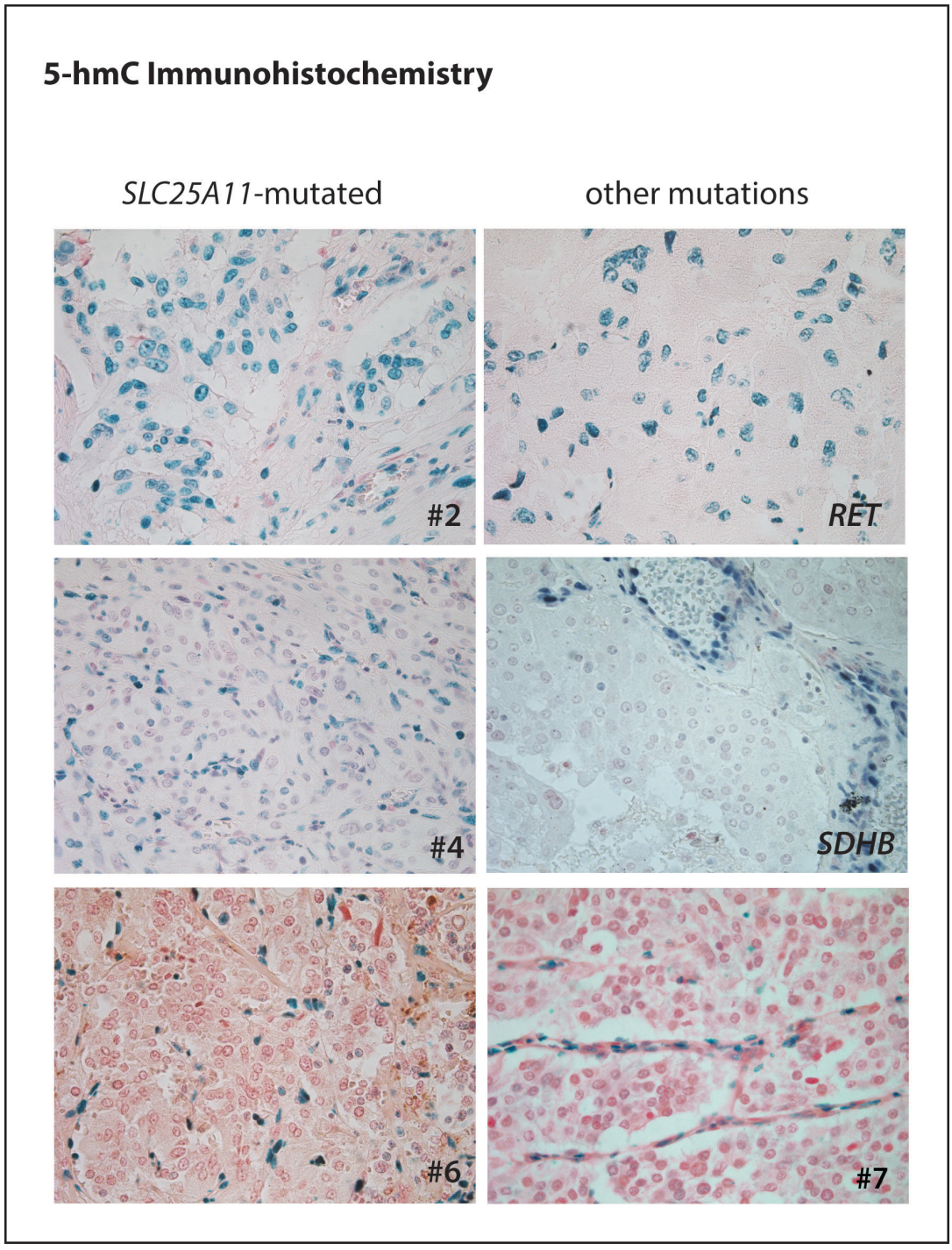

Fig. S5. **5hmC immunohistochemistry in *SLC25A11*-mutated tumors.** 5-hmC IHC of *SLC25A11* mutated PGL from patients #2, #4, #6 and #7 shows a low staining in the nuclei of all *SLC25A11*-mutated tumor cells except for one (patient #2), as compared to endothelial or sustentacular cells. Similar

immunostaining is observed in an *SDHB*-mutated PPGL whereas a *RET*-mutated tumor displays a homogeneously distributed positive 5-hmC labeling.

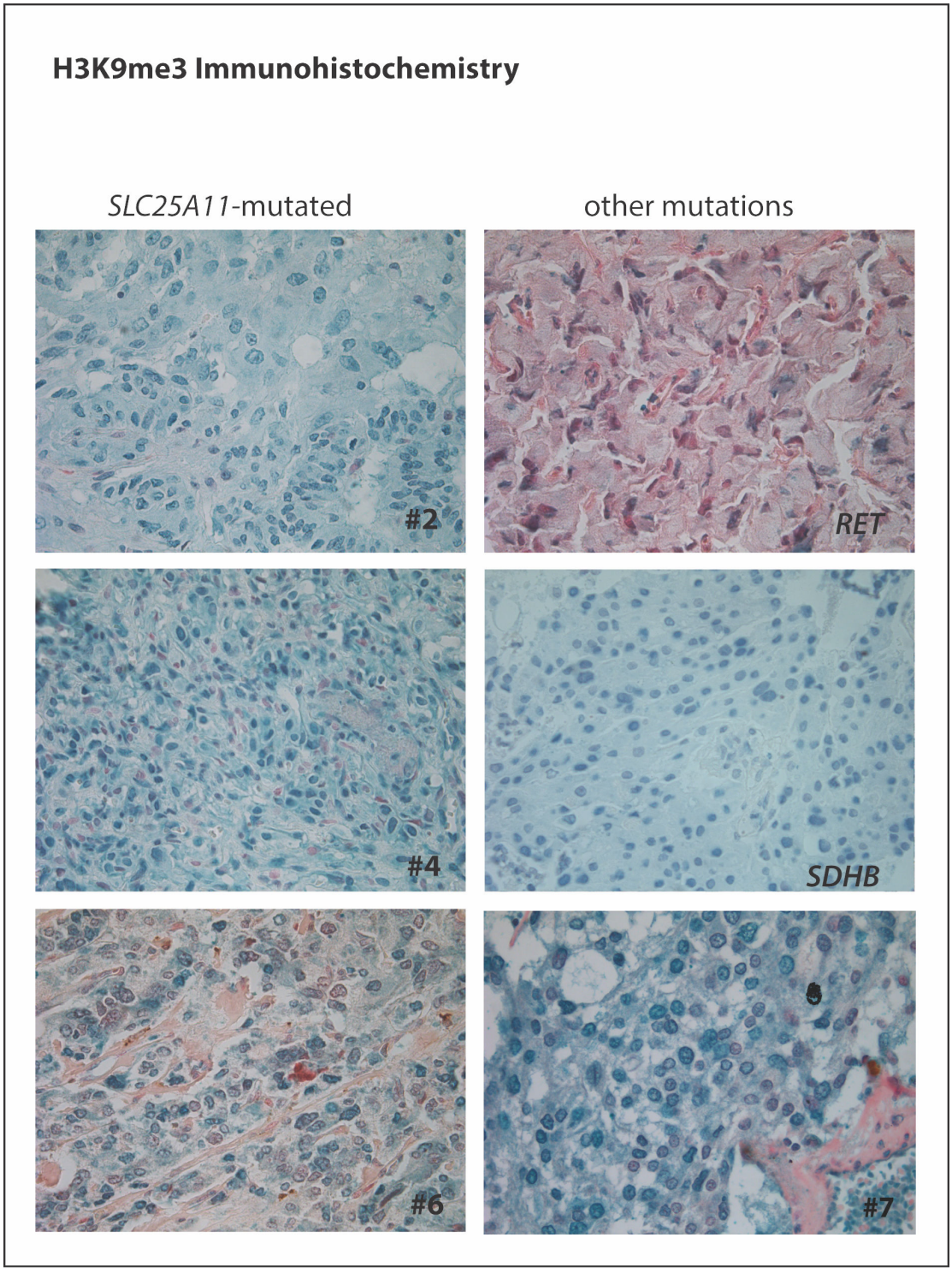

Fig. S6. H3K9me3 immunohistochemistry in *SLC25A11*-mutated tumors. Tumors from *SLC25A11*-mutated patients (#2, #4, #6 and #7) show a strong nuclear immunostaining, similar to that observed in a hypermethylated tumor carrying *SDHB* mutation. In contrast, control tumor with a *RET* mutation shows a negative or a low H3K9me3 labeling.

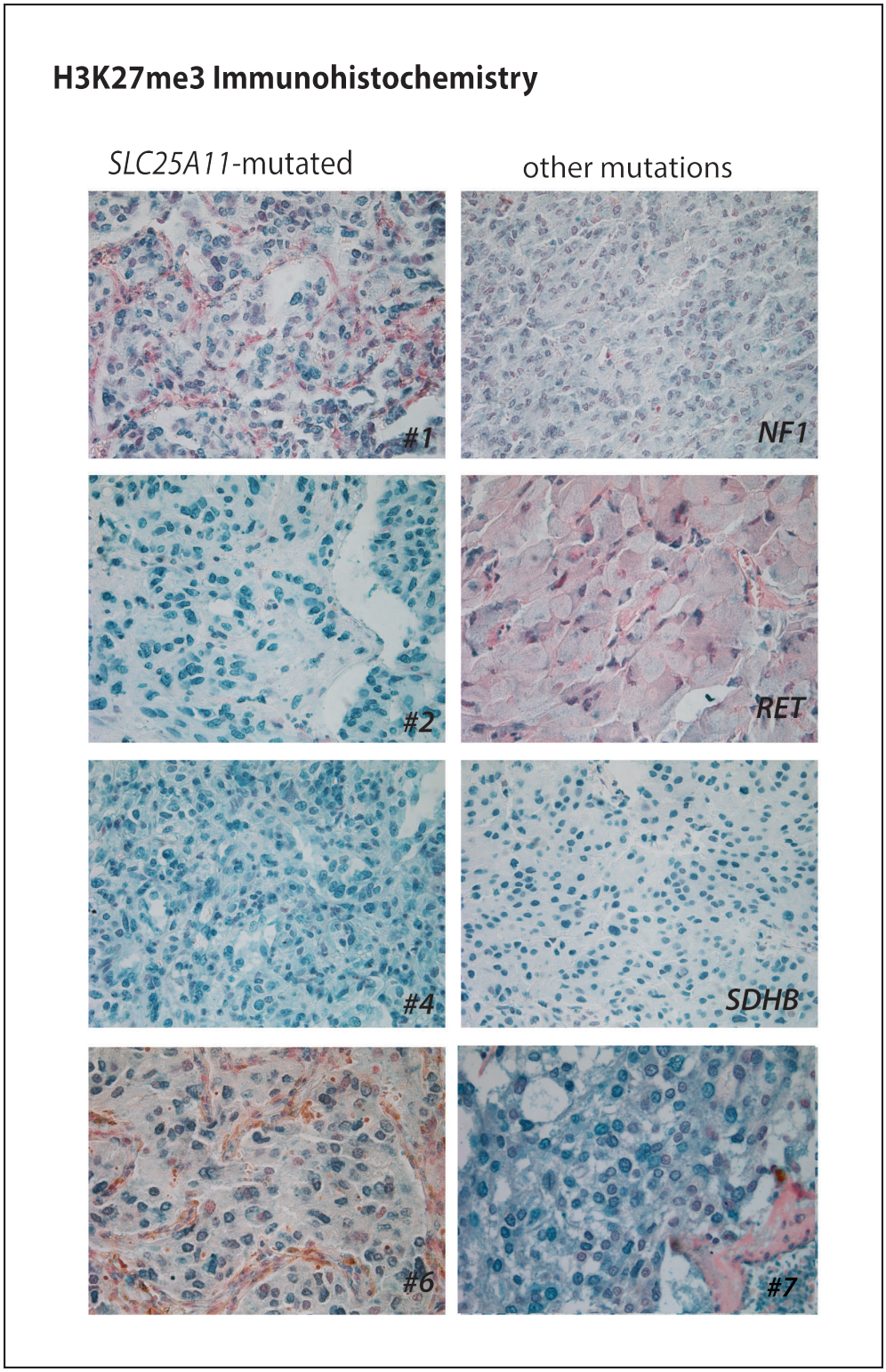

Fig. S7. H3K27me3 immunohistochemistry in *SLC25A11*-mutated tumors. Tumors from *SLC25A11*-mutated patients (#1, #2, #4, #6 and #7) show a strong nuclear immunostaining, similar to that observed in a hypermethylated tumor carrying *SDHB* mutation. In contrast, control tumors with *NF1* or *RET* mutations show a negative or a low H3K27me3 labeling.

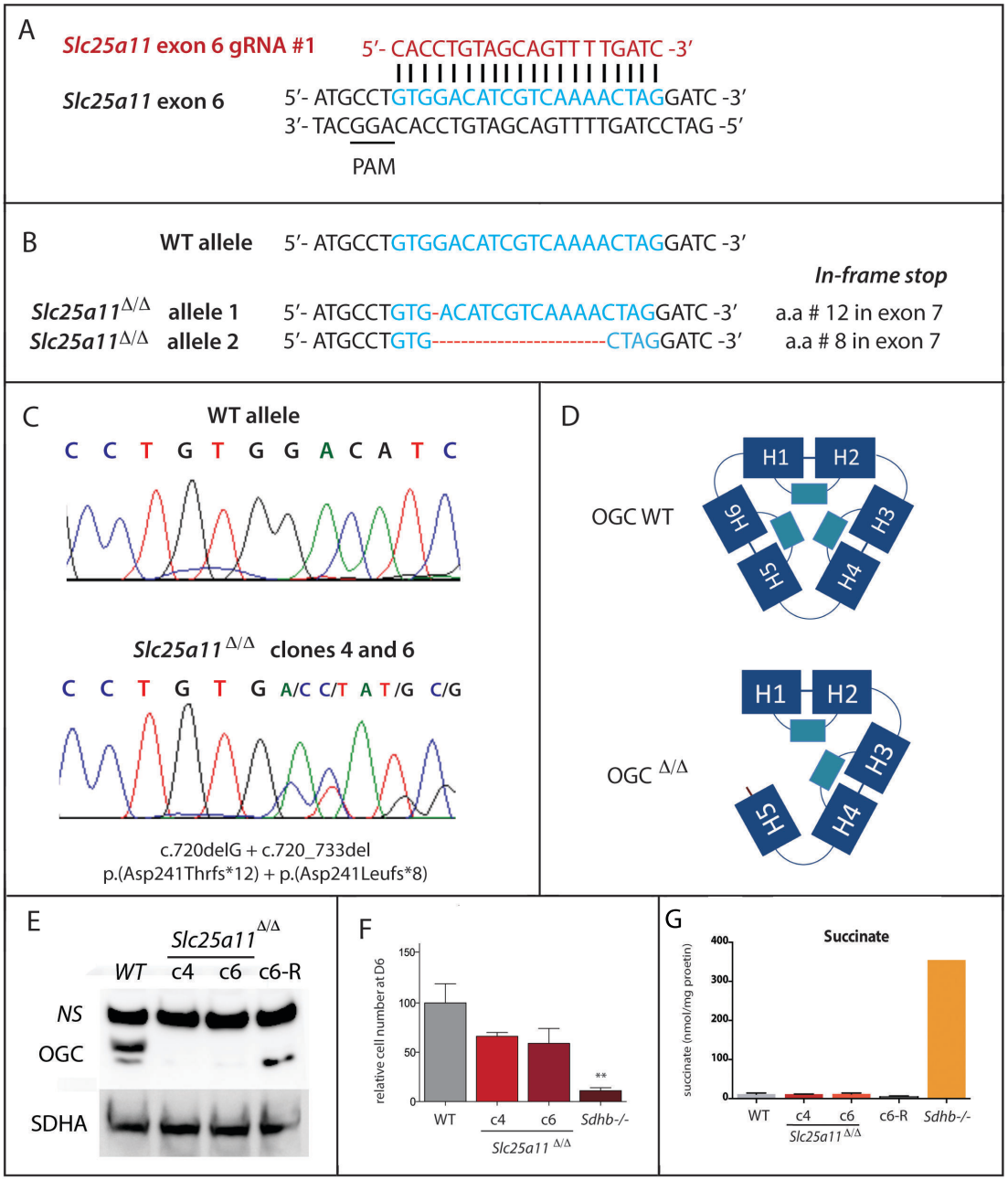

Fig. S8. CrispR-Cas9 design for the generation of *Slc25a11*$^{\Delta/\Delta}$ immortalized mouse chromaffin cells. gRNA sequence (in red) and targeted genomic *Slc25a11* sequence (in blue). PAM: Protospacer Adjacent Motif (A). Genomic alteration in *Slc25a11* gene in *Slc25a11*$^{\Delta/\Delta}$ imCCs. The first line represents the wild type (WT) sequence, and the two next lines the two alleles of *Slc25a11* gene in *Slc25a11*$^{\Delta/\Delta}$ imCCs. The deletion is drawn in red. The deletion in allele 1 leads to a stop codon 12 amino acids downstream in exon 7. The deletion in allele 2 results to a stop codon after 8 amino acids (B). Sequence electrophoregrams of the

targeted region in WT and in *Slc25a11*$^{\Delta/\Delta}$ imCCs (C). Schematic top view of WT and mutant OGC protein. The H1 to H6 transmembrane alpha helix chains are displayed in dark blue and the H12 to H56 matrix helix chains in light blue. In the *Slc25a11*$^{\Delta/\Delta}$ mutant, the H56 and H6 chains are deleted (D). Western Blot showing OGC and SDHA protein expression. NS: non-specific band (E). Cell proliferation (F). Succinate levels were not modified in *Slc25a11*$^{\Delta/\Delta}$ imCCs (G).

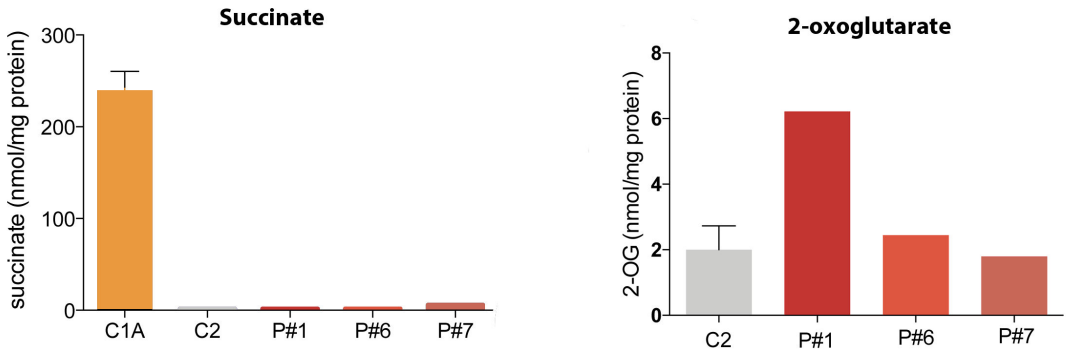

Fig. S9. Metabolomics analysis in human PPGL tumors shows no succinate increase in SLC25A11-mutated tumors from patients P#1, P#6 and P#7. 2-OG levels were highly variable and did not show significant differences between groups.

Gene	Name	Ref Seq	cDNA mutation	Protein alteration
ALKBH7	alkB homolog 7	NM_032306	c.419_420del	p.(Pro140Glnfs*28)
SHANK1	SH3 and multiple ankyrin repeat domains 1	NM_016148	c.102_130del	p.(Arg35Glnfs*6)
ZNF579	zinc finger protein 579	NM_152600	c.1109_1111del	p.(Gly370del)
TRIM50	tripartite motif containing 50	NM_178125	c.1074del	p.(Ser359Alafs*18)
OPRD1	opioid receptor delta 1	NM_000911	c.122G>A	p.(Arg41Gln)
DENND2C	DENN/MADD domain containing 2C	NM_001256404	c.68A>G	p.(Gln23Arg)
SLC25A11	2-oxoglutarate/malate carrier	NM_003562	c.715C>A	p.(Pro239Thr)
MYO19	myosin XIX	NM_025109	c.953C>T	p.(Ala318Val)
PNPLA6	patatin like phospholipase domain containing 6	NM_001166112	c.1667T>A	p.(Val556Glu)
LRRC8E	leucine-rich repeat containing 8 family member E	NM_025061	c.1753C>T	p.(Arg585Trp)
UBAP2	ubiquitin associated protein 2	NM_018449	c.2456C>T	p.(Ala819Val)

Table S1. Germline variations identified by whole-exome sequencing in patient #1's PGL. Only the variations that remained after filtration of whole-exome sequencing data, which were associated with a LOH on corresponding locus on SNP array data and predicted as being pathogenics *in silico* are shown.

Tumor ID	Gender	Malignancy	Mutation	OGC immunostaining
Patient 1	M	Benign	*SLC25A11*	Weak
CIT_207	F	Benign	*SDHC*	Positive
CIT_208	M	Metastatic	*SDHB*	Positive
CIT_158	M	Benign	*SDHD*	Positive
10H2558	F	Benign	*SDHB*	Positive
CIT_201	F	Metastatic	*SDHB*	Positive
14H21172	F	Benign	*SDHA*	Positive
CIT_121	F	Metastatic	*FH*	Positive
CIT_044	F	Benign	*RET*	Positive
CIT_133	F	Benign	*RET*	Positive
06H409	M	Benign	*RET*	Positive
CIT_072	F	Benign	*NF1s*	Positive
CIT_033	F	Benign	*NF1s*	Positive
CIT_120	F	Benign	*NF1s*	Positive
08h2722	F	Benign	*NF1*	Positive
166556	F	Benign	*TMEM127*	Positive
CIT_126	M	Benign	*MAX*	Positive
CIT_132	F	Benign	*MAXs*	Positive
CIT_059	F	Benign	*MAXs*	Positive
CIT_031	F	Benign		Positive
CIT_119	F	Benign		Positive

Table S2. Evaluation of OGC immunostaining in a series of PPGL with different genotypes. OGC expression is positive in all PPGL tissues, except in the *SLC25A11* mutated one.

SNV	Gene location	Protein location	Allele frequencies in this study (%)	EXAC allele frequencies (%)
rs138852681	c.262C>T	p.(Leu88Leu)	0.08	0.22
rs375769507	c.492G>C	p.(Val164Val)	0.16	0.01
rs201612668	c.547-34G>A	p.?	0.23	0.06
rs144541813	c.638-17C>T	p.?	0.08	0.01
rs73973661	c.738-14G>A	p.?	0.47	0.24
rs375082797	c.789+30G>C	p.?	0.23	0.02
rs145172608	c.849G>A	p.(Thr283Thr)	0.23	0.06

Table S3. Allelic frequencies of single nucleotide polymorphisms identified in *SLC25A11* gene by Sanger sequencing of 639 patients with PPGL and in the EXAC database (http://exac.broadinstitute.org/gene/ENSG00000108528).

REFERENCES

1. Letouze E, Martinelli C, Loriot C, Burnichon N, Abermil N, Ottolenghi C, et al. SDH mutations establish a hypermethylator phenotype in paraganglioma. Cancer cell. 2013;23:739-52.

2- **Dissection des mécanismes de tumorigenèse induits par l'inactivation de *SLC25A11 :* nouvelles données de métabolomique**

Suite à cette publication, notre objectif a été d'approfondir les connaissances sur les mécanismes moléculaires de la tumorigenèse *SLC25A11*-dépendante et les adaptations métaboliques mises en place par les cellules KO inactivées pour ce gène. En collaboration avec le Dr Daniel Tennant de l'Université de Birmingham, nous avons réalisé des dosages par spectrométrie de masse des différents métabolites présents dans les mitochondries des cellules WT et des cellules *Slc25a11*$^{\Delta/\Delta}$. L'objectif était de mieux comprendre les échanges de métabolites entre les compartiments cytosoliques et mitochondriaux secondaires à l'inactivation de ce transporteur mitochondrial, et plus précisément du 2-OG. En effet, notre hypothèse était que le 2-OG ne pouvait pas sortir de la mitochondrie, ce expliquerait la tumorigenèse secondaire à l'inactivation de *SLC25A11*.
Pour ce faire nous avons traité les cellules WT et *Slc25a11*$^{\Delta/\Delta}$ par la digitonine, ce traitement permettant de perméabiliser la membrane cellulaire et ainsi d'éliminer le contenu du cytosol. Les dosages réalisés après traitement sont donc le reflet des métabolites présents dans la mitochondrie.
La perméabilisation par la digitonine a été contrôlée par un Western blot utilisant les 3 anticorps primaires suivants, comme précédemment décrit (234) :
- anti-GAPDH (évalue l'élimination du cytosol),
- anti-cytochrome C (évalue l'intégrité de la membrane externe mitochondriale),
- anti-PCK2 (évalue l'intégrité de la membrane interne et la matrice mitochondriale).

Le premier essai réalisé en quadriplicats sur les cellules WT et les clones 6 *Slc25a11*$^{\Delta/\Delta}$ a montré une bonne perméabilisation par la digitonine (25 ug/ml pour les clone 6 et 30 ug/ml pour les WT) (**Figure 15**), et suggéré ainsi que le traitement n'avait pas lésé les mitochondries.

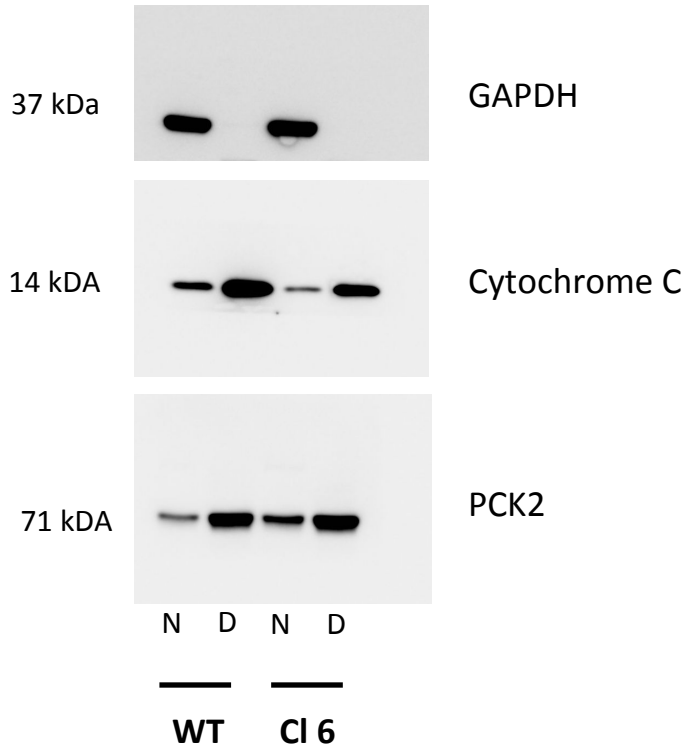

Figure 15 : Western blot anti-GAPDH, anti-PCK2 et anti-Cytochrome C sur les cellules WT et les clones 6 *Slc25a11*$^{\Delta/\Delta}$, traités ou non à la digitonine.
N : non traités par la digitonine, D : traités à la digitonine.

La quantification des métabolites intra-mitochondriaux par résonance magnétique montre que le 2-OG est à un niveau équivalent dans les mitochondries des cellules WT et des cellules *Slc25a11*$^{\Delta/\Delta}$. Nous avions pu démontrer dans l'article que le 2-OG dans les cellules entières était abaissé dans les cellules *Slc25a11*$^{\Delta/\Delta}$**.** Ces deux résultats suggèrent que le 2-OG ne peut pas sortir de la mitochondrie du fait du KO de *Slc25a11* (**Figure 16**). Ces premiers résultats, s'ils sont bien confirmés lors de la répétition de ces expériences et des dosages (en cours), expliqueraient la tumorigenèse secondaires à l'inactivation de *SLC25A11*, où l'appauvrissement en 2-OG cytosolique, dû à sa rétention dans la mitochondrie, conduirait à une perte d'activité des enzymes 2-OG dépendantes.

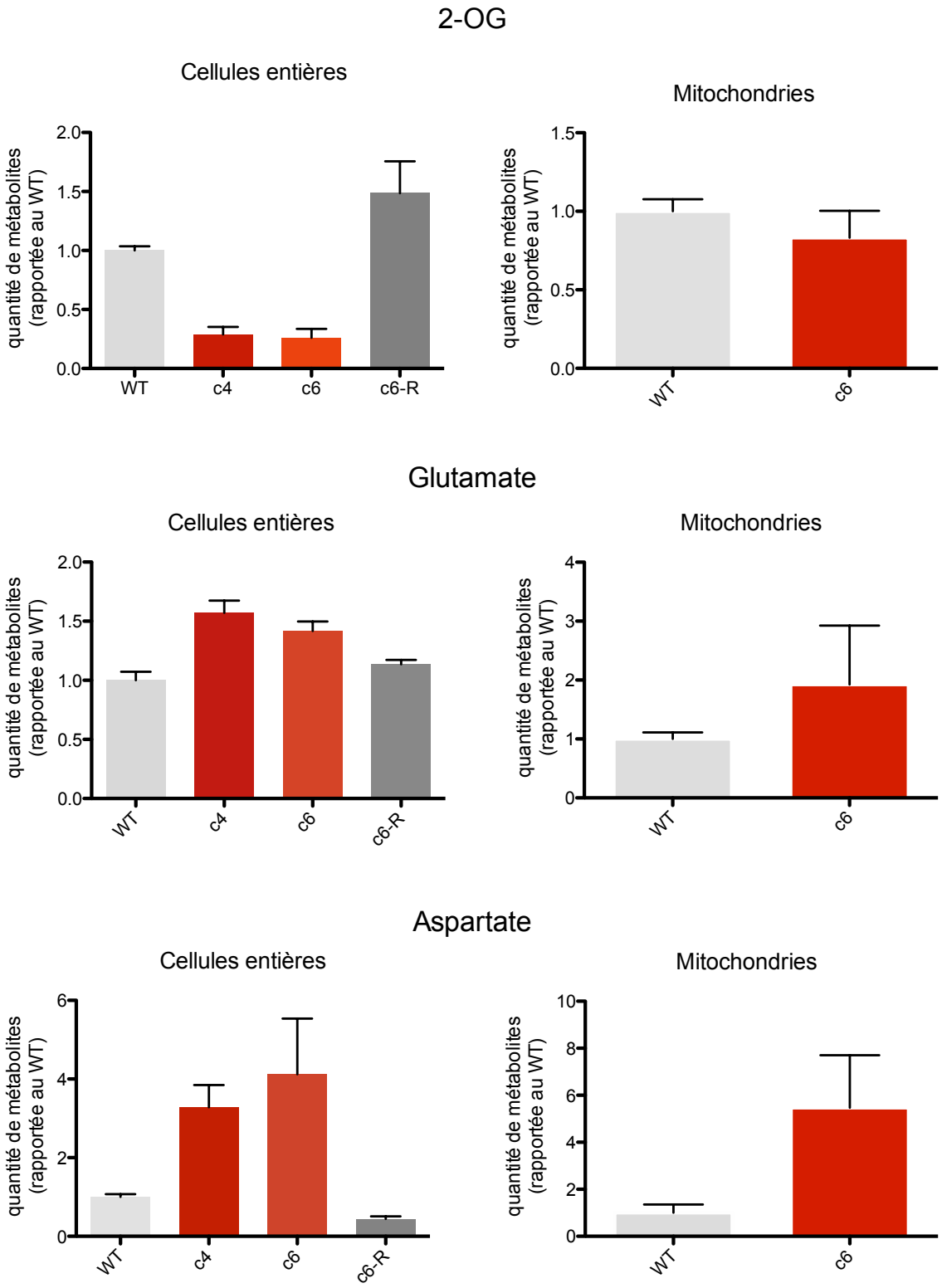

Figure 16 : Dosage de métabolites dans les cellules WT et *Slc25a11*$^{\Delta/\Delta}$ réalisé en cellules entières (à gauche) et sur la fraction mitochondriale (à droite).

Des flux métaboliques au glucose et à la glutamine marqués en C^{13} ont été également réalisés sur ces fractions mitochondriales. Leur analyse est en cours, les flux métaboliques sur cellules entières n'ayant montré que peu de différences (**Figure 17**).

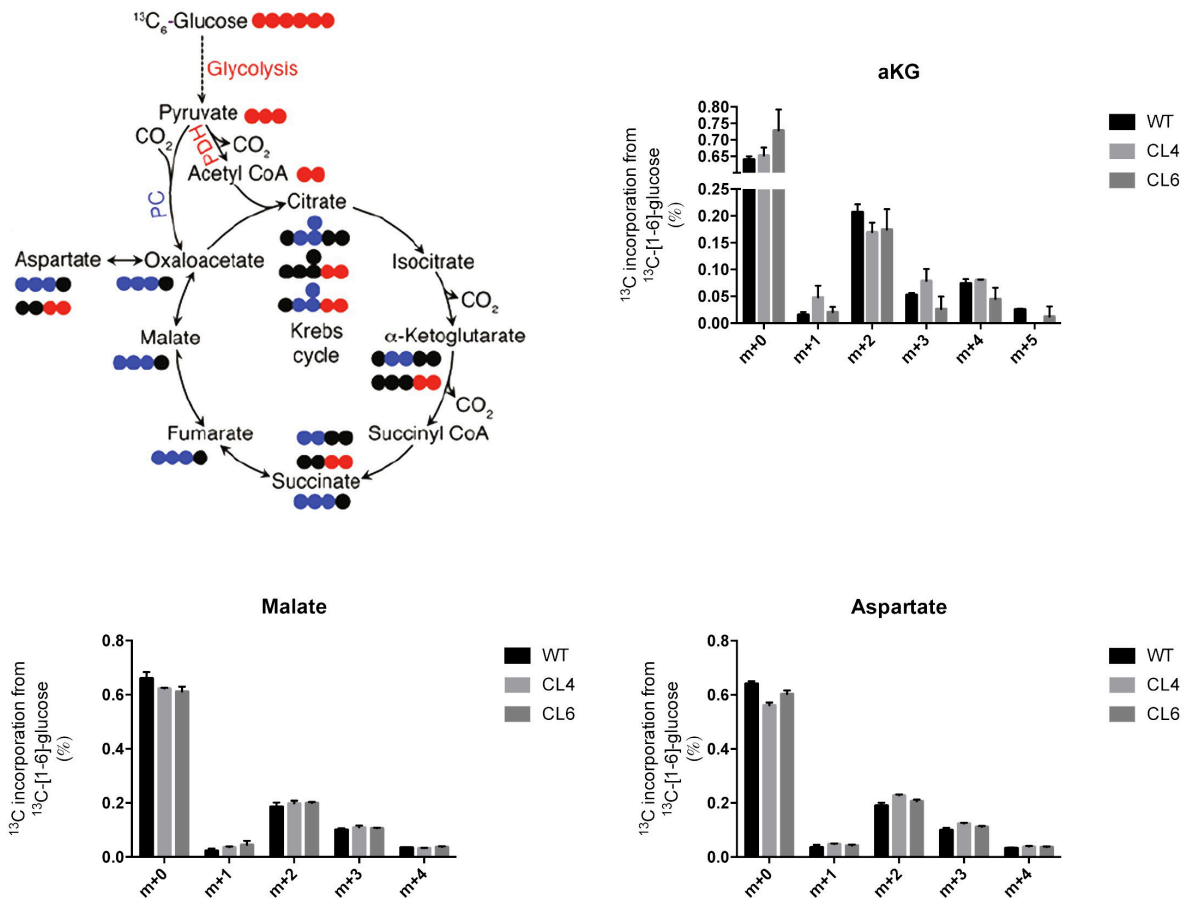

Figure 17 : Flux métaboliques après incorporation de ^{13}C-glucose et analyse par spectrométrie de masse dans les cellules WT et *Slc25a11*$^{\Delta/\Delta}$ (clones 4 et 6).

3- **Perspectives ouvertes par les résultats des autres whole-exome sequencing**

Je me suis ensuite intéressé aux résultats d'exome des 12 autres patients et j'ai trouvé une mutation somatique délétère du gène *CSDE1* (Cold shock domain-containing protein E1). Ce gène intervient dans le développement embryonnaire, la stabilité des ARNm et l'apoptose (235, 236). Comme mentionné dans l'introduction

de ce document, des mutations somatiques de *CSDE1* ont été décrites au cours de ma thèse par le TCGA chez quatre patients ayant des phéochromocytomes bénins dont le diagnostic a été fait au-delà de cinquante ans. Il s'agissait de quatre mutations perte de fonction associées à une perte d'hétérozygotie entrainant une diminution d'expression du transcrit de *CSDE1*. Les mutations de ce gène activeraient la voie Wnt-βcaténine (210).

J'ai identifié la mutation *CSDE1* chez HS_021, uniquement au niveau somatique (**Figure 18**). Il s'agit d'une mutation non-sens (c.2119C>T, p.Gln707Ter, NM_001242891) non décrite dans la base de données d'exomes GnomAD, située dans un domaine fonctionnel de la protéine. Le chromatographe est en faveur d'une perte d'hétérozygotie, et les données du transcriptome de la tumeur montrent une franche sous expression du transcrit de *CSDE1* (**Figure 18**), comme cela a été décrit précédemment (210). Pour valider l'implication de ce gène et la pathogénicité du variant nous allons réaliser une immunohistochimie anti-βcaténine prochainement.

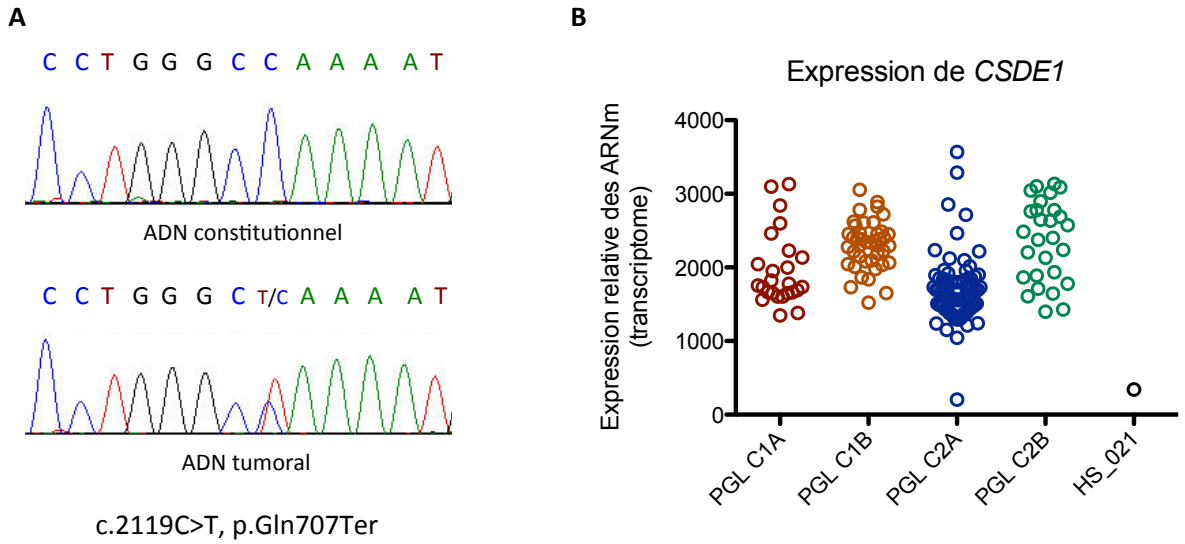

Figure 18 : Mutation somatique du gène *CSDE1* chez HS_021 (A), et expression de *CSDE1* dans les différents PGL du transcriptome (B).

A la suite de ces résultats, nous avons repris les données d'expression de CSDE1 issues du transcriptome de la collection de PPGL du réseau COMETE. De façon intéressante, nous avons observé qu'une des tumeurs classées par le transcriptome

dans le cluster C2A présente aussi une sous expression marquée de *CSDE1* **(Figure 18).** Nous avions précédemment mis en évidence une mutation somatique de *NF1* sur cette tumeur. Pour tester l'hypothèse d'un digénisme, nous allons séquencer *CSDE1* au niveau somatique et réaliser l'immunohistochimie anti-βcaténine sur ce phéochromocytome.

Enfin, dans les données des whole-exome sequencing j'ai identifié d'autres candidats. Toutefois ces gènes candidats n'ont pas été complétement validés à ce jour et feront l'objet de futures investigations.

CHAPITRE 3

Nouveaux mécanismes d'inactivation des gènes de prédisposition aux paragangliomes

I- CONTEXTE

Comme précédemment évoqué dans l'introduction, les mutations les plus souvent identifiées chez les patients avec un PGL sont localisées dans les des gènes *SDHx*, et une IHC SDHB peut permettre de détecter ces PGL *SDHx*-dépendants. Toutefois, une étude du réseau européen ENSAT a montré qu'environ 12 % des PGL avec une IHC SDHB négative n'ont pas de mutation constitutionnelle dans l'un des gènes *SDHx* (237). Il reste donc de nouveaux mécanismes d'inactivation des gènes *SDHx* à mettre en évidence.

Par ailleurs, les mutations des gènes *SDHx* peuvent également être responsables d'autres tumeurs, dont les tumeurs stromales gastrointestinales (GIST). La majorité des GIST, notamment chez l'adulte, sont secondaires à des mutations somatiques activatrices récurrentes dans les gènes *KIT* et *PDGFRA* qui sont les principaux *'drivers'* de cette pathologie tumorale (238, 239). Cependant, environ 15 % des GIST de l'adulte et 85 % des GIST pédiatriques n'ont pas de mutation dans ces deux gènes et sont individualisés sous la dénomination GIST *'Wild Type'* (183). De façon intéressante la majorité de ces GIST WT ont une IHC SDHB négative, et une mutation dans l'un des gènes *SDHx* est régulièrement retrouvée au niveau somatique ou constitutionnel chez ces patients (**Figure 19**) (183). La détermination de ce statut *SDHx* est importante pour ces patients qui ne répondent pas à l'imatinib contrairement aux GIST secondaires aux mutations dans les gènes *KIT* ou *PDGFRA* (240, 241).

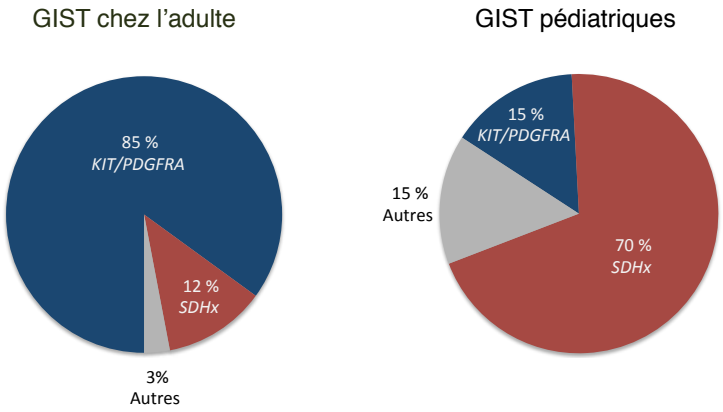

Figure 19 : Répartition des génotypes dans les GIST de l'adulte et les GIST pédiatriques d'après (183, 242).

Dans deux études publiées en 2014, il a été rapporté chez des patients avec des GIST à IHC SDHB négative et des dyades ou triades de Carney (qui sont l'association de PGL, GIST et chondromes pulmonaires pour la triade et de PGL et GIST pour la dyade), des épimutations du promoteur de *SDHC* (définie comme une altération épigénétique (dans ce cas une hyperméthylation spécifique du promoteur) menant à la répression transcriptionnelle de *SDHC*) (184, 243, 244).
Au début de ma thèse aucun patient avec un PGL n'avait été décrit avec une épimutation du promoteur de *SDHC*.
L'objectif de ce travail était de rechercher une épimutation du promoteur de *SDHC* parmi notre cohorte de patients ayant des PGL ou des GIST et une IHC anti-SDHB négative sans mutation identifiée dans un gène *SDHx*.

II- TRAVAUX EFFECTUES

1- **Patients et méthodes**

a- Patients

Nous avons sélectionné deux groupes de patients ayant déjà bénéficié de l'analyse constitutionnelle des gènes *SDHx* et d'une IHC anti-SDHB (**Table 11**):
- douze patients ayant un PGL avec une IHC anti-SDHB négative et sans mutation dans un gène *SDHx* identifiée sur les analyses constitutionnelles.
- sept patientes ayant une GIST avec IHC anti-SDHB négative. Deux patientes avaient une triade de Carney, deux une dyade de Carney, et trois des GIST isolées. Deux patientes avaient une mutation constitutionnelle dans le gène *SDHC* sans perte d'hétérozygotie dans le tissu tumoral.

PGL à IHC SDHB négative	**12**
Âge moyen au diagnostic	32 ans (19-52)
PGL unique	11
PGL multiples	1
Absence de mutation constitutionnelle *SDHx*	12
GIST à IHC SDHB négative	**7**
Âge moyen au diagnostic	17 ans (9-30)
PGL + GIST (Dyade de Carney)	2
PGL + GIST + Chondrome pulmonaire (Triade de Carney)	2
GIST isolée	3
Absence de mutation constitutionnelle *SDHx*	5
Mutation *SDHC* sans LOH	2

Table 11 : Caractéristiques cliniques et génétiques des deux groupes de patients étudiés.

Les âges sont exprimés en moyenne et valeurs extrêmes.

b- Conversion au bisulfite et pyroséquençage du promoteur de *SDHC*

L'ADN leucocytaire des patients des deux groupes a été extrait selon les protocoles standards, et l'analyse des gènes de prédisposition au PGL au niveau constitutionnel a été réalisée comme précédemment décrit (105, 229). L'ADN tumoral a été extrait avec les kits AllPrep pour les tumeurs congelées et DNA mini kit (Qiagen) pour les tumeurs incluses en paraffine.

Les ADN constitutionnels et tumoraux ont été traités au bisulfite en utilisant le kit EpiTect Plus DNA Bisulfite (Qiagen) selon le protocole du fabriquant.

Le pyroséquençage a été réalisé sur 7 CpG dans le promoteur du gène *SDHC*, qui ont été précédemment décrits comme hyperméthylés dans les précédentes publications (184, 244) : cinq CpG sont localisés avant le codon d'initiation de la traduction de *SDHC* et deux CpG au début de l'intron 1 (**Figure 20**). Les amorces permettant d'amplifier ces deux régions ainsi que les amorces utilisées pour le

séquençage ont été dessinées grâce au logiciel PyroMark Assay Design. Les PCR ainsi que le pyroséquençage ont été réalisés en utilisant les réactifs, équipements et logiciels PyroMark Q24 (Qiagen). Les résultats sont exprimés en moyenne de la méthylation des 7 CpG.

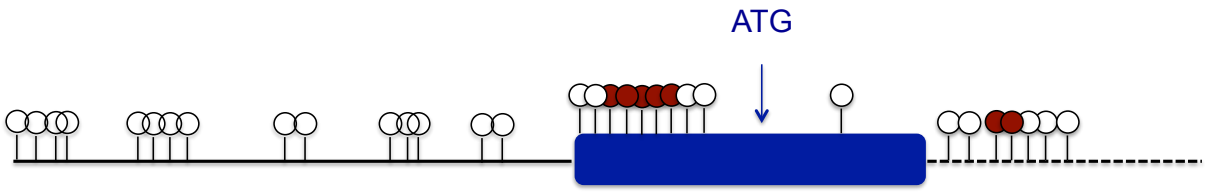

Figure 20 : Représentation schématique du promoteur de *SDHC* et de l'îlot CpG décrit comme méthylé dans les épimutations du promoteur de *SDHC*. Les CpG en rouge sont ceux explorés par pyroséquençage par les deux différentes PCR.

c- Séquençage haut débit des gènes *SDHx* sur l'ADN tumoral

Les exons et jonctions exons-introns des gènes de susceptibilité au PGL (*SDHx*, *VHL*, *EPAS1*, *EGLN1*, *EGLN2*, *NF1*, *RET*, *TMEM127*, *MAX*, *FH* et *MDH2*) ont été amplifiés en utilisant le kit SDH MASTR kit V2.0 (Multiplicom, Belgique). Les librairies ont été séquencées sur la plateforme MiSeq (Illumina, CA, USA) en utilisant la chimie v3 selon le protocole standard. Les alignements et le « variant calling » ont été réalisés en utilisant les logiciels SeqNEXT (JSI medical systems) et PolyDiag (Université Paris Descartes).

2- **Résultats**

La méthylation moyenne des 7 CpG explorés dans les tumeurs contrôles dont nous connaissons le génotype est toujours inférieure à 20 %. Nous n'avons pas mis en évidence d'hyperméthylation du promoteur de *SDHC* dans les régions explorées dans les ADN tumoraux des 12 patients avec un PGL à IHC SDHB-négative. Par contre, nous avons mis en évidence une épimutation du promoteur de *SDHC* au niveau tumoral chez 6 patientes sur 7 ayant une GIST à IHC anti-SDHB négative (**Figure 21**).

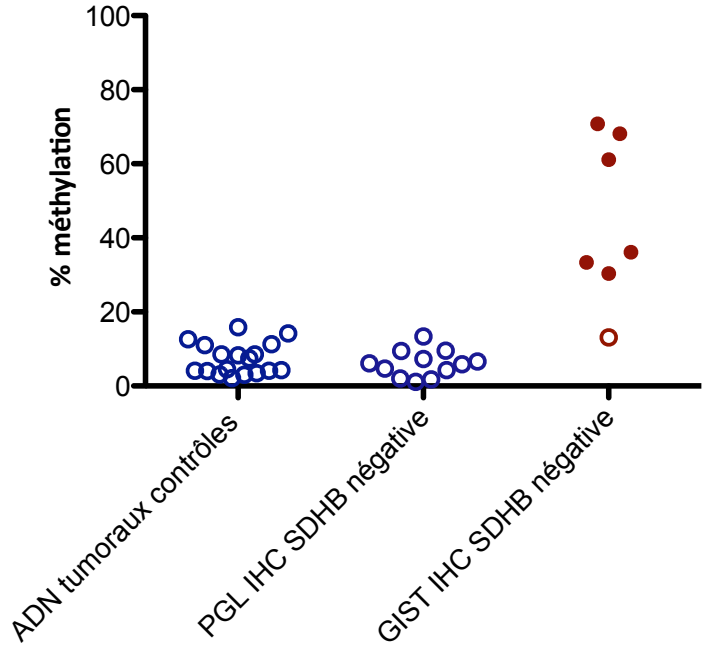

Figure 21 : Moyenne de la méthylation des 7 CpG explorés dans les ADN tumoraux contrôles et dans les deux groupes de patients.

Les points rouges pleins représentent les tumeurs dans lesquelles nous avons identifié une épimutation.

Trois des épimutations identifiées sont à l'état homozygote (les deux triades et une dyade de Carney) et trois épimutations sont à l'état hétérozygote (deux GIST isolées et une dyade de Carney). Parmi les trois patientes ayant une épimutation hétérozygote, deux d'entre elles étaient porteuses d'une mutation hétérozygote constitutionnelle de *SDHC* conduisant à une inactivation bi-allélique (**Table 12**).

Nous avons recherché un autre évènement mutationnel sur les gènes *SDHx* au niveau tumoral par séquençage haut débit (NGS *SDHx*) dans tous les GIST à IHC anti-SDHB négative, mais aucune autre mutation n'a été mise en évidence.

Patiente	Âge au diagnostic	Phénotype	épimutation *SDHC*	NGS *SDHx*
#1	14 ans	GIST multiples	Hétérozygote	Normal
#2	9 ans	GIST malins et PGL multiples	Hétérozygote	c.397C>T p.Arg133*
#3	15 ans	GIST multiples métastatiques	Hétérozygote	c.385T>C p.Trp129Arg
#4	15 ans	GIST et PGL multiples	Homozygote	Normal
#5	15 ans	GIST, PGL et chondromes pulmonaires multiples	Homozygote	Normal
#6	23 ans	GIST, PGL et chondromes pulmonaires multiples	Homozygote	Normal

Table 12 : Caractéristiques cliniques et génétiques des patientes ayant une épimutation du promoteur de *SDHC*. La recherche d 'épimutation et le NGS *SDHx* ont été fait sur l'ADN tumoral.

Nous avons ensuite évalué si ces épimutations étaient tumorales uniquement ou si elles étaient également présentes dans l'ADN constitutionnel, sous forme de mosaïque comme décrit dans 3 des 7 cas rapportés dans l'article de Killian *et al.* (184). L'épimutation n'était détectable dans l'ADN constitutionnel que dans un seul cas, chez la patiente #5 qui a une triade de Carney (**Figure 22**). En effet, la moyenne de la méthylation des 7 CpG au niveau constitutionnel était de 17 % dans l'ADN constitutionnel de cette patiente, alors que dans les ADN constitutionnels contrôles la méthylation était toujours inférieure à 10 %. De surcroit, nous avons pu mettre en évidence que l'épimutation était présente dans différents tissus tumoraux (GIST, chondrome pulmonaire) ou sain (rate) pour cette patiente, confirmant que l'épimutation de cette patiente était à l'état de mosaïque constitutionnelle (**Figure 23**).

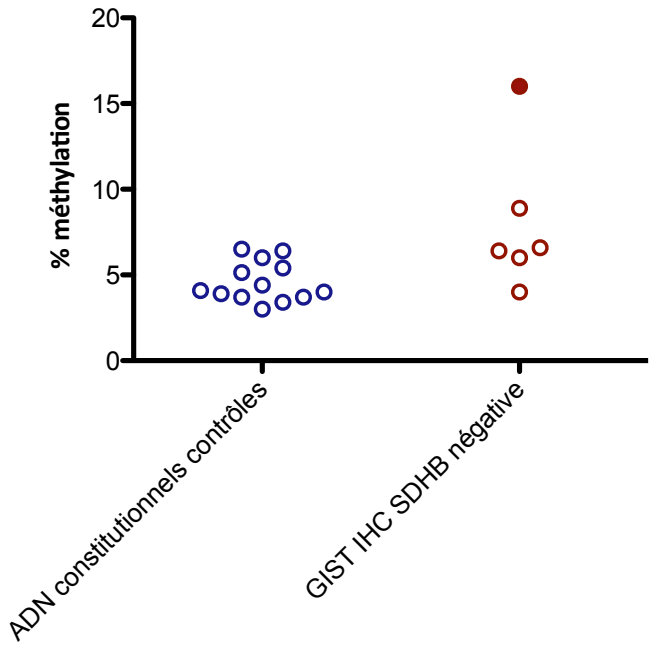

Figure 22 : Méthylation du promoteur de *SDHC* dans l'ADN constitutionnel des patientes porteuses d'une épimutation du promoteur de *SDHC* détectée dans l'ADN tumoral.

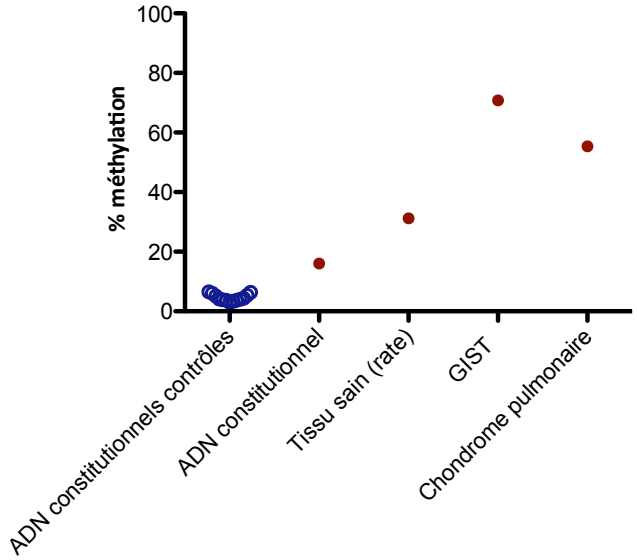

Figure 23 : Méthylation dans les différents tissus disponibles chez la patiente avec une épimutation détectable dans l'ADN constitutionnel (patiente #5).

3- **Discussion**

Nous avons mis en évidence une épimutation du promoteur de *SDHC* chez 6 patientes ayant développé une GIST et présentant une perte de l'expression de la protéine SDHB à l'IHC, dont un cas prouvé en mosaïque.

Ces épimutations seraient présentes dans 22 % des GIST WT et 25 % des GIST à IHC anti-SDHB négative selon les chiffres d'une étude récente sur 95 GIST WT publiée au cours de ma thèse (183). Toutefois cet évènement semble rare chez les patients avec PGL, car seules deux patientes ont été décrites jusqu'alors (207, 245). Il s'agit d'une patiente de 33 ans avec deux PGL abdominaux et d'une patiente avec une dyade de Carney (207). De façon étonnante, nous n'avons pas retrouvé d'épimutation du promoteur de *SDHC* dans notre cohorte de patients ayant un PGL avec une IHC anti-SDHB négative. Les deux PCR que j'ai utilisées couvrent deux des régions décrites comme hyperméthylées dans les épimutations du promoteur de *SDHC*. Ainsi la région en amont de l'ATG est la région explorée dans tous les articles publiés sur le sujet (184, 207, 244-246). Toutefois le papier princeps avait décrit une zone de 656 pb comme différentiellement méthylée, que nous n'avons pas explorée en intégralité ce qui explique peut-être une partie de ces résultats négatifs. De plus, ces PGL pourraient tout à fait être porteurs d'une autre épimutation sur un autre gène *SDHx*. Les premiers résultats du pyroséquençage du promoteur de *SDHB* que j'ai réalisé sur le même prélèvement ne semblent pas impliquer ce gène.

Des mutations du promoteur de *SDHD* ont été décrites dans les mélanomes (247-250). Nous avons recherché ces mutations récurrentes du promoteur de *SDHD* chez nos patients, mais sans succès.

De façon intéressante, la majorité des patients chez qui nous avons identifié une épimutation du promoteur de *SDHC* sont des femmes, ce qui est en accord avec les données de la littérature, où à notre connaissance un seul homme avec une GIST est porteur d'une épimutation du promoteur de *SDHC* (183, 184). Ce déséquilibre de

sexe ratio soulève la question de l'influence du chromosome X ou des hormones sexuelles sur la genèse de ces épimutations.

Le mécanisme de ces épimutations reste pour le moment mystérieux. Tout d'abord le caractère primaire ou secondaire de ces épimutations n'a pas été complètement démontré. En effet, les épimutations secondaires sont définies par une épimutation secondaire à un évènement mutationnel génétique en cis, comme par exemple dans les épimutations de *MSH2* secondaires aux délétions de *EPCAM* ou les épimutations de *MLH1* secondaires à des mutations du promoteur de *MLH1* ou des grands réarrangements du gène (251, 252). Dans le papier princeps, Killian et ses collaborateurs ont séquencé 130 kb autour de *SDHC* par séquençage haut débit de l'ADN tumoral des patients ayant une épimutation sans qu'un autre évènement n'ait été mis en évidence, ce qui suggèrent que ces épimutations seraient primaires (184). Nous n'avons pas pu confirmer ces résultats sur les tumeurs dans lesquelles nous avons mis en évidence une épimutation.

La détermination du statut primaire ou secondaire de ces épimutations est important pour la prédiction de la ségrégation familiale et donc pour le conseil génétique dans les familles des patients atteints. En effet, les épimutations secondaires se transmettent de façon autosomique dominante, alors que les épimutations primaires s'effacent au cours de la gamétogenèse, et donc ne se transmettront pas *a priori* à la descendance. Toutefois, deux cas exceptionnels de transmission familiale non mendélienne d'une épimutation primaire du promoteur de *MLH1* ont été décrites, toutes deux transmises par la mère (252).
Nos patientes ayant une épimutation du promoteur de *SDHC* n'ont pas d'histoire familiale de GIST ou de PGL, notamment la patiente #5 avec l'épimutation en mosaïque constitutionnelle. De plus le fait que cette épimutation soit présente à l'état de mosaïque rend peu probable la transmission par un de ses parents, mais n'élimine pas la possibilité d'une transmission à sa descendance.

Tous ces éléments semblent indiquer que la recherche d'épimutation du promoteur de *SDHC* doit être réalisée chez les patients avec une GIST ou un PGL ayant une IHC anti-SDHB négative, et cela d'autant plus qu'il s'agit d'une femme, que les GIST sont gastriques, multiples, métastatiques, qu'elles surviennent chez un enfant (pédiatriques) ou que le patient a une association d'une GIST et d'un PGL. Pour être le plus sensible possible, cette recherche d'épimutation doit débuter sur l'ADN tumoral.

CONCLUSIONS ET PERSPECTIVES

Mes travaux de thèse se sont articulés autour de deux grands projets :
1) un projet de recherche clinique, mené sur une grande cohorte de 221 patients suivis en France dans différents centres, qui a permis d'établir pour la première fois l'impact positif de la connaissance du statut génétique au moment du diagnostic du premier PGL sur la prise en charge et l'évolution des patients ;
2) un projet de recherche fondamentale qui a permis l'identification d'un nouveau gène de prédisposition au PGL d'une part et la confirmation de l'implication de nouveaux mécanismes d'inactivation de gènes de prédisposition préalablement connus d'autre part.

L'étude de recherche clinique que j'ai menée durant ma thèse a mis en lumière le bénéfice de l'identification d'une mutation constitutionnelle dans l'un des gènes majeurs de prédisposition au PGL chez les cas index. Ainsi, après des études ayant préalablement démontré l'impact sur la survie de la connaissance du statut mutationnel dans des cancers fréquents comme le cancer du sein/ovaires liés aux mutations sur les gènes *BRCA* et du colon secondaires aux mutations sur l'un des gènes *MMR* ou le gène *APC*, il s'agit de la première étude qui démontre le bénéfice de la connaissance du statut génétique pour les patients atteints d'un cancer rare (253, 254). Les résultats de notre étude renforcent les recommandations européennes et américaines de prise en charge du PGL qui recommandent, selon l'avis des experts, la réalisation d'un test génétique chez tous patients avec un PGL (21, 230).
La première perspective de ce travail est maintenant d'étudier l'impact d'un test génétique positif chez les apparentés asymptomatiques. A l'occasion des visites que j'ai effectuées dans les différents centres, j'ai pu recueillir les données phénotypiques et de suivi de cette population. Les recommandations actuelles de suivi des patients asymptomatiques porteurs d'une mutation identifiée chez un cas index de leur famille sont de réaliser un suivi adapté à leur génotype mais toutefois, elles ne décrivent pas les modalités précises (types d'examens et rythmicité) de cette surveillance. En effet, au moment de la rédaction de ces recommandations, il n'existait pas d'études menées sur ce thème, sur un grand nombre de sujets, disponibles dans la littérature.

Cette question des modalités de surveillance des sujets génétiquement prédisposés au PGL est l'une des grandes questions cliniques qu'il reste à résoudre. Les données contenues dans le registre national du paragangliome héréditaire, PGL.R, coordonné par mon laboratoire d'accueil et auquel j'ai contribué durant ma thèse, permettront au moins en partie de répondre à cette interrogation. Ce registre devrait aussi être le support de nouvelles études dédiées à évaluer la pénétrance des différentes mutations et gènes *SDHx*, et à rechercher de nouveaux variants et gènes modificateurs comme le variant p.E318K du gène *MITF* (255) (**voir l'article 6 donné en Annexes**), à l'aide des nouvelles technologies de puces à ADN qui permettent de génotyper un grand nombre de SNPs ou par whole-exome sequencing/whole-genome sequencing afin d'expliciter l'expressivité variable des mutations au sein des familles à risque et *in fine* d'améliorer le conseil génétique.

Mon projet de recherche fondamentale a bénéficié des études de whole-exome sequencing réalisées sur la cohorte de PGL collectée par le réseau COMETE. Ces études m'ont permis d'identifier *SLC25A11* comme nouveau gène de prédisposition aux PGL malins. Ce gène est le deuxième gène, en termes de fréquence, derrière *SDHB* et devant *FH*, associé à la malignité, ce qui justifie son exploration en routine chez les patients notamment en raison du risque de développement de métastases métachrones apparaissant après la chirurgie initiale.

Avec l'identification de *SLC25A11*, mon travail de thèse a mis en évidence un nouvel acteur qui joue un rôle important dans les relations entre le cycle de Krebs, le métabolisme cellulaire et la cancérogenèse. Nous avons une hypothèse forte pour expliciter le mécanisme initial de la tumorigenèse *SLC25A11*-dépendante, mais cette hypothèse doit être validée à l'aide de nouveaux dosages des métabolites dans les fractions mitochondriales et par l'évaluation des différents éléments du phénotype cellulaire après traitement au 2-oxoglutarate, comme nous l'avons réalisé précédemment pour l'étude de la migration collective publiée dans *Cancer Research*. De plus, les études de flux métaboliques actuellement en cours menées sur les cellules inactivées pour *Slc25a11* en collaboration avec Daniel Tennant (Université

de Cambridge) devraient permettre d'identifier les voies métaboliques permettant de compenser l'inactivation de SLC25A11 et donc de pouvoir envisager ensuite des expériences de létalité synthétique qui pourraient aboutir à plus long terme à l'émergence de nouveaux traitements spécifiques pour les patients porteurs d'une mutation *SLC25A11*.

Sur le plan clinique, la pénétrance des mutations de *SLC25A11* chez les patients n'est pas connue actuellement. Les enquêtes familiales en cours devraient nous permettre de l'estimer et ainsi d'affiner l'information délivrée aux familles lors du conseil génétique et de préciser le rythme et les modalités de surveillance à proposer aux patients asymptomatiques identifiés comme porteurs des mutations par le dépistage génétique familial. Enfin, les études du TCGA et les histoires familiales contenues dans les arbres généalogiques des patients chez qui les premières mutations ont été identifiées semblent suggérer que les mutations constitutionnelles de ce gène pourraient prédisposer à d'autres types de cancers, ce point important devra être précisé par les enquêtes familiales.

L'étude des données de whole-exome sequencing m'a aussi permis de confirmer l'implication des mutations *CSDE1* dans les PGL. Toutefois, la fréquence exacte des mutations somatiques de ce gène reste peu connue. Si l'étude pilote en cours menée sur la cohorte COMETE dédiée à évaluer les performances de l'immunohistochimie anti-βcatenine pour la détection des mutations *CSDE1* s'avère concluante, nous pourrons utiliser cette IHC sur la cohorte prospective de PGL collectée dans le cadre du PRTK COMETE TACTIC, pour déterminer la fréquence des mutations.

La quête de nouveaux gènes du PGL doit se poursuivre. Parmi les 11 premiers patients, sélectionnés à partir des données de génomique intégrative obtenues sur leur tumeur et pour lesquels des données de whole-exome sequencing ont été générées, j'ai identifié une mutation constitutionnelle potentiellement causale dans de nouveaux gènes candidats dans quelques cas , mais pas pour l'ensemble des patients ayant bénéficié de ces analyses, probablement parce que la majorité d'entre

eux avaient un PGL dont la présentation clinique était d'apparence sporadique. Plus récemment, nous avons sélectionné de nouveaux patients sur une suspicion clinique qu'ils soient porteurs d'une forme de PGL génétiquement déterminée car ils étaient atteints d'un PGL multiple ou qu'ils avaient des antécédents familiaux de PGL. Pour ces patients, le whole-exome sequencing sur le couple ADN constitutionnel/ADN tumoral, ainsi que le RNA-sequencing sur l'ARN tumoral ont été réalisés. Les variations génétiques déjà mises en évidence ainsi que celles qui seront identifiées grâce à l'interprétation des nouveaux séquençage d'exomes (dont l'interprétation sera facilitée par les résultats du RNA-sequencing), vont être validées en réalisant des analyses fonctionnelles au niveau tumoral, et en recherchant de nouveau patients porteurs de variations dans ces gènes parmi les patients testés dans le laboratoire de génétique. La poursuite de ce programme de recherche sera notamment confiée à une étudiante de Master 2 qui a obtenu une bourse de la Fondation pour la Recherche Médicale pour mener ce projet durant l'année 2018/2019 et que je participerai à encadrer.

À côté de ces nouveaux gènes de prédisposition, certains PGL sans cause génétique identifiée ont été finalement expliqués par des mécanismes mutationnels autres que des mutations ponctuelles dans les exons des gènes de prédisposition connus. Par exemple, durant ma thèse j'ai identifié des épimutations du promoteur de *SDHC* chez des patients ayant des GIST dont l'IHC anti-SDHB était négative, comme décrit préalablement dans la littérature à partir de données de méthylome, et transféré le protocole de pyroséquençage développé pour les mettre en évidence au laboratoire de génétique de l'HEGP afin que ce test soit accessible en routine diagnostique. Toutefois, ces épimutations ne sont pas l'explication de tous les cas de PGL ou GIST à IHC anti-SDHB négative, et l'exploration des promoteurs des autres gènes *SDHx* est à envisager, tant pour rechercher de nouvelles épimutations que de variations génétiques. Des altérations des zones régulatrices intra- ou inter-géniques des gènes *SDHx* pourraient également être impliquées, et nous prévoyons de réaliser l'analyse des interactions chromatine-chromatine à l'aide des nouvelles

techniques de capture de la conformation des chromosome couplées au séquençage haut débit (‘4C’ pour Chromosome Conformation Capture-on-Chip).

Enfin, au cours de ma thèse, il a aussi été décrit un nouveau mécanisme d’inactivation du gène *VHL*. En effet l’équipe de Betty Gardie a mis en évidence un nouvel exon, cryptique, du gène *VHL*, localisé dans l’intron 1. Cet exon E’1 est le siège de mutations chez des patients ayant un phénotype de maladie de von Hippel-Lindau sans mutation dans les trois exons connus du gène *VHL* (256) (**Voir l’article 7 donné en Annexes**). C’était le cas d’une famille de VHL de type 2C qui avait été vue en consultation d’oncogénétique à l’HEGP où le cas index était une petite fille de 11 ans avec un phéochromocytome et dont le père et le grand-père avaient développé des PGL. Cette famille était porteuse d’une variation apparemment silencieuse de *VHL*, qui entraine une rétention de cet exon cryptique. Nous coordonnons actuellement une grande étude internationale sur plus de 800 patients impliquant les principaux laboratoires Français d’oncogénétique du centre de référence de la maladie de von Hippel Lindau (PREDIR) ainsi que les équipes de Patricia Dahia à San Antonio (USA) et de Mercedes Robledo à Madrid (Espagne) afin de déterminer la fréquence des mutations de l’exon cryptique de *VHL* chez les patients porteurs de PGL/PH ou d’un pseudo-VHL. Nous avons identifié pour l’instant quatre mutations constitutionnelles de E’1 chez deux patients avec un PH et deux patients avec un PGL cervical parmi les 356 patients avec PGL que nous avons déjà analysés, ce qui suggère que le taux mutationnel pourrait se situer aux alentours de 1%.

Pour conclure, mon travail de thèse ainsi que les travaux de recherches menés par d’autres étudiants ou collaborateurs de mon équipe d’accueil et auxquels j’ai pu participer ces dernières années (donnés en Annexes) ont permis de faire avancer les connaissances sur la génétique des PGL/PH, mais aussi d’ouvrir de nouvelles perspectives de recherche intéressantes.

BIBLIOGRAPHIE

1. Lee KY, Oh YW, Noh HJ, Lee YJ, Yong HS, Kang EY, et al. Extraadrenal paragangliomas of the body: imaging features. AJR American journal of roentgenology. 2006;187:492-504.
2. Adams MS, Bronner-Fraser M. Review: the role of neural crest cells in the endocrine system. Endocrine pathology. 2009;20:92-100.
3. Knecht AK, Bronner-Fraser M. Induction of the neural crest: a multigene process. Nature reviews Genetics. 2002;3:453-61.
4. Furlan A, Dyachuk V, Kastriti ME, Calvo-Enrique L, Abdo H, Hadjab S, et al. Multipotent peripheral glial cells generate neuroendocrine cells of the adrenal medulla. Science. 2017;357.
5. Furlan A, Adameyko I. Schwann cell precursor: a neural crest cell in disguise? Developmental biology. 2018.
6. Flatmark T. Catecholamine biosynthesis and physiological regulation in neuroendocrine cells. Acta physiologica Scandinavica. 2000;168:1-17.
7. Schulz C, Eisenhofer G, Lehnert H. Principles of catecholamine biosynthesis, metabolism and release. Frontiers of hormone research. 2004;31:1-25.
8. Nagatsu T, Stjarne L. Catecholamine synthesis and release. Overview. Advances in pharmacology. 1998;42:1-14.
9. Stenstrom G, Svardsudd K. Pheochromocytoma in Sweden 1958-1981. An analysis of the National Cancer Registry Data. Acta medica Scandinavica. 1986;220:225-32.
10. Beard CM, Sheps SG, Kurland LT, Carney JA, Lie JT. Occurrence of pheochromocytoma in Rochester, Minnesota, 1950 through 1979. Mayo Clinic proceedings. 1983;58:802-4.
11. Anderson GH, Jr., Blakeman N, Streeten DH. The effect of age on prevalence of secondary forms of hypertension in 4429 consecutively referred patients. Journal of hypertension. 1994;12:609-15.
12. Luton JP, Martinez M, Coste J, Bertherat J. Outcome in patients with adrenal incidentaloma selected for surgery: an analysis of 88 cases investigated in a single clinical center. European journal of endocrinology. 2000;143:111-7.
13. Ariton M, Juan CS, AvRuskin TW. Pheochromocytoma: clinical observations from a Brooklyn tertiary hospital. Endocrine practice : official journal of the American College of Endocrinology and the American Association of Clinical Endocrinologists. 2000;6:249-52.
14. Lo CY, Lam KY, Wat MS, Lam KS. Adrenal pheochromocytoma remains a frequently overlooked diagnosis. American journal of surgery. 2000;179:212-5.
15. Amar L, Servais A, Gimenez-Roqueplo AP, Zinzindohoue F, Chatellier G, Plouin PF. Year of diagnosis, features at presentation, and risk of recurrence in patients with pheochromocytoma or secreting paraganglioma. The Journal of clinical endocrinology and metabolism. 2005;90:2110-6.
16. Lenders JW, Eisenhofer G, Mannelli M, Pacak K. Phaeochromocytoma. Lancet. 2005;366:665-75.
17. Plouin PF, Chatellier G, Delahousse M, Rougeot MA, Duclos JM, Pagny JY, et al. [Detection, diagnosis and localization of pheochromocytoma. 77 cases in a population of 21,420 hypertensive patients]. Presse medicale. 1987;16:2211-5.
18. Bravo EL, Tagle R. Pheochromocytoma: state-of-the-art and future prospects. Endocrine reviews. 2003;24:539-53.

19. Giavarini A, Chedid A, Bobrie G, Plouin PF, Hagege A, Amar L. Acute catecholamine cardiomyopathy in patients with phaeochromocytoma or functional paraganglioma. Heart. 2013;99:1438-44.
20. Capatina C, Ntali G, Karavitaki N, Grossman AB. The management of head-and-neck paragangliomas. Endocrine-related cancer. 2013;20:R291-305.
21. Lenders JW, Duh QY, Eisenhofer G, Gimenez-Roqueplo AP, Grebe SK, Murad MH, et al. Pheochromocytoma and paraganglioma: an endocrine society clinical practice guideline. The Journal of clinical endocrinology and metabolism. 2014;99:1915-42.
22. Eisenhofer G, Keiser H, Friberg P, Mezey E, Huynh TT, Hiremagalur B, et al. Plasma metanephrines are markers of pheochromocytoma produced by catechol-O-methyltransferase within tumors. The Journal of clinical endocrinology and metabolism. 1998;83:2175-85.
23. Eisenhofer G, Lenders JW. Clues to the diagnosis of pheochromocytoma from the differential tissue metabolism of catecholamines. Advances in pharmacology. 1998;42:374-7.
24. Lenders JW. Biochemical diagnosis of pheochromocytoma and paraganglioma. Annales d'endocrinologie. 2009;70:161-5.
25. Lenders JW, Pacak K, Walther MM, Linehan WM, Mannelli M, Friberg P, et al. Biochemical diagnosis of pheochromocytoma: which test is best? Jama. 2002;287:1427-34.
26. Peaston RT, Graham KS, Chambers E, van der Molen JC, Ball S. Performance of plasma free metanephrines measured by liquid chromatography-tandem mass spectrometry in the diagnosis of pheochromocytoma. Clinica chimica acta; international journal of clinical chemistry. 2010;411:546-52.
27. Unger N, Pitt C, Schmidt IL, Walz MK, Schmid KW, Philipp T, et al. Diagnostic value of various biochemical parameters for the diagnosis of pheochromocytoma in patients with adrenal mass. European journal of endocrinology. 2006;154:409-17.
28. Grouzmann E, Drouard-Troalen L, Baudin E, Plouin PF, Muller B, Grand D, et al. Diagnostic accuracy of free and total metanephrines in plasma and fractionated metanephrines in urine of patients with pheochromocytoma. European journal of endocrinology. 2010;162:951-60.
29. Pamporaki C, Darr R, Bursztyn M, Glockner S, Bornstein SR, Lenders JW, et al. Plasma-free vs deconjugated metanephrines for diagnosis of phaeochromocytoma. Clinical endocrinology. 2013;79:476-83.
30. Weismann D, Peitzsch M, Raida A, Prejbisz A, Gosk M, Riester A, et al. Measurements of plasma metanephrines by immunoassay vs liquid chromatography with tandem mass spectrometry for diagnosis of pheochromocytoma. European journal of endocrinology. 2015;172:251-60.
31. Rao D, Peitzsch M, Prejbisz A, Hanus K, Fassnacht M, Beuschlein F, et al. Plasma methoxytyramine: clinical utility with metanephrines for diagnosis of pheochromocytoma and paraganglioma. European journal of endocrinology. 2017;177:103-13.
32. van Duinen N, Corssmit EP, de Jong WH, Brookman D, Kema IP, Romijn JA. Plasma levels of free metanephrines and 3-methoxytyramine indicate a higher number of biochemically active HNPGL than 24-h urinary excretion rates of catecholamines and metabolites. European journal of endocrinology. 2013;169:377-82.

33. van Duinen N, Steenvoorden D, Kema IP, Jansen JC, Vriends AH, Bayley JP, et al. Increased urinary excretion of 3-methoxytyramine in patients with head and neck paragangliomas. The Journal of clinical endocrinology and metabolism. 2010;95:209-14.
34. Eisenhofer G, Lenders JW, Siegert G, Bornstein SR, Friberg P, Milosevic D, et al. Plasma methoxytyramine: a novel biomarker of metastatic pheochromocytoma and paraganglioma in relation to established risk factors of tumour size, location and SDHB mutation status. European journal of cancer. 2012;48:1739-49.
35. Darr R, Pamporaki C, Peitzsch M, Miehle K, Prejbisz A, Peczkowska M, et al. Biochemical diagnosis of phaeochromocytoma using plasma-free normetanephrine, metanephrine and methoxytyramine: importance of supine sampling under fasting conditions. Clinical endocrinology. 2014;80:478-86.
36. Eisenhofer G, Peitzsch M. Laboratory evaluation of pheochromocytoma and paraganglioma. Clinical chemistry. 2014;60:1486-99.
37. d'Herbomez M, Forzy G, Bauters C, Tierny C, Pigny P, Carnaille B, et al. An analysis of the biochemical diagnosis of 66 pheochromocytomas. European journal of endocrinology. 2007;156:569-75.
38. Plouin PF. Use of plasma chromogranin A and urine fractionated metanephrines to diagnose pheochromocytoma? Nature clinical practice Endocrinology & metabolism. 2008;4:314-5.
39. Brito JP, Asi N, Gionfriddo MR, Norman C, Leppin AL, Zeballos-Palacios C, et al. The incremental benefit of functional imaging in pheochromocytoma/paraganglioma: a systematic review. Endocrine. 2015;50:176-86.
40. Gimenez-Roqueplo AP, Caumont-Prim A, Houzard C, Hignette C, Hernigou A, Halimi P, et al. Imaging work-up for screening of paraganglioma and pheochromocytoma in SDHx mutation carriers: a multicenter prospective study from the PGL.EVA Investigators. The Journal of clinical endocrinology and metabolism. 2013;98:E162-73.
41. Ilias I, Chen CC, Carrasquillo JA, Whatley M, Ling A, Lazurova I, et al. Comparison of 6-18F-fluorodopamine PET with 123I-metaiodobenzylguanidine and 111in-pentetreotide scintigraphy in localization of nonmetastatic and metastatic pheochromocytoma. Journal of nuclear medicine : official publication, Society of Nuclear Medicine. 2008;49:1613-9.
42. Jacobson AF, Deng H, Lombard J, Lessig HJ, Black RR. 123I-meta-iodobenzylguanidine scintigraphy for the detection of neuroblastoma and pheochromocytoma: results of a meta-analysis. The Journal of clinical endocrinology and metabolism. 2010;95:2596-606.
43. Timmers HJ, Chen CC, Carrasquillo JA, Whatley M, Ling A, Havekes B, et al. Comparison of 18F-fluoro-L-DOPA, 18F-fluoro-deoxyglucose, and 18F-fluorodopamine PET and 123I-MIBG scintigraphy in the localization of pheochromocytoma and paraganglioma. The Journal of clinical endocrinology and metabolism. 2009;94:4757-67.
44. Elston MS, Meyer-Rochow GY, Conaglen HM, Clarkson A, Clifton-Bligh RJ, Conaglen JV, et al. Increased SSTR2A and SSTR3 expression in succinate dehydrogenase-deficient pheochromocytomas and paragangliomas. Human pathology. 2015;46:390-6.
45. Bustillo A, Telischi F, Weed D, Civantos F, Angeli S, Serafini A, et al. Octreotide scintigraphy in the head and neck. The Laryngoscope. 2004;114:434-40.
46. Bustillo A, Telischi FF. Octreotide scintigraphy in the detection of recurrent paragangliomas. Otolaryngology--head and neck surgery : official journal of American Academy of Otolaryngology-Head and Neck Surgery. 2004;130:479-82.

47. Taieb D, Sebag F, Barlier A, Tessonnier L, Palazzo FF, Morange I, et al. 18F-FDG avidity of pheochromocytomas and paragangliomas: a new molecular imaging signature? Journal of nuclear medicine : official publication, Society of Nuclear Medicine. 2009;50:711-7.
48. Favier J, Briere JJ, Burnichon N, Riviere J, Vescovo L, Benit P, et al. The Warburg effect is genetically determined in inherited pheochromocytomas. PloS one. 2009;4:e7094.
49. Timmers HJ, Chen CC, Carrasquillo JA, Whatley M, Ling A, Eisenhofer G, et al. Staging and functional characterization of pheochromocytoma and paraganglioma by 18F-fluorodeoxyglucose (18F-FDG) positron emission tomography. Journal of the National Cancer Institute. 2012;104:700-8.
50. Taieb D, Timmers HJ, Hindie E, Guillet BA, Neumann HP, Walz MK, et al. EANM 2012 guidelines for radionuclide imaging of phaeochromocytoma and paraganglioma. European journal of nuclear medicine and molecular imaging. 2012;39:1977-95.
51. Treglia G, Cocciolillo F, de Waure C, Di Nardo F, Gualano MR, Castaldi P, et al. Diagnostic performance of 18F-dihydroxyphenylalanine positron emission tomography in patients with paraganglioma: a meta-analysis. European journal of nuclear medicine and molecular imaging. 2012;39:1144-53.
52. King KS, Chen CC, Alexopoulos DK, Whatley MA, Reynolds JC, Patronas N, et al. Functional imaging of SDHx-related head and neck paragangliomas: comparison of 18F-fluorodihydroxyphenylalanine, 18F-fluorodopamine, 18F-fluoro-2-deoxy-D-glucose PET, 123I-metaiodobenzylguanidine scintigraphy, and 111In-pentetreotide scintigraphy. The Journal of clinical endocrinology and metabolism. 2011;96:2779-85.
53. Imani F, Agopian VG, Auerbach MS, Walter MA, Imani F, Benz MR, et al. 18F-FDOPA PET and PET/CT accurately localize pheochromocytomas. Journal of nuclear medicine : official publication, Society of Nuclear Medicine. 2009;50:513-9.
54. Fiebrich HB, Brouwers AH, Kerstens MN, Pijl ME, Kema IP, de Jong JR, et al. 6-[F-18]Fluoro-L-dihydroxyphenylalanine positron emission tomography is superior to conventional imaging with (123)I-metaiodobenzylguanidine scintigraphy, computer tomography, and magnetic resonance imaging in localizing tumors causing catecholamine excess. The Journal of clinical endocrinology and metabolism. 2009;94:3922-30.
55. Naswa N, Kumar A, Sharma P, Bal C, Malhotra A, Kumar R. Imaging carotid body chemodectomas with (6)(8)Ga-DOTA-NOC PET-CT. The British journal of radiology. 2012;85:1140-5.
56. Maurice JB, Troke R, Win Z, Ramachandran R, Al-Nahhas A, Naji M, et al. A comparison of the performance of (6)(8)Ga-DOTATATE PET/CT and (1)(2)(3)I-MIBG SPECT in the diagnosis and follow-up of phaeochromocytoma and paraganglioma. European journal of nuclear medicine and molecular imaging. 2012;39:1266-70.
57. Kroiss A, Shulkin BL, Uprimny C, Frech A, Gasser RW, Url C, et al. (68)Ga-DOTATOC PET/CT provides accurate tumour extent in patients with extraadrenal paraganglioma compared to (123)I-MIBG SPECT/CT. European journal of nuclear medicine and molecular imaging. 2015;42:33-41.
58. Han S, Suh CH, Woo S, Kim YJ, Lee JJ. Performance of (68)Ga-DOTA-Conjugated Somatostatin Receptor Targeting Peptide PET in Detection of Pheochromocytoma and Paraganglioma: A Systematic Review and Meta-Analysis. Journal of nuclear medicine : official publication, Society of Nuclear Medicine. 2018.

59. Janssen I, Blanchet EM, Adams K, Chen CC, Millo CM, Herscovitch P, et al. Superiority of [68Ga]-DOTATATE PET/CT to Other Functional Imaging Modalities in the Localization of SDHB-Associated Metastatic Pheochromocytoma and Paraganglioma. Clinical cancer research : an official journal of the American Association for Cancer Research. 2015;21:3888-95.
60. Janssen I, Chen CC, Taieb D, Patronas NJ, Millo CM, Adams KT, et al. 68Ga-DOTATATE PET/CT in the Localization of Head and Neck Paragangliomas Compared with Other Functional Imaging Modalities and CT/MRI. Journal of nuclear medicine : official publication, Society of Nuclear Medicine. 2016;57:186-91.
61. Tischler AS, deKrijger RR. 15 YEARS OF PARAGANGLIOMA: Pathology of pheochromocytoma and paraganglioma. Endocrine-related cancer. 2015;22:T123-33.
62. McNicol AM. Update on tumours of the adrenal cortex, phaeochromocytoma and extra-adrenal paraganglioma. Histopathology. 2011;58:155-68.
63. Plouin PF, Duclos JM, Soppelsa F, Boublil G, Chatellier G. Factors associated with perioperative morbidity and mortality in patients with pheochromocytoma: analysis of 165 operations at a single center. The Journal of clinical endocrinology and metabolism. 2001;86:1480-6.
64. Pacak K. Preoperative management of the pheochromocytoma patient. The Journal of clinical endocrinology and metabolism. 2007;92:4069-79.
65. Lim JY, Kim J, Kim SH, Lee S, Lim YC, Kim JW, et al. Surgical treatment of carotid body paragangliomas: outcomes and complications according to the shamblin classification. Clinical and experimental otorhinolaryngology. 2010;3:91-5.
66. Jansen TTG, Marres HAM, J HAMK, Kunst HPM. A meta-analysis on the surgical management of paraganglioma of the carotid body per Shamblin class. Clinical otolaryngology : official journal of ENT-UK ; official journal of Netherlands Society for Oto-Rhino-Laryngology & Cervico-Facial Surgery. 2018.
67. Sen I, Stephen E, Malepathi K, Agarwal S, Shyamkumar NK, Mammen S. Neurological complications in carotid body tumors: a 6-year single-center experience. Journal of vascular surgery. 2013;57:64S-8S.
68. Power AH, Bower TC, Kasperbauer J, Link MJ, Oderich G, Cloft H, et al. Impact of preoperative embolization on outcomes of carotid body tumor resections. Journal of vascular surgery. 2012;56:979-89.
69. Smith JD, Harvey RN, Darr OA, Prince ME, Bradford CR, Wolf GT, et al. Head and neck paragangliomas: A two-decade institutional experience and algorithm for management. Laryngoscope investigative otolaryngology. 2017;2:380-9.
70. Abu-Ghanem S, Yehuda M, Carmel NN, Abergel A, Fliss DM. Impact of preoperative embolization on the outcomes of carotid body tumor surgery: A meta-analysis and review of the literature. Head & neck. 2016;38 Suppl 1:E2386-94.
71. Smee RI, Jayasekara J, Williams JR, Hanna C. Paragangliomas: presentation and management by radiotherapy at the Prince of Wales Hospital. Journal of medical imaging and radiation oncology. 2015;59:229-35.
72. Zabel A, Milker-Zabel S, Huber P, Schulz-Ertner D, Schlegel W, Wannenmacher M, et al. Fractionated stereotactic conformal radiotherapy in the management of large chemodectomas of the skull base. International journal of radiation oncology, biology, physics. 2004;58:1445-50.
73. Cao KI, Feuvret L, Herman P, Bolle S, Jouffroy T, Goudjil F, et al. Protontherapy of head and neck paragangliomas: A monocentric study. Cancer radiotherapie : journal de la Societe francaise de radiotherapie oncologique. 2018;22:31-7.

74. Hescot S, Leboulleux S, Amar L, Vezzosi D, Borget I, Bournaud-Salinas C, et al. One-year progression-free survival of therapy-naive patients with malignant pheochromocytoma and paraganglioma. The Journal of clinical endocrinology and metabolism. 2013;98:4006-12.
75. Amar L, Fassnacht M, Gimenez-Roqueplo AP, Januszewicz A, Prejbisz A, Timmers H, et al. Long-term postoperative follow-up in patients with apparently benign pheochromocytoma and paraganglioma. Hormone and metabolic research = Hormon- und Stoffwechselforschung = Hormones et metabolisme. 2012;44:385-9.
76. Amar L, Baudin E, Burnichon N, Peyrard S, Silvera S, Bertherat J, et al. Succinate dehydrogenase B gene mutations predict survival in patients with malignant pheochromocytomas or paragangliomas. The Journal of clinical endocrinology and metabolism. 2007;92:3822-8.
77. Chrisoulidou A, Kaltsas G, Ilias I, Grossman AB. The diagnosis and management of malignant phaeochromocytoma and paraganglioma. Endocrine-related cancer. 2007;14:569-85.
78. Goldstein RE, O'Neill JA, Jr., Holcomb GW, 3rd, Morgan WM, 3rd, Neblett WW, 3rd, Oates JA, et al. Clinical experience over 48 years with pheochromocytoma. Annals of surgery. 1999;229:755-64; discussion 64-6.
79. Schovanek J, Martucci V, Wesley R, Fojo T, Del Rivero J, Huynh T, et al. The size of the primary tumor and age at initial diagnosis are independent predictors of the metastatic behavior and survival of patients with SDHB-related pheochromocytoma and paraganglioma: a retrospective cohort study. BMC cancer. 2014;14:523.
80. Ayala-Ramirez M, Feng L, Johnson MM, Ejaz S, Habra MA, Rich T, et al. Clinical risk factors for malignancy and overall survival in patients with pheochromocytomas and sympathetic paragangliomas: primary tumor size and primary tumor location as prognostic indicators. The Journal of clinical endocrinology and metabolism. 2011;96:717-25.
81. Assadipour Y, Sadowski SM, Alimchandani M, Quezado M, Steinberg SM, Nilubol N, et al. SDHB mutation status and tumor size but not tumor grade are important predictors of clinical outcome in pheochromocytoma and abdominal paraganglioma. Surgery. 2017;161:230-9.
82. Gimenez-Roqueplo AP, Favier J, Rustin P, Rieubland C, Crespin M, Nau V, et al. Mutations in the SDHB gene are associated with extra-adrenal and/or malignant phaeochromocytomas. Cancer research. 2003;63:5615-21.
83. Gimenez-Roqueplo AP, Favier J, Rustin P, Rieubland C, Kerlan V, Plouin PF, et al. Functional consequences of a SDHB gene mutation in an apparently sporadic pheochromocytoma. The Journal of clinical endocrinology and metabolism. 2002;87:4771-4.
84. Amar L, Bertherat J, Baudin E, Ajzenberg C, Bressac-de Paillerets B, Chabre O, et al. Genetic testing in pheochromocytoma or functional paraganglioma. Journal of clinical oncology : official journal of the American Society of Clinical Oncology. 2005;23:8812-8.
85. Kimura N, Takayanagi R, Takizawa N, Itagaki E, Katabami T, Kakoi N, et al. Pathological grading for predicting metastasis in phaeochromocytoma and paraganglioma. Endocrine-related cancer. 2014;21:405-14.
86. Agarwal A, Mehrotra PK, Jain M, Gupta SK, Mishra A, Chand G, et al. Size of the tumor and pheochromocytoma of the adrenal gland scaled score (PASS): can they predict malignancy? World journal of surgery. 2010;34:3022-8.

87. Thompson LD. Pheochromocytoma of the Adrenal gland Scaled Score (PASS) to separate benign from malignant neoplasms: a clinicopathologic and immunophenotypic study of 100 cases. The American journal of surgical pathology. 2002;26:551-66.
88. Wu D, Tischler AS, Lloyd RV, DeLellis RA, de Krijger R, van Nederveen F, et al. Observer variation in the application of the Pheochromocytoma of the Adrenal Gland Scaled Score. The American journal of surgical pathology. 2009;33:599-608.
89. Koh JM, Ahn SH, Kim H, Kim BJ, Sung TY, Kim YH, et al. Validation of pathological grading systems for predicting metastatic potential in pheochromocytoma and paraganglioma. PloS one. 2017;12:e0187398.
90. Favier J, Plouin PF, Corvol P, Gasc JM. Angiogenesis and vascular architecture in pheochromocytomas: distinctive traits in malignant tumors. The American journal of pathology. 2002;161:1235-46.
91. Oudijk L, van Nederveen F, Badoual C, Tissier F, Tischler AS, Smid M, et al. Vascular pattern analysis for the prediction of clinical behaviour in pheochromocytomas and paragangliomas. PloS one. 2015;10:e0121361.
92. van Hulsteijn LT, Niemeijer ND, Dekkers OM, Corssmit EP. (131)I-MIBG therapy for malignant paraganglioma and phaeochromocytoma: systematic review and meta-analysis. Clinical endocrinology. 2014;80:487-501.
93. Forrer F, Riedweg I, Maecke HR, Mueller-Brand J. Radiolabeled DOTATOC in patients with advanced paraganglioma and pheochromocytoma. The quarterly journal of nuclear medicine and molecular imaging : official publication of the Italian Association of Nuclear Medicine. 2008;52:334-40.
94. Kong G, Callahan J, Hofman MS, Pattison DA, Akhurst T, Michael M, et al. High clinical and morphologic response using (90)Y-DOTA-octreotate sequenced with (177)Lu-DOTA-octreotate induction peptide receptor chemoradionuclide therapy (PRCRT) for bulky neuroendocrine tumours. European journal of nuclear medicine and molecular imaging. 2017;44:476-89.
95. Pinato DJ, Black JR, Ramaswami R, Tan TM, Adjogatse D, Sharma R. Peptide receptor radionuclide therapy for metastatic paragangliomas. Medical oncology. 2016;33:47.
96. Ayala-Ramirez M, Feng L, Habra MA, Rich T, Dickson PV, Perrier N, et al. Clinical benefits of systemic chemotherapy for patients with metastatic pheochromocytomas or sympathetic extra-adrenal paragangliomas: insights from the largest single-institutional experience. Cancer. 2012;118:2804-12.
97. Huang H, Abraham J, Hung E, Averbuch S, Merino M, Steinberg SM, et al. Treatment of malignant pheochromocytoma/paraganglioma with cyclophosphamide, vincristine, and dacarbazine: recommendation from a 22-year follow-up of 18 patients. Cancer. 2008;113:2020-8.
98. Hadoux J, Favier J, Scoazec JY, Leboulleux S, Al Ghuzlan A, Caramella C, et al. SDHB mutations are associated with response to temozolomide in patients with metastatic pheochromocytoma or paraganglioma. International journal of cancer. 2014;135:2711-20.
99. Hadoux J, Terroir M, Leboulleux S, Deschamps F, Al Ghuzlan A, Hescot S, et al. Interferon-alpha Treatment for Disease Control in Metastatic Pheochromocytoma/Paraganglioma Patients. Hormones & cancer. 2017;8:330-7.
100. Ayala-Ramirez M, Chougnet CN, Habra MA, Palmer JL, Leboulleux S, Cabanillas ME, et al. Treatment with sunitinib for patients with progressive metastatic

pheochromocytomas and sympathetic paragangliomas. The Journal of clinical endocrinology and metabolism. 2012;97:4040-50.
101. Neumann HP, Berger DP, Sigmund G, Blum U, Schmidt D, Parmer RJ, et al. Pheochromocytomas, multiple endocrine neoplasia type 2, and von Hippel-Lindau disease. The New England journal of medicine. 1993;329:1531-8.
102. Baysal BE, Ferrell RE, Willett-Brozick JE, Lawrence EC, Myssiorek D, Bosch A, et al. Mutations in SDHD, a mitochondrial complex II gene, in hereditary paraganglioma. Science. 2000;287:848-51.
103. Niemann S, Muller U. Mutations in SDHC cause autosomal dominant paraganglioma, type 3. Nature genetics. 2000;26:268-70.
104. Astuti D, Latif F, Dallol A, Dahia PL, Douglas F, George E, et al. Gene mutations in the succinate dehydrogenase subunit SDHB cause susceptibility to familial pheochromocytoma and to familial paraganglioma. American journal of human genetics. 2001;69:49-54.
105. Burnichon N, Rohmer V, Amar L, Herman P, Leboulleux S, Darrouzet V, et al. The succinate dehydrogenase genetic testing in a large prospective series of patients with paragangliomas. The Journal of clinical endocrinology and metabolism. 2009;94:2817-27.
106. Brito JP, Asi N, Bancos I, Gionfriddo MR, Zeballos-Palacios CL, Leppin AL, et al. Testing for germline mutations in sporadic pheochromocytoma/paraganglioma: a systematic review. Clinical endocrinology. 2015;82:338-45.
107. Knudson AG, Jr. Mutation and cancer: statistical study of retinoblastoma. Proceedings of the National Academy of Sciences of the United States of America. 1971;68:820-3.
108. Lammert M, Friedman JM, Kluwe L, Mautner VF. Prevalence of neurofibromatosis 1 in German children at elementary school enrollment. Archives of dermatology. 2005;141:71-4.
109. Neurofibromatosis. Conference statement. National Institutes of Health Consensus Development Conference. Archives of neurology. 1988;45:575-8.
110. Hersh JH, American Academy of Pediatrics Committee on G. Health supervision for children with neurofibromatosis. Pediatrics. 2008;121:633-42.
111. Opocher G, Schiavi F. Genetics of pheochromocytomas and paragangliomas. Best practice & research Clinical endocrinology & metabolism. 2010;24:943-56.
112. Kepenekian L, Mognetti T, Lifante JC, Giraudet AL, Houzard C, Pinson S, et al. Interest of systematic screening of pheochromocytoma in patients with neurofibromatosis type 1. European journal of endocrinology. 2016;175:335-44.
113. Gruber LM, Erickson D, Babovic-Vuksanovic D, Thompson GB, Young WF, Jr., Bancos I. Pheochromocytoma and paraganglioma in patients with neurofibromatosis type 1. Clinical endocrinology. 2017;86:141-9.
114. Bausch B, Koschker AC, Fassnacht M, Stoevesandt J, Hoffmann MM, Eng C, et al. Comprehensive mutation scanning of NF1 in apparently sporadic cases of pheochromocytoma. The Journal of clinical endocrinology and metabolism. 2006;91:3478-81.
115. Moramarco J, El Ghorayeb N, Dumas N, Nolet S, Boulanger L, Burnichon N, et al. Pheochromocytomas are diagnosed incidentally and at older age in neurofibromatosis type 1. Clinical endocrinology. 2017;86:332-9.

116. Burnichon N, Buffet A, Parfait B, Letouze E, Laurendeau I, Loriot C, et al. Somatic NF1 inactivation is a frequent event in sporadic pheochromocytoma. Human molecular genetics. 2012;21:5397-405.
117. Gieldon L, Masjkur JR, Richter S, Darr R, Lahera M, Aust D, et al. Next-generation panel sequencing identifies NF1 germline mutations in three patients with pheochromocytoma but no clinical diagnosis of neurofibromatosis type 1. European journal of endocrinology. 2018;178:K1-K9.
118. Maxwell PH, Wiesener MS, Chang GW, Clifford SC, Vaux EC, Cockman ME, et al. The tumour suppressor protein VHL targets hypoxia-inducible factors for oxygen-dependent proteolysis. Nature. 1999;399:271-5.
119. Maher ER, Iselius L, Yates JR, Littler M, Benjamin C, Harris R, et al. Von Hippel-Lindau disease: a genetic study. Journal of medical genetics. 1991;28:443-7.
120. Maher ER, Neumann HP, Richard S. von Hippel-Lindau disease: a clinical and scientific review. European journal of human genetics : EJHG. 2011;19:617-23.
121. Binderup ML, Gimsing S, Kosteljanetz M, Thomsen C, Bisgaard ML. von Hippel-Lindau disease: deafness due to a non-MRI-visible endolymphatic sac tumor despite targeted screening. International journal of audiology. 2013;52:771-5.
122. Kim HJ, Butman JA, Brewer C, Zalewski C, Vortmeyer AO, Glenn G, et al. Tumors of the endolymphatic sac in patients with von Hippel-Lindau disease: implications for their natural history, diagnosis, and treatment. Journal of neurosurgery. 2005;102:503-12.
123. Maher ER, Webster AR, Richards FM, Green JS, Crossey PA, Payne SJ, et al. Phenotypic expression in von Hippel-Lindau disease: correlations with germline VHL gene mutations. Journal of medical genetics. 1996;33:328-32.
124. Nordstrom-O'Brien M, van der Luijt RB, van Rooijen E, van den Ouweland AM, Majoor-Krakauer DF, Lolkema MP, et al. Genetic analysis of von Hippel-Lindau disease. Human mutation. 2010;31:521-37.
125. Li L, Zhang L, Zhang X, Yan Q, Minamishima YA, Olumi AF, et al. Hypoxia-inducible factor linked to differential kidney cancer risk seen with type 2A and type 2B VHL mutations. Molecular and cellular biology. 2007;27:5381-92.
126. Ohh M, Park CW, Ivan M, Hoffman MA, Kim TY, Huang LE, et al. Ubiquitination of hypoxia-inducible factor requires direct binding to the beta-domain of the von Hippel-Lindau protein. Nature cell biology. 2000;2:423-7.
127. Maranchie JK, Afonso A, Albert PS, Kalyandrug S, Phillips JL, Zhou S, et al. Solid renal tumor severity in von Hippel Lindau disease is related to germline deletion length and location. Human mutation. 2004;23:40-6.
128. McNeill A, Rattenberry E, Barber R, Killick P, MacDonald F, Maher ER. Genotype-phenotype correlations in VHL exon deletions. American journal of medical genetics Part A. 2009;149A:2147-51.
129. Couve S, Ladroue C, Laine E, Mahtouk K, Guegan J, Gad S, et al. Genetic evidence of a precisely tuned dysregulation in the hypoxia signaling pathway during oncogenesis. Cancer research. 2014;74:6554-64.
130. Castro-Vega LJ, Letouze E, Burnichon N, Buffet A, Disderot PH, Khalifa E, et al. Multi-omics analysis defines core genomic alterations in pheochromocytomas and paragangliomas. Nature communications. 2015;6:6044.
131. Mannelli M, Castellano M, Schiavi F, Filetti S, Giacche M, Mori L, et al. Clinically guided genetic screening in a large cohort of italian patients with pheochromocytomas and/or functional or nonfunctional paragangliomas. The Journal of clinical endocrinology and metabolism. 2009;94:1541-7.

132. Boedeker CC, Erlic Z, Richard S, Kontny U, Gimenez-Roqueplo AP, Cascon A, et al. Head and neck paragangliomas in von Hippel-Lindau disease and multiple endocrine neoplasia type 2. The Journal of clinical endocrinology and metabolism. 2009;94:1938-44.
133. Mulligan LM. RET revisited: expanding the oncogenic portfolio. Nature reviews Cancer. 2014;14:173-86.
134. Brandi ML, Gagel RF, Angeli A, Bilezikian JP, Beck-Peccoz P, Bordi C, et al. Guidelines for diagnosis and therapy of MEN type 1 and type 2. The Journal of clinical endocrinology and metabolism. 2001;86:5658-71.
135. American Thyroid Association Guidelines Task F, Kloos RT, Eng C, Evans DB, Francis GL, Gagel RF, et al. Medullary thyroid cancer: management guidelines of the American Thyroid Association. Thyroid : official journal of the American Thyroid Association. 2009;19:565-612.
136. Wells SA, Jr., Asa SL, Dralle H, Elisei R, Evans DB, Gagel RF, et al. Revised American Thyroid Association guidelines for the management of medullary thyroid carcinoma. Thyroid : official journal of the American Thyroid Association. 2015;25:567-610.
137. Thosani S, Ayala-Ramirez M, Palmer L, Hu MI, Rich T, Gagel RF, et al. The characterization of pheochromocytoma and its impact on overall survival in multiple endocrine neoplasia type 2. The Journal of clinical endocrinology and metabolism. 2013;98:E1813-9.
138. Rodriguez JM, Balsalobre M, Ponce JL, Rios A, Torregrosa NM, Tebar J, et al. Pheochromocytoma in MEN 2A syndrome. Study of 54 patients. World journal of surgery. 2008;32:2520-6.
139. Peitzsch M, Pelzel D, Glockner S, Prejbisz A, Fassnacht M, Beuschlein F, et al. Simultaneous liquid chromatography tandem mass spectrometric determination of urinary free metanephrines and catecholamines, with comparisons of free and deconjugated metabolites. Clinica chimica acta; international journal of clinical chemistry. 2013;418:50-8.
140. Boedeker CC, Neumann HP, Offergeld C, Maier W, Falcioni M, Berlis A, et al. Clinical features of paraganglioma syndromes. Skull base : official journal of North American Skull Base Society [et al]. 2009;19:17-25.
141. Favier J, Gimenez-Roqueplo AP. Pheochromocytomas: the (pseudo)-hypoxia hypothesis. Best practice & research Clinical endocrinology & metabolism. 2010;24:957-68.
142. Percy MJ, Furlow PW, Lucas GS, Li X, Lappin TR, McMullin MF, et al. A gain-of-function mutation in the HIF2A gene in familial erythrocytosis. The New England journal of medicine. 2008;358:162-8.
143. Percy MJ, Sanchez M, Swierczek S, McMullin MF, Mojica-Henshaw MP, Muckenthaler MU, et al. Is congenital secondary erythrocytosis/polycythemia caused by activating mutations within the HIF-2 alpha iron-responsive element? Blood. 2007;110:2776-7.
144. Percy MJ, Zhao Q, Flores A, Harrison C, Lappin TR, Maxwell PH, et al. A family with erythrocytosis establishes a role for prolyl hydroxylase domain protein 2 in oxygen homeostasis. Proceedings of the National Academy of Sciences of the United States of America. 2006;103:654-9.
145. Ladroue C, Carcenac R, Leporrier M, Gad S, Le Hello C, Galateau-Salle F, et al. PHD2 mutation and congenital erythrocytosis with paraganglioma. The New England journal of medicine. 2008;359:2685-92.

146. Yang C, Zhuang Z, Fliedner SM, Shankavaram U, Sun MG, Bullova P, et al. Germ-line PHD1 and PHD2 mutations detected in patients with pheochromocytoma/paraganglioma-polycythemia. Journal of molecular medicine. 2015;93:93-104.
147. Zhuang Z, Yang C, Lorenzo F, Merino M, Fojo T, Kebebew E, et al. Somatic HIF2A gain-of-function mutations in paraganglioma with polycythemia. The New England journal of medicine. 2012;367:922-30.
148. Favier J, Buffet A, Gimenez-Roqueplo AP. HIF2A mutations in paraganglioma with polycythemia. The New England journal of medicine. 2012;367:2161; author reply -2.
149. Lorenzo FR, Yang C, Ng Tang Fui M, Vankayalapati H, Zhuang Z, Huynh T, et al. A novel EPAS1/HIF2A germline mutation in a congenital polycythemia with paraganglioma. Journal of molecular medicine. 2013;91:507-12.
150. Comino-Mendez I, de Cubas AA, Bernal C, Alvarez-Escola C, Sanchez-Malo C, Ramirez-Tortosa CL, et al. Tumoral EPAS1 (HIF2A) mutations explain sporadic pheochromocytoma and paraganglioma in the absence of erythrocytosis. Human molecular genetics. 2013;22:2169-76.
151. Buffet A, Smati S, Mansuy L, Menara M, Lebras M, Heymann MF, et al. Mosaicism in HIF2A-related polycythemia-paraganglioma syndrome. The Journal of clinical endocrinology and metabolism. 2014;99:E369-73.
152. Opotowsky AR, Moko LE, Ginns J, Rosenbaum M, Greutmann M, Aboulhosn J, et al. Pheochromocytoma and paraganglioma in cyanotic congenital heart disease. The Journal of clinical endocrinology and metabolism. 2015;100:1325-34.
153. Vaidya A, Flores SK, Cheng ZM, Nicolas M, Deng Y, Opotowsky AR, et al. EPAS1 Mutations and Paragangliomas in Cyanotic Congenital Heart Disease. The New England journal of medicine. 2018;378:1259-61.
154. Favier J, Amar L, Gimenez-Roqueplo AP. Paraganglioma and phaeochromocytoma: from genetics to personalized medicine. Nature reviews Endocrinology. 2015;11:101-11.
155. Neumann HP, Bausch B, McWhinney SR, Bender BU, Gimm O, Franke G, et al. Germ-line mutations in nonsyndromic pheochromocytoma. The New England journal of medicine. 2002;346:1459-66.
156. Hederstedt L. Structural biology. Complex II is complex too. Science. 2003;299:671-2.
157. Letouze E, Martinelli C, Loriot C, Burnichon N, Abermil N, Ottolenghi C, et al. SDH mutations establish a hypermethylator phenotype in paraganglioma. Cancer cell. 2013;23:739-52.
158. Pasini B, Stratakis CA. SDH mutations in tumorigenesis and inherited endocrine tumours: lesson from the phaeochromocytoma-paraganglioma syndromes. Journal of internal medicine. 2009;266:19-42.
159. Buffet A, Venisse A, Nau V, Roncellin I, Boccio V, Le Pottier N, et al. A decade (2001-2010) of genetic testing for pheochromocytoma and paraganglioma. Hormone and metabolic research = Hormon- und Stoffwechselforschung = Hormones et metabolisme. 2012;44:359-66.
160. Eisenhofer G, Lenders JW, Timmers H, Mannelli M, Grebe SK, Hofbauer LC, et al. Measurements of plasma methoxytyramine, normetanephrine, and metanephrine as discriminators of different hereditary forms of pheochromocytoma. Clinical chemistry. 2011;57:411-20.
161. Eisenhofer G, Timmers HJ, Lenders JW, Bornstein SR, Tiebel O, Mannelli M, et al. Age at diagnosis of pheochromocytoma differs according to catecholamine phenotype

and tumor location. The Journal of clinical endocrinology and metabolism. 2011;96:375-84.
162. Pigny P, Vincent A, Cardot Bauters C, Bertrand M, de Montpreville VT, Crepin M, et al. Paraganglioma after maternal transmission of a succinate dehydrogenase gene mutation. The Journal of clinical endocrinology and metabolism. 2008;93:1609-15.
163. Yeap PM, Tobias ES, Mavraki E, Fletcher A, Bradshaw N, Freel EM, et al. Molecular analysis of pheochromocytoma after maternal transmission of SDHD mutation elucidates mechanism of parent-of-origin effect. The Journal of clinical endocrinology and metabolism. 2011;96:E2009-13.
164. Bayley JP, Oldenburg RA, Nuk J, Hoekstra AS, van der Meer CA, Korpershoek E, et al. Paraganglioma and pheochromocytoma upon maternal transmission of SDHD mutations. BMC medical genetics. 2014;15:111.
165. Burnichon N, Mazzella JM, Drui D, Amar L, Bertherat J, Coupier I, et al. Risk assessment of maternally inherited SDHD paraganglioma and phaeochromocytoma. Journal of medical genetics. 2017;54:125-33.
166. Hensen EF, Jordanova ES, van Minderhout IJ, Hogendoorn PC, Taschner PE, van der Mey AG, et al. Somatic loss of maternal chromosome 11 causes parent-of-origin-dependent inheritance in SDHD-linked paraganglioma and phaeochromocytoma families. Oncogene. 2004;23:4076-83.
167. Baysal BE, McKay SE, Kim YJ, Zhang Z, Alila L, Willett-Brozick JE, et al. Genomic imprinting at a boundary element flanking the SDHD locus. Human molecular genetics. 2011;20:4452-61.
168. Ricketts CJ, Forman JR, Rattenberry E, Bradshaw N, Lalloo F, Izatt L, et al. Tumor risks and genotype-phenotype-proteotype analysis in 358 patients with germline mutations in SDHB and SDHD. Human mutation. 2010;31:41-51.
169. Benn DE, Gimenez-Roqueplo AP, Reilly JR, Bertherat J, Burgess J, Byth K, et al. Clinical presentation and penetrance of pheochromocytoma/paraganglioma syndromes. The Journal of clinical endocrinology and metabolism. 2006;91:827-36.
170. Andrews KA, Ascher DB, Pires DEV, Barnes DR, Vialard L, Casey RT, et al. Tumour risks and genotype-phenotype correlations associated with germline variants in succinate dehydrogenase subunit genes SDHB, SDHC and SDHD. Journal of medical genetics. 2018.
171. Castro-Vega LJ, Buffet A, De Cubas AA, Cascon A, Menara M, Khalifa E, et al. Germline mutations in FH confer predisposition to malignant pheochromocytomas and paragangliomas. Human molecular genetics. 2014;23:2440-6.
172. King KS, Prodanov T, Kantorovich V, Fojo T, Hewitt JK, Zacharin M, et al. Metastatic pheochromocytoma/paraganglioma related to primary tumor development in childhood or adolescence: significant link to SDHB mutations. Journal of clinical oncology : official journal of the American Society of Clinical Oncology. 2011;29:4137-42.
173. Bausch B, Wellner U, Bausch D, Schiavi F, Barontini M, Sanso G, et al. Long-term prognosis of patients with pediatric pheochromocytoma. Endocrine-related cancer. 2014;21:17-25.
174. Burnichon N, Briere JJ, Libe R, Vescovo L, Riviere J, Tissier F, et al. SDHA is a tumor suppressor gene causing paraganglioma. Human molecular genetics. 2010;19:3011-20.
175. van der Tuin K, Mensenkamp AR, Tops CMJ, Corssmit EPM, Dinjens WN, van de Horst-Schrivers AN, et al. Clinical Aspects of SDHA-Related Pheochromocytoma and

Paraganglioma: A Nationwide Study. The Journal of clinical endocrinology and metabolism. 2018;103:438-45.
176. Hao HX, Khalimonchuk O, Schraders M, Dephoure N, Bayley JP, Kunst H, et al. SDH5, a gene required for flavination of succinate dehydrogenase, is mutated in paraganglioma. Science. 2009;325:1139-42.
177. Kunst HP, Rutten MH, de Monnink JP, Hoefsloot LH, Timmers HJ, Marres HA, et al. SDHAF2 (PGL2-SDH5) and hereditary head and neck paraganglioma. Clinical cancer research : an official journal of the American Association for Cancer Research. 2011;17:247-54.
178. Bayley JP, Kunst HP, Cascon A, Sampietro ML, Gaal J, Korpershoek E, et al. SDHAF2 mutations in familial and sporadic paraganglioma and phaeochromocytoma. The Lancet Oncology. 2010;11:366-72.
179. Piccini V, Rapizzi E, Bacca A, Di Trapani G, Pulli R, Giache V, et al. Head and neck paragangliomas: genetic spectrum and clinical variability in 79 consecutive patients. Endocrine-related cancer. 2012;19:149-55.
180. Bausch B, Schiavi F, Ni Y, Welander J, Patocs A, Ngeow J, et al. Clinical Characterization of the Pheochromocytoma and Paraganglioma Susceptibility Genes SDHA, TMEM127, MAX, and SDHAF2 for Gene-Informed Prevention. JAMA oncology. 2017;3:1204-12.
181. Vanharanta S, Buchta M, McWhinney SR, Virta SK, Peczkowska M, Morrison CD, et al. Early-onset renal cell carcinoma as a novel extraparaganglial component of SDHB-associated heritable paraganglioma. American journal of human genetics. 2004;74:153-9.
182. Gill AJ, Hes O, Papathomas T, Sedivcova M, Tan PH, Agaimy A, et al. Succinate dehydrogenase (SDH)-deficient renal carcinoma: a morphologically distinct entity: a clinicopathologic series of 36 tumors from 27 patients. The American journal of surgical pathology. 2014;38:1588-602.
183. Boikos SA, Pappo AS, Killian JK, LaQuaglia MP, Weldon CB, George S, et al. Molecular Subtypes of KIT/PDGFRA Wild-Type Gastrointestinal Stromal Tumors: A Report From the National Institutes of Health Gastrointestinal Stromal Tumor Clinic. JAMA oncology. 2016;2:922-8.
184. Killian JK, Miettinen M, Walker RL, Wang Y, Zhu YJ, Waterfall JJ, et al. Recurrent epimutation of SDHC in gastrointestinal stromal tumors. Science translational medicine. 2014;6:268ra177.
185. Xekouki P, Pacak K, Almeida M, Wassif CA, Rustin P, Nesterova M, et al. Succinate dehydrogenase (SDH) D subunit (SDHD) inactivation in a growth-hormone-producing pituitary tumor: a new association for SDH? The Journal of clinical endocrinology and metabolism. 2012;97:E357-66.
186. Tomlinson IP, Alam NA, Rowan AJ, Barclay E, Jaeger EE, Kelsell D, et al. Germline mutations in FH predispose to dominantly inherited uterine fibroids, skin leiomyomata and papillary renal cell cancer. Nature genetics. 2002;30:406-10.
187. Muller M, Ferlicot S, Guillaud-Bataille M, Le Teuff G, Genestie C, Deveaux S, et al. Reassessing the clinical spectrum associated with hereditary leiomyomatosis and renal cell carcinoma syndrome in French FH mutation carriers. Clinical genetics. 2017.
188. Gardie B, Remenieras A, Kattygnarath D, Bombled J, Lefevre S, Perrier-Trudova V, et al. Novel FH mutations in families with hereditary leiomyomatosis and renal cell cancer (HLRCC) and patients with isolated type 2 papillary renal cell carcinoma. Journal of medical genetics. 2011;48:226-34.

189. Menko FH, Maher ER, Schmidt LS, Middelton LA, Aittomaki K, Tomlinson I, et al. Hereditary leiomyomatosis and renal cell cancer (HLRCC): renal cancer risk, surveillance and treatment. Familial cancer. 2014;13:637-44.
190. Clark GR, Sciacovelli M, Gaude E, Walsh DM, Kirby G, Simpson MA, et al. Germline FH mutations presenting with pheochromocytoma. The Journal of clinical endocrinology and metabolism. 2014;99:E2046-50.
191. Qin Y, Yao L, King EE, Buddavarapu K, Lenci RE, Chocron ES, et al. Germline mutations in TMEM127 confer susceptibility to pheochromocytoma. Nature genetics. 2010;42:229-33.
192. Deng Y, Qin Y, Srikantan S, Luo A, Cheng ZM, Flores SK, et al. The TMEM127 human tumor suppressor is a component of the mTORC1 lysosomal nutrient-sensing complex. Human molecular genetics. 2018;27:1794-808.
193. Abermil N, Guillaud-Bataille M, Burnichon N, Venisse A, Manivet P, Guignat L, et al. TMEM127 screening in a large cohort of patients with pheochromocytoma and/or paraganglioma. The Journal of clinical endocrinology and metabolism. 2012;97:E805-9.
194. Toledo SP, Lourenco DM, Jr., Sekiya T, Lucon AM, Baena ME, Castro CC, et al. Penetrance and clinical features of pheochromocytoma in a six-generation family carrying a germline TMEM127 mutation. The Journal of clinical endocrinology and metabolism. 2015;100:E308-18.
195. Yao L, Schiavi F, Cascon A, Qin Y, Inglada-Perez L, King EE, et al. Spectrum and prevalence of FP/TMEM127 gene mutations in pheochromocytomas and paragangliomas. Jama. 2010;304:2611-9.
196. Qin Y, Deng Y, Ricketts CJ, Srikantan S, Wang E, Maher ER, et al. The tumor susceptibility gene TMEM127 is mutated in renal cell carcinomas and modulates endolysosomal function. Human molecular genetics. 2014;23:2428-39.
197. Comino-Mendez I, Gracia-Aznarez FJ, Schiavi F, Landa I, Leandro-Garcia LJ, Leton R, et al. Exome sequencing identifies MAX mutations as a cause of hereditary pheochromocytoma. Nature genetics. 2011;43:663-7.
198. Grandori C, Cowley SM, James LP, Eisenman RN. The Myc/Max/Mad network and the transcriptional control of cell behavior. Annual review of cell and developmental biology. 2000;16:653-99.
199. Beaulieu ME, McDuff FO, Frappier V, Montagne M, Naud JF, Lavigne P. New structural determinants for c-Myc specific heterodimerization with Max and development of a novel homodimeric c-Myc b-HLH-LZ. Journal of molecular recognition : JMR. 2012;25:414-26.
200. Burnichon N, Cascon A, Schiavi F, Morales NP, Comino-Mendez I, Abermil N, et al. MAX mutations cause hereditary and sporadic pheochromocytoma and paraganglioma. Clinical cancer research : an official journal of the American Association for Cancer Research. 2012;18:2828-37.
201. Daly AF, Castermans E, Oudijk L, Guitelman MA, Beckers P, Potorac I, et al. Pheochromocytomas and pituitary adenomas in three patients with MAX exon deletions. Endocrine-related cancer. 2018;25:L37-L42.
202. Cascon A, Comino-Mendez I, Curras-Freixes M, de Cubas AA, Contreras L, Richter S, et al. Whole-exome sequencing identifies MDH2 as a new familial paraganglioma gene. Journal of the National Cancer Institute. 2015;107.
203. Calsina B, Curras-Freixes M, Buffet A, Pons T, Contreras L, Leton R, et al. Role of MDH2 pathogenic variant in pheochromocytoma and paraganglioma patients. Genetics in medicine : official journal of the American College of Medical Genetics. 2018.

204. Toledo RA, Qin Y, Cheng ZM, Gao Q, Iwata S, Silva GM, et al. Recurrent Mutations of Chromatin-Remodeling Genes and Kinase Receptors in Pheochromocytomas and Paragangliomas. Clinical cancer research : an official journal of the American Association for Cancer Research. 2016;22:2301-10.
205. Schlisio S, Kenchappa RS, Vredeveld LC, George RE, Stewart R, Greulich H, et al. The kinesin KIF1Bbeta acts downstream from EglN3 to induce apoptosis and is a potential 1p36 tumor suppressor. Genes & development. 2008;22:884-93.
206. Welander J, Andreasson A, Juhlin CC, Wiseman RW, Backdahl M, Hoog A, et al. Rare germline mutations identified by targeted next-generation sequencing of susceptibility genes in pheochromocytoma and paraganglioma. The Journal of clinical endocrinology and metabolism. 2014;99:E1352-60.
207. Remacha L, Comino-Mendez I, Richter S, Contreras L, Curras-Freixes M, Pita G, et al. Targeted Exome Sequencing of Krebs Cycle Genes Reveals Candidate Cancer-Predisposing Mutations in Pheochromocytomas and Paragangliomas. Clinical cancer research : an official journal of the American Association for Cancer Research. 2017;23:6315-24.
208. Remacha L, Curras-Freixes M, Torres-Ruiz R, Schiavi F, Torres-Perez R, Calsina B, et al. Gain-of-function mutations in DNMT3A in patients with paraganglioma. Genetics in medicine : official journal of the American College of Medical Genetics. 2018.
209. Burnichon N, Vescovo L, Amar L, Libe R, de Reynies A, Venisse A, et al. Integrative genomic analysis reveals somatic mutations in pheochromocytoma and paraganglioma. Human molecular genetics. 2011;20:3974-85.
210. Fishbein L, Leshchiner I, Walter V, Danilova L, Robertson AG, Johnson AR, et al. Comprehensive Molecular Characterization of Pheochromocytoma and Paraganglioma. Cancer cell. 2017;31:181-93.
211. Welander J, Larsson C, Backdahl M, Hareni N, Sivler T, Brauckhoff M, et al. Integrative genomics reveals frequent somatic NF1 mutations in sporadic pheochromocytomas. Human molecular genetics. 2012;21:5406-16.
212. Crona J, Delgado Verdugo A, Maharjan R, Stalberg P, Granberg D, Hellman P, et al. Somatic mutations in H-RAS in sporadic pheochromocytoma and paraganglioma identified by exome sequencing. The Journal of clinical endocrinology and metabolism. 2013;98:E1266-71.
213. Juhlin CC, Stenman A, Haglund F, Clark VE, Brown TC, Baranoski J, et al. Whole-exome sequencing defines the mutational landscape of pheochromocytoma and identifies KMT2D as a recurrently mutated gene. Genes, chromosomes & cancer. 2015;54:542-54.
214. Crona J, Nordling M, Maharjan R, Granberg D, Stalberg P, Hellman P, et al. Integrative genetic characterization and phenotype correlations in pheochromocytoma and paraganglioma tumours. PloS one. 2014;9:e86756.
215. Fishbein L, Khare S, Wubbenhorst B, DeSloover D, D'Andrea K, Merrill S, et al. Whole-exome sequencing identifies somatic ATRX mutations in pheochromocytomas and paragangliomas. Nature communications. 2015;6:6140.
216. Comino-Mendez I, Tejera AM, Curras-Freixes M, Remacha L, Gonzalvo P, Tonda R, et al. ATRX driver mutation in a composite malignant pheochromocytoma. Cancer genetics. 2016;209:272-7.
217. Korpershoek E, Favier J, Gaal J, Burnichon N, van Gessel B, Oudijk L, et al. SDHA immunohistochemistry detects germline SDHA gene mutations in apparently sporadic

paragangliomas and pheochromocytomas. The Journal of clinical endocrinology and metabolism. 2011;96:E1472-6.
218. van Nederveen FH, Gaal J, Favier J, Korpershoek E, Oldenburg RA, de Bruyn EM, et al. An immunohistochemical procedure to detect patients with paraganglioma and phaeochromocytoma with germline SDHB, SDHC, or SDHD gene mutations: a retrospective and prospective analysis. The Lancet Oncology. 2009;10:764-71.
219. Menara M, Oudijk L, Badoual C, Bertherat J, Lepoutre-Lussey C, Amar L, et al. SDHD immunohistochemistry: a new tool to validate SDHx mutations in pheochromocytoma/paraganglioma. The Journal of clinical endocrinology and metabolism. 2015;100:E287-91.
220. Richter S, Peitzsch M, Rapizzi E, Lenders JW, Qin N, de Cubas AA, et al. Krebs cycle metabolite profiling for identification and stratification of pheochromocytomas/paragangliomas due to succinate dehydrogenase deficiency. The Journal of clinical endocrinology and metabolism. 2014;99:3903-11.
221. Imperiale A, Moussallieh FM, Roche P, Battini S, Cicek AE, Sebag F, et al. Metabolome profiling by HRMAS NMR spectroscopy of pheochromocytomas and paragangliomas detects SDH deficiency: clinical and pathophysiological implications. Neoplasia. 2015;17:55-65.
222. Lussey-Lepoutre C, Bellucci A, Morin A, Buffet A, Amar L, Janin M, et al. In Vivo Detection of Succinate by Magnetic Resonance Spectroscopy as a Hallmark of SDHx Mutations in Paraganglioma. Clinical cancer research : an official journal of the American Association for Cancer Research. 2016;22:1120-9.
223. Varoquaux A, le Fur Y, Imperiale A, Reyre A, Montava M, Fakhry N, et al. Magnetic resonance spectroscopy of paragangliomas: new insights into in vivo metabolomics. Endocrine-related cancer. 2015;22:M1-8.
224. Sciacovelli M, Goncalves E, Johnson TI, Zecchini VR, da Costa AS, Gaude E, et al. Fumarate is an epigenetic modifier that elicits epithelial-to-mesenchymal transition. Nature. 2016;537:544-7.
225. Selak MA, Armour SM, MacKenzie ED, Boulahbel H, Watson DG, Mansfield KD, et al. Succinate links TCA cycle dysfunction to oncogenesis by inhibiting HIF-alpha prolyl hydroxylase. Cancer cell. 2005;7:77-85.
226. Loriot C, Domingues M, Berger A, Menara M, Ruel M, Morin A, et al. Deciphering the molecular basis of invasiveness in Sdhb-deficient cells. Oncotarget. 2015;6:32955-65.
227. Sulkowski PL, Sundaram RK, Oeck S, Corso CD, Liu Y, Noorbakhsh S, et al. Krebs-cycle-deficient hereditary cancer syndromes are defined by defects in homologous-recombination DNA repair. Nature genetics. 2018.
228. Castro-Vega LJ, Lepoutre-Lussey C, Gimenez-Roqueplo AP, Favier J. Rethinking pheochromocytomas and paragangliomas from a genomic perspective. Oncogene. 2016;35:1080-9.
229. Group NGSiPS, Toledo RA, Burnichon N, Cascon A, Benn DE, Bayley JP, et al. Consensus Statement on next-generation-sequencing-based diagnostic testing of hereditary phaeochromocytomas and paragangliomas. Nature reviews Endocrinology. 2017;13:233-47.
230. Plouin PF, Amar L, Dekkers OM, Fassnacht M, Gimenez-Roqueplo AP, Lenders JW, et al. European Society of Endocrinology Clinical Practice Guideline for long-term follow-up of patients operated on for a phaeochromocytoma or a paraganglioma. European journal of endocrinology. 2016;174:G1-G10.

231. Rohmer V, Vidal-Trecan G, Bourdelot A, Niccoli P, Murat A, Wemeau JL, et al. Prognostic factors of disease-free survival after thyroidectomy in 170 young patients with a RET germline mutation: a multicenter study of the Groupe Francais d'Etude des Tumeurs Endocrines. The Journal of clinical endocrinology and metabolism. 2011;96:E509-18.
232. Ardern-Holmes SL, North KN. Therapeutics for childhood neurofibromatosis type 1 and type 2. Current treatment options in neurology. 2011;13:529-43.
233. Plouin PF, Gimenez-Roqueplo AP, Bertagna X. [COMETE, a network for the study and management of hypersecreting adrenal tumors]. Bulletin de l'Academie nationale de medecine. 2008;192:73-82; discussion 3-5.
234. Salabei JK, Gibb AA, Hill BG. Comprehensive measurement of respiratory activity in permeabilized cells using extracellular flux analysis. Nature protocols. 2014;9:421-38.
235. Mihailovich M, Militti C, Gabaldon T, Gebauer F. Eukaryotic cold shock domain proteins: highly versatile regulators of gene expression. BioEssays : news and reviews in molecular, cellular and developmental biology. 2010;32:109-18.
236. Kobayashi H, Kawauchi D, Hashimoto Y, Ogata T, Murakami F. The control of precerebellar neuron migration by RNA-binding protein Csde1. Neuroscience. 2013;253:292-303.
237. Papathomas TG, Oudijk L, Persu A, Gill AJ, van Nederveen F, Tischler AS, et al. SDHB/SDHA immunohistochemistry in pheochromocytomas and paragangliomas: a multicenter interobserver variation analysis using virtual microscopy: a Multinational Study of the European Network for the Study of Adrenal Tumors (ENS@T). Modern pathology : an official journal of the United States and Canadian Academy of Pathology, Inc. 2015;28:807-21.
238. Heinrich MC, Corless CL, Demetri GD, Blanke CD, von Mehren M, Joensuu H, et al. Kinase mutations and imatinib response in patients with metastatic gastrointestinal stromal tumor. Journal of clinical oncology : official journal of the American Society of Clinical Oncology. 2003;21:4342-9.
239. Du CY, Shi YQ, Zhou Y, Fu H, Zhao G. The analysis of status and clinical implication of KIT and PDGFRA mutations in gastrointestinal stromal tumor (GIST). Journal of surgical oncology. 2008;98:175-8.
240. Patrikidou A, Domont J, Chabaud S, Ray-Coquard I, Coindre JM, Bui-Nguyen B, et al. Long-term outcome of molecular subgroups of GIST patients treated with standard-dose imatinib in the BFR14 trial of the French Sarcoma Group. European journal of cancer. 2016;52:173-80.
241. Miselli FC, Casieri P, Negri T, Orsenigo M, Lagonigro MS, Gronchi A, et al. c-Kit/PDGFRA gene status alterations possibly related to primary imatinib resistance in gastrointestinal stromal tumors. Clinical cancer research : an official journal of the American Association for Cancer Research. 2007;13:2369-77.
242. Boikos SA, Stratakis CA. The genetic landscape of gastrointestinal stromal tumor lacking KIT and PDGFRA mutations. Endocrine. 2014;47:401-8.
243. Sloane MA, Ward RL, Hesson LB. Defining the criteria for identifying constitutional epimutations. Clinical epigenetics. 2016;8:39.
244. Haller F, Moskalev EA, Faucz FR, Barthelmess S, Wiemann S, Bieg M, et al. Aberrant DNA hypermethylation of SDHC: a novel mechanism of tumor development in Carney triad. Endocrine-related cancer. 2014;21:567-77.
245. Richter S, Klink B, Nacke B, de Cubas AA, Mangelis A, Rapizzi E, et al. Epigenetic Mutation of the Succinate Dehydrogenase C Promoter in a Patient With Two

Paragangliomas. The Journal of clinical endocrinology and metabolism. 2016;101:359-63.
246. Urbini M, Astolfi A, Indio V, Heinrich MC, Corless CL, Nannini M, et al. SDHC methylation in gastrointestinal stromal tumors (GIST): a case report. BMC medical genetics. 2015;16:87.
247. Scholz SL, Horn S, Murali R, Moller I, Sucker A, Sondermann W, et al. Analysis of SDHD promoter mutations in various types of melanoma. Oncotarget. 2015;6:25868-82.
248. Populo H, Batista R, Sampaio C, Pardal J, Lopes JM, Soares P. SDHD promoter mutations are rare events in cutaneous melanomas but SDHD protein expression is downregulated in advanced cutaneous melanoma. PloS one. 2017;12:e0180392.
249. Zhang T, Xu M, Makowski MM, Lee C, Kovacs M, Fang J, et al. SDHD Promoter Mutations Ablate GABP Transcription Factor Binding in Melanoma. Cancer research. 2017;77:1649-61.
250. Weinhold N, Jacobsen A, Schultz N, Sander C, Lee W. Genome-wide analysis of noncoding regulatory mutations in cancer. Nature genetics. 2014;46:1160-5.
251. Leclerc J, Flament C, Lovecchio T, Delattre L, Ait Yahya E, Baert-Desurmont S, et al. Diversity of genetic events associated with MLH1 promoter methylation in Lynch syndrome families with heritable constitutional epimutation. Genetics in medicine : official journal of the American College of Medical Genetics. 2018.
252. Hitchins MP. Constitutional epimutation as a mechanism for cancer causality and heritability? Nature reviews Cancer. 2015;15:625-34.
253. Baretta Z, Mocellin S, Goldin E, Olopade OI, Huo D. Effect of BRCA germline mutations on breast cancer prognosis: A systematic review and meta-analysis. Medicine. 2016;95:e4975.
254. Barrow P, Khan M, Lalloo F, Evans DG, Hill J. Systematic review of the impact of registration and screening on colorectal cancer incidence and mortality in familial adenomatous polyposis and Lynch syndrome. The British journal of surgery. 2013;100:1719-31.
255. Castro-Vega LJ, Kiando SR, Burnichon N, Buffet A, Amar L, Simian C, et al. The MITF, p.E318K Variant, as a Risk Factor for Pheochromocytoma and Paraganglioma. The Journal of clinical endocrinology and metabolism. 2016;101:4764-8.
256. Lenglet M, Robriquet F, Schwarz K, Camps C, Couturier A, Hoogewijs D, et al. New lessons from an old gene: complex splicing and a novel cryptic exon in VHL gene cause erythrocytosis and VHL disease. Blood. 2018.

ANNEXES

ARTICLE 3

Multi-omics analysis defines core genomic alterations in pheochromocytomas and paragangliomas.

Castro-Vega LJ, Letouzé E, Burnichon N, Buffet A, Disderot PH, Khalifa E, Loriot C, Elarouci N, Morin A, Menara M, Lepoutre-Lussey C, Badoual C, Sibony M, Dousset B, Libé R, Zinzindohoue F, Plouin PF, Bertherat J, Amar L, de Reyniès A, Favier J, Gimenez-Roqueplo AP.

Nat Commun. 2015 Jan 27;6:6044

nature COMMUNICATIONS

ARTICLE

Received 11 Aug 2014 | Accepted 5 Dec 2014 | Published 27 Jan 2015

DOI: 10.1038/ncomms7044 OPEN

Multi-omics analysis defines core genomic alterations in pheochromocytomas and paragangliomas

Luis Jaime Castro-Vega[1,2,*], Eric Letouzé[3,*], Nelly Burnichon[1,2,4,*], Alexandre Buffet[1,2,4], Pierre-Hélie Disderot[1,2], Emmanuel Khalifa[1,2,4], Céline Loriot[1,2], Nabila Elarouci[3], Aurélie Morin[1,2], Mélanie Menara[1,2], Charlotte Lepoutre-Lussey[1,2,5], Cécile Badoual[1,2,6], Mathilde Sibony[2,7], Bertrand Dousset[2,8,9,10], Rossella Libé[2,9,10,11,12], Franck Zinzindohoue[2,13], Pierre François Plouin[1,2,5,12], Jérôme Bertherat[2,9,10,11,12], Laurence Amar[1,2,5], Aurélien de Reyniès[3], Judith Favier[1,2,§] & Anne-Paule Gimenez-Roqueplo[1,2,4,12,§]

Pheochromocytomas and paragangliomas (PCCs/PGLs) are neural crest-derived tumours with a very strong genetic component. Here we report the first integrated genomic examination of a large collection of PCC/PGL. SNP array analysis reveals distinct copy-number patterns associated with genetic background. Whole-exome sequencing shows a low mutation rate of 0.3 mutations per megabase, with few recurrent somatic mutations in genes not previously associated with PCC/PGL. DNA methylation arrays and miRNA sequencing identify DNA methylation changes and miRNA expression clusters strongly associated with messenger RNA expression profiling. Overexpression of the miRNA cluster 182/96/183 is specific in *SDHB*-mutated tumours and induces malignant traits, whereas silencing of the imprinted *DLK1-MEG3* miRNA cluster appears as a potential driver in a subgroup of sporadic tumours. Altogether, the complete genomic landscape of PCC/PGL is mainly driven by distinct germline and/or somatic mutations in susceptibility genes and reveals different molecular entities, characterized by a set of unique genomic alterations.

[1] INSERM, UMR970, Paris-Cardiovascular Research Center, F-75015 Paris, France. [2] Université Paris Descartes, Sorbonne Paris Cité, Faculté de Médecine, F-75006 Paris, France. [3] Programme Cartes d'Identité des Tumeurs, Ligue Nationale Contre Le Cancer, 75013 Paris, France. [4] Department of Genetics, Assistance Publique-Hôpitaux de Paris, Hôpital Européen Georges Pompidou, F-75015 Paris, France. [5] Hypertension Unit, Assistance Publique-Hôpitaux de Paris, Hôpital Européen Georges Pompidou, F-75015 Paris, France. [6] Department of Pathology, Assistance Publique-Hôpitaux de Paris, Hôpital Européen Georges Pompidou, F-75015 Paris, France. [7] Department of Pathology, Assistance Publique-Hôpitaux de Paris, Hôpital Cochin, F-75006 Paris, France. [8] Department of Digestive and Endocrine Surgery, Assistance Publique-Hôpitaux de Paris, Hôpital Cochin, F-75006 Paris, France. [9] INSERM, U1016, Institut Cochin, F-75006 Paris, France. [10] CNRS UMR8104, F-75006 Paris, France. [11] Department of Endocrinology, Assistance Publique-Hôpitaux de Paris, Hôpital Cochin, F-75006 Paris, France. [12] Rare Adrenal Cancer Network COMETE, F-75006 Paris, France. [13] Department of Surgery, Assistance Publique-Hôpitaux de Paris, Hôpital Européen Georges Pompidou, F-75015 Paris, France. * These authors contributed equally to this work. § These authors jointly supervised this work. Correspondence and requests for materials should be addressed to A.-P.G.-R. (email: anne-paule.gimenez-roqueplo@egp.aphp.fr).

Pheochromocytomas (PCCs) and paragangliomas (PGLs) are rare neuroendocrine tumours derived from chromaffin cells of the adrenal medulla and paraganglia of the autonomic nervous system, respectively. Most PCCs/PGLs are benign, but 10% of PCCs and up to 40% of PGLs become malignant with a 5-year survival rate below 50%. The malignant form of the disease remains difficult to predict and cure, as there are neither established histopathological criteria to assess the risk of progression nor effective treatment. Compared with other cancers, PCCs/PGLs are characterized by a remarkable genetic determinism[1]. To date, at least 12 susceptibility genes have been identified comprising two oncogenes (*RET* and *HIF2A*) and ten tumour suppressors (*NF1*, *VHL*, *SDHA*, *SDHB*, *SDHC*, *SDHD*, *SDHAF2*, *FH*, *TMEM127* and *MAX*). Up to 40% of affected patients carry a germline mutation in one of these genes[1]. Germline mutations in either *SDHB* or *FH* have been associated with an increased risk of metastasis[2–4]. On the other hand, loss-of-function mutations in *NF1* and *VHL*, as well as activating mutations in *RET*, *HIF2A* and *HRAS*, have been reported at the somatic level in about 30% of these tumours[5–9].

Transcriptome analyses identified expression clusters strongly correlated with known drivers[10–12]. Specifically, Clusters C1A and C1B, comprising *SDHx*- and *VHL*-mutated tumours, respectively, display a pseudohypoxic signature, whereas Cluster C2A, corresponding to *RET*-, *NF1*- and *TMEM127*-mutated tumours, displays activation of the RAS/mitogen-activated protein kinase (MAPK) signaling pathway. Clusters C2B and C2C are enriched in sporadic tumours. In addition, recent characterization of the methylation profile revealed that *SDHx* tumours display a hypermethylator phenotype[13]. Deregulated expression of microRNAs (miRNAs) and copy-number alterations (CNAs) have also been described[14–21]. However, to date, there is no study attempting to integrate multi-dimensional molecular data, which is necessary for a comprehensive understanding of the crucial mechanisms driving PCC/PGL tumorigenesis.

Here we present an integrated genomic analysis including whole-exome sequencing, single-nucleotide polymorphism (SNP) array, as well as mRNA, miRNA and DNA methylation profiling, aiming to characterize the major genomic alterations underlying PCCs/PGLs.

Results

Description and processing of the PCC/PGL COMETE cohort. A collection of 202 PCC/PGL samples from the French 'Cortico et Médullosurrénale: les Tumeurs Endocrines' (COMETE) Network was profiled on a set of genomic platforms. Tumour samples were collected from 190 patients, including 116 women and 74 men with a mean age at diagnosis of 42.4 years (range: 7–82 years; Supplementary Data 1). Overall, 168 (83.2%) tumours were PCCs, 25 (12.4%) were abdominal PGLs, 3 (1.5%) were thoracic PGLs and 6 (3%) were metastases. Twenty-seven (13.4%) tumours were from patients with a metastatic form of the disease. Importantly, all cases were previously genotyped for the presence or the absence of germline and somatic mutations in well-known susceptibility genes. For this study, we also screened the whole cohort for hotspot mutations of *HRAS* and found 10 of 202 (4.95%) mutated cases, corresponding exclusively to sporadic tumours (Supplementary Data 1).

SNP array (150 tumours), exome sequencing (31 tumour-normal pairs) and miRNA sequencing data (172 tumours) were generated specifically for this study, whereas DNA methylation (145 tumours) and mRNA expression data (188 tumours) were partially exploited in previous reports[5,6,13,22]. The collective molecular status derived from all of these platforms, excluding exome sequencing, was assigned to 128 tumours (Supplementary Fig. 1 and Supplementary Data 1).

Somatic CNAs. We first profiled somatic CNAs using SNP arrays. Overall, the degree of genome instability was low as determined by the fraction of aberrant arm score (median = 15%). The most frequent CNAs were broad deletions involving chromosome arms 1p, 3p, 3q, 11p, 11q, 17p, 21 and 22 (Fig. 1a). Chromosome gains were less frequent, mostly affecting chromosome arm 1q and chromosome 7. Strikingly, tumours belonging to the different molecular groups displayed characteristic CNA patterns (Fig. 1b). Specifically, *SDHx* tumours (Cluster C1A) displayed a significant enrichment of 1q gains (q-value <0.05, Supplementary Table 1). Loss of chromosomal arm 1p encompassing the *SDHB* locus, as well as losses of 11p—mostly present in *SDHD* tumours—and 17p were also frequent, yet not exclusive of *SDHx* tumours. *VHL* tumours (Cluster C1B) were characterized by a combined deletion of chromosome 3 (harbouring *VHL*) and arm 11p. *RET*, *NF1* and sporadic tumours (Cluster C2A) displayed a high frequency of 1q and 3q deletions, and a significant enrichment of 17q11 deletions (*NF1* locus). Deletions of arm 6q and chromosomes 21 and 22 were also frequent in this group. Sporadic tumours included in Cluster C2B were enriched in gains of chromosome 7. A copy-neutral loss of heterozygosity (LOH) at 14q32 was significantly associated with Clusters C2B and C2C.

Although PCC/PGL present a fairly low degree of chromosome instability, three tumours (37, 49 and 188) presented evidence of chromothripsis, consistent with the proportion of 2–3% observed in most cancers[23]. Notably, chromosome arms 1p and 17p were strongly rearranged in the three cases (Fig. 1c), suggesting chromosome shattering may lead to the loss or gain of important drivers in these regions.

For four patients (18, 25, 42 and 80), we obtained the SNP array profiles of two tumours: coexisting tumours or the primary tumour, and a relapse or metastasis. We also generated exome data for one tumour/metastasis pair. Using the TuMult algorithm[24], we reconstructed the order of copy-number changes in these tumours. We identified common alterations in every patient, confirming the clonal origin of their tumours. We could also distinguish early events, often comprising the loss of the wild-type copy of predisposing genes when a germline mutation is present, from late events that may be involved in tumour progression, including acquired somatic mutations and CNAs (Fig. 1d).

Somatic mutations. To gain insights from the mutational landscape of PCCs/PGLs, we performed whole-exome analysis of 30 tumour-normal DNA pairs and one trio including the primary tumour and a metastasis. We enriched the exome series in tumours belonging to the C1A expression cluster ($n=17$) and sporadic tumours included in the C2A ($n=3$) and C2B ($n=11$) clusters, aiming to establish comparisons between these tumour groups (Supplementary Data 1). Among them, 15 were *SDHx*-related tumours; 1 tumour, belonging to the Cluster C1A, carried 1 germline and 1 somatic mutation in the *FH* gene as previously reported[13]; 2 sporadic tumours from the C2A cluster displayed somatic mutations in *NF1*; 13 were sporadic tumours with no mutation in known predisposing genes. We sequenced 333,765 exons from 20,975 genes to a mean coverage of 80-fold (Supplementary Fig. 2). Mutations were considered as somatic if they were found only in the tumour sample without evidence in the germline data. We identified a total of 672 somatic variants in coding regions or exon/intron boundaries: 616 single-nucleotide variants (SNVs) and 56 indels (Supplementary Data 2).

PCCs/PGLs harboured a median of 3 synonymous and 9 non-synonymous mutations (range: 1–41 total mutations) (Fig. 2a), corresponding to a relatively low mutation rate of 0.3 mutations per megabase. The mutation rate did not differ between molecular subgroups or regarding the malignant status. The spectrum of mutations was enriched in C>T transitions (Fig. 2b), which are typically found in the majority of cancers analysed so far[25]. This result is compatible with spontaneous deamination rather than with a carcinogen-induced process. These mutations were also more frequent, yet not significant, in the transcribed strand.

We then combined damaging mutations (indels, nonsense or missense mutations predicted to be damaging by PolyPhen-2 software) and homozygous deletions obtained by SNP array (Supplementary Data 4), to identify putative driver genes in PCCs/PGLs. Seven genes presented at least two damaging events

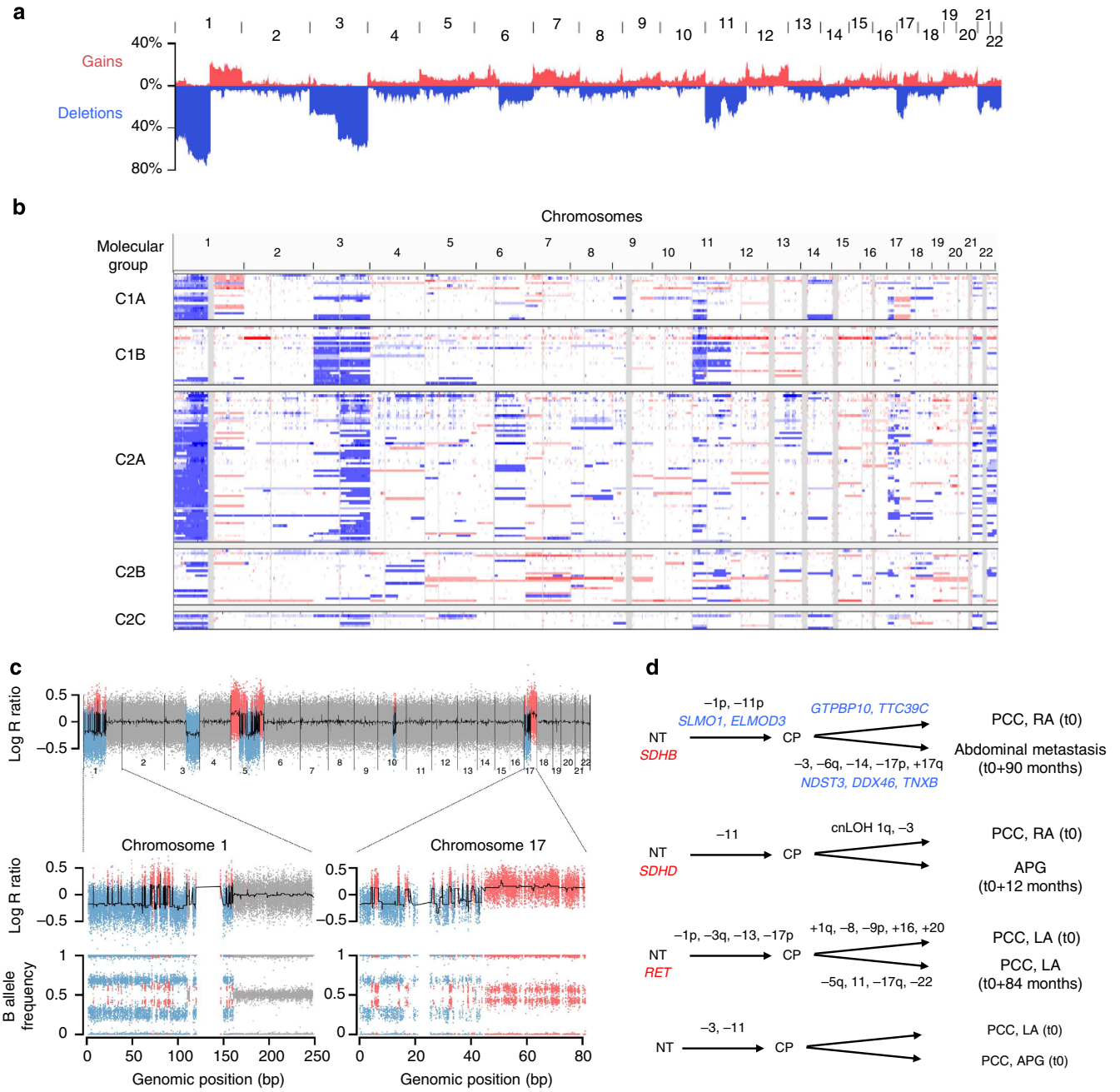

Figure 1 | Copy-number alterations in PCC/PGL. (**a**) Pan-genomic frequency of gains (in red) and deletions (in blue) among the complete set of 150 PCC/PGL. (**b**) Overview of the copy-number profiles exported from the Integrative Genomics Viewer. Each line represents the profile of a tumour, with gains in red and deletions in blue. Samples are ordered according to the mRNA expression cluster they belong to, as indicated on the left. (**c**) Copy-number profile of a tumour presenting chromothripsis on chromosomes 1, 5 and 17. Top: Pan-genomic log R ratio profile. Bottom: log R ratio and B allele frequency profiles of chromosomes 1 and 17. These chromosomes display numerous breakpoints and a copy number oscillating between two values, classical of chromothripsis events. (**d**) Tumour progression trees reconstructed for four patients with primary tumour and co-occurring tumour/relapse/metastasis data. Tumours of the first patient were also analysed by exome sequencing. APG, abdominal paraganglioma; cnLOH, copy neutral loss of heterozygosity; CP, common precursor; LA, left adrenal; NT, normal tissue; PCC, pheochromocytoma; RA, right adrenal. In red, germline mutations; in blue, somatic mutations.

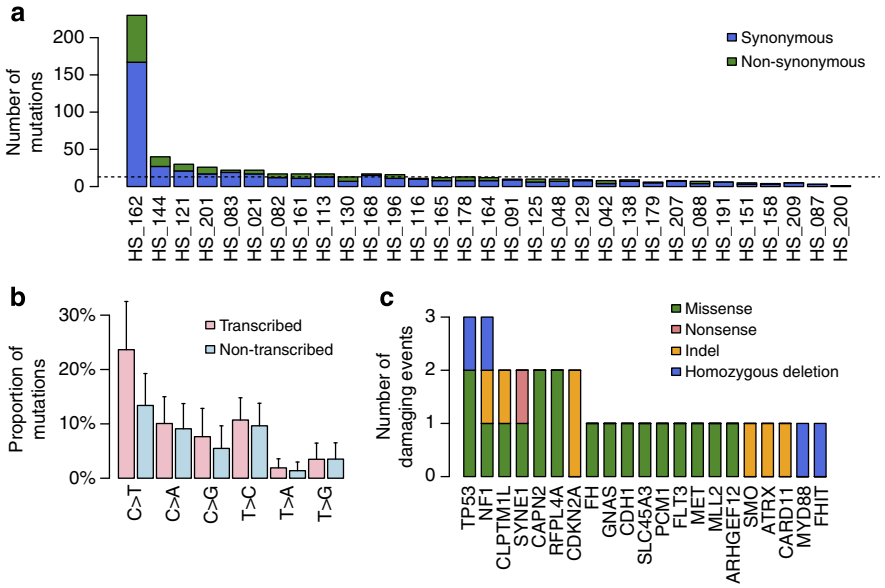

Figure 2 | Whole-exome sequencing analysis of 31 PCC/PGL. (**a**) Number of synonymous and non-synonymous somatic mutations in the 31 PCC/PGL samples. (**b**) Relative proportions of the 6 possible base-pair substitutions on the transcribed and non-transcribed strands among the 616 point mutations identified in the exome sequences of 31 PCC/PGL. Error bars denote the s.d. (**c**) Number and type of damaging events for 7 genes altered in at least 2 cases, and 14 genes belonging to the Cancer Gene Census and altered in a single tumour.

(Fig. 2c). As expected, we confirmed the *FH* and *NF1* mutations in corresponding tumours. Two other common cancer genes, *TP53* and *CDKN2A*, were altered in three (10%) and two (7%) cases, respectively, whereas the genes *CLPTM1L*, *SYNE1*, *CAPN2* and *RFPL4A* have not been yet implicated in cancer. Other genes of interest carrying damaging variants and listed in the Cancer Gene Census included *MET* (activating mutation p.E355K), *CDH1*, *ARHGEF12*, *SLC45A3*, *SMO*, *CARD11*, *MLL2*, *PCM1*, *ATRX*, *GNAS*, *FLT3* and *FHIT*. These genes were altered in a single tumour (Fig. 2c). Of note, the sample with the highest number of mutations (162) carries one somatic mutation in *POLE* and one in *POLD1*. All of these mutations were confirmed by Sanger sequencing (Supplementary Data 2). As expected, given the low mutation load of PCCs/PGLs, none of these variants was significantly mutated when MutSigCV was applied. To validate the exome-sequencing results, we screened the whole PCC/PGL cohort for mutations in *TP53*, *CDKN2A* and *MET* genes. In total, five (2.5%) tumours harbour hotspot mutations in *MET*, whereas no additional damaging variants were identified in *TP53* or *CDKN2A* genes (Supplementary Data 3).

DNA methylation profiling. We previously identified three homogeneous DNA methylation-based subgroups of PCCs/PGLs: the M1 group corresponding to *SDHx*- and *FH*-mutated cases and displaying a hypermethylator phenotype, the M2 group comprising exclusively *VHL*-mutated samples and the M3 group comprising mostly tumours of the C2 expression cluster. We have already extensively described the DNA methylation changes occurring in the M1 cluster[13]. Here we extended our analyses to DNA methylation changes present in the two other groups. We identified 88 genes significantly hypermethylated in the M2 cluster (*VHL* related). Of these genes, 84 (95%) were also hypermethylated in the M1 cluster (Supplementary Data 5). However, these changes had little impact on gene expression, as only two genes (*PNMT* and *NMNAT3*) were both hypermethylated and downregulated in M2 tumours. We found no significant CpG island hypermethylation in tumours belonging to cluster M3. In contrast, these tumours displayed a widespread hypomethylation outside CpG islands (Supplementary Fig. 3a). Hypomethylation of the same loci was also encountered in M2 tumours but with lower amplitude (Supplementary Fig. 3b). DNA hypomethylation outside CpG islands may thus result from a similar mechanism operating with different intensities in the two subgroups.

miRNA profiling. To further characterize gene expression patterns of PCC/PGL tumours, we assayed miRNA expression levels in our cohort by Illumina sequencing. Unsupervised classification using the miRNome data of 172 PCCs/PGLs revealed 7 homogeneous subgroups (Mi1 to Mi7, Fig. 3a) strongly associated with mRNA expression subgroups ($P = 1.8e-63$, χ^2-test) and mutations in known driver genes ($P = 6.1e-39$, χ^2-test, Fig. 3b). Clusters Mi1 and Mi2 were more closely associated and corresponded to mRNA expression Cluster C1, whereas clusters Mi3 to Mi7 corresponded to mRNA expression Cluster C2. Clusters Mi1 and Mi2 comprised *SDHx*- and *VHL*-mutated tumours, respectively, whereas cluster Mi3 was enriched in sporadic tumours belonging to the C2B mRNA expression cluster. We used the DESeq package[26] to identify differentially expressed miRNAs between the subgroups (Supplementary Data 6).

We found a significant upregulation of the miRNA cluster 182/96/183 in Mi1 (*SDHx*-related) tumours (Fig. 3c). We validated this finding using quantitative reverse transcription–PCR and confirmed that the highest expression is displayed by *SDHB*-mutated tumours (Supplementary Fig. 4). Of these, the miR-183 was significantly expressed in malignant cases (Fig. 3c). We demonstrated that ectopic expression of miR-183/96 but not miR-182 in immortalized mouse chromaffin cells (imCCs) induces an epithelial-to-mesenchymal transition (EMT) phenotype (Fig. 3d and Supplementary Fig. 5).

The Mi3 cluster, containing a subgroup of C2B, was characterized by a strong silencing of the imprinted *DLK1-MEG3* cluster (Fig. 3b,e). This genomic region harbours the largest cluster of miRNAs in the human genome[27]. Strikingly, 15 of 17 tumours belonging to cluster Mi3 displayed a LOH at the 14q32 locus harbouring *DLK1-MEG3*, compared with only 2 of 114 remaining cases ($P = 9.4e-16$, Fisher's exact test). We hypothesized that the loss of the maternal unmethylated allele

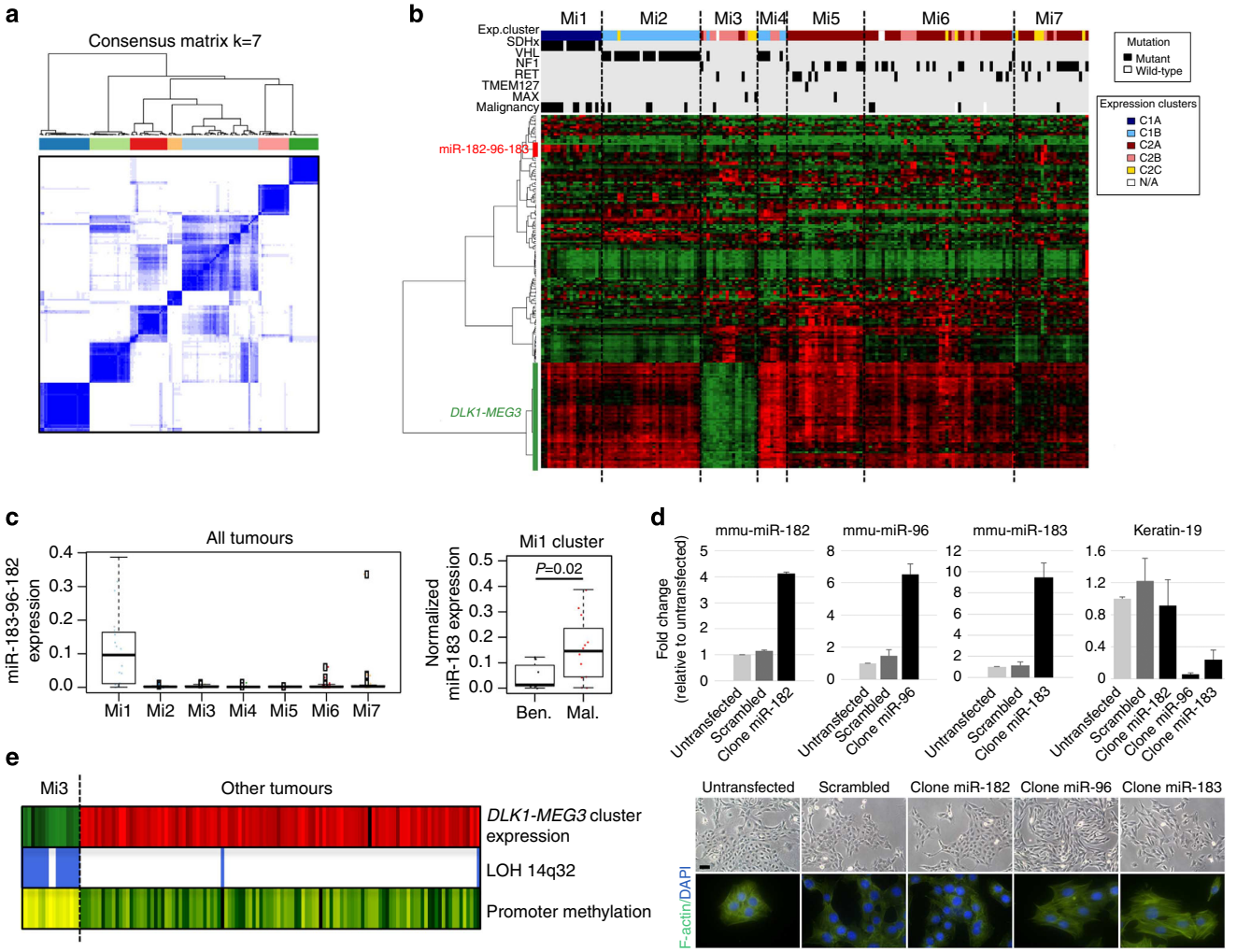

Figure 3 | miRNA profiling of 172 PCC/PGL. (**a**) Unsupervised classification of 172 PCC/PGL identifies 7 stable miRNA expression clusters. The consensus matrix represents the similarity between samples. Consensus index values range from 0 (highly dissimilar profiles, white) to 1 (highly similar profiles, dark blue). Samples are ordered on the *x* and *y* axes according to consensus clustering, which is depicted above the heat map. (**b**) Heat map of miRNA expression profiles. The expression levels of the miRNAs with the most variant expression are shown by colour (red for high expression and green for low expression). Samples are ordered by miRNA expression subgroup, with mRNA expression subgroup and mutations in known driver genes depicted above the heatmap. (**c**) Box-and-whisker plots show the distribution of miR-183-96-182 expression levels relative to each tumour subgroup (left), and of miR-183 relative to malignancy among Mi1 tumours (right). Middle bar, median; box, interquartile range; bars extend to 1.5 times the interquartile range. Ben., benign; Mal., malignant. Error bars denote the s.d. (**d**) Overexpression of miRNAs 96/183 in mouse chromaffin cells induces an EMT-like phenotype. Histograms show the relative expression of mature miRs and keratin-19 (used as EMT marker) detected by quantitative reverse transcription–PCR in clones obtained after stable transfections with plasmids containing either scrambled or miRNA sequences. Error bars denote the s.e.m. The bottom panel shows the corresponding morphology changes as determined by F-actin immunostaining. Scale bar, 20 μm. (**e**) Deregulation of the *DLK1-MEG3* cluster in PCC/PGL of the Mi3 group. The mean expression levels of miRNAs belonging to the *DLK1-MEG3* cluster are indicated, together with the presence of a LOH at the locus (blue, LOH; white, no LOH) and the methylation levels at the promoter CpG island (yellow, fully methylated; green, hemimethylated; dark green, unmethylated).

may explain the repression of this imprinted miRNA cluster, and we indeed identified a shift in *MEG3* promoter methylation from hemimethylation to full methylation, specifically in Mi3 cases ($P = 4.1e-11$, Wilcoxon rank-sum test, Fig. 3e).

Multi-omics integration. The combination of the main findings obtained with each omics data set defines the molecular portrait of each PCC/PGL subgroup (Fig. 4). C1A tumours are driven by germline mutations affecting *SDHx* genes. These tumours harbour frequent deletions of 1p and gains of 1q, display a hypermethylator phenotype and an overexpression of the miRNA cluster 182/96/183. This subgroup mostly comprises PGLs and malignant cases. C1B tumours are driven by *VHL* mutations. These tumours display a co-deletion of chromosome 3 and chromosome arm 11p, promoter hypermethylation of a few targets and a low-amplitude hypomethylation outside CpG islands. C2A tumours are mainly driven by *RET*, *NF1* and *HRAS* mutations. They harbour frequent 1p and 3q deletions, as well as 17q11 deletions in *NF1*-related cases. This group displays a strong hypomethylation outside CpG islands, such as the C2B and C2C groups. C2B tumours have no recurrent mutations but display frequent gains of chromosome 7, as well as a downregulation of the tumour suppressor *DLK1-MEG3* miRNA cluster following LOH at the 14q32 locus, also encountered in the C2C group. C2C tumours have only few CNAs, including deletions of 1p and 3q,

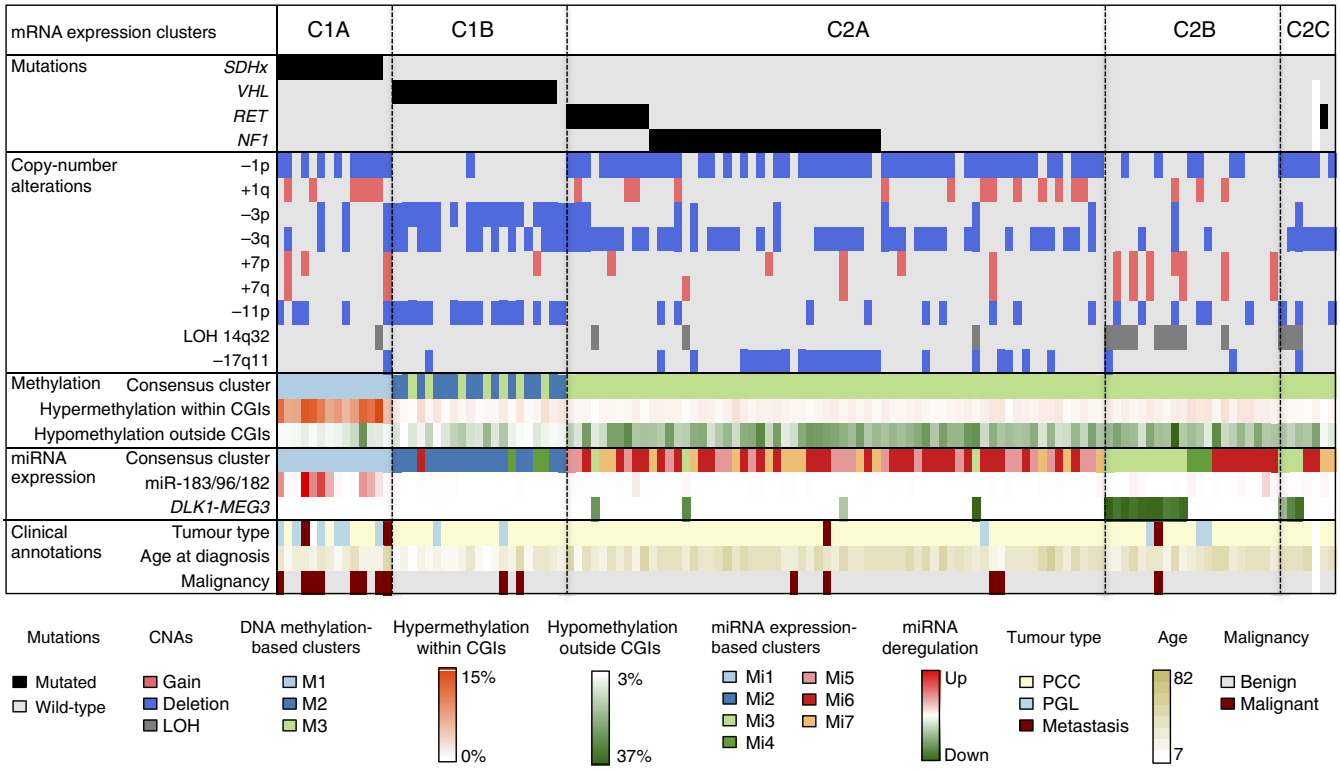

Figure 4 | Integrative genomic characterization of PCC/PGL. The main genetic, epigenetic and transcriptional changes affecting PCC/PGL are represented for the 128 samples analysed by SNP, DNA methylation, mRNA expression arrays, miRNA sequencing and targeted sequencing of known driver genes. Samples are ordered according to the mRNA cluster they belong to. Clinical features associated with molecular groups are also depicted at the bottom.

but no chromosomal gains. Overall, the C2 group comprises mainly benign PCCs with a later age of onset.

Discussion

The integrative genomic analysis of the well-annotated and genotyped COMETE cohort demonstrated that mutation status in PCC/PGL susceptibility genes is strongly correlated with multi-omics data. The somatic inactivation of the normal allele in PCC/PGL tumour suppressors such as *SDHx*, *VHL* and *NF1* tumours is driven by large deletions at the corresponding loci, but not by somatic mutations or epigenetic modifications. Given that these alterations involve large genomic segments, it remains challenging to identify other potential drivers and we cannot formally exclude the possibility that a concomitant loss of another tumour suppressor participates to tumorigenesis. Nevertheless, loss of 1p (*SDHB* locus) is broadly observed in PCC/PGL and was also encountered in cases displaying chromothripsis.

Regarding the mutational landscape, PCCs/PGLs are similar to other neural crest-derived tumours. Although they display a low mutation rate similar to neuroblastomas, medulloblastomas and ependymomas[28–31], PCCs/PGLs have mutations in *TP53*, *CDKN2A* and the RAS/MAPK signalling pathway that have also been found in melanomas and glioblastomas[32,33].

Importantly, we did not find any recurrent mutations in PCCs/PGLs, but it is expected that analysis of more samples could help identify significant genes of low mutation frequency[34]. In fact, our validation screening revealed frequent mutations in *MET*, particularly in C2A and C2B tumours. This gene encodes for a receptor with tyrosine kinase activity that triggers the RAS/MAPK signalling pathway frequently altered in PCCs/PGLs and therefore can be considered as a potential driver and theranostic biomarker[35]. We also point out mutations in *ATRX* and *MLL2*, two chromatin-remodelling genes, as they are frequently altered in gliomas, neuroblastomas, medulloblastomas and neuroendocrine tumours[28–30,36–40] and may therefore constitute a converging tumorigenic pathway for these related tumour types.

We previously found that *SDHx* and *FH* mutations establish a hypermethylator phenotype in PGLs[4,13]. In this regard, it is worth mentioning that similar results have been observed for at least two other neural crest-derived tumours, ependymomas and *IDH*-dependent glioblastomas[31,33], as well as in gastro-intestinal stromal tumours[41]. Increased CpG methylation induced by accumulation of metabolic intermediates (oncometabolites) reflects a block of the differentiation programme, thus probably promoting an increase in the number of stem and progenitor cells. Epigenetic modifiers would be a pertinent therapeutic strategy for this type of malignancy. On the other hand, the significance of the prevalent hypomethylation outside CpG islands found in Cluster 2 PCCs/PGLs remains unclear. Indeed, hypomethylation has classically been associated with genomic instability. In this subgroup of tumours, we have however not observed an increase in chromosome instability, and the pathophysiological consequences of this phenotype are still to be further investigated. In addition, we show here that *PNMT* gene encoding for the enzyme catalysing the conversion of noradrenaline to adrenaline is hypermethylated and downregulated in *VHL* tumours, suggesting that epigenetic silencing of this gene explains the noradrenergic phenotype of both *VHL*- and *SDHx*-mutated tumours[42].

Regarding miRNA expression changes, a high expression of miR-96 and miR-183 in *SDHB*-mutated tumours has been previously observed[17]. Here we extended this observation to the whole miRNA cluster miR-182/96/183 and further verified that

this overexpression is not related with CNA at this miR locus. Of these miRNAs, it seems that miR-183 is specific for malignant tumours, suggesting a potential prognostic value[16]. We previously reported that *SDHB*-mutated tumours display the activation of the EMT programme[43]. Here we further demonstrated that overexpression of miR-183 or miR-96 in mouse chromaffin cells induces an EMT-like phenotype. This miRNA cluster is upregulated in other invasive cancers including neural crest-derived tumours such as medulloblastomas, gliomas and melanomas[44–48]. Moreover, these miRs are highly expressed in neural stem cells and downregulated during differentiation[49]. Overexpression of miR-183 or miR-96 in PC12 cells blocks Nerve growth factor (NGF)-mediated differentiation[17]. Altogether, these observations suggest that these miRNAs may contribute to the maintenance of the undifferentiated state of *SDHB*-mutated tumours. The specific targets as well as the precise role of miR-182 await further functional characterization.

The miRNA profiling of PCC/PGL also uncovered a novel subgroup of sporadic tumours carrying a shutdown in the expression of the imprinted *DLK1-MEG3* cluster located in 14q32, an alteration previously associated with *MAX* tumours[17]. It is worth mentioning that this cluster is highly expressed in normal adrenal and other endocrine tissues[50]. The fact that both LOH and focal deletions of this genomic region were present, strongly suggests a tumour suppressor role of these miRNAs. Interestingly, in adrenocortical carcinoma, this alteration was also found in a benign subgroup without known driver mutation[51]. Therefore, downregulation of this cluster may be sufficient to trigger tumorigenesis in adrenal tissues.

In conclusion, this integrative genomic study provides evidence for strong concordance between multi-omics data and genetic status, thus demonstrating the crucial role of predisposing mutations as being the main drivers of PCCs/PGLs. This comprehensive analysis further illustrates the functional inter-dependence between genomic and epigenomic dysregulations. Ultimately, PCC/PGL subtypes can be defined by a set of unique genomic alterations and most probably represent different molecular entities. In the near future, omics-based tests should be developed to offer access to a precise molecular classification of PCCs/PGLs, to practicing clinicians. The knowledge of specific genomic alterations should provide a real help for individual patient management and should guide the choice of targeted therapy for malignant cases. Therefore, our findings pave the way towards omics-based clinical management and personalized medicine for patients with PCCs/PGLs.

Methods

Tumour samples. The tumour and blood samples were collected prospectively by the French COMETE Network. Ethical approval for the study was obtained from the institutional review board (Comité de Protection des Personnes Ile de France III, June 2012).

Written informed consent for the sample collection and subsequent analyses was obtained from all patients. The procedures used for PCC/PGL diagnosis were in accordance with both internal and international clinical practice guidelines[52,53]. Diagnosis was confirmed by histology in every case. A total of 202 consecutive cases of PCCs/PGLs, recruited over 15 years (1993–2008), were included in this study. Fresh tumour samples collected during surgery were immediately frozen and stored in liquid nitrogen until processing.

Nucleic acids extraction. Germline DNA was extracted from leukocytes using standard protocols. Tumour samples (30–50 mg) were powdered under liquid nitrogen. DNA was extracted and purified using a QIAamp DNA Mini Kit or an Allprep Kit (Qiagen) and RNA was extracted using an RNeasy Mini Kit (Qiagen). miRNA was extracted using a miRNeasy Mini Kit (Qiagen). Concentration of nucleic acids was determined using a Nanodrop ND-1000 instrument (Nyxor Biotech). RNA quality was assessed by electrophoresis on a Bioanalyzer 2100 (Agilent Technologies). A 28S/18S ratio above 1.5 was considered to rule out degradation.

Genetic testing and validation of somatic mutations. Mutation analysis of PCC/PGL susceptibility genes was performed as previously described[4–6]. Screening of *CDKN2A* gene and hotspot mutations in *HRAS* (exons 2, 3, 4 and 5), *TP53* (exons 4, 5, 6, 7, 8, 9, 10 and 11) and *MET* (exons 2, 14, 16 and 19) genes in the whole cohort, as well as validation of 20 mutations identified by exome sequencing in cancer genes (Supplementary Data 2) were performed by Sanger sequencing. The somatic nature of mutations was confirmed by sequencing tumour DNA and their paired blood DNA. The primer sequences and PCR conditions are available on request.

Analysis of copy-number data. DNA samples from 150 PCC/PGL (145 primary tumours and 5 relapses) were analysed with Illumina HumanCNV610-Quad v1.0. Hybridization was carried out by Integragen SA (Evry, France), following the manufacturer's recommendations. Raw fluorescent signals were launched into BeadStudio software (Illumina) and normalized[54] to obtain log R ratio and B allele frequency values. Genomic profiles were divided into homogeneous segments by applying the circular binary segmentation algorithm[55] to both log R ratio and B allele frequency values. The ploidy of each sample, the level of contamination with normal cells and the allele-specific copy number of each segment was determined using the Genome Alteration Print method[56]. The overall genomic instability of each sample was quantified as the fraction of aberrant arm score[57]. When several samples were available from the same patient, tumour progression trees were reconstructed using the TuMult algorithm[24].

Sequencing data processing and mutation detection. Whole-exome sequencing was performed in 30 pairs of PCCs/PGLs and matched normal samples (from blood), and 1 trio with a primary tumour and metastasis. In all tumour samples, the ratio of tumour cells to non-tumour cells was determined to be $>50\%$ and this value was confirmed by SNP array analysis. Sequence capture and exome sequencing were performed by Integragen as described elsewhere[57]. Briefly, Agilent in-solution enrichment (SureSelect Human All Exon Kit v4 + UTR) with the provided biotinylated oligonucleotide probe library (Human All Exon v4 + UTR–70 Mb) was used for DNA sequence capture, enrichment and elution from the tumour and matched blood DNA samples. The eluted fraction was amplified by PCR and sequenced on an Illumina HiSeq 2000 sequencer as paired-end 75-bp reads. Image analysis and base calling were performed using Illumina Real-Time Analysis Pipeline version 1.12.4.2 with default parameters. Illumina CASAVA 1.8.2 software was used to align reads against the hg19 genome build (GRCh37) and to detect SNVs and indels. We used the ELANDv2 algorithm for alignment. Targeted regions were sequenced to an average depth of $80\times$. We applied a previously described pipeline[51], with some modifications, to generate a list of somatic variants located in coding regions, plus four intronic bases corresponding to consensus splice sites. Quality-control filtering removed variants sequenced in <10 reads, with <3 variant calls or with QPHRED of <10. Variants were considered to be of somatic origin when the frequency of variant reads was $\geq 10\%$ in the tumour and $<5\%$ in the normal counterpart, with a significant enrichment of variant cells in the tumour as assessed through a Fisher's exact test. Common polymorphisms (with reported frequency of $>1\%$) were removed by comparison with dbSNP135, the 1000 Genomes Project database and a proprietary database of exomes from normal tissues. Missense variants were classified as 'benign', 'possibly damaging' or 'probably damaging' using PolyPhen-2 software (http://genetics.bwh.harvard.edu/pph2/). AlamutVisual Software version 2.4.6 (http://www.interactive-biosoftware.com/software.html) was used for nomenclature of gene variations. Somatic mutations occurring in at least two samples were validated visually using the Integrative Genomics Viewer[58]. The mean number of somatic mutations per sample (three silent and nine non-silent) comprised exonic SNVs and indels. The mutation rate in each tumour was evaluated by dividing the number of somatic mutations by the number of exonic bases covered by $\geq 10\times$ in both the tumour and normal samples. To identify mutations with transcriptional strand bias, we used a binomial test to assess whether the proportions of each type of somatic substitution occurring on the transcribed strand differed significantly from 0.5.

miRNA profiling. miRNA expression was performed in 172 PCC/PGL. Multiplexed miRNA libraries were prepared using a PCR barcoding method[59] and sequenced on an Illumina HiSeq 2000 sequencer. Image analysis, base calling, demultiplexing and conversion of BCL to FASTQ format were carried out using Illumina CASAVA 1.8.2 software. Adaptor sequences were removed using mirExpress software[60] and FASTA files for each sample were processed by miRanalyzer0.3 software[61], to quantify read counts for each miRNA referenced in mirBase74 v18. In total, 763 miRNAs were expressed (>10 reads) in at least 2 samples and were used for unsupervised classification. The miRNA count data were log2 transformed, divided by the total number of reads in each sample and centred on the mean expression level of each gene. Consensus clustering was then performed[62] and the optimal number of clusters ($K=7$) was determined from cumulative distribution function (CDF) curves. We used the Bioconductor DESeq package[26] to identify differentially expressed miRNAs. For validation of the expression of miRNA cluster 182/96/183 in tumour tissues and murine cell lines, we used the following TaqMan assays (Applied Biosystems): mmu-miR-183 (ID 002269), mmu-miR-96 (ID 000186), hsa-miR-182 (ID 002334) and mmu-miR-182

(ID 002599), hsa-miR-324-3p (ID 002161), has-miR-320 (ID 002277) and U6 snRNA (ID 001973). Briefly, 10 ng of RNA previously treated with Turbo DNase was reverse transcribed. Amplifications were performed in a StepOne Plus Real-Time PCR system. The expression of U6 or the mean expression of miR-320 and miR-324 were used as normalization control in murine cells and tumours, respectively.

Gene expression data. Gene expression profiles were available from a previous study, in which we identified five stable PGL/PCC subgroups, significantly associated with clinical features and gene mutations[6]. HG-U133 Plus 2.0 Affymetrix GeneChip data from this previous study are available online as ArrayExpress entry E-MTAB-733 (http://www.ebi.ac.uk/arrayexpress/).

DNA methylation arrays. Whole-genome DNA methylation was analysed in 145 tumour samples using the Illumina Infinium HumanMethylation27 assay as previously reported[13]. Data from this previous study are accessible through the NCBI's Gene Expression Omnibus series accession number GSE43298 (http://www.ncbi.nlm.nih.gov/geo).

Cellular assays. imCCs[13] were cultured in medium DMEM + Glutamax (GIBCO) supplemented with 10% fetal bovine serum (GIBCO) and maintained in a humidified 5% CO_2 atmosphere at 37 °C. For stable transfections of miRs, we used the Origen plasmid mmu-miR-183 (catalogue number SC400806), which also contains the mmu-miR-96 sequence, whereas both scrambled and mmu-miR-182 sequences were cloned in pCMV6-A-Puro Vectors. MegaTran 1.0 was used as transfection reagent (CliniSciences). Clones expressing one of the miRs belonging to the cluster 182/96/183 were obtained by limited dilution assays.

For immunofluorescence, microscope slides (Thermo scientific) were coated with Poly-D-lysine (100 μg ml^{-1}) for 3 h at 37 °C and washed with PBS 1 × without calcium. Cells seeded for 24 h were assayed for F-actin staining. Briefly, cells were fixed in 3% formaldehyde and 2% sucrose for 20 min at room temperature. Next, cells were washed twice with PBS 1 × and permeabilized for 10 min. A stock solution of phalloidin–tetramethylrhodamine isothiocyanate (Sigma) in dimethyl sulfoxide at 0.5 mg ml^{-1} was used at a concentration of 1:1,000 in PBS 1 × for 1 h at room temperature. Cells were washed several times to remove the conjugate and stained with 0.5 mg ml^{-1} 4′,6-diamidino-2-phenylindole.

Cell migration capacity of transfected imCC was assessed by performing *in vitro* scratch assays. Closure of the wounds was measured after 12 h[13]. For invasion assays, 75,000 cells per well (24-well format plates) were seeded on cell wall filters (8.0 μm pore size) containing a layer of growth factor reduced matrigel (BD Biosciences) diluted 1:4 in serum-free culture media. Cells were allowed to traverse the Matrigel for a period of 40 h after which they were fixed with methanol 15 min and then stained with toluidine blue 1% for 30 min. Cells were removed from the upper side of the chamber with cotton swabs. Images were taken from two independent experiments for quantifications.

References

1. Dahia, P. L. Pheochromocytoma and paraganglioma pathogenesis: learning from genetic heterogeneity. *Nat. Rev. Cancer.* **14,** 108–119 (2014).
2. Gimenez-Roqueplo, A. P. *et al.* Mutations in the SDHB gene are associated with extra-adrenal and/or malignant phaeochromocytomas. *Cancer Res.* **63,** 5615–5621 (2003).
3. Amar, L. *et al.* Succinate dehydrogenase B gene mutations predict survival in patients with malignant pheochromocytomas or paragangliomas. *J. Clin. Endocrinol. Metab.* **92,** 3822–3828 (2007).
4. Castro-Vega, L. J. *et al.* Germline mutations in FH confer predisposition to malignant pheochromocytomas and paragangliomas. *Hum. Mol. Genet.* **23,** 2440–2446 (2014).
5. Burnichon, N. *et al.* Somatic NF1 inactivation is a frequent event in sporadic pheochromocytoma. *Hum. Mol. Genet.* **21,** 5397–5405 (2012).
6. Burnichon, N. *et al.* Integrative genomic analysis reveals somatic mutations in pheochromocytoma and paraganglioma. *Hum. Mol. Genet.* **20,** 3974–3985 (2011).
7. Favier, J., Buffet, A. & Gimenez-Roqueplo, A. P. HIF2A mutations in paraganglioma with polycythemia. *N. Engl. J. Med.* **367,** 2161 author reply 2161-2162 (2012).
8. Crona, J. *et al.* Somatic mutations in H-RAS in sporadic pheochromocytoma and paraganglioma identified by exome sequencing. *J. Clin. Endocrinol. Metab.* **98,** E1266–E1271 (2013).
9. Oudijk, L. *et al.* H-RAS mutations are restricted to sporadic pheochromocytomas lacking specific clinical or pathological features: data from a multi-institutional series. *J. Clin. Endocrinol. Metab.* **99,** E1376–E1380 (2014).
10. Dahia, P. L. *et al.* A HIF1alpha regulatory loop links hypoxia and mitochondrial signals in pheochromocytomas. *PLoS Genet.* **1,** 72–80 (2005).
11. Favier, J. *et al.* The Warburg effect is genetically determined in inherited pheochromocytomas. *PLoS ONE* **4,** e7094 (2009).
12. Lopez-Jimenez, E. *et al.* Research resource: Transcriptional profiling reveals different pseudohypoxic signatures in SDHB and VHL-related pheochromocytomas. *Mol. Endocrinol.* **24,** 2382–2391 (2010).
13. Letouze, E. *et al.* SDH mutations establish a hypermethylator phenotype in paraganglioma. *Cancer Cell* **23,** 739–752 (2013).
14. Tombol, Z. *et al.* MicroRNA expression profiling in benign (sporadic and hereditary) and recurring adrenal pheochromocytomas. *Mod. Pathol.* **23,** 1583–1595 (2010).
15. Meyer-Rochow, G. Y. *et al.* MicroRNA profiling of benign and malignant pheochromocytomas identifies novel diagnostic and therapeutic targets. *Endocr. Relat. Cancer* **17,** 835–846 (2010).
16. Patterson, E. *et al.* The microRNA expression changes associated with malignancy and SDHB mutation in pheochromocytoma. *Endocr. Relat. Cancer* **19,** 157–166 (2012).
17. de Cubas, A. A. *et al.* Integrative analysis of miRNA and mRNA expression profiles in pheochromocytoma and paraganglioma identifies genotype-specific markers and potentially regulated pathways. *Endocr. Relat. Cancer* **20,** 477–493 (2013).
18. August, C. *et al.* CGH and CD 44/MIB-1 immunohistochemistry are helpful to distinguish metastasized from nonmetastasized sporadic pheochromocytomas. *Mod. Pathol.* **17,** 1119–1128 (2004).
19. Cascon, A. *et al.* A novel candidate region linked to development of both pheochromocytoma and head/neck paraganglioma. *Genes Chromosomes Cancer* **42,** 260–268 (2005).
20. van Nederveen, F. H. *et al.* Array-comparative genomic hybridization in sporadic benign pheochromocytomas. *Endocr. Relat. Cancer* **16,** 505–513 (2009).
21. Sandgren, J. *et al.* Recurrent genomic alterations in benign and malignant pheochromocytomas and paragangliomas revealed by whole-genome array comparative genomic hybridization analysis. *Endocr. Relat. Cancer* **17,** 561–579 (2010).
22. Burnichon, N. *et al.* SDHA is a tumor suppressor gene causing paraganglioma. *Hum. Mol. Genet.* **19,** 3011–3020 (2010).
23. Stephens, P. J. *et al.* Massive genomic rearrangement acquired in a single catastrophic event during cancer development. *Cell* **144,** 27–40 (2011).
24. Letouze, E., Allory, Y., Bollet, M. A., Radvanyi, F. & Guyon, F. Analysis of the copy number profiles of several tumor samples from the same patient reveals the successive steps in tumorigenesis. *Genome Biol.* **11,** R76 (2010).
25. Lawrence, M. S. *et al.* Mutational heterogeneity in cancer and the search for new cancer-associated genes. *Nature* **499,** 214–218 (2013).
26. Anders, S. & Huber, W. Differential expression analysis for sequence count data. *Genome Biol.* **11,** R106 (2010).
27. Benetatos, L. *et al.* The microRNAs within the DLK1-DIO3 genomic region: involvement in disease pathogenesis. *Cell Mol. Life Sci.* **70,** 795–814 (2013).
28. Pugh, T. J. *et al.* The genetic landscape of high-risk neuroblastoma. *Nat. Genet.* **45,** 279–284 (2013).
29. Molenaar, J. J. *et al.* Sequencing of neuroblastoma identifies chromothripsis and defects in neuritogenesis genes. *Nature* **483,** 589–593 (2012).
30. Jones, D. T. *et al.* Dissecting the genomic complexity underlying medulloblastoma. *Nature* **488,** 100–105 (2012).
31. Mack, S. C. *et al.* Epigenomic alterations define lethal CIMP-positive ependymomas of infancy. *Nature* **506,** 445–450 (2014).
32. Hodis, E. *et al.* A landscape of driver mutations in melanoma. *Cell* **150,** 251–263 (2012).
33. Brennan, C. W. *et al.* The somatic genomic landscape of glioblastoma. *Cell* **155,** 462–477 (2013).
34. Lawrence, M. S. *et al.* Discovery and saturation analysis of cancer genes across 21 tumour types. *Nature* **505,** 495–501 (2014).
35. Blumenschein, Jr. G. R., Mills, G. B. & Gonzalez-Angulo, A. M. Targeting the hepatocyte growth factor-cMET axis in cancer therapy. *J. Clin. Oncol.* **30,** 3287–3296 (2012).
36. Wu, G. *et al.* The genomic landscape of diffuse intrinsic pontine glioma and pediatric non-brainstem high-grade glioma. *Nat. Genet.* **46,** 444–450 (2014).
37. Schwartzentruber, J. *et al.* Driver mutations in histone H3.3 and chromatin remodelling genes in paediatric glioblastoma. *Nature* **482,** 226–231 (2012).
38. Parsons, D. W. *et al.* The genetic landscape of the childhood cancer medulloblastoma. *Science* **331,** 435–439 (2011).
39. Huether, R. *et al.* The landscape of somatic mutations in epigenetic regulators across 1,000 paediatric cancer genomes. *Nat. Commun.* **5,** 3630 (2014).
40. Karpathakis, A., Dibra, H. & Thirlwell, C. Neuroendocrine tumours: cracking the epigenetic code. *Endocr. Relat. Cancer* **20,** R65–R82 (2013).
41. Killian, J. K. *et al.* Succinate dehydrogenase mutation underlies global epigenomic divergence in gastrointestinal stromal tumor. *Cancer Discov.* **3,** 648–657 (2013).
42. Eisenhofer, G. *et al.* Measurements of plasma methoxytyramine, normetanephrine, and metanephrine as discriminators of different hereditary forms of pheochromocytoma. *Clin. Chem.* **57,** 411–420 (2011).

43. Loriot, C. *et al.* Epithelial to mesenchymal transition is activated in metastatic pheochromocytomas and paragangliomas caused by SDHB gene mutations. *J. Clin. Endocrinol. Metab.* **97,** E954–E962 (2012).
44. Cho, Y. J. *et al.* Integrative genomic analysis of medulloblastoma identifies a molecular subgroup that drives poor clinical outcome. *J. Clin. Oncol.* **29,** 1424–1430 (2011).
45. Weeraratne, S. D. *et al.* Pleiotropic effects of miR-183 ~ 96 ~ 182 converge to regulate cell survival, proliferation and migration in medulloblastoma. *Acta Neuropathol.* **123,** 539–552 (2012).
46. Bai, A. H. *et al.* MicroRNA-182 promotes leptomeningeal spread of non-sonic hedgehog-medulloblastoma. *Acta Neuropathol.* **123,** 529–538 (2012).
47. Tanaka, H. *et al.* MicroRNA-183 upregulates HIF-1alpha by targeting isocitrate dehydrogenase 2 (IDH2) in glioma cells. *J. Neurooncol.* **111,** 273–283 (2013).
48. Segura, M. F. *et al.* Aberrant miR-182 expression promotes melanoma metastasis by repressing FOXO3 and microphthalmia-associated transcription factor. *Proc. Natl Acad. Sci. USA* **106,** 1814–1819 (2009).
49. Stevanato, L. & Sinden, J. D. The effects of microRNAs on human neural stem cell differentiation in two- and three-dimensional cultures. *Stem Cell Res. Ther.* **5,** 49 (2014).
50. Liang, Y., Ridzon, D., Wong, L. & Chen, C. Characterization of microRNA expression profiles in normal human tissues. *BMC Genomics* **8,** 166 (2007).
51. Assie, G. *et al.* Integrated genomic characterization of adrenocortical carcinoma. *Nat. Genet.* **46,** 607–612 (2014).
52. Plouin, P. F., Gimenez-Roqueplo, A. P. & Bertagna, X. [COMETE, a network for the study and management of hypersecreting adrenal tumors]. *Bull. Acad. Natl Med.* **192,** 73–82 discussion 83-85 (2008).
53. Lenders, J. W. *et al.* Pheochromocytoma and paraganglioma: an endocrine society clinical practice guideline. *J. Clin. Endocrinol. Metab.* **99,** 1915–1942 (2014).
54. Bibikova, M. *et al.* Genome-wide DNA methylation profiling using Infinium(R) assay. *Epigenomics* **1,** 177–200 (2009).
55. Venkatraman, E. S. & Olshen, A. B. A faster circular binary segmentation algorithm for the analysis of array CGH data. *Bioinformatics* **23,** 657–663 (2007).
56. Popova, T. *et al.* Genome Alteration Print (GAP): a tool to visualize and mine complex cancer genomic profiles obtained by SNP arrays. *Genome Biol.* **10,** R128 (2009).
57. Guichard, C. *et al.* Integrated analysis of somatic mutations and focal copy-number changes identifies key genes and pathways in hepatocellular carcinoma. *Nat. Genet.* **44,** 694–698 (2012).
58. Robinson, J. T. *et al.* Integrative genomics viewer. *Nat. Biotechnol.* **29,** 24–26 (2011).
59. Vigneault, F. *et al.* High-throughput multiplex sequencing of miRNA. *Curr. Protoc. Hum. Genet.* **Chapter 11,** Unit 11.12.1–10 (2012).
60. Wang, W. C. *et al.* miREXpress: analyzing high-throughput sequencing data for profiling microRNA expression. *BMC Bioinformatics* **10,** 328 (2009).
61. Hackenberg, M., Rodriguez-Ezpeleta, N. & Aransay, A. M. miRanalyzer: an update on the detection and analysis of microRNAs in high-throughput sequencing experiments. *Nucleic Acids Res.* **39,** W132–W138 (2011).
62. Wilkerson, M. D. & Hayes, D. N. ConsensusClusterPlus: a class discovery tool with confidence assessments and item tracking. *Bioinformatics* **26,** 1572–1573 (2010).

Acknowledgements

This work is part of the 'Cartes d'Identité des Tumeurs (CIT) programme' funded and developed by 'La Ligue Nationale contre le Cancer' (http://cit.ligue-cancer.net). We thank Jacqueline Godet and Jacqueline Metral for their strong support within the CIT Program. We are grateful to Professors X. Jeunemaitre and Xavier Bertagna for continual support and helpful discussions. We also thank all members of the Genetics Department and Biological Resources Center and Tumor Bank Platform, Hôpital européen Georges Pompidou (BB-0033-00063), as well as Catherine Tritscher for administrative assistance. The work leading to these results has received funding from the Agence Nationale de la Recherche (ANR 08 GENOPATH 029 MitOxy and ANR-2011-JCJC-00701 MODEOMAPP), the Programme Hospitalier de Recherche Clinique grant COMETE 3 (AOM 06 179), the Plan Cancer : Appel projets Epigntique et Cancer 2013 (EPIG201303 METABEPIC) and from the European Union Seventh Framework Program (FP7/2007-2013) under grant agreement number 259735. C.L. is supported by 'La Fondation ARC' (DOC20130606831). C.L.-L. is funded by the Cancer Research for Personalized Medicine—CARPEM project (Site de Recherche Intégré sur le Cancer—SIRIC).

Author contributions

L.J.C.-V., E.L., N.B., J.F. and A.-P.G.-R. conceived and designed the study. E.L., N.E. and A.R. performed computational and statistical analyses. L.J.C.-V., N.B., A.B., P.-H.D., E.K., C.L., A.M. and M.M. performed experiments. C.B. and M.S. reviewed histopathology. C.L.-L., B.D., R.L., F.Z., J.B., P.-F.P., L.A. and A.-P.G.-R. recruited the subjects. P.-F.P. coordinated the COMETE Network. L.J.C.-V., E.L. and N.B. prepared figures and tables. L.J.C.-V., E.L., N.B., J.F. and A.-P.G.-R. wrote the manuscript. J.F. and A.-P.G.-R. supervised the study. All authors discussed the results and commented on the manuscript.

Additional information

Accession codes: Exome-sequencing data has been deposited in the European Genome-phenome Archive under the accession code EGAS00001000933. SNP array data has been deposited in ArrayExpress under the accession code E-MTAB-2817. miRNA sequencing data has been deposited in ArrayExpress under the accession code E-MTAB-2833.

Supplementary Information accompanies this paper at http://www.nature.com/naturecommunications

Competing financial interests: The authors declare no competing financial interests.

Reprints and permission information is available online at http://npg.nature.com/reprintsandpermissions/

How to cite this article: Castro-Vega, L. J. *et al.* Multi-omics analysis defines core genomic alterations in pheochromocytomas and paragangliomas. *Nat. Commun.* 6:6044 doi: 10.1038/ncomms7044 (2015).

ARTICLE 4

From Nf1 to Sdhb knockout: Successes and failures in the quest for animal models of pheochromocytoma.

Lepoutre-Lussey C, Thibault C, Buffet A, Morin A, Badoual C, Bénit P, Rustin P, Ottolenghi C, Janin M, Castro-Vega LJ, Trapman J, Gimenez-Roqueplo AP, Favier J.

Mol Cell Endocrinol. 2016 Feb 5;421:40-8

Molecular and Cellular Endocrinology 421 (2016) 40–48

Contents lists available at ScienceDirect

Molecular and Cellular Endocrinology

journal homepage: www.elsevier.com/locate/mce

From *Nf1* to *Sdhb* knockout: Successes and failures in the quest for animal models of pheochromocytoma

Charlotte Lepoutre-Lussey [a, b], Constance Thibault [a, b], Alexandre Buffet [a, b], Aurélie Morin [a, b], Cécile Badoual [a, b, c], Paule Bénit [d, e], Pierre Rustin [d, e], Chris Ottolenghi [b, f, g], Maxime Janin [b, f, g], Luis-Jaime Castro-Vega [a, b], Jan Trapman [h], Anne-Paule Gimenez-Roqueplo [a, b, i], Judith Favier [a, b, *]

[a] *INSERM, UMR970, Paris-Cardiovascular Research Center, F-75015 Paris, France*
[b] *Université Paris Descartes, Sorbonne Paris Cité, Faculté de Médecine, F-75006 Paris, France*
[c] *Assistance Publique-Hôpitaux de Paris, Hôpital Européen Georges Pompidou, Service d'anatomo-pathologie, F-75015 Paris, France*
[d] *INSERM, UMR1141, Hôpital Robert Debré, F-75019 Paris, France*
[e] *Université Paris 7, Faculté de Médecine Denis Diderot, Paris, France*
[f] *Metabolic Biochemistry, Hôpital Necker-Enfants Malades, Paris, France*
[g] *INSERM, Unit 1124, Paris, France*
[h] *Department of Pathology, Erasmus MC, University Medical Center Rotterdam, The Netherlands*
[i] *Assistance Publique-Hôpitaux de Paris, Hôpital Européen Georges Pompidou, Service de Génétique, F-75015 Paris, France*

ARTICLE INFO

Article history:
Received 10 April 2015
Received in revised form
2 June 2015
Accepted 2 June 2015
Available online 27 June 2015

Keywords:
Pheochromocytoma
Genetically engineered mouse
Knockout
Xenograft
Chromaffin cells

ABSTRACT

Pheochromocytomas and paragangliomas (PPGL) are rare neuroendocrine tumors characterized by a high frequency of hereditary forms. Based on transcriptome classification, PPGL can be classified in two different clusters. Cluster 1 tumors are caused by mutations in *SDHx*, *VHL* and *FH* genes and are characterized by a pseudohypoxic signature. Cluster 2 PPGL carry mutations in *RET, NF1, MAX* or *TMEM127* genes and display an activation of the MAPK and mTOR signaling pathways. Many genetically engineered and allografted mouse models have been generated these past 30 years to investigate the mechanisms of PPGL tumorigenesis and test new therapeutic strategies. Among them, only Cluster 2-related models have been successful while no Cluster 1-related knockout mouse was so far reported to develop a PPGL. In this review, we present an overview of existing, successful or not, PPGL models, and a description of our own experience on the quest of *Sdhb* knockout mouse models of PPGL.

1. Introduction

Pheochromocytomas (PCC) and paragangliomas (PPGL) are rare catecholamine-secreting tumors arising respectively from the adrenal medulla (PCC proper) or from extra-adrenal chromaffin tissues (PGL). PPGL occur in the context of inherited cancer syndromes in around 40% of cases. These hereditary syndromes include multiple endocrine neoplasia type 2 (caused by *RET* mutations), von Hippel Lindau disease (*VHL* gene mutations), neurofibromatosis type 1 (*NF1* gene mutations), hereditary PPGL syndrome (*SDHA, SDHB, SDHC, SDHD* (referred to *as SDHx*) and *SDHAF2* genes), familial pheochromocytoma (*TMEM127, MAX*), polycythemia paraganglioma syndrome (*EPAS1/HIF2A*), and Reed syndrome (*FH*) (Amar et al., 2005; Dahia, 2014; Favier et al., 2014; Gimenez-Roqueplo et al., 2012). Recently, *MDH2* was described as a novel PPGL susceptibility gene (Cascon et al., 2015). With the exceptions of *RET* and *HIF2A* which act as oncogenes, all PPGL susceptibility genes are considered as tumor suppressor genes: patients carry a heterozygous germline mutation and tumor development occurs following a somatic second hit that leads to loss of heterozygosity (LOH), and to the subsequent inactivation of the gene. The hereditary PPGL syndrome is the most frequent inherited condition, characterized by the occurrence of PCC or PGL usually at a young age, with a multifocal disease. Patients with *SDHB* mutations have an increased risk of recurrence, malignant disease and poor prognosis (Amar et al., 2007).

* Corresponding author. Centre de recherche cardiovasculaire de l'HEGP, 56 rue Leblanc, 75015 Paris.
E-mail address: judith.favier@inserm.fr (J. Favier).

http://dx.doi.org/10.1016/j.mce.2015.06.027
0303-7207/

Various large cohorts of patients have been generated worldwide with highly representative tumor collections permitting the implementation of genomic studies (Burnichon et al., 2011; Dahia et al., 2005; Eisenhofer et al., 2004; Favier et al., 2009; Lopez-Jimenez et al., 2010). Gene expression profiling obtained in these transcriptomic studies have been used to classify PPGLs, assigning them to either a hypoxic/angiogenic cluster (Cluster 1) or a kinase-signaling cluster (Cluster 2). Cluster 1 contains all *SDH*x-related tumors, the recently described *FH*- (Castro-Vega et al., 2014; Letouze et al., 2013) and *VHL*-mutated tumors. Cluster 2 consists in tumors related to *RET, NF1, TMEM127* and *MAX* genes mutations, as well as most of the sporadic tumors.

Many genetically engineered and allografted mouse models have been generated to investigate the mechanisms of PPGL tumorigenesis and test new therapeutic strategies (Table 1). Existing mouse models include inactivation of *Nf1, Rb, Vhl, Sdhd, Pten* and *InK4a* tumor suppressor genes (Bayley et al., 2009; Gnarra et al., 1997; Haase et al., 2001; Jacks et al., 1994; Korpershoek et al., 2009; Ma et al., 2003; Nikitin et al., 1999; Piruat et al., 2004; You et al., 2002) and mutations on *c-mos*, *Ret* and *ErbB2* proto-oncogenes(Lai et al., 2007; Schulz et al., 1992; Smith-Hicks et al., 2000). We describe here an overview of these existing predisposed and xenografted mouse models together with our local experience on the generation of *Sdhb* deficient mouse models.

2. Predisposed mouse models

2.1. Cluster 1

The Cluster C1 includes tumors carrying *SDHx, FH, VHL* and *HIF2A* genes mutations. Genes overexpressed in this cluster participate to the hypoxia-dependent signaling pathways promoting angiogenesis, proliferation and glycolysis (Favier et al., 2009). This "pseudo-hypoxic" signature is explained by the direct capacity of *SDHx, FH* and *VHL*-mutated cells to stabilize hypoxia-inducible factors (HIFs) in normoxic conditions. *VHL* encodes a member of an E3 ubiquitin ligase complex that targets HIFα proteins to proteasomal degradation in normoxia. *SDHA-D* genes encode the 4 subunits of succinate dehydrogenase (SDH) or mitochondrial complex II, an enzyme located at the crossroads between the mitochondrial electron transport chain and the tricarboxylic acid (TCA) cycle (Lancaster and Simon, 2002). The complete loss of SDH activity in the tumor is associated with succinate accumulation, which inhibits prolyl-hydroxylases activity that finally results in the abnormal stabilization of HIFαs under normoxic conditions (Briere et al., 2005). Succinate also inhibits TET DNA demethylases and JmJC histones demethylases, leading to global DNA and histones hypermethylation that has important consequences on gene expression (Letouze et al., 2013). *FH* is a tumor suppressor gene encoding fumarate hydratase (also known as fumarase), which

Table 1
Success and failures of predisposed mouse models of pheochromocytomas.

Transcription cluster	Human syndrome	Gene	Mouse model	PCC	Other phenotype	Cell lines	Reference
Cluster 1	Familial Paraganglioma	*SDHD*	*Sdhd*−/−	–	Embryonic lethal (E7)	–	Piruat et al., 2004
			Sdhd+/-	No	Carotid body hyperplasia	–	Bayley et al, 2009
		SDHB	Sdhb−/−	–	Embryonic lethal (E7)	imCC	Letouze et al., 2013
			Sdhb+/-	No	No	–	Present study
			Sdhdlox	No	No	–	
	Von Hippel Lindau	*VHL*	*Vhl*−/−	–	Embryonic lethal (E10.5 to 12.5)	–	Gnarra et al., 1997
			Vhl+/−; *Vhl*+/lox, albumin-Cre	No	Vascular tumours of multiple organs	–	Ma et al., 2003
			*Vhl*lox/−, ß-actin-CRE	No	Hepatic Hemangiomas	–	Haase et al., 2001
	HLRCC	*FH*	$Fh1^{-/-}$	–	Embryoniclethal (E6)	–	Pollard et al., 2007
			$Fh1^{lox/lox}$;Ksp1.3/Cre	No	renal cysts	–	
Cluster 2	Neurofibromatosis Type 1	*NF1*	*Nf1*−/−	–	Embryonic lethal (E13.5)	–	Jacks et al., 1994
			Nf1+/−	PCC in 10–20%, 15–28 months	Myeloid leukemia		
				–	–	MPC	Powers et al., 2000
	MEN2B	*RET*	Met918Thr (het)	Chromaffin cell hyperplasia (16%)	C-cell hyperplasia (up to 41% at 12 months)	–	Smith-Hicks et al., 2000
			Met918Thr (homo)	PCC in 100%, 6–10 months	C-cell hyperplasia (up to 60% at 10 months)	–	
						–	
	"MEN2-like"	*c-mos*	Transgenic	Bilateral PCC in 58%, 8 months	C-cell thyroid carcinomas; gliosis; axonal degeneration	–	Schulz et al., 1992
		Rb	*Rb* +/−	PCC in 71% (14% bilateral) 12 months	C-cell thyroid carcinomas 81% 12 months Pituitary, parathyroid, lung, pancreas tumors	–	Nikitin et al., 1999
	None	*ErbB2*	PB-*ErbB2*	Adrenal hypertrophy (5%), PCC in 5% of males, 15 months	Prostate intraepithelial neoplasia	–	Lai et al., 2007
		B-RAF	$B\text{-}Raf^{V600E}$	PCC and PGL in 80% at 5 months	cardio-facio-cutaneous syndrome	–	Urosevic et al., 2011
	Cowden Syndrome	*PTEN*	*Ink4a Arf*+/+ ; *Pten*+/-	PCC in 24%, 10.5 months	Prostate, breast and endometrial hyperplasia	–	You et al., 2002
			Ink4a Arf+/−; *Pten*+/-	PCC in 57%, 7.5 months			
			Ink4a Arf−/−; *Pten*+/-	PCC in 59%, 6 months	Lymphoma; pulmonary and colon carcinoma sarcoma		
			PSA-Cre; *Pten*loxP/loxP	PCC in 30% at 7–9 months and 100%, at 15–16 months	Prostate tumors	–	Korpershoek et al., 2009

converts fumarate into malate in the TCA cycle. As for SDH-related PPGL, *FH*-related paragangliomas present a pattern of global histone and DNA hypermethylation evocating that fumarate acts, like succinate, as an oncometabolite (Castro-Vega et al., 2014; Letouze et al., 2013; Morin et al., 2014).

2.1.1. SDH deficient mouse models

The first report of SDH complex inactivation in mouse was published in 2004 by Piruat et al. (Piruat et al., 2004). This model is embryonic lethal at E7 when the knockout (KO) of *Sdhd* is homozygous. Heterozygous *Sdhd* inactivation induces a slight increase in the percentage of glomus cells in the carotid body (CB) and a significant increase of spontaneous CB activity under normoxic conditions but does not lead to carotid body PGL nor PCC (Piruat et al., 2004). Several years later, a second team generated *Sdhd* gene knockout mice with the same results even after crossing them with a strain knocked-out for a candidate imprinted modifier gene (*H19* $^{+/-}$ mice) in order to mimic the "imprinted" inheritance of *SDHD* tumorigenesis observed in human (Bayley et al., 2009).

Our strategy was to inactivate *Sdhb* gene in order to generate an animal model of malignant PPGL as close as possible to the human disease.

Because embryonic death of nullizygous *Sdhb* mice was predictable, we used the Cre-Lox system to generate both a constitutive and a conditional inactivation of the gene. To that aim, LoxP sites were inserted on both sides of *Sdhb* exon 2 (Letouze et al., 2013). *Sdhb*-floxed mice were subsequently crossed with PGK-Cre^{m} mice (Lallemand, 1998) to generate the constitutive knockout model, and with tyrosine hydroxylase-Cre (TH-Cre) or human Prostate-Specific Antigen-Cre (PSA-Cre) mice to generate cell-specific conditional KO models. TH promoter is expected to drive Cre recombinase expression in all catecholaminergic cells (Gelman et al., 2003), while PSA, although supposedly specific of the prostate, actually drives expression in the adrenal medulla in mouse (Korpershoek et al., 2009) (see Section 2.2.2).

As expected, cross-breeding of *Sdhb*$^{+/-}$ animals did not lead to the expected Mendelian genotype ratios of 1:2:1 but to a heterozygous *Sdhb*$^{+/-}$ and wild type *Sdhb*$^{+/+}$ offspring (ratio 2:1) indicating that a complete inactivation of *Sdhb* results in embryonic lethality. Embryos isolated at day E7.5 onwards were found to have heterozygous *Sdhb*$^{+/-}$ or wild-type *Sdhb*$^{+/+}$ genotypes (N = 63) (Fig. 1A). At that time of embryonic development, about 25% of the embryo sacs were empty and only one homozygous *Sdhb*$^{-/-}$ embryo was retrieved and genotyped at E6.5 (Fig. 1A). These results are concordant with an embryonic lethality before E7.5 as previously reported for the *Sdhd* gene knockout (Piruat et al., 2004).

Expression of *Sdhb* mRNA (Fig. 1B) and SDH enzymatic activity (Fig. 1C) in several tissues were reduced in *Sdhb*$^{+/-}$ mice as compared with their wild type counterparts.

Heterozygous *Sdhb*$^{+/-}$ mice are fertile and viable. No bias was detected in the male/female ratio and the survival was comparable in the two groups. Evaluation of the cardiovascular phenotype of the mice (blood pressure and heart rate) revealed no significant differences compared to WT mice. Main organs (heart, kidney, lung, liver) and specific tissues of PGL emergence (adrenal, carotid body) were examined macroscopically and histologically and revealed no difference. A cohort of 231 mice was followed during a median period of 19 months (range 6–27 months) and sacrificed to analyze tumor development. This cohort included 106 wild type and 125 *Sdhb*$^{+/-}$ mice. No indication of chromaffin tumor development was apparent in any animal and only one heterozygous mouse died of natural causes (other than PCC) before sacrifice.

As for the heterozygous mice, TH-Cre/*Sdhb*$^{lox/lox}$ and TH-Cre/*Sdhb*$^{lox/-}$ (n = 51), as well as PSA-Cre/*Sdhb*$^{lox/lox}$ and PSA-Cre/*Sdhb*$^{lox/-}$ (N = 67) conditional knockout mice are viable, fertile and had no apparent phenotype (Table 2). Various tumors were identified in 5 mice (one schwannoma, one pancreatic cyst, one hepatocarcinoma, one lymphoma, one epidermoïd carcinoma) but none were pheochromocytoma and the median adrenal weight was 3.0 mg [range 1.0–7.9 mg], which is comparable to that of control mice.

Pten$^{+/-}$ mice were previously reported to be predisposed to PCC (You et al., 2002). Because of the absence of PCC or PGL in *Sdhb* KO mice, we crossed them under a *Pten* knockout background (*Pten*$^{+/-}$ mice generated by crossing *Pten*$^{+/lox}$ mice (Ma et al., 2005) with PGK-Cre^{m} mice). The aim was to generate a metastatic PCC experimental model harboring an inactivation of the *Sdhb* gene. Fifty-one constitutive double heterozygous (*Sdhb*$^{+/-}$/*Pten*$^{+/-}$) mice were studied and compared to 83 heterozygous *Pten*$^{+/-}$ mice. Among these mice, 26 died before sacrifice (11 *Sdhb*$^{+/-}$/*Pten*$^{+/-}$ including 1 necropsied and 15 *Pten*$^{+/-}$ including 3 necropsied). Necropsy was performed for the 68 remaining *Pten*$^{+/-}$ and 40 *Sdhb*$^{+/-}$/*Pten*$^{+/-}$ mice following sacrifice. Adrenals were retrieved in all cases and considered as a PCC if weighting more than 8 mg, as previously reported (Korpershoek et al., 2009). At 10 months, more than 70% of these mice developed a PCC detectable *in vivo* on MRI (Fig. 1E, F) and confirmed by histology (Fig. 1G) with no significant difference between the two groups regarding PCC frequency, adrenal median weight, median age of dissection, or death. Among the mice with PCC, lungs were examined on histological sections in 11/52 *Pten*$^{+/-}$ cases and 15/33 *Sdhb*$^{+/-}$/*Pten*$^{+/-}$ and lung micro-metastasis were found in 64% (7/11) and 73% (11/15) of cases, respectively (Fig. 1H). No other metastatic site was detected (lymph node or liver). Other cancer development was observed in accordance with *Pten* deficiency, with no difference between the two groups.

Finally, a double *Sdhb*/*Pten* conditional KO model expressing Cre recombinase under the control of PSA promoter was generated (Table 2). This promoter was chosen as its efficiency to promote PCC had previously been demonstrated in the *Pten* conditional KO (Korpershoek et al., 2009). Seventy-two double conditional KO mice were studied for PCC development. Among these mice one *PSA-Cre/Sdhb*$^{lox/-}$/*Pten*$^{lox/lox}$ died before sacrifice at 12 months old. In the end, necropsy was performed for 71 mice including 45 double conditional KO heterozygous for *Sdhb* deletion and 26 double conditional KO homozygous for *Sdhb* deletion (Table 2) at a median age of 12.9 months [range 8.3–14.6] and 9.7 months [range 7.6–11.9] respectively. The median adrenal weight and PCC development were significantly different between the 2 groups with a much lower tumor incidence in the group with double conditional KO homozygous for *Sdhb* deletion (Fig. 1E, Table 2). Indeed, in the double conditional KO heterozygous for *Sdhb* deletion, a high incidence of PCC was observed in comparable range to that of *Pten*$^{+/-}$ and *Sdhb*$^{+/-}$/*Pten*$^{+/-}$ mice (i.e. 64% in *PSA-Cre/Sdhb*$^{+/lox}$/*Pten*$^{+/lox}$ mice and 89% in *PSA-Cre/Sdhb*$^{+/lox}$/*Pten*$^{lox/lox}$). In contrast, there was a two-fold decrease in the incindence of PCC in the double conditional KO homozygous for *Sdhb* deletion (Table 2).

The succinate level was assessed by Gas chromatography–mass spectrometry (GC–MS) in 23 PCC from 13 *Pten*$^{+/-}$ mice and 9 double conditional KO (4 heterozygous and 5 homozygous for *Sdhb* deletion). In contrast with human PPGL (Pollard et al., 2005), no accumulation of succinate was detected in any of these tumors (Fig. 1I), demonstrating the persistence of an SDH activity, even in supposedly *Sdhb* homozygous knockout tumors. The high incidence of PCC in double conditional KO heterozygous for *Sdhb* deletion (*PSA-Cre/Sdhb*$^{+/lox}$/*Pten*$^{+/lox}$ mice and *PSA-Cre/Sdhb*$^{+/lox}$/*Pten*$^{lox/lox}$) shows that Cre-mediated recombination is highly efficient using the PSA promoter. Thus, the two-fold reduction in PCC incidence observed in the double conditional KO homozygous for *Sdhb* deletion, must be the consequence of a cell death induced by *Sdhb* complete deletion. Only cells in which a reduced Cre efficiency maintained a wild-type *Sdhb* allele were able to survive, leading to

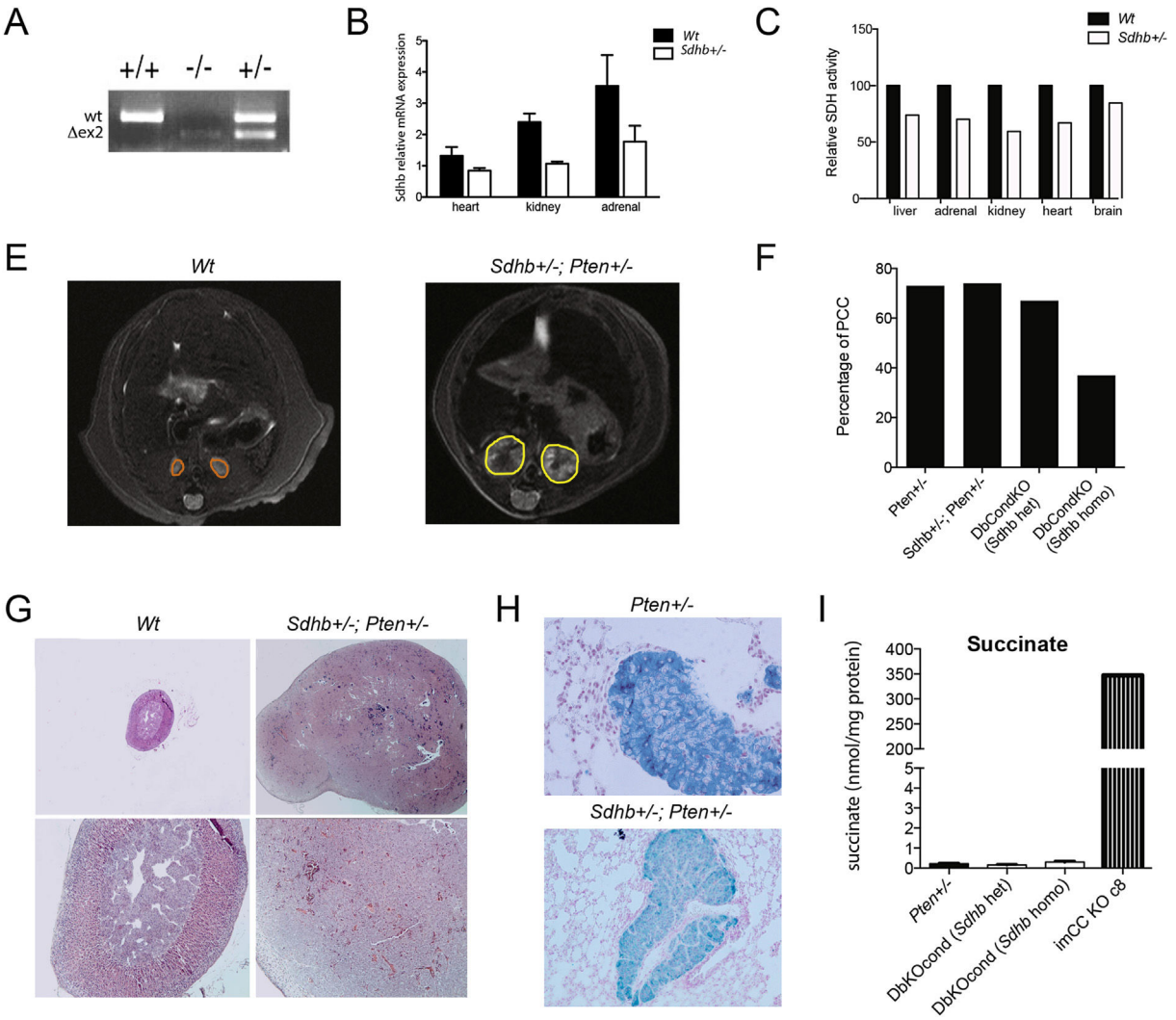

Fig. 1. Characterization of *Sdhb* constitutive and conditional knockout mice. Genotyping of *Sdhb* gene locus revealed the homozygous deletion of exon 2 (Δex2) in a single $Sdhb^{-/-}$ embryo at E7 (A). Quantitative RT-PCR confirmed the haploinsufficiency in the heart, kidney and adrenals of $Sdhb^{+/-}$ mice, compared to their wild-type (wt) littermates (B). $Sdhb^{+/-}$ mice displayed a 25–40% decrease in SDH activity measured by spectrophotometry (C). T2-weighted MRI reveals large adrenal masses in $Sdhb^{+/-}$; $Pten^{+/-}$ (yellow circles) as compared to a normal adrenal of a wt mouse (orange circles) (E). While more than 70% of $Pten^{+/-}$, $Sdhb^{+/-}$; $Pten^{+/-}$, and Double *Pten/Sdhb* PSA-Cre conditional knockout mouse (DbCondKO) heterozygous for *Sdhb* ($Sdhb^{+/lox}$) present a PCC, DbCondKO homozygous for *Sdhb* ($Sdhb^{lox/lox}$ *and* $Sdhb^{lox/-}$) only present a PCC in 38% of cases (F). Hematoxylin eosin staining of the adrenal of wt and $Sdhb^{+/-}$; $Pten^{+/-}$ mice confirms the diagnosis of PCC (G). Synaptophysin immunostaining reveals PCC micrometastases in the lungs of $Pten^{+/-}$ or $Sdhb^{+/-}$; $Pten^{+/-}$ (H). None of the PCC resected from these mouse models displays succinate accumulation measured by GS-MS (I).

Table 2
The quest for generating an *Sdhb* deficient mouse model predisposed to pheochromocytoma.

Mouse genotype	Expected genotype in adrenal medulla	PCC (%)	Nb of mice with PCC/Total
$Sdhb^{-/-}$	NA	NA	NA
$Sdhb^{+/-}$	$Sdhb^{+/-}$	0	0/125
TH-Cre/$Sdhb^{lox/lox}$	$Sdhb^{-/-}$	0	0/51
TH-Cre/$Sdhb^{lox/-}$			
PSA-Cre/$Sdhb^{lox/lox}$	$Sdhb^{-/-}$	0	0/67
PSA-Cre/$Sdhb^{lox/-}$			
$Pten^{+/-}$	$Pten^{+/-}$	73	52/71
$Sdhb^{+/-}$/$Pten^{+/-}$	$Sdhb^{+/-}$/$Pten^{+/-}$	80	33/41
PSA-Cre/$Sdhb^{+/lox}$/$Pten^{+/lox}$	$Sdhb^{+/-}$/$Pten^{+/-}$	64	23/36
PSA-Cre/$Sdhb^{+/lox}$/$Pten^{lox/lox}$	$Sdhb^{+/-}$/$Pten^{-/-}$	89	8/9
PSA-Cre/$Sdhb^{lox/lox}$/$Pten^{+/lox}$	$Sdhb^{-/-}$/$Pten^{+/-}$	33	4/12
PSA-Cre/$Sdhb^{lox/-}$/$Pten^{+/lox}$			
PSA-Cre/$Sdhb^{lox/lox}$/$Pten^{lox/lox}$	$Sdhb^{-/-}$ $Pten^{-/-}$	42	6/14
PSA-Cre/$Sdhb^{lox/-}$/$Pten^{lox/lox}$			
PSA-Cre/$Sdhb^{lox/-}$/$Pten^{lox/-}$			

PCC with normal SDH activity.

Altogether, these results suggest that *Sdhb* complete KO is lethal in mouse chromaffin cells *in vivo* and that the generation of an SDH-related model of PGL or PCC may not be feasible in mouse.

2.1.2. Other models targeting the pseudohypoxic pathway

Von Hippel–Lindau disease (VHL) is a rare autosomal dominant disease characterized in human by renal clear-cell carcinoma, PPGL and central nervous system or retinal haemangioblastomas associated with neuroendocrine pancreatic tumors or cysts, endolymphatic sac tumors, and epididymal and/or broad ligament cystadenomas (Maher et al., 2011). Homozygous disruption of *Vhl* in mice results in embryonic lethality from lack of placental vasculogenesis (Gnarra et al., 1997), while heterozygous *Vhl* mice have a phenotype strongly dependent on genetic background. Indeed, no phenotype was observed in $Vhl^{+/-}$ mice bred in a mixed C57BL6/c129 genetic background (Gnarra et al., 1997), while $Vhl^{+/-}$ in a BALB/c129 background developed cavernous liver hemangiomas with a high phenotypic penetrance (Haase et al., 2001). Haase et al. generated a conditional *Vhl* KO mouse model (Haase et al., 2001). They first targeted a disruption of *Vhl* in the liver leading to hepatic vascular tumors (cavernous hemangiomas) (Haase et al., 2001). Thereafter, different tissue-specific V*hl* KO strains were generated (in the kidney, epidermis, thymus …) with several vascular HIF1 and 2 dependent tumors. However, no specific chromaffin KO was generated and thus no PPGL was ever reported in these mice (for review see (Haase, 2005)).

Mutations in *FH* gene in human predispose to Reed syndrome, also known as multiple cutaneous and uterine leiomyomatosis (HLRCC) (Tomlinson et al., 2002; Toro et al., 2003). This autosomal dominant disease associates smooth muscle tumors (leiomyomas) in the skin and uterus. Some affected patients are at risk of developing benign renal cysts, type 2 papillary renal carcinoma, leiomyocarcinomas and, in exceptional cases, PPGL (Castro-Vega et al., 2014; Lehtonen et al., 2006; Tomlinson et al., 2002; Toro et al., 2003). The $Fh1^{-/-}$ mice generated by Pollard et al. died during early embryogenesis (Pollard et al., 2007). In this model, conditional targeting of *Fh1* in the kidney ($Fh1^{lox/lox}$;Ksp1.3/Cre animals), results in renal cysts as a direct consequence of HIF1α (and HIF2α) overexpression (Pollard et al., 2007). Nevertheless, while the link between tumor development and activation of the hypoxic pathway is clearly demonstrated in *Vhl* deficient animals (Rankin et al., 2005), the phenotype observed in *Fh* KO mice is not rescued, but even worsened by the inactivation of HIF1 (Adam et al., 2011). To our knowledge, a conditional model targeting *Fh* knockout in the adrenal medulla has not been generated yet.

2.2. Cluster 2A

Cluster C2A comprises *RET*-, *NF1*-, *MAX*- and *TMEM127*-mutated PCC, as well as most sporadic tumors. These tumors display activation of the RAS/mitogen-activated protein kinase (MAPK) signaling pathways (Fig. 2).

2.2.1. Predisposing genes in human

2.2.1.1. NF1. The *NF1* gene, located on chromosome 17q11.2, is one of the largest genes in humans. It encodes neurofibromin, a tumor suppressor that downregulates the RAS–RAF–MAPK signaling cascade (Viskochil et al., 1990). Neurofibromatosis type 1, also known as von Recklinghausen disease, is a frequent autosomic disorder that includes several clinical features among the following: café-au-lait spots, neurofibromas, freckling in the axillary or inguinal regions, optic glioma, Lisch nodules (iris hamartomas) and typical bone lesions (Gutmann et al., 1997). PCC are rare in patients with neurofibromatosis type 1 (0.1–5.7%).

Homozygous deletion of *Nf1* in mouse leads to embryonic lethality, while the heterozygous *Nf1* knockout mouse model is an incomplete reflection of the human pathology. Indeed, mice develop PCC at a much higher frequency (~10–20% lifetime incidence) but without any neurofibromas (Jacks et al., 1994). Nevertheless, important observations with this model were that PCC only arose in mice with a mixed genetic background, and that the lifetime tumor incidence was increased to ~80% by neonatal irradiation of rat pups harboring the mutant *Nf1* allele (Powers et al., 2000).

2.2.1.2. c-mos, Rb and ret. The *RET* proto-oncogene encodes a tyrosine kinase receptor activated by dimerization after binding of its ligands but also by phosphorylation of its tyrosine kinase domain. This leads to activation of the PI3K–AKT and MAPK–ERK signaling pathways (Ibanez, 2013; Wagner et al., 2012). RET can be constitutively activated in human by gain-of-function mutations causing the multiple endocrine neoplasia type 2 (MEN2). MEN2 is a rare autosomal dominant disorder bringing together two syndromes: MEN2A (or Sipple syndrome) characterized by medullary thyroid carcinoma (MTC), PCC and primary hyperparathyroidism, and MEN2B (or Gorlin syndrome, accounting only for 5% of MEN2 cases) assembling severe medullary thyroid carcinoma, PCC, Marfanoid habitus, mucosal neuromas and ganglioneuromatosis of the gut and intestine (Brandi et al., 2001).

Historically, Schulz et al. developed the first PCC mouse model in 1992 while they were studying 4 lines of transgenic *c-mos* mice (Schulz et al., 1992). In addition to severe neurological defects and lens abnormalities, 3 of 4 of these *mos* transgenic lines develop a pattern of tumor formation similar to the human MEN2 with a high frequency of bilateral PCC (58%) at 8 months associated with MTC. Thereafter, two mouse models of MEN2 were generated. The first was secondary to a heterozygous loss-of-function mutation in *Rb* with a phenotype dominated by MTC together with the development of PCC in 71% of *Rb* ± mice, 14% of which were bilateral (Nikitin et al., 1999). The second model was secondary to the activating mutation (Met918thyr) of the *RET* proto-oncogene involved in MEN2B (Smith-Hicks et al., 2000). At 6 months, 100% of the homozygous Ret^{MEN2B} mice developed a PCC. These mice also developed thyroid C-cell hyperplasia (the presumed precursor of carcinoma in human) but no MTC (Smith-Hicks et al., 2000).

2.2.2. Other genes: Pten/InK4a, ErbB2 and B-RAF

The *PTEN* tumor suppressor gene encodes a phosphatase that negatively regulates the phosphoinositide 3-kinase (PI3K), inhibiting the PI3K/AKT signaling pathway (Cantley and Neel, 1999). Mutations in this tumor suppressor gene in humans, cause, among others, Cowden syndrome which is characterized by several tumors (hamartomas, and in particular cancers of the breast, the thyroid gland, the endometrium) but no PCC (Puc et al., 2006; van Nederveen et al., 2006). Nevertheless, co-existing inactivation of *PTEN* and of *INK4a* are observed in several human cancers, although not yet in PPGL (Ali et al., 1999). *INK4A* gene encodes 2 tumor suppressor genes ($p16^{INK4a}$ and $p19^{ARF}$) that regulate p53 and pRb (Retinoblastoma) pathways. You et al. showed that the heterozygous inactivation of *Pten* predisposes to a broad spectrum of cancers in mice including PCC in 23% of cases at 7 months (rising to 60% when co-inactivated with *Ink4a* gene). Moreover, in contrast with the previously described mouse models predisposing mostly to benign PCC, these tumors present around 15% of malignancy (lung metastasis) (You et al., 2002).

Two models unexpectedly came from prostate cancer studies using targeting technologies driven by supposedly specific prostate promoters that actually leak in the adrenal medulla. First, Korpershoek et al. reported the conditional *Pten* KO using the PSA-Cre

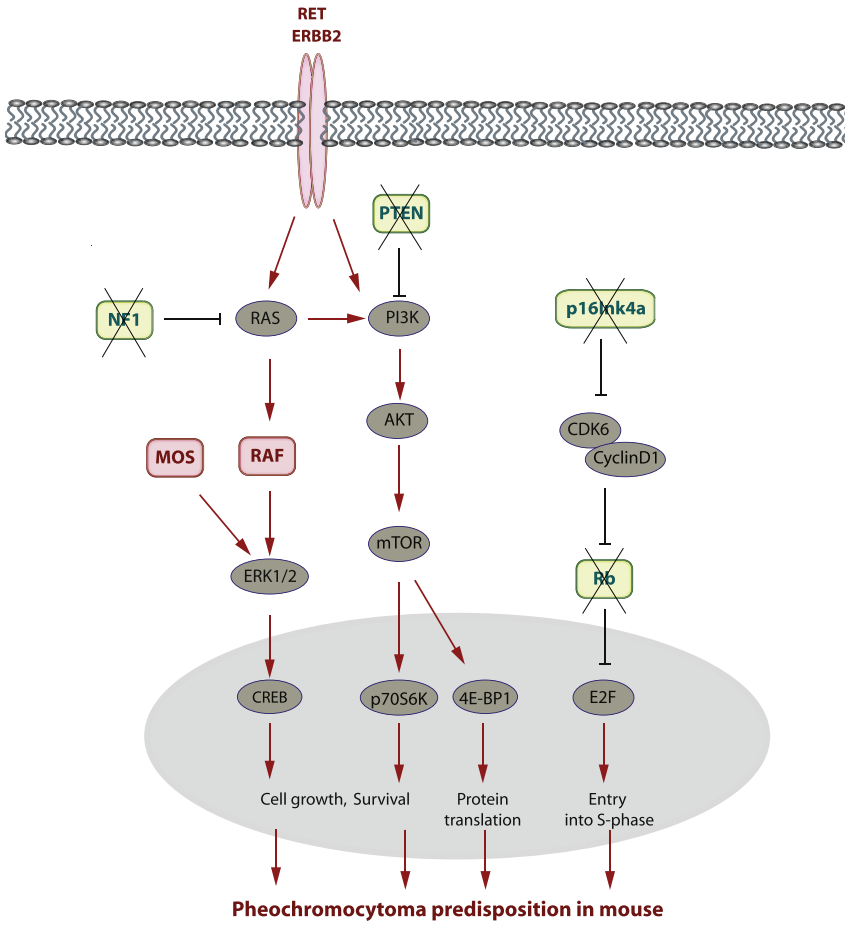

Fig. 2. Pathways involved in mouse models developing pheochromocytomas. Cluster 2-related models develop PCC at various frequencies. Targeted genes comprise transgenic activation of *Ret*, *c-mos*, *ErbB2* and *B-RAF* oncogenes and knock-out of *Nf1*, *Rb* and *Pten* or *Pten*/*InK4a* tumor suppressor genes.

system. These mice have proven to be a good model of PCC predisposition (78% of male mice developed a PCC, a number of whom had pulmonary metastases) (Korpershoek et al., 2009; Ma et al., 2003). Three years after, the same group crossed the *Pten* conditional KO mouse model with a *Trp53* conditional KO strain previously generated by *Marino* et al. (Marino et al., 2000). These double conditional KO mice developed metastatic PCC at a higher frequency (up to 67% lung metastases) and at a younger age (4–5months *vs* 11 months) (Korpershoek et al., 2012).

The second model is secondary to an ectopic expression of an activated *ErbB2* transgene, driven by the minimal rat probasin promoter (PB). The activation of this tyrosine kinase receptor results in bilateral PCC in approximately 5% of PB-*Erb2* male mice with an interesting decrease in the PTEN signaling pathway together with an increase in cycline D1 levels (Lai et al., 2007).

Finally it was recently shown that mice expressing a hypomorphic B-Raf^{V600E} allele, a constitutively active B-Raf kinase originally identified in human melanoma are predisposed to PPGL (Urosevic et al., 2011). This is the first model that develops both PGL and PCC, with a high incidence (80%) and at a relatively young age of onset (around 5 months). Twenty percent of these tumors eventually became metastatic to the stomach, pancreas, liver or lung. These results are particularly interesting, as around 10% of sporadic PCC have recently been shown to carry a somatic mutation in H-RAS (Castro-Vega et al., 2015b; Crona et al., 2013; Oudijk et al., 2014).

3. Allo- and xenografted mouse models

In parallel with these genetically predisposed models, allografted mice have been developed from the mouse pheochromocytoma cell (MPC) lines derived from a *Nf1* KO mouse tumor (Powers et al., 2000). Originally, a mouse model of metastatic PCC using intravenously injected MPC cells has been established, characterized by metastatic lesions predominantly in the liver, 4 weeks after injection (Ohta et al., 2008). In a second time, a more aggressive phenotype was obtained by isolating Mouse Tumor Tissue cells derived from an MPC liver metastasis (MTT cells) that can also be injected to athymic mice (Martiniova et al., 2009b). The extensive characterization of these two allografted models by multimodality imaging confirmed the metastatic phenotype, with a particular tropism for the liver (Giubellino et al., 2012; Martiniova et al., 2009a, 2009c, 2010, 2011b). Both models appear to be convenient for preclinical studies (Martiniova et al., 2011a; Pacak et al., 2012).

A second mouse xenograft model has recently been generated using rat pheochromocytoma PC12 cells injected subcutaneously into athymic Swiss nude nu/nu mice with a tumor development observed about 14 days after implantation. This model appears to be sensitive to both sunitinib and sorafenib treatments (Denorme et al., 2014).

Finally, a xenograft model using shRNA mediated SDHB knocked-down in 143B human osteosarcoma cells was generated by Guzy and colleagues (Guzy et al., 2008). Interestingly, they found an acceleration of tumor growth when inhibiting *SDHB*. Nevertheless, this model is not *stricto sensu* a PCC mouse model since the

cell types do not derived from a chromaffin tissue.

4. Preclinical trials

The main goal of developing animal models of PPGL is to evaluate the efficacy of candidate therapies *in vivo*, in conditions as close as possible to the human pathology. Management of patients with metastatic PPGL is indeed problematic as effective treatments are severely missing, the main therapeutic approach remaining surgery. The recent molecular findings related to the tumorigenic pathways associated with inherited forms of the disease have identified candidate targets that will need to be validated in appropriate experimental models. Although several genetically engineered mice have revealed a predisposition to PCC, none of these mice were yet reported in a preclinical study, and all *in vivo* therapeutic studies have been performed on allografted nude mice with MPC, MTT or PC12 cells.

A few studies have recently reported the assessment of anti-proliferative or anti-migratory effects of different compounds in MPC and MTT cells, as well as in non-proliferating human PPGL primary cell cultures. These reports were not always based on a strong rationale but have showed some efficacy. These included a small molecule inhibitor of serine/threonine protein phosphatase 2A (LB1) combined with Temozolomide (Martiniova et al., 2011a), Topoisomerase 1 inhibitors associated with 5-azacytidine (Powers et al., 2014), lipophilic statins (Fliedner et al., 2014), as well as some somatostatin analogues, LHRH and GHRH antagonists (Ziegler et al., 2013). Surprisingly, only a very few and recent reports have tested the efficacy of anti-cancer drugs *in vivo*. Following the hypothesis of a central role of the mTOR pathway in cluster 2 related PPGL, Giubellino et al. reported anti-tumor effects of AZD8055 (an mTORC1/2 inhibitor), in a metastatic model established with MTT cells expressing Luciferase and monitored by bioluminescence *in vivo* (Giubellino et al., 2013). The same group simultaneously reported important anti-metastatic effects of HSP90 inhibitors, both *in vitro* and on the metastatic spread of MTT cells injected in the tail vein of athymic mice. It was reported that HSP90 binds HIF1 and participates to its stabilization (Isaacs et al., 2002). In their study, Giubellino et al. showed that HSP90 inhibitors did promote a reduction of HIF1 levels. These observations suggest that HSP90 inhibition may be of interest for the management of Cluster 1 pseudohypoxic PPGL. Finally, only one report tested the effect of anti-angiogenic agents, such as the small tyrosine kinase inhibitor sunitinib, which is currently being evaluated in clinical trials in patients (http://clinicaltrials.gov/show/NCT01371201, and https://clinicaltrials.gov/ct2/show/NCT00843037). Denorme et al. showed that both sunitinib and sorafenib that target, among others, the VEGF receptors, were able to reduce microvessel density and tumor burden in a xenograft model of PC12 cells (Denorme et al., 2014).

5. Perspectives

Almost 20 years after the first publication of a mouse model of PCC predisposition, the number of studies evaluating the *in vivo* efficacy of candidate therapies remains very limited. In particular, the failure in generating human PPGL xenograft models and the lack of adequate experimental models of Cluster 1-related tumors have severely compromised the advances that could be applicable to malignant PPGL caused by *SDHB* mutations. Recently, an immortalized mouse chromaffin cell line harboring a complete *Sdhb* knockout has been generated and establishment of an *in vivo* model of allograft using these cells is currently underway. If successful, such a model would constitute the first cluster 1 model and will allow the assessment of the candidate targets identified by the numerous molecular studies reported over the past ten years (For review, see (Castro-Vega et al., 2015a)). These targets comprise demethylating agents such as 5-azacytidine and decitabine, which efficacy has partially been studied *in vitro* (Letouze et al., 2013; Powers et al., 2014), temozolomide, which was also evaluated in MPC and has shown some efficiency in *SDHB*-mutated patients (Hadoux et al., 2014) or 2-oxoglutarate, a metabolite that is expected to reverse all the tumorigenic effects mediated by oncometabolites such as succinate (in *SDHx* mutated tumors) or fumarate (in *FH* mutated tumors). The development of non-invasive imaging methods such as bioluminescence, small animal-dedicated MRI or PET-CT has recently permitted a major breakthrough in the capacities of research laboratories to evaluate therapeutic responses in small rodents. This will allow the launching of preclinical studies in the experimental models that are now available, and will most probably lead, in the next few years to major advances in the indication of molecular targeted therapies in malignant PPGL.

Acknowledgments

We are grateful to Dr Juliette Hadchouel and to the Mouse Clinical Institute (Illkirch) for helping in generating the *Sdhb* floxed mouse and to Dr Marcelo Rubinstein for providing the TH-Cre mouse. We thank Estelle Robidel and Maeva Ruel for technical assistance and Catherine Tritscher for administrative assistance. The work leading to these results has received funding from the GIST-Institut des Maladies rares, the Agence Nationale de la Recherche (ANR-2011-JCJC-00701 MODEOMAPP), the European Union Seventh Framework Programme (FP7/2007–2013) under grant agreement no 259735. C.L-L. is funded by the Cancer Research for Personalized Medicine – CARPEM project (Site de Recherche Intégré sur le Cancer – SIRIC).

References

Adam, J., Hatipoglu, E., O'Flaherty, L., Ternette, N., Sahgal, N., Lockstone, H., Baban, D., Nye, E., Stamp, G.W., Wolhuter, K., Stevens, M., Fischer, R., Carmeliet, P., Maxwell, P.H., Pugh, C.W., Frizzell, N., Soga, T., Kessler, B.M., El-Bahrawy, M., Ratcliffe, P.J., Pollard, P.J., 2011. Renal cyst formation in Fh1-deficient mice is independent of the Hif/Phd pathway: roles for fumarate in KEAP1 succination and Nrf2 signaling. Cancer Cell. 20, 524–537.

Ali, I.U., Schriml, L.M., Dean, M., 1999. Mutational spectra of PTEN/MMAC1 gene: a tumor suppressor with lipid phosphatase activity. J. Natl. Cancer Inst. 91, 1922–1932.

Amar, L., Bertherat, J., Baudin, E., Ajzenberg, C., Bressac-de Paillerets, B., Chabre, O., Chamontin, B., Delemer, B., Giraud, S., Murat, A., Niccoli-Sire, P., Richard, S., Rohmer, V., Sadoul, J.L., Strompf, L., Schlumberger, M., Bertagna, X., Plouin, P.F., Jeunemaitre, X., Gimenez-Roqueplo, A.P., 2005. Genetic testing in pheochromocytoma or functional paraganglioma. J. Clin. Oncol. 23, 8812–8818.

Amar, L., Baudin, E., Burnichon, N., Peyrard, S., Silvera, S., Bertherat, J., Bertagna, X., Schlumberger, M., Jeunemaitre, X., Gimenez-Roqueplo, A.P., Plouin, P.F., 2007. Succinate dehydrogenase B gene mutations predict survival in patients with malignant pheochromocytomas or paragangliomas. J. Clin. Endocrinol. Metab. 92, 3822–3828.

Bayley, J.P., van Minderhout, I., Hogendoorn, P.C., Cornelisse, C.J., van der Wal, A., Prins, F.A., Teppema, L., Dahan, A., Devilee, P., Taschner, P.E., 2009. Sdhd and SDHD/H19 knockout mice do not develop paraganglioma or pheochromocytoma. PLoS One 4, e7987.

Brandi, M.L., Gagel, R.F., Angeli, A., Bilezikian, J.P., Beck-Peccoz, P., Bordi, C., Conte-Devolx, B., Falchetti, A., Gheri, R.G., Libroia, A., Lips, C.J., Lombardi, G., Mannelli, M., Pacini, F., Ponder, B.A., Raue, F., Skogseid, B., Tamburrano, G., Thakker, R.V., Thompson, N.W., Tomassetti, P., Tonelli, F., Wells Jr., S.A., Marx, S.J., 2001. Guidelines for diagnosis and therapy of MEN type 1 and type 2. J. Clin. Endocrinol. Metab. 86, 5658–5671.

Briere, J.J., Favier, J., Benit, P., El Ghouzzi, V., Lorenzato, A., Rabier, D., Di Renzo, M.F., Gimenez-Roqueplo, A.P., Rustin, P., 2005. Mitochondrial succinate is instrumental for HIF1alpha nuclear translocation in SDHA-mutant fibroblasts under normoxic conditions. Hum. Mol. Genet. 14, 3263–3269.

Burnichon, N., Vescovo, L., Amar, L., Libe, R., de Reynies, A., Venisse, A., Jouanno, E., Laurendeau, I., Parfait, B., Bertherat, J., Plouin, P.F., Jeunemaitre, X., Favier, J., Gimenez-Roqueplo, A.P., 2011. Integrative genomic analysis reveals somatic mutations in pheochromocytoma and paraganglioma. Hum. Mol. Genet. 20, 3974–3985.

Cantley, L.C., Neel, B.G., 1999. New insights into tumor suppression: PTEN suppresses tumor formation by restraining the phosphoinositide 3-kinase/AKT pathway. Proc. Natl. Acad. Sci. U S A 96, 4240–4245.

Cascon, A., Comino-Mendez, I., Curras-Freixes, M., de Cubas, A.A., Contreras, L., Richter, S., Peitzsch, M., Mancikova, V., Inglada-Perez, L., Perez-Barrios, A., Calatayud, M., Azriel, S., Villar-Vicente, R., Aller, J., Setien, F., Moran, S., Garcia, J.F., Rio-Machin, A., Leton, R., Gomez-Grana, A., Apellaniz-Ruiz, M., Roncador, G., Esteller, M., Rodriguez-Antona, C., Satrustegui, J., Eisenhofer, G., Urioste, M., Robledo, M., 2015. Whole-exome sequencing identifies MDH2 as a new familial paraganglioma gene. J. Natl. Cancer Inst. 107.

Castro-Vega, L.J., Buffet, A., De Cubas, A.A., Cascon, A., Menara, M., Khalifa, E., Amar, L., Azriel, S., Bourdeau, I., Chabre, O., Curras-Freixes, M., Franco-Vidal, V., Guillaud-Bataille, M., Simian, C., Morin, A., Leton, R., Gomez-Grana, A., Pollard, P.J., Rustin, P., Robledo, M., Favier, J., Gimenez-Roqueplo, A.P., 2014. Germline mutations in FH confer predisposition to malignant pheochromocytomas and paragangliomas. Hum. Mol. Genet. 23, 2440–2446.

Castro-Vega, L.J., Lepoutre-Lussey, C., Gimenez-Roqueplo, A.P., Favier, J., 2015a Jun 1. Rethinking pheochromocytomas and paragangliomas from a genomic perspective. Oncogene. http://dx.doi.org/10.1038/onc.2015.172.

Castro-Vega, L.J., Letouze, E., Burnichon, N., Buffet, A., Disderot, P.H., Khalifa, E., Loriot, C., Elarouci, N., Morin, A., Menara, M., Lepoutre-Lussey, C., Badoual, C., Sibony, M., Dousset, B., Libe, R., Zinzindohoue, F., Plouin, P.F., Bertherat, J., Amar, L., de Reynies, A., Favier, J., Gimenez-Roqueplo, A.P., 2015b. Multi-omics analysis defines core genomic alterations in pheochromocytomas and paragangliomas. Nat. Commun. 6, 6044.

Crona, J., Delgado Verdugo, A., Maharjan, R., Stalberg, P., Granberg, D., Hellman, P., Bjorklund, P., 2013. Somatic mutations in H-RAS in sporadic pheochromocytoma and paraganglioma identified by exome sequencing. J. Clin. Endocrinol. Metab. 98, E1266–E1271.

Dahia, P.L., Ross, K.N., Wright, M.E., Hayashida, C.Y., Santagata, S., Barontini, M., Kung, A.L., Sanso, G., Powers, J.F., Tischler, A.S., Hodin, R., Heitritter, S., Moore, F., Dluhy, R., Sosa, J.A., Ocal, I.T., Benn, D.E., Marsh, D.J., Robinson, B.G., Schneider, K., Garber, J., Arum, S.M., Korbonits, M., Grossman, A., Pigny, P., Toledo, S.P., Nose, V., Li, C., Stiles, C.D., 2005. A HIF1alpha regulatory loop links hypoxia and mitochondrial signals in pheochromocytomas. PLoS Genet. 1, 72–80.

Dahia, P.L., 2014. Pheochromocytoma and paraganglioma pathogenesis: learning from genetic heterogeneity. Nat. Rev. Cancer 14, 108–119.

Denorme, M., Yon, L., Roux, C., Gonzalez, B.J., Baudin, E., Anouar, Y., Dubessy, C., 2014. Both sunitinib and sorafenib are effective treatments for pheochromocytoma in a xenograft model. Cancer Lett. 352, 236–244.

Eisenhofer, G., Huynh, T.T., Pacak, K., Brouwers, F.M., Walther, M.M., Linehan, W.M., Munson, P.J., Mannelli, M., Goldstein, D.S., Elkahloun, A.G., 2004. Distinct gene expression profiles in norepinephrine- and epinephrine-producing hereditary and sporadic pheochromocytomas: activation of hypoxia-driven angiogenic pathways in von Hippel-Lindau syndrome. Endocr. Relat. Cancer 11, 897–911.

Favier, J., Briere, J.J., Burnichon, N., Riviere, J., Vescovo, L., Benit, P., Giscos-Douriez, I., De Reynies, A., Bertherat, J., Badoual, C., Tissier, F., Amar, L., Libe, R., Plouin, P.F., Jeunemaitre, X., Rustin, P., Gimenez-Roqueplo, A.P., 2009. The Warburg effect is genetically determined in inherited pheochromocytomas. PLoS One 4, e7094.

Favier, J., Amar, L., Gimenez-Roqueplo, A., 2014. Paraganglioma and phaeochromocytoma: from genetics to personalized medicine. Nat. Rev. Endocrinol.

Fliedner, S.M., Engel, T., Lendvai, N.K., Shankavaram, U., Nolting, S., Wesley, R., Elkahloun, A.G., Ungefroren, H., Oldoerp, A., Lampert, G., Lehnert, H., Timmers, H., Pacak, K., 2014. Anti-cancer potential of MAPK pathway inhibition in paragangliomas-effect of different statins on mouse pheochromocytoma cells. PLoS One 9, e97712.

Gelman, D.M., Noain, D., Avale, M.E., Otero, V., Low, M.J., Rubinstein, M., 2003. Transgenic mice engineered to target Cre/loxP-mediated DNA recombination into catecholaminergic neurons. Genesis 36, 196–202.

Gimenez-Roqueplo, A.P., Dahia, P.L., Robledo, M., 2012. An update on the genetics of paraganglioma, pheochromocytoma, and associated hereditary syndromes. Horm. Metab. Res. 44, 328–333.

Giubellino, A., Woldemichael, G.M., Sourbier, C., Lizak, M.J., Powers, J.F., Tischler, A.S., Pacak, K., 2012. Characterization of two mouse models of metastatic pheochromocytoma using bioluminescence imaging. Cancer Lett. 316, 46–52.

Giubellino, A., Bullova, P., Nolting, S., Turkova, H., Powers, J.F., Liu, Q., Guichard, S., Tischler, A.S., Grossman, A.B., Pacak, K., 2013. Combined inhibition of mTORC1 and mTORC2 signaling pathways is a promising therapeutic option in inhibiting pheochromocytoma tumor growth: in vitro and in vivo studies in female athymic nude mice. Endocrinology 154, 646–655.

Gnarra, J.R., Ward, J.M., Porter, F.D., Wagner, J.R., Devor, D.E., Grinberg, A., Emmert-Buck, M.R., Westphal, H., Klausner, R.D., Linehan, W.M., 1997. Defective placental vasculogenesis causes embryonic lethality in VHL-deficient mice. Proc. Natl. Acad. Sci. U S A 94, 9102–9107.

Gutmann, D.H., Aylsworth, A., Carey, J.C., Korf, B., Marks, J., Pyeritz, R.E., Rubenstein, A., Viskochil, D., 1997. The diagnostic evaluation and multidisciplinary management of neurofibromatosis 1 and neurofibromatosis 2. J. Am. Med. Assoc. 278, 51–57.

Guzy, R.D., Sharma, B., Bell, E., Chandel, N.S., Schumacker, P.T., 2008. Loss of the SdhB, but not the SdhA, subunit of complex II triggers reactive oxygen species-dependent hypoxia-inducible factor activation and tumorigenesis. Mol. Cell. Biol. 28, 718–731.

Haase, V.H., Glickman, J.N., Socolovsky, M., Jaenisch, R., 2001. Vascular tumors in livers with targeted inactivation of the von Hippel-Lindau tumor suppressor. Proc. Natl. Acad. Sci. U S A 98, 1583–1588.

Haase, V.H., 2005. The VHL tumor suppressor in development and disease: functional studies in mice by conditional gene targeting. Semin. Cell. Dev. Biol. 16, 564–574.

Hadoux, J., Favier, J., Scoazec, J.Y., Leboulleux, S., Al Ghuzlan, A., Caramella, C., Deandreis, D., Borget, I., Loriot, C., Chougnet, C., Letouze, E., Young, J., Amar, L., Bertherat, J., Libe, R., Dumont, F., Deschamps, F., Schlumberger, M., Gimenez-Roqueplo, A.P., Baudin, E., 2014. SDHB mutations are associated with response to temozolomide in patients with metastatic pheochromocytoma or paraganglioma. Int. J. Cancer 135, 2711–2720.

Ibanez, C.F., 2013. Structure and physiology of the RET receptor tyrosine kinase. Cold Spring Harb. Perspect. Biol. 5.

Isaacs, J.S., Jung, Y.J., Mimnaugh, E.G., Martinez, A., Cuttitta, F., Neckers, L.M., 2002. Hsp90 regulates a von Hippel Lindau-independent hypoxia-inducible factor-1 alpha-degradative pathway. J. Biol. Chem. 277, 29936–29944.

Jacks, T., Shih, T.S., Schmitt, E.M., Bronson, R.T., Bernards, A., Weinberg, R.A., 1994. Tumour predisposition in mice heterozygous for a targeted mutation in Nf1. Nat. Genet. 7, 353–361.

Korpershoek, E., Loonen, A.J., Corvers, S., van Nederveen, F.H., Jonkers, J., Ma, X., Ziel-van der Made, A., Korsten, H., Trapman, J., Dinjens, W.N., de Krijger, R.R., 2009. Conditional Pten knock-out mice: a model for metastatic phaeochromocytoma. J. Pathol. 217, 597–604.

Korpershoek, E., Kloosterhof, N.K., Ziel-van der Made, A., Korsten, H., Oudijk, L., Trapman, J., Dinjens, W.N., de Krijger, R.R., 2012. Trp53 inactivation leads to earlier phaeochromocytoma formation in pten knockout mice. Endocr. Relat. Cancer 19, 731–740.

Lai, E.W., Rodriguez, O.C., Aventian, M., Cromelin, C., Fricke, S.T., Martiniova, L., Lubensky, I.A., Lisanti, M.P., Picard, K.L., Powers, J.F., Tischler, A.S., Pacak, K., Albanese, C., 2007. ErbB-2 induces bilateral adrenal pheochromocytoma formation in mice. Cell. Cycle 6, 1946–1950.

Lallemand, Y., 1998. Maternally expressed PGK-Cre transgene as a tool for early and uniform activation of the Cre site-specific recombinase. Transgenic Res. 7, 105–112.

Lancaster, C.R., Simon, J., 2002. Succinate:quinone oxidoreductases from epsilonproteobacteria. Biochim. Biophys. Acta 1553, 84–101.

Lehtonen, H.J., Kiuru, M., Ylisaukko-Oja, S.K., Salovaara, R., Herva, R., Koivisto, P.A., Vierimaa, O., Aittomaki, K., Pukkala, E., Launonen, V., Aaltonen, L.A., 2006. Increased risk of cancer in patients with fumarate hydratase germline mutation. J. Med. Genet. 43, 523–526.

Letouze, E., Martinelli, C., Loriot, C., Burnichon, N., Abermil, N., Ottolenghi, C., Janin, M., Menara, M., Nguyen, A.T., Benit, P., Buffet, A., Marcaillou, C., Bertherat, J., Amar, L., Rustin, P., De Reynies, A., Gimenez-Roqueplo, A.P., Favier, J., 2013. SDH mutations establish a hypermethylator phenotype in paraganglioma. Cancer Cell. 23, 739–752.

Lopez-Jimenez, E., Gomez-Lopez, G., Leandro-Garcia, L.J., Munoz, I., Schiavi, F., Montero-Conde, C., de Cubas, A.A., Ramires, R., Landa, I., Leskela, S., Maliszewska, A., Inglada-Perez, L., de la Vega, L., Rodriguez-Antona, C., Leton, R., Bernal, C., de Campos, J.M., Diez-Tascon, C., Fraga, M.F., Boullosa, C., Pisano, D.G., Opocher, G., Robledo, M., Cascon, A., 2010. Research resource: transcriptional profiling reveals different pseudohypoxic signatures in SDHB and VHL-related pheochromocytomas. Mol. Endocrinol. 24, 2382–2391.

Ma, W., Tessarollo, L., Hong, S.B., Baba, M., Southon, E., Back, T.C., Spence, S., Lobe, C.G., Sharma, N., Maher, G.W., Pack, S., Vortmeyer, A.O., Guo, C., Zbar, B., Schmidt, L.S., 2003. Hepatic vascular tumors, angiectasis in multiple organs, and impaired spermatogenesis in mice with conditional inactivation of the VHL gene. Cancer Res. 63, 5320–5328.

Ma, X., Ziel-van der Made, A.C., Autar, B., van der Korput, H.A., Vermeij, M., van Duijn, P., Cleutjens, K.B., de Krijger, R., Krimpenfort, P., Berns, A., van der Kwast, T.H., Trapman, J., 2005. Targeted biallelic inactivation of Pten in the mouse prostate leads to prostate cancer accompanied by increased epithelial cell proliferation but not by reduced apoptosis. Cancer Res. 65, 5730–5739.

Maher, E.R., Neumann, H.P., Richard, S., 2011. von Hippel-Lindau disease: a clinical and scientific review. Eur. J. Hum. Genet. 19, 617–623.

Marino, S., Vooijs, M., van Der Gulden, H., Jonkers, J., Berns, A., 2000. Induction of medulloblastomas in p53-null mutant mice by somatic inactivation of Rb in the external granular layer cells of the cerebellum. Genes. Dev. 14, 994–1004.

Martiniova, L., Kotys, M.S., Thomasson, D., Schimel, D., Lai, E.W., Bernardo, M., Merino, M.J., Powers, J.F., Ruzicka, J., Kvetnansky, R., Choyke, P.L., Pacak, K., 2009a. Noninvasive monitoring of a murine model of metastatic pheochromocytoma: a comparison of contrast-enhanced microCT and nonenhanced MRI. J. Magn. Reson Imaging 29, 685–691.

Martiniova, L., Lai, E.W., Elkahloun, A.G., Abu-Asab, M., Wickremasinghe, A., Solis, D.C., Perera, S.M., Huynh, T.T., Lubensky, I.A., Tischler, A.S., Kvetnansky, R., Alesci, S., Morris, J.C., Pacak, K., 2009b. Characterization of an animal model of aggressive metastatic pheochromocytoma linked to a specific gene signature. Clin. Exp. Metastasis 26, 239–250.

Martiniova, L., Lai, E.W., Thomasson, D., Kiesewetter, D.O., Seidel, J., Merino, M.J., Kvetnansky, R., Pacak, K., 2009c. Animal model of metastatic pheochromocytoma: evaluation by MRI and PET. Endocr. Regul. 43, 59–64.

Martiniova, L., Schimel, D., Lai, E.W., Limpuangthip, A., Kvetnansky, R., Pacak, K., 2010. In vivo micro-CT imaging of liver lesions in small animal models. Methods 50, 20–25.

Martiniova, L., Lu, J., Chiang, J., Bernardo, M., Lonser, R., Zhuang, Z., Pacak, K., 2011a. Pharmacologic modulation of serine/threonine phosphorylation highly

sensitizes PHEO in a MPC cell and mouse model to conventional chemotherapy. PLoS One 6, e14678.
Martiniova, L., Perera, S.M., Brouwers, F.M., Alesci, S., Abu-Asab, M., Marvelle, A.F., Kiesewetter, D.O., Thomasson, D., Morris, J.C., Kvetnansky, R., Tischler, A.S., Reynolds, J.C., Fojo, A.T., Pacak, K., 2011b. Increased uptake of [(1)(2)(3)I]meta-iodobenzylguanidine, [(1)(8)F]fluorodopamine, and [(3)H]norepinephrine in mouse pheochromocytoma cells and tumors after treatment with the histone deacetylase inhibitors. Endocr. Relat. Cancer 18, 143–157.
Morin, A., Letouze, E., Gimenez-Roqueplo, A.P., Favier, J., 2014. Oncometabolites-driven tumorigenesis: from genetics to targeted therapy. Int. J. Cancer 135, 2237–2248.
Nikitin, A.Y., Juarez-Perez, M.I., Li, S., Huang, L., Lee, W.H., 1999. RB-mediated suppression of spontaneous multiple neuroendocrine neoplasia and lung metastases in Rb+/- mice. Proc. Natl. Acad. Sci. U S A 96, 3916–3921.
Ohta, S., Lai, E.W., Morris, J.C., Pang, A.L., Watanabe, M., Yazawa, H., Zhang, R., Green, J.E., Chan, W.Y., Sirajuddin, P., Taniguchi, S., Powers, J.F., Tischler, A.S., Pacak, K., 2008. Metastasis-associated gene expression profile of liver and subcutaneous lesions derived from mouse pheochromocytoma cells. Mol. Carcinog. 47, 245–251.
Oudijk, L., de Krijger, R.R., Rapa, I., Beuschlein, F., de Cubas, A.A., Dei Tos, A.P., Dinjens, W.N., Korpershoek, E., Mancikova, V., Mannelli, M., Papotti, M., Vatrano, S., Robledo, M., Volante, M., 2014. H-RAS mutations are restricted to sporadic pheochromocytomas lacking specific clinical or pathological features: data from a multi-institutional series. J. Clin. Endocrinol. Metab. 99, E1376–E1380.
Pacak, K., Sirova, M., Giubellino, A., Lencesova, L., Csaderova, L., Laukova, M., Hudecova, S., Krizanova, O., 2012. NF-kappaB inhibition significantly upregulates the norepinephrine transporter system, causes apoptosis in pheochromocytoma cell lines and prevents metastasis in an animal model. Int. J. Cancer 131, 2445–2455.
Piruat, J.I., Pintado, C.O., Ortega-Saenz, P., Roche, M., Lopez-Barneo, J., 2004. The mitochondrial SDHD gene is required for early embryogenesis, and its partial deficiency results in persistent carotid body glomus cell activation with full responsiveness to hypoxia. Mol. Cell. Biol. 24, 10933–10940.
Pollard, P.J., Briere, J.J., Alam, N.A., Barwell, J., Barclay, E., Wortham, N.C., Hunt, T., Mitchell, M., Olpin, S., Moat, S.J., Hargreaves, I.P., Heales, S.J., Chung, Y.L., Griffiths, J.R., Dalgleish, A., McGrath, J.A., Gleeson, M.J., Hodgson, S.V., Poulsom, R., Rustin, P., Tomlinson, I.P., 2005. Accumulation of Krebs cycle intermediates and over-expression of HIF1alpha in tumours which result from germline FH and SDH mutations. Hum. Mol. Genet. 14, 2231–2239.
Pollard, P.J., Spencer-Dene, B., Shukla, D., Howarth, K., Nye, E., El-Bahrawy, M., Deheragoda, M., Joannou, M., McDonald, S., Martin, A., Igarashi, P., Varsani-Brown, S., Rosewell, I., Poulsom, R., Maxwell, P., Stamp, G.W., Tomlinson, I.P., 2007. Targeted inactivation of fh1 causes proliferative renal cyst development and activation of the hypoxia pathway. Cancer Cell. 11, 311–319.
Powers, J.F., Evinger, M.J., Tsokas, P., Bedri, S., Alroy, J., Shahsavari, M., Tischler, A.S., 2000. Pheochromocytoma cell lines from heterozygous neurofibromatosis knockout mice. Cell. Tissue Res. 302, 309–320.
Powers, J.F., Korgaonkar, P.G., Fliedner, S., Giubellino, A., Pacak, K., Sahagian, G.G., Tischler, A.S., 2014. Cytocidal activities of topoisomerase 1 inhibitors and 5-azacytidine against pheochromocytoma/paraganglioma cells in primary human tumor cultures and mouse cell lines. PLoS One 9, e87807.
Puc, J., Placha, G., Wocial, B., Podsypanina, K., Parsons, R., Gaciong, Z., 2006. Analysis of PTEN mutation in non-familial pheochromocytoma. Ann. N. Y. Acad. Sci. 1073, 317–331.
Rankin, E.B., Higgins, D.F., Walisser, J.A., Johnson, R.S., Bradfield, C.A., Haase, V.H., 2005. Inactivation of the arylhydrocarbon receptor nuclear translocator (Arnt) suppresses von Hippel-Lindau disease-associated vascular tumors in mice. Mol. Cell. Biol. 25, 3163–3172.
Schulz, N., Propst, F., Rosenberg, M.P., Linnoila, R.I., Paules, R.S., Kovatch, R., Ogiso, Y., Vande Woude, G., 1992. Pheochromocytomas and C-cell thyroid neoplasms in transgenic c-mos mice: a model for the human multiple endocrine neoplasia type 2 syndrome. Cancer Res. 52, 450–455.
Smith-Hicks, C.L., Sizer, K.C., Powers, J.F., Tischler, A.S., Costantini, F., 2000. C-cell hyperplasia, pheochromocytoma and sympathoadrenal malformation in a mouse model of multiple endocrine neoplasia type 2B. Embo J. 19, 612–622.
Tomlinson, I.P., Alam, N.A., Rowan, A.J., Barclay, E., Jaeger, E.E., Kelsell, D., Leigh, I., Gorman, P., Lamlum, H., Rahman, S., Roylance, R.R., Olpin, S., Bevan, S., Barker, K., Hearle, N., Houlston, R.S., Kiuru, M., Lehtonen, R., Karhu, A., Vilkki, S., Laiho, P., Eklund, C., Vierimaa, O., Aittomaki, K., Hietala, M., Sistonen, P., Paetau, A., Salovaara, R., Herva, R., Launonen, V., Aaltonen, L.A., Multiple Leiomyoma, C., 2002. Germline mutations in FH predispose to dominantly inherited uterine fibroids, skin leiomyomata and papillary renal cell cancer. Nat. Genet. 30, 406–410.
Toro, J.R., Nickerson, M.L., Wei, M.H., Warren, M.B., Glenn, G.M., Turner, M.L., Stewart, L., Duray, P., Tourre, O., Sharma, N., Choyke, P., Stratton, P., Merino, M., Walther, M.M., Linehan, W.M., Schmidt, L.S., Zbar, B., 2003. Mutations in the fumarate hydratase gene cause hereditary leiomyomatosis and renal cell cancer in families in North America. Am. J. Hum. Genet. 73, 95–106.
Urosevic, J., Sauzeau, V., Soto-Montenegro, M.L., Reig, S., Desco, M., Wright, E.M., Canamero, M., Mulero, F., Ortega, S., Bustelo, X.R., Barbacid, M., 2011. Constitutive activation of B-Raf in the mouse germ line provides a model for human cardio-facio-cutaneous syndrome. Proc. Natl. Acad. Sci. U S A 108, 5015–5020.
van Nederveen, F.H., Perren, A., Dannenberg, H., Petri, B.J., Dinjens, W.N., Komminoth, P., de Krijger, R.R., 2006. PTEN gene loss, but not mutation, in benign and malignant phaeochromocytomas. J. Pathol. 209, 274–280.
Viskochil, D., Buchberg, A.M., Xu, G., Cawthon, R.M., Stevens, J., Wolff, R.K., Culver, M., Carey, J.C., Copeland, N.G., Jenkins, N.A., et al., 1990. Deletions and a translocation interrupt a cloned gene at the neurofibromatosis type 1 locus. Cell 62, 187–192.
Wagner, S.M., Zhu, S., Nicolescu, A.C., Mulligan, L.M., 2012. Molecular mechanisms of RET receptor-mediated oncogenesis in multiple endocrine neoplasia 2. Clin. (Sao Paulo) 67 (Suppl. 1), 77–84.
You, M.J., Castrillon, D.H., Bastian, B.C., O'Hagan, R.C., Bosenberg, M.W., Parsons, R., Chin, L., DePinho, R.A., 2002. Genetic analysis of Pten and Ink4a/Arf interactions in the suppression of tumorigenesis in mice. Proc. Natl. Acad. Sci. U S A 99, 1455–1460.
Ziegler, C.G., Ullrich, M., Schally, A.V., Bergmann, R., Pietzsch, J., Gebauer, L., Gondek, K., Qin, N., Pacak, K., Ehrhart-Bornstein, M., Eisenhofer, G., Bornstein, S.R., 2013. Anti-tumor effects of peptide analogs targeting neuropeptide hormone receptors on mouse pheochromocytoma cells. Mol. Cell. Endocrinol. 371, 189–194.

ARTICLE 5

In Vivo Detection of Succinate by Magnetic Resonance Spectroscopy as a Hallmark of SDHx Mutations in Paraganglioma.

Lussey-Lepoutre C, Bellucci A, Morin A, Buffet A, Amar L, Janin M, Ottolenghi C, Zinzindohoué F, Autret G, Burnichon N, Robidel E, Banting B, Fontaine S, Cuenod CA, Benit P, Rustin P, Halimi P, Fournier L, Gimenez-Roqueplo AP, Favier J, Tavitian B.

Clin Cancer Res. 2016 Mar 1;22(5):1120-9.

Published OnlineFirst October 21, 2015; DOI: 10.1158/1078-0432.CCR-15-1576

Personalized Medicine and Imaging

Clinical Cancer Research

In Vivo Detection of Succinate by Magnetic Resonance Spectroscopy as a Hallmark of *SDHx* Mutations in Paraganglioma

Charlotte Lussey-Lepoutre[1,2], Alexandre Bellucci[1,2], Aurélie Morin[1,2], Alexandre Buffet[1,2], Laurence Amar[1,2,3], Maxime Janin[2,4,5], Chris Ottolenghi[2,4,5], Franck Zinzindohoué[2,6], Gwennhael Autret[1,2], Nelly Burnichon[1,2,7], Estelle Robidel[1,2], Benjamin Banting[8], Sébastien Fontaine[8], Charles-André Cuenod[1,2,8], Paule Benit[9,10], Pierre Rustin[9,10], Philippe Halimi[2,8], Laure Fournier[1,2,8], Anne-Paule Gimenez-Roqueplo[1,2,7], Judith Favier[1,2], and Bertrand Tavitian[1,2,8]

Abstract

Purpose: Germline mutations in genes encoding mitochondrial succinate dehydrogenase (SDH) are found in patients with paragangliomas, pheochromocytomas, gastrointestinal stromal tumors, and renal cancers. SDH inactivation leads to a massive accumulation of succinate, acting as an oncometabolite and which levels, assessed on surgically resected tissue are a highly specific biomarker of *SDHx*-mutated tumors. The aim of this study was to address the feasibility of detecting succinate *in vivo* by magnetic resonance spectroscopy.

Experimental Design: A pulsed proton magnetic resonance spectroscopy (^{1}H-MRS) sequence was developed, optimized, and applied to image nude mice grafted with $Sdhb^{-/-}$ or wild-type chromaffin cells. The method was then applied to patients with paraganglioma carrying ($n = 5$) or not ($n = 4$) an *SDHx* gene mutation. Following surgery, succinate was measured using gas chromatography/mass spectrometry, and SDH protein expression was assessed by immunohistochemistry in resected tumors.

Results: A succinate peak was observed at 2.44 ppm by ^{1}H-MRS in all $Sdhb^{-/-}$-derived tumors in mice and in all paragangliomas of patients carrying an *SDHx* gene mutation, but neither in wild-type mouse tumors nor in patients exempt of *SDHx* mutation. In one patient, ^{1}H-MRS results led to the identification of an unsuspected *SDHA* gene mutation. In another case, it helped define the pathogenicity of a variant of unknown significance in the *SDHB* gene.

Conclusions: Detection of succinate by ^{1}H-MRS is a highly specific and sensitive hallmark of *SDHx* mutations. This noninvasive approach is a simple and robust method allowing *in vivo* detection of the major biomarker of *SDHx*-mutated tumors. *Clin Cancer Res; 22(5); 1120–9. ©2015 AACR.*

[1]INSERM, UMR970, Paris Cardiovascular Research Center, Paris, France. [2]Université Paris Descartes, Sorbonne Paris Cité, Faculté de Médecine, Paris, France. [3]Assistance Publique-Hôpitaux de Paris, Hôpital Européen Georges Pompidou, Service d'hypertension artérielle et médecine vasculaire, Paris, France. [4]Assistance Publique-Hôpitaux de Paris, Hôpital Necker-Enfants Malades, Laboratoire de Biochimie Métabolique, Paris, France. [5]INSERM, U1124, Paris, France. [6]Assistance Publique-Hôpitaux de Paris, Hôpital Européen Georges Pompidou, Service de Chirurgie Digestive, Paris, France. [7]Assistance Publique-Hôpitaux de Paris, Hôpital Européen Georges Pompidou, Service de Génétique, Paris, France. [8]Assistance Publique-Hôpitaux de Paris, Hôpital Européen Georges Pompidou, Service de Radiologie, Paris, France. [9]INSERM, UMR1141, Hôpital Robert Debré, Paris, France. [10]Université Paris 7, Faculté de Médecine Denis Diderot, Paris, France.

Note: Supplementary data for this article are available at Clinical Cancer Research Online (http://clincancerres.aacrjournals.org/).

J. Favier and B. Tavitian share senior authorship of this article.

C. Lussey-Lepoutre and A. Bellucci contributed equally to this article.

Corresponding Author: Judith Favier, INSERM, 56 rue Leblanc, Paris 75015, France. Phone: 33153988041; Fax: 33144253987952; E-mail: judith.favier@inserm.fr

doi: 10.1158/1078-0432.CCR-15-1576

Introduction

Pheochromocytoma and paraganglioma are rare neuroendocrine tumors that arise in chromaffin cells of the adrenal medulla and in sympathetic and parasympathetic ganglia, respectively. The prevalence of pheochromocytoma and paraganglioma (PPGL) in patients with hypertension consulting at general outpatient clinics is estimated at 0.2% to 0.6%, but this number may be underestimated (1). Nearly 40% of patients with PPGL carry a germline mutation in one of the 13 PPGL predisposing genes identified so far (2), and mutations of *SDHx* genes (*SDHA, SDHB, SDHC, SDHD, SDHAF2*) are causative of approximately half of the genetically determined cases. *SDHx* mutations predispose to the hereditary PPGL syndrome but may also be found in patients with gastrointestinal stromal tumors (GIST; ref. 3) or renal clear cell carcinomas (4).

SDHA, B, C, and *D* genes encode the four subunits of succinate dehydrogenase (SDH), a mitochondrial enzyme of the tricarboxylic acid (TCA) cycle that oxidizes succinate into fumarate. They were the first genes encoding a mitochondrial enzyme demonstrated to act as tumor suppressor genes (5), an important finding supporting the hypothesis of a direct link between mitochondrial dysfunction and cancer proposed by Warburg in 1924 (6). Since

Published OnlineFirst October 21, 2015; DOI: 10.1158/1078-0432.CCR-15-1576

Translational Relevance

A large proportion of patients with paraganglioma/pheochromocytoma (PPGL) carry a germline mutation in an *SDHx* gene. Identification of *SDHx* mutations is important for the diagnostic work-up, the management, and the follow-up of patients with PPGL and their families, who are at risk of developing multiple paraganglioma. Moreover, *SDHB* gene mutations predispose to malignant, particularly aggressive forms of the disease. Therefore, a genetic counseling is now recommended for all patients suffering from PPGL. We here show that *in vivo* detection of succinate by proton magnetic resonance spectroscopy is a highly specific and sensitive hallmark of *SDHx* mutated tumors. This noninvasive approach will allow identifying and classifying *SDHx* mutations or variants of unknown significance. It may help for the characterization of inoperable tumors and suspicious lesions and serve as a surrogate biomarker in the assessment of tumor response to specific treatments.

then, mutations in genes encoding for the TCA enzymes fumarate hydratase (*FH*; ref. 7), isocitrate dehydrogenase (*IDH1* and *2*; ref. 8), and more recently malate dehydrogenase (*MDH2*), were reported to predispose to PPGL, renal cancers, leimyomas, or to be causative of sporadic gliomas (for review, see ref. 9).

Identification of *SDHx* mutations is important for the diagnostic work-up, the management, and the follow-up of index cases and their families. *SDHx* mutation carriers are at risk of developing multiple paraganglioma that can arise all along the embryonic migration way of neural crest cells, from the base of the skull to the pelvis (10). Moreover, the identification of *SDHB* gene mutations is of specific clinical importance as they predispose to malignant, particularly aggressive forms of the disease (11, 12), and a genetic counseling is now recommended for all patients suffering from PPGL (1). In familial PPGL patients carrying a germline heterozygous mutation on an *SDHx* gene, the somatic loss of the remaining allele induces a complete SDH loss-of-function, which results in the accumulation of succinate. Succinate acts as an oncometabolite and is suspected to mediate most, if not all, of the tumorigenic effects related to *SDHx* mutations (9, 13, 14). Development of specific tumor biomarkers allowing the rapid identification of these patients would be highly beneficial and particularly helpful for the characterization of inoperable tumors and suspicious lesions. Biomarkers could serve as surrogate markers in the assessment of tumor response to specific treatments. Until now, no *in vivo* method to assess the functional consequences of *SDHx* mutations was available, and all existing tests were performed on surgical resected specimens (15–22).

Succinate concentrations in the millimolar range—4 to 500 micromoles per gram depending on studies and procedures—have been reported in *SDHx*-mutated PPGL tumors, an increase of up to 100-fold compared with non-*SDHx*–mutated PPGL tumors (19, 21, 23). We hypothesized that these succinate levels could be detected noninvasively by *in vivo* proton magnetic resonance spectroscopy (^{1}H-MRS) in *SDHx*-mutated tumors, without the need for tissue sampling, similarly to 2-hydroxyglutarate in patients with *IDH1/2*-mutated gliomas (24–26). Here, we report a new method for SUCCinate Estimation by Spectroscopy (SUCCES) in patients with PPGL related or not to an *SDHx* mutation.

Materials and Methods

Optimization of SUCCES for succinate detection with ^{1}H-MRS

We first tested the SUCCES sequence at 4.7 T on a 3-cm-diameter spherical phantom tube containing 100 mmol/L sodium succinate dibasic hexahydrate, 100 mmol/L L-lactate, and animal fat. Spectra and signal intensities acquired with different echo times (TE) ranging from 12.8 to 792 ms are shown in Supplementary Fig. S1A and S1B. The gradual decrease of the lipid signal with increasing TE eventually unmasked the succinate peak at TE > 70 ms and the lactate peak at TE > 100 ms. As previously described (27), increasing TE reduced the succinate signal exponentially and the lactate peak sinusoidally due to scalar coupling effect (Supplementary Fig. S1B). To study both the succinate and lactate signals, we chose a TE of 272 ms that reduced fat contamination and yielded positive lactate and succinate peaks. We then performed ^{1}H-MRS spectra with decreasing (10–1 mmol/L) concentrations of succinate and lactate [repetition time (TR), 3000 ms; echo time (TE), 272 ms; average, 128; volume of interest (VOI) size, $5 \times 5 \times 5$ mm^3]. Water suppression was performed using VAPOR pulses (sinc RF pulses, 646 ms total duration, 700 Hz bandwidth), followed by crusher gradients (3 ms duration, 58 mT/m strength). Three-sinc–shaped RF pulses with 4 kHz bandwidth to obtain a spectral width of 20 ppm achieved VOI selection. Spectral resolution was 0.98 Hz/point. After zero filling and phase correction, data filtration was performed with a Gaussian function at the top of the Free Induction Decay, with a length band of 2 Hz and visualization was obtained with a Fourier transform. The area under the succinate peak measured from the spectra was linearly correlated with the succinate concentration (Supplementary Fig. S1C and S1D).

A similar procedure was performed in the 3T clinical scanner using 3-cm-diameter phantom tubes and a larger VOI size ($10 \times 10 \times 10$ mm^3), except that the TR was 2,500 ms and the TE was lowered to 144 ms to compensate the lower detection threshold and the decrease of the signal-to-noise ratio (Supplementary Fig. S1E). On the basis of these procedures, the threshold for succinate detection was found to be approximately 1 mmol/L in both magnets.

Generation of the allografted mouse model

No animal model of SDH-related PPGL being available, we generated an allografted mouse model by subcutaneous injection of 2.5×10^6 immortalized mouse chromaffin cells (imCC; ref. 13) carrying a homozygous knockout of the *Sdhb* gene ($Sdhb^{-/-}$, clone 8) or their wild-type (WT) counterparts ($Sdhb^{lox/lox}$) into the flanks of 10-week-old female NMRI-nu mice. Animal experiments were registered by the French Ethical committee under Number 14-041 and followed the ARRIVE guidelines of the National Centre for the Replacement, Refinement, and Reduction of Animals in Research (London, UK).

Tumors were allowed to grow until their size reached 0.6 cm^3. They were then resected and 8 mm^3 fragments were grafted in the dorsal fat pad of naïve nude mice. The tumors grew in 100% of mice and tumors were macroscopically visible after 2 weeks for WT and 1 month for $Sdhb^{-/-}$ tumors, in line with the reduced growth rate of $Sdhb^{-/-}$ cells observed *in vitro* (13). Immediately after magnetic resonance spectroscopy,

Published OnlineFirst October 21, 2015; DOI: 10.1158/1078-0432.CCR-15-1576

tumors were retrieved and snap-frozen in liquid nitrogen or fixed in 4% paraformaldehyde.

Succinate ^{1}H-MRS in a 4.7-T animal-dedicated MRI device

Imaging was performed 37 ± 11 days after the graft for the *Sdhb*$^{-/-}$ group versus 22 ± 7 days for the WT group. Mice were placed in prone position under isoflurane anesthesia (4% for induction and 1.5% for maintenance in 1 L/min air) with respiration monitoring.

^{1}H-MRS was performed in a dedicated small-animal 4.7-T MR system (Biospec 47/40 USR Bruker), using a ^{1}H quadrature transmit/receive body coil with a 3.5-cm inner diameter. An anatomical two-dimensional (2D) steady-state free precession sequence (True FISP) was first acquired in two orthogonal planes. ^{1}H-MRS was then carried out using an optimized asymmetric Point REsolved SpectroScopy (PRESS) monovoxel acquisition (Supplementary Fig. S1). Echo signals [TR, 3,000 ms; TE, 144 or 272 ms; average, 512, with a VOI size of 5 × 5 × 5 mm^3) were acquired during 25 minutes.

The MRS spectrum of succinic acid [HOOC-$(CH_2)_2$-COOH] presents a characteristic peak at 2.44 ppm, corresponding to the precession frequency of the CH_2 protons. The succinate peak was quantified by measuring the area under the peak using Topspin 2.0 software (Brüker Corporation).

Patients

Patients were recruited from the French COMETE (`Cortico et Médullosurrénale: les Tumeurs Endocrines') cohort of the Hypertension unit of the European Georges Pompidou Hospital (HEGP), Paris, France. Ethical approval for the study was obtained from the institutional review board [Comité de Protection des Personnes (CPP) Ile de France II], and written informed consent to participate in the study was obtained from all patients. The procedures used for PPGL diagnosis and genetic testing were in accordance with international clinical practice guidelines (1). Mutation analysis of PPGL susceptibility genes was performed as previously described (28). When patients underwent surgery for paraganglioma, fresh tumor samples were frozen immediately after surgical removal and stored in liquid nitrogen until processing following the COMETE collection procedures. Confirmation of diagnosis was performed by histology on paraffin-embedded, formalin-fixed samples.

Succinate detection by ^{1}H-MRS in patients at 3 T

Combined MR images and MR spectroscopic scans of patients were acquired in a 3 T MRI clinical scanner (Discovery MR750w GEMSOW, GE Medical Systems). ^{1}H-MRS spectra were acquired by PRESS on the basis of the PROBE monovoxel sequence (29) and optimized for succinate and lactate detection, with TR, 2,500 ms; TE, 144 ms; Nex: 512 (22-minute acquisition) or 1,024 (44-minute acquisition). The VOI (1.3–19 cm^3) was centered on the anatomical image to prevent lipid contamination from the tissue surrounding the tumor as previously described (30).

MR images were acquired using a whole body (GEM Chest/Body/Pelvis; Body 24 AA3) or a head and neck (GEM Head/Neck/Chest; Head 24) phased-array multi-coil.

Detection of tumors and VOI positioning was performed on thin-section high-resolution T2-weighted fast spin-echo imaging in at least two orthogonal planes with the following parameters: TR, 2,500 ms; TE, 85 ms; echo train length, 19; slice thickness, 3 mm; spacing, 0.3; field of view, 14 × 14 cm^2 for neck or 42 × 42 cm^2 for whole-body coil; matrix, 320 × 320.

If necessary, an anatomical 2D steady-state free precession sequence (FIESTA CINE) was acquired with TR, 3.7 ms; TE, 1.4 ms; TI, 210 ms; slice thickness, 5 mm; spacing, 1 mm; field of view, 14 × 14 cm^2 for neck or 42 × 42 cm^2 for whole-body coil and/or a 3D angio-MR at arterial phase, after contrast agent administration of gadoterate meglumine 0.2 mL/kg with TR, 11.4 ms; TE, 2.2 ms; slice thickness, 0.8 mm; spacing, 0.4 mm; field of view, 30 × 27 cm^2.

A prescan algorithm was first acquired to adapt the transmitter and receiver gains and center frequency, the homogeneity of the magnetic field was optimized with the three-plane auto-shim procedure, and water suppression and automatic shimming of the single voxel were performed.

Measurement of succinate by gas chromatography/mass spectrometry

Tumor samples from 15 mice (10 samples with *Sdhb* knockout and 5 WT controls) and from paragangliomas of four patients (patients #1, #5, #6, and #9) were processed by organic extraction with ethylacetate, derivatization with *N*,*O*-bis(trimethylsilyl) trifluoroacetamide with 1% trimethylchlorosilane, and analyzed by gas chromatography/tandem mass spectrometry (GC-MS) on a GC-MS triple quadrupole (Scion TQ, Brüker Daltonics). Analytes were identified according to retention time and mass spectrum in selected reaction monitoring mode on the basis of standard spectral reference libraries.

Immunohistochemistry

SDHA, SDHB, and SDHD protein expression were assessed on formalin-fixed, paraffin-embedded (FFPE) tumor samples by immunohistochemistry as previously described (16, 18, 22) using the following antibodies: anti-SDHA (ab14715, Abcam; 1:1,000), anti-SDHB (HPA002868, Sigma-Aldrich Corp; 1:500), and anti-SDHD (HPA045727, Sigma-Aldrich Corp; 1:50).

SDH activity

SDH activity was investigated on frozen tumor samples using a spectrophotometrical assay, as previously described (31).

Results

In vivo detection of succinate in murine allografted tumors

The ^{1}H-MRS sequence was optimized *in vitro* (Supplementary Fig. S1). To investigate whether *in vivo* detection of succinate could be assessed for the noninvasive identification of SDH-related tumors, a proof-of-concept pilot study was performed in a mouse model prior to patients' exploration. No animal model of SDH-related PPGL being available, we generated an allografted mouse model using imCC carrying a homozygous knockout of the *Sdhb* gene or their WT counterparts (13). *Sdhb* knockout in tumors was confirmed by genotyping (Fig. 1A) and measurement of SDH enzymatic activity (Fig. 1B). GC-MS showed a massive accumulation of succinate in SDH-deficient tumors: 28.3 ± 9.5 nmol per mg protein in the *Sdhb*$^{-/-}$ group, versus 0.6 ± 0.7 nmol/mg protein in the control groups (Fig. 1C), confirming inhibition of SDH activity in *Sdhb*$^{-/-}$ tumors. ^{1}H-MRS was first tested in mice using a TE = 272 ms and a fixed VOI size (125 mm^3) placed over the tumor mass of 13 *Sdhb*$^{-/-}$ and 16 WT allografted mice (Fig. 1D). The peak corresponding to lactate, indicative of anaerobic glycolysis, was always present regardless of the tumor type. In

Published OnlineFirst October 21, 2015; DOI: 10.1158/1078-0432.CCR-15-1576

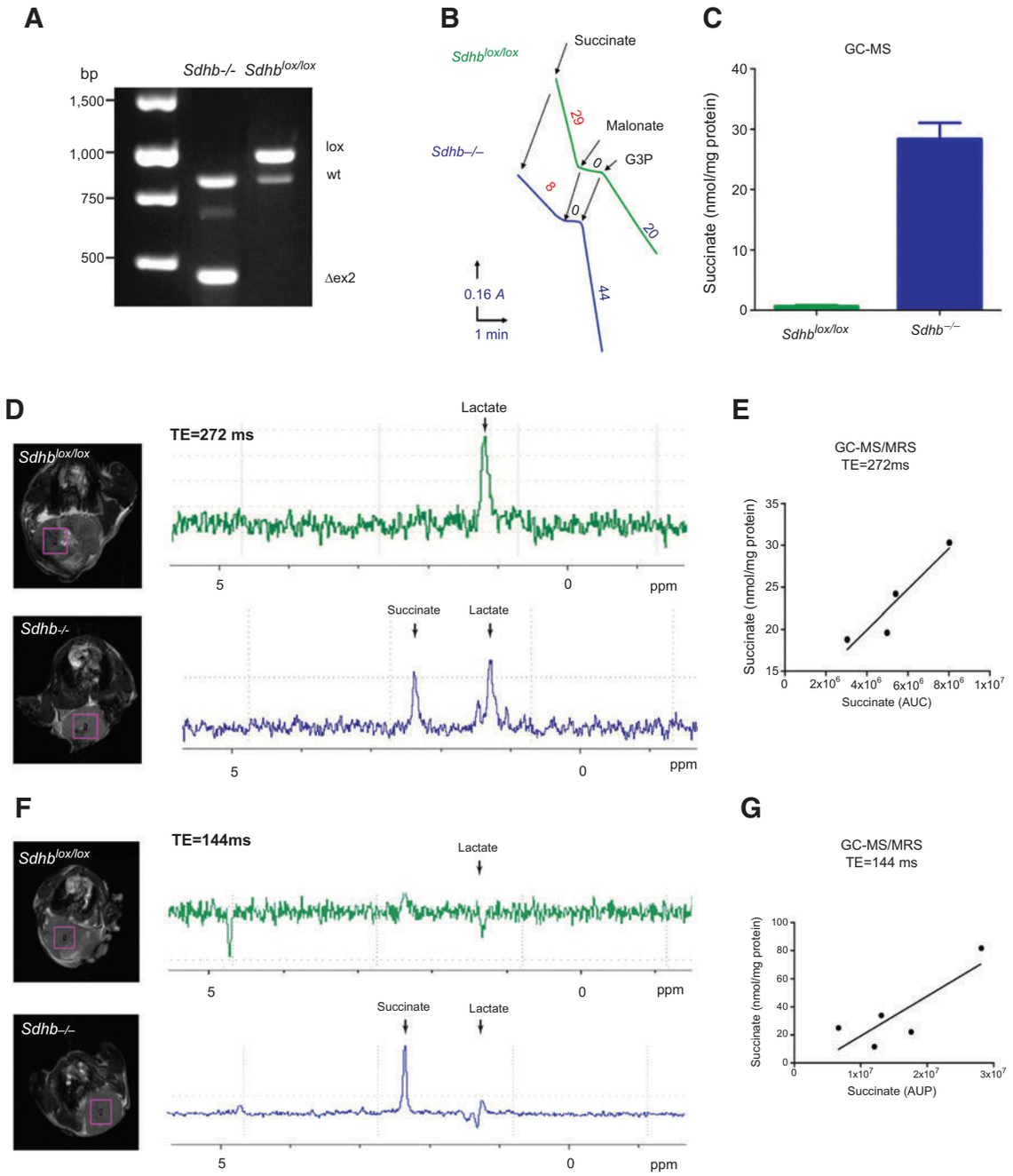

Figure 1.
SUCCES in *Sdhb*$^{-/-}$ allografted tumors in mice. A, genotyping of *Sdhb* gene locus in DNA extracted from tumors derived from *Sdhb*$^{-/-}$ and WT (*Sdhb*$^{lox/lox}$) cells allografted in mice. The deletion of exon 2 (ex2, 460 bp) is visible in tumors from *Sdhb*$^{-/-}$ grafted cells, whereas the floxed allele (900 bp) is shown in the *Sdhb*$^{lox/lox}$ grafted mice. In both tumor types, a WT DNA band (845 bp) originating from the supporting cells of the allografted mice (fibroblasts, endothelial cells) is visible. B, *Sdhb*$^{-/-}$ derived tumors display an unequivocal decrease in SDH activity measured by spectrophotometry. C, massive accumulation of succinate measured by GC-MS in *Sdhb*$^{-/-}$ derived tumors, which is not seen in *Sdhb*$^{lox/lox}$-derived tumors. D, ^{1}H-MRS spectra of tumor masses in mice allografted with WT (green spectra) or *Sdhb*$^{-/-}$ (blue spectra) cells using a TE = 272 ms. The lactate peak was present regardless of the tumor type, whereas the succinate peak was only detected in *Sdhb*$^{-/-}$ tumors. E, succinate levels measured *in vitro* by GC-MS correlate with the area under the succinate peaks (AUP) at TE = 272 ms. F, and G, the same data as in A and B, respectively, but at TE = 144 ms.

contrast, the succinate peak was only detected in *Sdhb*$^{-/-}$ tumors, with a sensitivity and specificity of 100% ($n = 13$), in agreement with succinate accumulation caused by SDH inhibition (Fig. 1D; Supplementary Fig. S2A). Measurements of succinate concentrations in *Sdhb*$^{-/-}$ tumor samples ($n = 4$) by GC-MS confirmed the MRS results. The succinate levels measured *in vitro* correlated with

Published OnlineFirst October 21, 2015; DOI: 10.1158/1078-0432.CCR-15-1576

Table 1. Characteristics of the 9 patients and 10 tumors analyzed by ^{1}H-MRS at 3 T

Patient	Gender	Age, y	Gene	Mutation type	Multiple locations	Type of tumor analyzed	Largest tumor diameter, mm	VOI size, cm^3	Succinate level on GC-MS, nmol/mg protein
1	M	33	*SDHB*	c.740T>Gp.Met247Arg	Yes	VPGL	80	4.6 and 1.5	ND
						APGL	94	19.2	89.3
2	M	70	*SDHC*	c.397C>Tp.Arg133Ter	No	VPGL	42	3.7	ND
3	F	32	*SDHD*	c.210G>Tp.Arg70Ser	Yes	CBPGL	24	1.5	ND
4	M	41	*SDHD*	c.325C>Tp.Gln109Ter	Yes	CBPGL	39	3.6	ND
5	M	25	none	NA	No	PCC	55	6.2	0.84
6	M	60	none	NA	No	APGL	35	4.2	0.54
7	F	74	none	NA	Yes	CBPGL	30	1.3	ND
8	M	47	none	NA	No	PCC	30	5.8	ND
9	M	48	*SDHA*	c.91C>Tp.Arg31Ter	No	APGL	50	12	72.17

Abbreviations: APGL, abdominal paraganglioma; CBPGL, carotid body paraganglioma; NA, not applicable; ND, not determined; PCC, pheochromocytoma; VPGL, vagal paraganglioma.

the area under the succinate peaks using a TE of 272 ms (r^2 = 0.88; Fig. 1E). The results obtained in the 4.7 T magnet with TE = 272 ms were repeated with TE = 144 ms in 5 *Sdhb*$^{-/-}$ and 3 WT tumors, (Fig. 1F; Supplementary Fig. S2B). At TE = 144 ms, lactate was hardly detectable, whereas succinate was specifically observed in *Sdhb*$^{-/-}$ tumors. Again, GC-MS quantification of succinate performed in *Sdhb*$^{-/-}$ resected samples (n = 5) correlated with *in vivo* measures (r^2 = 0.70; Fig. 1G).

In vivo detection of succinate in patients

Nine patients presenting with pheochromocytoma, cervical, and/or abdominal paragangliomas were recruited at the Hypertension unit of the European Georges Pompidou Hospital (Table 1). All patients benefited from genetic counseling in accordance with the Endocrine Society Clinical Practice Guidelines (1). Before undergoing SUCCES with ^{1}H-MRS, a germline *SDHx* gene mutation was identified in four patients (one *SDHB*, one *SDHC*, and two *SDHD*), whereas no mutation was identified for the other five patients.

Genetic testing identified a variant of unknown significance (VUS) in the *SDHB* gene of Patient #1 (c.740T>G = p.Met247Arg), a 33-year-old male with two paragangliomas and a predominant noradrenergic secretion profile. In the cervical paraganglioma of this patient, the ^{1}H-MRS signal of succinate was unequivocally discernable at 2.44 ppm using 1,024 averages and a 4.6 cm^3 VOI size (Fig. 2A). Sensitivity and specificity were explored by reducing the scan repeats from 1,024 to 512 averages and the VOI size from 4.6 to 1.5 cm^3: the succinate peak was still clearly detected in low sensitivity conditions in the cervical paraganglioma (Fig. 2A), as well as in the abdominal tumor mass (Fig. 2B), but not in the liver, showing the persistence of SDH activity in this healthy organ, expected to be heterozygous for the mutation (Fig. 2C). The pathogenicity of this newly described variant suggested by ^{1}H-MRS was supported by the LOH at the *SDHB* locus in DNA extracted from the resected abdominal paraganglioma (Fig. 2D) and confirmed by three functional tests: SDHB-negative (unspecific weak diffuse signal) and SDHD-positive immunohistochemistries (Fig. 2E), loss of SDH enzymatic activity (Fig. 2F), and succinate accumulation measured by GC-MS (Fig. 2G).

The succinate peak was observed in the tumors of the three other *SDHx* patients using scan repeats of 1,024 and 512 averages (Supplementary Fig. S3). Interestingly, a choline peak at 3.2 ppm was associated with the succinate peak in each of the *SDHx*-mutated tumors. In contrast, neither succinate nor choline peaks were observed in tumors from patients without *SDHx* mutations (Fig. 3; Supplementary Fig. S4). In Patient #5, immunohistochemistry of tumor samples showed SDHB- and SDHA-positive and SDHD-negative staining, whereas GC-MS analysis confirmed the absence of succinate accumulation (Fig. 3B and C).

Unexpected SDHA mutation identified by SUCCES

Surprisingly, a small but significant peak above baseline was detected in an abdominal paraganglioma from a patient with an apparently sporadic form of the disease (Fig. 4A.) This patient was a 48-year-old man suffering from a single abdominal paraganglioma with no family history of PPGL. Following comprehensive genetic counseling according to the international guidelines, the search for mutations of *SDHB*, *SDHC*, and *SDHD* genes returned negative. Nevertheless, the presence of a succinate peak in the tumor of this patient prompted us to sequence the *SDHA* gene of this patient, which identified a c.91C>T = p.Arg31Ter mutation (Fig. 4B), previously reported in Dutch patients with PPGL (16) or GIST (32). After the patient had undergone surgery, additional analyses of his tumor showed negative SDHA and SDHB and positive SDHD immunohistochemistry (Fig. 4C). GC-MS confirmed the accumulation of succinate (Table 1) and validated the rare and unexpected *SDHA*-mutated status of this patient that had been initially stratified as a sporadic case.

Discussion

Here, we report the noninvasive detection of succinate by *in vivo* MRS in tumors of patients with PPGL carrying *SDHx* genes mutations but not in those of patients without *SDHx* mutations. Interestingly, in an *Sdhb*$^{-/-}$ mouse tumor model, this succinate peak is correlated with the concentrations of succinate measured in the resected tumors by GC-MS.

Demonstration of SDH inactivation is currently based on *in vitro* analyses of tissue samples: immunohistochemical analyses of SDHB, SDHA, and SDHD expression in FFPE tissues (16, 18, 22), direct succinate measurements on frozen tumor samples by nuclear magnetic resonance (NMR) spectroscopy (15, 19, 20, 23), GC-MS, or liquid chromatography mass spectroscopy (LC-MS; refs. 13, 17, 21). Recently, Varoquaux and colleagues reported *in vivo* detection of succinate using ^{1}H-MRS in 6 patients with head and neck paraganglioma (3 *SDHD*, 1 *SDHB*, and 2 sporadic cases). Although the spectra quality was considered as low in the 2 sporadic cases and uninterpretable in one *SDHD*-mutated tumor, a succinate peak was also only

Published OnlineFirst October 21, 2015; DOI: 10.1158/1078-0432.CCR-15-1576

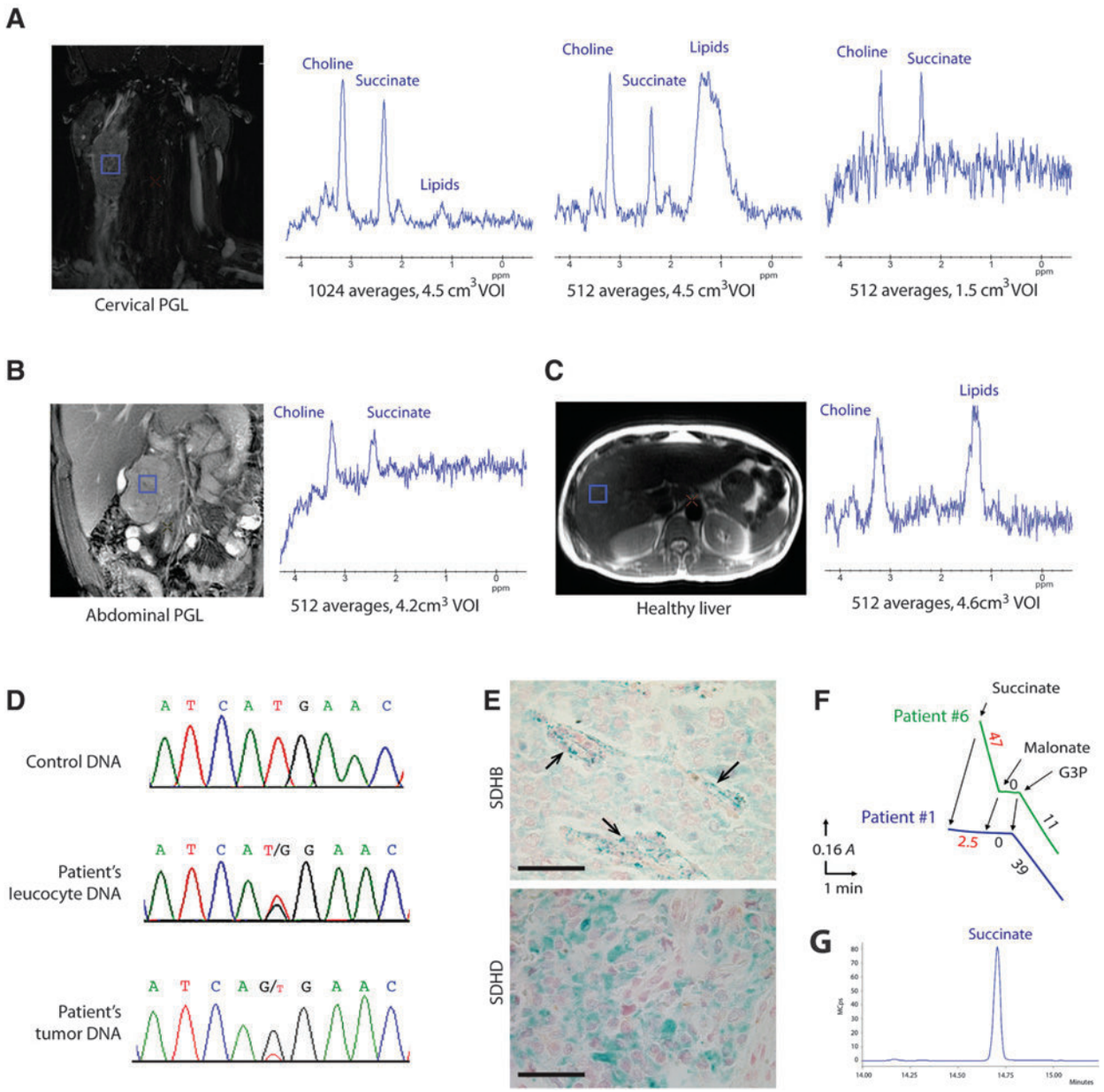

Figure 2.
SUCCES in a patient with an *SDHB* gene mutation. A, ^{1}H-MRS spectra of the right cervical paraganglioma (PGL) of Patient #1. A succinate peak was detected in the cervical PGL with two different averages (1,024 and 512) and two different VOI sizes (4.6 and 1.5 cm^{3}). B, applying the PRESS sequence to the abdominal tumor mass of the same patient permits to detect a succinate peak. C, in the healthy liver, the absence of a peak demonstrates the specificity of the method. D, genetic testing identified a variant of unknown significance in the *SDHB* gene with an LOH in tumor DNA extracted from the resected abdominal PGL. E, SDHB immunochemistry (IHC) leads to an unspecific weak diffuse signal in tumor cells, whereas endothelial cells (arrows) are strongly labeled (top part). A positive staining is shown after SDHD IHC (bottom part). Scale bar, 50 μm. F, significant reduction of SDH activity in Patient #1 (blue line) as compared with Patient #6, a case without *SDHx* mutation (green line). G, High level of succinate in the abdominal PGL of Patient #1 measured by GC-MS.

detected in three *SDHx*-mutated tumors (33). In the present study, we show that ^{1}H-MRS also detects succinate in abdominal paraganglioma and in genes encoding all four SDH subunits. Moreover, we performed longer acquisition time (512 and 1,024 averages, vs. 120 in the Varoquaux and colleagues study), which allowed an immediate interpretation of spectra, without the need of postprocessing the data.

The benefits of assessing this tumor hallmark in patients with *SDHx*-related tumors are important in several aspects. SUCCES would allow stratifying these patients or classifying VUS as deleterious mutations with no need of tissue sampling. Patient #9 carried a single abdominal paraganglioma diagnosed at age 48, without a family history for this disease. According to international guidelines, *SDHB*, *SDHC*, and *SDHD* genetic testing were

Published OnlineFirst October 21, 2015; DOI: 10.1158/1078-0432.CCR-15-1576

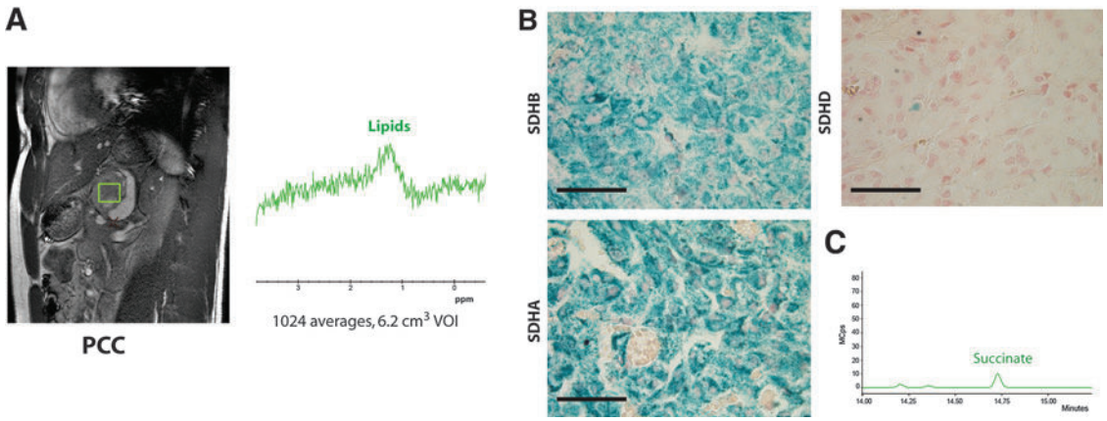

Figure 3.
SUCCES in a patient without *SDHx* gene mutation. A, absence of a succinate peak in the ^{1}H-MRS spectrum of Patient #5's pheochromocytoma (PCC) with 1,024 averages. B, unequivocal positive granular staining after SDHB and SDHA IHC (left) and negativity of SDHD IHC (right). Scale bar, 50 μm. C, low level of succinate in the tumor measured by GC-MS.

performed in this patient, but not *SDHA*, which would have been prescribed only after surgery, in case of SDHA negative immunohistochemistry (1). In such a case, exploring the patient with ^{1}H-MRS and detecting the succinate peak orientated us without hesitation toward *SDHA* sequencing, leading to early identification of the mutation. SDHA immunohistochemistry is not included in international guidelines and is not a standard procedure, thus it is likely that this mutation would have been missed in most instances. In Patient #1, an *SDHB* gene VUS was identified, whereas SDHB immunohistochemistry showed a potentially misleading, weak diffuse signal, previously reported in some PPGL with *SDHx* genes mutations (18). Hence, in this other case, the ^{1}H-MRS succinate peak was particularly informative to validate the functionality of the *SDHB* mutation.

SDHx mutation carriers are at risk of developing multiple paragangliomas, and *SDHB*-mutated carriers are predisposed to metastatic forms of the disease. Knowledge of the *SDHx*-mutated status is critical for the follow-up and clinical management of patients and of their relatives. On the basis of an early knowledge of the *SDHx* mutational status, surgeons may decide to

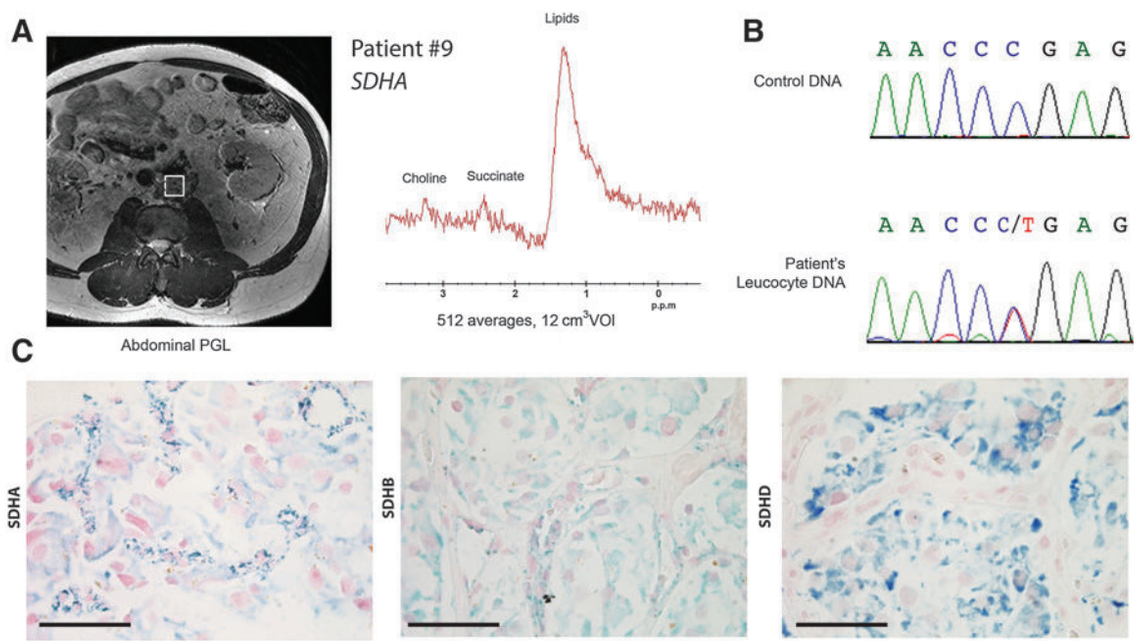

Figure 4.
SUCCES in a patient with an *SDHA* gene mutation. A, ^{1}H-MRS spectra in Patient #9's abdominal paraganglioma (PGL). A small succinate peak was detected with 512 averages and a 12 cm^{3} VOI size. B, results of genetic testing that identified a c. 91C>T variant in the *SDHA* gene. C, SDHA and SDHB immunochemistry (IHC) lead to unspecific weak diffuse signals in tumor cells whereas endothelial cells are strongly labeled. In contrast, SDHD IHC shows a positive staining. Scale bars, 50 μm.

Published OnlineFirst October 21, 2015; DOI: 10.1158/1078-0432.CCR-15-1576

adapt their procedures, especially for *SDHB* cases. For nonoperable tumors, therapeutic choices may also take advantage from this information. For example, studies have suggested that *SDHB* mutation carriers may be better responders to high doses of ^{131}I-MIBG (34), sunitinib (35), or temozolomide treatments (36). Although these results will need to be evaluated in larger, prospective, and comparative studies, they nevertheless pave the way toward personalized medicine for inherited PPGL.

Overall, the clinical value of SUCCES lies in its capacity to assess for the presence of succinate repeatedly over the time course of the disease, for clinical surveillance, postoperative follow-up, and evaluation of treatment efficacy (17). *In vivo* estimation of succinate could help classifying a dubious lesion detected during surveillance and to demonstrate the causality of SDH deficiency in tumors identified in *SDHx*-mutated patients. This would be particularly helpful in cases for which surgery is not necessary, such as prolactin-secreting pituitary adenomas recently described in *SDHx* mutation carriers (37). Because of the small size of these tumors, the feasibility of SUCCESS may however be more difficult in these cases.

Animal experiments demonstrated that the area under the succinate peak of the ^{1}H-MRS spectra is correlated with the concentrations of succinate measured in the resected tumors by GC-MS. Future studies in larger groups will be needed to show whether this correlation holds also in patients. If this turned out to be the case and given that succinate concentrations in tumors reflect the metabolic activity of SDH-deficient tumor cells, then SUCCES would produce a quantifiable surrogate marker of radiation and/or chemotherapy efficacy for the patients.

Interestingly, other metabolites have been shown *in vitro* to discriminate between different types of inherited PPGL (20). In future studies, it may also be addressed whether these metabolites can also be observed by ^{1}H-MRS and used as supplemental tools. For example, Imperiale and colleagues recently reported in a case of sporadic pheochromocytoma that catecholamines are indeed detectable by ^{1}H-MRS (38).

The present proof-of-concept study has shown that SUCCES is highly sensitive, reliable, and specific for the detection of the *SDHx* mutations that lead to inhibition of SDH activity. The next step to fully define the place of this new method in the clinical management of PPGL is to test the method in larger series of patients and define the best conditions for routine clinical applications. In that respect, we occasionally observed, in both groups of patients, a blunt signal centered at 1.2 ppm. This signal corresponds to adipose tissue surrounding the tumor that is not always straightforward to avoid even with strict intratumor positioning of the VOI in which ^{1}H-MRS is performed. Because MRS data are usually displayed with a γ scale normalized on the highest peak of the spectrum, the presence of a significant lipid signal may modify the threshold for succinate detection in small lesions. Averaging more spectra increases the signal-to-noise ratio but also increases scan duration, which may not be applicable to all patients. For abdominal tumors, respiratory gating should be considered to reduce the lipid peak and improve the quality of spectra, as previously reported for *in vivo* catecholamine detection (38). Using 512 scan averages appears to be sufficient for reliable succinate detection in tumors with *SDHx* genes mutation. However, this may limit the quality of spectra for small or highly necrotic tumors, as shown in the case of patient #3 (Supplementary Fig. S3B), for whom successful interpretation could only be achieved after 1,024 scan averages. Therefore, the minimal tumor size for reliable measurements of succinate needs to be addressed in future prospective studies. Fortunately, this ^{1}H-MRS sequence is easy to implement in any clinical MRI scanner using standard hardware and software already in place in many imaging departments.

Finally, it is noteworthy that the succinate peak was always associated in human PPGL with a peak resonating at 3.2 ppm on the ^{1}H-MRS spectra, most probably corresponding to choline. Such a peak was only seen in tumors from the patients carrying *SDHx* mutations. Previous *in vitro* NMR studies never reported such a choline increase in SDH-related tumors. However, a similar peak is also observed in the spectra of both *SDHx*-mutated paraganglioma evaluated by *in vivo* ^{1}H-MRS in the Varoquaux and colleagues study (33). The accuracy of this observation will need to be further validated both *in vivo* and *in vitro*, in SDH as well as in other oncogenic mutations of metabolic pathways. It is worth noting that choline is a methyl donor in the *S*-adenosylmethionine pathway involved in DNA and histone methylation. Hence, if confirmed, the choline peak that we observed here may be related to the disrupted methylation phenotype recently identified in SDH-deficient tumors (13).

In conclusion, we present here a robust and simple method that can be used routinely to demonstrate the presence of succinate in the tumors of patients with PPGL. Considering its excellent sensitivity, specificity, and innocuousness, SUCCES deserves to be tested in large multicentric series to define its place in the clinical guidelines of PPGL management as well as in other SDH-related tumors such as GIST and renal clear cell carcinomas.

Disclosure of Potential Conflicts of Interest

No potential conflicts of interest were disclosed.

Authors' Contributions

Conception and design: C. Lussey-Lepoutre, A. Morin, L. Amar, F. Zinzindohoué, A.-P. Gimenez-Roqueplo, J. Favier, B. Tavitian

Development of methodology: C. Lussey-Lepoutre, A. Bellucci, A. Morin, L. Amar, M. Janin, G. Autret, C.-A. Cuenod, J. Favier, B. Tavitian

Acquisition of data (provided animals, acquired and managed patients, provided facilities, etc.): C. Lussey-Lepoutre, A. Bellucci, A. Morin, A. Buffet, L. Amar, M. Janin, C. Ottolenghi, F. Zinzindohoué, G. Autret, N. Burnichon, E. Robidel, B. Banting, S. Fontaine, C.-A. Cuenod, P. Benit, P. Rustin, P. Halimi, J. Favier

Analysis and interpretation of data (e.g., statistical analysis, biostatistics, computational analysis): C. Lussey-Lepoutre, A. Bellucci, N. Burnichon, P. Halimi, B. Tavitian, J. Favier

Writing, review, and/or revision of the manuscript: C. Lussey-Lepoutre, L. Amar, M. Janin, C. Ottolenghi, F. Zinzindohoué, G. Autret, N. Burnichon, C.-A. Cuenod, P. Halimi, L. Fournier, A.-P. Gimenez-Roqueplo, J. Favier, B. Tavitian

Administrative, technical, or material support (i.e., reporting or organizing data, constructing databases): C. Lussey-Lepoutre, A. Morin, F. Zinzindohoué, E. Robidel, B. Banting, S. Fontaine, L. Fournier, A.-P. Gimenez-Roqueplo, J. Favier

Study supervision: C. Lussey-Lepoutre, A.-P. Gimenez-Roqueplo, J. Favier, B. Tavitian

Acknowledgments

The authors thank Prof. Pierre-François Plouin and Dr. Guillaume Bobrie for their clinical contribution to the study and Prof. Catherine Oppenheim and Stephanie Lion for sharing their expertise. They also thank Daniel Balvay for helpful discussions, Brigitte Lambert (Radiology, HEGP) and Marion Uettwiller (General Electrics Healthcare) for technical assistance, and Catherine Tritscher for administrative assistance. They thank the technical staff of the Genetic department of HEGP (especially Françoise Le Quellec, Caroline Travers, Nirubiah Thurairajasingam) led by Prof. Xavier Jeunemaitre, Jean-Michaël

Published OnlineFirst October 21, 2015; DOI: 10.1158/1078-0432.CCR-15-1576

Mazzella, and Samir Jocelyn Do Rego for their contribution to the study. They thank Daniel Tennant for helpful discussion.

Grant Support

This work received funding from the Cancer Research for Personalized Medicine—CARPEM project (Site de Recherche Intégré sur le Cancer- SIRIC), the Agence Nationale de la Recherche (ANR-2011-JCJC-00701 MODEOMAPP), the European Union Seventh Framework Programme (FP7/2007-2013) under grant agreement no. 259735, and the Institut National du Cancer et la Direction Générale de l'Offre de Soins (INCa-DGOS_8663) for the COMETE network. C. Lepoutre-Lussey is funded by the CARPEM project. A. Bellucci received a fellowship from Fondation pour la Recherche Médicale. A. Buffet received a fellowship from the ITMO Cancer - Plan Cancer 2014-2019.

The costs of publication of this article were defrayed in part by the payment of page charges. This article must therefore be hereby marked *advertisement* in accordance with 18 U.S.C. Section 1734 solely to indicate this fact.

Received July 2, 2015; revised September 16, 2015; accepted October 6, 2015; published OnlineFirst October 21, 2015.

References

1. Lenders JW, Duh QY, Eisenhofer G, Gimenez-Roqueplo AP, Grebe SK, Murad MH, et al. Pheochromocytoma and paraganglioma: an endocrine society clinical practice guideline. J Clin Endocrinol Metab 2014;99:1915–42.
2. Favier J, Amar L, Gimenez-Roqueplo AP. Paraganglioma and phaeochromocytoma: from genetics to personalized medicine. Nat Rev Endocrinol 2015;11:101–11.
3. Janeway KA, Kim SY, Lodish M, Nose V, Rustin P, Gaal J, et al. Defects in succinate dehydrogenase in gastrointestinal stromal tumors lacking KIT and PDGFRA mutations. Proc Natl Acad Sci U S A 2011;108:314–8.
4. Vanharanta S, Buchta M, McWhinney SR, Virta SK, Peczkowska M, Morrison CD, et al. Early-onset renal cell carcinoma as a novel extraparaganglial component of SDHB-associated heritable paraganglioma. Am J Hum Genet 2004;74:153–9.
5. Baysal BE, Ferrell RE, Willett-Brozick JE, Lawrence EC, Myssiorek D, Bosch A, et al. Mutations in SDHD, a mitochondrial complex II gene, in hereditary paraganglioma. Science 2000;287:848–51.
6. Warburg O. Ueber den stoffwechsel der tumoren. Constable, London. 1930.
7. Tomlinson IP, Alam NA, Rowan AJ, Barclay E, Jaeger EE, Kelsell D, et al. Germline mutations in FH predispose to dominantly inherited uterine fibroids, skin leiomyomata and papillary renal cell cancer. Nat Genet 2002;30:406–10.
8. Yan H, Parsons DW, Jin G, McLendon R, Rasheed BA, Yuan W, et al. IDH1 and IDH2 mutations in gliomas. N Eng J Med 2009;360:765–73.
9. Morin A, Letouze E, Gimenez-Roqueplo AP, Favier J. Oncometabolites-driven tumorigenesis: From genetics to targeted therapy. Int J Cancer 2014;135:2237–48.
10. Gimenez-Roqueplo AP, Caumont-Prim A, Houzard C, Hignette C, Hernigou A, Halimi P, et al. Imaging work-up for screening of paraganglioma and pheochromocytoma in SDHx mutation carriers: a multicenter prospective study from the PGL.EVA Investigators. J Clin Endocrinol Metab 2013;98:E162–73.
11. Amar L, Baudin E, Burnichon N, Peyrard S, Silvera S, Bertherat J, et al. Succinate dehydrogenase B gene mutations predict survival in patients with malignant pheochromocytomas or paragangliomas. J Clin Endocrinol Metab 2007;92:3822–8.
12. Gimenez-Roqueplo AP, Favier J, Rustin P, Rieubland C, Crespin M, Nau V, et al. Mutations in the SDHB gene are associated with extra-adrenal and/or malignant phaeochromocytomas. Cancer Res 2003;63:5615–21.
13. Letouze E, Martinelli C, Loriot C, Burnichon N, Abermil N, Ottolenghi C, et al. SDH mutations establish a hypermethylator phenotype in paraganglioma. Cancer Cell 2013;23:739–52.
14. Selak MA, Armour SM, MacKenzie ED, Boulahbel H, Watson DG, Mansfield KD, et al. Succinate links TCA cycle dysfunction to oncogenesis by inhibiting HIF-alpha prolyl hydroxylase. Cancer Cell 2005;7:77–85.
15. Imperiale A, Moussallieh FM, Roche P, Battini S, Cicek AE, Sebag F, et al. Metabolome profiling by HRMAS NMR spectroscopy of pheochromocytomas and paragangliomas detects SDH deficiency: clinical and pathophysiological implications. Neoplasia 2015;17:55–65.
16. Korpershoek E, Favier J, Gaal J, Burnichon N, van Gessel B, Oudijk L, et al. SDHA immunohistochemistry detects germline SDHA gene mutations in apparently sporadic paragangliomas and pheochromocytomas. J Clin Endocrinol Metab 2011;96:E1472–6.
17. Lendvai N, Pawlosky R, Bullova P, Eisenhofer G, Patocs A, Veech RL, et al. Succinate-to-fumarate ratio as a new metabolic marker to detect the presence of SDHB/D-related paraganglioma: initial experimental and ex vivo findings. Endocrinology 2014;155:27–32.
18. Menara M, Oudijk L, Badoual C, Bertherat J, Lepoutre-Lussey C, Amar L, et al. SDHD immunohistochemistry: a new tool to validate SDHx mutations in pheochromocytoma/paraganglioma. J Clin Endocrinol Metab 2015;100:E287–91.
19. Rao JU, Engelke UF, Rodenburg RJ, Wevers RA, Pacak K, Eisenhofer G, et al. Genotype-specific abnormalities in mitochondrial function associate with distinct profiles of energy metabolism and catecholamine content in pheochromocytoma and paraganglioma. Clin Cancer Res 2013;19:3787–95.
20. Rao JU, Engelke UF, Sweep FC, Pacak K, Kusters B, Goudswaard AG, et al. Genotype-specific differences in the tumor metabolite profile of pheochromocytoma and paraganglioma using untargeted and targeted metabolomics. J Clin Endocrinol Metab 2015;100:E214–22.
21. Richter S, Peitzsch M, Rapizzi E, Lenders JW, Qin N, de Cubas AA, et al. Krebs cycle metabolite profiling for identification and stratification of pheochromocytomas/paragangliomas due to succinate dehydrogenase deficiency. J Clin Endocrinol Metab 2014;99:3903–11.
22. van Nederveen FH, Gaal J, Favier J, Korpershoek E, Oldenburg RA, de Bruyn EM, et al. An immunohistochemical procedure to detect patients with paraganglioma and phaeochromocytoma with germline SDHB, SDHC, or SDHD gene mutations: a retrospective and prospective analysis. Lancet Oncol 2009;10:764–71.
23. Pollard PJ, Briere JJ, Alam NA, Barwell J, Barclay E, Wortham NC, et al. Accumulation of Krebs cycle intermediates and over-expression of HIF1alpha in tumours which result from germline FH and SDH mutations. Hum Mol Genet 2005;14:2231–9.
24. Andronesi OC, Kim GS, Gerstner E, Batchelor T, Tzika AA, Fantin VR, et al. Detection of 2-hydroxyglutarate in IDH-mutated glioma patients by *in vivo* spectral-editing and 2D correlation magnetic resonance spectroscopy. Sci Transl Med 2012;4:116ra4.
25. Choi C, Ganji SK, DeBerardinis RJ, Hatanpaa KJ, Rakheja D, Kovacs Z, et al. 2-hydroxyglutarate detection by magnetic resonance spectroscopy in IDH-mutated patients with gliomas. Nat Med 2012;18:624–9.
26. Elkhaled A, Jalbert LE, Phillips JJ, Yoshihara HA, Parvataneni R, Srinivasan R, et al. Magnetic resonance of 2-hydroxyglutarate in IDH1-mutated low-grade gliomas. Sci Translat Med 2012;4:116ra5.
27. Harada K, Honmou O, Liu H, Bando M, Houkin K, Kocsis JD. Magnetic resonance lactate and lipid signals in rat brain after middle cerebral artery occlusion model. Brain Res 2007;1134:206–13.
28. Burnichon N, Vescovo L, Amar L, Libe R, de Reynies A, Venisse A, et al. Integrative genomic analysis reveals somatic mutations in pheochromocytoma and paraganglioma. Hum Mol Genet 2011;20:3974–85.
29. Webb PG, Sailasuta N, Kohler SJ, Raidy T, Moats RA, Hurd RE. Automated single-voxel proton MRS: technical development and multisite verification. Magn Reson Med 1994;31:365–73.
30. Agarwal M, Chawla S, Husain N, Jaggi RS, Husain M, Gupta RK. Higher succinate than acetate levels differentiate cerebral degenerating cysticerci from anaerobic abscesses on in-vivo proton MR spectroscopy. Neuroradiology 2004;46:211–5.
31. Rustin P, Chretien D, Bourgeron T, Gerard B, Rotig A, Saudubray JM, et al. Biochemical and molecular investigations in respiratory chain deficiencies. Clin Chim Acta 1994;228:35–51.
32. Oudijk L, Gaal J, Korpershoek E, van Nederveen FH, Kelly L, Schiavon G, et al. SDHA mutations in adult and pediatric wild-type gastrointestinal stromal tumors. Mod Pathol 2013;26:456–63.

Published OnlineFirst October 21, 2015; DOI: 10.1158/1078-0432.CCR-15-1576

33. Varoquaux A, le Fur Y, Imperiale A, Reyre A, Montava M, Fakhry N, et al. Magnetic resonance spectroscopy of paragangliomas: new insights into *in vivo* metabolomics. Endocr Relat Cancer 2015;22: M1–8.
34. Gonias S, Goldsby R, Matthay KK, Hawkins R, Price D, Huberty J, et al. Phase II study of high-dose [131I]metaiodobenzylguanidine therapy for patients with metastatic pheochromocytoma and paraganglioma. J Clin Oncol 2009;27:4162–8.
35. Jimenez C, Rohren E, Habra MA, Rich T, Jimenez P, Ayala-Ramirez M, et al. Current and future treatments for malignant pheochromocytoma and sympathetic paraganglioma. Curr Oncol Rep 2013;15: 356–71.
36. Hadoux J, Favier J, Scoazec JY, Leboulleux S, AlGhuzlan A, Caramella C, et al. SDHB mutations are associated with response to temozolomide in patients with metastatic pheochromocytoma or paraganglioma. Int J Cancer 2014;135:2711–20.
37. Xekouki P, Szarek E, Bullova P, Giubellino A, Quezado M, Mastroyannis SA, et al. Pituitary adenoma with paraganglioma/pheochromocytoma (3PAs) and succinate dehydrogenase defects in human and mice. J Clin Endocrinol Metab 2015:jc20144297.
38. Imperiale A, Battini S, Averous G, Mutter D, Goichot B, Bachellier P, et al.. *In vivo* detection of catecholamines by magnetic resonance spectroscopy: a potential specific biomarker for the diagnosis of pheochromocytoma. Surgery. 2015 May 1. [Epub ahead of print].

Published OnlineFirst October 21, 2015; DOI: 10.1158/1078-0432.CCR-15-1576

Clinical Cancer Research

In Vivo Detection of Succinate by Magnetic Resonance Spectroscopy as a Hallmark of *SDHx* Mutations in Paraganglioma

Charlotte Lussey-Lepoutre, Alexandre Bellucci, Aurélie Morin, et al.

Clin Cancer Res 2016;22:1120-1129. Published OnlineFirst October 21, 2015.

REVUE 1

Pheochromocytoma and paraganglioma: molecular testing and personalized medicine.

Burnichon N, Buffet A, Gimenez-Roqueplo AP.

Curr Opin Oncol. 2016 Jan;28(1):5-10.

TITLE PAGE

Title of review article:

Pheochromocytoma and paraganglioma: Molecular testing and personalized medicine

Authors:

Nelly Burnichon[a,b,c], Alexandre Buffet [a,b], Anne-Paule Gimenez-Roqueplo[a,b,c]

Authors' affiliations:

[a]INSERM, UMR970, Paris-Cardiovascular Research Center, F-75015, Paris, France

[b]Faculté de Médecine, Université Paris Descartes, Sorbonne Paris Cité, F-75006 Paris, France

[c]Assistance Publique-Hôpitaux de Paris, Hôpital Européen Georges Pompidou, Department of Genetics, F-75015, Paris, France

Author of correspondence:

Nelly Burnichon
INSERM, UMR970
Paris-Cardiovascular Research Center
F-75015, Paris, France
Tel: +33 1 53 98 80 41
Fax: +33 1 53 98 79 52
email: nelly.burnichon@inserm.fr

ABSTRACT

Purpose of review:

Pheochromocytomas and paragangliomas (PPGL) are rare tumours, strongly associated with inherited susceptibility gene mutations, and presenting limited therapeutic options for patients with metastatic disease. This review discusses the recent developments in the characterization of PPGL genetic heterogeneity and associated tumourigenesis pathways, together with their potential clinical relevance.

Recent findings:

The mutational landscape of PPGL is now well defined, especially with the contribution of next generation sequencing (NGS). Up to 70% of these tumours harbour a germline or a somatic mutation in one of the numerous predisposing gene. In parallel, "omics" analyses have identified mutation-linked subsets of tumours substantially associated with molecular signatures suggesting new therapeutic targets for patients with a malignant transformation of the disease.

Summary:

In the near future, extended molecular testing of PPGL could be used to determine therapeutic approaches and assess diagnosis and prognosis biomarkers. Considering the current development of NGS-based genetic screening, this technology appears as a good option to improve both PPGL molecular diagnosis and patient management.

KEYWORDS

Paragangliomas; genetic testing; personalized medicine; next generation sequencing

INTRODUCTION

Pheochromocytomas (PCC) and paragangliomas (PGL) are rare neuroendocrine tumours that arise from neural crest cells and can develop either in the adrenal medulla (PCC), or in paraganglionic tissues (PGL) located from the skull base to the pelvic region.

Paraganglioma and pheochromocytoma (PPGL) can be classified as syndromic, familial or sporadic. The understanding of inherited forms of PPGL has dramatically changed over the past 15 years. Since the first description of mutations in the *SDHD* gene in patients with PPGL in 2000 [1], a dozen of susceptibility genes have been identified. It is currently accepted that roughly 40% of PPGL are associated with an inherited mutation [2]. Moreover, major advances in genomic analyses have shown that up to 30% of tumours actually carry somatic mutations in these known susceptibility genes [3, 4**] (Figure 1).

In contrast, the genetic events that drive the malignant progression of the disease are yet poorly understood, and malignancy is still defined by the presence of distant metastases. The risk of malignancy is about 10 to 20% with a 5-year survival rate estimated to 50% [5]. To date, no reliable predictors for malignant potential nor molecular or histological markers for malignancy exist. Therapeutic options are limited and mainly restricted to palliative management [6*].

The large genetic heterogeneity of PPGL is directly linked to the heterogeneity in subsequently activated cancer pathways. The identification of such pathways

paves the way to molecular targeted therapies and to the implementation of diagnosis and prognosis markers of malignancy.

Herein, we review the mutational landscape of PPGL at both germline and somatic levels. A molecular oriented strategy for targeted therapy will be discussed.

MAIN SUSCEPTIBILITY GENES AND ASSOCIATED TUMOURIGENIC PATHWAYS

Traditionally, pheochromocytomas were considered to have a syndromic presentation in about 10% of cases, as part of neurofibromatosis type 1 (due to mutations in the *NF1* gene), multiple endocrine neoplasia type 2 (associated with activating *RET* mutations) or von Hippel Lindau (caused by mutations in *VHL* gene) syndromic diseases. The description of familial form of PPGL and the improvement in molecular biology methods have led to the identification of *SDHx* [1, 7-10] and, more recently, *TMEM127* [11], *MAX* [12] and *MDH2* [13**] as PPGL tumour suppressor genes (Figure 1).

During the last few years, several large-scale genomic analyses, including CGH and SNP array, mRNA and microRNA expression studies and methylation profiling, have been conducted worldwide on independent series. Concordantly, these approaches have led to the description of well-defined tumour subtypes and their corresponding tumourigenic pathways.

Gene expression profiling initially revealed that PPGL could be separated in two main clusters (C1 and C2) each subdivided into sub-clusters (C1A and 1B; C2A, 2B and 2C) by unsupervised analysis [14-16]. These different groups were

defined according to their mutational status and strongly associated with specific tumourigenic pathways. In a same way, DNA methylation and miRNA profiling revealed a major influence of the main genetic drivers on the somatic molecular phenotype [4**, 17-19**].

Cluster 1-related genes

Unsupervised analyses distinguished two groups defined as C1A and C1B sub-clusters mainly corresponding to *SDHx*- and *VHL*-related tumours, respectively.

SDHx genes comprise *SDHA*, *SDHB*, *SDHC* and *SDHD* genes encoding the four subunits of succinate dehydrogenase (SDH, mitochondrial complex II), and *SDHAF2*, which encodes an SDH assembly factor, responsible for the flavination of SDHA protein. Germline mutations in these tumour suppressor genes cause hereditary paragangliomas with familial or sporadic presentation. It is worthy of note that mutation in *SDHB* is a risk factor for malignancy and poor prognosis [20, 21]. *SDHD* and *SDHAF2* mutations are mainly found in patients with a family history of head and neck paragangliomas in the paternal branch while mutations in *SDHA* have been described in sporadic form of the disease only. *SDHA*, *SDHAF2* and *SDHC*-related PPGL remain unfrequent. Somatic mutations in *SDHx* are extremely rare, if ever [22].

Germline *VHL* mutations predispose to the von Hippel Lindau disease, a systemic cancer syndrome that gives rise to clear-cell renal cell carcinoma, PPGL and other tumours in many organs including central nervous system, eyes and pancreas. *VHL*-associated PPGL are frequently early-onset pheochromocytomas that can be bilateral and/or recurrent. Head and neck paragangliomas have been more rarely described.

Very high similarities in gene expression profiles inside each subgroup led to the discovery of germline mutations in *FH* [17] and *MDH2* [13**] genes in apparently sporadic tumours clustering with C1A and the identification of somatic mutations in *VHL* [16] and *EPAS1* [23] in sporadic C1B-tumors.

FH and *MDH2* encode the fumarate hydratase and the malate dehydrogenase, respectively, two enzymes belonging to the tricarboxylic acid cycle. Mutations in *FH* predispose to hereditary leiomyomatosis and renal cell carcinoma (HLRCC), associating cutaneous and uterine leiomyomatosis and type 2 papillary renal carcinoma. The incidence of *FH* mutation in PPGL is estimated at 1%. Interestingly, about 40% of cases carrying germline *FH* mutation presented a metastatic disease [24, 25*]. To date, only one germline *MDH2* mutation has been identified in a patient with multiple malignant PPGL. Larger international cohort studies are now required to determine the prevalence of *MDH2* mutations and to confirm a possible association with malignancy, as already demonstrated for *SDHB* and *FH*.

Gain of function mutations of *EPAS1* (encoding the hypoxia-inducible factor 2α) have been described recently in PPGL at the somatic level [26, 27*]. Additional studies revealed that these hot spot mutations could actually be mosaic or germline mutations [28]. In that case, affected patients can present associated polycythemia and somastinoma.

Germline or somatic mutations in cluster 1 genes lead to a pseudo-hypoxic signature [14-16] with overexpression of angiogenesis factors as one consequence. Thus, antiangiogenic drugs are promising candidates for targeted therapies in malignant PPGL, especially those belonging to the C1 cluster. Several phase II clinical trials evaluating tyrosine kinase inhibitors sunitinib and axitinib

are currently in progress and should determine the efficacy of such therapies [6*].

Gene expression and methylation profiling studies have allowed differentiating tumorigenesis mechanisms in C1A from C1B. Glycolysis is activated in *VHL*-related tumours while DNA and histone hypermethylation is observed in *SDHx*-, *FH*- and *MDH2*-linked tumours. For therapeutic purpose, the hypermethylator phenotype of C1A tumours suggests that DNA-demethylating drugs such as 5-aza-2'-deoxycytidine or histone methyl transferase inhibitors could be an effective approach. Moreover, temozolomide, an alkylating agent, has been shown, in a limited cohort, to be more effective in patients with *SDHB* malignant tumours compared with non-*SDHB* patients. This increased response is probably explained by the extinction of the repair enzyme MGMT which promoter is highly methylated in this subgroup of tumours [29**].

Cluster 2-related genes

Cluster 2 includes tumours carrying mutations in *NF1*, *RET*, *TMEM127* and *MAX* genes as well as a large set of sporadic tumours.

Mutations in the *NF1* tumour suppressor gene lead to neurofibromatosis type 1 (NF1), a frequent autosomal dominant syndrome (prevalence estimated to 1/3,000). PPGL occurrence is rare in NF1 and is in general restricted to unique pheochromocytoma. Mutation analysis of the large *NF1* gene is not indicated in the majority of cases as clinical diagnosis is mostly obvious. Interestingly, *NF1* is the most somatically mutated gene in sporadic pheochromocytomas with a somatic mutation rate estimated between 20 and 40% [30, 31].

Activating mutations in the *RET* proto-oncogene cause multiple endocrine neoplasia type 2 (MEN2). MEN2A, which accounts for 95% of MEN2 cases, can associate medullary thyroid carcinoma (MTC), PPGL and parathyroid adenomas while MEN2B is characterized by MTC, PPGL and clinical abnormalities such as ganglioneuromas of the lips, tongue and colon but without hyperparathyroidism. Causative mutations are hot-spot missense mutations classified into three risk of developing MTC categories according to the recently revised American Thyroid Association guidelines [32**]: highest risk (MEN2B and the *RET* p.Met918Thr mutation), high risk (MEN2A and the *RET* codon Arg634 mutations) and moderate risk (other mutations). Pheochromocytomas associated with *RET* mutations are frequently bilateral while paragangliomas are reported to be rare [33]. Somatic *RET* gain-of-function mutations have been reported in about 5% of sporadic PPGL [16].

Mutations in *TMEM127* and *MAX* genes are found in about 1-2% of cases [11, 12, 34**], primarily in PPGL with family history but also in apparently sporadic forms of the disease. Somatic mutations have been described in *MAX* [35] but not in *TMEM127*.

PPGL presenting mutations in *RET*, *NF1*, *TMEM127* and *MAX* but also sporadic tumours classifying in cluster 2A share the overexpression of the RAS/MAPK and PI3K-AKT-mTOR signalling pathways. The use of mTOR inhibitors or other drugs targeting the RAS-RAF pathway might be of interest in cluster 2 malignant PPGL but needs to be evaluated in adapted clinical trials.

CONTRIBUTION OF HIGH THROUGHPUT SEQUENCING

Multiple technological advances in molecular genetics have allowed the development of high throughput sequencing, referred to as "next generation sequencing" (NGS). Among them, whole exome sequencing (WES) revealed *MAX*, *FH* and *MDH2* as new susceptibility genes [12, 13**, 17] (Figure 1).

With the aim of identifying novel disease causing genes or new driver mutations, several WES studies have been performed on PPGL tumour tissue during the last years.

In 2013, WES conducted on 4 cases of benign apparently sporadic tumours revealed 2 tumours with hotspot mutations in *H-RAS* [36]. Targeted *H-RAS* direct sequencing in larger cohorts showed a somatic mutation rate of 5-15% in sporadic PPGL [4, 36, 37*, 38*].

Fishbein and colleagues [39**] recently published WES of 21 matched tumour/ germline DNA pairs. They confirmed the high prevalence of somatic *NF1* mutations in sporadic PPGL (3 of 7) and reported somatic *ATRX* mutations. *ATRX* encodes a SWI/SNF chromatin remodelling protein playing a role in telomere maintenance and chromosome integrity. In a validation cohort, 12.6% of tumours exhibited a somatic *ATRX* mutation, comprising several tumours with germline *SDHx* mutations. Again, this finding suggests association between epigenetic regulation and clinically aggressive features in PPGL.

WES of a set of 30 tumour-normal DNAs pairs and one trio (including the primary tumour and a metastasis) allowed identifying somatic mutations in various cancer genes including *TP53* (10%), *CDKN2A* (7%), *MET* (2.5%), *CDH1*, *MLL2*, *ATRX*, *GNAS* and *FHIT* [4**]. Recurrent mutations were also found in *CLPTML, SYNE1, CAPN2* and *RFPL4A* genes, which have not been related to

cancer yet. Additional studies are required to determine the role of these genes in PPGL tumourigenesis and the prevalence of their mutations.

Somatic mutations in *ATRX* and *TP53* genes have been confirmed in an independent WES analysis of 40 PPGL [40**]. Additional known cancer genes have been involved such as *STAG2*, *PALB2* and *STAT3* genes but still with low frequencies.

Finally, the most recent publication reporting PPGL exome sequencing identified recurrent *MLL2* (=*KMT2D*) variants in 14 of 99 explored tumours with 6 of them co-occurring with somatic or germline mutations in *NF1*, *RET* or *TMEM127* [41**]. As occurrence of *KMT2D* mutation has not been confirmed in a cohort of 13 abdominal PGL, future studies are needed to elucidate whether identified *KMT2D* missense variants are activating, deleterious or without pathogenic significance and to determine the implication of *KMT2D* in PPGL tumourigenesis [42].

All these WES studies indicate that PPGL harbour limited somatic single nucleotide variants (SNV), counting for less than 40 mutations in coding regions per tumour. They concordantly show very low mutation frequencies in multiple genes suggesting that no major underlying driver is responsible for PPGL tumourigenesis or malignant transformation in addition to mutations occurring in known PPGL susceptibility genes. However, further studies exploring non coding regions such as whole genome sequencing, could detect recurrent promoter, intronic or intergenic variants of interest. To date, only *TERT* promoter C228T mutations have been reported in metastatic *SDHx*-deficient tumours, including extra-adrenal PGLs but also adrenocortical carcinomas and gastrointestinal stromal tumours (GIST) [43*, 44].

Next generation sequencing in clinical practice

Recent published guidelines on PPGL recommend that genetic testing should be considered in all patients with PPGL, given that about 40% of all patients with PPGL have disease-causing germline mutations [34**]. A sequential strategy using a clinical feature-driven diagnostic algorithm is generally applied to prioritize the analysis, as conventional Sanger sequencing remains expensive and time consuming.

The use of NGS now allows a simultaneous screening of all PPGL genes of interest. Recent publications demonstrated that targeted NGS using gene panels but also whole exome sequencing are sensitive, time efficient and cost-effective methods, which can be used as a reliable alternative to Sanger sequencing [45-49**]. Such a strategy is now relevant in laboratory routine and should rapidly lead to a more widespread PPGL diagnostic genetic testing in all at-risk individuals.

Regarding diagnosis, using an NGS-based assay including the less commonly involved genes should improve the knowledge of mutation prevalence for all genes and associated phenotypes. As NGS test is feasible on germline DNA but also on DNA extracted from frozen or from formalin-fixed paraffin embedded (FFPE) tissues, this method will be relevant from a clinical perspective. Indeed, it will certainly be helpful to identify appropriate targeted therapy as indications are usually based on somatic DNA sequencing results. Finally, when biomarkers for response and resistance to therapy will be identified, NGS analysis would be decisive for follow-up and treatment adjustment if required. Moreover, although it is still technically challenging, detection and characterization of circulating

tumour cells and cell free circulating tumour DNA might play a role in malignant PPGL management in the next future. These precise technologies could help defining and estimating the degree of inter- and intra-tumour heterogeneity in PPGL of the same patient as recently demonstrated [4**, 40**, 50**]. At the beginning of the development of precision medicine in patients with aggressive disease, the implication of genetic PPGL heterogeneity needs to be clarified, as it would have a direct impact on the interpretation of detected biomarkers for diagnosis, prognosis and response to therapy.

CONCLUSION

During the past 15 years, mutations associated with PPGL have been described in more than 15 genes, at germline and/or somatic levels with very different mutational frequencies according to the nature of the gene. Despite this complex mutational landscape, different "omics" analyses have shown that mutations in major susceptibility genes are driver events in PPGL tumourigenesis revealing at least three groups of tumours exhibiting distinct molecular profiles. The genetic and genomic hallmarks characterizing each tumour could ultimately be used as diagnosis and prognosis biomarkers and should allow personalized treatment. In that perspective, next generation sequencing testing in germline and tumour DNA should be used in PPGL patient management as a major tool.

KEY POINTS

- PPGLs are characterized by a high rate of heritability and a strong genetic heterogeneity.
- Using genomic hallmarks, PPGLs can be classified in tumour subtypes associated with distinctive and targetable tumourigenic signatures.
- Genomics-driven therapy is a pertinent perspective for patients with malignant PPGL, comprising antiangiogenic drugs for cluster 1-tumours and mTOR or RAS-RAF pathway inhibitors for tumours belonging to cluster 2.
- Next generation sequencing recently contributed to the identification of new susceptibility genes and, in a near future, should be commonly used to detect driver mutations at germline and somatic levels and to determine biomarkers useful for patient care.

ACKNOWLEDGEMENTS

1. Acknowledgements: We thank Dr Judith Favier for English-language assistance. We apologize to colleagues in the field whose contribution was not cited due to space limitations or oversight.

2. Financial support and sponsorship: Our research team is currently supported by Assistance Publique-Hôpitaux de Paris and by the Institut National du Cancer (INCA-DGOS-8663) in the context of the Programme Hospitalier de Recherche Clinique 2014, grant COMETE-TACTIC; by the European Union Seventh Framework Program (FP7/2007-2013, agreement #259735); and by the

European Union's Horizon 2020 research and innovation program (agreement #633983).

3. Conflicts of interest: None

REFERENCE SECTION

Papers of particular interest, published within the annual period of review, (18 months/ 2014-2015) have been highlighted as:

* of special interest

** of outstanding interest

1. Baysal BE, Ferrell RE, Willett-Brozick JE *et al*. Mutations in SDHD, a mitochondrial complex II gene, in hereditary paraganglioma. Science 2000; 287:848-851.
2. Dahia PL. Pheochromocytoma and paraganglioma pathogenesis: learning from genetic heterogeneity. Nat Rev Cancer 2014; 14:108-119.
3. Crona J, Nordling M, Maharjan R *et al*. Integrative genetic characterization and phenotype correlations in pheochromocytoma and paraganglioma tumours. PLoS One 2014; 9:e86756.
**4. Castro-Vega LJ, Letouze E, Burnichon N *et al*. Multi-omics analysis defines core genomic alterations in pheochromocytomas and paragangliomas. Nat Commun 2015; 6:6044.
Integrative genomic examination of a large collection of PPGLs including WES for 31 tumors.
5. Jimenez C, Rohren E, Habra MA *et al*. Current and future treatments for malignant pheochromocytoma and sympathetic paraganglioma. Curr Oncol Rep 2013; 15:356-371.
*6. Baudin E, Habra MA, Deschamps F *et al*. Therapy of endocrine disease: treatment of malignant pheochromocytoma and paraganglioma. Eur J Endocrinol 2014; 171:R111-122.
Review about management and therapeutical options for patients with metastatic PPGL.
7. Astuti D, Latif F, Dallol A *et al*. Gene mutations in the succinate dehydrogenase subunit SDHB cause susceptibility to familial pheochromocytoma and to familial paraganglioma. Am J Hum Genet 2001; 69:49-54.
8. Burnichon N, Briere JJ, Libe R *et al*. SDHA is a tumor suppressor gene causing paraganglioma. Hum Mol Genet 2010; 19:3011-3020.
9. Hao HX, Khalimonchuk O, Schraders M *et al*. SDH5, a gene required for flavination of succinate dehydrogenase, is mutated in paraganglioma. Science 2009; 325:1139-1142.
10. Niemann S, Muller U. Mutations in SDHC cause autosomal dominant paraganglioma, type 3. Nat Genet 2000; 26:268-270.
11. Qin Y, Yao L, King EE *et al*. Germline mutations in TMEM127 confer susceptibility to pheochromocytoma. Nat Genet 2010; 42:229-233.

12. Comino-Mendez I, Gracia-Aznarez FJ, Schiavi F *et al*. Exome sequencing identifies MAX mutations as a cause of hereditary pheochromocytoma. Nat Genet 2011; 43:663-667.
**13. Cascon A, Comino-Mendez I, Curras-Freixes M *et al*. Whole-exome sequencing identifies MDH2 as a new familial paraganglioma gene. J Natl Cancer Inst 2015; 107:
Identification of germline MDH2 mutation in PPGL.
14. Dahia PL, Ross KN, Wright ME *et al*. A HIF1alpha regulatory loop links hypoxia and mitochondrial signals in pheochromocytomas. PLoS Genet 2005; 1:72-80.
15. Lopez-Jimenez E, Gomez-Lopez G, Leandro-Garcia LJ *et al*. Research resource: Transcriptional profiling reveals different pseudohypoxic signatures in SDHB and VHL-related pheochromocytomas. Mol Endocrinol 2010; 24:2382-2391.
16. Burnichon N, Vescovo L, Amar L *et al*. Integrative genomic analysis reveals somatic mutations in pheochromocytoma and paraganglioma. Hum Mol Genet 2011; 20:3974-3985.
17. Letouze E, Martinelli C, Loriot C *et al*. SDH mutations establish a hypermethylator phenotype in paraganglioma. Cancer Cell 2013; 23:739-752.
18. de Cubas AA, Leandro-Garcia LJ, Schiavi F *et al*. Integrative analysis of miRNA and mRNA expression profiles in pheochromocytoma and paraganglioma identifies genotype-specific markers and potentially regulated pathways. Endocr Relat Cancer 2013; 20:477-493.
**19. de Cubas AA, Korpershoek E, Inglada-Perez L *et al*. DNA Methylation Profiling in Pheochromocytoma and Paraganglioma Reveals Diagnostic and Prognostic Markers. Clin Cancer Res 2015; 21:3020-3030.
DNA methylation study in metastatic PPGLs identifying prognostic markers
20. Amar L, Baudin E, Burnichon N *et al*. Succinate dehydrogenase B gene mutations predict survival in patients with malignant pheochromocytomas or paragangliomas. J Clin Endocrinol Metab 2007; 92:3822-3828.
21. Gimenez-Roqueplo AP, Favier J, Rustin P *et al*. Mutations in the SDHB gene are associated with extra-adrenal and/or malignant phaeochromocytomas. Cancer Res 2003; 63:5615-5621.
22. Pasini B, Stratakis CA. SDH mutations in tumorigenesis and inherited endocrine tumours: lesson from the phaeochromocytoma-paraganglioma syndromes. J Intern Med 2009; 266:19-42.
23. Zhuang Z, Yang C, Lorenzo F *et al*. Somatic HIF2A gain-of-function mutations in paraganglioma with polycythemia. N Engl J Med 2012; 367:922-930.
24. Castro-Vega LJ, Buffet A, De Cubas AA *et al*. Germline mutations in FH confer predisposition to malignant pheochromocytomas and paragangliomas. Hum Mol Genet 2014; 23:2440-2446.
*25. Clark GR, Sciacovelli M, Gaude E *et al*. Germline FH mutations presenting with pheochromocytoma. J Clin Endocrinol Metab 2014; 99:E2046-2050.
Identification of rare FH germline mutations in PPGLs.
26. Comino-Mendez I, de Cubas AA, Bernal C *et al*. Tumoral EPAS1 (HIF2A) mutations explain sporadic pheochromocytoma and paraganglioma in the absence of erythrocytosis. Hum Mol Genet 2013; 22:2169-2176.

*27. Welander J, Andreasson A, Brauckhoff M *et al*. Frequent EPAS1/HIF2alpha exons 9 and 12 mutations in non-familial pheochromocytoma. Endocr Relat Cancer 2014; 21:495-504.
Identification of EPAS1 mutations in PPGLs.
28. Buffet A, Smati S, Mansuy L *et al*. Mosaicism in HIF2A-related polycythemia-paraganglioma syndrome. J Clin Endocrinol Metab 2014; 99:E369-373.
**29. Hadoux J, Favier J, Scoazec JY *et al*. SDHB mutations are associated with response to temozolomide in patients with metastatic pheochromocytoma or paraganglioma. Int J Cancer 2014; 135:2711-2720.
Demonstration that temozolomide is an effective treatment in SDHB-related malignant PPGLs.
30. Burnichon N, Buffet A, Parfait B *et al*. Somatic NF1 inactivation is a frequent event in sporadic pheochromocytoma. Hum Mol Genet 2012; 21:5397-5405.
31. Welander J, Larsson C, Backdahl M *et al*. Integrative genomics reveals frequent somatic NF1 mutations in sporadic pheochromocytomas. Hum Mol Genet 2012; 21:5406-5416.
**32. Wells SA, Jr., Asa SL, Dralle H *et al*. Revised American Thyroid Association guidelines for the management of medullary thyroid carcinoma. Thyroid 2015; 25:567-610.
Updated guidelines for the management of MTC.
33. Amar L, Bertherat J, Baudin E *et al*. Genetic testing in pheochromocytoma or functional paraganglioma. J Clin Oncol 2005; 23:8812-8818.
**34. Lenders JW, Duh QY, Eisenhofer G *et al*. Pheochromocytoma and paraganglioma: an endocrine society clinical practice guideline. J Clin Endocrinol Metab 2014; 99:1915-1942.
Clinical practices guidelines for PPGL.
35. Burnichon N, Cascon A, Schiavi F *et al*. MAX mutations cause hereditary and sporadic pheochromocytoma and paraganglioma. Clin Cancer Res 2012; 18:2828-2837.
36. Crona J, Delgado Verdugo A, Maharjan R *et al*. Somatic mutations in H-RAS in sporadic pheochromocytoma and paraganglioma identified by exome sequencing. J Clin Endocrinol Metab 2013; 98:E1266-1271.
*37. Luchetti A, Walsh D, Rodger F *et al*. Profiling of somatic mutations in phaeochromocytoma and paraganglioma by targeted next generation sequencing analysis. Int J Endocrinol 2015; 2015:138573.
NGS analysis of 85 PPGL tumour samples for "mutation hotspots" in 50 human cancer genes.
*38. Curras-Freixes M, Inglada-Perez L, Mancikova V *et al*. Recommendations for somatic and germline genetic testing of single pheochromocytoma and paraganglioma based on findings from a series of 329 patients. J Med Genet 2015;
Sanger sequencing-based genetic testing strategy in PPGLs.
**39. Fishbein L, Khare S, Wubbenhorst B *et al*. Whole-exome sequencing identifies somatic ATRX mutations in pheochromocytomas and paragangliomas. Nat Commun 2015; 6:6140.
Identification of ATRX somatic mutations in PPGL.

**40. Flynn A, Benn D, Clifton-Bligh R *et al*. The genomic landscape of phaeochromocytoma. J Pathol 2015; 236:78-89.
Study of 40 PPGL tumour tissues using RNA-Seq , WES and SNP array.
**41. Juhlin CC, Stenman A, Haglund F *et al*. Whole-exome sequencing defines the mutational landscape of pheochromocytoma and identifies KMT2D as a recurrently mutated gene. Genes Chromosomes Cancer 2015; 54:542-554.
Identification of KMT2D mutations in sporadic PPGLs using a WES strategy.
42. Stenman A, Juhlin CC, Haglund F *et al*. Absence of KMT2D/MLL2 mutations in abdominal paraganglioma. Clin Endocrinol (Oxf) 2015;
*43. Papathomas TG, Oudijk L, Zwarthoff EC *et al*. Telomerase reverse transcriptase promoter mutations in tumors originating from the adrenal gland and extra-adrenal paraganglia. Endocr Relat Cancer 2014; 21:653-661.
Prevalence of TERT promoter mutations in adrenal tumours and PGL.
44. Liu T, Brown TC, Juhlin CC *et al*. The activating TERT promoter mutation C228T is recurrent in subsets of adrenal tumors. Endocr Relat Cancer 2014; 21:427-434.
45. Casey R, Garrahy A, Tuthill A *et al*. Universal genetic screening uncovers a novel presentation of an SDHAF2 mutation. J Clin Endocrinol Metab 2014; 99:E1392-1396.
46. Crona J, Verdugo AD, Granberg D *et al*. Next-generation sequencing in the clinical genetic screening of patients with pheochromocytoma and paraganglioma. Endocr Connect 2013; 2:104-111.
47. Rattenberry E, Vialard L, Yeung A *et al*. A comprehensive next generation sequencing-based genetic testing strategy to improve diagnosis of inherited pheochromocytoma and paraganglioma. J Clin Endocrinol Metab 2013; 98:E1248-1256.
**48. Welander J, Andreasson A, Juhlin CC *et al*. Rare germline mutations identified by targeted next-generation sequencing of susceptibility genes in pheochromocytoma and paraganglioma. J Clin Endocrinol Metab 2014; 99:E1352-1360.
Targeted NGS analysing 14 PPGL predisposing genes in 86 tumor samples.
**49. Toledo RA, Dahia PL. Next-generation sequencing for the diagnosis of hereditary pheochromocytoma and paraganglioma syndromes. Curr Opin Endocrinol Diabetes Obes 2015; 22:169-179.
Review about NGS approaches for inherited PPGL diagnosis.
**50. Crona J, Backman S, Maharjan R *et al*. Spatio-temporal heterogeneity characterizes the genetic landscape of pheochromocytoma and defines early events in tumourigenesis. Clin Cancer Res 2015;
Investigation of 136 PPGL tumour samples demonstrating a genetic heterogeneity between patients, between tumours of one patient and within tumour lesions.

FIGURE TITLE AND LEGEND

Figure 1: Identification of the major genes involved in PPGL tumourigenesis

ARTICLE 6

The MITF, p.E318K Variant, as a Risk Factor for Pheochromocytoma and Paraganglioma.

Castro-Vega LJ, Kiando SR, Burnichon N, Buffet A, Amar L, Simian C, Berdelou A, Galan P, Schlumberger M, Bouatia-Naji N, Favier J, Bressac-de Paillerets B, Gimenez-Roqueplo AP.

J Clin Endocrinol Metab. 2016 Dec;101(12):4764-4768.

The *MITF*, p.E318K Variant, as a Risk Factor for Pheochromocytoma and Paraganglioma

Luis Jaime Castro-Vega, Soto Romuald Kiando, Nelly Burnichon, Alexandre Buffet, Laurence Amar, Christophe Simian, Amandine Berdelou, Pilar Galan, Martin Schlumberger, Nabila Bouatia-Naji, Judith Favier,* Brigitte Bressac-de Paillerets,* and Anne-Paule Gimenez-Roqueplo*

INSERM (L.J.C.-V., S.R.K., N.K., A.B., L.A., N.B.-N., J.F., A.-P.G.-R.), UMR970, Paris-Cardiovascular Research Center, F-75015, Paris, France; Université Paris Descartes (L.J.C.-V., S.R.K., N.B., A.B., L.A., N.B.-N., J.F., A.-P.G.-R.), PRES Sorbonne Paris Cité, Faculté de Médecine, F-75006 Paris, France; Service de Génétique, Hôpital Européen Georges Pompidou, Assistance Publique-Hôpitaux de Paris (N.B., C.S., A.-P.G.-R.), F-75015, Paris, France; Unité Hypertension artérielle (L.A.), Hôpital Européen Georges Pompidou, Assistance Publique-Hôpitaux de Paris, F-75015, Paris, France; Département de Cancérologie endocrinienne and Université Paris-Saclay (A.B., M.S.), Gustave Roussy, Villejuif, F-94805, France; Université Paris 13 (P.G.), Equipe de Recherche en Epidémiologie Nutritionnelle (EREN), Centre d'Epidémiologie et Statistiques Sorbonne Paris Cité, INSERM (U1153), Inra (U1125), Cnam, COMUE Sorbonne Paris Cité, Bobigny; INSERM (B.B.-d.P.), U1186, Université Paris-Sud, Université Paris-Saclay, Villejuif, F-94805, France; Département de Biopathologie (B.B.-d.P.), Gustave Roussy, Villejuif, F-94805, France; and Rare Adrenal Cancer Network COMETE (L.A., A.-P.G.-R.), F-75006, Paris, France

Context: The microphthalmia-associated transcription factor (MITF) regulates the survival, proliferation, and differentiation of neural crest-derived lineages. Recent studies reported an increased risk of melanoma in individuals carrying the rare variant *MITF*, p.E318K (rs149617956). Whether this variant plays a role in other neural crest-derived tumors is unknown.

Objective: In the present study, we aimed at determining the prevalence of the *MITF*, p.E318K variant, in a well-characterized French cohort of pheochromocytomas/paragangliomas (PCC/PGL).

Design and Methods: Genomic DNA from 555 unrelated patients with PCC/PGL was genotyped for the p.E318K variant in *MITF* using Sanger sequencing.

Main Outcome Measure: The prevalence of the mutation in the PCC/PGL cohort was compared with a population-based sample of 2348 ethnically matched controls.

Results: We identified seven carriers (five patients with sporadic PCCs, two with PGLs). The prevalence of the *MITF*, p.E318K variant, was higher in the PCC/PGL cohort than in controls, and appears to be a significant risk factor (odds ratio, 3.19; 95% confidence interval, 1.34–7.59; $P = .005$). Noteworthy, two patients were homozygous for the p.E318K risk allele, a patient with metastatic PCC and an *SDHB*-mutated patient with PGL.

Conclusion: Our results indicate that the germline variant *MITF*, p.E318K is associated with an increased risk of other neural crest-derived tumors such as PCC/PGL. **(*J Clin Endocrinol Metab* 101: 4764–4768, 2016)**

ISSN Print 0021-972X ISSN Online 1945-7197
Printed in USA

Received May 13, 2016. Accepted September 21, 2016.
First Published Online September 28, 2016

* J.F., B.B.-d.P., and A.-P.G.R. contributed equally to the study.

Abbreviations: CI, confidence interval; MITF, microphthalmia-associated transcription factor; OR, odds ratio; PCC, pheochromocytoma; PGL, paraganglioma; SUMO, small-ubiquitin-like modifier.

The microphthalmia-associated transcription factor (MITF), a basic helix-loop-helix, leucine-zipper transcription factor, is a master regulator of neural crest development (1). MITF plays a role in the survival, proliferation, and differentiation of neural crest-derivative cells such as melanocytes (2). Genetic alterations including somatic copy number gains and mutations in *MITF* were initially reported in metastatic melanomas, thus indicating a potential oncogenic effect (3, 4). More recently, two studies reported that a rare germline variant in the *MITF* gene (c.952G>A, p.Glu318Lys, rs149617956, usually abbreviated as p.E318K) (National Center for Biotechnology Information accession NM_000248.3; NP_000239.1) is associated with increased risk of melanoma (5, 6) and renal cell carcinoma (5). This association was later replicated in different populations and extended to pancreatic carcinomas (7). The *MITF*, p.E318K variant, cosegregated with melanomas in some but not all familial cases, demonstrating incomplete penetrance and a role as a moderate susceptibility risk gene. Functional analyses demonstrated that the variant changes the binding affinity of small-ubiquitin-like modifier (SUMO) proteins for the canonical site ($\psi K^{316}XE^{318}$), and ultimately modifies the MITF transcriptional activity on downstream targets (5, 6). Whether this variant plays a role in other neural crest-derived tumors remains unknown.

Pheochromocytomas and paragangliomas (PCC/PGL) are rare neural crest-derived tumors with an approximate incidence of 1:300,000/year. The only environmental risk factor described so far is chronic hypoxia in populations living at high altitude. These tumors are characterized by a strong genetic determinism. To date, germline mutations in 13 susceptibility genes comprising *SDHA*, *SDHB*, *SDHC*, *SDHD*, *SDHAF2*, *FH*, *MDH2*, *EPAS1*, *VHL*, *NF1*, *RET*, *TMEM127*, and *MAX* have been shown to account for up to 40% of cases, whereas the genetic basis of most PCC/PGL remains unknown (8). Although rare genetic variants with a moderately penetrant risk could substantially contribute to unexplained PCC/PGL heritability, the possible effect of such variants has not yet been assessed. PCC/PGL display genetic alterations common to other neural crest-derived tumors including melanomas (9), suggesting that converging tumorigenic pathways could be common to these related tumor types. We hypothesized that *MITF*, p.E318K, a low-frequency variant and well-established melanoma risk factor, might also play a role in PCC/PGL tumorigenesis, and we investigated its prevalence in a large cohort of PCC/PGL cases and in controls.

Materials and Methods

Patients and controls

Blood samples from 555 patients with PCC and/or PGL, collected prospectively (1993–2012) in the Department of Genetics, Georges Pompidou European Hospital, Paris, France, were included in this study (Table 1). Written informed consent as well as clinical data and confirmed diagnosis of PCC/PGL by conventional tests (clinical, biological, imaging, or histopathology) were obtained for each patient. This study was formally approved by the institutional review board [Comité de Protection des Personnes (CPP) Ile de France III, June 2012].

Controls were 2348 individuals ascertained from the SU.VI.MAX study, a national sample of healthy volunteers living in France and enrolled between 1996 and 2001 in a randomized, placebo-controlled trial testing the benefit of antioxidants nutrients on the incidence of cancers and cardiovascular diseases (10). Of these, 689 samples were genotyped using the Illumina HumanExome-12v1_A Beadchip platform, whereas genotypes of 1659 DNAs were assayed on single-nucleotide polymorphism arrays (Illumina) as previously described (5).

MITF, p.E318K variant, genotyping

Genomic DNA was extracted from leukocytes according to standard protocols. PCR was performed for the exon 9 of *MITF* isoform M, (NM_000248.3) using the JumpStart Taq ReadyMix (Sigma). The sequences of forward and reverse primers (5′–3′) were CAGTGACATTTCATTATCCT and TATATCCTG GGCTATTGATA, respectively. Sequencing reactions in both directions were performed using BigDye terminator v3.1 (Life Technologies) in an Applied Biosystems 3730xl machine. DNA sequencing chromatograms were obtained and analyzed with the Sequencher 4.10.1 software. Deletions affecting the MITF locus (3p13) in the two MITF carriers presenting the homozygous status were ruled out by using the multiplex ligation-dependent probe amplification assay SALSA multiplex ligation-dependent probe amplification probe mix P186-C1 (MRC-Holland).

Statistical analyses

The *MITF*, p.E318K allele frequencies in cases and controls were compared using a standard χ^2 test. The odds ratios (ORs) and 95% confidence intervals (CIs) associated with *MITF*, p.E318K carrier status were calculated using a logistic regression test under the additive and dominant genetic models. Differences between patients carrying or not the *MITF*, p.E318K variant,

Table 1. Clinical Characteristics of Patients From the PCC/PGL Cohort

Total Patients	**n = 555**
Mean age at diagnosis	44.6
PCC	400
PGL	136
PCC and PGL	19
Genetically determined	299
Sporadic	256
Single	457
Multiple	98
Metastatic	58
Nonmetastatic	497
Total controls	**n = 2348**

Table 2. Association Between rs1496117956 and PCC/PGL

	Genotypes					Allelic[a]		Additive[b]		Dominant[b]	
	N	GG	AG	AA	EAF (A)	OR (95% CI)	*P* Value	OR (95% CI)	*P* Value	OR (95% CI)	*P* Value
Cases	555	548	5	2	0.008	3.19 (1.34–7.59)	.005	2.65 (1.18–5.96)	.018	2.49 (0.97–6.34)	.057
Controls	2348	2336	12	0	0.003						

Abbreviation: EAF, effect allele frequency.

[a] χ-squared test (two-sided) for the differences in rs1496117956 allele frequency between cases and controls.

[b] Logistic regression tests under the additive and dominant genetic models.

regarding age at diagnosis, frequency of multiple tumors and malignancy were analyzed using Student *t* test or Fisher's exact tests. To evaluate MITF expression levels in PCC/PGL tumors, we used our previously generated transcriptome data (ArrayExpress entry E-MTAB-733). Differences in expression between tumor subtypes and between malignant vs nonmalignant tumors were assessed using ANOVA Bonferroni and Student *t* test, respectively. All statistic tests were two-tailed with significance threshold set to $P < .05$. The computations of single-nucleotide polymorphism association tests were carried out using the PLINK software (v1.07) (11).

Results

We identified seven germline carriers of the *MITF*, p.E318K variant, present in five patients with PCCs and two with PGLs. The variant was enriched in the PCC/PGL cohort (n = 555; allele frequency, 0.008) compared with the population-based sample of controls (n = 2348; allele frequency, 0.003) (Table 2). The rs149617956 [A] allele was significantly more prevalent in PCC/PGL patients compared to controls (OR, 3.19; 95% CI, 1.34–7.59; $P = 5.58 \times 10^{-3}$) (Table 2). Of note, we report for the first time two homozygous carriers for the risk [A] allele that were present in a patient suffering from sporadic PCC with evidence of metastatic disease, and in an *SDHB*-germline mutation (p.Arg46Gly) carrier (Figure 1; Table 3). We verified that this homozygosity was not an artifactual effect of *MITF* deletions using a multiplex ligation-dependent probe amplification assay (data not shown). In marked contrast, despite the relatively large sample, none of the controls analyzed was found to carry the rs149617956 variant at the homozygous state. The risk association was also significant under the additive model of penetrance ($P = .018$), with an OR of 2.65 (95% CI, 1.18–5.96), and on the boundary of significance when the dominant model was tested ($P = .057$), with an OR of 2.49 (95% CI, 0.97–6.34) (Table 2). Regarding the mutation status in the carriers of the *MITF*, p.E318K variant, five corresponded to sporadic PCCs without mutations in a predisposing gene, whereas the other two cases presented either *NF1* or *SDHB* germline mutations (Table 3). Finally, no significant differences between *MITF*, p.E318K carriers and noncarriers, were found regarding clinical characteristics such as frequency of multiple tumors, age at diagnosis, or malignant status ($P > .05$).

Discussion

In the current genetic association case-control study, we demonstrated that the *MITF*, p.E318K germline variant, is associated with a more than 3-fold increased risk of PCC/PGL development in a French population. The strength of this result relies on the reliable comparison of a large and well-characterized cohort of PCC/PGL patients with a 4-fold greater number of controls.

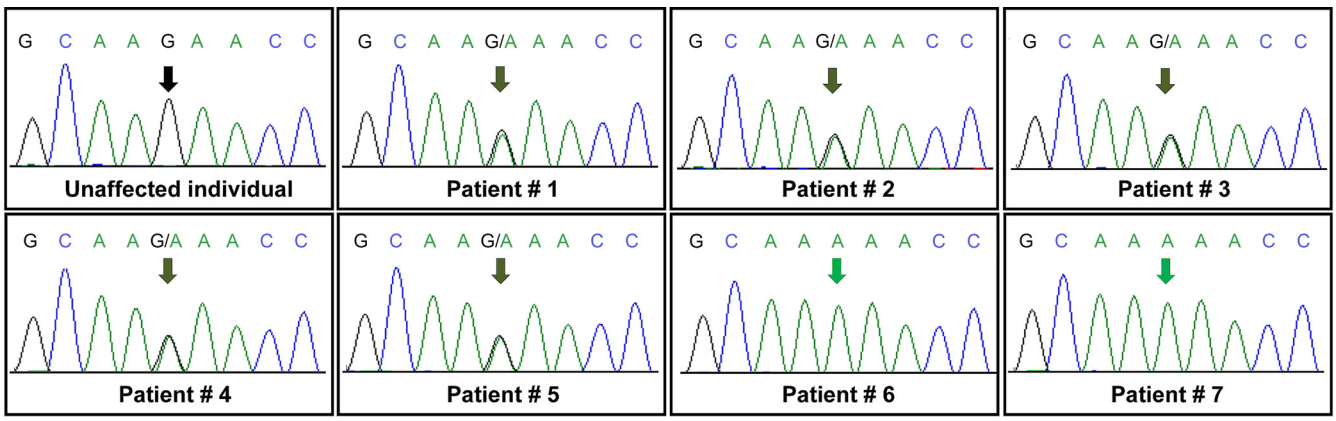

Figure 1. Chromatograms corresponding to one *MITF* wild-type sample from an unaffected individual, and the *MITF*, p.E318K variant, found in PCC/PGL patients in either heterozygous or homozygous states.

Table 3. Clinical Characteristics of the Seven *MITF,* p.E318K Variant, Carriers Identified in the PCC/PGL Cohort

Patient	Sex	Age	Tumor Type	Single	Sporadic	Metastases	Genotype p.E318K
1	M	41	PCC	Yes	Yes	No	AG
2	M	54	PCC	Yes	Yes	No	AG
3	F	71	PCC	Yes	Yes	No	AG
4	F	54	PCC	Yes	NF1	No	AG
5	M	39	PGL (TA)	Yes	Yes	No	AG
6	M	58	PGL (H&N)	Yes	SDHB	No	AA
7	M	62	PCC	Yes	Yes	Yes	AA

Abbreviations: F, female; H&N, head and neck; M, male; TA, thoracic/abdominal.

Previous studies estimated that carriers of the *MITF*, p.E318K variant, have an increased risk of melanoma (OR, 2.09–4.78) in different cohorts from Australia, the United Kingdom, France, Italy, and Denmark (7). The familial studies demonstrated a dominant model of inheritance and incomplete penetrance, compatible with a medium-risk variant (6).

Our results extend the association of this variant effect to the development of another neural crest-derived tumor type. Further studies are needed in other populations to confirm this finding and to quantify relative and lifetime risk of *MITF*, p.E318K carriers.

In contrast to melanoma, where the MITF variant has been associated with multiple tumors and malignancy, we did not observe differences between MITF carriers and noncarriers in the PCC/PGL cohort regarding frequency of multiple tumors, age at diagnosis, or malignant status. Given the limited statistical power of our current sample of patients, and the low prevalence of the p.E318K variant, more cases are needed to confidently conclude about these genotype/phenotype correlations in PCC/PGL.

Although infrequent, the association of PCC with malignant melanoma has been previously described (12) and a rigorous screening of phenotypic risk manifestations of melanoma should therefore not be overlooked. Conversely, screening of PCC/PGL carriers should be performed in *MITF*, p.E318K carriers, with melanoma.

Interestingly, we found two homozygous carriers of the *MITF*, p.E318K variant, one of which with evidence of metastatic disease. This result suggests a more pronounced effect

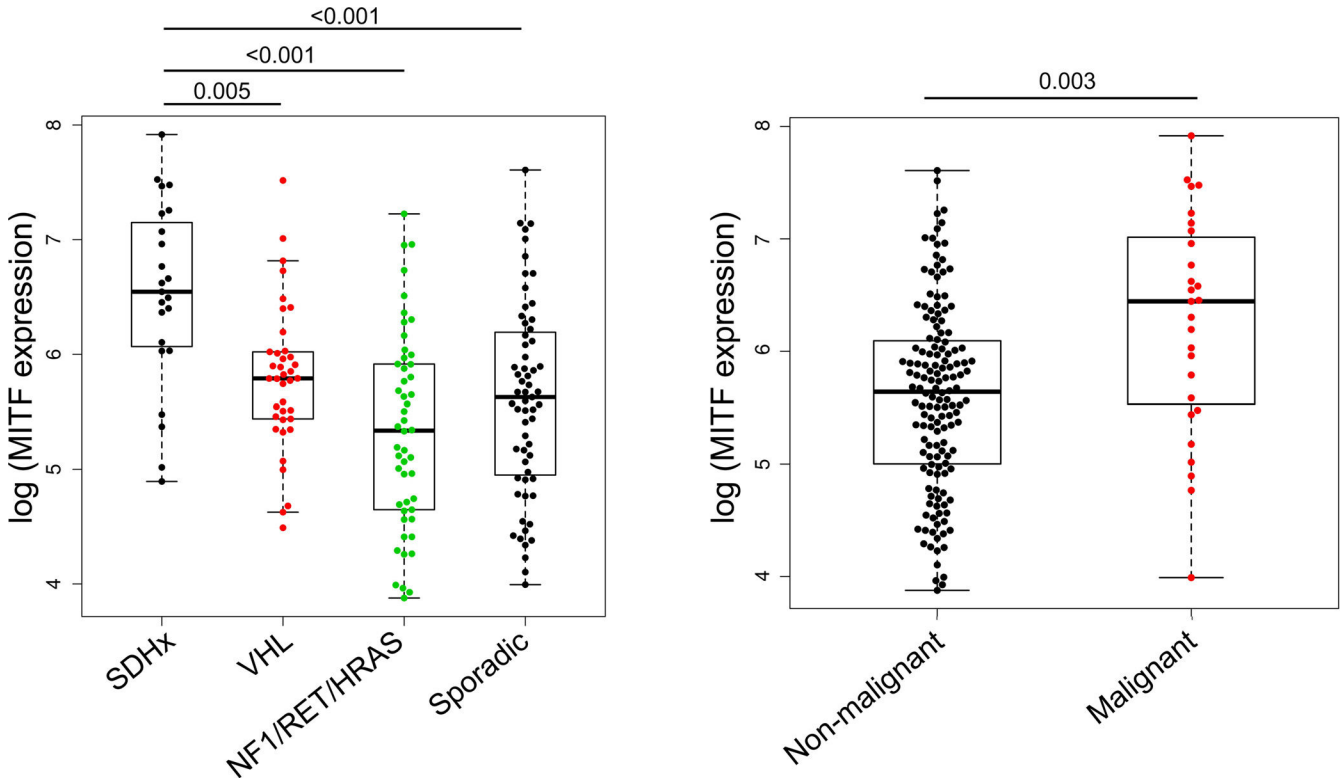

Figure 2. Analysis of transcriptome data, ArrayExpress entry E-MTAB-733. The box plots show the expression data of MITF among the different PCC/PGL tumor subtypes (left) and between nonmalignant and malignant tumors (right). ANOVA Bonferroni and two-tailed Student *t* tests were performed, respectively, for the comparisons. HRAS, Harvey rat sarcoma viral oncogene homolog; RET, rearranged during transfection protooncogene; SDHx, succinate dehydrogenase complex subunit gene; VHL, Von Hippel-Lindau tumor suppressor.

of the risk allele when homozygote, which is supported by the fact that the association fits with the additive genetic model. Regarding the second homozygous carrier, there is no evidence of metastasis at present. This patient also carries a germline mutation in *SDHB*, which is known to confer risk of progression and therefore it will be difficult to ascertain the effect of the *MITF*, p.E318K variant, in such a genetic background. Whether the *MITF* mutation could act as a genetic modifier of *SDHB* needs further investigation.

Mechanistically, it has demonstrated a gain-of-function effect for the *MITF*, p.E318K variant, that, in agreement with the somatic amplifications and mutations of this locus found in both primary and metastatic melanomas, supports an oncogenic role for MITF (5, 6). In PCC/PGL, although 3p deletions are frequent in *VHL*-mutated tumors (9), the highest expression of MITF is present in *SDHx*-mutated tumors as well as in malignant tumors (Figure 2).

A role for MITF in cell survival appears to predominate (13), which in turn can be crucial for facing the constraints imposed by a hostile microenvironment. It has been shown that MITF signaling is modulated by the hypoxic tumor microenvironment (14–16) and plays a role in oxidative metabolism (17, 18). Of note, hypoxia and mitochondrial dysfunction are also predominant scenarios in PCC/PGL tumorigenesis (19). Specifically, *MITF*, p.E318K activates more efficiently *EPAS1* promoter than *MITF* wild-type. On the other hand, *EPAS1* is being targeted by renal cancer susceptibility genes including *VHL*, which also predisposes to PCC/PGL (8). Given that SUMOylation is a global cellular answer to allow proper adaptation to stress (20), a possible role of the *MITF*, p.E318K hypo-SUMOylable form, in PCC/PGL tumorigenesis is not surprising.

In conclusion, we present the *MITF*, p.E318K as the first low-frequency genetic variant associated with an increased risk of PCC/PGL. It will be important to confirm this finding in other populations and to address the role of *MITF* as modifier gene in hereditary PCC/PGL by genotype.

Acknowledgments

The authors thank the technical staff from the Department of Genetics, George Pompidou European Hospital, led by Prof. Xavier Jeunemaitre.

Address all correspondence and requests for reprints to: Luis Jaime Castro-Vega, MD, PhD, Postdoctoral Fellow, INSERM, UMR970, Paris-Cardiovascular Research Center, F-75015, Paris, France, 20-40 rue Leblanc, 75015 Paris, France. E-mail: luis-jaime.castro-vega@inserm.fr.

This work was supported by the Agence Nationale de la Recherche (ANR-2011-JCJC-00701 MODEOMAPP), the European Union Seventh Framework Programme (FP7/2007-2013) under grant agreement no. 259735, and the Institut National du Cancer et la Direction de l'Offre de Soins (INCa-DGOS_8663) for the COMETE network.

Disclosure Summary: The authors have nothing to disclose.

References

1. **Hou L, Pavan WJ.** Transcriptional and signaling regulation in neural crest stem cell-derived melanocyte development: do all roads lead to Mitf? *Cell Res*. 2008;18:1163–1176.
2. **Bertolotto C, Abbe P, Hemesath TJ, et al.** Microphthalmia gene product as a signal transducer in cAMP-induced differentiation of melanocytes. *J Cell Biol*. 1998;142:827–835.
3. **Garraway LA, Widlund HR, Rubin MA, et al.** Integrative genomic analyses identify MITF as a lineage survival oncogene amplified in malignant melanoma. *Nature*. 2005;436:117–122.
4. **Cronin JC, Wunderlich J, Loftus SK, et al.** Frequent mutations in the MITF pathway in melanoma. *Pigment Cell Melanoma Res*. 2009;22:435–444.
5. **Bertolotto C, Lesueur F, Giuliano S, et al.** A SUMOylation-defective MITF germline mutation predisposes to melanoma and renal carcinoma. *Nature*. 2011;480:94–98.
6. **Yokoyama S, Woods SL, Boyle GM, et al.** A novel recurrent mutation in MITF predisposes to familial and sporadic melanoma. *Nature*. 2011;480:99–103.
7. **Read J, Wadt KA, Hayward NK.** Melanoma genetics. *J Med Genet*. 2016;53:1–14.
8. **Favier J, Amar L, Gimenez-Roqueplo A.** Paraganglioma and phaeochromocytoma: from genetics to personalized medicine. *Nat Rev Endocrinol*. 2015;11:101–111.
9. **Castro-Vega LJ, Lepoutre-Lussey C, Gimenez-Roqueplo AP, Favier J.** Rethinking pheochromocytomas and paragangliomas from a genomic perspective. *Oncogene*. 2016;35:1080–1089.
10. **Hercberg S, Galan P, Preziosi P, et al.** The SU.VI.MAX Study: a randomized, placebo-controlled trial of the health effects of antioxidant vitamins and minerals. *Arch Intern Med*. 2004;164:2335–2342.
11. **Purcell S, Neale B, Todd-Brown K, et al.** PLINK: a tool set for whole-genome association and population-based linkage analyses. *Am J Hum Genet*. 2007;81:559–575.
12. **Lamovec J, Frkovic-Grazio S, Bracko M.** Nonsporadic cases and unusual morphological features in pheochromocytoma and paraganglioma. *Arch Pathol Lab Med*. 1998;122:63–68.
13. **Hartman ML, Czyz M.** Pro-survival role of MITF in melanoma. *J Invest Dermatol*. 2015;135:352–358.
14. **Busca R, Berra E, Gaggioli C, et al.** Hypoxia-inducible factor 1{alpha} is a new target of microphthalmia-associated transcription factor (MITF) in melanoma cells. *J Cell Biol*. 2005;170:49–59.
15. **Feige E, Yokoyama S, Levy C, et al.** Hypoxia-induced transcriptional repression of the melanoma-associated oncogene MITF. *Proc Natl Acad Sci U S A*. 2011;108:E924–E933.
16. **Cheli Y, Giuliano S, Fenouille N, et al.** Hypoxia and MITF control metastatic behaviour in mouse and human melanoma cells. *Oncogene*. 2012;31:2461–2470.
17. **Vazquez F, Lim JH, Chim H, et al.** PGC1alpha expression defines a subset of human melanoma tumors with increased mitochondrial capacity and resistance to oxidative stress. *Cancer Cell*. 2013;23:287–301.
18. **Haq R, Shoag J, Andreu-Perez P, et al.** Oncogenic BRAF regulates oxidative metabolism via PGC1alpha and MITF. *Cancer Cell*. 2013;23:302–315.
19. **Favier J, Gimenez-Roqueplo AP.** Pheochromocytomas: the (pseudo)-hypoxia hypothesis. *Best Pract Res Clin Endocrinol Metab*. 2010;24:957–968.
20. **Guo C, Henley JM.** Wrestling with stress: roles of protein SUMOylation and deSUMOylation in cell stress response. *IUBMB Life*. 2014;66:71–77.

REVUE 2

Mitochondrial Deficiencies in the Predisposition to Paraganglioma.

Lussey-Lepoutre C, Buffet A, Gimenez-Roqueplo AP, Favier J.

Metabolites. 2017 May 4;7(2).

metabolites

MDPI

Review

Mitochondrial Deficiencies in the Predisposition to Paraganglioma

Charlotte Lussey-Lepoutre [1,2,3], Alexandre Buffet [1,2,4], Anne-Paule Gimenez-Roqueplo [1,2,4,5] and Judith Favier [1,2,4,*]

1 INSERM UMR970, Paris-Cardiovascular Research Center at HEGP, F-75015 Paris, France; charlotte.lussey@inserm.fr (C.L.-L.); alexander.buffet@inserm.fr (A.B.); anne-paule.gimenez-roqueplo@aphp.fr (A.-P.G.-R.)
2 Equipe Labellisée Ligue contre le Cancer, F-75015 Paris, France
3 Faculté de Médecine, Université Pierre et Marie Curie, F-75006 Paris, France
4 Faculté de Médecine, Sorbonne Paris Cité, Paris Descartes, F-75006 Paris, France
5 APHP, Hôpital Européen Georges Pompidou, Service de Génétique, F-75015 Paris, France
* Correspondence: judith.favier@inserm.fr; Tel.: +33-1-5398-8041

Academic Editor: Madhu Basetti
Received: 30 March 2017; Accepted: 30 April 2017; Published: 4 May 2017

Abstract: Paragangliomas and pheochromocytomas are rare neuroendocrine tumours with a very strong genetic component. It is estimated that around 40% of all cases are caused by a germline mutation in one of the 13 predisposing genes identified so far. Half of these inherited cases are intriguingly caused by mutations in genes encoding tricarboxylic acid enzymes, namely *SDHA*, *SDHB*, *SDHC*, *SDHD*, and *SDHAF2* genes, encoding succinate dehydrogenase and its assembly protein, *FH* encoding fumarate hydratase, and *MDH2* encoding malate dehydrogenase. These mutations may also predispose to other type of cancers, such as renal cancer, leiomyomas, or gastro-intestinal stromal tumours. SDH, which is also the complex II of the oxidative respiratory chain, was the first mitochondrial enzyme to be identified having tumour suppressor functions, demonstrating that 80 years after his initial proposal, Otto Warburg may have actually been right when he hypothesized that low mitochondrial respiration was the origin of cancer. This review reports the current view on how such metabolic deficiencies may lead to cancer predisposition and shows that the recent data may lead to the development of innovative therapeutic strategies and establish precision medicine approaches for the management of patients affected by these rare diseases.

Keywords: SDH; paraganglioma; pheochromocytoma

1. Introduction

Paragangliomas (PGLs) are rare tumours that may occur in non-chromaffin cells of the parasympathetic ganglia, typically in the head and neck region (glomus tympanicus, glomus jugulare, carotid body). These tumours can also arise in chromaffin cells of the sympathetic nervous system in the chest, abdomen, or pelvis (organ of Zuckerkandl, urinary bladder). Pheochromocytomas (PCCs) are particular PGLs that develop in the adrenal medulla. While head and neck PGLs are usually non-functional, PCCs and functional PGLs secrete catecholamines (epinephrine, norepinephrine, dopamine) in the circulation and can induce severe lethal cardiovascular and cerebrovascular complications. The prevalence of pheochromocytomas/paragangliomas (PPGLs) in patients with hypertension consulting at general outpatient clinics is estimated at 0.2% to 0.6%, but this number is probably underestimated [1]. Most PPGLs are benign, with a 10-year overall survival rate of ~96%. However, 10% of PCC patients and up to 40% of PGL patients develop a metastatic disease with

a five-year survival rate below 50%. Currently, there are no histopathological criteria to predict malignancy [2], and current treatments for the metastatic forms of the disease are generally ineffective.

Approximately 40% of patients with PPGLs carry a germline mutation in one of the 13 PPGL predisposing genes identified so far, including the *RET* proto-oncogene and the *NF1*, *VHL*, and *SDHx* genes. Other rare cases involve germline mutations in the *FH*, *TMEM127*, *MAX*, and *MDH2* genes [3–6]. In addition, somatic mutations have been reported in 30% of cases, involving the *VHL*, *RET*, *NF1*, *HIF2A*, *ATRX* and *HRAS* genes [4]. Predisposing mutations can occur in apparently sporadic tumours (12–15%) or in the context of a hereditary cancer syndrome mostly represented by the following three genetic syndromes: multiple endocrine neoplasia type 2, Von Hippel–Lindau disease, and neurofibromatosis type I [7,8]. Activating mutations in the *RET* proto-oncogene lead to multiple endocrine neoplasia type 2 (MEN2), characterized by the development of medullary thyroid carcinoma, often associated with PCCs and hyperparathyroidism. The *NF1* gene, one of the largest genes in humans (60 exons) [9], encodes neurofibromin, which is a tumour suppressor that downregulates the RAS–RAF–MAPK signalling cascade. Mutations in this gene cause neurofibromatosis type 1, also known as Von Recklinghausen disease, a frequent autosomal disorder (prevalence of 1 in 3000 to 1 in 4000 people in the general population and a high penetrance) characterized by pigmentary abnormalities and neoplastic growth of neural crest-derived cells, such as multiple dermal neurofibromas and very rarely PCCs (0.1–5.7% of patients with NF1) [10]. The Von Hippel Lindau disease is a hereditary neoplastic syndrome caused by mutations in the *VHL* tumour suppressor gene, which are responsible for a predisposition to renal cell carcinoma (RCC), retinal or central nervous system hemangioblastomas, pancreatic cysts, and PCCs [11]. VHL type 1 families have a greatly reduced risk of PCC, but can develop all the other tumour types generally associated with the disease. VHL type 2 families develop PCCs, but have either a low-risk (type 2A) or high-risk (type 2B) for RCC. VHL type 2C families have PPGLs only, without the other hallmarks of VHL disease. More recently, integrative genomic approaches identified germline mutations in two new tumour suppressor genes: *TMEM127* [12] and *MAX* [13] genes which predispose to familial, bilateral, or apparently sporadic PCCs.

In 2000, the description of the first mutations in the *SDHD* gene [14] in patients with PPGL was a major breakthrough, not only in the understanding of PPGL tumorigenesis but in cancer in general [14,15]. Indeed, *SDHx* genes were the first genes encoding a mitochondrial protein implicated in the development of cancer, supporting the hypothesis of a direct link between mitochondrial dysfunction and cancer, as proposed by Otto Warburg at the beginning of the 20th century [16] and underlying the important role of metabolism as a "new" hallmark of cancer [17].

2. Genetically-Determined Mitochondrial Deficiencies

SDHx genes (*SDHA*, *SDHB*, *SDHC*, *SDHD*, and *SDHAF2*) represent almost half of the germline mutated genes in PPGL [6] (Table 1). *SDHA-D* are nuclear genes that encode the four subunits of succinate dehydrogenase (SDH), a mitochondrial enzyme located in the inner mitochondrial membrane. It catalyses the oxidation of succinate into fumarate within the tricarboxylic acid (TCA) cycle and transfers electrons to the ubiquinone pool in the respiratory chain. Succinate dehydrogenase contains two anchorage proteins (SDHC and SDHD) and two catalytic proteins (SDHA and SDHB). SDHAF2 is responsible for the flavination of the SDHA subunit, which is essential for the assembly of the complex.

SDHx genes behave as tumour suppressor genes in keeping with Knudson's "two-hit" model. Hence, patients carry a germline heterozygous loss-of-function mutation and subsequent loss of heterozygosity (LOH) at somatic level, leads to the complete inactivation of the gene [18,19]. These two events are responsible for the loss of function of succinate dehydrogenase activity leading to massive succinate accumulation in the cytoplasm [20].

Previous studies have reported that germline mutations in one of the *SDHx* genes lead to PPGL predisposition in patients [7,21,22], which is transmitted in an autosomal dominant fashion for *SDHA*, *SDHB*, and *SDHC* genes mutations and in an autosomal dominant fashion with maternal imprinting

for *SDHD* and *SDHAF2* genes. In *SDHx*-related PPGL, the great majority of patient have a mutation in *SDHB* and *SDHD* genes (more than 60%), while mutation in *SDHC* and *SDHA* are rare [22,23]. Patients carrying an *SDHx* germline mutation develop PPGLs at a mean age of 36 years old, while sporadic PPGLs usually occur around 50 years old [7,8]. *SDHx* germline mutations have an incomplete penetrance, and genotype-phenotype correlations have been described. *SDHD* germline mutations have a penetrance of 86% at the age of 50 and are frequently associated with the development of multiple head and neck PGL and with family history of PPGLs in the paternal branch. In contrast, *SDHB* germline mutations have an estimated penetrance of 50% at the age of 50 [24,25], frequently predispose to abdominal PGLs, and to malignant forms of the disease in 50% of cases. On the contrary, malignant PPGLs are only found in 5% of *SDHD* or *SDHC* mutation carriers [8,25].

Table 1. Genes encoding mitochondrial proteins implicated in pheochromocytomas/paragangliomas (PPGL) susceptibility.

Genes	Enzyme	Phenotype	Mutation Frequency
SDHA	Succinate dehydrogenase	Paraganglioma/pheochromocytoma	20%
SDHB		Renal cell carcinoma	0.05–0.2%
SDHC		Gastrointestinal stromal tumour	12% (adult forms)
SDHD		Gastrointestinal stromal tumour	70% (paediatric forms)
SDHAF2			
FH	Fumarate hydratase	HRLCC syndrome	70–90%
		Paraganglioma	1%
MDH2	Malate dehydrogenase	Paraganglioma	One patient

Germline *SDHB* mutations are found in 36% of all malignant PPGLs, and *SDHB*-related malignant PPGLs have a worst prognosis than all other types of malignant PPGL. The median overall survival of patients with an *SDHB*-related malignant PPGL is of 42 months after the diagnosis of the first metastasis, while it is of 244 months for non-*SDHB* malignant PPGL [26]. The reason for this phenotypic characteristic of *SDHB* mutants is still unclear.

Germline mutation in *SDHC* gene are rare and may be associated with any type of PPGL. Finally, *SDHA* and *SDHAF2* mutations have been described in only few patients and predispose to abdominal PPGL and head and neck PGL, respectively [27,28].

Because of the genetic complexity of PPGL and of the large number of variants of unknown significance (VUS) identified in patients, immunochemical analyses of SDHA [29], SDHB [30], and SDHD [31] are now used in pathology department worldwide to validate the genetic analyses.

Germline mutations in *SDHx* genes have also been implicated in other tumours such as renal cell carcinoma (RCC) and gastro-intestinal stromal tumour (GIST) (Table 1). In 2004, Vanharata et al. described the first cases of RCC secondary to an *SDHB* germline mutation, which co-segregated with PPGL in a family [32]. Since, *SDHx* genes mutations have been implicated in 0.05 to 0.2% of renal cancers, and *SDHB* mutations are the most frequent [33]. It had recently been recognized as a subtype of renal cancer by the World Health Organization (WHO, 2016). In this subtype of RCC, various histological types have been described (chromophobe RCC, clear cell RCC, papillary RCC, and sarcomatoïd RCC). Multiple forms are described in 30% of cases [34]. In patients carrying the *SDHB* gene mutation, the lifetime risk of RCC has been estimated as 14% [24].

The great majority of GISTs are secondary to somatic mutation in *KIT* or *PDGFRA* genes. However, 85% of paediatric forms and 15% of adult forms have a so-called Wild-Type (WT) GIST, i.e., without *KIT* or *PDFGRA* mutations [35]. In these WT GISTs, more than 85% are secondary to an *SDHx* gene mutation [36]. The great majority are germline mutation (82%) and *SDHA* mutations represent more than a half of the identified mutations. *SDHx* related GISTs are more frequent in women, are always located in the gastric wall, and are multiple in 40% of cases. Malignant evolution is observed in 45% of patients, but with an indolent evolution [36]. Recently, epimutations of the *SDHC* gene promoter

have been proposed as a new mechanism of SDH loss of function in WT GIST with a negative SDHB immunochemistry and without any mutations in germline or somatic DNA [37,38]. These epimutations are germline or somatic mosaic, and represent almost the quarter of *SDHx* related GIST [36]. They are more frequent in female patients and are multiple in 70% of cases. They are characterized by an *SDHC* promoter-specific CpG island hypermethylation associated with subsequent gene silencing. Recently, a patient with multiple PPGL has been described with an epimutation of the *SDHC* promotor [39].

Additional to *SDHx* genes, other genes encoding enzymes of the TCA cycle have been implicated in tumorigenesis. Fumarate hydratase, encoded by the *FH* gene, is a TCA cycle enzyme that catalyses the step immediately following SDH in the cycle, converting fumarate into malate. Germline mutations in this tumour suppressor gene were first described in the predisposition to HRLCC syndrome (hereditary leiomyomatosis and renal cell cancer) also known as Reed Syndrome [40]. More than 70% of *FH*-mutation carriers develop cutaneous leiomyoma, and women are prone to uterine leiomyoma in more than 82% of cases. In 18% of cases, FH patients develop very aggressive papillary type II renal cancer associated with poor prognosis [41,42]. More recently, it was demonstrated that *FH* gene germline mutations can also predispose to PPGL [43] and lead to malignant or multiple forms of the disease [44,45].

Finally, Cascon et al. have recently described the first *MDH2* gene germline mutation in a patient with a multiple and malignant PGL. This gene encodes malate dehydrogenase, which converts the malate into oxaloacetate in the TCA cycle [3]. Until now, this is the only case of *MDH2* mutation ever described in the predisposition to cancer.

3. Tumorigenesis

In 2000, the demonstration of *SDHD* being a tumour suppressor gene showed that Warburg view was actually true, at least in these very specific cases of inherited cancer predisposition, and that a defect in a central metabolic function could be the origin of cancer. Intriguingly, genetic disorders associated with this type of dysfunction had before that, been associated with neurodegenerative diseases rather than with a proliferative phenotype. Indeed, *SDHA* and *FH* germline homozygous mutations had been shown to respectively cause Leigh syndrome, a progressive brain disorder that appears in infancy or early childhood and multiple severe neurologic abnormalities in the so-called "Fumarate hydratase deficiency". How mutations in the same genes lead to a proliferative disease was a real surprise. One explanation is that patients affected with Leigh syndrome or fumarate hydratase deficiency carry homozygous germline mutations that maintain some residual enzymatic activity, allowing these mutations to be viable and mediating the neurologic phenotype. In contrast, mutations predisposing to cancer susceptibility are heterozygous, require a second somatic genetic event (most generally the loss of the chromosomal region harbouring the wild-type allele), and then lead to the complete and selective loss of the enzymatic activity. Recently, Lorendeau et al addressed this question and suggest that tumorigenesis requires the combine loss of SDH and complex I activity, while SDH inhibition alone would solely lead to the neurodegenerative phenotype [46].

The first key allowing understanding the tumorigenesis pathways associated with TCA cycle mutations was the description, in the first French family of *SDHD*-related PGL, of increased angiogenesis and overexpression of the hypoxia inducible factor 2α (HIF2α) and one of its target, the vascular endothelial growth factor (VEGF) [18]. Transcriptomic studies further confirmed this initial observation by demonstrating that unsupervised classification of PPGL tumours allowed separating them into two major clusters of expression: cluster 1, characterized by a hypoxic signature, which comprised all TCA cycle mutations (cluster 1A) on one side and *VHL* and *HIF2A* mutated tumours (cluster 1B) on the other side, and cluster 2, regrouping *RET*, *NF1*, *MAX*, and *TMEM127* related tumours, as well as most of the sporadic cases [47,48]. The *VHL* gene encodes an E3 ubiquitin ligase that is implicated in the ubiquitination of HIF1α and HIF2α transcription factors leading to their proteosomal degradation (Figure 1). The recognition of HIFs by pVHL requires their hydroxylation on two highly conserved proline residues by the so called HIF-prolyl hydroxylases

(PHDs or EGLN) that belong to the family of 2-oxoglutarate (2-OG) dependent dioxygenases. The reaction of hydroxylation uses O_2 as a co-substrate, explaining the stabilization of HIFs in hypoxic conditions. In VHL-mutants, loss of pVHL function leads to the abnormal stabilization of HIFs, even in the presence of oxygen, leading to a pseudohypoxic drive. In SDH and FH-deficient tumours, it was subsequently shown that the massive accumulation of their respective substrates, namely succinate and fumarate is responsible for the inhibition of PHD activity, also leading to a pseudohypoxic response. Indeed, succinate and fumarate, which are very similar to 2-OG, act as competitive inhibitors of 2-OG dependent dioxygenases. In addition, another hydroxylase is implicated in the modulation of HIF activity in normal conditions. This so-called Factor Inhibiting HIF (FIH) is an asparagyl hydroxylase that hydroxylates an asparagine residue located on the carboxy-terminal transactivation domain of HIFs, preventing the recruitment of the coactivator proteins p300 and CBP, thereby attenuating HIF-dependent transcription [49]. The inhibition of FIH activity by succinate and fumarate may as well increase the HIF-mediated transcriptional response thereby modulating the expression of a wide variety of target genes, the products of which being implicated in the regulation of angiogenesis, tumour growth, energy metabolism, survival, and migration.

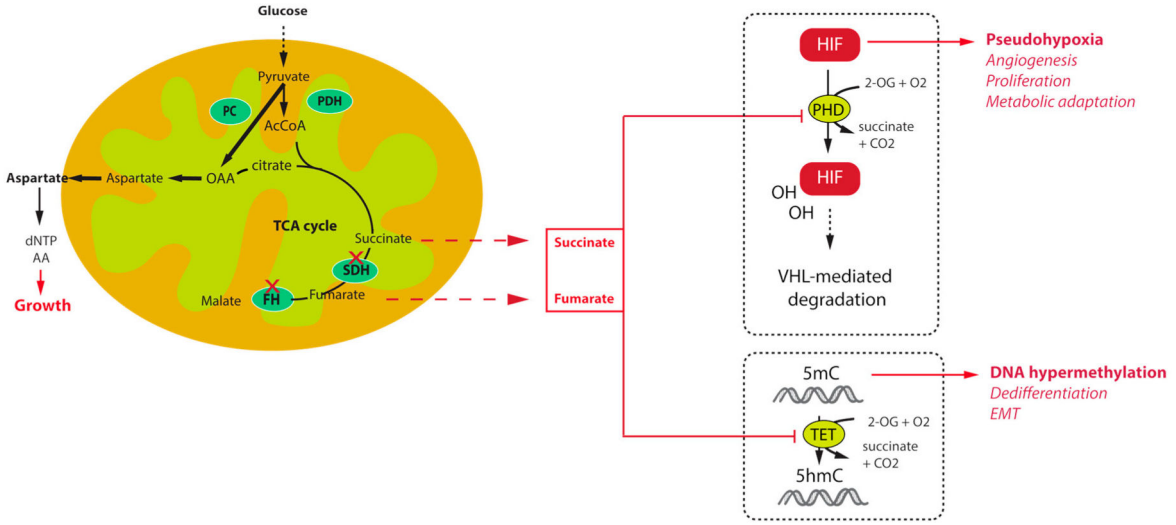

Figure 1. Mechanisms of tumorigenesis and survival associated with tricarboxylic acid (TCA) cycle mutations in paraganglioma.

Other important members of the 2-OG dependent dioxygenases family are the DNA and histone demethylases, namely the ten eleven translocation (TET) enzymes and histone lysine demethylase (KDM) family of JmjC-domain containing proteins. Oxidative demethylation of DNA is mediated by TET enzymes, which hydroxylate 5-methylcytosine (5mC) into 5-hydroxy-methylcytosine (5hmC) [50,51]. It was shown that inhibition of TET enzymes by succinate leads to a high abundance of DNA methylation and a low abundance of DNA hydroxymethylation in *SDH*-related PPGL [43] and GIST [52] (Figure 1). This has massive consequences on gene expression as hypermethylation of CpG islands within the promoter regions of genes is frequently associated with the repression of transcription. Hence, *SDH* mutant cells, by reprogramming the transcriptome at the whole genome scale, foster tumorigenesis by repressing the expression of genes that promote cancer stem cell identity [53], and Epithelial-to-Mesenchymal Transition (EMT) [54]. An EMT like phenotype has indeed been described in both *SDHB*-mutated metastatic human PPGL [55] and cells [56], as well as in FH-deficient cells [57]. This phenotype is regulated by epigenetic modifications, that comprise the hypermethylator phenotype, but also the dysregulation of key target microRNAs [4,57]. Because of their central role in the acquisition of tumour hallmarks by SDH- and FH-deficient cells, succinate and

fumarate are now referred to as "oncometabolites", as 2-hydroxyglutarate, the organic acid generated by mutant isocitrate dehydrogenase mutants in gliomas and acute myeloid leukaemia [58].

4. Innovative Strategies and Future Directions

As discussed earlier, *SDHx* mutation carriers are at risk of developing multiple PPGLs, and *SDHB*-mutation carriers are predisposed to metastatic forms of the disease. Malignant PPGLs respond very poorly to classical chemotherapies, and the complete surgical resection of the tumour is still the only curative treatment. For non-operable or metastatic PPGLs, therapeutic choices may take into account the particular metabolic reprogramming of these tumours.

4.1. New Therapeutic Strategies for SDHx-Deficient Metastatic PPGL

One promising strategy is based on an antiangiogenic approach that appears appropriate regarding the highly vascularized pattern and the activation of a VEFG-dependant angiogenesis of PPGL carrying *SDHx* mutations. The first six case reports of metastatic PPGLs treated with sunitinib were published almost simultaneously by four different teams showing extended partial response in patients carrying *SDHB* mutations [59–62]. The most comprehensive study reported so far is a retrospective review of medical records of 17 patients (including eight with an *SDHB* mutation and one *VHL* patient) with metastatic PPGLs who were treated with sunitinib [63]. Among the 14 patients without early toxicity, three had a partial response and five had stable disease, while the disease progressed in the other six patients. Partial response or stable disease were observed in the patient with a *VHL* mutation and five of the six evaluable patients with an *SDHB* mutation, suggesting that patients with cluster 1 disease might be better responders to antiangiogenic treatments than patients with cluster 2 tumours. These observations need to be confirmed in larger cohorts of patients and compared with appropriate placebo conditions. To that aim, the first randomized double blind phase II international multicentre study (the FIRSTMAPPP study) is currently ongoing and will hopefully enable such validations. The FIRSTMAPPP study is a randomized double-blind phase II international multicentre study that is evaluating the efficacy of sunitinib versus placebo in patients with progressive malignant PPGL (http://clinicaltrials.gov/ct2/show/NCT01371201), and two nonrandomized phase II studies that are evaluating the response to sunitinib (https://clinicaltrials.gov/ct2/show/NCT00843037) and axitinib (https://clinicaltrials.gov/ct2/show/NCT01967576).

Directly inhibiting HIF2α, instead of its targets like VEGF, appears to be a good strategy. Recently, two independent teams published the results of PT2399, a selective HIF-2 antagonist, in a preclinical model of clear cell renal carcinoma (ccRCC) [64,65]. Further studies are needed to evaluate if these new molecules will be effective in the PPGL field.

Other pathways identified by "OMICs" approaches are promising candidates for precision medicine. Epigenetic alterations play major roles in establishing and maintaining aberrant gene expression profiles in cancer cells and in particular in the hypermethylated cluster M1 involving all PPGL with *SDHx* and *FH* mutations [43]. Targeting epigenetic alterations in cancer cells (epigenetic therapy) is a new frontier in drug discovery. Reversion of DNA methylation by epidrugs such as 5-aza-2′-deoxycytidine (Decitabine) or histone methylation by histone methyl transferase inhibitors, is clearly an attractive strategy for carriers of *SDHx* or *FH* mutations. The efficacy of these drugs has led to their approval as monotherapy in haematological malignancies [66]. Although no study is yet available in humans, some promising results are now starting to bear fruit from in vitro studies, suggesting that drugs targeting epigenetic pathways might constitute useful alternative treatments for *SDHx*-related or *FH*-related malignant PPGLs in the future [43]. Hence, a statistically significant effect of decitabine on the cell migration was previously demonstrated in a model of hypermethylated *Sdhb*-knockout mouse chromaffin cells (ImCC) [43]. In primary cultures of human PCCs and in another PCC-derived mouse cell line (MPC), the 5-aza-cytidine DNA methylation inhibitor increased the efficacy of the proapoptotic Topoisomerase1 inhibitor (camptothecin) agent when used as a complementary drug [67].

Furthermore, the hypermethylated phenotype of *SDHB*-related tumours apparently affects the promoter of the MGMT gene encoding the O6-methylguanine-DNA methyltransferase, the repression of which is a biomarker of a good response to alkylating agents such as temozolomide [68,69]. Indeed, in the first report involving a small retrospective cohort of 15 patients with progressive metastatic PPGL, temozolomide treatment was more effective in patients carrying *SDHB* mutations than in those without *SDHB* mutations [70]. Although these data are promising, the findings will need to be confirmed in a prospective clinical trial.

4.2. The Explorative Way of Metabolic Reprogramming

Metabolic reprogramming is emerging as a core hallmark of cancer [71]. During the last decade, many studies have shown that the majority of oncogenes and tumour suppressor genes are involved in cell metabolism and that mutations in these genes facilitate cell survival and proliferation by promoting the use of nutrients [72]. As a central metabolic actor, alterations of enzymes in the TCA cycle result in important metabolic re-wiring in order to respond to bioenergetics and anabolic requests of cancer cells. Main changes rely on an increase of glucose and glutamine consumption and an increased anaerobic glycolysis. Hence, mutations in *SDHx* genes were demonstrated to mediate a rise in contribution of glucose to ATP production and glutamine to TCA cycle intermediates in an ovarian cancer model [73,74]. Recently, two independent studies demonstrated that loss of SDH activity through *Sdhb* deletion in a mouse cellular model results in their dependence on the pyruvate carboxylase (PC) enzyme, responsible for pyruvate carboxylation to synthesize oxaloacetate (OAA) (Figure 1). Despite the TCA cycle truncation, cells can use OAA as a TCA cycle intermediate in order to produce aspartate, a key metabolic pivot in the cell (the main precursor for protein and nucleotide biosynthesis) [75,76]. Moreover, in vitro silencing of PC resulted in complete ablation of proliferation and loss of viability [75,76]. Although it is unlikely that PC targeting would be appropriate in patients, deciphering the metabolic pathways associated with TCA cycle mutations may reveal important and novel therapeutic targets for the management of these tumours. In FH deficient renal cells, similar experiments revealed that argininosuccinate was produced from arginine and fumarate by the reverse activity of the urea cycle enzyme argininosuccinate lyase (ASL), making these cells auxotophic for arginine [77]. Fumarate also promotes protein succination that alters the function of multiple proteins, including aconitase, thus promoting to the dysregulated metabolism observed in these cells [78]. Hence, although these observations should also be confirmed in PPGL cells, they may also provide potential new therapeutic interventions or biomarkers for these cancers.

4.3. New Biomarkers for Diagnosis, Prognosis, and Early Response to Treatment

Increase in anaerobic glycolysis in most cancer cells and particularly in cells with an interruption of the TCA cycle lead to a wide utilisation in oncology imaging of the radionuclide ^{18}F-Fluorodeoxyglucose (^{18}F-FDG), a glucose analogue labelled with a positron emitter (^{18}F) permitting its detection by positron emission tomography (PET) imaging. In contrast to its uptake in other neuroendocrine tumours, ^{18}F-FDG uptake in PPGL provides the most sensitive functional imaging with a sensitivity on a patient basis of more than 80% [79]. Furthermore, ^{18}F-FDG uptake is higher in *SDH*-deficient PGL [80,81]. ^{18}F-FDG PET/CT is therefore already considered a standard examination for complete staging in patients with an *SDHx* mutation and for the evaluation of early response to treatment [82–84]. Nevertheless, the limitation of ^{18}F-FDG PET/CT is the lack of specificity.

SDH inactivation leads to a massive accumulation of succinate, acting as an oncometabolite, and its levels, assessed on surgically resected tissues, are a highly specific biomarker of *SDHx*-mutated tumours. Succinate presents a characteristic peak at 2.44 ppm in spectral analysis that can be detected noninvasively by in vivo proton magnetic resonance spectroscopy (^{1}H-MRS). ^{1}H-MRS is an analytical technique for the observation of tissue compounds after elimination of water protons with a saturation pulse. Until now, ^{1}H-MRS has been mostly studied in the field of cerebral tumours, especially gliomas. The majority (50–86%) of gliomas diagnosed in younger adults (<45 years old) have recurrent

somatic mutations in one of the genes encoding isocitrate dehydrogenase (*IDH1* and *IDH2*) leading to the overproduction of 2-hydroxyglutarate, an oncometabolite that plays a key role in malignant transformation and is interestingly detectable in vivo by ^{1}H-MRS [85,86]. A pulse ^{1}H-MRS sequence was previously developed to measure succinate in an allografted mouse model of *Sdhb*-deficient tumours and used in a pilot study performed in nine patients with PPGL (five with *SDHx* mutations and four sporadic cases). That pilot study demonstrated the feasibility of detecting succinate in vivo by ^{1}H-MRS as a very specific biomarker of *SDHx* mutations [87]. Moreover, animal experiments demonstrated that the area under the succinate peak of the ^{1}H-MRS spectra in vivo was correlated with the concentrations of succinate measured in the resected tumours by GC-MS in vitro, allowing quantifying succinate levels in vivo. Future studies are needed to show whether this correlation holds in patients. If this turned out to be the case, and given that succinate concentrations in tumours reflect the metabolic activity of SDH-deficient tumour cells, this new innovative and innocuous imaging method could produce a quantifiable surrogate marker of early response to treatment for the patients.

Acknowledgments: Authors of this review received funding by the Institut National du Cancer and by the Direction Générale de l'Offre de Soins (PRT-K 2014, COMETE-TACTIC, INCa-DGOS_8663), the Paradifference Foundation. A. Buffet received a financial support from ITMO Cancer AVIESAN (Alliance Nationale pour les Sciences de la Vie et de la Santé, National Alliance for Life Sciences & Health) within the framework of the Cancer Plan.

Conflicts of Interest: The authors declare no conflict of interest.

References

1. Lenders, J.W.; Duh, Q.Y.; Eisenhofer, G.; Gimenez-Roqueplo, A.P.; Grebe, S.K.; Murad, M.H.; Naruse, M.; Pacak, K.; Young, W.F., Jr.; Endocrine, S. Pheochromocytoma and paraganglioma: An endocrine society clinical practice guideline. *J. Clin. Endocrinol. Metab.* **2014**, *99*, 1915–1942. [CrossRef] [PubMed]
2. Louis, D.; Ohgaki, H.; Wiestler, O.; Cavenee, W. *WHO Classification of Tumours of the Central Nervous System*, 4th ed.; IARC Press: Lyon, France, 2007.
3. Cascon, A.; Comino-Mendez, I.; Curras-Freixes, M.; de Cubas, A.A.; Contreras, L.; Richter, S.; Peitzsch, M.; Mancikova, V.; Inglada-Perez, L.; Perez-Barrios, A.; et al. Whole-exome sequencing identifies MDH2 as a new familial paraganglioma gene. *J. Natl. Cancer Inst.* **2015**, *107*. [CrossRef] [PubMed]
4. Castro-Vega, L.J.; Letouze, E.; Burnichon, N.; Buffet, A.; Disderot, P.H.; Khalifa, E.; Loriot, C.; Elarouci, N.; Morin, A.; Menara, M.; et al. Multi-omics analysis defines core genomic alterations in pheochromocytomas and paragangliomas. *Nat. Commun.* **2015**, *6*, 6044. [CrossRef] [PubMed]
5. Dahia, P.L. Pheochromocytoma and paraganglioma pathogenesis: Learning from genetic heterogeneity. *Nat. Rev. Cancer* **2014**, *14*, 108–119. [CrossRef] [PubMed]
6. Favier, J.; Amar, L.; Gimenez-Roqueplo, A. Paraganglioma and phaeochromocytoma: From genetics to personalized medicine. *Nat. Rev. Endocrinol.* **2014**, *11*, 101–111. [CrossRef] [PubMed]
7. Amar, L.; Bertherat, J.; Baudin, E.; Ajzenberg, C.; Bressac-de Paillerets, B.; Chabre, O.; Chamontin, B.; Delemer, B.; Giraud, S.; Murat, A.; et al. Genetic testing in pheochromocytoma or functional paraganglioma. *J. Clin. Oncol.* **2005**, *23*, 8812–8818. [CrossRef] [PubMed]
8. Burnichon, N.; Rohmer, V.; Amar, L.; Herman, P.; Leboulleux, S.; Darrouzet, V.; Niccoli, P.; Gaillard, D.; Chabrier, G.; Chabolle, F.; et al. The succinate dehydrogenase genetic testing in a large prospective series of patients with paragangliomas. *J. Clin. Endocrinol. Metab.* **2009**, *94*, 2817–2827. [CrossRef] [PubMed]
9. Viskochil, D.; Buchberg, A.M.; Xu, G.; Cawthon, R.M.; Stevens, J.; Wolff, R.K.; Culver, M.; Carey, J.C.; Copeland, N.G.; Jenkins, N.A.; et al. Deletions and a translocation interrupt a cloned gene at the neurofibromatosis type 1 locus. *Cell* **1990**, *62*, 187–192. [CrossRef]
10. Gutmann, D.H.; Aylsworth, A.; Carey, J.C.; Korf, B.; Marks, J.; Pyeritz, R.E.; Rubenstein, A.; Viskochil, D. The diagnostic evaluation and multidisciplinary management of neurofibromatosis 1 and neurofibromatosis 2. *JAMA* **1997**, *278*, 51–57. [CrossRef] [PubMed]
11. Kim, W.Y.; Kaelin, W.G. Role of VHL gene mutation in human cancer. *J. Clin. Oncol.* **2004**, *22*, 4991–5004. [CrossRef] [PubMed]

12. Qin, Y.; Yao, L.; King, E.E.; Buddavarapu, K.; Lenci, R.E.; Chocron, E.S.; Lechleiter, J.D.; Sass, M.; Aronin, N.; Schiavi, F.; et al. Germline mutations in TMEM127 confer susceptibility to pheochromocytoma. *Nat. Genet.* **2010**, *42*, 229–233. [CrossRef] [PubMed]
13. Comino-Mendez, I.; Gracia-Aznarez, F.J.; Schiavi, F.; Landa, I.; Leandro-Garcia, L.J.; Leton, R.; Honrado, E.; Ramos-Medina, R.; Caronia, D.; Pita, G.; et al. Exome sequencing identifies max mutations as a cause of hereditary pheochromocytoma. *Nat. Genet.* **2011**, *43*, 663–667. [CrossRef] [PubMed]
14. Baysal, B.E.; Ferrell, R.E.; Willett-Brozick, J.E.; Lawrence, E.C.; Myssiorek, D.; Bosch, A.; van der Mey, A.; Taschner, P.E.; Rubinstein, W.S.; Myers, E.N.; et al. Mutations in SDHD, a mitochondrial complex II gene, in hereditary paraganglioma. *Science* **2000**, *287*, 848–851. [CrossRef] [PubMed]
15. Astuti, D.; Latif, F.; Dallol, A.; Dahia, P.L.; Douglas, F.; George, E.; Skoldberg, F.; Husebye, E.S.; Eng, C.; Maher, E.R. Gene mutations in the succinate dehydrogenase subunit SDHB cause susceptibility to familial pheochromocytoma and to familial paraganglioma. *Am. J. Hum. Genet.* **2001**, *69*, 49–54. [CrossRef] [PubMed]
16. Warburg, O. On respiratory impairment in cancer cells. *Science* **1956**, *124*, 269–270. [PubMed]
17. Hanahan, D.; Weinberg, R.A. Hallmarks of cancer: The next generation. *Cell* **2011**, *144*, 646–674. [CrossRef] [PubMed]
18. Gimenez-Roqueplo, A.P.; Favier, J.; Rustin, P.; Mourad, J.J.; Plouin, P.F.; Corvol, P.; Rotig, A.; Jeunemaitre, X. The R22X mutation of the sdhd gene in hereditary paraganglioma abolishes the enzymatic activity of complex II in the mitochondrial respiratory chain and activates the hypoxia pathway. *Am. J. Hum. Genet.* **2001**, *69*, 1186–1197. [CrossRef] [PubMed]
19. Gimenez-Roqueplo, A.P.; Favier, J.; Rustin, P.; Rieubland, C.; Crespin, M.; Nau, V.; Khau Van Kien, P.; Corvol, P.; Plouin, P.F.; Jeunemaitre, X. Mutations in the sdhb gene are associated with extra-adrenal and/or malignant phaeochromocytomas. *Cancer Res.* **2003**, *63*, 5615–5621. [PubMed]
20. Pollard, P.J.; Briere, J.J.; Alam, N.A.; Barwell, J.; Barclay, E.; Wortham, N.C.; Hunt, T.; Mitchell, M.; Olpin, S.; Moat, S.J.; et al. Accumulation of krebs cycle intermediates and over-expression of HIF1α in tumours which result from germline FH and SDH mutations. *Hum. Mol. Genet.* **2005**, *14*, 2231–2239. [CrossRef] [PubMed]
21. Neumann, H.P.; Bausch, B.; McWhinney, S.R.; Bender, B.U.; Gimm, O.; Franke, G.; Schipper, J.; Klisch, J.; Altehoefer, C.; Zerres, K.; et al. Germ-line mutations in nonsyndromic pheochromocytoma. *N. Engl. J. Med.* **2002**, *346*, 1459–1466. [CrossRef] [PubMed]
22. Pasini, B.; Stratakis, C.A. SDH mutations in tumorigenesis and inherited endocrine tumours: Lesson from the phaeochromocytoma-paraganglioma syndromes. *J. Intern. Med.* **2009**, *266*, 19–42. [CrossRef] [PubMed]
23. Buffet, A.; Venisse, A.; Nau, V.; Roncellin, I.; Boccio, V.; Le Pottier, N.; Boussion, M.; Travers, C.; Simian, C.; Burnichon, N.; et al. A decade (2001–2010) of genetic testing for pheochromocytoma and paraganglioma. *Horm. Metab. Res.* **2012**, *44*, 359–366. [CrossRef] [PubMed]
24. Ricketts, C.J.; Forman, J.R.; Rattenberry, E.; Bradshaw, N.; Lalloo, F.; Izatt, L.; Cole, T.R.; Armstrong, R.; Kumar, V.K.; Morrison, P.J.; et al. Tumor risks and genotype-phenotype-proteotype analysis in 358 patients with germline mutations in SDHB and SDHD. *Hum. Mutat.* **2010**, *31*, 41–51. [CrossRef] [PubMed]
25. Benn, D.E.; Gimenez-Roqueplo, A.P.; Reilly, J.R.; Bertherat, J.; Burgess, J.; Byth, K.; Croxson, M.; Dahia, P.L.; Elston, M.; Gimm, O.; et al. Clinical presentation and penetrance of pheochromocytoma/paraganglioma syndromes. *J. Clin. Endocrinol. Metab.* **2006**, *91*, 827–836. [CrossRef] [PubMed]
26. Amar, L.; Baudin, E.; Burnichon, N.; Peyrard, S.; Silvera, S.; Bertherat, J.; Bertagna, X.; Schlumberger, M.; Jeunemaitre, X.; Gimenez-Roqueplo, A.P.; et al. Succinate dehydrogenase b gene mutations predict survival in patients with malignant pheochromocytomas or paragangliomas. *J. Clin. Endocrinol. Metab.* **2007**, *92*, 3822–3828. [CrossRef] [PubMed]
27. Burnichon, N.; Briere, J.J.; Libe, R.; Vescovo, L.; Riviere, J.; Tissier, F.; Jouanno, E.; Jeunemaitre, X.; Benit, P.; Tzagoloff, A.; et al. SDHA is a tumor suppressor gene causing paraganglioma. *Hum. Mol. Genet.* **2010**, *19*, 3011–3020. [CrossRef] [PubMed]
28. Hao, H.X.; Khalimonchuk, O.; Schraders, M.; Dephoure, N.; Bayley, J.P.; Kunst, H.; Devilee, P.; Cremers, C.W.; Schiffman, J.D.; Bentz, B.G.; et al. SDH5, a gene required for flavination of succinate dehydrogenase, is mutated in paraganglioma. *Science* **2009**, *325*, 1139–1142. [CrossRef] [PubMed]
29. Korpershoek, E.; Favier, J.; Gaal, J.; Burnichon, N.; van Gessel, B.; Oudijk, L.; Badoual, C.; Gadessaud, N.; Venisse, A.; Bayley, J.P.; et al. SDHA immunohistochemistry detects germline SDHA gene mutations in apparently sporadic paragangliomas and pheochromocytomas. *J. Clin. Endocrinol. Metab.* **2011**, *96*, E1472–E1476. [CrossRef] [PubMed]

30. Van Nederveen, F.H.; Gaal, J.; Favier, J.; Korpershoek, E.; Oldenburg, R.A.; de Bruyn, E.M.; Sleddens, H.F.; Derkx, P.; Riviere, J.; Dannenberg, H.; et al. An immunohistochemical procedure to detect patients with paraganglioma and phaeochromocytoma with germline SDHB, SDHC, or SDHD gene mutations: A retrospective and prospective analysis. *Lancet Oncol.* **2009**, *10*, 764–771. [CrossRef]
31. Menara, M.; Oudijk, L.; Badoual, C.; Bertherat, J.; Lepoutre-Lussey, C.; Amar, L.; Iturrioz, X.; Sibony, M.; Zinzindohoue, F.; de Krijger, R.; et al. SDHD immunohistochemistry: A new tool to validate SDHx mutations in pheochromocytoma/paraganglioma. *J. Clin. Endocrinol. Metab.* **2015**, *100*, E287–E291. [CrossRef] [PubMed]
32. Vanharanta, S.; Buchta, M.; McWhinney, S.R.; Virta, S.K.; Peczkowska, M.; Morrison, C.D.; Lehtonen, R.; Januszewicz, A.; Jarvinen, H.; Juhola, M.; et al. Early-onset renal cell carcinoma as a novel extraparaganglial component of SDHB-associated heritable paraganglioma. *Am. J. Hum. Genet.* **2004**, *74*, 153–159. [CrossRef] [PubMed]
33. Kuroda, N.; Yorita, K.; Nagasaki, M.; Harada, Y.; Ohe, C.; Jeruc, J.; Raspollini, M.R.; Michal, M.; Hes, O.; Amin, M.B. Review of succinate dehydrogenase-deficient renal cell carcinoma with focus on clinical and pathobiological aspects. *Pol. J. Pathol.* **2016**, *67*, 3–7. [CrossRef] [PubMed]
34. Gill, A.J.; Hes, O.; Papathomas, T.; Sedivcova, M.; Tan, P.H.; Agaimy, A.; Andresen, P.A.; Kedziora, A.; Clarkson, A.; Toon, C.W.; et al. Succinate dehydrogenase (SDH)-deficient renal carcinoma: A morphologically distinct entity: A clinicopathologic series of 36 tumors from 27 patients. *Am. J. Surg. Pathol.* **2014**, *38*, 1588–1602. [CrossRef] [PubMed]
35. Stratakis, C.A.; Carney, J.A. The triad of paragangliomas, gastric stromal tumours and pulmonary chondromas (carney triad), and the dyad of paragangliomas and gastric stromal sarcomas (carney-stratakis syndrome): Molecular genetics and clinical implications. *J. Intern. Med.* **2009**, *266*, 43–52. [CrossRef] [PubMed]
36. Boikos, S.A.; Pappo, A.S.; Killian, J.K.; LaQuaglia, M.P.; Weldon, C.B.; George, S.; Trent, J.C.; von Mehren, M.; Wright, J.A.; Schiffman, J.D.; et al. Molecular subtypes of KIT/PDGFRA wild-type gastrointestinal stromal tumors: A report from the national institutes of health gastrointestinal stromal tumor clinic. *JAMA Oncol.* **2016**, *2*, 922–928. [CrossRef] [PubMed]
37. Killian, J.K.; Miettinen, M.; Walker, R.L.; Wang, Y.; Zhu, Y.J.; Waterfall, J.J.; Noyes, N.; Retnakumar, P.; Yang, Z.; Smith, W.I., Jr.; et al. Recurrent epimutation of SDHC in gastrointestinal stromal tumors. *Sci. Transl. Med.* **2014**, *6*. [CrossRef] [PubMed]
38. Haller, F.; Moskalev, E.A.; Faucz, F.R.; Barthelmess, S.; Wiemann, S.; Bieg, M.; Assie, G.; Bertherat, J.; Schaefer, I.M.; Otto, C.; et al. Aberrant DNA hypermethylation of SDHC: A novel mechanism of tumor development in carney triad. *Endocr. Relat. Cancer* **2014**, *21*, 567–577. [CrossRef] [PubMed]
39. Richter, S.; Klink, B.; Nacke, B.; de Cubas, A.A.; Mangelis, A.; Rapizzi, E.; Meinhardt, M.; Skondra, C.; Mannelli, M.; Robledo, M.; et al. Epigenetic mutation of the succinate dehydrogenase c promoter in a patient with two paragangliomas. *J. Clin. Endocrinol. Metab.* **2016**, *101*, 359–363. [CrossRef] [PubMed]
40. Tomlinson, I.P.; Alam, N.A.; Rowan, A.J.; Barclay, E.; Jaeger, E.E.; Kelsell, D.; Leigh, I.; Gorman, P.; Lamlum, H.; Rahman, S.; et al. Germline mutations in FH predispose to dominantly inherited uterine fibroids, skin leiomyomata and papillary renal cell cancer. *Nat. Genet.* **2002**, *30*, 406–410. [CrossRef] [PubMed]
41. Gardie, B.; Remenieras, A.; Kattygnarath, D.; Bombled, J.; Lefevre, S.; Perrier-Trudova, V.; Rustin, P.; Barrois, M.; Slama, A.; Avril, M.F.; et al. Novel FH mutations in families with hereditary leiomyomatosis and renal cell cancer (HLRCC) and patients with isolated type 2 papillary renal cell carcinoma. *J. Med. Genet.* **2011**, *48*, 226–234. [CrossRef] [PubMed]
42. Menko, F.H.; Maher, E.R.; Schmidt, L.S.; Middelton, L.A.; Aittomaki, K.; Tomlinson, I.; Richard, S.; Linehan, W.M. Hereditary leiomyomatosis and renal cell cancer (HLRCC): Renal cancer risk, surveillance and treatment. *Fam. Cancer* **2014**, *13*, 637–644. [CrossRef] [PubMed]
43. Letouze, E.; Martinelli, C.; Loriot, C.; Burnichon, N.; Abermil, N.; Ottolenghi, C.; Janin, M.; Menara, M.; Nguyen, A.T.; Benit, P.; et al. SDH mutations establish a hypermethylator phenotype in paraganglioma. *Cancer Cell* **2013**, *23*, 739–752. [CrossRef] [PubMed]
44. Castro-Vega, L.J.; Buffet, A.; De Cubas, A.A.; Cascon, A.; Menara, M.; Khalifa, E.; Amar, L.; Azriel, S.; Bourdeau, I.; Chabre, O.; et al. Germline mutations in FH confer predisposition to malignant pheochromocytomas and paragangliomas. *Hum. Mol. Genet.* **2014**, *23*, 2440–2446. [CrossRef] [PubMed]

45. Clark, G.R.; Sciacovelli, M.; Gaude, E.; Walsh, D.M.; Kirby, G.; Simpson, M.A.; Trembath, R.C.; Berg, J.N.; Woodward, E.R.; Kinning, E.; et al. Germline FH mutations presenting with pheochromocytoma. *J. Clin. Endocrinol. Metab.* **2014**, *99*, E2046–E2050. [CrossRef] [PubMed]
46. Lorendeau, D.; Rinaldi, G.; Boon, R.; Spincemaille, P.; Metzger, K.; Jager, C.; Christen, S.; Dong, X.; Kuenen, S.; Voordeckers, K.; et al. Dual loss of succinate dehydrogenase (SDH) and complex i activity is necessary to recapitulate the metabolic phenotype of SDH mutant tumors. *Metab. Eng.* **2016**. [CrossRef] [PubMed]
47. Burnichon, N.; Vescovo, L.; Amar, L.; Libe, R.; de Reynies, A.; Venisse, A.; Jouanno, E.; Laurendeau, I.; Parfait, B.; Bertherat, J.; et al. Integrative genomic analysis reveals somatic mutations in pheochromocytoma and paraganglioma. *Hum. Mol. Genet.* **2011**, *20*, 3974–3985. [CrossRef] [PubMed]
48. Dahia, P.L.; Ross, K.N.; Wright, M.E.; Hayashida, C.Y.; Santagata, S.; Barontini, M.; Kung, A.L.; Sanso, G.; Powers, J.F.; Tischler, A.S.; et al. A HIF1α regulatory loop links hypoxia and mitochondrial signals in pheochromocytomas. *PLoS Genet.* **2005**, *1*, 72–80. [CrossRef] [PubMed]
49. Lando, D.; Peet, D.J.; Gorman, J.J.; Whelan, D.A.; Whitelaw, M.L.; Bruick, R.K. FIH-1 is an asparaginyl hydroxylase enzyme that regulates the transcriptional activity of hypoxia-inducible factor. *Genes Dev.* **2002**, *16*, 1466–1471. [CrossRef] [PubMed]
50. Tahiliani, M.; Koh, K.P.; Shen, Y.; Pastor, W.A.; Bandukwala, H.; Brudno, Y.; Agarwal, S.; Iyer, L.M.; Liu, D.R.; Aravind, L.; et al. Conversion of 5-methylcytosine to 5-hydroxymethylcytosine in mammalian DNA by MLL partner TET1. *Science* **2009**, *324*, 930–935. [CrossRef] [PubMed]
51. Ito, S.; D'Alessio, A.C.; Taranova, O.V.; Hong, K.; Sowers, L.C.; Zhang, Y. Role of Tet proteins in 5mC to 5hmC conversion, ES-cell self-renewal and inner cell mass specification. *Nature* **2010**, *466*, 1129–1133. [CrossRef] [PubMed]
52. Killian, J.K.; Kim, S.Y.; Miettinen, M.; Smith, C.; Merino, M.; Tsokos, M.; Quezado, M.; Smith, W.I., Jr.; Jahromi, M.S.; Xekouki, P.; et al. Succinate dehydrogenase mutation underlies global epigenomic divergence in gastrointestinal stromal tumor. *Cancer Discov.* **2013**, *3*, 648–657. [CrossRef] [PubMed]
53. Tarayrah, L.; Chen, X. Epigenetic regulation in adult stem cells and cancers. *Cell Biosci.* **2013**, *3*, 41. [CrossRef] [PubMed]
54. Grassian, A.R.; Lin, F.; Barrett, R.; Liu, Y.; Jiang, W.; Korpal, M.; Astley, H.; Gitterman, D.; Henley, T.; Howes, R.; et al. Isocitrate dehydrogenase (IDH) mutations promote a reversible zeb1/microrna (MIR)-200-dependent epithelial-mesenchymal transition (EMT). *J. Biol. Chem.* **2012**, *287*, 42180–42194. [CrossRef] [PubMed]
55. Loriot, C.; Burnichon, N.; Gadessaud, N.; Vescovo, L.; Amar, L.; Libe, R.; Bertherat, J.; Plouin, P.F.; Jeunemaitre, X.; Gimenez-Roqueplo, A.P.; et al. Epithelial to mesenchymal transition is activated in metastatic pheochromocytomas and paragangliomas caused by SDHB gene mutations. *J. Clin. Endocrinol. Metab.* **2012**, *97*, E954–E962. [CrossRef] [PubMed]
56. Loriot, C.; Domingues, M.; Berger, A.; Menara, M.; Ruel, M.; Morin, A.; Letouzé, E.; Bemelmans, A.P.; Larue, L.; Gimenez-Roqueplo, A.P.; et al. Deciphering the molecular basis of invasiveness in SDHB-deficient cells. *Oncotarget* **2015**, *6*, 32955–32965. [PubMed]
57. Sciacovelli, M.; Goncalves, E.; Johnson, T.I.; Zecchini, V.R.; da Costa, A.S.; Gaude, E.; Drubbel, A.V.; Theobald, S.J.; Abbo, S.R.; Tran, M.G.; et al. Fumarate is an epigenetic modifier that elicits epithelial-to-mesenchymal transition. *Nature* **2016**, *537*, 544–547. [CrossRef] [PubMed]
58. Dang, L.; White, D.W.; Gross, S.; Bennett, B.D.; Bittinger, M.A.; Driggers, E.M.; Fantin, V.R.; Jang, H.G.; Jin, S.; Keenan, M.C.; et al. Cancer-associated IDH1 mutations produce 2-hydroxyglutarate. *Nature* **2009**, *462*, 739–744. [CrossRef] [PubMed]
59. Hahn, N.M.; Reckova, M.; Cheng, L.; Baldridge, L.A.; Cummings, O.W.; Sweeney, C.J. Patient with malignant paraganglioma responding to the multikinase inhibitor sunitinib malate. *J. Clin. Oncol.* **2009**, *27*, 460–463. [CrossRef] [PubMed]
60. Jimenez, C.; Cabanillas, M.E.; Santarpia, L.; Jonasch, E.; Kyle, K.L.; Lano, E.A.; Matin, S.F.; Nunez, R.F.; Perrier, N.D.; Phan, A.; et al. Use of the tyrosine kinase inhibitor sunitinib in a patient with von hippel-lindau disease: Targeting angiogenic factors in pheochromocytoma and other von hippel-lindau disease-related tumors. *J. Clin. Endocrinol. Metab.* **2009**, *94*, 386–391. [CrossRef] [PubMed]
61. Joshua, A.M.; Ezzat, S.; Asa, S.L.; Evans, A.; Broom, R.; Freeman, M.; Knox, J.J. Rationale and evidence for sunitinib in the treatment of malignant paraganglioma/pheochromocytoma. *J. Clin. Endocrinol. Metab.* **2009**, *94*, 5–9. [CrossRef] [PubMed]

62. Park, K.S.; Lee, J.L.; Ahn, H.; Koh, J.M.; Park, I.; Choi, J.S.; Kim, Y.R.; Park, T.S.; Ahn, J.H.; Lee, D.H.; et al. Sunitinib, a novel therapy for anthracycline- and cisplatin-refractory malignant pheochromocytoma. *Jpn. J. Clin. Oncol.* **2009**, *39*, 327–331. [CrossRef] [PubMed]
63. Ayala-Ramirez, M.; Chougnet, C.N.; Habra, M.A.; Palmer, J.L.; Leboulleux, S.; Cabanillas, M.E.; Caramella, C.; Anderson, P.; Al Ghuzlan, A.; Waguespack, S.G.; et al. Treatment with sunitinib for patients with progressive metastatic pheochromocytomas and sympathetic paragangliomas. *J. Clin. Endocrinol. Metab.* **2012**, *97*, 4040–4050. [CrossRef] [PubMed]
64. Chen, W.; Hill, H.; Christie, A.; Kim, M.S.; Holloman, E.; Pavia-Jimenez, A.; Homayoun, F.; Ma, Y.; Patel, N.; Yell, P.; et al. Targeting renal cell carcinoma with a HIF-2 antagonist. *Nature* **2016**, *539*, 112–117. [CrossRef] [PubMed]
65. Cho, H.; Du, X.; Rizzi, J.P.; Liberzon, E.; Chakraborty, A.A.; Gao, W.; Carvo, I.; Signoretti, S.; Bruick, R.K.; Josey, J.A.; et al. On-target efficacy of a HIF-2α antagonist in preclinical kidney cancer models. *Nature* **2016**, *539*, 107–111. [CrossRef] [PubMed]
66. Taby, R.; Issa, J.P. Cancer epigenetics. *Cancer J. Clin.* **2010**, *60*, 376–392. [CrossRef] [PubMed]
67. Powers, J.F.; Korgaonkar, P.G.; Fliedner, S.; Giubellino, A.; Pacak, K.; Sahagian, G.G.; Tischler, A.S. Cytocidal activities of topoisomerase 1 inhibitors and 5-azacytidine against pheochromocytoma/paraganglioma cells in primary human tumor cultures and mouse cell lines. *PLoS ONE* **2014**, *9*, e87807. [CrossRef] [PubMed]
68. Esteller, M.; Garcia-Foncillas, J.; Andion, E.; Goodman, S.N.; Hidalgo, O.F.; Vanaclocha, V.; Baylin, S.B.; Herman, J.G. Inactivation of the DNA-repair gene mgmt and the clinical response of gliomas to alkylating agents. *N. Engl. J. Med.* **2000**, *343*, 1350–1354. [CrossRef] [PubMed]
69. Hegi, M.E.; Diserens, A.C.; Gorlia, T.; Hamou, M.F.; de Tribolet, N.; Weller, M.; Kros, J.M.; Hainfellner, J.A.; Mason, W.; Mariani, L.; et al. Mgmt gene silencing and benefit from temozolomide in glioblastoma. *N. Engl. J. Med.* **2005**, *352*, 997–1003. [CrossRef] [PubMed]
70. Hadoux, J.; Favier, J.; Scoazec, J.Y.; Leboulleux, S.; Al Ghuzlan, A.; Caramella, C.; Deandreis, D.; Borget, I.; Loriot, C.; Chougnet, C.; et al. Sdhb mutations are associated with response to temozolomide in patients with metastatic pheochromocytoma or paraganglioma. *Int. J. Cancer* **2014**, *135*, 2711–2720. [CrossRef] [PubMed]
71. Ward, P.S.; Thompson, C.B. Metabolic reprogramming: A cancer hallmark even warburg did not anticipate. *Cancer Cell* **2012**, *21*, 297–308. [CrossRef] [PubMed]
72. Tennant, D.A.; Duran, R.V.; Boulahbel, H.; Gottlieb, E. Metabolic transformation in cancer. *Carcinogenesis* **2009**, *30*, 1269–1280. [CrossRef] [PubMed]
73. Aspuria, P.J.; Lunt, S.Y.; Varemo, L.; Vergnes, L.; Gozo, M.; Beach, J.A.; Salumbides, B.; Reue, K.; Wiedemeyer, W.R.; Nielsen, J.; et al. Succinate dehydrogenase inhibition leads to epithelial-mesenchymal transition and reprogrammed carbon metabolism. *Cancer Metab.* **2014**, *2*, 21. [CrossRef] [PubMed]
74. Laurenti, G.; Tennant, D.A. Isocitrate dehydrogenase (IDH), succinate dehydrogenase (SDH), fumarate hydratase (FH): Three players for one phenotype in cancer? *Biochem. Soc. Trans.* **2016**, *44*, 1111–1116. [CrossRef] [PubMed]
75. Lussey-Lepoutre, C.; Hollinshead, K.E.; Ludwig, C.; Menara, M.; Morin, A.; Castro-Vega, L.J.; Parker, S.J.; Janin, M.; Martinelli, C.; Ottolenghi, C.; et al. Loss of succinate dehydrogenase activity results in dependency on pyruvate carboxylation for cellular anabolism. *Nat. Commun.* **2015**, *6*, 8784. [CrossRef] [PubMed]
76. Cardaci, S.; Zheng, L.; MacKay, G.; van den Broek, N.J.; MacKenzie, E.D.; Nixon, C.; Stevenson, D.; Tumanov, S.; Bulusu, V.; Kamphorst, J.J.; et al. Pyruvate carboxylation enables growth of SDH-deficient cells by supporting aspartate biosynthesis. *Nat. Cell Biol.* **2015**, *17*, 1317–1326. [CrossRef] [PubMed]
77. Zheng, L.; Mackenzie, E.D.; Karim, S.A.; Hedley, A.; Blyth, K.; Kalna, G.; Watson, D.G.; Szlosarek, P.; Frezza, C.; Gottlieb, E. Reversed argininosuccinate lyase activity in fumarate hydratase-deficient cancer cells. *Cancer Metab.* **2013**, *1*, 12. [CrossRef] [PubMed]
78. Ternette, N.; Yang, M.; Laroyia, M.; Kitagawa, M.; O'Flaherty, L.; Wolhulter, K.; Igarashi, K.; Saito, K.; Kato, K.; Fischer, R.; et al. Inhibition of mitochondrial aconitase by succination in fumarate hydratase deficiency. *Cell Rep.* **2013**, *3*, 689–700. [CrossRef] [PubMed]
79. Timmers, H.J.; Chen, C.C.; Carrasquillo, J.A.; Whatley, M.; Ling, A.; Eisenhofer, G.; King, K.S.; Rao, J.U.; Wesley, R.A.; Adams, K.T.; et al. Staging and functional characterization of pheochromocytoma and paraganglioma by ^{18}F-fluorodeoxyglucose (^{18}F-FDG) positron emission tomography. *J. Natl. Cancer Inst.* **2012**, *104*, 700–708. [CrossRef] [PubMed]

80. Taieb, D.; Sebag, F.; Barlier, A.; Tessonnier, L.; Palazzo, F.F.; Morange, I.; Niccoli-Sire, P.; Fakhry, N.; De Micco, C.; Cammilleri, S.; et al. ^{18}F-FDG avidity of pheochromocytomas and paragangliomas: A new molecular imaging signature? *J. Nucl. Med.* **2009**, *50*, 711–717. [CrossRef] [PubMed]
81. Timmers, H.J.; Kozupa, A.; Chen, C.C.; Carrasquillo, J.A.; Ling, A.; Eisenhofer, G.; Adams, K.T.; Solis, D.; Lenders, J.W.; Pacak, K. Superiority of fluorodeoxyglucose positron emission tomography to other functional imaging techniques in the evaluation of metastatic SDHB-associated pheochromocytoma and paraganglioma. *J. Clin. Oncol.* **2007**, *25*, 2262–2269. [CrossRef] [PubMed]
82. Plouin, P.F.; Amar, L.; Dekkers, O.M.; Fassnacht, M.; Gimenez-Roqueplo, A.P.; Lenders, J.W.; Lussey-Lepoutre, C.; Steichen, O.; Guideline Working, G. European society of endocrinology clinical practice guideline for long-term follow-up of patients operated on for a phaeochromocytoma or a paraganglioma. *Eur. J. Endocrinol.* **2016**, *174*, G1–G10. [CrossRef] [PubMed]
83. Lepoutre-Lussey, C.; Caramella, C.; Bidault, F.; Deandreis, D.; Berdelou, A.; Al Ghuzlan, A.; Hartl, D.; Borget, I.; Gimenez-Roqueplo, A.P.; Dumont, F.; et al. Screening in asymptomatic SDHx mutation carriers: Added value of ^{18}F-FDG PET/CT at initial diagnosis and 1-year follow-up. *Eur. J. Nucl. Med. Mol. Imaging* **2015**, *42*, 868–876. [CrossRef] [PubMed]
84. Taieb, D.; Timmers, H.J.; Hindie, E.; Guillet, B.A.; Neumann, H.P.; Walz, M.K.; Opocher, G.; de Herder, W.W.; Boedeker, C.C.; de Krijger, R.R.; et al. EANM 2012 guidelines for radionuclide imaging of phaeochromocytoma and paraganglioma. *Imaging* **2012**, *39*, 1977–1995. [CrossRef] [PubMed]
85. Andronesi, O.C.; Kim, G.S.; Gerstner, E.; Batchelor, T.; Tzika, A.A.; Fantin, V.R.; Vander Heiden, M.G.; Sorensen, A.G. Detection of 2-hydroxyglutarate in idh-mutated glioma patients by in vivo spectral-editing and 2D correlation magnetic resonance spectroscopy. *Sci. Transl. Med.* **2012**, *4*, 116ra114. [CrossRef] [PubMed]
86. Choi, C.; Ganji, S.K.; DeBerardinis, R.J.; Hatanpaa, K.J.; Rakheja, D.; Kovacs, Z.; Yang, X.L.; Mashimo, T.; Raisanen, J.M.; Marin-Valencia, I.; et al. 2-hydroxyglutarate detection by magnetic resonance spectroscopy in idh-mutated patients with gliomas. *Nat. Med.* **2012**, *18*, 624–629. [CrossRef] [PubMed]
87. Lussey-Lepoutre, C.; Bellucci, A.; Morin, A.; Buffet, A.; Amar, L.; Janin, M.; Ottolenghi, C.; Zinzindohoue, F.; Autret, G.; Burnichon, N.; et al. In vivo detection of succinate by magnetic resonance spectroscopy as a hallmark of SDHx mutations in paraganglioma. *Clin. Cancer Res.* **2015**, *22*, 1120–1129. [CrossRef] [PubMed]

REVUE 3

Rodent models of pheochromocytoma, parallels in rodent and human tumorigenesis.

Lussey-Lepoutre C, Buffet A, Morin A, Goncalves J, Favier J.

Cell Tissue Res. 2018 May;372(2):379-392.

Cell and Tissue Research (2018) 372:379–392
https://doi.org/10.1007/s00441-018-2797-y

REVIEW

Rodent models of pheochromocytoma, parallels in rodent and human tumorigenesis

Charlotte Lussey-Lepoutre[1,2] · Alexandre Buffet[2,3] · Aurélie Morin[2,3] · Judith Goncalves[2,3] · Judith Favier[2,3]

Received: 10 November 2017 / Accepted: 16 January 2018 / Published online: 9 February 2018

Abstract

Paragangliomas and pheochromocytomas are rare neuroendocrine tumors characterized by a large spectrum of hereditary predisposition. Based on gene expression profiling classification, they can be classically assigned to either a hypoxic/angiogenic cluster (cluster 1 including tumors with mutations in *SDHx*, *VHL* and *FH* genes) or a kinase-signaling cluster (cluster 2 consisting in tumors related to *RET*, *NF1*, *TMEM127* and *MAX* genes mutations, as well as most of the sporadic tumors). The past 15 years have seen the emergence of an increasing number of genetically engineered and grafted models to investigate tumorigenesis and develop new therapeutic strategies. Among them, only cluster 2-related predisposed models have been successful but grafted models are however available to study cluster 1-related tumors. In this review, we present an overview of existing rodent models targeting predisposition genes involved or not in human pheochromocytoma/paraganglioma susceptibility and their contribution to the improvement of pheochromocytoma experimental research.

Keywords Pheochromocytoma · Paraganglioma · Mouse models

Introduction

Pheochromocytoma (PCC) and paraganglioma (PGL) are rare neuroendocrine tumors that arise in chromaffin cells of the adrenal medulla and in sympathetic and parasympathetic paraganglia, respectively. Nearly 40% of patients with pheochromocytoma and/or paraganglioma (PPGL) carry a germline mutation in one of the 13 PPGL predisposing genes identified so far (Favier et al. 2014), including *RET* (leading to multiple endocrine neoplasia type 2A and 2B), *NF1* (causing neurofibromatosis type 1), *VHL* (Von Hippel Lindau disease) and *SDHx* genes (*SDHA*, *SDHB*, *SDHC*, *SDHD*, *SDHAF2*, responsible for hereditary PGL syndrome). Other rare cases involve germline or mosaic mutations in the *FH*, *TMEM127*, *MAX*, *HIF2A* and *MDH2* genes (Cascon et al. 2015; Castro-Vega et al. 2015; Dahia 2014; Favier et al. 2014). In addition, somatic mutations have been reported in 30% of cases, involving the *VHL*, *RET*, *NF1*, *HIF2A*, *ATRX* and *HRAS* genes (Castro-Vega et al. 2015). With the exception of *RET* and *HIF2A* that act as oncogenes, all PPGL susceptibility genes are tumor suppressor genes: patients carry a heterozygous germline mutation and tumor development occurs following a somatic second hit that leads to loss of heterozygosity (LOH) and to the subsequent inactivation of the gene's function.

Over the past few years, gene expression profiling of these rare tumors enabled discovering new PPGL predisposition genes (Burnichon et al. 2010; Cascon et al. 2015; Comino-Mendez et al. 2011; Favier et al. 2012; Letouze et al. 2013; Qin et al. 2010) and classifying PPGLs by classically assigning them to either a hypoxic/angiogenic cluster (cluster 1) or a kinase-signaling cluster (cluster 2) (Burnichon et al. 2011; Dahia et al. 2005; Eisenhofer et al. 2004; Favier et al. 2009; Lopez-Jimenez et al. 2010). Cluster 1 contains all *SDHx*-, *VHL*- and *FH*-mutated tumors (Castro-Vega et al. 2014; Letouze et al. 2013). Cluster 2 comprises tumors related to *RET*, *NF1*, *TMEM127* and *MAX* genes mutations, as well as most of the sporadic tumors.

Between 10% (PCC) to 40% (PGL) of patients will present a malignant progression of their disease, defined by the occurrence of the first metastasis (Lenders et al. 2014) and with a 5-

✉ Judith Favier
judith.favier@inserm.fr

[1] Université Pierre et Marie Curie, Faculté de Médecine, Service de Médecine Nucléaire Hôpital Pitié-Salpêtrière, Paris, France

[2] INSERM UMR970, Paris-Cardiovascular Research Center, Equipe Labellisée Ligue Contre le Cancer, 56 rue Leblanc, F-75015 Paris, France

[3] Sorbonne Paris Cité, Faculté de Médecine, Université Paris Descartes, F-75006 Paris, France

year survival rate below 50%. Mutations in the *SDHB* gene are associated with metastatic, aggressive forms of PPGL (Amar et al. 2007; Gimenez-Roqueplo et al. 2003). Indeed, more than one third of patients with metastatic PPGL carry a germline *SDHB* mutation and half of *SDHB*-mutated patients will ultimately develop a metastatic disease.

Many genetically engineered and grafted mouse models have been generated to investigate the mechanisms of PPGL tumorigenesis, develop new diagnostic biomarkers or test innovative therapeutic strategies. Existing mouse models include mutations on *c-mos*, *Ret*, *ErbB2* and *B-Raf* proto-oncogenes (Lai et al. 2007; Schulz et al. 1992; Smith-Hicks et al. 2000; Urosevic et al. 2011) and inactivation of *Nf1*, *Rb*, *Trp53 Vhl*, *Sdhd*, *Pten* and *InK4a* tumor suppressor genes (Bayley et al. 2009; Gnarra et al. 1997; Haase et al. 2001; Jacks et al. 1994; Korpershoek et al. 2009; Ma et al. 2003; Nikitin et al. 1999; Piruat et al. 2004; You et al. 2002). This review focuses on these existing models aiming at deciphering human tumor development and improving malignant PPGL early diagnosis and treatment.

Predisposed mouse models

Cluster 1

The cluster C1 comprises tumors carrying mutations on *SDHx*, *FH*, *VHL* and *HIF2A* genes. Genes overexpressed in the C1 cluster promote a "pseudo-hypoxic" signature secondary to the direct capacity of *SDHx* and *VHL*-mutated cells to stabilize hypoxia-inducible factors (HIFs) in normoxic conditions, thereby stimulating angiogenesis, proliferation and glycolysis pathways (Favier et al. 2009). *VHL* encodes a member of an E3 ubiquitin ligase complex that addresses HIFα proteins to proteasomal degradation in normoxia. *SDHA-D* genes encode the four subunits of succinate dehydrogenase (SDH) or mitochondrial complex II, an enzyme located at the crossroads between the mitochondrial electron transport chain and the tricarboxylic acid (TCA) cycle (Lancaster and Simon 2002). In PPGL patients carrying a germline heterozygous mutation on a *SDHx* gene, somatic loss of the remaining allele induces a complete SDH loss-of-function, which results in the accumulation of its substrate, succinate in the tumor. Succinate acts as an oncometabolite that is suspected to mediate the tumorigenic effects related to *SDHx* mutations (Letouze et al. 2013): its accumulation inhibits prolyl-hydroxylases activity that finally results in the abnormal stabilization of HIFαs under normoxic conditions (Briere et al. 2005). *SDHx* mutations also impair DNA and histone demethylation processes. Succinate inhibits TET DNA and JmJC histones demethylases, leading to global DNA and histones hypermethylation that has important consequences on gene expression (Letouze et al. 2013). *FH* is also a tumor suppressor gene involved in the TCA cycle, encoding fumarase (or fumarate hydratase), which converts fumarate into malate. As for SDH-related PPGL, fumarate accumulation acts as an oncometabolite (Castro-Vega et al. 2014; Letouze et al. 2013) (Morin et al. 2014) leading to a global histone and DNA hypermethylation in *FH*-related paragangliomas, a high rate of malignancy and a poor prognosis. Altogether these findings underlie the medical need for a reliable preclinical model of "cluster 1-like" tumors.

The (desperate) quest for an SDH-deficient mouse model

Piruat et al. published the first report of SDH complex inactivation in a mouse model in 2004 (Piruat et al. 2004). In this model, the homozygous knockout (KO) of *Sdhd* was lethal at an embryonic stage (E7) while heterozygous *Sdhd* inactivation induces a slight hyperplasia of the carotid body (CB) and a significant increase of spontaneous CB activity under normoxic conditions but without any CB PGL nor PCC (Piruat et al. 2004). Several years later, a second *Sdhd*-knockout mouse model was generated. They observed the same results even after crossing them with a strain knocked-out for a candidate imprinted modifier gene ($H19^{+/-}$ mice) in order to mimic the "imprinted" inheritance of *SDHD* tumorigenesis observed in human (Bayley et al. 2009). Finally, two conditional *Sdhd* KO were reported. One allowed a tissue-specific Sdhd deletion driven by the tyrosine hydroxylase promoter in the catecholaminergic system and the other one a tamoxifen-induced LOH at adulthood. None of these models resulted in PPGL. In contrast, they led to a reduced size of carotid bodies and to decreased cell numbers in the adrenal medulla (Diaz-Castro et al. 2012).

Two different teams reported negative results regarding engineering a *Sdhb*-deficient mouse model (Lepoutre-Lussey et al. 2015; Maher III et al. 2011).

Maher et al. did not observe any PPGL development in their heterozygous constitutional *Sdhb*-deficient mouse model, even after crossing them with a mouse deficient for *Bub 1*, *a* gene playing a key role in the mitotic checkpoint (Maher III et al. 2011).

As embryonic death of nullizygous *Sdhb* mice was predictable, our strategy was to use the Cre-Lox system to generate both a constitutive and a conditional inactivation of the gene. To that aim, LoxP sites were inserted on both sides of *Sdhb* exon 2 (Lepoutre-Lussey et al. 2015; Letouze et al. 2013). The constitutive knockout model was obtained by crossing *Sdhb*-floxed mice with PGK-Crem mice and two tissue-specific conditional KO models were generated using tyrosine hydroxylase-Cre (TH-Cre), expected to drive Cre recombinase expression in all catecholaminergic cells (Gelman et al. 2003) or human Prostate-Specific Antigen-Cre (PSA-Cre), supposedly specific of the prostate in human but actually driving expression in the adrenal medulla in

mouse (Korpershoek et al. 2009). Unfortunately, after a long-life follow-up of a large cohort including heterozygous constitutive and tissue specific Sdhb KO mice, no indication of chromaffin tumor development was apparent in any animal (Lepoutre-Lussey et al. 2015).

In a second step, because of the failure of the pure *Sdhb* KO model, we crossed them under a *Pten* KO background, which was previously reported to be predisposed to PCC (You et al. 2002), in order to generate a metastatic PCC experimental model harboring an inactivation of the Sdhb gene. At 10 months, 37% of the double conditional KO homozygous for Sdhb deletion mice (Ptenlox/lox, Sdhblox/lox, PSA-Cre and Pten+/lox, Sdhblox/lox, PSA-Cre) developed a PCC (instead of more than 70% in the Pten+/− KO mouse model) but in contrast with human tumors (Pollard et al. 2005), no accumulation of succinate was detected in any of these tumors suggesting the absence of Sdhb deletion in the tumor. This result, together with the lower incidence of PCC, suggest a cellular lethality of Sdhb complete KO in mouse, as shown for the *Sdhd* conditional KO (Diaz-Castro et al. 2012). The generation of a predisposed SDH-related model of PGL or PCC probably requires a "second hit" that would allow paraganglioma tumorigenesis in rodents.

Vhl- and *Fh*-deficient mice

The Von Hippel Lindau disease is a rare autosomal dominant hereditary neoplastic syndrome caused by mutations in the *VHL* tumor suppressor gene, which are responsible for a predisposition to renal cell carcinoma (RCC), retinal or central nervous system hemangioblastomas, pancreatic cysts and PPGL (Kim and Kaelin 2004).

The homozygous KO of *Vhl* in mice results in embryonic lethality secondary to a lack of placental vasculogenesis (Gnarra et al. 1997), while the phenotype of heterozygous *Vhl* mice is strongly dependent on their genetic background. Indeed, no phenotype was observed in $Vhl^{+/-}$ mice bred in a mixed C57BL6/c129 genetic background (Gnarra et al. 1997), while $Vhl^{+/-}$ in a BALB/c129 background developed cavernous liver hemangiomas with a high phenotypic penetrance (Haase et al. 2001). Several tissue-specific V*hl* KO models were generated (first in the liver (Haase et al. 2001) and then in the kidney, epidermis, thymus…) leading to several vascular tumors and renal cysts (for review see Haase 2005). Although about 90% of clear cell renal cell carcinomas (RCC) harbor biallellic inactivation of *VHL* (Sato et al. 2013), most of renal cell-specific *Vhl* KO failed to develop RCC. Recently, Harlander et al. showed that the development of RCC in *Vhl*-deficient mice needed the combination of 2 other combined deletions in *Trp53* and *Rb1* genes suggesting that *Vhl* deficiency is not sufficient for RCC formation (Harlander et al. 2017).

To our knowledge, only one specific *Vhl* KO in catecholaminergic cells was generated using the TH promoter (Macias et al. 2014). Interestingly, in contrast with the expected role of *VHL* as a tumor suppressor gene in human, conditional *Vhl* inactivation in catecholaminergic mouse cells did not lead to a tumor development but in the contrary to an important atrophy of targeted organs such as CB, adrenomedulla and sympathetic ganglia. These impairments were also associated with intolerance to hypoxia in the absence of hypoxia-induced CB hypertrophy in adult mice (Macias et al. 2014). These results were confirmed, to a lesser extend but always without any PPGL development, with a conditional *Vhl* KO during adulthood thanks to an inducible conditional KO (TH-CRE^{ER}-VHL^{KO}) (Macias et al. 2014).

Germline mutations in the tumor suppressor gene *FH* predispose in human to Reed syndrome, also known as Hereditary leiomyomatosis and renal cell cancer (HLRCC) (Tomlinson et al. 2002; Toro et al. 2003). This autosomal dominant disease associates smooth muscle tumors (leiomyomas) in the skin (more than 70% of *FH*-mutation carriers develop cutaneous leiomyoma) and uterus (about 82% of women develop uterine leiomyoma). Affected patients are at risk of developing benign renal cysts and type 2 papillary renal carcinoma. Recently, we demonstrated that *FH* gene germline mutations can also predispose to PPGL (Letouze et al. 2013) and, as in patients with *SDHB* mutation, lead to malignant or multiple forms of the disease (Castro-Vega et al. 2014; Clark et al. 2014).

Pollard et al. generated a mouse model of FH deficiency with a particular interest in kidney cancer development (Pollard et al. 2007). Again, $Fh1^{-/-}$ mice died during early embryogenesis, while tissue-specific targeting of *Fh1* in the kidney ($Fh1^{lox/lox}$;Ksp1.3/Cre animals), results in renal cysts but no RCC, as a direct consequence of HIF1α (and HIF2α) overexpression (Pollard et al. 2007) but without a clear demonstration of the link between tumor development and activation of the hypoxic pathway while the phenotype observed in *Fh* KO mice is not rescued but even worsened by the inactivation of HIF1 (Adam et al. 2011). No specific *Fh* inactivation in the adrenal medulla has been performed so far.

Cluster 2A

Cluster C2A comprises *RET*-, *NF1*-, *MAX*- and *TMEM127*-mutated tumors, as well as most sporadic tumors, including the recently described hotspot somatic mutation in *HRAS* (Castro-Vega et al. 2015). These tumors display activation of the RAS/mitogen-activated protein kinase (MAPK) and IGF1 signaling pathways, predisposing in human to the development of usually benign PCC with a very low incidence of PGL and malignant tumors (Table 1, Fig. 1).

Table 1 Rodent models of pheochromocytomas

Model type	Human expression cluster	Human syndrome	Gene	Mouse model	PPGL (%) and age of onset	Other phenotype	Cell lines	References
Genetically predisposed mouse models	Cluster 1	No model						
	Cluster 2	NF1	*NF1*	*Nf1−/−*	–	Embryonic lethal (E13.5)	–	Jacks 1994
				Nf1+/−	PCC (10–20%), 15–28 months	Myeloid leukemia		
					–	–	MPC	Powers 2000
		MEN2B	*RET*	Met918Thr (het)	Chromaffin cell hyperplasia (16%)	C-cell hyperplasia (up to 41% at 12 months)	–	Smith-Hicks 2000
				Met918Thr (homo)	PCC (100%), 6–10 months	C-cell hyperplasia (up to 60% at 10 months)	–	
							–	
		Retinoblastoma	*Rb*	*Rb +/−*	PCC 71% (14% bilateral) 12 months	C-cell thyroid carcinomas 81% 12 months. Pituitary, parathyroid, lung, pancreas tumors	–	Nikitin 1999
				Rb1F2/F2:Trp53F2–10/F2–10:TEC1	Bilateral PCC (100%), 4 months		–	Tonks 2010
		None	*c-mos*	Transgenic	Bilateral PCC (58%), 8 months	C-cell thyroid carcinomas; gliosis; axonal degeneration	–	Schultz 1992
		None	*B-Raf*	*B-RafV600E*	PCC and PGL (80%), 5 months	Cardio-faciocutaneous syndrome		Urosevic 2011
		None	*CerS2*	*CerS2$^{GT/GT}$ (CerS2null)*	Medullary hyperplasia (100%) Bilateral PCC (54%)	Hepatopathy, emphysema, demyelination	–	Park 2015
		None	*ErbB2*	PB-*ErbB2*	Adrenal hypertrophy (5%) PCC (5% of males), 15 months	Prostate intraepithelial neoplasia	–	Lai 2007
		Cowden syndrome	*PTEN*	*Ink4a Arf+/+; Pten+/−*	PCC (24%), 10.5 months	Prostate, breast and endometrial hyperplasia. Lymphoma; pulmonary and colon carcinoma sarcoma	–	You 2002
				Ink4a Arf+/−; Pten+/−	PCC (57%), 7.5 months			
				Ink4a Arf−/−; Pten+/−	PCC (59%), 6 months			
				PSA-Cre; *Pten*loxP/loxP	PCC from 30%, 7–9 months to 100%, 15–16 months	Prostate tumors	–	Korpershoek 2009
Xeno- and allografted tumors	Cluster 1	Familial PGL	*SDHB*	Allograft *Sdhb −/−*	Subcutaneous tumors	–	Immortalized mouse chromaffin cells "ImCC"	Lussey-Lepoutre 2016
				Xenograft ShRNA-*SDHB*	Subcutaneous tumors	–	143B human osteosarcoma	Guzy 2008

Table 1 (continued)

Model type	Human expression cluster	Human syndrome	Gene	Mouse model	PPGL (%) and age of onset	Other phenotype	Cell lines	References
				Xenograft human PGL and a human PGL-liver metastasis	Small subcutaneous tumors	–	–	Powers 2017
	Cluster 2	NF1	*NF1*	Allograft *Nf1*+/–	Subcutaneous and metastatic tumors	–	Mouse PCC cells "MPC"	Ohta 2008
					Metastatic tumors	–	Mouse tumor tissue "MTT"	Martiniova 2009
		Familial PCC	*MAX*	Xenograft *Max* −/–	Subcutaneous tumors	–	Rat PC 12 cells	Denorme 2015
		Sporadic PGL	–	Xenograft human sporadic PGL	Small subcutaneous tumors	–	–	Powers 2017

PCC pheochromocytoma, *PGL* paraganglioma, *NF1* neurofibromatosis type 1, *MEN* multiple endocrine neoplasia

Genes linked to PPGL predisposition in human

Nf1 *NF1* is a very large gene (60 exons) (Viskochil et al. 1990) encoding neurofibromin, a repressor of the RAS–RAF–MAPK signaling cascade. Heterozygous mutations in this gene were identified in the early nineties as being responsible for neurofibromatosis type 1, also known as Von Recklinghausen disease, one of the most frequent autosomic disorders (prevalence of 1 in 3000 to 1 in 4000 people in the general population and a high penetrance) characterized by pigmentary abnormalities and neoplastic growth of neural crest-derived cells, such as multiple dermal neurofibromas and very rarely PCC (0.1–5.7% of patients with NF1) (Gutmann et al. 1997).

As an important tumor suppressor, homozygous deletion of Nf1 in mouse leads to embryonic lethality. The heterozygous Nf1 knockout mouse model partially mimics the human syndrome as mice develop PCC (but at a much higher frequency, ~ 10–20% lifetime incidence) without any neurofibromas (Jacks et al. 1994). However, an interesting observation with this model is that, as already observed in the Vhl mice, the great influence of the genetic background. Indeed, PCC only arose in mice with a mixed genetic background (Powers et al. 2000). One possible explanation for this is the varying levels of neurofibromin expression depending on the mouse strain. Indeed, strain-dependent tissue-specific modifiers may modulate Nf1 expression to levels comparable to that of mutation of one *Nf1* allele. Hence, haploinsufficient models may be extremely different from one another depending on the genetic background (Hawes et al. 2007).

Ret *RET is a* proto-oncogene encoding a tyrosine kinase receptor activating, after binding of its ligands, the PI3K–AKT and MAPK–ERK signaling pathways (Ibanez 2013; Wagner et al. 2012). Gain-of-function mutations in *RET* proto-oncogene cause multiple endocrine neoplasia type 2 (MEN2), a rare autosomal dominant disorder comprising 2 syndromes: MEN2A, associating medullary thyroid carcinoma, PCC and hyperparathyroidism and caused by several germline mutations frequently affecting codon 634 and MEN 2B (accounting only for 5% of MEN2 cases) defined by severe medullary thyroid carcinoma, PCC, Marfanoid habitus, mucosal neuromas and ganglioneuromatosis of the gut and the intestine and exclusively secondary to a unique point mutation at codon 918 (M918T) (Carlson et al. 1994) .

Only one PCC model was secondary to a direct activating mutation (Met918thr) of the *RET* proto-oncogene, the mutation involved in MEN2B in human (Smith-Hicks et al. 2000). At 6 months, 100% of the homozygous RetMEN2B mice developed a PCC. In contrast with the human phenotype, these mice developed thyroid C-cell hyperplasia (the presumed precursor of carcinoma in human) but no MTC (Smith-Hicks et al. 2000). MEN 2A mouse models secondary

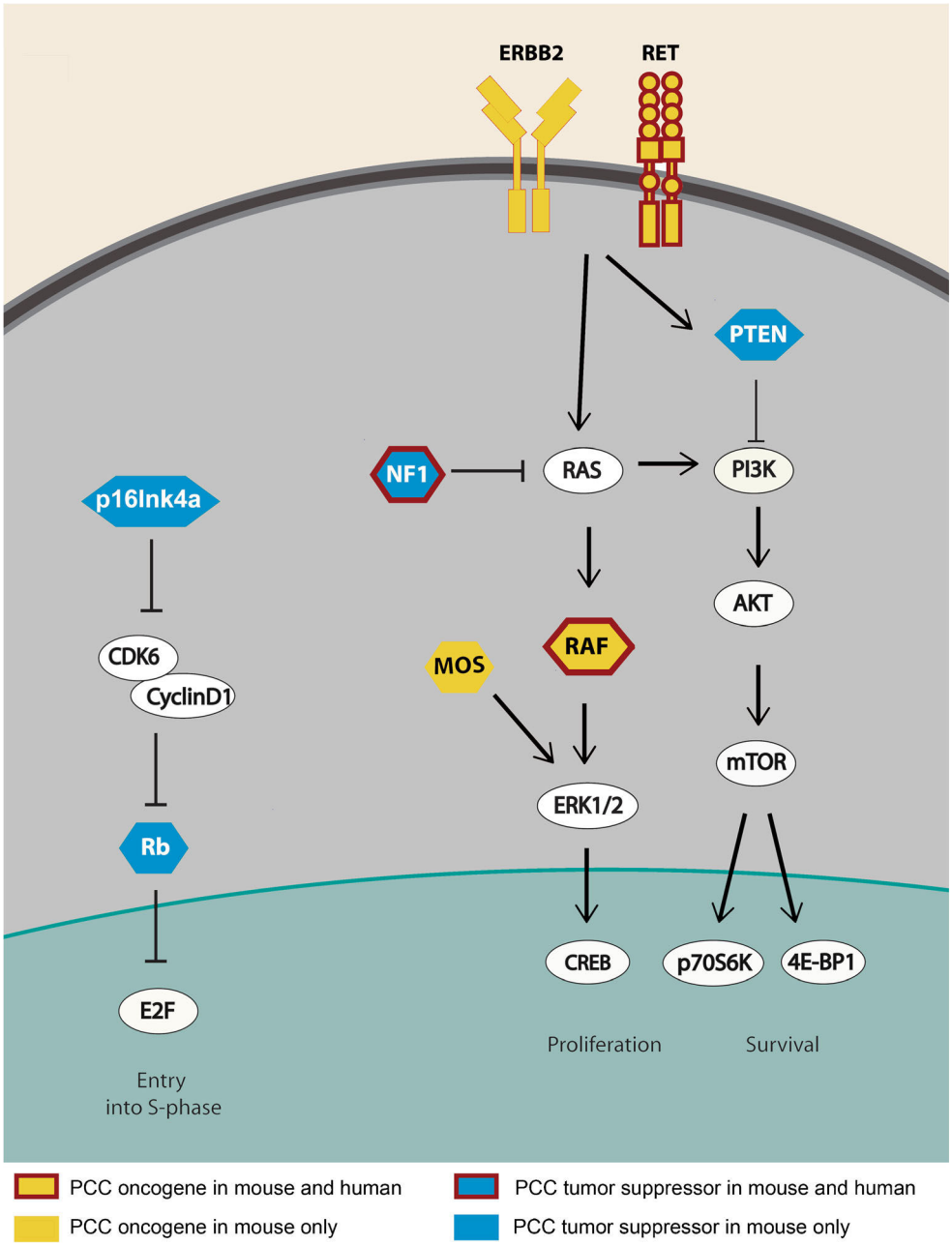

Fig. 1 Signaling pathways associated with the development of pheochromocytomas in mouse

to RET mutations affecting codon 634 predispose to MTC but without chromaffin tumor (Michiels et al. 1997; Reynolds et al. 2001). These different phenotypes may be explained by the different consequences of MEN 2A and MEN 2B causing mutations. Indeed, all MEN 2 mutations result in a stimulation of RET tyrosine kinase receptor but through different mechanisms of activation. MEN 2A 634 mutations involve cysteine residues in the RET extracellular domain resulting in ligand-independent dimerization and constitutive activation of the phosphorylating cascade. In contrast, the M918T substitution seems to convert the substrate-binding pocket of RET to resemble those of non-receptor src-related tyrosine kinases. More recently, it was shown to increase intrinsic kinase activity, partially release kinase autoinhibition and facilitate ligand-independent phosphorylation of 2B-RET receptors (Gujral et al. 2006).

Predisposing genes in mice without parallel human PPGL disease: *c-mos*, *Rb*, *B-Raf*, *Pten/InK4a*, *p53*, *Rb*, *ErbB2* and *CerS2*

Other genetically engineered mice with mutations not associated with PPGL susceptibility in humans have surprisingly been shown to be predisposed to PPGL.

The very first report of a PCC mouse model was linked to the RET signaling pathway, when Schultz et al. studied four

lines of transgenic *c-mos* mice in 1992 (Schulz et al. 1992). In addition to severe neurological defects and lens abnormalities, three of these *mos* transgenic lines presented neuroendocrine tumors similar to the human MEN2 associating a high frequency of bilateral PCC (58%) with MTC. Thereafter, a mouse with a heterozygous loss-of-function mutation of the retinoblastoma tumor suppressor (*Rb+/−*) developed a phenotype combining MTC and 71% of PCC (14% bilateral) (Nikitin et al. 1999). This later pathway is strongly associated with PCC in mouse as the dual loss of *Rb1* and *Trp53* in the adrenal medulla (using a Tyrosinase promoter driven Cre) also leads to PCC, without metastasis (Tonks et al. 2010).

Mutations in the *PTEN* tumor suppressor gene (involved in the negative regulation of the PI3K/AKT signaling pathway) have as main consequences in humans the Cowden syndrome associating several tumors (hamartomas, breast, thyroid and endometrium cancers) but no PCC (Puc et al. 2006; van Nederveen et al. 2006). Co-existing inactivation of *PTEN* and of *INK4a*, (which encodes 2 tumor suppressors (p16INK4a and p19ARF) that regulate p53 and pRb pathways) are observed in several human cancers, although not yet in PPGL (Ali et al. 1999). The heterozygous inactivation of *Pten* predisposes to a broad spectrum of cancers in mice including PCC in 23% of cases at 7 months, a frequency that rises to 60% when *Pten* and *Ink4a* are co-inactivated. Furthermore, this is one of the rare mouse models predisposing to malignant PCC, with around 15% of malignancy (lung metastasis) (You et al. 2002).

Surprisingly prostate cancer studies led to two tissue-specific PCC mouse models using technologies driven by supposedly specific prostate promoters that actually leak in the mouse adrenal medulla. First, Korpershoek et al. reported the conditional *Pten* KO driven by a PSA (prostate-specific antigen)-Cre recombinase. These mice are predisposed to PCC with an incidence of 78% in males, a number of whom with pulmonary metastases (Korpershoek et al. 2009; Ma et al. 2003). The same group also generated a double conditional KO mouse by crossing the *Pten* conditional KO with a Trp53 conditional KO previously generated by Marino et al. (2000). This model is more severe with a higher frequency of metastatic PCC (up to 67% lung metastases) and with a younger age of onset (4–5 months vs 11 months) (Korpershoek et al. 2012).

The second model results from an ectopic expression of an activated *ErbB2* transgene, driven by the minimal rat probasin promoter (PB). The activation of this tyrosine kinase receptor results in a decrease in the PTEN signaling pathway together with an increase in cycline D1 levels and leads to bilateral PCC in approximately 5% of male mice (Lai et al. 2007).

BRAF encodes a serine/threonine protein kinase involved in the RAS-RAF-MEK-ERK signaling pathway. The BRAF V600E mutation is the most common activating mutation in cancer, leading to constitutive BRAF kinase activity, phosphorylation of MEK and ERK kinases and sustained MAPK pathway signaling. *BRAF* V600E somatic mutations have been identified in several solid tumors, including malignant melanoma, colorectal cancer, differentiated thyroid cancers, breast and lung carcinomas, with a usually poor prognosis (Davies et al. 2002; Ikenoue et al. 2003; Namba et al. 2003). This mutation is not directly involved in human hereditary PPGL but around 10% of sporadic PCC have recently been shown to carry a somatic mutation in H-RAS (Castro-Vega et al. 2015; Crona et al. 2013; Oudijk et al. 2014). Interestingly, it was recently shown that mice expressing the hypomorphic B-RafV600E allele are predisposed to PPGL (Urosevic et al. 2011). Very interestingly, this is the first model that develops a high incidence (80% at 5 months of age) of both PGL and PCC with a 20% rate of metastatic phenotype.

Finally, the *CerS2* gene, encoding ceramide synthase 2, an enzyme involved in sphingolipid (SL) biosynthesis, has recently been implicated in PCC predisposition in mice (Park et al. 2015). Indeed, the CerS2 null mice, which are unable to synthetize very long-chain ceramides, develop lesions in several organs (hepatopathy, emphysema, demyelination) and are prone to bilateral PCC in more than 50% at 19 months of age with a 100% of medullary hyperplasia. The mechanism responsible for PCC tumorigenesis is not known but appears to be linked with changes in the SL profile with a reduction level of very long-chain SL together with an accumulation of long-chain SL and sphinganine that lead to the inhibition of mitochondrial complex IV activity and subsequent oxidative stress (Zigdon et al. 2013). Nevertheless, none of the classical signaling pathways usually incriminated in PPGL development seem to be involved: no upregulation of HIF-1α, no phosphorylation of Akt or mTor (Park et al. 2015). In human, only one patient harboring a deletion in one allele of *CerS2* has been reported with no evidence of PCC occurrence (Mosbech et al. 2014).

Conclusions on predisposed mouse models

The struggle for developing animal models of PPGL predisposition has shown that mice and men display some similarities but also major differences. Hence, all the models that have been successful are related to cluster 2 tumors and cause pheochromocytomas, with the exception of some paragangliomas in B-*Raf*$^{+/LSLV600E}$ mice. These mutations that mostly promote the activation of the MAPK and AKT/mTOR pathways do seem to be strongly oncogenic in adrenal chromaffin cells in mouse (Fig. 1). Actually, their impact is even more important than in humans as some genes of these pathways such as *Pten*, *c-mos*, *Rb*, *Erbb2* cause PCC in mouse but have not been associated with PCC predisposition in patients. To the best of our knowledge, none of the knockout mice of the cluster 1 mutated genes has ever been described with PPGL. Actually, at least 90% of tumors developed in SDH

patients are paragangliomas, which appears to be extremely rare in rodents. This may partly explain the failure in generating SDH-related tumors in mouse. However, *VHL*-mutated patients mostly develop PCC and PGL in only 20% of cases or so. Hence, it appears that the pathways associated with tumorigenesis in cluster 1 related tumors (pseudo-hypoxia in both SDH and VHL and DNA hypermethylation in SDH but also, to a lesser extent in VHL tumors) seem to be poorly efficient to promote tumorigenesis in mice. The reason for this discrepancy is quite puzzling but difficult to investigate experimentally. Whether it is linked to the genetic backgrounds used to generate these animals or to the lack of an associated chromosomal event, not reproduced in these models, is still a question that has not been properly addressed and that may provide some answers. Anyhow, the urge to generate such models has led researchers in the field to develop graft models using mouse or human cells.

Grafted mouse models

In a grafted model, human (xenograft) or animal (xeno-/allograft) cancer cells are transplanted either under the skin (ectopic) or into the organ of tumor origin (orthotopic) using immunodeficient rodents such as athymic nude mice or severely compromised immunodeficient (SCID) mice. Metastatic models can further be developed by injecting cells into the circulation (through the tail vein or in the heart) or in the spleen, the latter leading to a typical liver tropism. As compared with naturally occurring tumors, these models generally show a rapid tumor growth with an easy follow-up in particular for ectopic grafts. Although very useful for preclinical studies, most of these models do not recapitulate the typical slow growth of PPGL in humans and do not mimic the natural history of the tumor. In addition, they imply the use of immunodeficient mice and are thus inappropriate for studying the role of the immune microenvironment and the use of biotherapies targeting the immune checkpoint. Anyhow, the recent development of several cell lines and graft models has allowed significant advances in the understanding of PPGL tumorigenesis and in the launching of preclinical studies.

Allografted models

The first mouse model was developed by allografting the mouse pheochromocytoma cells (MPC) derived from an *Nf1* KO mouse tumor (Powers et al. 2000). This mouse model of metastatic PCC was established using intravenously injected MPC cells leading to metastatic lesions predominantly in the liver, 4 weeks after injection (Ohta et al. 2008). One year after, the same team obtained an allografted mouse model with a more aggressive phenotype by injecting into athymic mice the mouse tumor tissue (MTT) cells derived from an MPC liver metastasis (Martiniova et al. 2009). These two allografted models were extensively characterized by multimodality imaging confirming the metastatic phenotype, with a particular tropism for the liver (Giubellino et al. 2012; Martiniova et al. 2009, 2009, 2010, 2011) and both models appear to be suitable for preclinical studies (Martiniova et al. 2011; Pacak et al. 2012). More recently, the MPC cell line was stably transduced with a far-red-flurorescent-tagged lentivirus (MPC-mCherry cell line) and subcutaneously allografted to nude mice in order to elaborate a mouse model suitable for preclinical studies without the need for dedicated small animal imaging strategies only available in specialized research centers (Ullrich et al. 2014).

Nevertheless, there was still an unmet medical need for experimental models of cluster 1-related tumors that would reproduce malignant PPGL caused by *SDHB* mutations. Hence, because of the failure to develop a predisposed SDH-related animal model, our lab recently generated an allografted mouse model by subcutaneous injection of immortalized mouse chromaffin cells (imCC) (Letouze et al. 2013) carrying a homozygous knockout of the *Sdhb* gene into the fat-pad of female NMRI-nu mice (Lussey-Lepoutre et al. 2015). This mouse model reproduces the succinate accumulation and the particular vascular pattern observed in human *SDHx*-dependent PPGL. However, imCC have lost some differentiation markers of chromaffin cells and are likely not secreting anymore. Another allograft model has also been reported using *Sdhb*−/− renal cells (Cardaci et al. 2015).

Xenografted mouse models

One xenograft mouse model has recently been generated using rat pheochromocytoma PC12 cells injected subcutaneously into athymic Swiss nude nu/nu mice with a tumor development observed about 14 days after implantation. PC12 cells are historically the first cell line elaborated from an irradiated rat that spontaneously developed a PCC (Greene and Tischler 1976). About 20 years after, a deletion in *Max*, a gene also involved in human PCC (cluster C2) was identified as potentially responsible for tumorigenesis in these cells (Hopewell and Ziff 1995).

An adequate experimental model for a preclinical study would have been human xenograft of primary or metastatic PPGL. An interesting xenograft model using shRNA mediated *SDHB* knock-down in 143B human osteosarcoma cells was generated by Guzy et al. (2008). Interestingly, they found an acceleration of tumor growth when inhibiting *SDHB*. Nevertheless, this model is not *stricto* sensu a PCC mouse model since the cell type is not derived from a chromaffin tissue. Unfortunately, generating such a model appears to be challenging and until now, only one human xenografted model has been reported (Powers et al. 2017). Indeed, Powers et al. succeeded in growing xenografts of human PPGL in a

particular strain of immunodeficient mice: NOD-scid gamma (NGS) mice, which lack functional B cells, T cells and NK cells, paving the way for a new hope in this quest. Nevertheless, a limit of these human xenografts is that their progression is extremely slowly. Therefore, while they might faithfully replicate the growth rate of PPGL in their human hosts, which is often measured in years for a single doubling, this also makes them impractical for reproducible studies.

Did rodent models give new insights in the human PPGL struggle?

The objective of developing animal models includes deciphering tumorigenesis, developing new diagnosis tools and testing new therapeutic strategies in vivo, in conditions as close as possible to the human pathology.

Tumorigenesis

Surprisingly, PCC predisposed models in mouse have been only minimally utilized for mechanistic studies following their initial reports. Indeed, the molecular pathways implicated in cluster 2 tumors are mostly very well known, with the activation of the canonical signaling pathways involving MAPK or mTOR. In contrast, the more puzzling cluster 1 group of tumors could never be reproduced in a rodent knockout model and has therefore not beneficiated from such tools, allowing the study of the tumor's natural history. Current knowledge on these tumors, such as the identification of the pseudohypoxic pathway or the hypermethylator phenotype, have basically been obtained through the study of human tumor samples, or using in vitro cell lines. Xenograft models have however allowed some progress in the demonstration of the functionality of these pathways in vivo. Indeed, Guzy et al. demonstrated that targeting the hypoxic response in *Sdhb* knockdown cells did lead to a reduction of their growth in immunodeficient mice (Guzy et al. 2008).

Innovating diagnosis tools and therapeutic preclinical studies

The recent development of numerous graft models has allowed the launching of an increasing number of preclinical and in vivo imaging studies. One main advance in PPGL imaging issued from a preclinical model was the development last year of a new method to detect succinate accumulation in vivo by proton magnetic resonance spectroscopy (^{1}H-MRS) (Lussey-Lepoutre et al. 2015). Indeed, SDH inactivation leads to a massive accumulation of succinate that, assessed on surgically resected tissues, is a highly specific biomarker of *SDHx*-mutated tumors (Pollard et al. 2005; Rao et al. 2013; Richter et al. 2014). We optimized a pulse ^{1}H-MRS sequence to measure succinate in the allografted mouse model of *Sdhb*-deficient tumors. Following this initial preclinical step, we demonstrated, in patients, the feasibility of detecting succinate in vivo by ^{1}H-MRS as a very specific biomarker of *SDHx* mutations and as a quantifiable surrogate marker putatively enabling to monitor early response to treatment (Lussey-Lepoutre et al. 2015).

Other reports studied functional imaging with the ultimate objective of radionuclide therapy. *Martinova* et al. showed an increased uptake in ^{123}MIBG (meta-iodobenzylguanidine) and 18F–Fluorodopamine detected by scintigraphy in the metastatic allografted MPC mouse model following treatment with histone deacetylase (HDAC) inhibitors (Martiniova et al. 2011). HDAC inhibitors actually amplified the amount of norepinephrine transporter expressed in the tumors, potentially enhancing the efficacy of ^{131}MIBG therapy, one current therapeutic option in malignant PPGL (Martiniova et al. 2011). Nevertheless, until now, no therapeutic combination of HDAC and ^{131}MIBG therapy has been published either in this mouse model or in patients.

As a neuroendocrine tumor, PPGL abundantly express somatostatin receptor (sst) promoting great interest for new imaging using Gallium-68 labeled somatostatin analogues that recently showed interesting performance for PPGL evaluation (Archier et al. 2016; Janssen et al. 2015; Janssen et al. 2016; Kroiss et al. 2013, 2015). These good results support peptide receptor-targeting radionuclide therapies, mostly tested in gastroenteropancreatic neuroendocrine tumors (Strosberg et al. 2017) but also in metastatic or inoperable PPGL, although only in small series (Forrer et al. 2008; Puranik et al. 2015; Zovato et al. 2012). Recently, a German team demonstrated promising results of ^{177}Lu-Dotatate therapy in parallel to a high rate of ^{64}Cu-DOTATATE tumor uptake visualized on microPET imaging in the MPC-mCherry allografted mouse model (Ullrich et al. 2014), hence providing a basis for future clinical trials (Ullrich et al. 2016).

A few studies tested specific therapeutic agents in in vivo models. The effect of AZD8055 (an mTORC1/2 inhibitor) was assessed in the metastatic model established with MTT cells expressing Luciferase and monitored by in vivo bioluminescence imaging (Giubellino et al. 2013). This showed a reduction in the primary tumor burden as well as of the number of lung and liver metastases. The same authors reported the effects of HSP90 inhibitors in the metastatic spread of MTT cells injected in the tail vein of immunodeficient mice (Isaacs et al. 2002) and showed a reduction of HIF1 levels, suggesting that such inhibitor may be of interest for the management of cluster 1 pseudohypoxic PPGL. Finally, Denorme et al. used the xenograft model of PC12 cells to study the effect of the anti-angiogenic molecules, sorafenib and sunitinib (which is still being evaluated in clinical trials in patients (http://clinicaltrials.gov/show/NCT01371201 and https://clinicaltrials.gov/ct2/show/NCT00843037)) and showed that

both molecules promoted a reduction in microvessel density and of tumor growth (Denorme et al. 2014).

Conclusion and perspectives

In conclusion, the past 10 or 15 years have seen the emergence of an increasing number of models and studies that have been able to generate a pertinent and efficient animal model of PPGL that allows studying their natural history and launching preclinical assays. These studies have now demonstrated that if mice are strongly susceptible to the development of cluster 2-like pheochromocytomas (mediated by activating mutations in *Ret*, *Erbb2*, *Raf* or *c-mos* or by knockout of *Nf1*, *Rb*, *Pten*, *p16Ink4a*), it is still impossible to generate a cluster 1-like model through knockouts of *Sdhx*, *Fh*, or *Vhl* genes. For now, allografts with murine cell lines remain the only feasible option to study in vivo the behavior of such tumors. The recent progress allowed by the TALEN, CRISPR/Cas9, or induced pluripotent stem cells (iPSCs) technologies will surely promote, in the next future, an acceleration of such models. The Tischler Lab has already generated heterozygous *Sdhb*+/– rats that may be more prone to the development of SDH-related PPGL. Also, new mouse or human chromaffin or PPGL cell lines or grafts will eventually become available to permit experimental research for the treatment of this rare disease.

The international pheochromocytoma/paraganglioma research consortium PRESSOR encourages and attempts to foster collaboration on development of new experimental models. The webpage of the PRESSOR Tumor Models working Group can be accessed at www.PRESSOR.org.

References

Adam J, Hatipoglu E, O'Flaherty L, Ternette N, Sahgal N, Lockstone H, Baban D, Nye E, Stamp GW, Wolhuter K, Stevens M, Fischer R, Carmeliet P, Maxwell PH, Pugh CW, Frizzell N, Soga T, Kessler BM, El-Bahrawy M, Ratcliffe PJ, Pollard PJ (2011) Renal cyst formation in Fh1-deficient mice is independent of the Hif/Phd pathway: roles for fumarate in KEAP1 succination and Nrf2 signaling. Cancer Cell 20:524–537

Ali IU, Schriml LM, Dean M (1999) Mutational spectra of PTEN/MMAC1 gene: a tumor suppressor with lipid phosphatase activity. J Natl Cancer Inst 91:1922–1932

Amar L, Baudin E, Burnichon N, Peyrard S, Silvera S, Bertherat J, Bertagna X, Schlumberger M, Jeunemaitre X, Gimenez-Roqueplo AP, Plouin PF (2007) Succinate dehydrogenase B gene mutations predict survival in patients with malignant pheochromocytomas or paragangliomas. J Clin Endocrinol Metab 92:3822–3828

Archier A, Varoquaux A, Garrigue P, Montava M, Guerin C, Gabriel S, Beschmout E, Morange I, Fakhry N, Castinetti F, Sebag F, Barlier A, Loundou A, Guillet B, Pacak K, Taieb D (2016) Prospective comparison of (68)Ga-DOTATATE and (18)F-FDOPA PET/CT in patients with various pheochromocytomas and paragangliomas with emphasis on sporadic cases. Eur J Nucl Med Mol Imaging 43:1248–1257

Bayley JP, van Minderhout I, Hogendoorn PC, Cornelisse CJ, van der Wal A, Prins FA, Teppema L, Dahan A, Devilee P, Taschner PE (2009) Sdhd and SDHD/H19 knockout mice do not develop paraganglioma or pheochromocytoma. PLoS One 4:e7987

Briere JJ, Favier J, Benit P, El Ghouzzi V, Lorenzato A, Rabier D, Di Renzo MF, Gimenez-Roqueplo AP, Rustin P (2005) Mitochondrial succinate is instrumental for HIF1alpha nuclear translocation in SDHA-mutant fibroblasts under normoxic conditions. Hum Mol Genet 14:3263–3269

Burnichon N, Briere JJ, Libe R, Vescovo L, Riviere J, Tissier F, Jouanno E, Jeunemaitre X, Benit P, Tzagoloff A, Rustin P, Bertherat J, Favier J, Gimenez-Roqueplo AP (2010) SDHA is a tumor suppressor gene causing paraganglioma. Hum Mol Genet 19:3011–3020

Burnichon N, Vescovo L, Amar L, Libe R, de Reynies A, Venisse A, Jouanno E, Laurendeau I, Parfait B, Bertherat J, Plouin PF, Jeunemaitre X, Favier J, Gimenez-Roqueplo AP (2011) Integrative genomic analysis reveals somatic mutations in pheochromocytoma and paraganglioma. Hum Mol Genet 20:3974–3985

Cardaci S, Zheng L, MacKay G, van den Broek NJ, MacKenzie ED, Nixon C, Stevenson D, Tumanov S, Bulusu V, Kamphorst JJ, Vazquez A, Fleming S, Schiavi F, Kalna G, Blyth K, Strathdee D, Gottlieb E (2015) Pyruvate carboxylation enables growth of SDH-deficient cells by supporting aspartate biosynthesis. Nat Cell Biol 17:1317–1326

Carlson KM, Dou S, Chi D, Scavarda N, Toshima K, Jackson CE, Wells SA Jr, Goodfellow PJ, Donis-Keller H (1994) Single missense mutation in the tyrosine kinase catalytic domain of the RET protooncogene is associated with multiple endocrine neoplasia type 2B. Proc Natl Acad Sci U S A 91:1579–1583

Cascon A, Comino-Mendez I, Curras-Freixes M, de Cubas AA, Contreras L, Richter S, Peitzsch M, Mancikova V, Inglada-Perez L, Perez-Barrios A, Calatayud M, Azriel S, Villar-Vicente R, Aller J, Setien F, Moran S, Garcia JF, Rio-Machin A, Leton R, Gomez-Grana A, Apellaniz-Ruiz M, Roncador G, Esteller M, Rodriguez-Antona C, Satrustegui J, Eisenhofer G, Urioste M, Robledo M (2015) Whole-exome sequencing identifies MDH2 as a new familial paraganglioma gene. J Natl Cancer Inst 107

Castro-Vega LJ, Buffet A, De Cubas AA, Cascon A, Menara M, Khalifa E, Amar L, Azriel S, Bourdeau I, Chabre O, Curras-Freixes M, Franco-Vidal V, Guillaud-Bataille M, Simian C, Morin A, Leton R, Gomez-Grana A, Pollard PJ, Rustin P, Robledo M, Favier J, Gimenez-Roqueplo AP (2014) Germline mutations in FH confer predisposition to malignant pheochromocytomas and paragangliomas. Hum Mol Genet 23:2440–2446

Castro-Vega LJ, Lepoutre-Lussey C, Gimenez-Roqueplo AP, Favier J (2015) Rethinking pheochromocytomas and paragangliomas from a genomic perspective. Oncogene

Castro-Vega LJ, Letouze E, Burnichon N, Buffet A, Disderot PH, Khalifa E, Loriot C, Elarouci N, Morin A, Menara M, Lepoutre-Lussey C, Badoual C, Sibony M, Dousset B, Libe R, Zinzindohoue F, Plouin PF, Bertherat J, Amar L, de Reynies A, Favier J, Gimenez-Roqueplo AP (2015) Multi-omics analysis defines core genomic alterations in pheochromocytomas and paragangliomas. Nat Commun 6:6044

Clark GR, Sciacovelli M, Gaude E, Walsh DM, Kirby G, Simpson MA, Trembath RC, Berg JN, Woodward ER, Kinning E, Morrison PJ, Frezza C, Maher ER (2014) Germline FH mutations presenting with pheochromocytoma. J Clin Endocrinol Metab 99:E2046–E2050

Comino-Mendez I, Gracia-Aznarez FJ, Schiavi F, Landa I, Leandro-Garcia LJ, Leton R, Honrado E, Ramos-Medina R, Caronia D, Pita G, Gomez-Grana A, de Cubas AA, Inglada-Perez L, Maliszewska A, Taschin E, Bobisse S, Pica G, Loli P, Hernandez-Lavado R, Diaz JA, Gomez-Morales M, Gonzalez-Neira A, Roncador G, Rodriguez-Antona C, Benitez J, Mannelli M,

Opocher G, Robledo M, Cascon A (2011) Exome sequencing identifies MAX mutations as a cause of hereditary pheochromocytoma. Nat Genet 43:663–667

Crona J, Delgado Verdugo A, Maharjan R, Stalberg P, Granberg D, Hellman P, Bjorklund P (2013) Somatic mutations in H-RAS in sporadic pheochromocytoma and paraganglioma identified by exome sequencing. J Clin Endocrinol Metab 98:E1266–E1271

Dahia PL (2014) Pheochromocytoma and paraganglioma pathogenesis: learning from genetic heterogeneity. Nat Rev Cancer 14:108–119

Dahia PL, Ross KN, Wright ME, Hayashida CY, Santagata S, Barontini M, Kung AL, Sanso G, Powers JF, Tischler AS, Hodin R, Heitritter S, Moore F, Dluhy R, Sosa JA, Ocal IT, Benn DE, Marsh DJ, Robinson BG, Schneider K, Garber J, Arum SM, Korbonits M, Grossman A, Pigny P, Toledo SP, Nose V, Li C, Stiles CD (2005) A HIF1alpha regulatory loop links hypoxia and mitochondrial signals in pheochromocytomas. PLoS Genet 1:72–80

Davies H, Bignell GR, Cox C, Stephens P, Edkins S, Clegg S, Teague J, Woffendin H, Garnett MJ, Bottomley W, Davis N, Dicks E, Ewing R, Floyd Y, Gray K, Hall S, Hawes R, Hughes J, Kosmidou V, Menzies A, Mould C, Parker A, Stevens C, Watt S, Hooper S, Wilson R, Jayatilake H, Gusterson BA, Cooper C, Shipley J, Hargrave D, Pritchard-Jones K, Maitland N, Chenevix-Trench G, Riggins GJ, Bigner DD, Palmieri G, Cossu A, Flanagan A, Nicholson A, Ho JW, Leung SY, Yuen ST, Weber BL, Seigler HF, Darrow TL, Paterson H, Marais R, Marshall CJ, Wooster R, Stratton MR, Futreal PA (2002) Mutations of the BRAF gene in human cancer. Nature 417:949–954

Denorme M, Yon L, Roux C, Gonzalez BJ, Baudin E, Anouar Y, Dubessy C (2014) Both sunitinib and sorafenib are effective treatments for pheochromocytoma in a xenograft model. Cancer Lett 352:236–244

Diaz-Castro B, Pintado CO, Garcia-Flores P, Lopez-Barneo J, Piruat JI (2012) Differential impairment of catecholaminergic cell maturation and survival by genetic mitochondrial complex II dysfunction. Mol Cell Biol 32:3347–3357

Eisenhofer G, Huynh TT, Pacak K, Brouwers FM, Walther MM, Linehan WM, Munson PJ, Mannelli M, Goldstein DS, Elkahloun AG (2004) Distinct gene expression profiles in norepinephrine- and epinephrine-producing hereditary and sporadic pheochromocytomas: activation of hypoxia-driven angiogenic pathways in von Hippel-Lindau syndrome. Endocr Relat Cancer 11:897–911

Favier J, Amar L, Gimenez-Roqueplo A (2014) Paraganglioma and phaeochromocytoma: from genetics to personalized medicine. Nat Rev Endocrinol

Favier J, Briere JJ, Burnichon N, Riviere J, Vescovo L, Benit P, Giscos-Douriez I, De Reynies A, Bertherat J, Badoual C, Tissier F, Amar L, Libe R, Plouin PF, Jeunemaitre X, Rustin P, Gimenez-Roqueplo AP (2009) The Warburg effect is genetically determined in inherited pheochromocytomas. PLoS One 4:e7094

Favier J, Buffet A, Gimenez-Roqueplo AP (2012) HIF2A mutations in paraganglioma with polycythemia. N Engl J Med 367:2161 **author reply 2161-2162**

Forrer F, Riedweg I, Maecke HR, Mueller-Brand J (2008) Radiolabeled DOTATOC in patients with advanced paraganglioma and pheochromocytoma. The quarterly journal of nuclear medicine and molecular imaging: official publication of the Italian Association of Nuclear Medicine 52:334–340

Gelman DM, Noain D, Avale ME, Otero V, Low MJ, Rubinstein M (2003) Transgenic mice engineered to target Cre/loxP-mediated DNA recombination into catecholaminergic neurons. Genesis 36: 196–202

Gimenez-Roqueplo AP, Favier J, Rustin P, Rieubland C, Crespin M, Nau V, Khau Van Kien P, Corvol P, Plouin PF, Jeunemaitre X, Network C (2003) Mutations in the SDHB gene are associated with extra-adrenal and/or malignant phaeochromocytomas. Cancer Res 63: 5615–5621

Giubellino A, Bullova P, Nolting S, Turkova H, Powers JF, Liu Q, Guichard S, Tischler AS, Grossman AB, Pacak K (2013) Combined inhibition of mTORC1 and mTORC2 signaling pathways is a promising therapeutic option in inhibiting pheochromocytoma tumor growth: in vitro and in vivo studies in female athymic nude mice. Endocrinology 154:646–655

Giubellino A, Woldemichael GM, Sourbier C, Lizak MJ, Powers JF, Tischler AS, Pacak K (2012) Characterization of two mouse models of metastatic pheochromocytoma using bioluminescence imaging. Cancer Lett 316:46–52

Gnarra JR, Ward JM, Porter FD, Wagner JR, Devor DE, Grinberg A, Emmert-Buck MR, Westphal H, Klausner RD, Linehan WM (1997) Defective placental vasculogenesis causes embryonic lethality in VHL-deficient mice. Proc Natl Acad Sci U S A 94:9102–9107

Greene LA, Tischler AS (1976) Establishment of a noradrenergic clonal line of rat adrenal pheochromocytoma cells which respond to nerve growth factor. Proc Natl Acad Sci U S A 73:2424–2428

Gujral TS, Singh VK, Jia Z, Mulligan LM (2006) Molecular mechanisms of RET receptor-mediated oncogenesis in multiple endocrine neoplasia 2B. Cancer Res 66:10741–10749

Gutmann DH, Aylsworth A, Carey JC, Korf B, Marks J, Pyeritz RE, Rubenstein A, Viskochil D (1997) The diagnostic evaluation and multidisciplinary management of neurofibromatosis 1 and neurofibromatosis 2. JAMA 278:51–57

Guzy RD, Sharma B, Bell E, Chandel NS, Schumacker PT (2008) Loss of the SdhB, but not the SdhA, subunit of complex II triggers reactive oxygen species-dependent hypoxia-inducible factor activation and tumorigenesis. Mol Cell Biol 28:718–731

Haase VH (2005) The VHL tumor suppressor in development and disease: functional studies in mice by conditional gene targeting. Semin Cell Dev Biol 16:564–574

Haase VH, Glickman JN, Socolovsky M, Jaenisch R (2001) Vascular tumors in livers with targeted inactivation of the von Hippel-Lindau tumor suppressor. Proc Natl Acad Sci U S A 98:1583–1588

Harlander S, Schonenberger D, Toussaint NC, Prummer M, Catalano A, Brandt L, Moch H, Wild PJ, Frew IJ (2017) Combined mutation in Vhl, Trp53 and Rb1 causes clear cell renal cell carcinoma in mice. Nat Med

Hawes JJ, Tuskan RG, Reilly KM (2007) Nf1 expression is dependent on strain background: implications for tumor suppressor haploinsufficiency studies. Neurogenetics 8:121–130

Hopewell R, Ziff EB (1995) The nerve growth factor-responsive PC12 cell line does not express the Myc dimerization partner Max. Mol Cell Biol 15:3470–3478

Ibanez CF (2013) Structure and physiology of the RET receptor tyrosine kinase. Cold Spring Harbor Perspect in Biol 5

Ikenoue T, Hikiba Y, Kanai F, Tanaka Y, Imamura J, Imamura T, Ohta M, Ijichi H, Tateishi K, Kawakami T, Aragaki J, Matsumura M, Kawabe T, Omata M (2003) Functional analysis of mutations within the kinase activation segment of B-Raf in human colorectal tumors. Cancer Res 63:8132–8137

Isaacs JS, Jung YJ, Mimnaugh EG, Martinez A, Cuttitta F, Neckers LM (2002) Hsp90 regulates a von Hippel Lindau-independent hypoxia-inducible factor-1 alpha-degradative pathway. J Biol Chem 277: 29936–29944

Jacks T, Shih TS, Schmitt EM, Bronson RT, Bernards A, Weinberg RA (1994) Tumour predisposition in mice heterozygous for a targeted mutation in Nf1. Nat Genet 7:353–361

Janssen I, Blanchet EM, Adams K, Chen CC, Millo C, Herscovitch P, Taieb D, Kebebew E, Lehnert H, Fojo AT, Pacak K (2015) Superiority of [68Ga]-DOTATATE PET/CT to other functional imaging modalities in the localization of SDHB-associated metastatic pheochromocytoma and paraganglioma. Clin Cancer Res: Off J Am Assoc Cancer Res

Janssen I, Chen CC, Millo CM, Ling A, Taieb D, Lin FI, Adams KT, Wolf KI, Herscovitch P, Fojo AT, Buchmann I, Kebebew E, Pacak K

(2016) PET/CT comparing (68)Ga-DOTATATE and other radiopharmaceuticals and in comparison with CT/MRI for the localization of sporadic metastatic pheochromocytoma and paraganglioma. Eur J Nucl Med Mol Imaging 43:1784–1791

Kim WY, Kaelin WG (2004) Role of VHL gene mutation in human cancer. Journal of clinical oncology : official journal of the American Society of Clinical Oncology 22:4991–5004

Korpershoek E, Kloosterhof NK, Ziel-van der Made A, Korsten H, Oudijk L, Trapman J, Dinjens WN, de Krijger RR (2012) Trp53 inactivation leads to earlier phaeochromocytoma formation in pten knockout mice. Endocr Relat Cancer 19:731–740

Korpershoek E, Loonen AJ, Corvers S, van Nederveen FH, Jonkers J, Ma X, Ziel-van der Made A, Korsten H, Trapman J, Dinjens WN, de Krijger RR (2009) Conditional Pten knock-out mice: a model for metastatic phaeochromocytoma. J Pathol 217:597–604

Kroiss A, Putzer D, Frech A, Decristoforo C, Uprimny C, Gasser RW, Shulkin BL, Url C, Widmann G, Prommegger R, Sprinzl GM, Fraedrich G, Virgolini IJ (2013) A retrospective comparison between 68Ga-DOTA-TOC PET/CT and 18F-DOPA PET/CT in patients with extra-adrenal paraganglioma. Eur J Nucl Med Mol Imaging 40:1800–1808

Kroiss A, Shulkin BL, Uprimny C, Frech A, Gasser RW, Url C, Gautsch K, Madleitner R, Nilica B, Sprinzl GM, Gastl G, Fraedrich G, Virgolini IJ (2015) (68)Ga-DOTATOC PET/CT provides accurate tumour extent in patients with extraadrenal paraganglioma compared to (123)I-MIBG SPECT/CT. Eur J Nucl Med Mol Imaging 42:33–41

Lai EW, Rodriguez OC, Aventian M, Cromelin C, Fricke ST, Martiniova L, Lubensky IA, Lisanti MP, Picard KL, Powers JF, Tischler AS, Pacak K, Albanese C (2007) ErbB-2 induces bilateral adrenal pheochromocytoma formation in mice. Cell Cycle 6:1946–1950

Lancaster CR, Simon J (2002) Succinate:quinone oxidoreductases from epsilon-proteobacteria. Biochim Biophys Acta 1553:84–101

Lenders JW, Duh QY, Eisenhofer G, Gimenez-Roqueplo AP, Grebe SK, Murad MH, Naruse M, Pacak K, Young WF Jr, Endocrine S (2014) Pheochromocytoma and paraganglioma: an endocrine society clinical practice guideline. J Clin Endocrinol Metab 99:1915–1942

Lepoutre-Lussey C, Thibault C, Buffet A, Morin A, Badoual C, Benit P, Rustin P, Ottolenghi C, Janin M, Castro-Vega LJ, Trapman J, Gimenez-Roqueplo AP, Favier J (2015) From Nf1 to Sdhb knockout: successes and failures in the quest for animal models of pheochromocytoma. Mol Cell Endocrinol

Letouze E, Martinelli C, Loriot C, Burnichon N, Abermil N, Ottolenghi C, Janin M, Menara M, Nguyen AT, Benit P, Buffet A, Marcaillou C, Bertherat J, Amar L, Rustin P, De Reynies A, Gimenez-Roqueplo AP, Favier J (2013) SDH mutations establish a hypermethylator phenotype in paraganglioma. Cancer Cell 23:739–752

Lopez-Jimenez E, Gomez-Lopez G, Leandro-Garcia LJ, Munoz I, Schiavi F, Montero-Conde C, de Cubas AA, Ramires R, Landa I, Leskela S, Maliszewska A, Inglada-Perez L, de la Vega L, Rodriguez-Antona C, Leton R, Bernal C, de Campos JM, Diez-Tascon C, Fraga MF, Boullosa C, Pisano DG, Opocher G, Robledo M, Cascon A (2010) Research resource: transcriptional profiling reveals different pseudohypoxic signatures in SDHB and VHL-related pheochromocytomas. Mol Endocrinol 24:2382–2391

Lussey-Lepoutre C, Bellucci A, Morin A, Buffet A, Amar L, Janin M, Ottolenghi C, Zinzindohoue F, Autret G, Burnichon N, Robidel E, Banting B, Fontaine S, Cuenod CA, Benit P, Rustin P, Halimi P, Fournier L, Gimenez-Roqueplo AP, Favier J, Tavitian B (2015) In vivo detection of succinate by magnetic resonance spectroscopy as a Hallmark of SDHx mutations in paraganglioma. Clin Cancer Res: Off J Am Assoc Cancer Res

Ma W, Tessarollo L, Hong SB, Baba M, Southon E, Back TC, Spence S, Lobe CG, Sharma N, Maher GW, Pack S, Vortmeyer AO, Guo C, Zbar B, Schmidt LS (2003) Hepatic vascular tumors, angiectasis in multiple organs, and impaired spermatogenesis in mice with conditional inactivation of the VHL gene. Cancer Res 63:5320–5328

Macias D, Fernandez-Aguera MC, Bonilla-Henao V, Lopez-Barneo J (2014) Deletion of the von Hippel-Lindau gene causes sympathoadrenal cell death and impairs chemoreceptor-mediated adaptation to hypoxia. EMBO molecular medicine 6:1577–1592

Maher III LJ, Smith EH, Rueter EM, Becker NA, Bida JP, Nelson-Holte M, Piruat Palomo JI, García-Flores P, López-Barneo O, Van Deursen J (2011) Mouse models of human familial paraganglioma. In: Martin JF (ed) Pheochromocytoma—a new view of the old problem. InTech

Marino S, Vooijs M, van Der Gulden H, Jonkers J, Berns A (2000) Induction of medulloblastomas in p53-null mutant mice by somatic inactivation of Rb in the external granular layer cells of the cerebellum. Genes Dev 14:994–1004

Martiniova L, Kotys MS, Thomasson D, Schimel D, Lai EW, Bernardo M, Merino MJ, Powers JF, Ruzicka J, Kvetnansky R, Choyke PL, Pacak K (2009) Noninvasive monitoring of a murine model of metastatic pheochromocytoma: a comparison of contrast-enhanced microCT and nonenhanced MRI. Journal of magnetic resonance imaging : JMRI 29:685–691

Martiniova L, Lai EW, Elkahloun AG, Abu-Asab M, Wickremasinghe A, Solis DC, Perera SM, Huynh TT, Lubensky IA, Tischler AS, Kvetnansky R, Alesci S, Morris JC, Pacak K (2009) Characterization of an animal model of aggressive metastatic pheochromocytoma linked to a specific gene signature. Clin Exp Metastasis 26:239–250

Martiniova L, Lai EW, Thomasson D, Kiesewetter DO, Seidel J, Merino MJ, Kvetnansky R, Pacak K (2009) Animal model of metastatic pheochromocytoma: evaluation by MRI and PET. Endocr Regul 43:59–64

Martiniova L, Lu J, Chiang J, Bernardo M, Lonser R, Zhuang Z, Pacak K (2011) Pharmacologic modulation of serine/threonine phosphorylation highly sensitizes PHEO in a MPC cell and mouse model to conventional chemotherapy. PLoS One 6:e14678

Martiniova L, Perera SM, Brouwers FM, Alesci S, Abu-Asab M, Marvelle AF, Kiesewetter DO, Thomasson D, Morris JC, Kvetnansky R, Tischler AS, Reynolds JC, Fojo AT, Pacak K (2011) Increased uptake of [(1)(2)(3)I]meta-iodobenzylguanidine, [(1)(8)F]fluorodopamine, and [(3)H]norepinephrine in mouse pheochromocytoma cells and tumors after treatment with the histone deacetylase inhibitors. Endocr Relat Cancer 18:143–157

Martiniova L, Schimel D, Lai EW, Limpuangthip A, Kvetnansky R, Pacak K (2010) In vivo micro-CT imaging of liver lesions in small animal models. Methods 50:20–25

Michiels FM, Chappuis S, Caillou B, Pasini A, Talbot M, Monier R, Lenoir GM, Feunteun J, Billaud M (1997) Development of medullary thyroid carcinoma in transgenic mice expressing the RET protooncogene altered by a multiple endocrine neoplasia type 2A mutation. Proc Natl Acad Sci U S A 94:3330–3335

Morin A, Letouze E, Gimenez-Roqueplo AP, Favier J (2014) Oncometabolites-driven tumorigenesis: from genetics to targeted therapy. Int J Cancer 135:2237–2248

Mosbech MB, Olsen AS, Neess D, Ben-David O, Klitten LL, Larsen J, Sabers A, Vissing J, Nielsen JE, Hasholt L, Klein AD, Tsoory MM, Hjalgrim H, Tommerup N, Futerman AH, Moller RS, Faergeman NJ (2014) Reduced ceramide synthase 2 activity causes progressive myoclonic epilepsy. Annals of clinical and translational neurology 1:88–98

Namba H, Nakashima M, Hayashi T, Hayashida N, Maeda S, Rogounovitch TI, Ohtsuru A, Saenko VA, Kanematsu T, Yamashita S (2003) Clinical implication of hot spot BRAF mutation, V599E, in papillary thyroid cancers. J Clin Endocrinol Metab 88:4393–4397

Nikitin AY, Juarez-Perez MI, Li S, Huang L, Lee WH (1999) RB-mediated suppression of spontaneous multiple neuroendocrine

neoplasia and lung metastases in Rb+/− mice. Proc Natl Acad Sci U S A 96:3916–3921

Ohta S, Lai EW, Morris JC, Pang AL, Watanabe M, Yazawa H, Zhang R, Green JE, Chan WY, Sirajuddin P, Taniguchi S, Powers JF, Tischler AS, Pacak K (2008) Metastasis-associated gene expression profile of liver and subcutaneous lesions derived from mouse pheochromocytoma cells. Mol Carcinog 47:245–251

Oudijk L, de Krijger RR, Rapa I, Beuschlein F, de Cubas AA, Dei Tos AP, Dinjens WN, Korpershoek E, Mancikova V, Mannelli M, Papotti M, Vatrano S, Robledo M, Volante M (2014) H-RAS mutations are restricted to sporadic pheochromocytomas lacking specific clinical or pathological features: data from a multi-institutional series. J Clin Endocrinol Metab 99:E1376–E1380

Pacak K, Sirova M, Giubellino A, Lencesova L, Csaderova L, Laukova M, Hudecova S, Krizanova O (2012) NF-kappaB inhibition significantly upregulates the norepinephrine transporter system, causes apoptosis in pheochromocytoma cell lines and prevents metastasis in an animal model. International journal of cancer Journal international du cancer 131:2445–2455

Park WJ, Brenner O, Kogot-Levin A, Saada A, Merrill AH Jr, Pewzner-Jung Y, Futerman AH (2015) Development of pheochromocytoma in ceramide synthase 2 null mice. Endocr Relat Cancer 22:623–632

Piruat JI, Pintado CO, Ortega-Saenz P, Roche M, Lopez-Barneo J (2004) The mitochondrial SDHD gene is required for early embryogenesis, and its partial deficiency results in persistent carotid body glomus cell activation with full responsiveness to hypoxia. Mol Cell Biol 24: 10933–10940

Pollard PJ, Briere JJ, Alam NA, Barwell J, Barclay E, Wortham NC, Hunt T, Mitchell M, Olpin S, Moat SJ, Hargreaves IP, Heales SJ, Chung YL, Griffiths JR, Dalgleish A, McGrath JA, Gleeson MJ, Hodgson SV, Poulsom R, Rustin P, Tomlinson IP (2005) Accumulation of Krebs cycle intermediates and over-expression of HIF1alpha in tumours which result from germline FH and SDH mutations. Hum Mol Genet 14:2231–2239

Pollard PJ, Spencer-Dene B, Shukla D, Howarth K, Nye E, El-Bahrawy M, Deheragoda M, Joannou M, McDonald S, Martin A, Igarashi P, Varsani-Brown S, Rosewell I, Poulsom R, Maxwell P, Stamp GW, Tomlinson IP (2007) Targeted inactivation of fh1 causes proliferative renal cyst development and activation of the hypoxia pathway. Cancer Cell 11:311–319

Powers JF, Evinger MJ, Tsokas P, Bedri S, Alroy J, Shahsavari M, Tischler AS (2000) Pheochromocytoma cell lines from heterozygous neurofibromatosis knockout mice. Cell Tissue Res 302:309–320

Powers JF, Pacak K, Tischler AS (2017) Pathology of human pheochromocytoma and paraganglioma xenografts in NSG mice. Endocr Pathol 28:2–6

Puc J, Placha G, Wocial B, Podsypanina K, Parsons R, Gaciong Z (2006) Analysis of PTEN mutation in non-familial pheochromocytoma. Ann N Y Acad Sci 1073:317–331

Puranik AD, Kulkarni HR, Singh A, Baum RP (2015) Peptide receptor radionuclide therapy with (90)Y/ (177)Lu-labelled peptides for inoperable head and neck paragangliomas (glomus tumours). Eur J Nucl Med Mol Imaging 42:1223–1230

Qin Y, Yao L, King EE, Buddavarapu K, Lenci RE, Chocron ES, Lechleiter JD, Sass M, Aronin N, Schiavi F, Boaretto F, Opocher G, Toledo RA, Toledo SP, Stiles C, Aguiar RC, Dahia PL (2010) Germline mutations in TMEM127 confer susceptibility to pheochromocytoma. Nat Genet 42:229–233

Rao JU, Engelke UF, Rodenburg RJ, Wevers RA, Pacak K, Eisenhofer G, Qin N, Kusters B, Goudswaard AG, Lenders JW, Hermus AR, Mensenkamp AR, Kunst HP, Sweep FC, Timmers HJ (2013) Genotype-specific abnormalities in mitochondrial function associate with distinct profiles of energy metabolism and catecholamine content in pheochromocytoma and paraganglioma. Clinical cancer research : an official journal of the American Association for Cancer Research 19:3787–3795

Reynolds L, Jones K, Winton DJ, Cranston A, Houghton C, Howard L, Ponder BA, Smith DP (2001) C-cell and thyroid epithelial tumours and altered follicular development in transgenic mice expressing the long isoform of MEN 2A RET. Oncogene 20:3986–3994

Richter S, Peitzsch M, Rapizzi E, Lenders JW, Qin N, de Cubas AA, Schiavi F, Rao JU, Beuschlein F, Quinkler M, Timmers HJ, Opocher G, Mannelli M, Pacak K, Robledo M, Eisenhofer G (2014) Krebs cycle metabolite profiling for identification and stratification of pheochromocytomas/paragangliomas due to succinate dehydrogenase deficiency. J Clin Endocrinol Metab 99:3903–3911

Sato Y, Yoshizato T, Shiraishi Y, Maekawa S, Okuno Y, Kamura T, Shimamura T, Sato-Otsubo A, Nagae G, Suzuki H, Nagata Y, Yoshida K, Kon A, Suzuki Y, Chiba K, Tanaka H, Niida A, Fujimoto A, Tsunoda T, Morikawa T, Maeda D, Kume H, Sugano S, Fukayama M, Aburatani H, Sanada M, Miyano S, Homma Y, Ogawa S (2013) Integrated molecular analysis of clear-cell renal cell carcinoma. Nat Genet 45:860–867

Schulz N, Propst F, Rosenberg MP, Linnoila RI, Paules RS, Kovatch R, Ogiso Y, Vande Woude G (1992) Pheochromocytomas and C-cell thyroid neoplasms in transgenic c-mos mice: a model for the human multiple endocrine neoplasia type 2 syndrome. Cancer Res 52:450–455

Smith-Hicks CL, Sizer KC, Powers JF, Tischler AS, Costantini F (2000) C-cell hyperplasia, pheochromocytoma and sympathoadrenal malformation in a mouse model of multiple endocrine neoplasia type 2B. EMBO J 19:612–622

Strosberg J, El-Haddad G, Wolin E, Hendifar A, Yao J, Chasen B, Mittra E, Kunz PL, Kulke MH, Jacene H, Bushnell D, O'Dorisio TM, Baum RP, Kulkarni HR, Caplin M, Lebtahi R, Hobday T, Delpassand E, Van Cutsem E, Benson A, Srirajaskanthan R, Pavel M, Mora J, Berlin J, Grande E, Reed N, Seregni E, Oberg K, Lopera Sierra M, Santoro P, Thevenet T, Erion JL, Ruszniewski P, Kwekkeboom D, Krenning E, Investigators N-T (2017) Phase 3 trial of 177Lu-Dotatate for midgut neuroendocrine tumors. N Engl J Med 376:125–135

Tomlinson IP, Alam NA, Rowan AJ, Barclay E, Jaeger EE, Kelsell D, Leigh I, Gorman P, Lamlum H, Rahman S, Roylance RR, Olpin S, Bevan S, Barker K, Hearle N, Houlston RS, Kiuru M, Lehtonen R, Karhu A, Vilkki S, Laiho P, Eklund C, Vierimaa O, Aittomaki K, Hietala M, Sistonen P, Paetau A, Salovaara R, Herva R, Launonen V, Aaltonen LA, Multiple Leiomyoma C (2002) Germline mutations in FH predispose to dominantly inherited uterine fibroids, skin leiomyomata and papillary renal cell cancer. Nat Genet 30:406–410

Tonks ID, Mould AW, Schroder WA, Cotterill A, Hayward NK, Walker GJ, Kay GF (2010) Dual loss of rb1 and Trp53 in the adrenal medulla leads to spontaneous pheochromocytoma. Neoplasia 12:235–243

Toro JR, Nickerson ML, Wei MH, Warren MB, Glenn GM, Turner ML, Stewart L, Duray P, Tourre O, Sharma N, Choyke P, Stratton P, Merino M, Walther MM, Linehan WM, Schmidt LS, Zbar B (2003) Mutations in the fumarate hydratase gene cause hereditary leiomyomatosis and renal cell cancer in families in North America. Am J Hum Genet 73:95–106

Ullrich M, Bergmann R, Peitzsch M, Cartellieri M, Qin N, Ehrhart-Bornstein M, Block NL, Schally AV, Pietzsch J, Eisenhofer G, Bornstein SR, Ziegler CG (2014) In vivo fluorescence imaging and urinary monoamines as surrogate biomarkers of disease progression in a mouse model of pheochromocytoma. Endocrinology 155:4149–4156

Ullrich M, Bergmann R, Peitzsch M, Zenker EF, Cartellieri M, Bachmann M, Ehrhart-Bornstein M, Block NL, Schally AV, Eisenhofer G, Bornstein SR, Pietzsch J, Ziegler CG (2016) Multimodal somatostatin receptor theranostics using [(64)Cu]Cu

−/[(177)Lu]Lu-DOTA-(Tyr(3))octreotate and AN-238 in a mouse pheochromocytoma model. Theranostics 6:650–665

Urosevic J, Sauzeau V, Soto-Montenegro ML, Reig S, Desco M, Wright EM, Canamero M, Mulero F, Ortega S, Bustelo XR, Barbacid M (2011) Constitutive activation of B-Raf in the mouse germ line provides a model for human cardio-facio-cutaneous syndrome. Proc Natl Acad Sci U S A 108:5015–5020

van Nederveen FH, Perren A, Dannenberg H, Petri BJ, Dinjens WN, Komminoth P, de Krijger RR (2006) PTEN gene loss, but not mutation, in benign and malignant phaeochromocytomas. J Pathol 209: 274–280

Viskochil D, Buchberg AM, Xu G, Cawthon RM, Stevens J, Wolff RK, Culver M, Carey JC, Copeland NG, Jenkins NA et al (1990) Deletions and a translocation interrupt a cloned gene at the neurofibromatosis type 1 locus. Cell 62:187–192

Wagner SM, Zhu S, Nicolescu AC, Mulligan LM (2012) Molecular mechanisms of RET receptor-mediated oncogenesis in multiple endocrine neoplasia 2. Clinics 67(Suppl 1):77–84

You MJ, Castrillon DH, Bastian BC, O'Hagan RC, Bosenberg MW, Parsons R, Chin L, DePinho RA (2002) Genetic analysis of Pten and Ink4a/Arf interactions in the suppression of tumorigenesis in mice. Proc Natl Acad Sci U S A 99:1455–1460

Zigdon H, Kogot-Levin A, Park JW, Goldschmidt R, Kelly S, Merrill AH Jr, Scherz A, Pewzner-Jung Y, Saada A, Futerman AH (2013) Ablation of ceramide synthase 2 causes chronic oxidative stress due to disruption of the mitochondrial respiratory chain. J Biol Chem 288:4947–4956

Zovato S, Kumanova A, Dematte S, Sansovini M, Bodei L, Di Sarra D, Casagranda E, Severi S, Ambrosetti A, Schiavi F, Opocher G, Paganelli G (2012) Peptide receptor radionuclide therapy (PRRT) with 177Lu-DOTATATE in individuals with neck or mediastinal paraganglioma (PGL). Hormone and metabolic research = Hormon- und Stoffwechselforschung = Hormones et metabolisme 44:411–414

ARTICLE 7

New lessons from an old gene: complex splicing and a novel cryptic exon in VHL gene cause erythrocytosis and VHL disease.

Lenglet M, Robriquet F, Schwarz K, Camps C, Couturier A, Hoogewijs D, Buffet A, Knight SJ, Gad S, Couvé S, Chesnel F, Pacault M, Lindenbaum P, Job S, Dumont S, Besnard T, Cornec M, Dreau H, Pentony M, Kvikstad E, Deveaux S, Burnichon N, Ferlicot S, Vilaine M, Mazzella JM, Airaud F, Garrec C, Heidet L, Irtan S, Mantadakis E, Bouchireb K, Debatin KM, Redon R, Bezieau S, Bressac-de Paillerets B, Teh BT, Girodon F, Randi ML, Putti MC, Bours V, Van Wijk R, Göthert JR, Kattamis A, Janin N, Bento C, Taylor JC, Arlot-Bonnemains Y, Richard S, Gimenez-Roqueplo AP, Cario H, Gardie B.

Blood. 2018 Jun 11. pii: blood-2018-03-838235.

Blood First Edition Paper, prepublished online June 11, 2018; DOI 10.1182/blood-2018-03-838235

TITLE:

New lessons from an old gene: complex splicing and a novel cryptic exon in *VHL* gene cause erythrocytosis and VHL disease

RUNNING TITLE:

Complex genetics in VHL disease and erythrocytosis

AUTHORS:

Marion Lenglet,[1,2,3§] Florence Robriquet,[2,3§] Klaus Schwarz,[4] Carme Camps,[5,6] Anne Couturier,[7] David Hoogewijs,[8] Alexandre Buffet,[9,10] Samantha JL. Knight,[5,6] Sophie Gad,[1,11] Sophie Couvé,[1,11] Franck Chesnel,[7] Mathilde Pacault,[2,12] Pierre Lindenbaum,[3] Sylvie Job,[13] Solenne Dumont,[2] Thomas Besnard,[3,12] Marine Cornec,[3] Helene Dreau,[14] Melissa Pentony,[5,6] Erika Kvikstad,[5,6] Sophie Deveaux,[15,16] Nelly Burnichon,[9,10,16,17] Sophie Ferlicot,[18,19] Mathias Vilaine,[2] Jean-Michaël Mazzella,[9,10,16,17] Fabrice Airaud,[12] Céline Garrec,[12] Laurence Heidet,[20] Sabine Irtan,[21] Elpis Mantadakis,[22] Karim Bouchireb,[20] Klaus-Michael Debatin,[23] Richard Redon,[3] Stéphane Bezieau,[3,12] Brigitte Bressac-de Paillerets,[24] Bin Tean Teh,[25] François Girodon,[26-27,36] Maria-Luigia Randi,[28] Maria Caterina Putti,[29] Vincent Bours,[30] Richard Van Wijk,[31] Joachim R. Göthert,[32] Antonis Kattamis,[33] Nicolas Janin,[34] Celeste Bento,[35] Jenny C. Taylor,[5,6] Yannick Arlot-Bonnemains,[7] Stéphane Richard,[1,11,15,16ß] Anne-Paule Gimenez-Roqueplo,[9,10,16,17ß], Holger Cario,[23]* Betty Gardie,[1,2,3, 36]*.

CORRESPONDENCE

Correspondence should be addressed to Betty Gardie: betty.gardie@inserm.fr

AFFILIATIONS

§ ß * These authors contributed equally to this work.

1- Ecole Pratique des Hautes, EPHE, PSL research University, France.
2- CRCINA, INSERM, Université de Nantes, Université d'Angers, Nantes, France.
3- L'institut du thorax, INSERM, CNRS, UNIV Nantes, Nantes, France.
4- Institute for Transfusion Medicine, University of Ulm and Institute for Clinical Transfusion Medicine and Immunogenetics Ulm, German Red Cross Blood Service Baden-Württemberrg-Hessen, Ulm, Germany.
5- Wellcome Centre for Human Genetics, University of Oxford, Oxford, UK.
6- Oxford NIHR Biomedical Research Centre, Oxford, UK.

7- Univ Rennes, CNRS, IGDR (Institut de génétique et développement de Rennes) - UMR 6290, F- 35000 Rennes, France.
8- Department of Medicine/Physiology, University of Fribourg, 1700 Fribourg, Switzerland.
9- INSERM UMR970, Paris-Cardiovascular Research Center at HEGP, Paris, France.
10- Université Paris Descartes, Faculté de Médecine, Paris, France, Equipe labellisée Ligue contre le Cancer.
11- INSERM UMR 1186, Institut Gustave Roussy, Université Paris-Saclay, Villejuif, France.
12- Service de Génétique Médicale, CHU de Nantes, Nantes, France.
13- Programme Cartes d'Identité des Tumeurs, Ligue Nationale Contre le Cancer, F-75013 Paris, France.
14- Molecular Diagnostics Laboratories, Molecular Haematology Dept, Oxford University Hospitals Trust, Oxford, UK.
15- Faculté de Médecine Paris-Sud, Le Kremlin-Bicêtre, France.
16- Réseau Expert National pour Cancers Rares de l'Adulte INCa "PREDIR" and Réseau d'Oncogénétique National INCa "Maladie de VHL et prédispositions au cancer du rein," Service d'Urologie, Assistance publique, Hôpitaux de Paris, Hôpital Bicêtre, Le Kremlin-Bicêtre, France.
17- Assistance Publique Hôpitaux de Paris, Hôpital européen Georges Pompidou, Service de Génétique, Paris, France.
18- Pathology Department, Hôpitaux Universitaires Paris Sud, Assistance Publique Hôpitaux de Paris, Le Kremlin Bicêtre, France.
19- Université Paris 11, Faculté de Médecine Paris Sud, Le Kremlin Bicêtre, France.
20- Assistance Publique Hôpitaux de Paris Centre de Référence des Maladies Rénales Héréditaires de l'Enfant et de l'Adulte (MARHEA), Service de Néphrologie Pédiatrique, Hôpital Universitaire Necker-Enfants malades, Paris, France
21- Assistance Publique Hôpitaux de Paris, Département de Chirurgie Pédiatrique, Hôpital Universitaire Necker-Enfants malades, Université Paris Descartes-Sorbonne Paris Cité, Paris, France.
22- Democritus University of Thrace Faculty of Medicine Alexandroupolis, Thrace, Greece.
23- Department of Pediatrics and Adolescent Medicine, University Medical Center Ulm, Ulm, Germany.
24- Gustave Roussy and INSERM U1186, Université Paris Saclay, Département de Biologie et Pathologies Médicales, Villejuif, F-94805, France.
25- SingHealth/Duke-NUS Institute of Precision Medicine, National Heart Centre Singapore, Singapore.
26- Service d'hématologie Biologique, Pôle Biologie, CHU Dijon, Dijon, France.
27- Inserm UMR1231 "Lipides Nutrition Cancer" équipe "Protéines de Stress et Cancer", FCS Bourgogne Franche Comté, LipSTIC Labex, F-21000 Dijon, France.
28- First Medical Clinic, Department of Medicine- DIMED, University of Padua, Padua, Italy.
29- Clinic of Pediatric Hemato-Oncology, Department of Woman's and Child's Health, University of Padua, Padua, Italy.
30- Service de génétique humaine du CHU Sart Tilman, B-4000 Liège, Belgium.
31- Department of Clinical Chemistry and Haematology, University Medical Center Utrecht, Utrecht, The Netherlands.
32- Department of Hematology, West German Cancer Center, University Hospital Essen, Essen, Germany.
33- First Department of Pediatrics, National and Kapodistrian University of Athens, Greece
34- Centre de Génétique Humaine, Cliniques universitaires Saint-Luc, B-1200 Bruxelles,

Belgium.
35- Department of Hematology, Centro Hospitalar e Universitario de Coimbra, Coimbra, Portugal.
36- Laboratory of Excellence GR-Ex.

Abstract:

Chuvash polycythemia is an autosomal recessive form of erythrocytosis associated with a homozygous p.Arg200Trp mutation in the von Hippel-Lindau (*VHL*) gene. Since this discovery, additional *VHL* mutations have been identified in patients with congenital erythrocytosis, in a homozygous or compound-heterozygous state. *VHL* is a major tumor suppressor gene, mutations in which were first described in patients presenting with von Hippel–Lindau disease, which is characterized by the development of highly vascularized tumors. Here, we identified a new *VHL* cryptic-exon (termed E1') deep in intron 1 that is naturally expressed in many tissues. More importantly, we identified mutations in E1' in seven families with erythrocytosis (one homozygous case and six compound-heterozygous cases with a mutation in E1' in addition to a mutation in *VHL* coding sequences) and in one large family with typical VHL disease but without any alteration in the other *VHL* exons. In this study we have shown that the mutations induced a dysregulation of the *VHL* splicing with excessive retention of E1' and are associated with a downregulation of VHL protein expression. In addition, we have demonstrated a pathogenic role for synonymous mutations in *VHL*-Exon 2 that alter splicing through E2-skipping in five families with erythrocytosis or VHL disease. In all the studied cases, the mutations differentially impact splicing, correlating with phenotype severity. This study demonstrates that cryptic-exon-retention or exon-skipping are new *VHL* alterations and reveals a novel complex splicing regulation of the *VHL* gene. These findings open new avenues for diagnosis and research into the VHL-related-hypoxia-signaling pathway.

Key points
• Mutations in a *VHL* cryptic exon may be found in patients with familial erythrocytosis or von Hippel-Lindau disease
• Synonymous mutations in *VHL* exon 2 may induce exon-skipping and cause familial erythrocytosis or von Hippel-Lindau disease

Introduction:

Congenital erythrocytosis represents a heterogeneous group of rare disorders. Genetic changes affecting all parts of the regulatory pathway of erythropoiesis, including oxygen sensing, erythropoietin sensitivity, or hemoglobin oxygen affinity have been described in patients with congenital erythrocytosis. The detection of underlying genetic changes in patients with presumed hematological pathology may have important implications for an adequate clinical management. However, even with the use of NGS panel diagnostics, the underlying genetic cause of presumed congenital erythrocytosis has been identified in less than one third of the patients in most published cohorts.

The molecular basis of VHL-related congenital erythrocytosis was first described in the autonomous Russian Republic of Chuvashia where this condition is an endemic disorder.[1] Chuvash polycythemia is frequently associated with rubor, vertebral hemangiomas, varicose veins and low blood pressure. Chuvash patients have reduced survival rates associated with a higher prevalence of arterial and venous thromboses and pulmonary hypertension in addition to hemorrhagic events.[2]

Chuvash polycythemia arose from a homozygous c.598C>T, p.Arg200Trp (R200W) mutation in the *VHL* gene. This specific *VHL*-R200W mutation has also been identified in combination with other *VHL* mutations (compound-heterozygosity) in Chuvash polycythemia. Subsequently, other missense *VHL* mutations in both alleles have been described in patients with congenital erythrocytosis.[3,4] Interestingly, it has been described some unexplained cases of patients with erythrocytosis in which only one heterozygous *VHL* mutation has been identified to date.[4-6]

VHL is located on 3p25-26 and has been reported to contain three exons (E1, E2, E3). The commonly described *VHL* transcript contains the three spliced exons that encode a 213 amino-acid (aa) protein (pVHL213 also termed pVHL30) and a smaller isoform (pVHL160 or pVHL19) initiated from an in-frame internal translation start site.[7] A naturally occurring splice variant, expressed at low levels in some tissues, comprises E1 directly spliced to E3 and is translated into a protein product termed pVHL172 (pVHLΔE2), the functions of which are still under investigation.[8-12] pVHL213 and pVHL160 are involved in a variety of functions, the most studied being the regulation of the cellular oxygen-sensing pathway. The main player of this pathway is the Hypoxia Inducible Factor (HIF). Under normal oxygen supply, the α–subunits of HIF (HIF-

1α, 2α and 3α) are hydroxylated by the prolyl-4 hydroxylase domain enzymes (PHD1, 2 and 3) and subsequently targeted by pVHL, a subunit of an E3 ubiquitin-ligase complex that promotes HIF-α ubiquitination and subsequent proteasomal degradation.[13,14] Under hypoxic conditions or when *VHL* is mutated, HIF-α remains stable and heterodimerizes with HIF-β, constituting a functional HIF factor. HIF transcriptionally activates a variety of genes involved in adaptation to reduced oxygen supply (e.g. erythropoiesis, angiogenesis, metabolism and cell survival). Dysregulation of the hypoxia pathway[13,14] is central to the development of erythrocytosis[1,4] (via upregulation of erythropoietin (EPO), a HIF2α target gene), but also in the development of tumors.[15] Indeed, *VHL* is a tumor suppressor gene, heterozygous mutations of which are associated with von Hippel-Lindau disease (Figure 1A).[16,17] The VHL disease, described in 1936, is an autosomal dominant disorder with high penetrance characterized by the development of highly vascularized tumors like central nervous system and retinal haemangioblastomas, pancreatic neuroendocrine tumors, pheochromocytomas and clear-cell renal cell carcinomas (ccRCC).[18-20]

In patients carrying *VHL* mutations, the precise mechanistic aspects that underpin the different phenotypes remain obscure. Although most patients carry mutations in the *VHL* gene that induce a partial or complete loss of protein function, some cases remain unsolved. Indeed, some patients with erythrocytosis have been found to be heterozygous rather than homozygous for the expected alteration[4-6] or carry homozygous synonymous mutations that leave the amino-acid sequence intact. In addition, some patients present with VHL disease in the absence of identified mutations or deletions in *VHL*, or carry heterozygous synonymous mutations. Here, we report an investigation of twelve families linked to unexplained disease, including nine families with erythrocytosis and three families with VHL disease (Figure 1A). This study has led to the discovery of a novel cryptic-exon in the *VHL* gene and a complex regulation of *VHL* splicing.

Methods:

Complete materials and methods are detailed in supplemental data.

Study approval

Informed consent for medical diagnosis and research was obtained from the patients and their relatives. This study was agreed by the CCPPRB (French Ethical Committee) Paris-Sud at Bicêtre Hospital.

Sanger sequencing

Exons and exon-intron junctions of the *VHL* gene were sequenced from DNA extracted from whole blood, as previously described.[21]

Whole Genome Sequencing

Whole genome sequencing (for Families F2, F3, F7) was performed at the clinically accredited Molecular Diagnostics Laboratory at the John Radcliffe Hospital using the Hi-Seq 4000 platform (Illumina Inc., San Diego, CA) in high-throughput mode.[22,23] Analysis of single nucleotide variants, short insertions/deletions and copy number variants was conducted and is explained in detail in the supplemental methods.

Transcript detection and quantification

After reverse-transcription reactions (ThermoScientific), exon-specific PCR was performed using primers localized to flanking E1 and E3 exons. Taqman real-time PCR were performed on 20 ng of cDNA with the qPCR Mastermix (Eurogentec). Quantification of *RPLP0* transcripts was used as internal control. The thresholds were determined using dilutions of plasmids containing coding sequences of each gene.

RNA sequencing

Library construction was performed with SureSelect Strand-Specific RNA Library Prep for the Illumina Multiplexed-kit (Agilent-Technologies). After purification (Macherey-Nagel), the fragment size of libraries was controlled using the 2200 TapeStation system (Agilent-

Technologies). Ten pM of each library were pooled and prepared according to the denaturing and diluting libraries protocol for the Hiseq and GAIIx (Illumina) for cluster generation on the cBot™ system. Paired-end sequencing was carried out in a single lane on the HiSeq® 2500 system (Illumina). Processing of reads is detailed in Supplemental methods.

Reporter assays

The plasmid encoding the wild-type HA-VHL was kindly provided by Prof. William G. Kaelin Jr. An expression plasmid for the hypothetical X1-protein was constructed by subcloning the coding sequence following its synthesis (LifeTechnologies). Mutations of interest were introduced by site-directed mutagenesis (New-England Biolabs). 786-O cells were transfected (Polyplus) with constructs encoding wild-type or mutant proteins, Firefly-luciferase under the control of Hypoxia-Response-Elements (HRE-luciferase), and Renilla-luciferase for normalization.[24] After 24h, luciferase assays were performed using a Dual-Luciferase®Reporter Assay System (Promega).

Western Blotting

Cell lysates from the luciferase reporter assay were loaded into a Bis-Tris Mini Gel (4-12%) (Invitrogen). After transfert, the membrane (GE-Healthcare) was subsequently incubated with a mouse anti-HA antibody (BioLegend), and then a goat anti-mouse HRP-conjugated antibody (Jackson-Immuno-Research). Western blot using the mouse monoclonal antibody JD-1956 (Patent No. 14305925.1-1402-2014; CNRS-EFS) raised against human VHL was performed as described.[8]

Minigene experiments

Minigene constructs were prepared in pCas2 plasmid, containing two artificial exons A and B (as described[25]), between which *VHL*-Exon1' or *VHL*-Exon2 with intronic flanking sequences were cloned. Cells were transfected (Polyplus) or nucleofected (Lonza). RNA were extracted 24h after transfection and reverse transcribed. PCR amplification was performed using the PCR GoTaqQ2 kit (Promega) with primers against artificial (A and B) exons. PCR products were resolved in a 2% agarose gel.

Results:

Identification of new VHL spliced isoforms containing a cryptic-exon.

We first focused our study on a patient with erythrocytosis in whom a synonymous *VHL* c.429C>T, p.Asp143Asp (D143D) mutation in the heterozygous state had previously been identified (Family 1, Table 1). No other mutations in the three *VHL* canonical exons had been identified in genomic DNA of this patient. A RT-PCR using primers in E1 and E3 was performed using mRNA samples extracted from lymphoblastoid cell lines (LCL) established from different family members. The results showed a strong decrease of the E1E2E3 isoform and an upregulation of the E1E3 isoform (Figure 1B) compared with wild-type LCL. Some minor extra fragments of larger size were observed in this patient and his mother's sample. Subcloning and sequencing of these fragments allowed us to identify new *VHL* transcripts that contained intronic sequences. This intronic sequence, which we termed the E1' cryptic-exon, is spliced to E1 at its 5' end, and to either E2 or E3 at its 3' terminus (Figure 1C). We showed that these isoforms are expressed in a variety of tissues and cell lines (Supplemental Fig.1). Their translation may theoretically lead to the production of a protein of 193 aa that contains the first 114 aa encoded by E1[26], and 79 additional aa of unknown function encoded by E1'. During the course of our study, data from an automated computational analysis for an isoform containing the E1' cryptic-exon (E1E1'E2 isoform), was deposited in NCBI. This isoform was predicted to encode a protein of 193 aa, named X1 (XP_011532380.1) with the sequence described above. The analysis of this region revealed strong conservation in primates, but a moderate to low conservation in more distant species (Supplemental Fig.2A-C); notably, the splice sites are identical to canonical sites (ttc**ag**/TC, AG/**gt**aag), and are highly conserved. *In silico* analysis of the donor (SD) and acceptor (SA) splice sites of E1' showed similar consensus values compared to other *VHL* exons (Figure 1C, upper panel). The capacity to translate a potential X1 protein is only conserved in higher primates (Supplemental Fig.2D). The deposited sequence has now been removed and replaced by a non-coding isoform containing E1' spliced with *VHL*-E2 and E3 (ENST00000477538.1) (Figure 1C, isoform on the bottom). This isoform may be initiated by an alternative promoter. Indeed, the sequence located at the 5' end of E1' represents a transcriptionally active region, as illustrated by epigenetic marks (Supplemental Fig.3). We confirmed the expression of an additional transcript initiated from the upstream region of E1' (that we termed "Upstream E1'") in different tissues and cell lines (Supplemental Fig.1).

The new E1' cryptic-exon is mutated in patients with erythrocytosis or von Hippel-Lindau disease.

Sanger sequencing of this new cryptic-exon in the proband (F1-II.1) identified a variant which had not been reported in databases: c.340+770T>C (Figure 2B, Table 1, Supplemental Fig.4). Sequencing of the germline DNA of the mother revealed the same variant, indicating that the propositus F1-II.1 is compound heterozygous. This result prompted us to sequence additional patients with erythrocytosis described as heterozygous for *VHL* mutations.

We investigated Chuvash polycythemia patients for whom the *VHL*-R200W had been found in a heterozygous state. Sanger sequencing identified the identical intronic variant c.340+770T>C in a singleton (F2)[5] and two affected brothers (F3) (Figure 2B). In addition, we identified a duplication c.340+694_711dup in the proband of F4 and F5[6] previously described as *VHL*-R200W/wt and *VHL*-G144R/wt respectively (Figure 2B). In F6, previously diagnosed as *VHL*-Q164H/wt, we identified a genetic variant c.340+574A>T that altered the consensus splice-acceptor (SA) site **ag**/TC of E1'. This variant is described as a rare polymorphism (rs98274567) in the NCBI database (Table 1).

As biological material from the parents of F2 and F3 was not available, we cloned the intronic region containing the E1' variant and the Chuvash core-haplotype SNP (single nucleotide polymorphism) rs779808 associated with the *VHL*-R200W mutation (described[27] to be located downstream of E1', in position c.340+1150). Segregation analysis (F4, F5, F6) or Chuvash core-haplotype analysis (F2, F3) demonstrated that all patients are compound heterozygous, with one mutation being inherited from each parent (Supplemental Fig.5).

In a parallel independent study, whole genome sequencing (WGS) was being used to investigate patients with Chuvash polycythemia, heterozygous for the *VHL*-R200W mutation (F2 and F3). The intronic variant c.340+770T>C was the only rare variant identified in the *VHL* gene in these patients. Other WGS filtering strategies (Supplemental Methods) did not identify any further significant mutations in biologically relevant genes (Supplemental Fig.6). This study also conducted WGS for a trio with congenital erythrocytosis for which prior whole exome sequencing (WES) had not identified any mutations (F7). No rare biologically relevant variants

were identified using the filtering strategy described in Supplemental Methods. However, further inspection of the new cryptic-exon led to the identification of a c.340+816A>C variant in the homozygous state in the proband, with both parents being heterozygous for this mutation.

In addition to these patients with erythrocytosis, in which no variants in *VHL* were initially detected, screening of patients with von Hippel-Lindau disease may also fail to detect mutations in canonical *VHL* exons. An example of such family, F8, with hereditary hemangioblastoma, clear-cell renal-cell carcinoma and pheochromocytoma has been studied. Microsatellite analysis demonstrated a co-segregation of markers surrounding the *VHL* region with the disease (Supplemental Fig.7). Sequencing of the new E1' cryptic-exon in this family identified two heterozygous variants in E1': a previously unreported c.340+617C>G variant and a c.340+648T>C variant described as a rare polymorphism in databases (Table 1). These variants segregate in six patients who developed the disease, and were absent in four healthy tested descendants, indicating their presence on a single disease-associated allele (Figure 2B). Sequencing of tumor DNAs did not display loss of heterozygosity (LOH), suggesting that a wild-type *VHL* deletion (as observed in classic VHL disease) may not be prerequisite in cells of patients with this specific *VHL* genotype (Supplemental Fig.4).

Expression study of the new VHL isoforms in patients' cells.

RNA-sequencing (RNA-Seq) analysis of patients' LCL and tumors demonstrated that genomic variants in E1' are associated with an up-regulation of transcripts containing the E1' cryptic-exon compared with controls (Figure 3A, Supplemental Fig.8). In addition, the mutated allele is preferentially expressed (more than 70%), suggesting a causal relationship between the genetic variants and the E1' retention (Supplemental Fig.8C).

We performed quantitative RT-PCR using TaqMan probes specific for the different splicing junctions or for the region upstream of E1' (location of probes Figure 1C), which showed a strong upregulation of a unique isoform containing E1' spliced with E1 in LCL and tumors from patients of F8 compared with controls (Figure 3B). The study therefore focused on the isoform E1-E1'. Transcripts that retain E1' spliced with E1 contain (in-frame with E1) a premature termination codon (Figure 1C) and are likely targeted for degradation according to nonsense-mediated mRNA Decay (NMD) mechanisms. We therefore investigated the expression of transcripts that

contain E1 spliced with E1' in the absence or presence of puromycin, an inhibitor of NMD. Without puromycin, higher levels of expression were seen in samples with mutated E1' (Figure 3C) compared with samples containing WT-E1'. Exposure to puromycin resulted in a profound induction of isoforms containing E1 spliced with E1' *versus* other isoforms (Figure 3C, Supplemental Fig.9). These results indicated that isoforms with E1-E1' junction are degraded by NMD and may fail to produce proteins. We performed RT-PCR on LCL sample of F6 carrying the mutation in the SA site, using primers in *VHL* exons E1 and E3. We observed fragments of larger size in samples from patients carrying the mutation, which were highly visible in presence of puromycin (Figure 3D). Cloning and sequencing of these fragments demonstrated a dysregulated splicing of E1' with the use of an alternative SA site located 15 nucleotides downstream (Supplemental Fig.10).

In order to measure the impact of the splicing dysregulation on pVHL expression, we performed an immunoblot with an antibody able to recognize the aa encoded by E1 and, therefore, able to detect the different pVHL isoforms.[8] The antibody detected overexpressed exogenous X1 protein following transfection of plasmid encoding X1 (Figure 4A). However, it failed to detect the endogenous protein, even in patients' samples that overexpress the mRNA containing E1-E1'. Instead, the immunoblots showed a lower expression of all the VHL protein isoforms in patients with mutated E1' (Figures 4A and 4B).

Functional characterization of the mutated VHL-E1'.

As the hypoxia pathway represents the major pathway involved in the genesis of the secondary erythrocytosis and VHL disease[13-15,28], we performed functional studies of the hypothetical wild-type or mutated X1 proteins using Hypoxia Response Element (HRE)-dependent reporter assays. These functional tests failed to reveal any substantial effects of X1 on this pathway, either alone or in competition with pVHL (Figure 4C, Supplemental Fig.11). We next focused our study on a potential impact of the E1' variants on splicing by performing splicing reporter minigene assays in various cell lines. The experiments showed that splicing of the wild-type E1' is barely detected (Figure 4D). Interestingly, higher molecular weight bands corresponding to the expected spliced isoforms containing E1' appeared in the presence of the mutations. Cloning and sequencing of the isoforms confirmed a retention of E1' at the expected

splicing sites. The level of expression of the upper isoform, specific to E1' inclusion, was higher for mutations associated with cancers than for those with erythrocytosis, independently of the cell lines. Notably, the combination of both variants associated with cancer has a more pronounced effect than each variant individually (the SNP showing very low effect), suggesting a synergistic effect of the variants on splicing (Supplemental Fig.12). *In silico* analysis of the c.340+617C>G consistently predicted a severe alteration of splicing by the creation of an Exonic Splicing Enhancer (ESE) site (Supplemental Fig.13).

The minigene experiment performed with the mutated E1' at the SA site (F6) confirmed the inclusion of E1' during splicing (Figure 4D, right panel), using the same dowstream alternative SA site identified in mRNA extracted from patients' LCL (Supplemental Fig.10).

Synonymous mutations in VHL-Exon 2 induce exon-skipping.

We then focused our study on the synonymous heterozygous D143D mutation in E2, identified in the proband of F1. This mutation was also identified in the homozygous state in two patients with erythrocytosis (F9, F10, Figure 5A, Table 1). The mRNAs extracted from LCLs established from the different members of these two families were reverse transcribed and sequenced. Comparison of chromatograms obtained by sequencing of DNA *versus* cDNA displayed a weaker peak of the mutated allele in cDNA, reflecting a decreased expression of the mRNA transcripts carrying the mutation.

A different synonymous mutation in E2, c.414A>G, p.Pro138Pro (P138P), has been identified in two families (F11, F12) with von Hippel-Lindau disease (Figure 5B). This heterozygous mutation segregates with the disease in three generations. Sequencing of DNA extracted from the pheochromocytoma of F11-III.1 showed a loss of the wild-type allele in the tumor, demonstrating LOH as currently described in classical VHL disease.

Suspecting an effect of the synonymous mutations on splicing, we next assessed the expression of the *VHL* transcripts in patients' samples by RT-PCR (Figure 5C). We showed a significant change in the ratio of expressed *VHL* isoforms, with a higher expression of the E1-E3 transcripts in LCL of patients homozygous for D143D and in the pheochromocytomas with P138P mutation. These results suggested an effect of the mutation on splicing regulatory elements, leading to E2

skipping. *In silico* analysis of the synonymous mutations indicated a potential effect on Exonic-Splicing Enhancer (ESE) motifs (Supplemental Fig.14).

In order to specifically quantify the different *VHL* isoforms, we performed quantitative RT-PCR on LCL using Taqman probes complementary to the *VHL* E1-E2 or E1-E3 junctions (Figure 5D). All mutated samples displayed an increase of the isoform with skipped E2 (E1-E3). The patients carrying a homozygous D143D mutation presented a severe decrease of the wild-type isoform expression level. These results demonstrated that synonymous mutations in E2 affect mRNA isoform production.

In order to evaluate a potential impact on protein expression, we performed a western blot analysis. We did not observe any overexpression of the pVHL172 isoform as expected from mRNA quantification studies. However, in patients homozygous for D143D, we detected a strong downregulation of all the pVHL isoforms, which was also observed to a lesser extent in LCL samples from heterozygous patients (Figure 5E).

Proportion of VHL-E2 skipping is correlated to disease severity in minigene experiments.

In order to study the impact of the synonymous E2 mutations on splicing in different cell lines, we performed minigene assays. We tested the implications of the D143D and P138P mutations on splicing in addition to the nearby mutations described in patients with erythrocytosis (P138L and G144R).[4,6,29] Indeed, these mutations may also impact splicing rather than VHL protein function. We first evaluated the loss-of-function of these mutants by reporter assays. We showed that these could downregulate HIF in a manner similar to the wild-type protein, in contrast to VHL proteins lacking E2 (pVHLΔE2) which are described to be non-functional in terms of their regulation of HIF activity[8-10,12] (Figure 6A). Minigene experiments were performed in a variety of cell lines relevant to the studied diseases, using LCLs as control (Figure 6B). We demonstrated that all mutations cause E2-skipping in LCLs. In other cell lines, these experiments demonstrated a major impact on the *VHL*-E2 splicing of the P138P mutation which is associated with cancer. The mutations P138L, D143D and G144R, which are all associated with erythrocytosis, displayed a weaker effect on splicing, with slight variations among cell lines but with a stronger effect in the erythroid cell line (UT7 cultured with EPO).

Splicing dysregulation of VHL is causal in the developement of disease.

RNA-seq confirmed that the synonymous mutations were not silent but instead induce potent E2-skipping (Figure 6C, Supplemental Fig.15A). Further transcriptome analyses of the pheochromocytoma carrying P138P showed an upregulation of HIF target genes (typically seen in *VHL*-related pheochromocytomas) compared with the pheochromocytoma carrying a *RET* mutation (Supplemental Fig.15B)[30]. We then re-analyzed our independent cohort of pheochromocytomas[30] using RNA-Seq data from both tumors. After unsupervised classification, we observed a segregation of the P138P pheochromocytoma with other *VHL* related-tumors (C1B cluster) whereas the control pheochromocytoma bearing the *RET* mutation was grouped with other *RET* related-tumors (Figure 6D).

Discussion:

The hypoxia pathway plays a central role in erythrocytosis or tumors developed by patients carrying *VHL* mutations. Nevertheless, the full molecular mechanisms at the origin of these different phenotypes remain to be elucidated. To date, the functional studies of *VHL* mutants have been performed on missense mutations. We describe here, for the first time, functional studies of *VHL* mutations which do not have an impact on the coding sequence, but which influence the *VHL* splicing. We discovered a complex regulation of *VHL* splicing that may help to explain the complexity of genotype/phenotype correlations observed in VHL-related disorders. Notably, we demonstrated that synonymous variants (D143D or P138P) can have an impact on *VHL* splicing and should be considered as pathogenic mutations. Our study points to a particular region in the E2 that may be considered as a splicing regulatory domain. Therefore, it would be interesting to evaluate the impact of all the nucleotide changes described in *VHL*-E2[17] on splicing, in the same way as we described for two missense mutations (P138L, G144R). We observed that, depending on the mutation in this region, the impact on splicing can be moderate (D143D, G144R, P138L) or severe (P138P), which correlates with the severity of the disease seen in individuals carrying these *VHL* mutations (erythrocytosis *versus* cancers). This observation confirms the hypothesis of a continuum model of tumor suppression by *VHL*.[21,31]
Regarding the erythrocytosis developed in patients homozygous for D143D, both probands (F9 II.1 and F10 II.1) present mutations in the beta-globin gene (*HBB*) that induce hemoglobin

instability or thalassemia (Table 1). This may compensate the strong erythropoiesis associated with a very high serum erythropoietin level associated with the D143D mutation.

More importantly, we discovered a new *VHL* cryptic-exon, E1', expressed in healthy tissues. Our study led to the identification of E1' heterozygous mutations occurring in the second allele of six families with an erythrocytosis previously associated with a heterozygous mutation in *VHL* rather than a homozygous mutation. Our investigations further confirmed that polycythemia associated with *VHL* mutation is definitely an autosomal recessive disease. In addition, we identified an E1' homozygous mutation in a patient with an erythrocytosis of unknown origin. This result demonstrates the causal role of the alteration in this new cryptic-exon in the pathophysiology of erythrocytosis. Importantly, we also identified E1' mutations in patients with unexplained VHL disease.

This *VHL*-E1' exon remained unidentified until this point because of its low expression and the fact that this deep intronic region was never explored or represented in WES data. Our data showed that these newly described E1'-containing transcripts may be polyadenylated (as they are captured by polydT in RNAseq) but are also likely to be subjected to NMD and may therefore fail to produce a protein. However, we cannot exclude the possibility that they are translated into a new protein (X1) not expressed in sufficient quantity to be detected by western blot. This potential X1 isoform would contain the VHL-E1 that encodes the NH2-terminal part of pVHL, including 16 residues involved in HIF binding from the 17 described.[26] Nonetheless, the hypoxia-dependent reporter assays failed to identify a potential direct role of this isoform on the HIF pathway. Instead, our results provide compelling evidence that mutations in E1' induce a severe retention of this E1'cryptic-exon which correlates with a defect in global VHL protein expression. Therefore, our study strongly favors a dysregulation of splicing with a consequent downregulation of pVHL expression as the underlying cause of the diseases observed. Here, insufficient pVHL levels but not a reduced HIF binding by the mutant pVHL (as seen in the Chuvash polycythemia mutation *VHL*-R200W[1]) may lead to an impairment of HIF degradation. Of note is the fact that the functional study of mutations identified in E1' in association with erythrocytosis resulted in a less severe impact on splicing than the mutations associated with cancer, confirming that polycythemia is associated with *VHL* hypomorphic mutations.

Our findings may have broad implications for patients with presumed congenital erythrocytosis. First, the underlying cause of congenital erythrocytosis has been identified in only about one third of the patients in most published studies. However, previous studies have focused on missense and nonsense changes in coding regions and known regulatory domains of candidate genes. This has also been the case in patients with suspected VHL disease. Our study shows that synonymous exonic changes, as well as changes within intronic sequences affecting exon splicing, may be responsible for these disorders and should be considered during the diagnostic process. Notably, the *VHL*-E1' exon should be added in the list of regions routinely sequenced in patients with congenital erythrocytosis. Second, the detection of molecular changes has implications for the clinical management of patients. For example, phlebotomy in patients with VHL- or HIF2α-related erythrocytosis may even worsen the clinical situation by increasing the risk and severity of pulmonary hypertension in these patients.[32] Third, the confirmation of the continuum model of tumor suppression by VHL helps to understand the very low frequency of secondary tumors in patients with VHL-related erythrocytosis.[33] On the other hand, this also means that later occurrence of such neoplasms cannot be definitely excluded. Therefore, the clinical management of these patients should include regular follow-up to assess the risk for thromboembolic complications, pulmonary hypertension, and cardiovascular disease, as well as regular examinations to check for the presence of typical VHL-related tumors. Patients with VHL disease due to E1' mutations will also benefit from regular screening for tumors. Finally, the detection of these new genetic changes will also allow appropriate genetic counselling of affected patients and their families.

In conclusion, *VHL* is a major tumor suppressor gene that plays a pivotal role in the oxygen-sensing pathway which is involved in multiple physiological (e.g. angiogenesis, erythropoiesis) and pathological (e.g. cancer) processes. Our findings regarding the complex splicing regulation of this gene in erythrocytosis and tumorigenesis may therefore open new avenues for diagnosis of these conditions as well as research in biological mechanisms related to the hypoxia-signaling pathway. Notably, we suggest further targeted exploration of the *VHL*-E1' region in unresolved cases of congenital erythrocytosis, inherited kidney cancers, hereditary

paraganglioma/pheochromocytoma syndrome, hemangioblastomas, in addition to all types of sporadic tumors with altered hypoxia signaling.

Acknowledgments:
This study was supported by grants from the Région Pays de la Loire, project "EryCan"; the ANR (PRTS 2015 "GenRED"); the labex GR-Ex, reference ANR-11-LABX-0051 and the Ligue Nationale contre le Cancer (Comités de la Loire Atlantique et des Côtes d'Armor). In addition, we acknowledge funding from the Oxford NIHR Biomedical Research Centre and the Health Innovation Challenge Fund scheme. The views expressed in this manuscript are those of the authors and not necessarily those of Wellcome Trust and Department of Health. We acknowledge also funding contribution from the Wellcome Trust Core Award Grant Number 203141/Z/16/Z. AB received a financial support from ITMO Cancer AVIESAN (Alliance Nationale pour les Sciences de la Vie et de la Santé, National Alliance for Life Sciences & Health) within the framework of the Cancer Plan. DH is supported by the National Center of Competence in Research Kidney.CH. The authors thank Richard Breathnach, Jean Feunteun, Judith Favier, Sylvie Hermouet for scientific discussions; Helena M Silva, Caroline Abadie, Sophie Giraud, Florence Fellmann, Pascal Pigny, Vinciane Dideberg, Segers Karine for patient recruitment and medical advices; Amandine Le Roy, Isabelle Barbieux, Christophe Simian, Marie-Laure Clenet and Stéphanie Lebeau for technical assistance in addition to the Genomics and Bioinformatics Core Facility of Nantes (GenoBiRD, Biogenouest) for its technical support**.** We are grateful to Mario Tosi, Pascaline Gaildrat, and Alexandra Martins (Inserm U1079-IRIB, University of Rouen, Rouen, France) for kindly providing the pCAS2 minigene plasmid.
We would also like to thank the European COST Networks MPN&MPNr-EuroNet (COST Action BM0902 "Molecular Diagnosis of MyeloProliferative Neoplasms Euronet") and Hypoxianet (COST Action action TD0901 "Hypoxia sensing, signaling and adaptation").

Authorship contributions:

ML, FR, KS, AC, DH, AB, SG, SC, FC, MP, TB, SF, MV, YAB, BG performed experiments; CC, SJLK, JCT, MP, EK and HD conducted genome sequencing or data analysis & interpretation; PL, MC, SDu, SJ, ML performed bioinformatics analyses; HC, KS, SDe, NB, JMM, FA, CG, LH, SI, EM, KB, KMD, BBdP, FG, MLR, MCP, VB, RVW, JG, AK, NJ, CB, APGR, SR conducted the medical study; BG, DH, ML, FR wrote the manuscripts; BG, HC, designed the study; BG directed the study; all authors contributed to the research and approved the final manuscript.

Disclosure of Conflicts of Interests:

The authors declare no competing financial interests.

References:

1. Ang SO, Chen H, Hirota K, et al. Disruption of oxygen homeostasis underlies congenital Chuvash polycythemia. *Nat Genet*. 2002;32(4):614-621.
2. Gordeuk VR, Sergueeva AI, Miasnikova GY, et al. Congenital disorder of oxygen sensing: association of the homozygous Chuvash polycythemia VHL mutation with thrombosis and vascular abnormalities but not tumors. *Blood*. 2004;103(10):3924-3932.
3. Bento C, Cario H, Gardie B, Hermouet S, McMullin MF. Congenital Erythrocytosis and Hereditary Thrombocytosis. *Book MPN & MPNrEuroNet COST final publication, 2015*. 2015.
4. Bento C, Percy MJ, Gardie B, et al. Genetic basis of congenital erythrocytosis: mutation update and online databases. *Hum Mutat*. 2014;35(1):15-26.
5. Cario H, Schwarz K, Jorch N, et al. Mutations in the von Hippel-Lindau (VHL) tumor suppressor gene and VHL-haplotype analysis in patients with presumable congenital erythrocytosis. *Haematologica*. 2005;90(1):19-24.
6. Randi ML, Murgia A, Putti MC, et al. Low frequency of VHL gene mutations in young individuals with polycythemia and high serum erythropoietin. *Haematologica*. 2005;90(5):689-691.
7. Schoenfeld A, Davidowitz EJ, Burk RD. A second major native von Hippel-Lindau gene product, initiated from an internal translation start site, functions as a tumor suppressor. *Proc Natl Acad Sci U S A*. 1998;95(15):8817-8822.
8. Chesnel F, Hascoet P, Gagne JP, et al. The von Hippel-Lindau tumour suppressor gene: uncovering the expression of the pVHL172 isoform. *Br J Cancer*. 2015;113(2):336-344.
9. Clifford SC, Cockman ME, Smallwood AC, et al. Contrasting effects on HIF-1alpha regulation by disease-causing pVHL mutations correlate with patterns of tumourigenesis in von Hippel-Lindau disease. *Hum Mol Genet*. 2001;10(10):1029-1038.
10. Gnarra JR, Tory K, Weng Y, et al. Mutations of the VHL tumour suppressor gene in renal carcinoma. *Nat Genet*. 1994;7(1):85-90.
11. Hascoet P, Chesnel F, Jouan F, et al. The pVHL172 isoform is not a tumor suppressor and up-regulates a subset of pro-tumorigenic genes including TGFB1 and MMP13. *Oncotarget*. 2017;8(44):75989-76002.
12. Richards FM, Schofield PN, Fleming S, Maher ER. Expression of the von Hippel-Lindau disease tumour suppressor gene during human embryogenesis. *Hum Mol Genet*. 1996;5(5):639-644.
13. Maxwell PH, Wiesener MS, Chang GW, et al. The tumour suppressor protein VHL targets hypoxia-inducible factors for oxygen-dependent proteolysis. *Nature*. 1999;399(6733):271-275.
14. Stebbins CE, Kaelin WG, Jr., Pavletich NP. Structure of the VHL-ElonginC-ElonginB complex: implications for VHL tumor suppressor function. *Science*. 1999;284(5413):455-461.
15. Iliopoulos O, Kibel A, Gray S, Kaelin WG, Jr. Tumour suppression by the human von Hippel-Lindau gene product. *Nat Med*. 1995;1(8):822-826.

16. Latif F, Tory K, Gnarra J, et al. Identification of the von Hippel-Lindau disease tumor suppressor gene. *Science*. 1993;260(5112):1317-1320.
17. Nordstrom-O'Brien M, van der Luijt RB, van Rooijen E, et al. Genetic analysis of von Hippel-Lindau disease. *Hum Mutat*. 2010;31(5):521-537.
18. Kaelin WG, Jr. Molecular basis of the VHL hereditary cancer syndrome. *Nat Rev Cancer*. 2002;2(9):673-682.
19. Maher ER, Kaelin WG, Jr. von Hippel-Lindau disease. *Medicine (Baltimore)*. 1997;76(6):381-391.
20. Richard S, Gardie B, Couve S, Gad S. Von Hippel-Lindau: how a rare disease illuminates cancer biology. *Semin Cancer Biol*. 2013;23(1):26-37.
21. Couve S, Ladroue C, Laine E, et al. Genetic evidence of a precisely tuned dysregulation in the hypoxia signaling pathway during oncogenesis. *Cancer Res*. 2014;74(22):6554-6564.
22. Camps C, Petousi N, Bento C, et al. Gene panel sequencing improves the diagnostic work-up of patients with idiopathic erythrocytosis and identifies new mutations. *Haematologica*. 2016;101(11):1306-1318.
23. Rimmer A, Phan H, Mathieson I, et al. Integrating mapping-, assembly- and haplotype-based approaches for calling variants in clinical sequencing applications. *Nat Genet*. 2014;46(8):912-918.
24. Ladroue C, Hoogewijs D, Gad S, et al. Distinct deregulation of the hypoxia inducible factor by PHD2 mutants identified in germline DNA of patients with polycythemia. *Haematologica*. 2012;97(1):9-14.
25. Gaildrat P, Killian A, Martins A, Tournier I, Frebourg T, Tosi M. Use of splicing reporter minigene assay to evaluate the effect on splicing of unclassified genetic variants. *Methods Mol Biol*. 2010;653:249-257.
26. Czyzyk-Krzeska MF, Meller J. von Hippel-Lindau tumor suppressor: not only HIF's executioner. *Trends Mol Med*. 2004;10(4):146-149.
27. Liu E, Percy MJ, Amos CI, et al. The worldwide distribution of the VHL 598C>T mutation indicates a single founding event. *Blood*. 2004;103(5):1937-1940.
28. Kondo K, Kim WY, Lechpammer M, Kaelin WG, Jr. Inhibition of HIF2alpha is sufficient to suppress pVHL-defective tumor growth. *PLoS Biol*. 2003;1(3):E83.
29. Lanikova L, Lorenzo F, Yang C, et al. Novel homozygous VHL mutation in exon 2 is associated with congenital polycythemia but not with cancer. *Blood*. 2013;121(19):3918-3924.
30. Burnichon N, Vescovo L, Amar L, et al. Integrative genomic analysis reveals somatic mutations in pheochromocytoma and paraganglioma. *Hum Mol Genet*. 2011;20(20):3974-3985.
31. Berger AH, Knudson AG, Pandolfi PP. A continuum model for tumour suppression. *Nature*. 2011;476(7359):163-169.
32. Sable CA, Aliyu ZY, Dham N, et al. Pulmonary artery pressure and iron deficiency in patients with upregulation of hypoxia sensing due to homozygous VHL(R200W) mutation (Chuvash polycythemia). *Haematologica*. 2012;97(2):193-200.
33. Woodward ER, Wall K, Forsyth J, Macdonald F, Maher ER. VHL mutation analysis in patients with isolated central nervous system haemangioblastoma. *Brain*. 2007;130(Pt 3):836-842.

Family n°/patient	nucleotide variant on allele 1 / allele 2	Impact on protein	Year of birth/Age at diag	Sex	Hb	Ht	Red cells	EPO	Phenotye	Other mutation
F1, II.1	c.429C>T/ c.340+770T>C	VHL p.Asp143Asp/ X1 p.Ser179Pro?	1991/ 15 years	M	16.6	57	6.9	163	Erythrocytosis, kidney ischemic infarct	-
F2, II.1	c.598C>T/ c.340+770T>C	VHL p.Arg200Trp/ X1 p.Ser179Pro?	1957/ 21 years	M	19.9	67		22.2	Erythrocytosis	-
F3, II.1	c.598C>T/ c.340+770T>C	VHL p.Arg200Trp/ X1 p.Ser179Pro?	2003/ 4 months	M	17.9	54	7,5	60	Erythrocytosis	-
F3, II.2	c.598C>T/ c.340+770T>C	VHL p.Arg200Trp/ X1 p.Ser179Pro?	2005/ 6months	M	14.6	45			Erythrocytosis	-
F4, II.1	c.598C>T/ c.340+694_711dup	VHL p.Arg200Trp/ X1 p.Trp159X?	1990/ 7 years	M	20.6	64	8.25	49.9	Erythrocytosis, deep vein thrombosis, intracerebral hemorrhage	FV Leiden
F5, , II.2	c.430G>A/ c.340+694_711dup	VHL p.Gly144Arg/ X1 p.Trp159X?	1975/ 13 years	M	16.2	60	5.9		Erythrocytosis	-
F6 , II.1	c.492G>T/ c.340+574A>T♦	VHL p.Gln164His/ SA	2014/ 6 months	M	15.6	49	6.9	1167	Splenomegaly	-
F7	c.340+816A>C/ c.340+816A>C	X1 p.*194Serext*24/ X1 p.*194Serext*24	7 years	M	20	64	8.09	33	Erythrocytosis	-
F8	c.340+617C>G + c.340+648T>C♦♦/ WT	X1 p.Leu128Val+ X1 p.Leu138Pro/WT			N	N	N	N	VHL disease	-
F9, II.1	c.429C>T/ c.429C>T	VHL p.Asp143Asp/ VHL p.Asp143Asp	1997/ 5 months	M	16.2	49.3	5.2	186	Erythrocytosis	Hb Sitia
F10, II.1	c.429C>T/ c.429C>T	VHL p.Asp143Asp/ VHL p.Asp143Asp	2002/ 4.5 years	F	22.5	64-77.4	12.6	264	Erythrocytosis, Splenomegaly	β thalassemia
F11	c.414A>G/WT	VHL p.Pro138Pro/WT			N	N	N	N	VHL disease	-
F12	c.414A>G/WT	VHL p.Pro138Pro/WT			N	N	N	N	VHL disease	-

Table Legend:

Table 1. Description of variants identified in *VHL*-E1' and *VHL*-E2 with associated clinical manifestations. The second column indicates the position of the nucleotide variants identified in the *VHL* gene regarding the current nomenclature (sequence encoded by the *VHL* E1-E2-E3). WT: wild-type. ♦: the nucleotide change has been reported as rs982745672 with a global MAF that corresponds to T=0.00007/2 (TOPMED). ♦♦: the nucleotide change has been reported as rs73024533 with a global MAF that corresponds to C=0.0026/13 (1000 Genomes) and C=0.0050/147 (TOPMED). The third column indicates the impact either on the VHL protein (for variants located in E1, E2 or E3), or on the potential X1 protein, if encoded by E1-E1' (for variants located in E1'). SA: mutation in splice acceptor site; Diag: diagnosis, M: Male, F: Female, N: normal values. The normal values corresponds to: Hb (Hemoglobin) (g/dL) = M: 13-18 and F: 12-15; Ht (hematocrit) (%)= M: 40-52, F: 37-47; Red cells (million/mm^3)= M: 4.2-5.7, F: 4.2-5.2; EPO (mU/ml)= 5-25.

Figures Legend:

Figure 1: Clinical manifestations of patients carrying *VHL* mutations and identification of a new *VHL* spliced isoform containing a cryptic-exon.

(A) Mutations in the *VHL* gene predispose to different phenotypes. Von Hippel–Lindau disease is characterized by the development of central nervous system (CNS) and retinal hemangioblastomas, neuroendocrine pancreatic tumors, pheochromocytomas and clear-cell renal cell carcinomas. Chuvash polycythemia (erythrocytosis) is characterized by an elevated red blood cell number. This study describes families with typical VHL-related phenotypes associated with an unexpected *VHL* status (i.e. either synonymous mutations or no alterations in *VHL*). (B) RT-PCR using primers specific for E1 and E3 was performed on mRNA extracted from lymphoblastoid cell line (LCL) established from Controls and patients of the Family 1. WT: wild-type. *: denotes larger fragments that were subsequently cloned and sequenced. (C) Schematic representation of the *VHL* gene and its products. The different *VHL* exons are represented on a scale: E1: 340bp from the ATG initiation codon, E1': 259bp, E2: 123 bp, E3: 179bp to the Stop termination codon. The full-length *VHL* mRNA isoform encodes pVHL213 (also named

pVHL30). *VHL*-E1 contains an internal translation initiation codon that initiates the production of pVHL160 protein (pVHL19). *: the isoforms containing E1' spliced with *VHL* exons have been identified by cloning and sequencing in the laboratory but have been described later on by NCBI as transcripts able to produce a protein termed X1. Consensus values of donor (SD) and acceptor (SA) splice sites sequences are indicated above the *VHL* gene, as calculated by the Human Splicing Finder *in silico* tool. Horizontal blue lines indicate the location of probes used in Taqman assays.

Figure 2: Identification of mutations in the new *VHL* cryptic-exon in seven patients with erythrocytosis and a large family with the VHL disease.

(A) Schematic representation of the *VHL* gene and location of the identified mutations in the new *VHL* cryptic-exon E1'. (B) Pedigree of families with erythrocytosis or von Hippel Lindau disease. The genotypes have been elucidated by sequencing both parents and proband (F1, F5, F6), deduced by sequencing of one parent and proband (F4, the mutation deduced being under brackets), or deduced from allele cloning of proband carrying the conserved Chuvash mutation and core haplotype (F2, F3) confirming the transmission of the mutations by one of each parents (for F2 and F3, the identity of the transmitting parent being unknown, the mutation is represented by a white circle under brackets). The genotype of parents from F7 has been elucidated from WGS data. The numbers in italics (F8) indicate the age of the patient at tumor diagnosis.

Figure 3: Expression study of the new *VHL* transcripts isoforms in patient cells.

(A) Sashimi plots from RNA-Seq data obtained from samples (LCLs or pheochromocytoma, Pheo), of three patients from F8. The positions of the different *VHL* exons are indicated, with the maximal number of reads indicated at the right. Splice junctions are denoted by the horizontal links, with details provided in Supplemental Fig. 8. (B) TaqMan quantification of the different *VHL* isoforms from samples of F8 performed using probes specific to the *VHL* E1-E2, the translated sequence upstream E1' or E1-E1' junctions. Relative gene expression has been normalized to LCL control (C1) fixed at 1 (mean results of technical duplicates). C: healthy control. (C) TaqMan quantification of the different *VHL* isoforms in LCLs (established from two independent controls and from patients of F1, F2 and F8) cultured in the absence or presence of puromycin, an inhibitor of Nonsense-Mediated mRNA Decay. TaqMan probes are specific to the

VHL E1-E1' or E1-E2 junctions. The graph resumes experiments performed on LCL cultured independently 3 times and quantified in duplicates. Data are represented as the mean +/- SEM. Statistical p value: * p<0.05, ** p<0.01 based on a *t*-test. (D) RT-PCR using primers specific for E1 and E3 was performed on mRNA extracted from LCLs established from controls and patients of the Family 6 (carrying the mutation c.340+574A>T that targets the Splice Acceptor (SA) site of E1'). Patients with erythrocytosis are indicated in red. On the right, the spliced isoforms are schematically represented. *: denotes larger fragments that contains E1' spliced with E1, but with 15 nucleotides deleted (represented in red) by the use of an alternative SA site (sequences of the cloned bands are detailed in Supplemental Fig.10).

Figure 4: Functional studies of mutations in *VHL*-E1'.

(A, B) Immunoblot analysis of patient LCLs. A representative immunoblot (A) and quantification of 3 different immunoblots are presented (B). Relative gene expression has been normalized to GAPDH expression and results obtained with LCL control (C1) have been fixed at 100%. Data are represented as the mean +/- SEM. ** p<0.01, *** p<0.001, **** p<0.0001 based on a *t*-test. A VHL-antibody which recognized VHL-E1 was able to detect the hypothetical X1 protein. In the most left lane, control LCLs were transfected with an expression vector containing the coding sequence for X1. Five µg of proteins were blotted *vs.* 45µg for other samples to avoid signal saturation with overexpressed X1. Patients with erythrocytosis are indicated in red. (C) Functional HRE-dependent reporter assays were performed in 786-O cells (i.e. *VHL* negative cells that constitutively express HIF-2α). The results are expressed as relative Firefly luciferase activity with *Renilla* luciferase as an internal control. 1.0 unit denotes the basal activity of endogenous HIF-2α using the HRE-luciferase reporter plasmid. The ability of wild-type and mutated X1 to downregulate Firefly luciferase activity (related to HIF activity) was compared to pVHL and in competition with pVHL. An immunoblot using an antibody specific to the hemagglutinin tag was used to detect HA-VHL and HA-X1. The X1-L128V+L138P corresponds to a potential impact of the c.340+648T>C and c.340+617C>G mutations on the hypothetical X1 protein. Three independent experiments were performed. ** p<0.01, based on *t*-test. (D) Characterization of *VHL*-E1' retention by the Minigene experiment (representative picture of agarose gel from n=3). RT-PCR was performed on mRNA obtained from cell lines transfected with a minigene construct containing *VHL*-E1' (wild-type or mutated) flanked by large intronic

sequences cloned between the *SERPING1* exons (exons A and B, targeted by the RT-PCR primers). The plasmids were transfected and the expression of the spliced chimeric transcripts (containing EA and EB with or without E1') was analyzed. Two wild-type constructs containing E1' were used; one contains SNP rs779808, 340+1150T>C. Bands corresponding to EA and EB spliced together or with *VHL*-E1' are indicated on the right. * corresponds to unspecific bands verified by sequencing. The minigene experiment performed with the construction carrying the mutation c.340+574A>T (that targets the Splice Acceptor (SA) site of E1' in F6) confirmed the use of an alternative SA site (right panel) with the deletion of 15 nucleotides (represented in red).

Figure 5: Genetic and expression study of synonymous mutations in *VHL*-E2.

(A, B) Pedigree and sequence chromatograms of germline DNA, tumor (pheochromocytoma) DNA or cDNA prepared from two families (F9, F10) with erythrocytosis (A), and two families (F11, F12) with von Hippel-Lindau disease. (C) Results of RT-PCR using mRNA extracted from LCLs (F9, F10) and leukocytes and tumor material (pheochromocytoma) (F11, F12). (D) TaqMan quantification of the different *VHL* isoforms in LCLs (established from patients of F9, F10 and F11) cultured in the absence or presence of puromycin. TaqMan probes are specific to the *VHL* E1-E2 or E1-E3 junctions. Relative gene expression has been normalized to LCL control (C1). C: healthy control, F: Families. ** $P < 0.01$, *** $P < 0.001$ (E) Immunoblot analysis of patient LCLs. Patients with erythrocytosis are indicated in red. A representative immunoblot (upper panel) and quantification of 4 different immunoblots are displayed (lower panel). Relative gene expression has been normalized to GAPDH expression and results obtained with LCL control (C1) have been fixed at 100%. Data are represented as the mean +/- SEM. ** $p<0.01$, *** $p<0.001$, **** $p<0.0001$ based on a *t*-test.

Figure 6: Functional study of synonymous mutations in *VHL*-E2.

(A) Functional HRE-dependent reporter assays were performed in 786-O cells to evaluate the impact of *VHL* mutations in E2 (P138L and G144R) on VHL protein activity. The VHL protein lacking E2 (pVHL172/VHLΔE2) is used as a negative controle. The results are expressed as Firefly luciferase activity relative to Renilla luciferase as an internal control. 1.0 unit denotes the basal activity of endogenous HIF-2α using the HRE-luciferase reporter plasmid. Immunoblots using an antibody specific for the hemagglutinin tag were used to detect HA-VHL. (B)

Characterization of *VHL* E2-skipping by minigene analyses. Minigene experiments were performed in a variety of cell lines relevant to the studied diseases: renal (293T, 786-O, HK2), pheochromocytoma (PC12), erythroid cell line (UT7 cultured with EPO); and LCL. RT-PCR was performed on mRNA obtained from cell lines transfected with a minigene construct containing *VHL*-E2 flanked by intronic sequences cloned between the *SERPING1* exons (exons A and B, targeted by the RT-PCR primers). Bands corresponding to EA and EB spliced together or with *VHL*-E2 are indicated on the right (C) Sashimi plots from RNA-Seq data. The positions of the different *VHL* exons are indicated, with the maximum number of reads for each exon indicated at the right. Splice junctions are denoted by the horizontal links, with details provided in Supplemental Fig. 15A. (D) Heatmap of pheochromocytoma transcriptome data. A comparison of transcriptome data for the pheochromocytoma from patient F11 III.1 (with P138P mutation) *vs.* Affymetrix data from the largest available cohort of paraganglioma/pheochromocytomas (recruited by the French COMETE network) that identified homogeneous molecular subgroups associated with susceptibility genes (Burnichon et al., 2011). exp: relative expression compared to the median.

Figure 1

A

Phenotype :

Healthy | Erythrocytosis | von Hippel-Lindau Disease (2C | 2A | 2B | 1)

- Pheocromocytoma
- Neuroendocrine Pancreatic tumor
- CNS Hemangioblastoma
- Retinal Hemangioblastoma
- Renal cell carcinoma

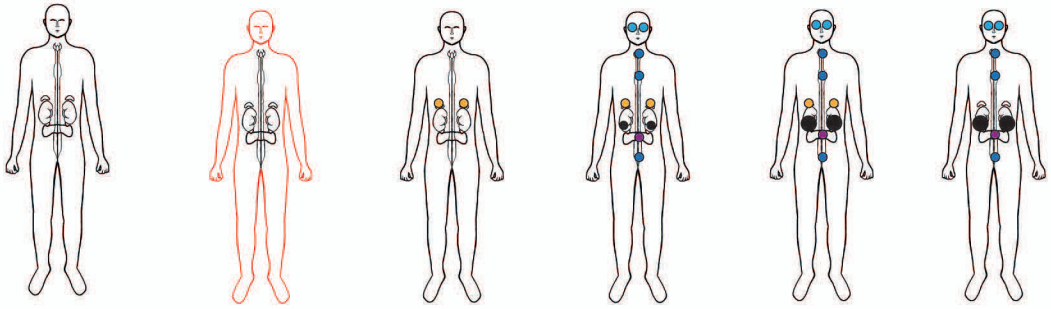

Representative Genotype : R200W/WT | R200W/R200W | L188V/WT | Y98H/WT | R167Q/WT | C162F/WT

Genotype of unsolved cases :

F1 : D143D/WT?
F2,F3, F4 : R200W/WT?
F5 : G144R/WT?
F6 : Q164H/WT
F7 : WT/WT?
F9,F10 : D143D/D143D
F8 : WT/WT?
F11, F12 : P138P/WT

B

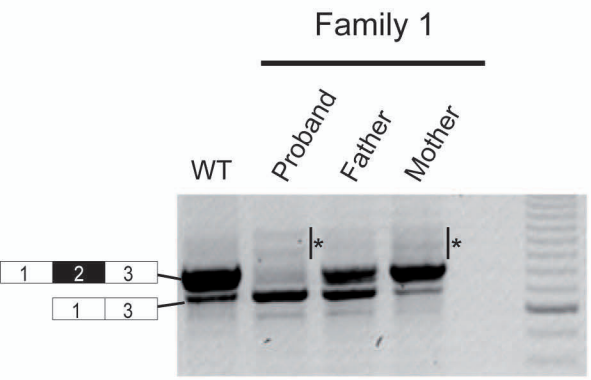

C

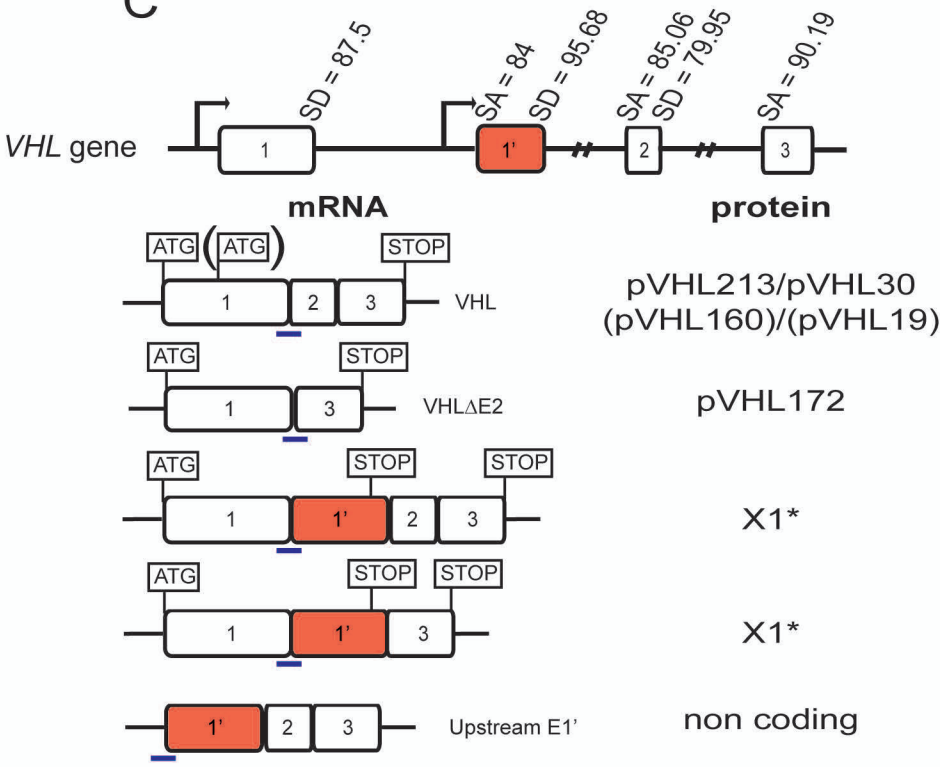

Figure 2

A

- c.340+574A>T
- c.340+694_711dup
- c.340+770T>C
- c.340+816A>C

Erythrocytosis

- c.340+617C>G + c.340+648T>C

VHL disease

B

Family 1

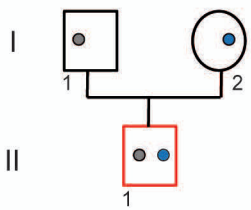

- c.429C>T, p.Asp143Asp
- c.340+770T>C

Family 2

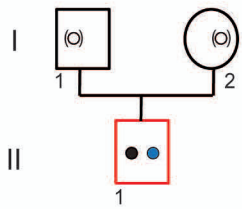

- c.598C>T, p.Arg200Trp
- c.340+770T>C

Family 3

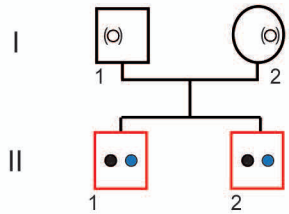

- c.598C>T, p.Arg200Trp
- c.340+770T>C

Family 4

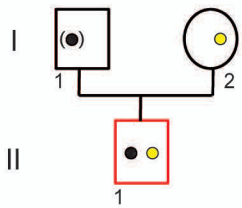

- c.598C>T, p.Arg200Trp
- c.340+694_711dup

Family 5

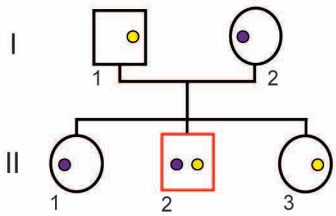

- c.430G>A, p.Gly144Arg
- c.340+694_711dup

Family 6

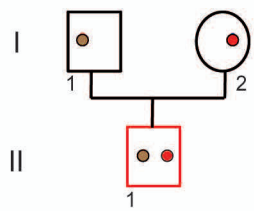

- c.492G>T, p.Gln164His
- c.340+574A>T

Family 7

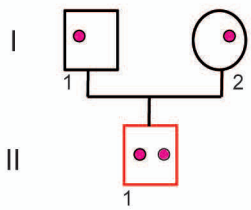

- c.340+816A>C

Family 8

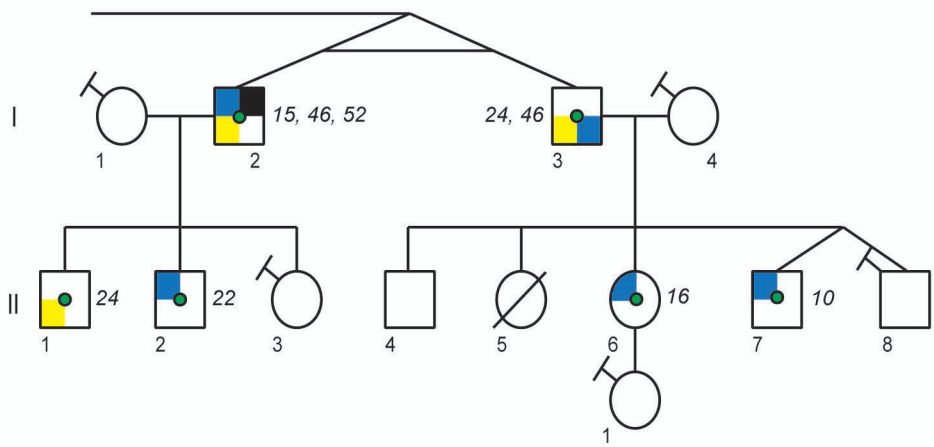

Legend:

- Erythrocytosis
- Retinal Hemangioblastoma
- Pheochromocytoma
- CNS Hemangioblastoma
- Renal cell carcinoma
- c.340+617C>G c.340+648T>C
- Genetically tested, *VHL* WT

Figure 3

A

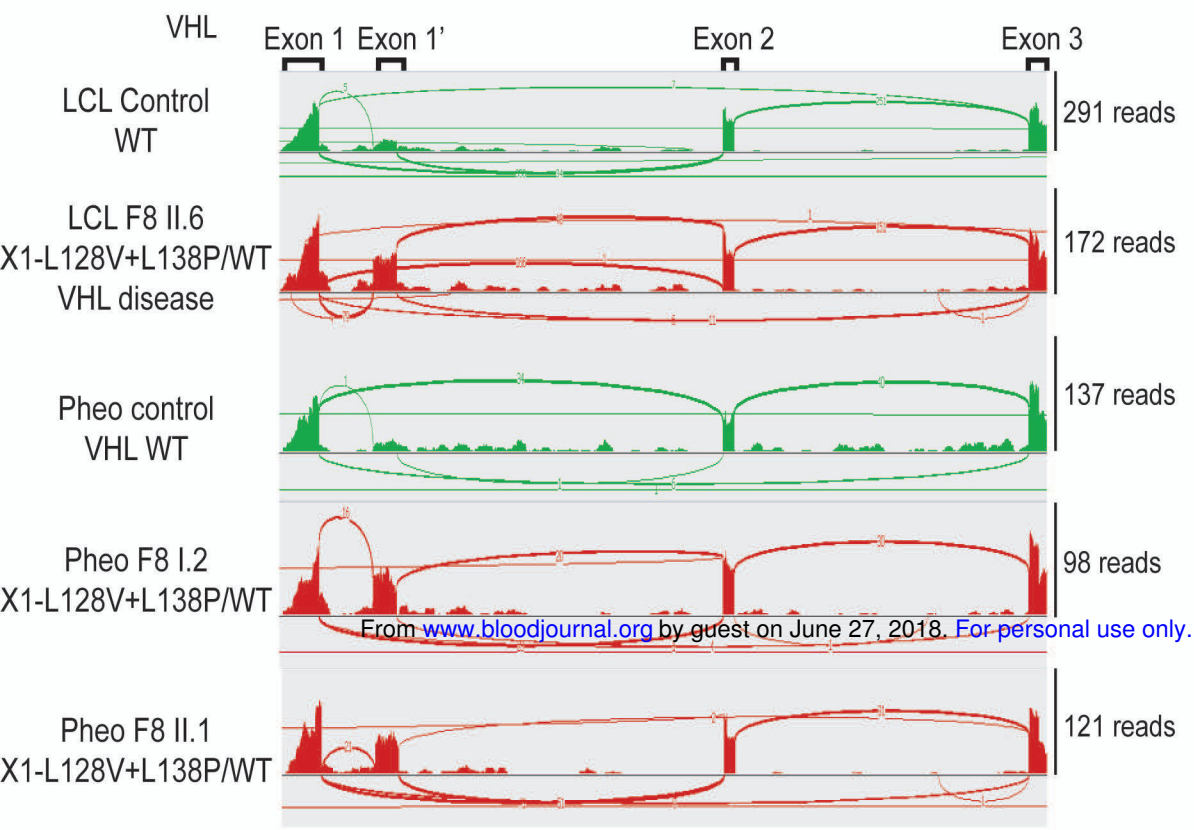

B

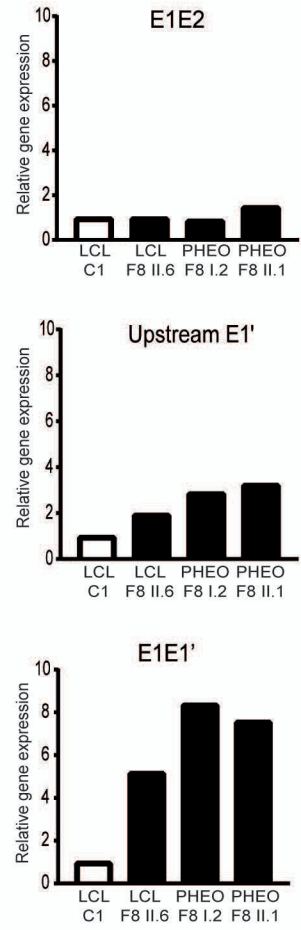

C

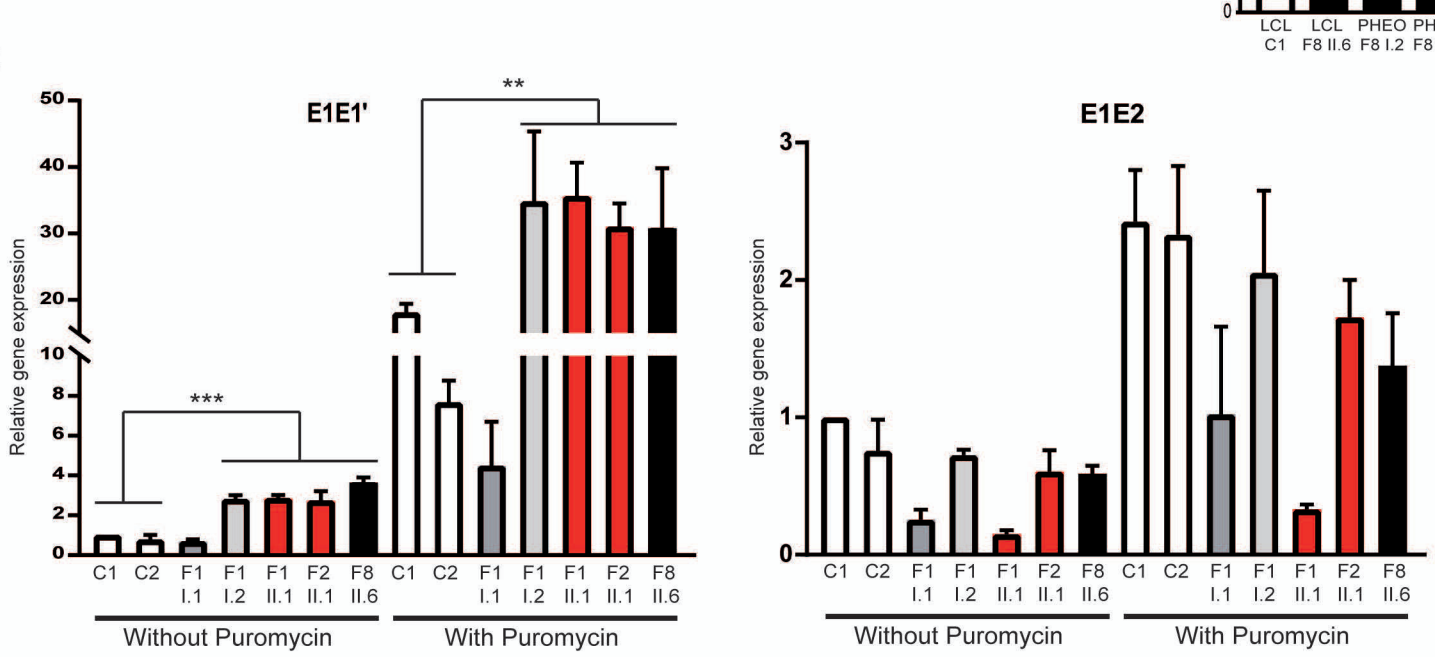

D

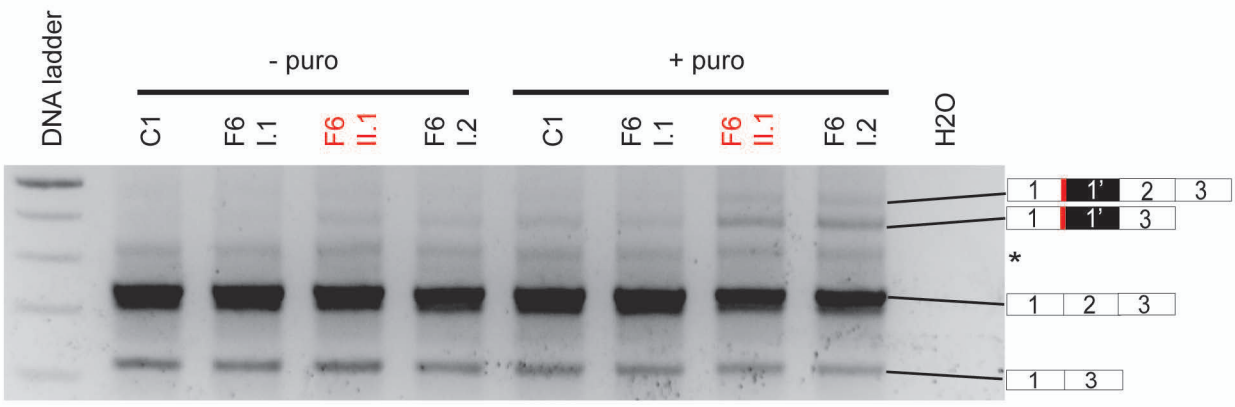

Figure 4

A

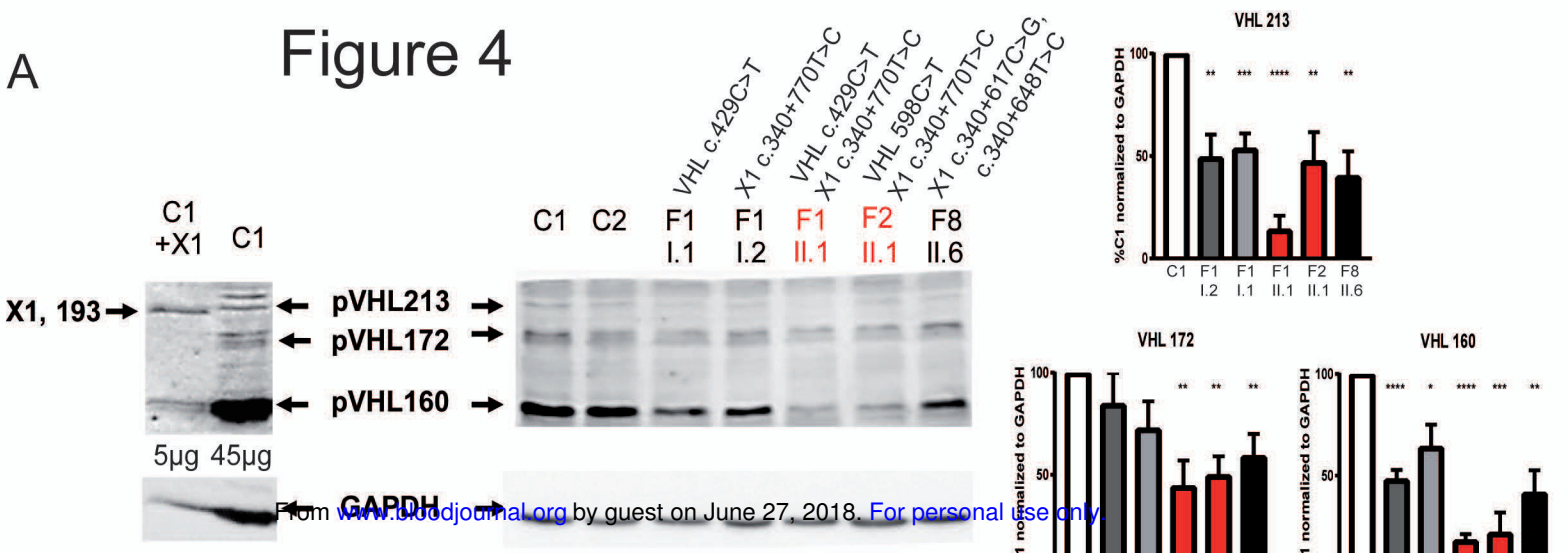

B

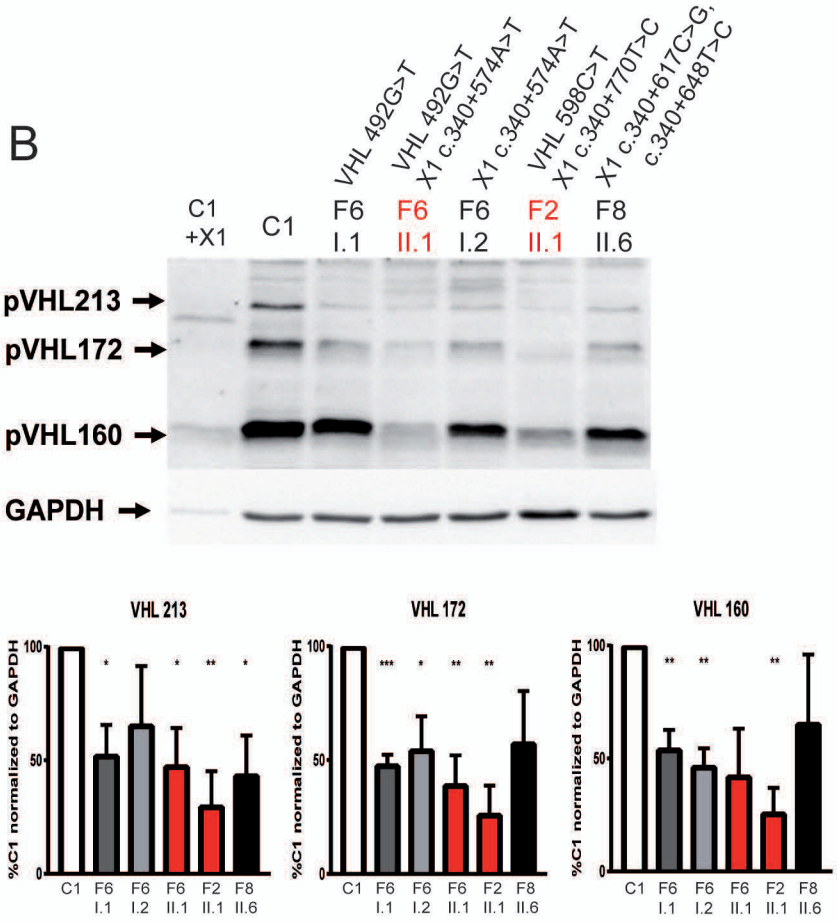

C

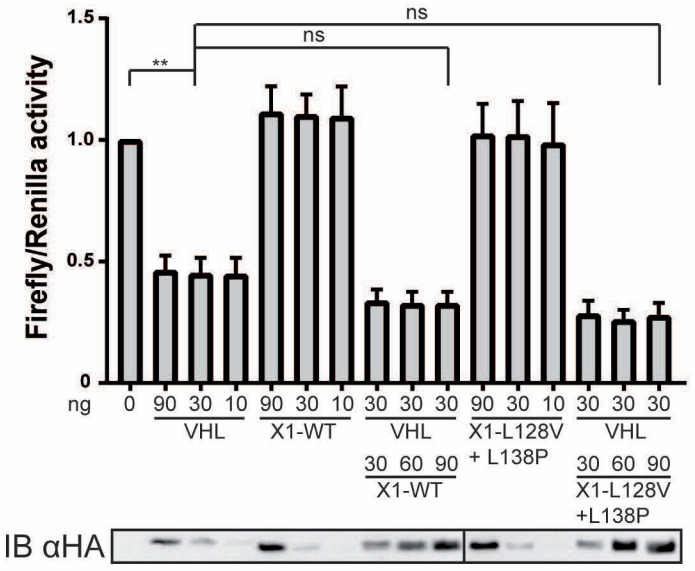

D

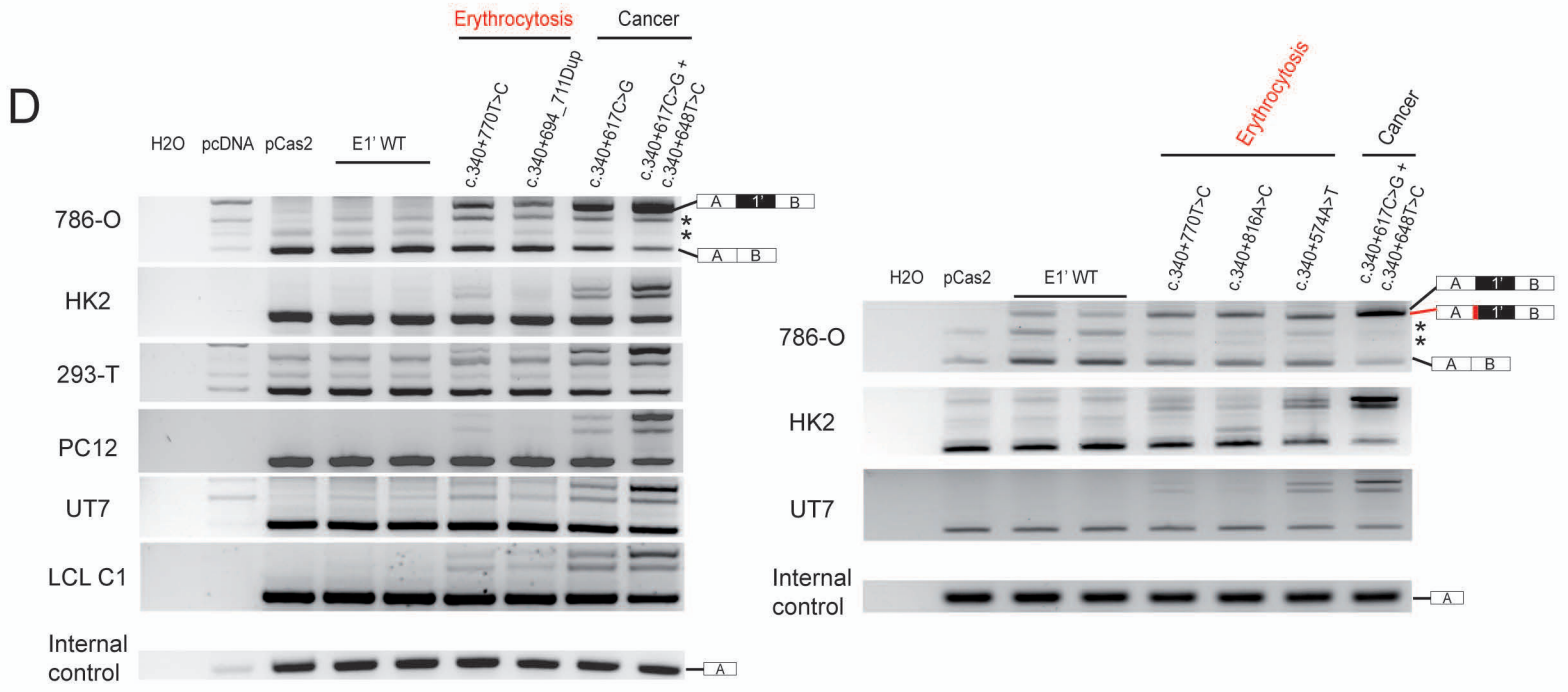

Figure 5

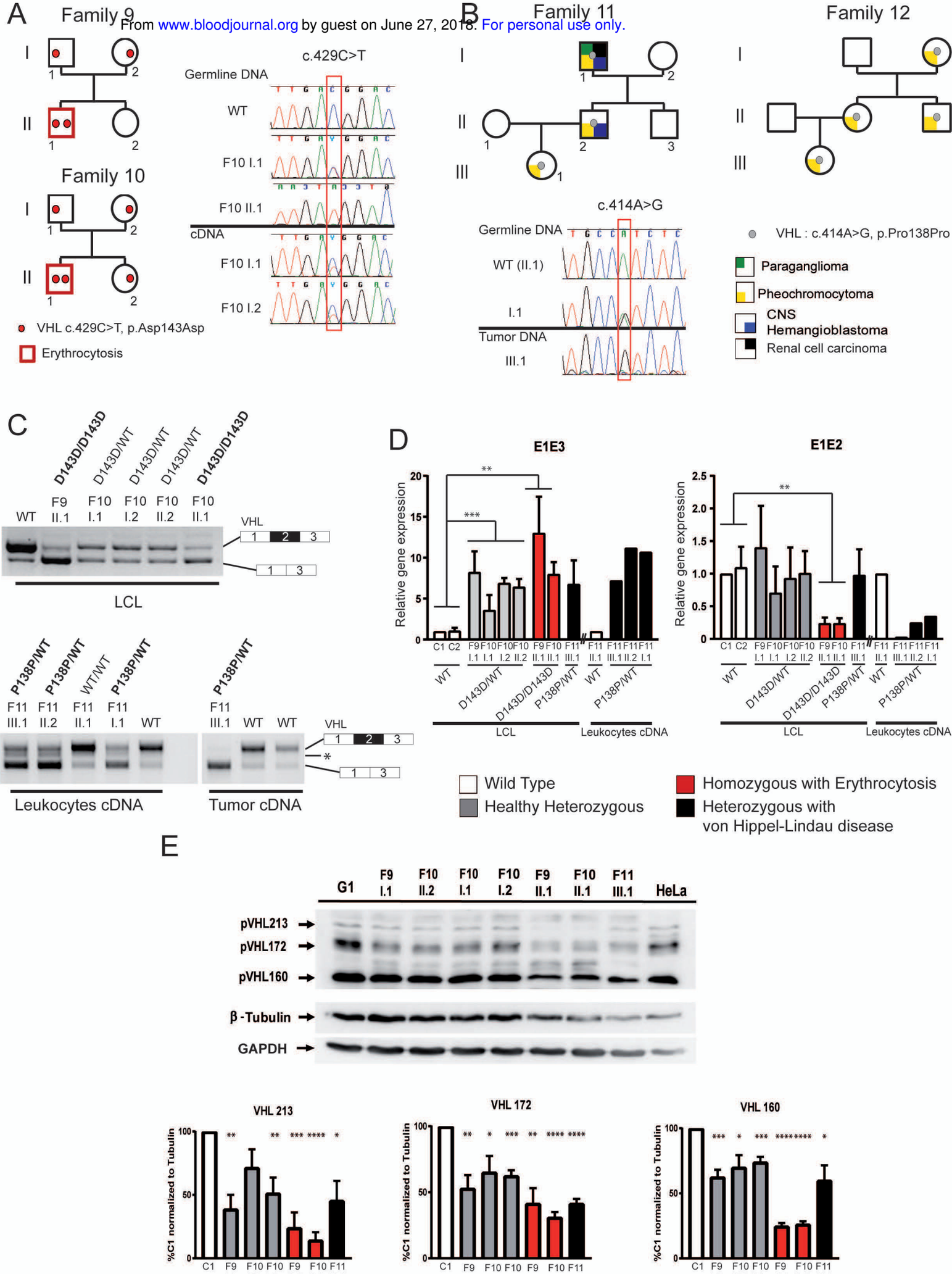

Figure 6

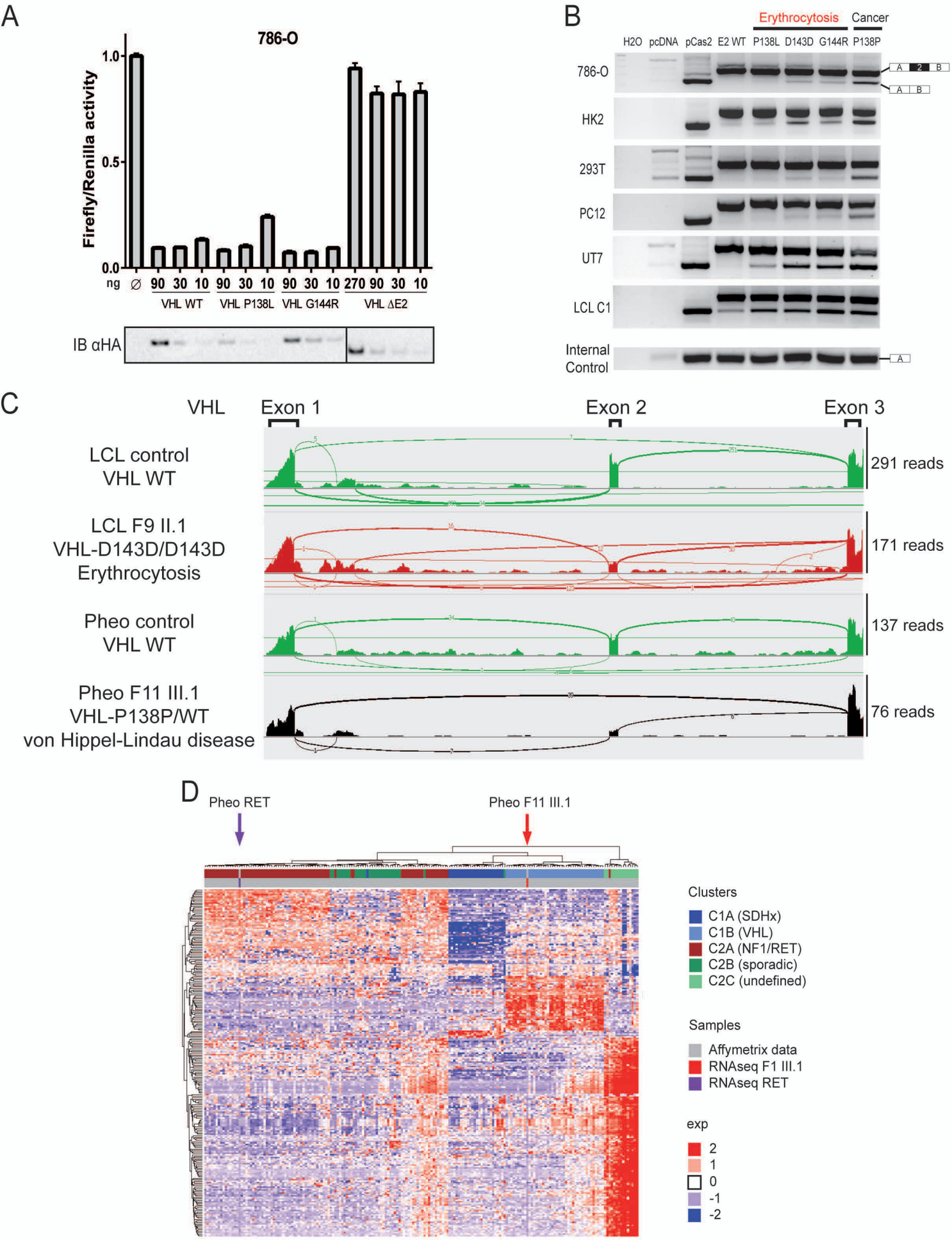

Prepublished online June 11, 2018;
doi:10.1182/blood-2018-03-838235

New lessons from an old gene: complex splicing and a novel cryptic exon in VHL gene cause erythrocytosis and VHL disease

Marion Lenglet, Florence Robriquet, Klaus Schwarz, Carme Camps, Anne Couturier, David Hoogewijs, Alexandre Buffet, Samantha JL. Knight, Sophie Gad, Sophie Couvé, Franck Chesnel, Mathilde Pacault, Pierre Lindenbaum, Sylvie Job, Solenne Dumont, Thomas Besnard, Marine Cornec, Helene Dreau, Melissa Pentony, Erika Kvikstad, Sophie Deveaux, Nelly Burnichon, Sophie Ferlicot, Mathias Vilaine, Jean-Michaël Mazzella, Fabrice Airaud, Céline Garrec, Laurence Heidet, Sabine Irtan, Elpis Mantadakis, Karim Bouchireb, Klaus-Michael Debatin, Richard Redon, Stéphane Bezieau, Brigitte Bressac-de Paillerets, Bin Tean Teh, François Girodon, Maria-Luigia Randi, Maria Caterina Putti, Vincent Bours, Richard Van Wijk, Joachim R. Göthert, Antonis Kattamis, Nicolas Janin, Celeste Bento, Jenny C. Taylor, Yannick Arlot-Bonnemains, Stéphane Richard, Anne-Paule Gimenez-Roqueplo, Holger Cario and Betty Gardie Dr

Blood (print ISSN 0006-4971, online ISSN 1528-0020), is published weekly by the American Society of Hematology, 2021 L St, NW, Suite 900, Washington DC 20036.

ARTICLE 8

Role of MDH2 pathogenic variant in pheochromocytoma and paraganglioma patients.

Calsina B, Currás-Freixes M, Buffet A, Pons T, Contreras L, Letón R, Comino-Méndez I, Remacha L, Calatayud M, Obispo B, Martin A, Cohen R, Richter S, Balmaña J, Korpershoek E, Rapizzi E, Deutschbein T, Vroonen L, Favier J, de Krijger RR, Fassnacht M, Beuschlein F, Timmers HJ, Eisenhofer G, Mannelli M, Pacak K, Satrústegui J, Rodríguez-Antona C, Amar L, Cascón A, Dölker N, Gimenez-Roqueplo AP, Robledo M.

Genet Med. 2018 Jul 16, Epub ahead of print.

Title: Role of *MDH2* mutations in pheochromocytoma and paraganglioma patients

Running Title: Role of *MDH2* mutations in pheochromocytoma and paraganglioma patients

Authors: Bruna Calsina, MSc*[1], Maria Currás-Freixes, M.D., PhD*[1], Alexandre Buffet, MSc[2], Tirso Pons, PhD[3,4], Laura Contreras, PhD[5,6], Rocío Letón, BSc[1], Iñaki Comino-Méndez, PhD[1], Laura Remacha, MSc[1], María Calatayud, M.D.[7], Berta Obispo, M.D.[8], Antoine Martin, M.D.[9,10], Regis Cohen, M.D.[11,12], Susan Richter, PhD[13], Judith Balmaña, M.D., PhD[14], Esther Korpershoek, PhD[15], Elena Rapizzi, PhD[16], Timo Deutschbein, M.D.[17], Laurent Vroonen, M.D.[18], Judith Favier, PhD[2], Ronald R. de Krijger, M.D., PhD[19,20], Martin Fassnacht, M.D., PhD[17], Felix Beuschlein, M.D.[21,22], Henri J. Timmers, M.D., PhD[23], Graeme Eisenhofer, PhD[13,24], Massimo Mannelli, M.D., PhD[16], Karel Pacak, M.D., PhD[25], Jorgina Satrústegui, PhD[5,6], Cristina Rodríguez-Antona, PhD[1,6], Laurence Amar, M.D., PhD[2,26], Alberto Cascón, PhD[1,6], Nicole Dölker, PhD[3], Anne-Paule Gimenez-Roqueplo, M.D., PhD[2,27], Mercedes Robledo, PhD[1,6]

Authors' Affiliations:

[1] Hereditary Endocrine Cancer Group, Spanish National Cancer Research Centre (CNIO), Madrid, Spain;

[2] INSERM, UMR970, Paris Cardiovascular Research Center and Université Paris Descartes, Sorbonne Paris Cité, Faculté de Médecine; Equipe labellisée Ligue contre le cancer, Paris, France;

[3] Structural Biology and BioComputing Programme, Spanish National Cancer Research Centre (CNIO), Madrid, Spain;

[4] Department of Immunology and Oncology, National Centre for Biotechnology (CNB-CSIC), Madrid, Spain;

[5] Departamento de Biología Molecular, Centro de Biología Molecular Severo Ochoa UAM-CSIC, Universidad Autónoma de Madrid and Instituto de Investigación Sanitaria Fundación Jiménez Díaz, Madrid, Spain;

[6] Centro de Investigación Biomédica en Red de Enfermedades Raras (CIBERER), Madrid, Spain;

[7] Department of Endocrinology and Nutrition Service, Hospital Universitario 12 de Octubre, Madrid, Spain;

[8] Servicio Oncología Médica, Hospital Infanta Leonor, Vallecas, Madrid;

[9] Assistance Publique Hôpitaux de Paris; Hôpital Avicenne, Service d'anatomie et cytologie pathologiques, Bobigny, France;

[10] INSERM, U978, Université Paris 13, Sorbonne Paris Cité, Bobigny, France;

[11] Assistance Publique-Hôpitaux de Paris, Hôpital Avicenne, Service de Médecine Interne, Bobigny, France;

[12] Université Paris 13, Sorbonne Paris Cité, Bobigny, France;

[13] Institute of Clinical Chemistry and Laboratory Medicine, University Hospital Carl Gustav Carus, Medical Faculty Carl Gustav Carus, Technische Universität Dresden, Dresden, Germany;

[14] High Risk and Cancer Prevention Group, Medical Oncology Department, Vall d'Hebron University Hospital and Vall d'Hebron Institute of Oncology, Barcelona, Spain;

[15] Department of Pathology, Erasmus Medical Center Cancer Institute, University Medical Center Rotterdam, Rotterdam, The Netherlands;

[16] Department of Experimental and Clinical Medicine, University of Florence, Italy;

[17] Department of Internal Medicine I, Division of Endocrinology and Diabetes, University Hospital, University of Würzburg, Würzburg, Germany;

[18] Department of Endocrinology, Centre Hospitalier Universitaire (CHU) de Liège, Belgium;

[19] Department of Pathology, Erasmus University Medical Center, Rotterdam, the Netherlands;

[20] Department of Pathology, Reinier de Graaf Hospital, Delft, the Netherlands;

[21] Medizinische Klinik und Poliklinik IV, Klinikum der Universität München, Ludwig-Maximilians-Universität München, Munich, Germany;

[22] Klinik für Endokrinologie, Diabetologie und Klinische Ernährung, Universitätsspital Zürich, Zürich, Switzerland;

[23] Department of Internal Medicine, Radboud University Medical Centre, Nijmegen, The Netherlands;

[24] Department of Medicine III, University Hospital and Medical Faculty Carl Gustav Carus, Dresden University of Technology, Dresden, Germany;

[25] Section on Medical Neuroendocrinology, *Eunice Kennedy Shriver* National Institute of Child Health and Human Development, NIH, Bethesda, Maryland, USA;

[26] Assistance Publique-Hôpitaux de Paris, Hôpital Européen Georges Pompidou, Hypertension Unit, Paris, France;

[27] Assistance Publique-Hôpitaux de Paris, Hôpital Européen Georges Pompidou (HEGP), Department of Genetics, Paris, France;

* Bruna Calsina and Maria Currás-Freixes contributed equally to this work

Corresponding Author: Mercedes Robledo, Spanish National Cancer Center (CNIO), Calle Melchor Fernandez Almagro 3, Madrid 28029, Spain. Phone 34- 917-328000; Fax. 34-912-246972; E-mail: mrobledo@cnio.es

Conflict of interest: The authors declare no conflict of interest.

ABSTRACT

Purpose: *MDH2* (malate dehydrogenase 2) has recently been proposed as a novel potential pheochromocytoma/paraganglioma (PPGL) susceptibility gene, but its role in the disease has not been addressed. This study aimed to determine the prevalence of *MDH2* mutations among PPGL patients and determine the associated phenotype.

Methods: Eight hundred thirty patients with PPGLs, negative for the main PPGL driver genes, were included in the study. Interpretation of variants of unknown significance (VUS) was performed using an algorithm based on twenty computational predictions, by implementing cell-based enzymatic and immunofluorescence assays, and/or by using a molecular dynamics simulation approach.

Results: Five variants with potential involvement in pathogenicity were identified: three missense (p.Arg104Gly, p.Val160Met and p.Ala256Thr), one in-frame deletion (p.Lys314del), and a splice-site variant (c.429+1G>T). All were germline and those with available biochemical data, corresponded to noradrenergic PPGL.

Conclusion: This study suggests that *MDH2* mutations may play a role in PPGL susceptibility and that they might be responsible for less than 1% of PPGLs in patients without mutations in other major PPGL driver genes, a prevalence similar to the one recently described for other PPGL genes. However, more epidemiological data are needed to recommend *MDH2* testing in patients negative for other major PPGL genes.

Key words: MDH2; pheochromocytoma and paraganglioma; variants of unknown significance; dominant negative effect; molecular dynamics

INTRODUCTION

Pheochromocytomas (PCCs) and paragangliomas (PGLs), abbreviated as PPGLs, are very rare neuroendocrine tumors characterized by a high degree of genetic and clinical heterogeneity[1,2].

Since the description of *NF1* in 1990 as the first driver gene related to PPGL development, thirty-five additional genes have been identified to be involved in the disease, establishing PPGLs as the human neoplasia with the highest degree of heritability. Among PPGL-associated genes, seven have been found almost exclusively mutated in the germline (*SDHA*, *SDHB*, *SDHC*, *SDHD*, *SDHAF2*, *FH* and *TMEM127*), four either in the germline or somatically (*RET*, *VHL*, *NF1* and *MAX*), one postzygotically or somatically (*EPAS1*) and the last one only somatically (*HRAS*) [1,3]. Furthermore, there are twenty two more susceptibility genes for which the contribution to the disease remains unclear: *IDH1, KIF1B, MEN1, BAP1, EGLN1/PHD2, EGLN2/PHD1, ATRX, KMT2D/MLL2, MET, TP53, BRAF, JMJD1C, KDM2B, MERTK, H3F3A, SETD2, EZH2, FGFR1, MITF*, *CSDE1*, *GOT2* and *IDH3B*[1,4–12]. In addition, other mechanisms such as point mutations in the promoter region of *TERT*[13,14], *SDHC* promoter epimutations[15], or rearrangements involving *MAML3, BRAF, NGFR,* and *NF1* have been also described[11].

Recently, our group added malate dehydrogenase 2 (*MDH2*) to the list of potential PPGL susceptibility genes. *MDH2* encodes the mitochondrial malate dehydrogenase (MDH), essential for the conversion of malate to oxaloacetate as part of the proper functioning of the Krebs cycle. A single *MDH2* mutation affecting a donor splice-site (c.429+1G>A) was identified in a 55 year-old man with multiple noradrenergic PGLs associated with bone metastasis[16], and in one apparently unaffected relative with a positive biochemical diagnosis of the disease. Loss of heterozygosity (LOH) and significant reduction of MDH activity in the tumors suggested that *MDH2* acts as a tumor suppressor gene. As alterations in Krebs cycle genes have been associated with a higher metastatic risk of the disease, an early genetic diagnosis of unaffected carriers in these families seems to be crucial. However, that study did not

address the contribution of *MDH2* to the global PPGL susceptibility or the clinical features associated with mutations in this gene.

One of the main challenges for genetic screening is the classification of variants of unknown significance (VUS) to improve genetic counseling and clinical follow-up of mutation carriers. The pathogenicity assessment of VUS requires taking into account the frequency reported in several databases, *in silico* effect prediction and functional assays.

In this international collaborative study, we determined the prevalence of germline and/or somatic *MDH2* mutations, and the associated phenotype in 830 unrelated PPGL index patients, negative for at least the main 13 driver PPGL susceptibility genes. Secondly, we developed a workflow of *in silico* predictions and simulations, and functional studies for assessing the functional impact of *MDH2* VUS identified.

All *MDH2* genetic changes, except one in-frame deletion and one variant affecting a donor splice-site, consisted of single nucleotide substitutions leading to missense, synonymous or intronic changes, for which we assessed their functional impact. Those *MDH2* VUS were analyzed with one to five approaches: (i) applying 20 computational methods to predict their effect at the level of protein structure and function, implementing an enzymatic assay to assess: (ii) MDH2 activity and (iii) MDH2 affinity, (iv) designing an immunofluorescence assay to evaluate MDH2 localization changes, and (v) using a molecular dynamics (MD) simulation approach to examine the potential changes in protein structure and dynamics for the most controversial variants. This sequential scheme aimed to categorize the vast majority of *MDH2* VUS found in an extensive setting.

MATERIALS AND METHODS

Patients

Diagnosis of PPGL was established following conventional methods (including clinical, biochemical, imaging and pathological data). A new series of 561 PPGL index cases negative for at least 13 major PPGL genes (*RET, VHL*, SDH genes, *NF1*, *HRAS*, *EPAS1*, *MAX*, *TMEM127*, and *FH*) and not previously tested for *MDH2* were screened by Sanger (SS) or a Next-Generation (NGS) sequencing panel (PheoSeq[17]). In order to establish the prevalence of *MDH2* mutations and classify *MDH2* VUS, we also considered 269 previously reported patients with negative genetic screening for the 13 PPGL genes, but including 4 carriers of *MDH2* VUS[17]. This outstanding series of 830 unrelated PPGL index patients was recruited through a collaborative effort from 11 participating centers: 10 of the European Network for the Study of Adrenal Tumors (ENS@T) consortium (Madrid, Paris, Liège, Würzburg, Munich, Dresden, Florence, Rotterdam, Delft and Nijmegen), and one in the USA (Bethesda).

Clinical data were collected as previously described[18]. Table 1 summarizes the clinical characteristics of patients, who provided informed consent to collect clinical and genetic data, in accordance with institutional ethical –approved protocols for each center. In addition, tumor tissues from the Erasmus MC (Rotterdam, The Netherlands) and the Radboud University Medical Centre (Nijmegen, The Netherlands) were used according to the code of conduct: “Proper Secondary Use of Human Tissue” established by the Dutch Federation of Medical Scientific Societies.

Samples

A total of 849 DNA samples from the 830 patients were available for this study. DNA was obtained exclusively from blood in 641 patients, tumor in 170 patients and matched tumor-blood in 19 patients (Table 1). Tumor samples were formalin-fixed paraffin-embedded (FFPE) tissues in 80 (42.3%) and frozen tissues in 109 (57.7%) of the cases.

Germline DNA was extracted from peripheral blood samples following a standard method (FlexiGene DNA Kit, Qiagen). DNeasy Blood & Tissue Kit (Qiagen) and truXTRAC FFPE DNA microTUBE Kit (Covaris, Massachusetts, USA) were used to extract DNA from frozen tumor tissue and from FFPE tumor samples, respectively, following the manufacturer's instructions.

Molecular genetic analyses

MDH2 genetic screening was performed in the CNIO (Madrid) and in the HEGP (Paris), either by NGS panel or SS. Primers sequences spanning the nine exons and intron-exon boundaries of *MDH2* were those previously described[16].

MDH2 gross deletions were tested in 216 cases with good germline DNA quality using a semi-quantitative multiplex-PCR method with labeled primers, as previously described for other genes[16,19].

The variant calling was based on the *MDH2* transcript ENST00000315758.9. The frequency of *MDH2* variants was investigated in public databases: dbSNP (https://www.ncbi.nlm.nih.gov/SNP), COSMIC (http://cancer.sanger.ac.uk/cosmic), and gnomAD (http://gnomad.broadinstitute.org/).

MDH2 variants identified in <0.1% of the population and without homozygotes described were included in the study and used for further analyses. LOH of the *MDH2* variants in tumor DNA was assessed by direct sequencing (if material available).

MDH2 *expression by immunohistochemistry*

Immunohistochemistry was performed as described in supplemental methods.

Computational prediction of functional impact

Three distinct *in silico* approaches were used to assess the functional and three-dimensional (3D) structural effect of the missense variants: 1) measure of the evolutionary conservation in the genome of vertebrate and mammalian species (i.e. phyloP, phastCons, GERP++), 2) prediction of the impact of amino acid substitutions in protein function (i.e. SIFT, Polyphen2, LRT, MutationAssessor, fathmm-

MKL, PROVEAN, MetaSVM, MetaLR, MutationTaster), and 3) prediction of protein 3D destabilization (i.e. PoPMuSiCv3.1, CUPSAT, I-Mutant v3.0, MAESTRO, INPS-3D).

A consensus interpretation was established according to the number of tools predicting a damaging effect versus a benign or tolerated one. The consensus was given if at least 70% (functional impact: 7 out of 10; 3D stability: 4 out of 5) of the predictors agreed in the variant classification. Otherwise, the results were considered as inconclusive.

Moreover, we included functional annotations (e.g. ligand binding sites, catalytic residues, post-translational modifications of proteins, residues in protein-protein interaction interfaces) retrieved by the Structure-PPi system[20]. Structure-PPi also considers residues in physical proximity (at a distance of 5Å) to amino-acid changes found in other type of cancers.

ESEFinder and RESCUE-ESE using Alamut Visual software version 2.7 (Interactive Biosoftware, Rouen, France) were used to predict splicing changes in synonymous and intronic variants.

***RBP1* gene expression analysis**

The low expression of retinol binding protein 1 (*RBP1)* is a marker of Krebs cycle disruption[21]. Its assessment is detailed in supplemental methods.

Plasmids and cell culture

QuickChange Lightning Site-Directed Mutagenesis Kit (Agilent) was used to generate missense variants in pCMV6-AC-MDH2 (Origene), a plasmid containing the full cDNA sequence (NM_005918) of the human *MDH2* gene. We generated a polymorphism with a MAF=0.037 in gnomAD (rs10256: p.Lys301Arg), to be used as control. Primers used to generate mutated vectors are described in Table S1. The introduction of the mutation of interest was confirmed by SS (Figure S1).

Sh8561 *MDH2* knock down Hela cells[16] (*MDH2* KD cells) culture conditions are specified in supplemental methods.

Microscopic analysis

For immunofluorescence imaging, 300,000 cells were seeded 24h before transfection on coverslips in 12-well plates. Cells were transiently transfected with 2µg of plasmids mutated with each variant using Lipofectamine 2000 (Invitrogen) following the vendor's manual. Twenty-four hours after transfection cells were stained as described in supplemental methods and analyzed by confocal microscopy (Leica TCS SP5 X).

***In silico* molecular dynamics (MD) simulations**

The initial model of the system used the crystal structure of a tetramer of oxaloacetate and NADH-bound MDH2 (PDBid: 4wlo). The structure contains coordinates for residues 24-337 of each monomer. The dimer formed by monomers A and B was extracted and ligands and crystal waters were removed. Missing hydrogen atoms were added using the H++ server[22], and in the case of the mutants, the point mutations were introduced using Pymol[23]. The systems were placed in dodecahedral boxes, being the minimal distance between the protein and the borders of the box was 10Å. The systems were solvated with TIP3P waters[24], and Na^+/CL^- was added to neutralize them to obtain a physiological salt concentration of 0.15mol/l. First, the systems were minimized during 500 steps, applying the steepest descent algorithm. Consequently, the solvent was equilibrated for 100ps in the NVT ensemble, followed by another 100ps in the isobaric-isothermal (NpT) ensemble. The resulting configurations were used for MD production runs of 400ns for each system. The trajectories were analyzed by Principal Component Analysis (PCA) (see supplemental methods).

Simulations and analyses of the trajectories were performed as described in supplemental methods.

Enzymatic activity assay

MDH2 KD cells were seeded in T150 flasks at $16 \cdot 10^6$ cells/ flask 24h before transfection. Each flask was transiently transfected with 20µg of each variant plasmid using Lipofectamine 2000 (Invitrogen), according to the manufacturer's recommendations. *MDH2* KD cells transfected either with wild-type

(WT) cDNA (pCMV6-AC-*MDH2*), *MDH2* KD cells with pCMV6-AC empty vector (EV) or *MDH2* KD cells with pCMV6-AC-*MDH2*-c.902A>G vector, were used as controls. To mimic the heterozygous state of p.Arg104Gly patient, we co-transfected 10µg pCMV6-AC-*MDH2* and 10µg pCMV6-AC-*MDH2*-c.310A>G plasmids; as control, we used cells co-transfected with 10µg pCMV6-AC-*MDH2* and 10µg pCMV6-AC EV, and 20µg EV alone. 24h after transfection, enzymatic activity assay was performed as described in supplemental methods.

RESULTS

MDH2 variants and computational analyses

Twelve *MDH2* heterozygous variants (Figure 1) were found, demonstrating a germline origin for 11 of them (only tumor DNA was available in the remaining case). Clinical data of the *MDH2* carriers are detailed in Table S3. None of the patients had family history of the disease.

Five of the 12 were missense (41.7%), one synonymous (8.3%), four were located in the intronic region (33.3%), one was an in-frame deletion (8.3%), and one affected a donor splice-site (8.3%) (Figure 1). Five of them were unreported variants (3 missense, 1 intronic and 1 in-frame deletion), six showed a low allele frequency ($<1 \cdot 10^{-3}$) and no homozygotes in gnomAD, and the donor splice-site mutation had been previously suggested to be pathogenic[16] (Table 2; Table S5). The two probands with the splice-site *MDH2* mutation are not related.

The synonymous variant (p.Phe333Phe), found in a patient with a non-functional T-PGL, had no effect according to *in silico* splicing predictors (Table S5). Similarly, the splicing for three of the four intronic variants (c.320-26A>C, c.733+47G>A and c.734- 5C>A) was not predicted affected, while it was anticipated as altered in the remaining intronic variant (c.319+37G>A) identified in a 48-year-old patient with a noradrenergic PCC. RNA of this patient was not available to confirm this prediction.

Of the 5 *MDH2* missense variants identified (Table 2), only one (p.Ser3Phe) was outside the functional domains in the transit peptide to mitochondria. The variants p.Arg104Gly, p.Gln130Arg and p.Val160Met were positioned in the lactate/malate dehydrogenase, NAD binding domain; and, p.Ala256Thr in the lactate/malate dehydrogenase, alpha/beta C-terminal domain. Furthermore, they affected conserved positions in vertebrate and mammalian species, as indicated by phyloP, phastCons and GERP++ methods. Indeed, p.Arg104Gly is positioned in the NAD-binding site.

Three of the missense variants (p.Arg104Gly, p.Val160Met and p.Ala256Thr) were predicted to have a damaging effect (*impaired* functional predictions and *destabilization* of the 3D structure) (Table 2;

Table S4). The variant p.Ser3Phe was classified as *inconclusive* according to the functional impact predictions and the corresponding 3D structural predictions could not be performed (residue not present in the crystal structure [PDB ID: 2DFD]). The variant p.Gln130Arg was categorized as *neutral* and *inconclusive* according to the functional and 3D structure predictions, respectively. Moreover, COSMIC database reported *MDH2* somatic mutations in other cancers in neighbor positions (d≤5Å), as indicated by Structure-PPi (Figure S2), for all the variants except for p.Ser3Phe.

The variants p.Arg104Gly and p.Ala256Thr were found in two young patients (25 and 29 years old, respectively) with norepinephrine-producing PCC both diagnosed during pregnancy. One of them developed metachronous bone metastases. The p.Val160Met was identified in a PCC-patient without biochemical data. The remaining two missense variants (p.Ser3Phe and p.Gln130Arg) were found in patients older than 45 years, diagnosed with PCC; the former involving an adrenergic tumor and the latter without evidence of excess in catecholamine production (Table S3).

A previously unreported in-frame deletion (p.Lys314del) was found in a 55-year-old patient, with multiple noradrenergic PGLs. It affected a conserved residue, for which mutations in neighboring residues have been described in several cancers (Table 2; Figure S2); LOH was demonstrated in the tumor.

Furthermore, the c.429+1G>T variant, previously described[16], was found in a 57-year-old patient diagnosed with a PCC and liver metastases.

***MDH2* immunohistochemistry**

MDH2 IHC it is not useful to classify VUS or select patients for *MDH2* screening (see supplemental results).

***RBP1* expression in *MDH2* variants**

RBP1 measurement was performed in four available tumors (p.Ser3Phe, p.Arg104Gly, p.Val160Met and p.Lys314del–tumor), observing a reduced *RBP1* expression in three tumors compared to controls:

93.86±1.83% (p=0.007), 83.18±0.65% (p=0.007) and 82.44±19.72% (p=0.030) for p.Lys314del-, p.Arg104Gly-, and p.Val160Met-tumor, respectively (Figure S3).

MDH2 localization

None of the variants was associated with an altered MDH2 localization, or mitochondrial quantity and morphology (see supplemental results).

Enzymatic activity characterization

Only variant p.Arg104Gly displayed a significant lower MDH2 enzymatic activity at saturating concentration of substrates (p<0.0001) compared to WT, comparable to the activity detected in the KD cells not expressing *MDH2* (Figure 2A). On the other hand, citrate synthase activity, present exclusively in the mitochondria, was similar for all variants (Table S2), suggesting that none of them produced an increased mitochondrial biogenesis to compensate the possible aberrant *MDH2* variant. Thus, this functional assay only supported pathogenicity for p.Arg104Gly, having an incomplete functional proof of *in silico* predictions.

Enzymatic activity assay to check a dominant-negative effect.

LOH was not detected in any of the tumors carrying the missense variants. In order to evaluate if *MDH2* variants could exert a dominant-negative effect on MDH2 WT, we took as a model the p.Arg104Gly variant. We co-transfected WT plasmid, p.Arg104Gly plasmid, and a combination of both to mimic the heterozygous state of the mutated patient. EV was used to achieve the same amount of total transfected plasmid (20ug in each co-transfection). Cells co-transfected with both WT and p.Arg104Gly plasmids exhibited lower enzymatic activity in comparison with those co-transfected with WT and EV ones (27.8%±22.6; p=0.0002) (Figure 2B).

***MDH2* missense variants affinity characterization**

Another assay was designed to evaluate if p.Val160Met and p.Ala256Thr variants affected the affinity of the enzyme for the substrates, instead of the maximal activity. We used the p.Arg104Gly variant as

positive control. A tendency of reduced enzymatic activity when decreasing malate concentration was observed for p.Val160Met, significant at 5mM (5-fold reduction to malate saturating concentration, p=0.0256) (Fig 2C) and at 2.5mM (10-fold reduction to malate saturating concentration, p=0.0047) (Fig 2D). Furthermore, a subtle decrease in the activity was observed for p.Ala256Thr when diminishing concentration of NAD+ (Fig 2F) and malate (Fig 2D) to 20-fold (p=0.0464) and 10-fold (p=0.0366), respectively. No significant changes were observed at higher NAD+ concentrations (0.5mM) (Fig 2E).

Molecular dynamics (MD) simulations

Simulations of the dimers of the WT apoenzyme, and the p.Ala256Thr and p.Val160Met variants revealed differences in their principal motions. In the WT, we observed movements of the two monomers relative to each other, and large conformational changes in one of the helices of the substrate-binding site and its adjacent loop (Figure S5A). In the p.Ala256Thr mutant, the character of the main motions was conserved (Figure S5B), whereas in the p.Val160Met mutant the relative movement of the monomers was strongly reduced (Figure S5C).

Although the dynamics of the p.Ala256Thr variant were similar to that of the WT, closer inspection revealed conformational changes. In the WT and p.Val160Met variant, the side chain of Phe260, neighboring Ala/Thr256, switches between two orientations, while in the p.Ala256Thr mutant it remains immobile (Figure 3A). On a larger scale, the opening between the two monomers becomes slightly enlarged (Figure 3B).

Even on a short time scale, the MD simulations revealed changes in conformation and dynamics of the variants, compared to the WT. The results suggest that the p.Ala256Thr variant affects the conformation of the neighboring residues, which contribute to the dimeric interface. This implies that the p.Ala256Thr variant may affect dimerization of MDH2. In the p.Val160Met variant changes in the dynamics of the substrate binding site may affect substrate affinity.

DISCUSSION

After the identification of major susceptibility PPGL genes, the list of other genes with modest contributions to the disease has kept growing and it is likely that this number will continue to increase over the near future[3]. Examples include *SDHA*[32], *TMEM127*[33], *MAX*[34] or *FH*[35]. The use of NGS panels[36] to offer a comprehensive genetic diagnosis, multiple VUS are identified, for which the functional interpretation represents a crucial challenge in an accurate genetic counseling. Herein, we aimed to determine the prevalence and the clinical characteristics of *MDH2* mutation-carriers in 830 patients with PPGL without mutation in major PPGL susceptibility genes and to investigate the potential pathogenicity of every identified *MDH2* variant. We were able to classify 2 *MDH2* variants as pathogenic and provide evidence that suggests an altered molecular function of MDH2 in 2 others (which have been designated as likely pathogenic mutations), following the criteria established by the American College of Medical Genetics and Genomics and the Association for Molecular Pathology guidelines[37]. Furthermore, a new patient, carrying the already reported c.429+1G>T *MDH2* variant, was identified.

RBP1 expression in the tumor, bioinformatics predictions and functional assays, suggested that p.Arg104Gly is a pathogenic mutation located in the highly conserved NAD-binding site and significantly impairing MDH2 activity. This variant was found in a young patient with a noradrenergic PCC. Mutations in neighboring positions are reported in different cancers, supporting the implication of mutations at this residue in the neoplastic process. However, neither LOH, nor any other somatic mutation was found in the corresponding tumor sample. Enzymatic assays performed by co-transfection of WT and p.Arg104Gly plasmids resembling the heterozygous character of this mutation, suggested a dominant-negative effect of the p.Arg104Gly-mutant.

The two other missense variants, p.Ala256Thr and p.Val160Met, reported as rare SNPs and located in conserved residues, were predicted to produce protein 3D structure destabilization and impaired the MDH2 molecular function. The p.Val160Met was detected in a 54-year-old PCC patient, whose tumor

showed low *RBP1* expression. The p.Ala256Thr tumor sample was not available, so the interpretation of this variant was based exclusively on functional assays. This latter variant was found in a 29-year-old female with a noradrenergic metastatic PCC. The substitutions at residues Val160 and Ala256 could also affect the substrate binding affinity and protein 3D stability, and therefore, neither the enzymatic assay nor the immunofluorescence experiments are able to evaluate the effect. Because of that, we conducted MD simulations only with these variants, which suggested that p.Val160Met could be modifying malate binding to the catalytic site, and consequently affecting MDH2 affinity for its substrate. This was demonstrated *in vitro*, as MDH2 activity decreased when we reduced malate concentration, pointing to a lower affinity of the mutated enzyme for malate. For variant p.Ala256Thr, MD simulations predicted that it could be affecting enzyme dimerization. We observed a slight decrease in MDH2 activity when reducing both malate and NAD+ down to low concentrations, which could be related to impaired dimerization. A second somatic hit was not observed in the tumor of p.Val160Met-related patient and p.Ala256Thr-related tumor was not available. A dominant-negative effect for p.Val160Met and p.Ala256Thr variants might be the underlying mechanism as occurs with the p.Arg104Gly variant, although this has not been tested in this study. Thus, the p.Ala256Thr variant could be classified as likely pathogenic. Regarding the p.Val160Met variant, although most of our analyses suggested a potential pathogenic role as well, it was also classified as likely pathogenic due to the high number of alleles found (46/277206) in general population.

For the two other novel missense variants (p.Ser3Phe and p.Gln130Arg) identified, computational analyses did not reach a consensus. In addition, patients carrying these variants had predominant adrenaline production or non-functional tumors, which is in discordance with *MDH2*-mutated patient[16] and other Krebs cycle genes. The high *RBP1* expression in the p.Ser3Phe-tumor supported that this variant is not pathogenic. Thus, we classified these two variants as likely neutral.

The four intronic variants and the synonymous one were not classified, as no RNA was available. The computational tools indicated no agreement, highlighting the relevance of having access to tissue tumor sample to study at least the *RBP1* and/or *MDH2* expression.

The p.Lys314del, identified in a patient with multiple noradrenergic PGLs, was classified as pathogenic, as it affects a conserved amino acid, and LOH and low *RBP1* expression in the tumor sample were found.

Finally, a 57-year-old patient with a metastatic pheochromocytoma, clinical phenotype similar to the patient reported[16], was identified to carry the same variant affecting a donor splice-site (c.429+1G>A).

In summary, taking into account only those *MDH2* variants identified which display characteristics supportive of a pathogenicity potential, we provide more evidences that suggest the potential role of *MDH2* in PPGL predisposition, and indicate that *MDH2* germline mutations could be responsible for 0.6% of PPGL cases, prevalence comparable to that reported for other recently described PPGL genes. The apparent lack of family history in four pedigrees investigated suggests an incomplete penetrance of *MDH2*, similar to the one observed in other Krebs cycle genes, such as *SDHA* or *FH*. Furthermore, there are other similarities worthy to mention. In this regard, families affected with encephalopathy due to recessive MDH2 deficiency have been described[38]. One could expect to find PPGL patients in these families, but as it happens in pedigrees affected with the Leigh syndrome (OMIM 256000) associated with autosomal-recessive pathogenic mutations in *SDHA*[39], their members do not develop either these tumors.

On the other hand, it is worthy to note that *MDH2* variants were found in metastatic cases, as two out of five patients (three out of six, if we include the reported *MDH2* patient[16]) developed metastases. Taking into account the low prevalence of *MDH2* mutations, as well as the low penetrance, its genetic testing could be considered in a research direction manner until providing further epidemiological and segregation data that would confirm the implication of *MDH2* mutations in PPGL susceptibility.

NGS is becoming the rational tool to apply to PPGL genetic diagnosis, and unavoidably it leads to an increasing number of VUS reported. The task of classifying VUS for genetic counseling is especially complex when considering genes scarcely analyzed, which exhibit a high ratio of missense variants, as previously shown for *MAX*[40]. In this study, we were able to demonstrate a functional impact for two variants (p.Arg104Gly and p.Lys314del) and suggested an altered molecular function for other two (p.Val160Met and p.Ala256Thr), but there were insufficient evidences to consider them pathogenic even after applying up to five approaches to classify them. Although, it is likely that this rational is unapproachable in the clinical setting when tumor tissue is unavailable, we demonstrated that *MDH2* variants could be classified by a multidisciplinary approach.

ACKNOWLEDGEMENTS

We gratefully acknowledge Diego Megias and all Confocal Microscopy Core Unit (CNIO) team for their technical support and advice, as well as Santiago Ramón-Maiques from Structural Bases of Genome Integrity Group (CNIO) for fruitful discussions. This work was supported by the Instituto de Salud Carlos III (ISCIII), Acción Estratégica en Salud, (projects PI14/00240 and PI17/01796), co-financed by Fondo Europeo de Desarrollo Regional (FEDER), GETNE (Grupo Español de Tumores Neuroendocrinos), the European Union Seventh Framework Programme (FP7/2007-2013) under grant agreement no. 259735, the Paradifference foundation, and the Intramural Research Program of the NIH, NICHD. Bruna Calsina is supported by the Becas de excelencia Rafael del Pino 2017, Maria Currás-Freixes was supported by the Severo Ochoa Excellence Programme (project SEV-2011-0191), Laura Contreras by a CIBERER contract, Alexandre Buffet received a financial support from ITMO Cancer AVIESAN (Alliance Nationale pour les Sciences de la Vie et de la Santé, National Alliance for Life Sciences & Health) within the framework of the Cancer Plan and Susan Richter by the Deutsche Forschungsgemeinschaft (RI 2684/1-1).

REFERENCES

1. Dahia, P. L. M. Pheochromocytoma and paraganglioma pathogenesis: learning from genetic heterogeneity. *Nat. Rev. Cancer* **14,** 108–19 (2014).

2. Crona, J. *et al.* Spatiotemporal heterogeneity characterizes the genetic landscape of pheochromocytoma and defines early events in tumorigenesis. *Clin. Cancer Res.* **21,** 4451–4460 (2015).

3. Favier, J., Amar, L. & Gimenez-Roqueplo, A.-P. Paraganglioma and phaeochromocytoma: from genetics to personalized medicine. *Nat. Rev. Endocrinol.* **11,** (2014).

4. Gaal, J. *et al.* Isocitrate dehydrogenase mutations are rare in pheochromocytomas and paragangliomas. *J. Clin. Endocrinol. Metab.* **95,** 1274–1278 (2010).

5. Yang, C. *et al.* Germ-line PHD1 and PHD2 mutations detected in patients with pheochromocytoma/paraganglioma-polycythemia. *J. Mol. Med.* **93,** 93–104 (2014).

6. Fishbein, L. *et al.* Whole-exome sequencing identifies somatic ATRX mutations in pheochromocytomas and paragangliomas. *Nat. Commun.* **6,** 6140 (2015).

7. Castro-Vega, L. J. *et al.* Multi-omics analysis defines core genomic alterations in pheochromocytomas and paragangliomas. *Nat Commun* **6,** 6044 (2015).

8. Luchetti, A. *et al.* Profiling of somatic mutations in phaeochromocytoma and paraganglioma by targeted next generation sequencing analysis. *Int. J. Endocrinol.* **2015,** (2015).

9. Toledo, R. a. *et al.* Recurrent Mutations of Chromatin-Remodeling Genes and Kinase Receptors in Pheochromocytomas and Paragangliomas. *Clin. Cancer Res.* 1–11 (2015). doi:10.1158/1078-0432.CCR-15-1841

10. Castro-Vega LJ, Kiando SR, Burnichon N, Buffet A, Amar L, Simian C, B., A, Galan P, Schlumberger M, Bouatia-Naji N, Favier J, B. P. B. & AP., G.-R. The MITF, p.E318K variant as a risk factor for pheochromocytoma and paraganglioma. *J Clin Endocrinol Metab.* **Sep 28:jc2,**

(2016).

11. Fishbein, L. *et al.* Comprehensive Molecular Characterization of Pheochromocytoma and Paraganglioma. *Cancer Cell* **31,** 181–193 (2017).

12. Remacha, L. *et al.* Targeted exome sequencing of Krebs cycle genes reveals candidate cancer predisposing mutations in pheochromocytomas and paragangliomas. *Clin. Cancer Res.* clincanres.2250.2016 (2017). doi:10.1158/1078-0432.CCR-16-2250

13. Papathomas, T. G. *et al.* Telomerase reverse transcriptase promoter mutations in tumors originating from the adrenal gland and extra-adrenal paraganglia. *Endocr. Relat. Cancer* **21,** 653–661 (2014).

14. Liu, T. *et al.* The activating TERT promoter mutation C228T is recurrent in subsets of adrenal tumors. *Endocr. Relat. Cancer* **21,** 427–434 (2014).

15. Richter, S. *et al.* Epigenetic Mutation of the Succinate Dehydrogenase C Promoter in a Patient With Two Paragangliomas. *J Clin Endocrinol Metab.* **Feb;101(2),** 359–363 (2016).

16. Cascón, A. *et al.* Whole-exome sequencing identifies MDH2 as a new familial paraganglioma gene. *J. Natl. Cancer Inst.* **107,** 1–5 (2015).

17. Currás-Freixes, M. *et al.* PheoSeq: A Targeted Next-Generation Sequencing Assay for Pheochromocytoma and Paraganglioma Diagnostics. *J. Mol. Diagnostics* **19,** (2017).

18. Currás-Freixes, M. *et al.* Recommendations for somatic and germline genetic testing of single pheochromocytoma and paraganglioma based on findings from a series of 329 patients. *J. Med. Genet.* **52,** 647–656 (2015).

19. Cascón, A. *et al.* Gross SDHB deletions in patients with paraganglioma detected by multiplex PCR: A possible hot spot? *Genes Chromosom. Cancer* **45,** 213–219 (2006).

20. V??zquez, M., Valencia, A. & Pons, T. Structure-PPi: A module for the annotation of cancer-related single-nucleotide variants at protein-protein interfaces. *Bioinformatics* **31,** 2397–2399

(2015).

21. Chou, A. P. *et al.* Identification of retinol binding protein 1 promoter hypermethylation in isocitrate dehydrogenase 1 and 2 mutant gliomas. *J. Natl. Cancer Inst.* **104,** 1458–1469 (2012).

22. Gordon, J. C. *et al.* H++: A server for estimating pKas and adding missing hydrogens to macromolecules. *Nucleic Acids Res.* **33,** (2005).

23. DeLano, W. L. The PyMOL Molecular Graphics System. *Schrödinger LLC wwwpymolorg* **Version 1.,** http://www.pymol.org (2002).

24. Mahoney, M. W. & Jorgensen, W. L. A five-site model for liquid water and the reproduction of the density anomaly by rigid, nonpolarizable potential functions. *J. Chem. Phys.* **112,** 8910 (2000).

25. Van Der Spoel, D. *et al.* GROMACS: Fast, flexible, and free. *Journal of Computational Chemistry* **26,** 1701–1718 (2005).

26. Hess, B., Kutzner, C., Van Der Spoel, D. & Lindahl, E. GRGMACS 4: Algorithms for highly efficient, load-balanced, and scalable molecular simulation. *J. Chem. Theory Comput.* **4,** 435–447 (2008).

27. Abraham, M. J. *et al.* Gromacs: High performance molecular simulations through multi-level parallelism from laptops to supercomputers. *SoftwareX* **1–2,** 19–25 (2015).

28. Lindorff-Larsen, K. *et al.* Improved side-chain torsion potentials for the Amber ff99SB protein force field. *Proteins Struct. Funct. Bioinforma.* **78,** 1950–1958 (2010).

29. Best, R. B. & Hummer, G. Optimized molecular dynamics force fields applied to the helix-coil transition of polypeptides. *J. Phys. Chem. B* **113,** 9004–9015 (2009).

30. Bussi, G., Donadio, D. & Parrinello, M. Canonical sampling through velocity rescaling. *J. Chem. Phys.* **126,** (2007).

31. Parrinello, M. & Rahman, A. Polymorphic transitions in single crystals: A new molecular dynamics method. *J. Appl. Phys.* **52,** 7182–7190 (1981).

32. Korpershoek, E. *et al.* SDHA immunohistochemistry detects germline SDHA gene mutations in apparently sporadic paragangliomas and pheochromocytomas. *J. Clin. Endocrinol. Metab.* **96,** (2011).

33. Qin, Y. *et al.* Germline mutations in TMEM127 confer susceptibility to pheochromocytoma. *Nat. Genet.* **42,** 229–33 (2010).

34. Comino-Méndez, I. *et al.* Exome sequencing identifies MAX mutations as a cause of hereditary pheochromocytoma. *Nat. Genet.* **43,** 663–667 (2011).

35. Castro-Vega, L. J. *et al.* Germline mutations in FH confer predisposition to malignant pheochromocytomas and paragangliomas. *Hum. Mol. Genet.* **23,** 2440–2446 (2014).

36. Toledo, R. A. *et al.* Consensus Statement on next-generation-sequencing-based diagnostic testing of hereditary phaeochromocytomas and paragangliomas. *Nat. Rev. Endocrinol.* **13,** 233–247 (2016).

37. Richards, S. *et al.* Standards and guidelines for the interpretation of sequence variants: A joint consensus recommendation of the American College of Medical Genetics and Genomics and the Association for Molecular Pathology. *Genet. Med.* **17,** 405–424 (2015).

38. Ait-El-Mkadem, S. *et al.* Mutations in MDH2, Encoding a Krebs Cycle Enzyme, Cause Early-Onset Severe Encephalopathy. *Am. J. Hum. Genet.* **100,** 151–159 (2017).

39. Renkema, G. H. *et al.* SDHA mutations causing a multisystem mitochondrial disease: Novel mutations and genetic overlap with hereditary tumors. *Eur. J. Hum. Genet.* **23,** 202–209 (2015).

40. Comino-Méndez, I. *et al.* Functional and in silico assessment of MAX variants of unknown significance. *J. Mol. Med.* **93,** 1247–1255 (2015).

TABLES

Table 1. Clinical characteristics of the patients included in the study.

	NUMBER (percentage)				
PATIENTS	830				
DNA germline	641 (77.2%)	Total DNA samples: 849			
DNA tumor	170 (20.5%)				
DNA matched tumor-germline	19 (2.3%)				
SEX					
Female	449 (57.8%)				
Male	328 (42.2%)				
No data	53				
AGE AT PRESENTATION					
Median (IQR)	39 (29-56) years				
Younger than 35	334 (40.2 %)				
FAMILIAL PPGL	13 (1.7%)				
LOCATION					
SINGLE	678 (85.2%)	**MULTIPLE**	118 (14.8%)	**No data**	34
PCC	427	PCC	32		
HN-PGL	146	HN-PGL	27		
A-PGL	83	A-PGL	18		
T-PGL	12	T-PGL	1		
No data	10	A- and T-PGL	4		
		A- and HN-PGL	6		
		HN- and T-PGL	1		
		PCC and A-PGL	22		
		PCC and T-PGL	4		
		PCC and HN-PGL	1		
		No data	2		
METASTASIS					
No	756 (91.1%)				
Yes	74 (8.9%)				
PREDOMINANTLY BIOCHEMICAL SECRETION					
Adrenergic	60	No secretion	176		
Noradrenergic	237	High, but unspecified	132		
Dopaminergic	4	No data	221		

IQR: interquartile range. PCC: pheochromocytoma. PGL: paraganglioma. HN: head and neck. A: Abdominal. T: thoracic.

Table 2. Summary of the *in silico* and *in vitro* analyses in *MDH2* missense and deletion VUS

VUS		V-1 p.Ser3Phe	V-2 p.Arg104Gly	V-5 p.Gln130Arg	V-6 p.Val160Met	V-9 p.Ala256Thr	V-10 p.Lys314del
SNP ID ExAC allele freq. gnomAD* allele freq. 1000 Genomes*		not described	not described	not described	rs138541865 $1{,}66{\cdot}10^{-4}$; 0 hom -	rs147655350 $4{,}69{\cdot}10^{-5}$; 0 hom -	not described
Evolutionary conservation *Interpretation* (a)		Conserved position	Conserved position	Conserved position	Conserved position	Conserved position	Conserved position ¤
Functional domain		NA (Low complexity region)	Ldh_1_N domain (PF00056)	Ldh_1_N domain (PF00056)	Ldh_1_N domain (PF00056)	Ldh_1_C domain (PF02866)	Ldh_1_C domain (PF02866)
Protein function prediction *Interpretation* (a)		Inconclusive (5/9)	**Impaired (10/10)**	Neutral (3/10)	**Impaired (8/10)**	**Impaired (9/10)**	NA
3D structural annotations (Structure-PPi)		Transit peptide to Mitochondria (aa 1-24)	NAD-binding site	α-helix	NA	α-helix	α-helix
3D structural prediction *Interpretation* (a)		No effect	**Destabilize (4/5)**	Inconclusive (3/5)	**Destabilize (5/5)**	**Destabilize (5/5)**	NA
Neighbor positions mutated in other cancers (b) (Structure-PPi)		NA	Malignant melanoma, Ovary carcinoma, Colon carcinoma, Endometrium carcinoma	Breast carcinoma	Stomach carcinoma	Endometrium carcinoma, Head and neck squamous cell carcinoma	Endometrioid Carcinoma (p.Ser310Ser), Prostate carcinoma (p.Ser317Leu), Oral carcinoma (p.Ala319Ser)
***RBP1* expression** (c)		+++	**+**	NA	**+**	NA	**+**
LOH		no	no	NA	no	NA	**Yes**
MDH2 subcelular localization (d)		M	M	M	M	M	NA
Enzymatic activity	**with saturating [NAD+] and [malate]** (e)	+++	**+**	+++	+++	+++	NA
	co-transfection experiment (e)	NA	**++**	NA	NA	NA	NA
	Affinity assay: with lower [NAD+] and [malate] (f)	NA	**Impaired for malate and NAD^+**	NA	**Likely impaired for malate**	**Likely impaired for malate and NAD+**	NA
Molecular dynamics simulations		NA	NA	NA	**Substrate binding site likely affected**	**Dimerization likely affected**	NA
Classification of VUS		**LIKELY BENIGN**	**PATHOGENIC**	**LIKELY BENIGN**	**LIKELY PATHOGENIC**	**LIKELY PATHOGENIC**	**PATHOGENIC**

Results in dark gray highlight and bold indicate major alterations. V-: variant; NA: not available. Ldh_1_N domain: lactate/malate dehydrogenase, NAD binding domain (Pfam accession: PF00056); Ldh_1_C domain: lactate/malate dehydrogenase, alpha/beta C-terminal domain (Pfam accession: PF02866).

(a) See Table S4 for breakdown of the different computational predictors. In brackets, it is shown the number of tools predicting a damaging effect.

(b) See Figure S2 for mapping of the mutations onto the crystal structure.

(c) *RBP1* mRNA expression relative to tumors with mutations in non-Krebs cycle genes: +++ corresponds non-significant *RBP1* expression reduction, + corresponds to significant ($p<0.05$) *RBP1* expression reduction

(d) M: mitochondrial

(e) from *in vitro* MDH2 enzymatic activity (Fig 2A, 2B): +++ corresponds to MDH2 activity >75% compared to control, ++ 25-75% and + 0-25%.

(f) from *in vitro* MDH2 enzymatic affinity assay (Fig 2C-F)

* http://gnomad.broadinstitute.org/ and http://www.internationalgenome.org/ (Last accessed: Jun 07, 2017)

¤Despite the variant p.K314del is not annotated in the dbNSFP database, we infers the evolutionary conservation of this position considering the annotated variants at this position (i.e., p.K314Q, p.K314E, p.K314*, p.K314T, p.K314R, p.K314M and p.K314N). For each method, the lowest and the highest scores are included

FIGURE LEGENDS

Figure 1. Graphical representation of the variants identified in *MDH2* and the residues of the protein affected. The mutation previously reported[16] is indicated with ★ . Missense variants are framed in continuous line; in-frame deletion is framed in discontinuous line; synonymous variant is shown in the upper part of the figure; intronic variants are shown in the lower part of the figure.

Figure 2. MDH2 activity measured in *MDH2* KD cells transfected with different vectors containing the VUS in *MDH2*. A: Enzymatic activities at saturating concentrations of malate (25mM) and NAD+ (2mM) in p.R104G (p.Arg104Gly), p.Q130R (p.Gln130Arg), p.V160M (p.Val160Met) and p.S3F (p.Ser3Phe) variants, plus C (p.K301R-p.Lys301Arg) which is a polymorphism with minor allele frequency of 0.037), KD and WT as controls, are expressed as mean (nmol/min/mg) ± SD of 3 paired independent experiments in quadruplicate. Different shadings indicate the only variants tested in experiments from fig C-F. B: Enzymatic activities at saturating concentrations of cells co-transfected with WT, EV and/or p.R104G plasmids expressed as mean of fold-change over activity in cells co-transfected with WT and EV (control) ± SD of 2 paired independent experiments at least in quadruplicate; µg of plasmid DNA transfected for each condition are showed in the figure. C-F: Enzymatic activities in p.A256T, p.V160M, p.R104G and control (p.K301R) expressed as mean of fold-change over control ± SD of at least 2-paired independent experiments in triplicate. Assays performed with reduced concentrations of malate or NAD+: C) 5-fold reduction malate (5mM), D) 10-fold reduction malate (2.5mM), E) 4-fold reduction of NAD+ (0.5mM) and F) 20-fold reduction of NAD+ (0.1mM). *****: *p*-value<0.0001; ****: p-value<0.001; ***: *p*-value<0.01; **: *p*-value<0.03 and *: *p*-value<0.05 based on a two-sided Mann-Whitney U test.

Figure 3. Molecular dynamics simulations in MDH2 p.Ala256Thr and p.Val160Met VUS versus wt. A: Distance between the Cζ atom of F260 and the Cβ atom of A/T256 for both monomers of wt MDH2 (magenta, upper pannels), Ala256Thr (blue, middle pannels) and V160M (green, lower pannels) during the simulations. A short distance corresponds to the F260 down conformation, and a long distance to the F260 up conformation (inset). B and C: Distribution of the distance between the Cα atoms of K269 of the two monomers of the Ala256Thr (A) and Val160Met (B) variants from snapshots from the simulation trajectories, compared to wt.

The authors of the manuscript declare no conflicts of interest.

Figure 1

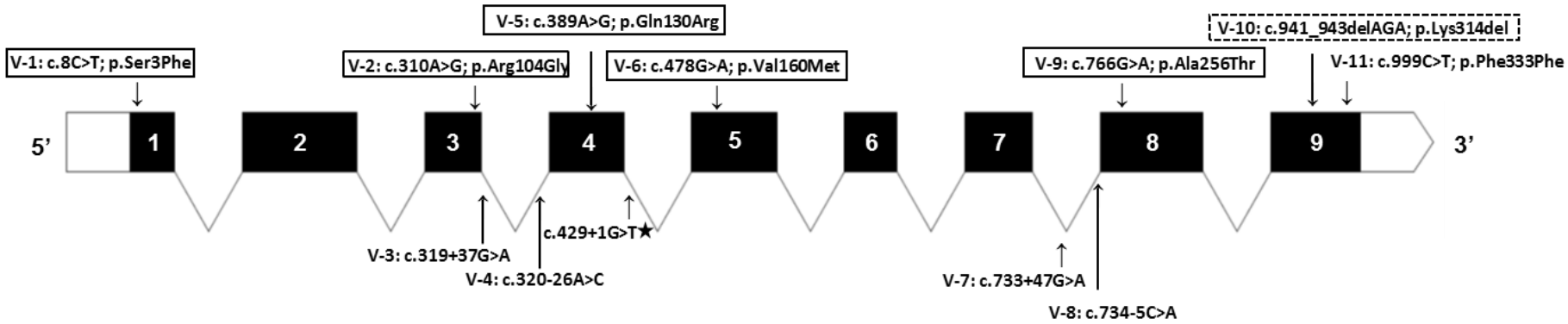
V-1: c.8C>T; p.Ser3Phe
V-2: c.310A>G; p.Arg104Gly
V-5: c.389A>G; p.Gln130Arg
V-6: c.478G>A; p.Val160Met
V-9: c.766G>A; p.Ala256Thr
V-10: c.941_943delAGA; p.Lys314del
V-11: c.999C>T; p.Phe333Phe
5'
1
2
3
4
5
6
7
8
9
3'
V-3: c.319+37G>A
V-4: c.320-26A>C
c.429+1G>T★
V-7: c.733+47G>A
V-8: c.734-5C>A

Figure 2

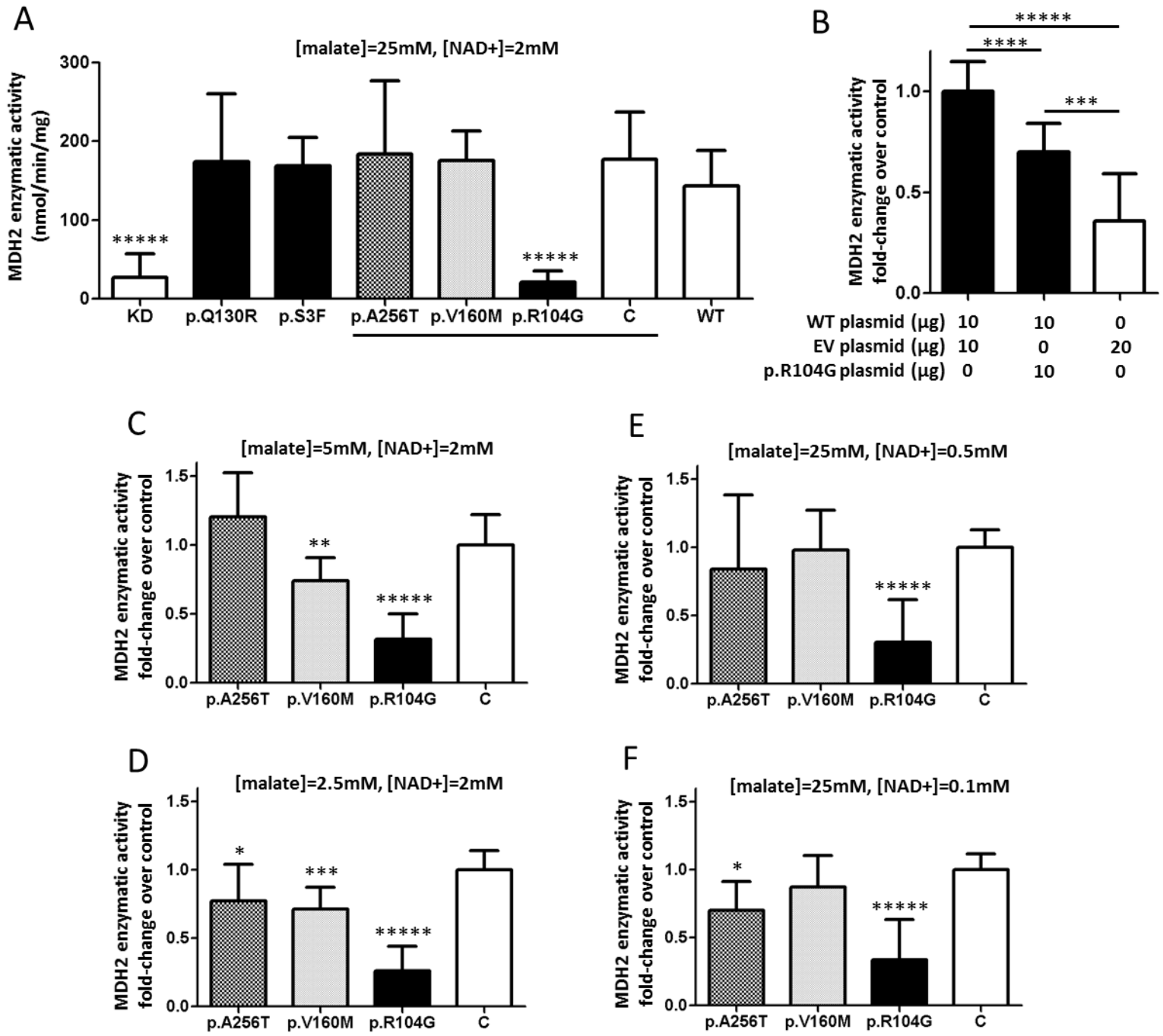
A
[malate]=25mM, [NAD+]=2mM
MDH2 enzymatic activity (nmol/min/mg)
300
200
100
0
*****
*****
KD
p.Q130R
p.S3F
p.A256T
p.V160M
p.R104G
C
WT
B
*****
****
***
MDH2 enzymatic activity fold-change over control
1.0
0.5
0.0
WT plasmid (µg) 10 10 0
EV plasmid (µg) 10 0 20
p.R104G plasmid (µg) 0 10 0
C
[malate]=5mM, [NAD+]=2mM
MDH2 enzymatic activity fold-change over control
1.5
1.0
0.5
0.0
**
*****
p.A256T
p.V160M
p.R104G
C
E
[malate]=25mM, [NAD+]=0.5mM
MDH2 enzymatic activity fold-change over control
1.5
1.0
0.5
0.0
*****
p.A256T
p.V160M
p.R104G
C
D
[malate]=2.5mM, [NAD+]=2mM
MDH2 enzymatic activity fold-change over control
1.5
1.0
0.5
0.0
*
***
*****
p.A256T
p.V160M
p.R104G
C
F
[malate]=25mM, [NAD+]=0.1mM
MDH2 enzymatic activity fold-change over control
1.5
1.0
0.5
0.0
*
*****
p.A256T
p.V160M
p.R104G
C

Figure 3

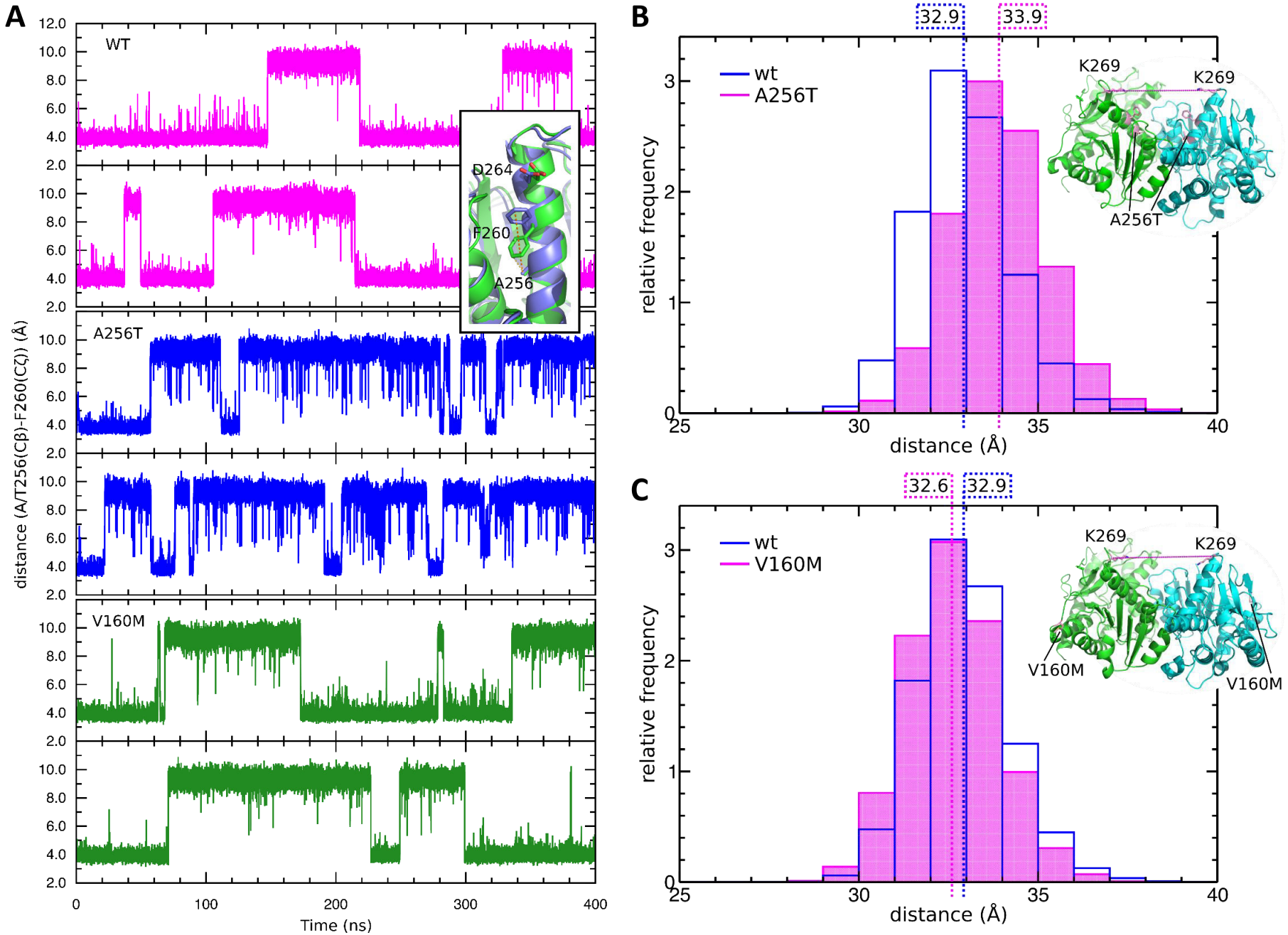
A
WT
A256T
V160M
D264
F260
A256
distance (A/T256(Cβ)-F260(Cζ)) (Å)
Time (ns)
B
32.9
33.9
wt
A256T
relative frequency
distance (Å)
K269
K269
A256T
C
32.6
32.9
wt
V160M
relative frequency
distance (Å)
K269
K269
V160M
V160M

REVUE 4

Génétique des phéochromocytomes et paragangliomes

Buffet A, Gimenez-Roqueplo AP.

EMC -Endocrinologie-Nutrition 2018;0(0):1-8 [Article 10-015-B-55].

Génétique des phéochromocytomes et paragangliomes

A. Buffet, A.-P. Gimenez-Roqueplo

Les paragangliomes (PGL) sont des tumeurs neuroendocrines rares caractérisées par un fort déterminisme génétique. En effet, la génétique des PGL a évolué de façon majeure ces 15 dernières années. Il est actuellement considéré qu'environ 40 % des PGL sont génétiquement déterminés, secondaires à des mutations constitutionnelles de transmission autosomique dominante dans la quinzaine de gènes de prédisposition connus à ce jour. Plus de la moitié des mutations siègent sur un des gènes SDHx *(*SDHA, SDHB, SDHC, SDHD, SDHAF2*) qui codent pour les différentes sous-unités de la succinate déshydrogénase, une enzyme mitochondriale. Ces différents gènes prédisposent à des formes précoces (*VHL, RET, SDHD, EPAS1*), syndromiques (*RET, VHL, EPAS1, NF1, FH*), multiples (*SDHD, TMEM127, MAX*) ou malignes (*SDHB, FH*) de PGL. Ces différents gènes activent des voies de tumorigenèse/cancérogenèse différentes. La mise en évidence d'une mutation dans un de ces gènes de prédisposition va changer la prise en charge du patient et sa surveillance et aussi permettre le dépistage génétique familial et d'organiser une surveillance présymptomatique de la maladie chez les apparentés porteurs de la mutation.*

Mots-clés : Phéochromocytome ; Paragangliome ; Mutation constitutionnelle ; Gènes SDHx ; Enquête familiale

Plan

Introduction

Les paragangliomes (PGL) sont des tumeurs endocrines rares qui se développent aux dépens des systèmes ortho- et parasympathiques, et se répartissent le plus souvent le long des grands axes vasculaires. Ils peuvent s'étendre des ganglions parasympathiques (au niveau cervical) à la chaîne ganglionnaire sympathique (au niveau thoraco-abdomino-pelvien). Les PGL localisés dans la médullo-surrénale sont appelés phéochromocytomes (PH).

Ces tumeurs peuvent se révéler par un syndrome de compression (atteintes des nerfs crâniens pour les PGL cervicaux), ou par un syndrome sécrétant. En effet, les PGL et PH peuvent sécréter des catécholamines (dopamine, noradrénaline, adrénaline) et être alors révélées par des signes ou complications cardio- ou cérébrovasculaires.

Dix à 15 % des PGL sont d'évolution maligne. Le diagnostic de malignité est porté sur la présence d'une métastase ou d'une dissémination métastatique à distance d'un site paraganglionnaire (classification WHO 2004 révisée en 2017).

Une des grandes spécificités de cette tumeur est son fort déterminisme génétique puisqu'il est considéré aujourd'hui que le PGL est la tumeur neuroendocrine la plus impactée par la génétique. Environ 40 % des PGL sont génétiquement déterminés, secondaires à des mutations constitutionnelles de transmission autosomique dominante dans une quinzaine de gènes de prédisposition connus en 2017. De plus, une méta-analyse réalisée par la Mayo Clinic a démontré qu'environ 12 % des patients ayant une présentation apparemment sporadique de la maladie (PGL ou PH unique, survenu à un âge tardif, et sans contexte familial) sont porteurs d'une mutation dans un de ces gènes de prédispositions [1]. Mis à part les gènes *RET* et *HIF2A* qui sont des oncogènes, tous les autres gènes sont des gènes suppresseurs de tumeurs (GST), c'est-à-dire que le mécanisme de tumorigenèse nécessite l'association d'une mutation constitutionnelle et d'une perte d'hétérozygotie somatique ou d'une seconde mutation sur l'autre allèle, conformément au modèle des « two hits » de Knudson [2].

Volume 0 > n°0 > xxx 2018
http://dx.doi.org/10.1016/S1155-1941(18)83576-4

Tableau 1.
Critères de diagnostic d'une neurofibromatose de type 1 (NF1) selon le consensus du National Institutes of Health (NIH).

Deux critères ou plus, parmi la liste ci-dessous, sont suffisants pour poser le diagnostic de NF1
≥ 6 tâches café au lait (> 0,5 cm avant la puberté, > 1,5 cm après la puberté)
Éphélides axillaires ou inguinales
≥ 2 neurofibromes quel que soit le type ou 1 neurofibrome plexiforme
≥ 2 nodules de Lisch
Une lésion osseuse évocatrice (dysplasie des ailes du sphénoïde, etc.)
Un gliome des voies optiques
Un apparenté au premier degré avec une NF1

Tableau 2.
Phénotype (hors paragangliome) de la maladie de von Hippel-Lindau et des néoplasies endocriniennes multiples de type 2 (NEM2).

Maladie de von Hippel-Lindau	**NEM2**
Hémangioblastome rétinien	**NEM2A**
Hémangioblastome du SNC	CMT, hyperparathyroïdie
Carcinome rénal à cellules claires	**NEM2B**
Tumeur endocrine pancréatique	CMT
Kystes pancréatiques	Habitus marfanoïde
Tumeur du sac endolymphatique	Gangliomatose digestive
Cystadénome épididymaire ou du ligament large	Neurome muqueux

SNC : système nerveux central ; CMT : carcinome médullaire de la thyroïde.

■ Génétique constitutionnelle des paragangliomes

Formes syndromiques

Neurofibromatose de type 1 (gène *NF1*)

Les mutations constitutionnelles du gène *NF1* sont responsables de la neurofibromatose de type 1 (NF1), appelée aussi maladie de von Recklinghausen, pathologie à forte pénétrance de transmission autosomique dominante dont la prévalence est estimée à 1/3000. Le diagnostic est clinique et repose sur les sept critères du consensus du National Institutes of Health (NIH) (Tableau 1) [3]. Le diagnostic de NF1 peut être posé dans 95 % des cas sur l'association d'au moins deux de ces critères cliniques dès l'âge de 11 ans [4].

Les patients avec une NF1 développent des PGL dans 0,1 à 5,7 % des cas, le plus souvent à l'âge adulte dans la quatrième décade [5, 6]. Les patients présentent dans la grande majorité des cas des PH, de découverte incidente dans 30 % des cas [5]. Chez un patient avec un PH, le diagnostic de NF1 est souvent simple cliniquement. Toutefois, deux études ont mis en évidence une mutation constitutionnelle de *NF1* chez quatre patients ayant un PH d'apparence sporadique au diagnostic. Ces patients avaient cependant des critères phénotypiques frustres de la maladie lors de la réévaluation clinique spécialisée [7, 8].

Maladie de von Hippel-Lindau (gène *VHL*)

Les mutations constitutionnelles du gène *VHL* mènent à la maladie de von Hippel-Lindau (VHL), maladie de transmission autosomique dominante dont l'incidence est de 1/36 000. Cette pathologie est caractérisée par le développement, avec une pénétrance variable, de différentes tumeurs (Tableau 2).

Deux grands cadres phénotypiques ont été décrits chez les patients avec un VHL, fondés sur le risque de développer un PH : le VHL de type 1, où le risque de développer un PH est bas, et où les mutations mises en évidence sont plus fréquemment des mutations tronquantes du gène *VHL*, et le VHL de type 2, où le risque de développer un PH est important. Ce VHL de type 2 est subdivisé en trois sous-groupes : le type 2A où le risque de cancer du rein est important, le type 2B où le risque de cancer du rein est faible et, enfin, le type 2C où les patients ne développeront a priori que des PH ou des PGL [9, 10]. Dans le VHL de type 2, les mutations causales sont plutôt des mutations faux-sens menant à une altération forte (2A et 2B) ou faible (2C) de la fonction de la protéine VHL [11, 12].

Les patients porteurs d'une mutation dans le gène *VHL* ont des PGL volontiers précoces (avant 20 ans), de localisations surrénaliennes ou abdominales et fréquemment bilatéraux (40 à 60 % des cas). On retrouve des antécédents familiaux de VHL et/ou des lésions syndromiques chez deux tiers des patients (Tableau 3) [6, 13].

Néoplasies endocriniennes multiples de type 2 (gène *RET*)

Les mutations gain de fonction du gène *RET* sont responsables des néoplasies endocriniennes multiples de type 2 (NEM2), touchant 1/30 000 individus. Ces mutations de transmission autosomique dominante sont des mutations récurrentes survenant dans les exons 8, 10, 11, 13, 14, 15, 16, qui entraînent une auto-activation du récepteur tyrosine kinase RET. Trois tableaux cliniques différents sont possibles selon le siège de la mutation. Les corrélations génotype-phénotype sont décrites dans le Tableau 2 : les NEM2A ou syndrome de Sipple (70 à 80 % des cas), les NEM2B ou syndrome de Gorlin (5 % des cas), et les carcinomes médullaires de la thyroïde familiaux ou syndrome de Farndon (10 à 12 % des cas) [14].

Les carcinomes médullaires de la thyroïde (CMT) font la gravité de la NEM2. L'agressivité du CMT est corrélée au génotype et les mutations *RET* sont classées selon l'agressivité du CMT en trois niveaux (*moderate, high, highest*) par l'American Thyroid Association [15].

Les PH sont présents dans environ 50 % des patients avec une NEM2 [14] et peuvent être révélateurs d'une NEM2 dans 6 à 13 % des cas [16].

Syndromes paragangliomes-polyglobulie (gènes *EPAS1* et *EGLN1*)

Des mutations constitutionnelles gain de fonction de *EPAS1* (codant pour la protéine *hypoxia inducible factor* 2A [HIF2A]) et perte de fonction de *EGLN1* (codant pour la protéine *prolyl hydroxylase domain 2* [PHD2]) ont été décrites dans des polyglobulies congénitales de transmission autosomique dominante [17, 18].

Depuis 2008, deux patients ont été décrits avec des PGL abdominaux associés à une polyglobulie et une mutation *EGLN1* [19, 20].

L'équipe de Karel Pacak a décrit en 2012 les premières mutations de *EPAS1*. Ces mutations sont des mutations gain de fonction et ont été retrouvées chez des patients avec polyglobulie congénitale, somatostatinome et PGL [21]. Depuis, d'autres équipes ont confirmé ces données. Les patients avec mutations *EPAS1* ont des PGL ou des PH multiples dans la moitié des cas et volontiers précoces [22]. Une polyglobulie est retrouvée dans moins de la moitié des cas et des somatostatinomes uniques ou multiples sont présents dans un quart des cas. Ces différentes mutations sont présentes soit au niveau tumoral, soit à l'état de mosaïque somatique, et sont donc potentiellement transmissibles à la descendance que si la mutation est présente dans les cellules germinales [22].

Paragangliomes héréditaires

Gènes *SDHx*

Les gènes *SDHx* (*SDHA, SDHB, SDHC, SDHD* et *SDHAF2*) représentent presque la moitié des gènes porteurs d'une mutation au niveau constitutionnel dans les PGL [6, 13, 23]. Ces gènes codent pour la succinate déshydrogénase (SDH) ou complexe 2 mitochondrial, qui intervient dans deux voies métaboliques, le cycle de Krebs et la chaîne respiratoire mitochondriale. La SDH permet d'oxyder le succinate en fumarate dans le cycle de Krebs, et le complexe 2 mitochondrial intervient dans le transfert d'électrons dans la chaîne respiratoire. La SDH contient deux sous-unités d'ancrage SDHC, SDHD, et deux sous-unités catalytiques, SDHA et SDHB. SDHAF2 est responsable de la flavination de SDHA, qui est essentielle à l'assemblage du complexe.

Tableau 3.
Corrélations génotype-phénotype.

Gène	*NF1*	*VHL*	*RET*	*EPAS1*	*EGLN1*	*SDHA*	*SDHB*	*SDHC*	*SDHD*	*SDHAF2*	*FH*	*TMEM127*	*MAX*
Localisation	17q11	3p25	10q11	2p21	14q42	5p15	1p36	1q23	11q23	11q13	1q42	2q11	14q23
Fréquence des mutations	3 %	7 %	6 %	1 %	2 patients	< 1 %	10 %	1 %	9 %	< 1 %	1 %	1–2 %	1 %
Âge de diagnostic du PGL/PH	40–50 ans	20–30 ans	30–40 ans	20–30 ans	NC	35–40 ans	30–40 ans	35–40 ans	30–40 ans	30–40 ans	30–40 ans	35–40 ans	35–40 ans
Localisation préférentielle du PGL/PH	PH	PH ou PGL	PH	PH ou PGL TAP	PGL A	PGL A	PGL A (60 %), PGL C (40 %)	PGL C	PGL C	PGL C	PGL A	PH	PH
Fréquence PGL/PH multiples	20–40 %	40–60 %	66 %	50 %	NC	NC	20 %	30 %	66 %	75 %	40 %	15–66 %	50 %
Fréquence PGL/PH métastatique	Rare	Rare	Rare	Rare	NC	Rare	40 %	Rare	Rare	NC	40 %	Rare	Rare
Sécrétion	Ad	Norad	Ad	Norad ou EPO	Norad	Norad, Dopa, NS	Norad, Dopa, NS	Norad, Dopa, NS	Norad, Dopa, NS	NS	Norad, NS	Ad	Norad
Autres tumeurs	Cf. Tableau 1	Cf. Tableau 2	Cf. Tableau 2	PG, ST	PG	GIST, CR	GIST, CR	GIST, CR	GIST, CR	Non	LC, LU, CR	CR	Non

PH : phéochromocytome ; PGL : paragangliome ; PGL TAP : paragangliome thoraco-abdomino-pelvien ; PGL C : PGL cervical ; PGL A : PGL abdominal ; NC : non connu ; Ad : sécrétion d'adrénaline ; Norad : sécrétion de noradrénaline ; Dopa : sécrétion de dopamine ; NS : non sécrétant ; GIST : tumeur stromale gastro-intestinale ; CR : cancer du rein ; PG : polyglobulie ; ST : somatostatinome ; LC : léiomyome cutané ; LU : léiomyome utérin.

Une mutation constitutionnelle dans l'un des gènes *SDHx* associée à une perte d'hétérozygotie au niveau somatique mène à une perte de l'activité enzymatique de la SDH et à une accumulation de succinate dans le cytoplasme, qui va se comporter comme un oncométabolite [24]. Ces mutations se transmettent de façon autosomique dominante pour les gènes *SDHA*, *SDHB* et *SDHC*, et de façon autosomique dominante soumis à empreinte maternelle pour *SDHD* et *SDHAF2*. La majorité des PGL secondaires aux mutations *SDHx* sont secondaires à des mutations dans les gènes *SDHD* et *SDHB* [23]. Des différences de phénotype peuvent être observées selon le gène *SDHx* muté et l'origine parentale de la mutation (Tableau 3).

Les mutations dans le gène *SDHD*, quand elles sont héritées de la branche paternelle, favorisent le développement de PGL cervicaux (chez plus de 97 % des patients) multiples, dont la pénétrance est de 86 % à l'âge de 50 ans [25, 26], alors que les sujets ayant reçu une mutation *SDHD* transmise par la branche maternelle développent exceptionnellement la maladie [27].

Les mutations dans le gène *SDHB* ont une pénétrance de 50 % à l'âge de 50 ans [28] et prédisposent à la malignité. En effet, environ la moitié des patients porteurs d'un PGL *SDHB*-dépendant ont une forme métastatique, et une mutation constitutionnelle du gène *SDHB* est retrouvée chez 36 % des patients avec un PGL malin, alors qu'une forme maligne n'est retrouvée que chez moins de 5 % des patients porteurs d'une mutation dans les gènes *SDHD* et *SDHC* [25, 26]. De plus, les patients ayant un PGL malin *SDHB*-dépendant ont un plus mauvais pronostic que les patients ayant un PGL malin non *SDHB*-dépendant [29].

Les mutations dans les gènes *SDHC, SDHA, SDHAF2* sont rares et prédisposent au développement de PGL cervicaux ou abdominaux selon le génotype (Tableau 3) [30, 31].

Ces mutations *SDHx* prédisposent à d'autres types de cancers rares. Elles sont impliquées dans 0,05 à 0,2 % des cancers du rein, principalement à cellules claires [32]. Elles sont également impliquées dans les tumeurs gastro-intestinales stromales (GIST) sans mutation dans *PDGFRA* et *KIT*, où elles prédisposent principalement à des formes pédiatriques, gastriques, multiples et malignes [33]. Ces GIST secondaires aux mutations *SDHx* ou à une épimutation du promoteur de *SDHC* (hyperméthylation du promoteur de *SDHC*) peuvent être isolées ou s'intégrer dans la triade de Carney (association GIST, PGL et chondrome pulmonaire) ou du syndrome de Carney-Stratakis associant GIST et PGL [33, 34].

Enfin, les mutations des gènes *SDHx* pourraient être impliquées dans la prédisposition aux adénomes hypophysaires, mais cette implication est controversée, notamment car l'activité de la SDH dans les tumeurs est conservée et les immunohistochimies anti-SDHB et anti-SDHD sont contradictoires par rapport à ce qui est décrit dans les PGL et PH [35, 36].

Gène *FH*

Le gène *FH* code pour la fumarate hydratase, une enzyme qui catalyse l'étape qui suit celle de la SDH dans le cycle de Krebs.

Les mutations constitutionnelles de ce gène étaient connues pour être responsables du syndrome *hereditary leiomyomatosis and renal cell cancer* (HRLCC) [37]. Les patients ayant ce syndrome développent, dans deux tiers des cas, des léiomyomes cutanés et les femmes présentent dans plus de 80 % des cas des léiomyomes utérins dès l'âge de 30 ans. Enfin, dans environ 20 % des cas, il est retrouvé un carcinome papillaire de type 2, qui est de mauvais pronostic [38].

L'équipe des auteurs a récemment montré que le gène *FH* était également impliqué dans les PGL. Des mutations constitutionnelles de ce gène ont été identifiées chez des patients avec un phénotype *SDHB-like* [24, 39] et peu ou pas de léiomyomes ou de carcinome rénal associés.

Phéochromocytomes familiaux : les gènes *TMEM127* et *MAX*

Les mutations du gène *TMEM127* prédisposent quasi exclusivement aux PH, souvent bilatéraux, parfois familiaux et qui se développent généralement après 35 ans [40].

Ce gène est également impliqué dans la prédisposition aux carcinomes rénaux à cellules claires [41].

Les mutations du gène *MAX*, quant à elles, prédisposent aux PH ou aux PGL abdominaux se développant souvent avant 35 ans. La moitié des patients ont une forme bilatérale, et une histoire familiale est retrouvée dans 40 % des cas [42].

Gènes rares

Certains gènes n'ont été impliqués que pour un nombre très limité de patients, comme par exemple *MDH2, MET, H3F3A, MERTK*, *KMT2D* et *KIF1B*, et la réalité de leur implication reste encore à démontrer dans des études plus larges [43–46].

■ Génétique tumorale

À côté des mutations constitutionnelles, il a été décrit des mutations dans l'acide désoxyribonucléique (ADN) extrait du tissu tumoral dans différents gènes de prédisposition aux PGL (*VHL, RET, EPAS1* et, surtout, *NF1*) ou dans d'autres gènes impliqués dans l'oncogenèse (*HRAS, TP53, CDKN2A, FGFR1*, etc.), expliquant jusqu'à 30 % des PGL sans mutation constitutionnelle, ce qui porte à 60–70 % le nombre de PGL génétiquement déterminés, ce qui en fait la tumeur avec le plus fort déterminisme génétique [7, 47, 48]. Bien qu'il n'y ait pas de risque de transmission de ces mutations somatiques à la descendance, la connaissance de ces mutations est importante pour connaître la biologie de la tumeur du patient et expliquer, entre autres, le phénotype sécrétoire de ces PGL/PH. En effet, un PGL avec une mutation somatique dans le gène *VHL* sécrète préférentiellement de la noradrénaline, alors qu'un PGL avec une mutation somatique *NF1* ou *RET* sécrète préférentiellement de l'adrénaline [7, 47]. De surcroît, certaines données récentes suggèrent que l'identification d'une mutation somatique dans les gènes *ATRX*, ou *KMT2D* pourrait être un prédicteur de l'agressivité de la tumeur [49, 50].

■ Génétique et tumorigenèse (Fig. 1)

Les données récentes issues des études de génomique ont permis de mieux comprendre les mécanismes de tumorigenèse des PGL. En effet, il a été démontré, grâce aux études de transcriptomique, que les PGL se répartissent en trois différents clusters, reflétant des mécanismes de tumorigenèse différents [47, 51] : le cluster pseudo-hypoxique, le cluster *mitogen-activated protein kinase* (MAPK) et le cluster Wnt/β-caténine. Le premier cluster regroupe les tumeurs secondaires aux mutations *SDHx*, *FH*, *VHL* et *HIF2A*. Ce groupe est caractérisé par une activation de la voie de l'angiogenèse et de l'hypoxie du fait d'une stabilisation anormale des facteurs de transcription de réponse à l'hypoxie HIF-1 et HIF-2 et mène à une pseudo-hypoxie. Les protéines HIF associent une sous-unité exprimée de façon constitutionnelle (HIFβ) à une des sous-unités induite par l'hypoxie (HIF1α ou HIF2α). En situation physiologique et normoxique, les HIFα sont dégradées rapidement grâce à l'hydroxylation de deux prolines par les PHD, permettant la fixation de VHL et ainsi leur polyubiquitination et leur dégradation dans le protéasome. En absence d'oxygène, les PHD ne peuvent plus assurer l'hydroxylation des HIFα, qui sont donc stabilisés et transloqués dans le noyau. Les mutations des gènes *SDHx* et *FH* mènent à l'accumulation de succinate et de fumarate dans les PGL respectivement, qui jouent un rôle d'inhibiteur compétitif des dioxygénases dépendantes du 2-oxyglutarate (dont les PHD), et conduit donc à une stabilisation anormale des HIF [52, 53]. L'activation de la pseudo-hypoxie induit l'activation de gènes cibles, impliqués entre autres dans la prolifération cellulaire, l'angiogenèse, la survie et la transition épithélio-mésenchymateuse [54]. Par ailleurs, l'équipe des auteurs a démontré que des modifications épigénétiques intervenaient également dans les PGL *SDHx* et *FH*. En effet, l'accumulation de succinate et de fumarate dans ces PGL est responsable de l'inhibition de l'activité d'autres dioxygénases dépendantes du 2-oxoglutarate, les enzymes *ten-eleven translocation* (TET),

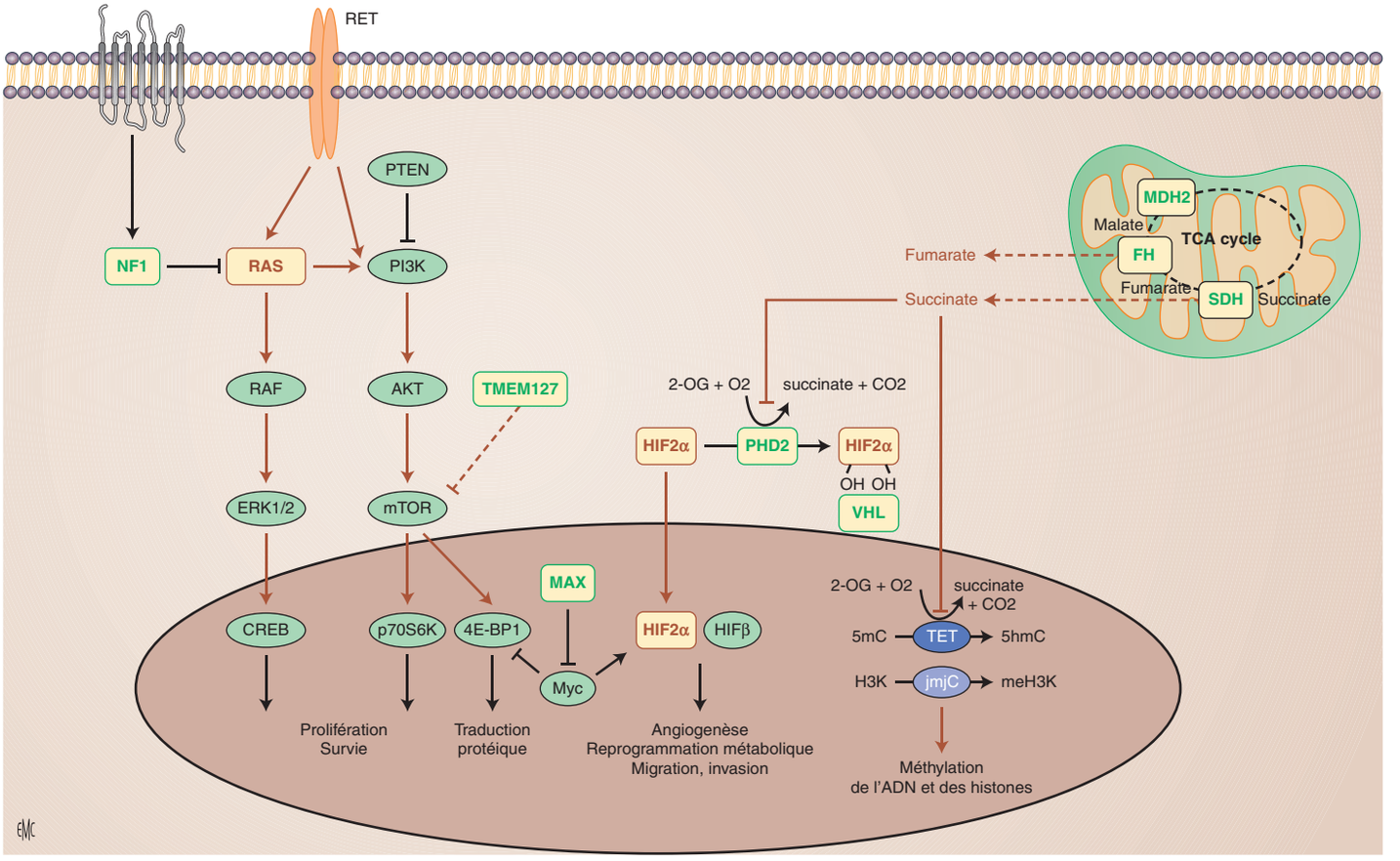

Figure 1. Voie de tumorigenèse des paragangliomes selon le génotype. Les protéines entourées en vert sont codées par des gènes suppresseurs de tumeur et celles entourées en rouge par des oncogènes. ADN : acide désoxyribonucléique ; TCA : cycle des acides tricarboxyliques ; NF1 : neurofibromatose de type 1 ; HIF2α : *hypoxia inducible factor* 2α.

impliquées dans la déméthylation de l'ADN, et les déméthylases des histones, conduisant ainsi à une hyperméthylation globale de l'ADN et à des modifications structurelles de la chromatine. Ces modifications mènent à la sous-expression de différents gènes, notamment de GST, et de gènes répresseurs des processus métastatiques, ainsi que la sous-expression des gènes impliqués dans la différenciation chromaffine [24].

Le deuxième grand mécanisme de tumorigenèse des PGL implique la voie des MAPK et la voie *mechanistic target of rapamycin* (mTOR), retrouvées activées dans les PGL secondaires aux mutations des gènes *RET*, *NF1*, *TMEM127*, et *MAX*. Le gène *RET* code pour un récepteur à activité tyrosine kinase activant la voie des MAPK. La guanosine triphosphate (GTP)ase NF1 est impliquée dans la régulation de la voie de l'oncogène Ras, première étape de la voie des MAPK et qui régule la voie protéine kinase B (AKT)/mTOR. Les mécanismes exacts de l'activation de ces voies dans les PGL secondaires aux mutations *MAX* et *TMEM127* ne sont pas encore bien connus mais font également intervenir la signalisation mTOR [42, 47].

Enfin, il a été récemment mis en évidence un troisième *cluster* sur le transcriptome marqué par une activation de la voie Wnt/β-caténine, une voie impliquée dans la genèse de nombreuses tumeurs [51].

■ Implications des avancées de la génétique pour les patients ayant un paragangliome

Test génétique

Devant cette forte composante génétique dans la genèse des PGL, il doit être systématiquement proposé à chaque patient atteint de bénéficier de l'analyse de ces différents gènes au niveau constitutionnel. Les tests étaient antérieurement faits de façon séquentielle, et orientés selon le phénotype du patient ainsi que, dans certains cas, sur les résultats d'immunohistochimies anti-SDHB, SDHA, MAX [42, 55, 56]. En effet, un immunomarquage anti-SDHB négatif est en faveur d'une mutation dans un des gènes *SDHx*, alors qu'un immunomarquage anti-SDHA ou anti-MAX négatif oriente respectivement vers une mutation du gène *SDHA*, ou une mutation tronquante du gène *MAX*.

Cette approche est de moins en moins utilisée avec la généralisation des panels de séquençage haut débit, permettant de séquencer en une fois l'intégralité des gènes du PGL [57]. Toutefois, la description détaillée du phénotype du patient et les analyses immunohistochimiques peuvent permettre de valider les variations génétiques de signification inconnue identifiées qui sont beaucoup plus fréquentes avec les nouvelles techniques de séquençage haut débit (*next generation sequencing* [NGS]). Des recommandations internationales ont été récemment publiées pour la réalisation du test génétique du PGL par NGS [57].

Intérêt du statut génétique pour le suivi du patient et de ses apparentés

Les recommandations américaines et européennes sur la prise en charge du PGL ont mis l'accent sur le fait que les patients avec une forme génétique de PGL devaient être suivis de façon adaptée à leur génotype [58, 59].

La mise en évidence d'une mutation constitutionnelle va permettre de surveiller l'occurrence des différentes lésions syndromiques, de proposer une surveillance à vie du fait des risques de récurrences et de malignité [59], et d'orienter sur le type d'examens qui composent le suivi chez ces patients (par exemple, les patients ayant un PGL métastatique *SDHB*-dépendant peuvent

Tableau 4.
Proposition de suivi des patients asymptomatiques porteurs d'une mutation dans un des principaux gènes de prédisposition aux paragangliome/phéochromocytome.

Gène	Surveillance des adultes asymptomatiques
SDHB	Pression artérielle annuelle Dosage des dérivés méthoxylés plasmatiques ou urinaires annuel IRM corps entier tous les deux à trois ans TEP ^{18}FDG-TEP si anomalie à l'IRM
SDHD	Pression artérielle annuelle Dosage des dérivés méthoxylés plasmatiques ou urinaires annuel IRM corps entier tous les deux à trois ans TEP fluoro-DOPA si anomalie à l'IRM
SDHC ou *SDHA*	Pression artérielle annuelle Dosage des dérivés méthoxylés plasmatiques ou urinaires annuel IRM corps entier tous les deux à trois ans
VHL	Pression artérielle annuelle Dosage des dérivés méthoxylés plasmatiques ou urinaires annuel Examen du fond de l'œil annuel IRM du SNC tous les deux ans IRM abdominale ou échographie abdominale en alternance annuelle
FH	Pression artérielle annuelle Dosage des dérivés méthoxylés plasmatiques ou urinaires annuel Examen gynécologique et dermatologique annuel IRM abdominale annuelle
RET	Pression artérielle annuelle Dosage de la calcémie annuel Dosage de la thyrocalcitonine annuel (en l'absence de thyroïdectomie) Dosage des dérivés méthoxylés plasmatiques ou urinaires annuel
NF1	Pression artérielle annuelle Si HTA : dosage des dérivés méthoxylés plasmatiques ou urinaires et imagerie abdominale
TMEM127 ou *MAX*	Pression artérielle annuelle Dosage des dérivés méthoxylés plasmatiques ou urinaires annuel IRM abdominale tous les deux à trois ans

SNC : système nerveux central ; IRM : imagerie par résonance magnétique ; HTA : hypertension artérielle ; TEP ^{18}FDG : tomographie à émission de positrons au 18-fluorodésoxyglucose.

bénéficier d'un suivi régulier, entre autres composé d'une tomographie à émission de positrons au 18-fluorodésoxyglucose [TEP ^{18}FDG] [58, 60, 61], voire d'orienter le traitement en cas de forme métastatique [62]).

Finalement, la mise en évidence d'une mutation dans un de ces gènes de prédisposition permet de proposer, comme il s'agit d'une maladie de transmission autosomique dominante, un dépistage présymptomatique aux apparentés dans le cadre prévu par la loi (article R.1131-5 du Code la santé publique) et, s'ils sont porteurs de la mutation, les faire entrer dans un protocole de suivi adapté dans un centre expert. Des recommandations de suivis selon le génotype ont été proposées [23, 59] mais malheureusement ne reposent uniquement que sur des avis d'experts. Une proposition de suivi de ces patients est reportée dans le Tableau 4.

Conclusion

L'évolution de la connaissance de la génétique du PGL ces 15 dernières années a permis de mieux comprendre la tumorigenèse de ces tumeurs et surtout de mieux surveiller et prendre en charge les patients porteurs d'une forme génétique ainsi que leurs apparentés.

Points essentiels

- Les paragangliomes ont une forte prédisposition génétique nécessitant de proposer à tous les patients une consultation de génétique.
- La grande majorité des mutations surviennent dans les gènes *SDHD* et *SDHB.*
- Les mutations constitutionnelles du gène *SDHD* prédisposent aux paragangliomes cervicaux multiples.
- Les mutations constitutionnelles du gène *SDHB* prédisposent aux paragangliomes malins.
- L'identification d'une mutation sur un gène de prédisposition doit permettre au patient d'avoir un suivi adapté à son risque génétique.

Déclaration de liens d'intérêts : les auteurs déclarent ne pas avoir de liens d'intérêts en relation avec cet article.

Références

[1] Brito JP, Asi N, Bancos I, Gionfriddo MR, Zeballos-Palacios CL, Leppin AL, et al. Testing for germline mutations in sporadic pheochromocytoma/paraganglioma : a systematic review. *Clin Endocrinol (Oxf)* 2015;**82**:338–45.

[2] Knudson Jr AG. Mutation and cancer: statistical study of retinoblastoma. *Proc Natl Acad Sci U S A* 1971;**68**:820–3.

[3] Neurofibromatosis. Conference statement. National Institutes of Health Consensus Development Conference. *Arch Neurol* 1988;**45**:575–8.

[4] Hersh JH, American Academy of Pediatrics Committee on Genetics. Health supervision for children with neurofibromatosis. *Pediatrics* 2008;**121**:633–42.

[5] Gruber LM, Erickson D, Babovic-Vuksanovic D, Thompson GB, Young Jr WF, Bancos I. Pheochromocytoma and paraganglioma in patients with neurofibromatosis type 1. *Clin Endocrinol (Oxf)* 2017;**86**:141–9.

[6] Amar L, Bertherat J, Baudin E, Ajzenberg C, Bressac-de Paillerets B, Chabre O, et al. Genetic testing in pheochromocytoma or functional paraganglioma. *J Clin Oncol* 2005;**23**:8812–8.

[7] Burnichon N, Buffet A, Parfait B, Letouzé E, Laurendeau I, Loriot C, et al. Somatic NF1 inactivation is a frequent event in sporadic pheochromocytoma. *Hum Mol Genet* 2012;**21**:5397–405.

[8] Bausch B, Koschker AC, Fassnacht M, Stoevesandt J, Hoffmann MM, Eng C, et al. Comprehensive mutation scanning of NF1 in apparently sporadic cases of pheochromocytoma. *J Clin Endocrinol Metab* 2006;**91**:3478–81.

[9] Maher ER, Webster AR, Richards FM, Green JS, Crossey PA, Payne SJ, et al. Phenotypic expression in von Hippel-Lindau disease: correlations with germline VHL gene mutations. *J Med Genet* 1996;**33**:328–32.

[10] Nordstrom-O'Brien M, van der Luijt RB, van Rooijen E, van den Ouweland AM, Majoor-Krakauer DF, Lolkema MP, et al. Genetic analysis of von Hippel-Lindau disease. *Hum Mutat* 2010;**31**:521–37.

[11] Li L, Zhang L, Zhang X, Yan Q, Minamishima YA, Olumi AF, et al. Hypoxia-inducible factor linked to differential kidney cancer risk seen with type 2A and type 2B VHL mutations. *Mol Cell Biol* 2007;**27**:5381–92.

[12] Ohh M, Park CW, Ivan M, Hoffman MA, Kim TY, Huang LE, et al. Ubiquitination of hypoxia-inducible factor requires direct binding to the beta-domain of the von Hippel-Lindau protein. *Nat Cell Biol* 2000;**2**:423–7.

[13] Mannelli M, Castellano M, Schiavi F, Filetti S, Giacche M, Mori L, et al. Clinically guided genetic screening in a large cohort of Italian patients with pheochromocytomas and/or functional or nonfunctional paragangliomas. *J Clin Endocrinol Metab* 2009;**94**:1541–7.

[14] Brandi ML, Gagel RF, Angeli A, Bilezikian JP, Beck-Peccoz P, Bordi C, et al. Guidelines for diagnosis and therapy of MEN type 1 and type 2. *J Clin Endocrinol Metab* 2001;**86**:5658–71.

[15] Wells Jr SA, Asa SL, Dralle H, Elisei R, Evans DB, Gagel RF, et al. Revised American Thyroid Association guidelines for the management of medullary thyroid carcinoma. *Thyroid* 2015;**25**:567–610.

[16] Thosani S, Ayala-Ramirez M, Palmer L, Hu MI, Rich T, Gagel RF, et al. The characterization of pheochromocytoma and its impact on overall survival in multiple endocrine neoplasia type 2. *J Clin Endocrinol Metab* 2013;**98**:E1813–9.

[17] Percy MJ, Furlow PW, Lucas GS, Li X, Lappin TR, McMullin MF, et al. A gain-of-function mutation in the HIF2A gene in familial erythrocytosis. *N Engl J Med* 2008;**358**:162–8.

[18] Percy MJ, Zhao Q, Flores A, Harrison C, Lappin TR, Maxwell PH, et al. A family with erythrocytosis establishes a role for prolyl hydroxylase domain protein 2 in oxygen homeostasis. *Proc Natl Acad Sci U S A* 2006;**103**:654–9.

[19] Ladroue C, Carcenac R, Leporrier M, Gad S, Le Hello C, Galateau-Salle F, et al. PHD2 mutation and congenital erythrocytosis with paraganglioma. *N Engl J Med* 2008;**359**:2685–92.

[20] Yang C, Zhuang Z, Fliedner SM, Shankavaram U, Sun MG, Bullova P, et al. Germ-line PHD1 and PHD2 mutations detected in patients with pheochromocytoma/paraganglioma-polycythemia. *J Mol Med* 2015;**93**:93–104.

[21] Zhuang Z, Yang C, Lorenzo F, Merino M, Fojo T, Kebebew E, et al. Somatic HIF2A gain-of-function mutations in paraganglioma with polycythemia. *N Engl J Med* 2012;**367**:922–30.

[22] Buffet A, Smati S, Mansuy L, Menara M, Lebras M, Heymann MF, et al. Mosaicism in HIF2A-related polycythemia-paraganglioma syndrome. *J Clin Endocrinol Metab* 2014;**99**:E369–73.

[23] Favier J, Amar L, Gimenez-Roqueplo AP. Paraganglioma and phaeochromocytoma: from genetics to personalized medicine. *Nat Rev Endocrinol* 2015;**11**:101–11.

[24] Letouze E, Martinelli C, Loriot C, Burnichon N, Abermil N, Ottolenghi C, et al. SDH mutations establish a hypermethylator phenotype in paraganglioma. *Cancer Cell* 2013;**23**:739–52.

[25] Burnichon N, Rohmer V, Amar L, Herman P, Leboulleux S, Darrouzet V, et al. The succinate dehydrogenase genetic testing in a large prospective series of patients with paragangliomas. *J Clin Endocrinol Metab* 2009;**94**:2817–27.

[26] Pasini B, Stratakis CA. SDH mutations in tumorigenesis and inherited endocrine tumours : lesson from the phaeochromocytoma-paraganglioma syndromes. *J Intern Med* 2009;**266**:19–42.

[27] Burnichon N, Mazzella JM, Drui D, Amar L, Bertherat J, Coupier I, et al. Risk assessment of maternally inherited SDHD paraganglioma and phaeochromocytoma. *J Med Genet* 2017;**54**:125–33.

[28] Ricketts CJ, Forman JR, Rattenberry E, Bradshaw N, Lalloo F, Izatt L, et al. Tumor risks and genotype-phenotype-proteotype analysis in 358 patients with germline mutations in SDHB and SDHD. *Hum Mutat* 2010;**31**:41–51.

[29] Amar L, Baudin E, Burnichon N, Peyrard S, Silvera S, Bertherat J, et al. Succinate dehydrogenase B gene mutations predict survival in patients with malignant pheochromocytomas or paragangliomas. *J Clin Endocrinol Metab* 2007;**92**:3822–8.

[30] Burnichon N, Briere JJ, Libe R, Vescovo L, Riviere J, Tissier F, et al. SDHA is a tumor suppressor gene causing paraganglioma. *Hum Mol Gen* 2010;**19**:3011–20.

[31] Hao HX, Khalimonchuk O, Schraders M, Dephoure N, Bayley JP, Kunst H, et al. SDH5, a gene required for flavination of succinate dehydrogenase, is mutated in paraganglioma. *Science* 2009;**325**(5944):1139–42.

[32] Gill AJ, Hes O, Papathomas T, Sedivcova M, Tan PH, Agaimy A, et al. Succinate dehydrogenase (SDH) -deficient renal carcinoma: a morphologically distinct entity: a clinicopathologic series of 36 tumors from 27 patients. *Am J Surg Pathol* 2014;**38**:1588–602.

[33] Boikos SA, Pappo AS, Killian JK, LaQuaglia MP, Weldon CB, George S, et al. Molecular subtypes of KIT/PDGFRA wild-type gastrointestinal stromal tumors: a report from the National Institutes of Health Gastrointestinal Stromal Tumor Clinic. *JAMA Oncol* 2016;**2**:922–8.

[34] Killian JK, Miettinen M, Walker RL, Wang Y, Zhu YJ, Waterfall JJ, et al. Recurrent epimutation of SDHC in gastrointestinal stromal tumors. *Sci Transl Med* 2014;**6**(268), 268ra177.

[35] Xekouki P, Pacak K, Almeida M, Wassif CA, Rustin P, Nesterova M, et al. Succinate dehydrogenase (SDH) D subunit (SDHD) inactivation in a growth-hormone-producing pituitary tumor: a new association for SDH? *J Clin Endocrinol Metab* 2012;**97**:E357–66.

[36] Menara M, Oudijk L, Badoual C, Bertherat J, Lepoutre-Lussey C, Amar L, et al. SDHD immunohistochemistry: a new tool to validate SDHx mutations in pheochromocytoma/paraganglioma. *J Clin Endocrinol Metab* 2015;**100**:E287–91.

[37] Tomlinson IP, Alam NA, Rowan AJ, Barclay E, Jaeger EE, Kelsell D, et al. Germline mutations in FH predispose to dominantly inherited uterine fibroids, skin leiomyomata and papillary renal cell cancer. *Nat Genet* 2002;**30**:406–10.

[38] Muller M, Ferlicot S, Guillaud-Bataille M, Le Teuff G, Genestie C, Deveaux S, et al. Reassessing the clinical spectrum associated with hereditary leiomyomatosis and renal cell carcinoma syndrome in French FH mutation carriers. *Clin Genet* 2017;**92**:606–15.

[39] Castro-Vega LJ, Buffet A, De Cubas AA, Cascon A, Menara M, Khalifa E, et al. Germline mutations in FH confer predisposition to malignant pheochromocytomas and paragangliomas. *Hum Mol Genet* 2014;**23**:2440–6.

[40] Yao L, Schiavi F, Cascon A, Qin Y, Inglada-Perez L, King EE, et al. Spectrum and prevalence of FP/TMEM127 gene mutations in pheochromocytomas and paragangliomas. *JAMA* 2010;**304**:2611–9.

[41] Qin Y, Deng Y, Ricketts CJ, Srikantan S, Wang E, Maher ER, et al. The tumor susceptibility gene TMEM127 is mutated in renal cell carcinomas and modulates endolysosomal function. *Hum Mol Genet* 2014;**23**:2428–39.

[42] Burnichon N, Cascon A, Schiavi F, Morales NP, Comino-Mendez I, Abermil N, et al. MAX mutations cause hereditary and sporadic pheochromocytoma and paraganglioma. *Clin Cancer Res* 2012;**18**:2828–37.

[43] Cascon A, Comino-Mendez I, Curras-Freixes M, de Cubas AA, Contreras L, Richter S, et al. Whole-exome sequencing identifies MDH2 as a new familial paraganglioma gene. *J Natl Cancer Inst* 2015;**107**.

[44] Toledo RA, Qin Y, Cheng ZM, Gao Q, Iwata S, Silva GM, et al. Recurrent mutations of chromatin-remodeling genes and kinase receptors in pheochromocytomas and paragangliomas. *Clin Cancer Res* 2016;**22**:2301–10.

[45] Schlisio S, Kenchappa RS, Vredeveld LC, George RE, Stewart R, Greulich H, et al. The kinesin KIF1Bbeta acts downstream from EglN3 to induce apoptosis and is a potential 1p36 tumor suppressor. *Genes Dev* 2008;**22**:884–93.

[46] Welander J, Andreasson A, Juhlin ML, Wiseman RW, Backdahl M, Hoog A, et al. Rare germline mutations identified by targeted next-generation sequencing of susceptibility genes in pheochromocytoma and paraganglioma. *J Clin Endocrinol Metab* 2014;**99**:E1352–60.

[47] Burnichon N, Vescovo L, Amar L, Libe R, de Reynies A, Venisse A, et al. Integrative genomic analysis reveals somatic mutations in pheochromocytoma and paraganglioma. *Hum Mol Genet* 2011;**20**:3974–85.

[48] Castro-Vega LJ, Letouze E, Burnichon N, Buffet A, Disderot PH, Khalifa E, et al. Multi-omics analysis defines core genomic alterations in pheochromocytomas and paragangliomas. *Nat Commun* 2015;**6**:6044.

[49] Juhlin ML, Stenman A, Haglund F, Clark VE, Brown TC, Baranoski J, et al. Whole-exome sequencing defines the mutational landscape of pheochromocytoma and identifies KMT2D as a recurrently mutated gene. *Genes Chromosomes Cancer* 2015;**54**:542–54.

[50] Comino-Mendez I, Tejera AM, Curras-Freixes M, Remacha L, Gonzalvo P, Tonda R, et al. ATRX driver mutation in a composite malignant pheochromocytoma. *Cancer Genet* 2016;**209**:272–7.

[51] Fishbein L, Leshchiner I, Walter V, Danilova L, Robertson AG, Johnson AR, et al. Comprehensive molecular characterization of pheochromocytoma and paraganglioma. *Cancer Cell* 2017;**31**:181–93.

[52] Sciacovelli M, Goncalves E, Johnson TI, Zecchini VR, da Costa AS, Gaude E, et al. Fumarate is an epigenetic modifier that elicits epithelial-to-mesenchymal transition. *Nature* 2016;**537**(7621):544–7.

[53] Selak MA, Armour SM, MacKenzie ED, Boulahbel H, Watson DG, Mansfield KD, et al. Succinate links TCA cycle dysfunction to oncogenesis by inhibiting HIF-alpha prolyl hydroxylase. *Cancer Cell* 2005;**7**:77–85.

[54] Loriot C, Domingues M, Berger A, Menara M, Ruel M, Morin A, et al. Deciphering the molecular basis of invasiveness in Sdhb-deficient cells. *Oncotarget* 2015;**6**:32955–65.

[55] van Nederveen FH, Gaal J, Favier J, Korpershoek E, Oldenburg RA, de Bruyn EM, et al. An immunohistochemical procedure to detect patients with paraganglioma and phaeochromocytoma with germline SDHB, SDHC, or SDHD gene mutations: a retrospective and prospective analysis. *Lancet Oncol* 2009;**10**:764–71.

[56] Korpershoek E, Favier J, Gaal J, Burnichon N, van Gessel B, Oudijk L, et al. SDHA immunohistochemistry detects germline SDHA gene mutations in apparently sporadic paragangliomas and pheochromocytomas. *J Clin Endocrinol Metab* 2011;**96**:E1472–6.

[57] NGS in PPGL (NGSnPPGL) Study Group, Toledo RA, Burnichon N, Cascon A, Benn DE, Bayley JP, et al. Consensus Statement on next-generation-sequencing-based diagnostic testing of hereditary phaeochromocytomas and paragangliomas. *Nat Rev Endocrinol* 2017;**13**:233–47.

[58] Lenders JW, Duh QY, Eisenhofer G, Gimenez-Roqueplo AP, Grebe SK, Murad MH, et al. Pheochromocytoma and paraganglioma: an endocrine society clinical practice guideline. *J Clin Endocrinol Metab* 2014;**99**:1915–42.

[59] Plouin PF, Amar L, Dekkers OM, Fassnacht M, Gimenez-Roqueplo AP, Lenders JW, et al. European Society of Endocrinology Clinical Practice Guideline for long-term follow-up of patients operated on for a phaeochromocytoma or a paraganglioma. *Eur J Endocrinol* 2016;**174**:G1–10.

[60] Gimenez-Roqueplo AP, Caumont-Prim A, Houzard C, Hignette C, Hernigou A, Halimi P, et al. Imaging work-up for screening of paraganglioma and pheochromocytoma in SDHx mutation carriers: a multicenter prospective study from the PGL.EVA Investigators. *J Clin Endocrinol Metab* 2013;**98**:E162–73.

[61] Taieb D, Tessonnier L, Sebag F, Niccoli-Sire P, Morange I, Colavolpe C, et al. The role of 18F-FDOPA and 18F-FDG-PET in the management of malignant and multifocal phaeochromocytomas. *Clin Endocrinol* 2008;**69**:580–6.

[62] Hadoux J, Favier J, Scoazec JY, Leboulleux S, Al Ghuzlan A, Caramella C, et al. SDHB mutations are associated with response to temozolomide in patients with metastatic pheochromocytoma or paraganglioma. *Int J Cancer* 2014;**135**:2711–20.

A. Buffet (alexandre.buffet@inserm.fr).
Inserm, UMR970, Paris-Centre de recherche cardiovasculaire, 75015 Paris, France.
Faculté de médecine, Université Paris Descartes, PRES Sorbonne Paris Cité, 75006 Paris, France.

A.-P. Gimenez-Roqueplo.
Inserm, UMR970, Paris-Centre de recherche cardiovasculaire, 75015 Paris, France.
Faculté de médecine, Université Paris Descartes, PRES Sorbonne Paris Cité, 75006 Paris, France.
Service de génétique, Hôpital européen Georges-Pompidou, AP–HP, 56, rue Leblanc, 75015 Paris, France.
Centre expert national COMETE-Cancer de la surrénale, 75014 Paris, France.

Toute référence à cet article doit porter la mention : Buffet A, Gimenez-Roqueplo AP. Génétique des phéochromocytomes et paragangliomes. EMC - Endocrinologie-Nutrition 2018;0(0):1-8 [Article 10-015-B-55].